

بسم الله الرحمن الرحيم

*For the soul of my father who planted and firmed in myself  
the significance of scientific research for our life*

**THE SEISMIC ANALYSIS OF STATICALLY DESIGNED TALL  
REINFORCED CONCRETE BUILDINGS USING THE FINITE  
ELEMENT METHOD**

by

**TAHER MOKHTAR AHMED EL-KHAWANKY**

Advanced Engineering Research Institute  
School of Computing, Science & Engineering  
University Of Salford, Salford, UK

A thesis Submitted for the degree of Doctor of Philosophy

September 2003





2.2.3.1	Forms of Earthquake Loads in Analysis and Design of Structures .....	35
2.2.3.2	Effects of Earthquake Loads on RC Buildings .....	37
2.3	Seismic Analysis of Multi-Storey RC Buildings Using the FEM .....	40
2.3.1	Elastic Analysis of Multi-Storey RC Buildings Under Earthquake Loading .....	49
2.3.1.1	Time – History Analysis of Three-Dimensional Multi-Storey RC Buildings (Direct Integration Method) .....	49
2.3.2	Inelastic Analysis of Multi-Storey RC Buildings Under Earthquake Loading .....	52
2.3.3	Modelling and Analysis of Structures Using the Finite Element Method .....	53
2.3.3.1	Review of Finite Element Method (FEM) .....	54
2.3.4	Assessment of Seismic Performance of Existing Multi-Storey RC Buildings Designed to Normal Design Codes .....	55
2.4	Seismic Design .....	57
2.4.1	Philosophy of Seismic Design of RC Buildings According to Modern Design Codes .....	60
2.4.2	Conceptual Design of Tall RC Buildings .....	64
2.4.3	Structural Systems of Tall RC Buildings Against Earthquakes ...	65
2.4.3.1	Ductility System of Buildings .....	65
2.4.3.2	Structural Wall System .....	68
2.4.3.3	Dual Systems .....	69
Chapter 3	Verification of ANSYS (Preliminary Analysis) .....	70
3.1	ANSYS Overview .....	70
3.1.1	Basic Analysis Procedures of ANSYS .....	70
3.1.2	Structural Analyses of ANSYS .....	72
3.1.2.1	Nonlinear Analysis .....	73
3.1.2.2	Static Analysis .....	76
3.1.2.3	Modal Analysis .....	77
3.1.2.4	Transient Dynamic Analysis .....	77
3.2	Capability Check of ANSYS to Perform Nonlinear Analysis .....	79
3.3	ANSYS Analysis of an unbraced 5-storey RC Building .....	80
3.3.1	Three Dimensional Static Analysis .....	83

3.3.2	Three Dimensional Modal Analysis .....	84
3.3.2.1	Analytical Calculations of Natural Frequencies .....	89
3.3.3	Three Dimensional Transient Dynamic Analysis .....	90
3.3.3.1	Input Ground Motion .....	91
3.3.3.2	Analysis Under Horizontal Earthquake .....	92
3.3.3.3	Analysis Under both Horizontal and Vertical Earthquake Together .....	99
3.4	ANSYS Analysis of a braced 5-storey RC Building .....	102
3.4.1	Three Dimensional Static Analysis .....	104
3.4.2	Three Dimensional Modal Analysis .....	104
3.4.2.1	Rayleigh Damping Coefficients .....	108
3.4.3	Three Dimensional Transient Dynamic Analysis .....	110
3.4.3.1	Analysis Under Horizontal Earthquake .....	111
3.4.3.2	Analysis Under both Horizontal and Vertical Earthquake Together .....	114
3.4.3.3	Verification of Results Using Analytical Calculations ..	116
3.5	Discussion of Seismic Response of the unbraced and braced 5-storey RC Building .....	117
3.5.1	Effects Study of Gravity Loads, Damping Ratio, and Infill Walls .....	118
3.5.2	Probabilities of Formation of Soft Storey (Building Stiffness) .....	121
Chapter 4	Three Dimensional Modelling and Analysis .....	123
4.1	Static Design of the Ten-Storey RC Building .....	123
4.1.1	Description of the Building .....	124
4.2	Three Dimensional Finite Element Modelling of the Global Building Structure .....	126
4.2.1	Modelling Approach .....	127
4.2.2	Generation of the Finite Element Model .....	128
4.3	Linear Static Analysis of the FCTS and SCTS Model .....	133
4.4	Modal Analysis of the FCTS and SCTS Model .....	137
4.5	Transient Linear Dynamic Analysis of the FCTS and SCTS Model .....	146

<b>Chapter 5</b>	<b>Seismic Assessment</b>	<b>150</b>
5.1	Philosophy of Assessment	150
5.2	Assessment of the FCTS Model	155
5.2.1	Discussion and Evaluation of Assessment Results (Collapse Mechanism)	155
5.2.2	Conservatism of the Assessment Technique for the Seismic Analysis Results	159
5.3	Assessment of the SCTS Model	161
5.3.1	Discussion and Evaluation of Assessment Results (Collapse Mechanism)	162
5.4	Response Spectra of the FCTS and SCTS model	166
5.4.1	Under Horizontal Earthquake Only	166
5.4.2	Under both Horizontal and Vertical Earthquake Together	169
<b>Chapter 6</b>	<b>Discussion of Results</b>	<b>172</b>
6.1	Introduction	172
6.2	Investigation of the Affecting Factors on Collapse Mechanisms of the FCTS and SCTS Model	173
6.2.1	Soft Storey	173
6.2.2	Vertical Earthquake	176
6.2.3	Building Response	177
6.3	Significance of the Three Dimensional Simulation of Buildings	178
<b>Chapter 7</b>	<b>Conclusion and Future Work</b>	<b>180</b>
7.1	General Conclusion	180
7.1.1	Choice of the Earthquake Accelerogram	180
7.1.2	Consideration of Soil Structure Interaction	181
7.2	Assessment	181
7.2.1	Conservatism in the Loading	182
7.2.2	Conservatism in the Code Assessment	184
7.3	Model Behaviour – Static vs Seismic Design	184
7.4	Future Work	186



References ..... 188

Appendix I : Static Linear and Nonlinear Analyses of Steel Fixed Beam  
& One-Storey Steel Portal Frame ..... 193

Appendix II : Design Calculation Sheet of Ten-Storey Reinforced  
Concrete Building ..... 207

Appendix III : ANSYS Input Data Batch File of Transient Dynamic  
Analysis of FCTS Under both Horizontal and Vertical  
Earthquake Together ..... 274

Appendix IV : Spreadsheet of Assessment Results ..... 291

Appendix V : Analytical Calculations for the Seismic Performance of  
the 10 Storey RC Building ..... 307

## LIST OF FIGURES

- Fig.2.1 Short-term design stress - strain curve for normal-weight concrete
- Fig.2.2 Short-term design stress - strain curve for reinforcement
- Fig.2.3 Influence of stress and strain rate on concrete properties in compression
- Fig.2.4 Influence of strain rate on yield stress of hot rolled reinforcing steel bars
- Fig.2.5 Linear elastic stress & strain distribution of a beam section under service loading
- Fig.2.6 Stress & strain distribution of a beam section at first yield and at RC failure
- Fig.2.7 Illustration of ductile behaviour during cyclic horizontal loading
- Fig.2.8 Collapse beam mechanism and collapse combined mechanism for RC portal frame
- Fig.2.9 Possible collapse mechanisms of reinforced concrete portal frame
- Fig.2.10 Collapse mechanisms
- Fig.2.11 Soft -storey sway mechanism, 1990 Philippine earthquake
- Fig.2.12 Formation of a soft and weak storey, 1999 Turkey earthquake
- Fig.2.13 Mathematical model for one-storey structure excited by an external force
- Fig.2.14 Mathematical model for a one-storey structure excited at its base
- Fig.2.15 Mode shapes of a free vibration three-storey frame
- Fig.2.16 Characteristic deformation
- Fig.2.17 Maximum horizontal shear response for Bank of New Zealand building
- Fig.2.18 North-south component of the El Centro earthquake, California, 1940
- Fig.2.19 Typical UK design response spectra
- Fig.2.20 Global seismic hazard map of the world
- Fig.2.21 Types of failure at beam-column joints during the earthquake
- Fig.2.22 Relationship between the ductility and concrete compressive strength
- Fig.2.23 Different types of finite element with nodal degrees of freedom shown at a typical node only
- Fig.2.24 Isolated building structures supported on laminated rubber springs

Fig.3.1	The finite element model of unbraced five-storey RC building (UFS)
Fig.3.2	The floor plan of storeys of UFS
Fig.3.3	Sway mode of UFS model in x-direction
Fig.3.4	Torsional mode shape of UFS model and its longitudinal stresses
Fig.3.5	Comparison between theoretical and ANSYS modal analysis results of the UFS model
Fig.3.6	Typical displacement time-history input motion
Fig.3.7	Acceleration response spectra of horizontal input motion using ANSYS
Fig.3.8	Acceleration response spectra of horizontal input motion using the computer program
Fig.3.9	Displacement time-histories of building floors and input motion
Fig.3.10	Maximum displacements of building floors during seismic excitation
Fig.3.11	Maximum shear forces at building floors during seismic excitation
Fig.3.12	Maximum moments of columns at joints during seismic excitation
Fig.3.13	Comparison between maximum moments and axial loads of building columns under earthquake
Fig.3.14	Inter-storey drifts of UFS model at maximum displacement of upper floor under earthquake
Fig.3.15	Deformed and undeformed shape of UFS model at maximum displacement of upper floor under earthquake
Fig.3.16	Response envelopes of elastic lateral displacements and columns moments of 20-storey RC building under an earthquake
Fig.3.17	Maximum vertical displacement of building floors during concurrent components of earthquake
Fig.3.18	Comparison between maximum moments and axial loads of building columns under horizontal & vertical earthquake
Fig.3.19	Variation of the fundamental period with time step for the UFS model under horizontal earthquake only & under both horizontal and vertical earthquake together
Fig.3.20	The finite element model of braced five-storey RC building (BFS)
Fig.3.21	Sway mode of BFS model in x-direction
Fig.3.22	Torsional mode shape of BFS model and its longitudinal stresses

Fig.3.23	Rayleigh damping coefficients of the UFS model
Fig.3.24	Displacement time-histories of building floors and input motion
Fig.3.25	Acceleration response spectra of BFS floors under horizontal earthquake
Fig.3.26	Maximum displacements of building floors during seismic excitation
Fig.3.27	Maximum shear forces at building floors during seismic excitation
Fig.3.28	Maximum moments of columns at joints during seismic excitation
Fig.3.29	Comparison between maximum moments and axial loads of building columns under earthquake
Fig.3.30	Maximum vertical displacement of building floors during concurrent components of earthquake
Fig.3.31	Comparison between maximum moments and axial loads of building columns under horizontal & vertical earthquake
Fig.3.32	Acceleration response spectra of slabs of building floors under both horizontal and vertical earthquake together
Fig.3.33	Analytical calculations of PGA for the BFS model under horizontal earthquake only
Fig.3.34	Comparison between excited displacement time histories of upper floor for the UFS & BFS model under horizontal earthquake only
Fig.3.35	Deformed shape of the UFS & BFS model at maximum drift of the upper floor under horizontal earthquake only
Fig.3.36	Comparison between acceleration response spectra of the upper floor for the UFS & BFS model under horizontal earthquake only
Fig.3.37	Comparison between axial load time histories of ground floor columns for the UFS & BFS model under horizontal earthquake only
Fig.3.38	Displaced shape of the BFS model at maximum moment of the first floor columns during the horizontal earthquake
Fig.4.1	The ten-storey RC building
Fig.4.2	The ANSYS finite element type Beam 4
Fig.4.3	The ANSYS finite element type Beam 44
Fig.4.4	The ANSYS finite element type Shell 63
Fig.4.5	The ANSYS finite element type Link 8



Fig.4.6	The 3D finite element model of the ten-storey RC building (FCTS)
Fig.4.7	Base numbers of the FCTS & SCTS models
Fig.4.8	Sway mode of FCTS model in x-direction
Fig.4.9	Torsional mode of FCTS model in y-direction
Fig.4.10	Rayleigh damping coefficients of the FCTS model
Fig.4.11	Rayleigh damping coefficients of the SCTS model
Fig.4.12	Loading steps of the gravitational constant 9.81 m/s/s in ANSYS for applying the gravity loads of model
Fig.5.1	Realistic seismic response of the FCTS model under horizontal earthquake only
Fig.5.2	Realistic seismic response of the FCTS model under both horizontal & vertical earthquake together
Fig.5.3	Columns axes of the ground floor of the FCTS & SCTS model
Fig.5.4	Columns axes of the above floors of the FCTS & SCTS model
Fig.5.5	Realistic seismic response of the SCTS model under horizontal earthquake only
Fig.5.6	Realistic seismic response of the SCTS model under both horizontal & vertical earthquake together
Fig.5.7	Horizontal acceleration secondary response spectra of FCTS floors under horizontal earthquake
Fig.5.8	Horizontal acceleration secondary response spectra of SCTS floors under horizontal earthquake
Fig.5.9	Vertical acceleration secondary response spectra of FCTS floors under concurrent horizontal & vertical earthquake
Fig.5.10	Vertical acceleration secondary response spectra of SCTS floors under concurrent horizontal & vertical earthquake
Fig.6.1	Margin values of the front left corner column and its surrounding columns of the FCTS model under the vertical earthquake

- Fig.6.2 Margin values of the front internal column and its surrounding columns of the FCTS model under the horizontal earthquake only
- Fig.6.3 Margin values of the front left corner column and its surrounding columns of the SCTS model under the vertical earthquake
- Fig.6.4 Maximum axial loads of floor corner columns of the FCTS model under horizontal earthquake only & under concurrent horizontal and vertical earthquake
- 
- Fig.I.1 The steel fixed ended beam
- Fig.I.2 The stress distribution of beam section of the studied cases
- Fig.I.3 The elastic bending moment distribution of the beam
- Fig.I.4 The collapse mechanism of the beam
- Fig.I.5 The deformed shape of the beam under a vertical point load and its horizontal stresses
- 
- Fig.I.6 Comparison between analytical and ANSYS results of the node 1
- Fig.I.7 Comparison between analytical and ANSYS results of the node 2
- Fig.I.8 Comparison between analytical and ANSYS results of the node 3
- Fig.I.9 The geometry and loads of the steel portal frame (general case)
- Fig.I.10 The moment distribution diagrams of the steel portal frame (linear analyses cases)
- Fig.I.11 (a) The beam mechanism of the steel portal frame and its bending moment diagram
- Fig.I.11 (b) The sway mechanism of the steel portal frame and its bending moment diagram
- Fig.I.11 (c) The combined mechanism of the steel portal frame and its bending moment diagram
- Fig.I.12 Comparison between analytical and ANSYS results of the node 1 for the linear analysis cases
- Fig.I.13 Comparison between analytical and ANSYS results of the node 1 for the nonlinear analysis cases
- Fig.I.14 Comparison between theoretical and ANSYS results of the formation of combined collapse mechanism

Fig.II.1	Details of the building
Fig.II.2	Plan of the ground floor slab
Fig.II.3	Plan of every floor slab for the floors from the first to ninth

**LIST OF TABLES**

Table 2.1	Mechanical properties of concrete and reinforcing steel bars
Table 2.2	The MSK intensity scale
Table 3.1	Design details of model of UF
Table 3.2	Analytical and ANSYS results of static linear analysis of UFS
Table 3.3	Sum of effective masses of all modes in each direction for UFS
Table 3.4	Modal analysis results of UFS
Table 3.5	Modal analysis results of the UFS model
Table 3.6	Natural frequencies of the UFS model from analytical and ANSYS modal analysis
Table 3.7	Comparison between mode shapes from modal analysis and displaced shapes of transient dynamic analysis of UFS model
Table 3.8	Analytical and ANSYS results of static linear analysis of BFS
Table 3.9	Sum of effective masses of all modes in each direction for BFS
Table 3.10	Modal analysis results of BFS
Table 3.11	Modal analysis results of the BFS model
Table 4.1	General details of the ten-storey RC building
Table 4.2	Analytical and ANSYS results for mass of FCTS & SCTS
Table 4.3	ANSYS static analysis results of FCTS
Table 4.4	ANSYS static analysis results of SCTS
Table 4.5	Comparison between design and analysis forces of transfer beams
Table 4.6	ANSYS modal analysis of the FCTS model
Table 4.7	ANSYS modal analysis of the SCTS model
Table 4.8	Modal analysis results of the FCTS & SCTS model
Table 5.1	Seismic response of the transfer beam of the FCTS model
Table 5.2	Seismic response of the transfer beam of the SCTS model

Table I.1	Description of steel fixed ended beam
Table I.2	Comparison between the results of analytical and ANSYS program analyses of the beam
Table I.3	The load cases and analysis types of the steel portal frame
Table I.4	Comparison between the results of analytical and ANSYS program analyses of the steel portal frame
Table I.5	Comparison between the results of analytical and ANSYS program analyses of the steel portal frame

## **ACKNOWLEDGEMENTS**

I would like to thank Dr. L.Weekes for his valuable aid and advise throughout the research and I am also gratefully acknowledge the support & encouragement received from him.

I owe special thanks to Prof. C. Melbourne for his helpfulness throughout the research, his expert advise on matters of Structural Engineering. Also, I owe many thanks to all my colleagues who have helped & supported me throughout this research.

To my wife, who has given unconditional support at home, with my family & research, I owe much debt of gratitude.

Lastly but not least. For my mother who has encouraged me throughout my life to aspire to much heights.

## **DECLARATION**

None of the material contained in this thesis has been submitted in support of an application for another degree of qualification of this or other university or institution of learning.

**Taher Mokhtar El-Khawanky**

**July 2003**



**ABBREVIATIONS**

SDOF	Single degree of freedom
RC	Reinforced concrete
EC8	Eurocode 8
ZPA	Zero period acceleration
PGA	Peak ground acceleration
PA	Peak acceleration
UFS	Unbraced five storey reinforced concrete building
BFS	Braced five storey reinforced concrete building
$f_y$	Characteristic strength of reinforcement
$f_{cu}$	Characteristic cube strength of concrete
$\gamma_m$	Partial safety factor for materials
$E_c$	Modulus of elasticity of concrete
$E_s$	Modulus of elasticity of steel
$\epsilon_{cu}$	Ultimate concrete strain in compression
$\epsilon_s$	Tensile strain in tension reinforcement
$\nu_c$	Poisson's ratio of concrete
$\nu_s$	Poisson's ratio of steel
$\phi_u$	Curvature of section of reinforced concrete member at ultimate moment
$\phi_y$	Curvature of section of reinforced concrete member at first yield
$M_p$	Plastic moment capacity
$\sigma$	Stress
$g$	Acceleration of gravity
FCTS	First case ten-storey reinforced concrete building
SCTS	Second case ten-storey reinforced concrete building



## **ABSTRACT**

Earthquakes present one of the most devastating hazards on the planet. They threaten the safety of civilians in seismically active regions, and are of extreme concern in applications that demand a high level of safety, i.e. the nuclear industry. However in nearly all cases, the fatalities that occur are as a result of the collapse of man-made structures. Hence the problems facing Civil Engineers who are concerned with seismic mitigation is evident. The dynamic behaviour of their structures must now be accounted for in the design. As our knowledge broadens, structures can, and are being designed to be earthquake resistant. However there are many buildings still standing in seismically active regions which have been designed for static load cases only, or are now of substandard design.

Seismic engineering research and application has progressed rapidly over the last few decades, not least in part due to the evolution of computer technology, and our ability to produce computer models which aid us in the design and analysis processes. Hence the research presented focuses on the global behaviour of a typical statically designed tall reinforced concrete building.

A literature review has been performed to investigate current mathematical and experimental work which has been carried out with regard to reinforced concrete structures under seismic/cyclic loading. The main point to note from this is that most of the current research has focussed on local behaviour rather than overall global response. The majority of models incorporating global 3D finite element modelling using time-history analysis are being created in the Nuclear Industry.

After verification work, the ANSYS general purpose finite element computer package has been used to analyse a statically designed 10-storey reinforced concrete building (designed to the rules of BS8110) for static, modal and time-history analyses under a typical (synthetic) earthquake. Certain features have been incorporated in the model with the foresight that these might cause problems under dynamic loading (i.e. soft-storeys). The global response of the building has then been investigated, backed up with supporting 'hand' calculations.

A 'margins' assessment was carried out mainly on the columns to the requirements of a static code. This enabled the identification the problematic areas of the building, giving insight into the collapse behaviour and possible areas where design upgrade, attention to workmanship or retrofit may be required. In this process the potential for redistribution and overload capacity of the structure is also demonstrated.

In conclusion, a number of suggestions for future work using global response models are made, and the benefits of using the global model approach adopted are discussed in detail. The global response, as opposed to local effects are captured providing insight into the potential for partial or total collapse.

# CHAPTER 1 INTRODUCTION

## 1.1 Background

The collapse of structures due to sudden dynamic transient load effects such as earthquakes are considered as one of the most serious problems which face civil engineers around the world today. The earthquake is considered as the independent natural phenomenon of vibration of the ground and becomes a dangerous phenomenon when it is considered in relation to structures. Many earthquake related disasters are due to the failure of important man-made structures such as multi-storey reinforced concrete buildings. These types of buildings are vulnerable to failure during earthquakes due mainly to their structural form and properties.

Earthquakes present one of the most devastating hazards on the planet. They threaten the safety of civilians in seismically active region since the collapse of tall reinforced concrete buildings suddenly due to earthquake loads can result in a catastrophic loss of life. In recent years, seismic regions have extended to new parts of the world, which has led to an increase in seismic hazard for people in many areas which were thought previously to be low risk. Reinforced concrete structures constitute the common types of construction for some of these areas (such as the Middle East area which includes Egypt) due to the abundance of reinforced concrete material resources. Although these areas are now prone to seismic activity, the design of multi-storey RC buildings is still carried out in accordance with the static design codes. In general, the countries which are situated in these areas contain many RC buildings which have been designed for static load cases only, and are now possibly of substandard design. Consequently, the interest and research into the behaviour and analysis of existing multi-storey reinforced concrete buildings (which were designed according to the static design codes) under dynamic action such as earthquakes has seen an increase in recent years due to failure of such structures under seismic loads.

In recent decades, earthquakes having an intensity range from moderate to high were occurred in Egypt. In 1988, a detailed presentation of the regulations for earthquake resistant design of RC buildings was published by the Egyptian society for earthquake engineering. In 1989, the simplest form of these regulations (depending mainly on static

analysis and design) was included in the Egyptian code for the design & construction of reinforced concrete buildings. The standard seismic analysis and design of buildings is limited for the structures of particular importance to the community that require a more exact analysis.

Many years ago research has begun regarding the seismic engineering field and much research has been carried out since to study the effects of earthquakes on tall reinforced concrete buildings with regard to their dynamic behaviour. These studies yielded useful results, which could be subsequently, used in seismic design. The incorporation of seismic design procedures in building design was first adopted in a general sense in the 1920s and 1930s, when the importance of inertial loadings of buildings began to be appreciated. In the absence of reliable measurements of ground accelerations and as a consequence of the lack of detailed knowledge of the dynamic response of structures, the magnitude of seismic inertia forces could not be estimated with any reliability. Typically, design for lateral forces corresponding to about 10% of the building weight was adopted.

By the 1960s accelerograms giving detailed information on the ground acceleration occurring in earthquakes were becoming more generally available. The advent of design philosophies, and development of sophisticated computer-based analytical procedures facilitated a much closer examination of the seismic response of structures. In recent years the evolution of computer technology has advanced to the stage where the finite element method (through codes such as 'ANSYS') can realistically be used to model full-scale buildings and subject them to a variety of loads, including seismic. Modelling through a detailed finite element discretisation of the structure can provide a more realistic representation of the actual seismic behaviour of RC buildings (which cannot be readily obtained through experimental testing).

## **1.2 Research Objectives**

Seismic risk mitigation is an essential requirement of contemporary structural design and assessment of existing structures, and seismic ground motions are a major cause for concern when considering their damaging effects on multi-storey reinforced concrete buildings. The exact characteristics of the earthquake ground motions that may occur at a given site cannot be predicted with certainty, and it is difficult to evaluate all



factors affecting the complete behaviour of a complex structure such as these buildings when subjected to the earthquake. Nevertheless, it is possible to seismically analyse these buildings using FE and subsequently assess its seismic behaviour to understand the possible collapse mechanisms that may occur. Determination of the realistic collapse mechanism extensively contributes in improving the seismic performance of tall RC buildings and mitigation of the seismic risk.

The designed mode of failure for multi-storey reinforced concrete buildings during earthquakes involves the formation of sufficient plastic hinges at the joints to produce a mechanism. Structural collapse mechanisms depend mainly on the deformation capacity (ductility), location and number of plastic hinges in the structure. Plastic hinges may be designed to form at the end regions of nearly all beams in a high-rise building, causing a global sway mechanism for whole building. At the other extreme, plastic hinges may concentrate in a single storey at the two ends of all its columns, causing a 'soft-storey' or 'column-sway' mechanism. This mechanism accounts for numerous collapses of existing multi-storey framed buildings in recent earthquakes, and many examples of this exist.

Hence, the main objective of this research is to determine the realistic collapse mechanism of an existing statically designed multi-storey RC building containing a soft storey using finite element analysis. The other objectives are as follows:

1. Using the finite element method (ANSYS computer package) to develop a three dimensional model for the seismic analysis of statically designed structures such as multi-storey RC buildings
2. Perform an assessment to appropriate codes (i.e. BS8110) to examine the relative performance of the building under a prescribed earthquake
3. Identify the vulnerable areas of the buildings and study the effects of the structural members stiffnesses to improve the seismic performance of such buildings
4. Examine the damaging effects of the vertical component of the earthquake on the RC buildings

5. To examine any mitigating circumstances or conservatism inherent within the analysis and assessment of the model which may improve seismic withstand, and demonstrate that good static design can provide significant overload capacity (depending on the quality of workmanship & detailing provided)

The implemented approach in this research for achieving these objectives is demonstrated throughout the next chapters as follows:

- Chapter 2 presents a complete review for the available previous works (which have been carried out experimentally or theoretically) concerning the static & dynamic analysis and design of tall RC buildings. Also this chapter discusses the implemented previous works for study of the complete seismic behaviour of multi-storey RC buildings global structures. It was noted that the previous & current research of the overall global seismic response are mainly focussed on the study of local seismic behaviour. The study of the global seismic response of multi-storey RC buildings constitutes the main objective of this research.
- Chapter 3 addresses the verification of ANSYS to be used to satisfy the objectives of this research. Not only does the findings of this chapter confirm the use of ANSYS for subsequent analysis, but many useful preliminary models are produced from which much about seismic behaviour in general has been learned. The results of these analyses are included in the chapter and Appendix I.
- Chapter 4 presents the static design (according to BS8110) of the main models of the research (ten-storey RC buildings: FCTS & SCTS) and the calculation sheet is included in the Appendix II. Also this chapter presents the three-dimensional modelling technique of these models using the ANSYS program, and the linear static & dynamic analysis of the ten-storey RC buildings is discussed (the ANSYS input data batch file of the transient dynamic analysis of FCTS under both horizontal & vertical earthquake together is included in the Appendix III).
- Chapter 5 discusses and evaluates the structural assessment of the transient dynamic analysis results of the FCTS & SCTS model to determine the factors affecting the seismic behaviour and the possible collapse mechanisms of these buildings during the prescribed earthquake. A sample of the spreadsheet of the

assessment process for the models is involved in the Appendix IV. The resulting response spectra of these models under earthquakes are presented and verified using the analytical calculations that are included in the Appendix V.

- Chapter 6 discusses the results of the seismic analysis & assessment of the models and examines the effects of some significant factors on the seismic behaviour of multi-storey RC buildings.
- Chapters 7 contains the conclusions which were drawn from this research work and a number of recommended suggestions for the future work.

In general, it is difficult to evaluate all aspects of the complete seismic behaviour of structures (such as multi-storey RC buildings) due to the complexity and number of parameters involved. However this research is focussed on the overall global seismic behaviour of high-rise RC buildings in order to provide both the seismic engineering research field and industry with a methodology for analysis & assessment which may be used reliably & conservatively to estimate global seismic behaviour.

## CHAPTER 2 REVIEW OF PREVIOUS WORKS

### 2.1 Reinforced Concrete

Historical surveys of reinforced concrete reveals that this composite material was discovered as a construction material in the mid eighteenth century in France, England and United States of America. Throughout the entire period 1850-1900, relatively little researches were conducted to test this material theoretically and experimentally to understand its physical and mechanical behaviour in the construction field. In the first decade of the twentieth century, progress in reinforced concrete was rapid especially after determination the behaviour of structural elements of reinforced concrete such as beams, columns and slabs. Since the mid twentieth century, reinforced concrete has become the most important building material and much research still has been (and is being) carried out regarding its development.

Understanding of reinforced concrete behaviour is still far from complete; building codes and specification that give design procedures are continually changing to reflect latest knowledge, Wang and Salmon, ref. [1].

Reinforced concrete is a composite material consisting of concrete reinforced with steel bars. This material makes use of tensile strength of the steel & compressive strength of the concrete (concrete on its own has low tensile capacity) therefore providing an appropriate material for construction. Concrete, unlike any other structural building material, allows the architects and engineers to choose not only its mode of production, but also control its structural behaviour i.e. ductility & strength as well to resist the most onerous of loading effects. When architects and engineers specify a concrete structural system, they must also specify a multitude of variables, such as its strength, durability, forming techniques, hardening characteristics, nature and extent of reinforcement, aesthetics and much more, Ali, ref. [2]. Reinforced concrete can be used for all standard buildings both single storey and multistory and for containment / retaining structures and bridges.

Concrete has low tensile strength and a high compressive strength. The Steel reinforcement is provided to effectively overcome the deficiencies in the tensile strength of the concrete. So the reinforcing steel must have adequate tensile properties and form



a strong bond with the concrete since the concrete transmits load to the steel by longitudinal shearing stresses, in structures such as beams & columns. The bond is purely mechanical and arises from surface roughness and friction.

The behaviour of hardened reinforced concrete is influenced by the properties of concrete and steel bars under the type of applied loading. This behaviour under static loading is well known and there are many different design codes around the world governing the behaviour of reinforced concrete structures to guard against sudden failure. In recent years, dynamic loading such as that which may be caused by earthquakes presents dangerous effects on reinforced concrete structures, potentially causing collapse. Much research has focussed on understanding the behaviour of reinforced concrete under such dynamic actions.

This research is focussed on the behaviour of tall reinforced concrete buildings under earthquakes loads such that is types of common reinforced concrete structures found in many countries prone to seismic activity. The following sections present a review of previous research concerned with the behaviour of reinforced concrete structures under static and dynamic loading.

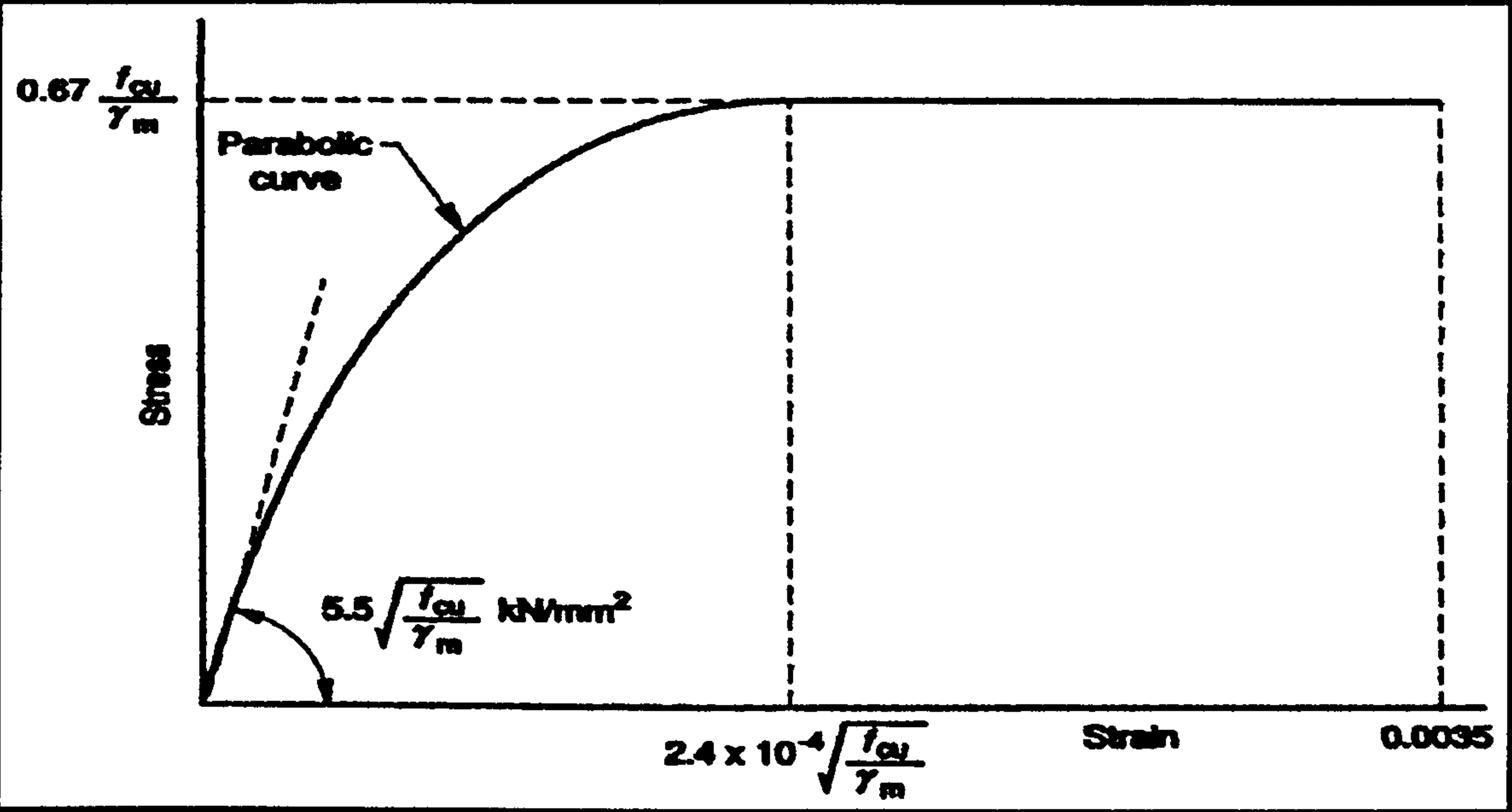
### **2.1.1 Static & Dynamic Behaviour of Reinforced Concrete**

According to the type of loading, behaviour of reinforced concrete is divided into static and dynamic behaviour. The design codes which regulate the behaviour of reinforced concrete buildings are also divided depending on loading type into static codes (normal codes) such as BS-8110, ref. [3] and dynamic codes (modern codes) such as Eurocode 8, ref. [4]. In general, the behaviour of reinforced concrete is mainly analysed and recognised based on the properties of concrete and reinforcing steel bars under loading, properties such as modulus of elasticity (Young's modulus) & Poisson's ratio in the elastic deformation zone and the ductility & strength in the inelastic deformation zone.

#### **Static Properties of Reinforced Concrete**

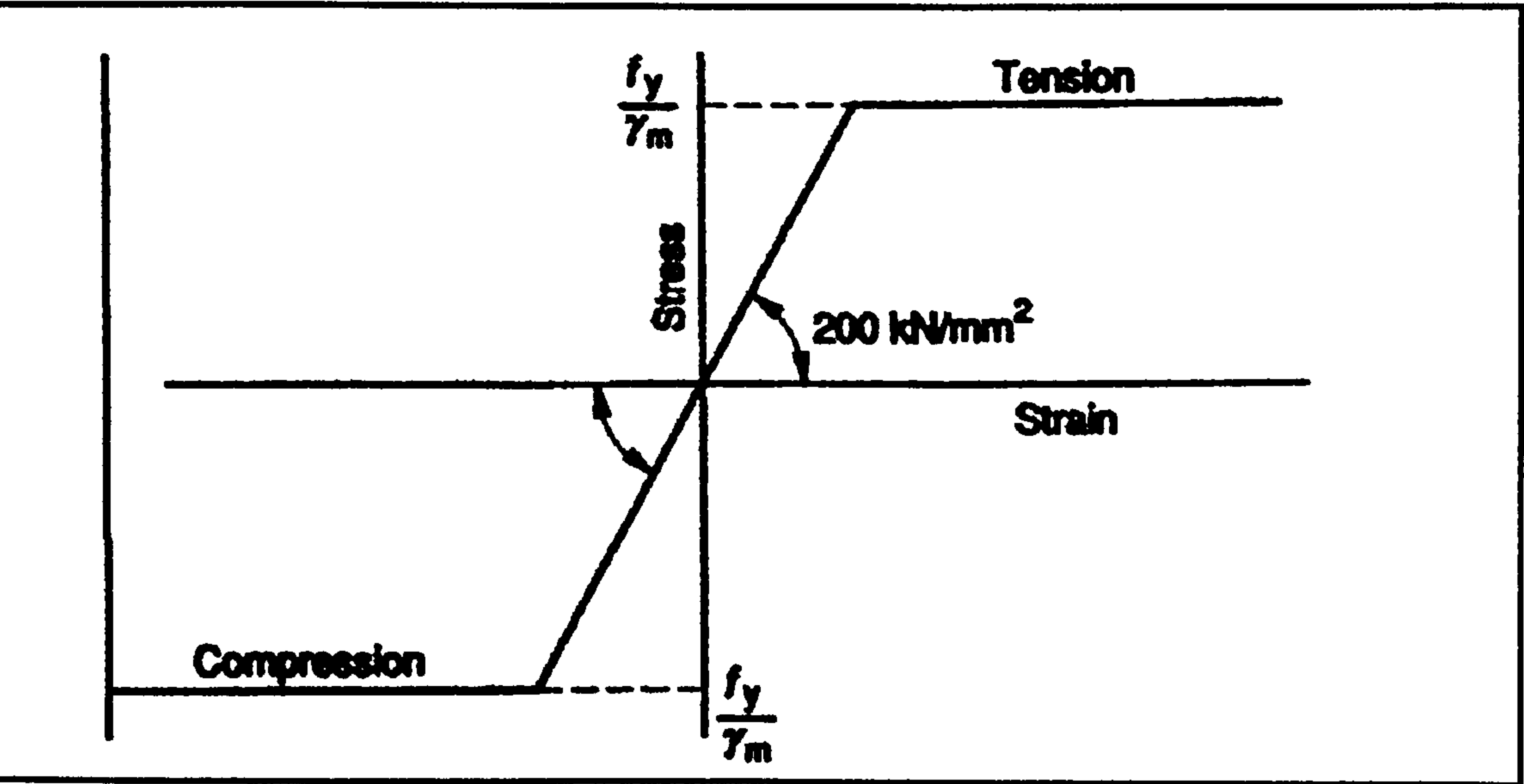
Determination of the properties of reinforced concrete material depends on the stress-strain curves for concrete and reinforcement. Fig. (2.1) and Fig. (2.2) show the idealized

stress-strain relationships for concrete and steel reinforcement according to BS-8110: part1, ref. [3], for design purposes. There are two types of reinforcing steel bars, hot rolled mild steel bars and hot rolled high yield steel bars, the ductility of hot rolled mild steel bars is greater than hot rolled high yield steel bars. Table (2.1) shows the mechanical properties of concrete and reinforcing steel bars according to BS-8110: part1, ref. [3], Kong & Evans, ref. [5] and MACGinley & Choo, ref. [6].



Note:  $f_{cu}$  is in  $\text{N/mm}^2$ .

Figure 2.1 Short-term design stress - strain curve for normal-weight concrete (BS 8110: part1, ref. [3])



Note:  $f_y$  is in  $\text{N/mm}^2$ .

Figure 2.2 Short-term design stress - strain curve for reinforcement (BS 8110: part1, ref. [3])

Mechanical properties	Concrete (In compression)	Steel bars (In compression and tension)	
		Hot rolled mild steel bars	Hot rolled high yield steel bars
Yield stress (N/mm <sup>2</sup> )	$f_y = 0.67f_{cu} / \gamma_m$	$f_y = 250$	$f_y = 460$
Young's modulus (KN/mm <sup>2</sup> )	$E_c = 20$	$E_s = 200$	$E_s = 200$
Strain at yield	$\epsilon_{cu} = 0.0035$	$\epsilon_s = 0.0011$	$\epsilon_s = 0.002$
Poisson's ratio	$\nu_c = 0.2$	$\nu_s = 0.3$	$\nu_s = 0.3$

Note:  $\gamma_m$  is equal 1.5 for concrete and 1.05 for steel bars.

**Table 2.1** Mechanical properties of concrete and reinforcing steel bars  
(BS 8110: part1, ref. [3])

The exact shape of the stress-strain curve of concrete is much dependent on its strength but for design purposes and practical use of concrete in the building construction, BS 8110 idealizes the stress-strain curves of concrete and reinforcement as shown in Fig. 2.1 and 2.2. Maximum compression stress in the concrete is given in the table (2.1) that the coefficient 0.67 takes account of the relation between the cube strength and the bending strength in a flexural member. The strain of concrete at yield that depends on the concrete grade remains constant with increasing load until a strain of 0.0035 is reached when the concrete fails. Young's modulus ( $E_c$ ) of the concrete is an important property in the elastic deformation zone since this property is a measure for stiffness, deformation and deflection of the concrete. The initial elastic modulus is approximately equal to 20 kN/mm<sup>2</sup> for concrete grade 30 N/mm<sup>2</sup>. Also Poisson's ratio ( $\nu_c$ ), which is the ratio of the lateral strain to the associated axial strain of concrete varies from 0.1 to 0.3 since the value of 0.2 is commonly used, MACGinley & Choo, ref. [6]. The yield strains of reinforcing steel bars at yield stress of 250 N/mm<sup>2</sup> is equal (0.0011) and of 460 N/mm<sup>2</sup> is (0.002) as given in table 2.1.

**Dynamic Properties of Reinforced Concrete**

Important properties of reinforced concrete such as Young's modulus, strength and

strain limits under dynamic actions (dynamic loading such as earthquakes in this research) change to a greater or lesser extent, when compared with the corresponding values for static loading. This change is usually expressed as a function of the strain rate and in some cases also as a function of the stress rate.

$$\dot{\epsilon} = \frac{d\epsilon}{dt}$$

$\dot{\epsilon}$  : The strain rate

$$\dot{\sigma} = \frac{d\sigma}{dt}$$

$\dot{\sigma}$  : The stress rate

The fatigue resistance of reinforced concrete is an important property when considering dynamic cyclic loading. The change in the fatigue resistance of reinforced concrete can also be expressed as a function of the strain & stress rate and the rate of loading. The strain rate rarely exceeds the limit value  $0.1 \text{ s}^{-1}$  in most normal cases of dynamic loading which result in moderate changes in reinforced concrete properties. In the cases of strong dynamic loads, the strain rate becomes much larger and varies from  $1$  to  $10 \text{ s}^{-1}$ . Variation of the reinforced concrete properties under dynamic actions is analysed and illustrated using the properties value at the static case of loading, Bachmann...et al, ref. [7].

In 1995, Ammann and Nussbaumer, ref. [7], outlined the behaviour of concrete and reinforcing steel bars in compression & tension under dynamic loading. In compression, the modulus of elasticity ( $E$ ) of concrete increases with the stress and strain rate according to the following formulas that depends on the relations plotted in Fig.2.3.

$$E_{dyn}/E_{stat} = (\dot{\sigma} / \dot{\sigma}_0)^{0.025} \text{ with initial stress rate } \dot{\sigma}_0 = 1 \text{ N/mm}^2 \text{ s or}$$

$$E_{dyn}/E_{stat} = (\dot{\epsilon} / \dot{\epsilon}_0)^{0.026} \text{ with initial strain rate } \dot{\epsilon}_0 = 30 \cdot 10^{-6} \text{ s}^{-1}$$

Fig. 2.3 shows that the ratio between dynamic and static Young's modulus ( $E_{dyn}$ ,  $E_{stat}$ ) increases with the stress and strain rate. The figure also shows the influence of stress and strain rate on the compressive strength ( $f_{dyn}$ ,  $f_{stat}$ ) and ultimate strain ( $\epsilon_{u, dyn}$ ,  $\epsilon_{u, stat}$ ) of concrete under dynamic loads and that appears clearly beyond the strain rate of  $30 \text{ s}^{-1}$  where increase of the compressive strength and ultimate strain is very pronounced. The formulas that reveal effects of the stress and strain rate on compressive strength and ultimate strain are

$$f_{dyn}/f_{stat} = (\dot{\epsilon} / \dot{\epsilon}_0)^{1.026\alpha} \text{ with } \alpha = 1 / (5 + 3 f_{cm}/4) \text{ for } \dot{\epsilon}_0 \leq 30 \text{ s}^{-1}$$

$$f_{cm} = \text{mean static cube strength of concrete (N/mm}^2\text{)}$$



$$\epsilon_{u,dyn} / \epsilon_{u,stat} = (\dot{\epsilon} / \dot{\epsilon}_0)^{0.020} \text{ with initial strain rate } \dot{\epsilon}_0 = 30 \cdot 10^{-6} \text{ s}^{-1}$$

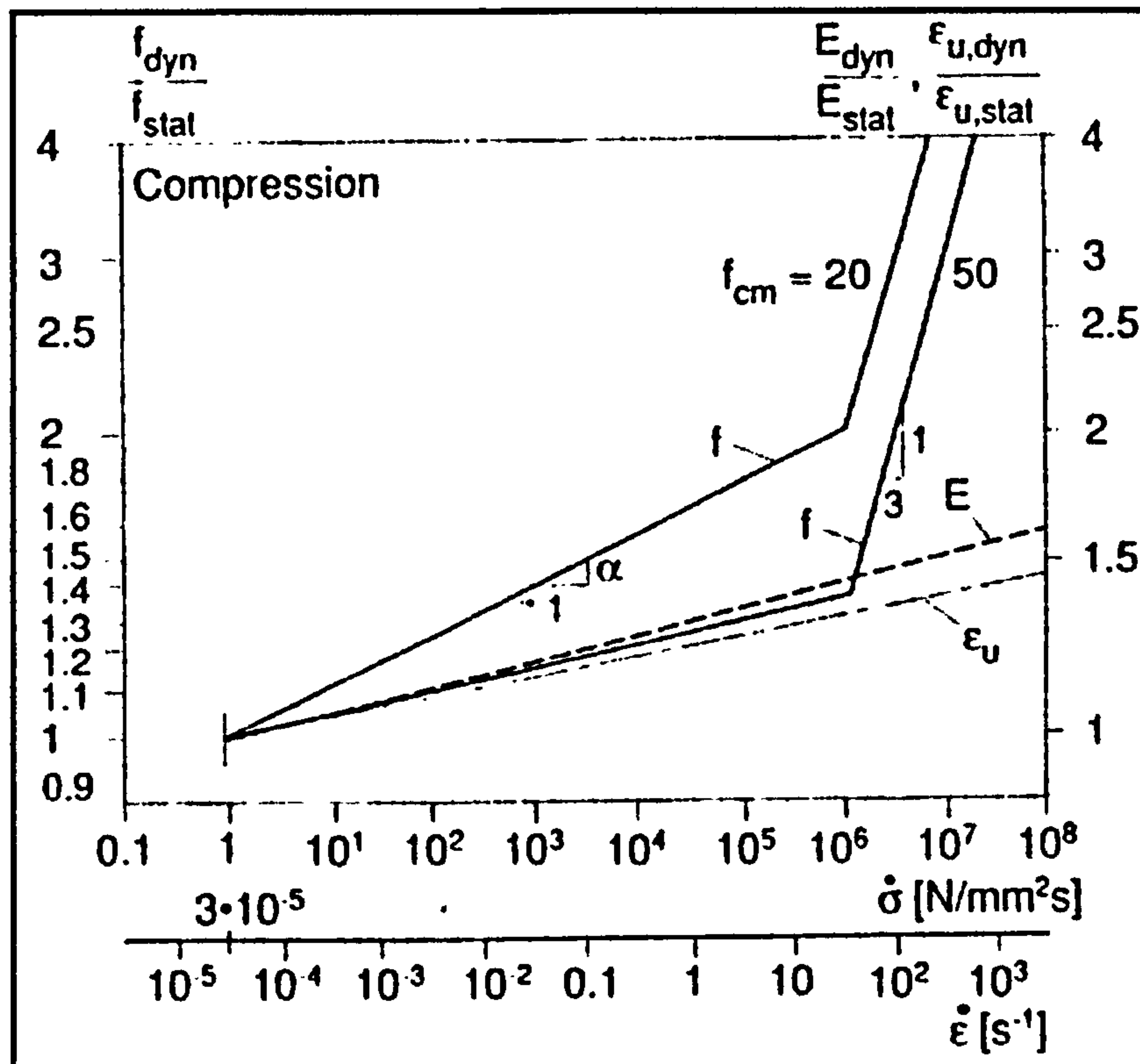


**Figure 2.3** Influence of stress and strain rate on concrete properties in compression  
(Bachmann...et al, ref. [7])

Modulus of elasticity (Young's modulus) of reinforcing steel bars remains unchanged under dynamic loads in tension and compression. In tension, the yield strength of reinforcing steel bars increases with strain rate but this change is not pronounced for some types of steel bars such as cold worked steel. Fig. 2.4 shows the effects of strain rate on yield stress of hot rolled reinforcing steel bars.

As this research is focussed on the behaviour of tall reinforced concrete buildings under earthquake (dynamic) loads, previous research regarding the ductility of reinforced concrete has been reviewed. The ductility constitutes one of the fundamental requirements regarding the dynamic behaviour of reinforced concrete structures to resist the earthquakes, Penelis and Kappos, ref. [8]. The use of reinforced concrete as a ductile material began in the early 1960s with the publication of Blume, Newmark & Corning (1961) which established that properly detailed reinforced concrete beams and columns would respond to dynamic forces in a ductile manner and would sustain a number of cycles of stress reversal. The same conclusion was later drawn for shear walls,

principally the work of Professor R. Park and Professor T. Paulay at the University of Canterbury in New Zealand during the 1970s, Key, ref. [9]. The ductility as an important property of reinforced concrete material relevant to seismic analysis will be discussed later in Section 2.1.1.2.1.

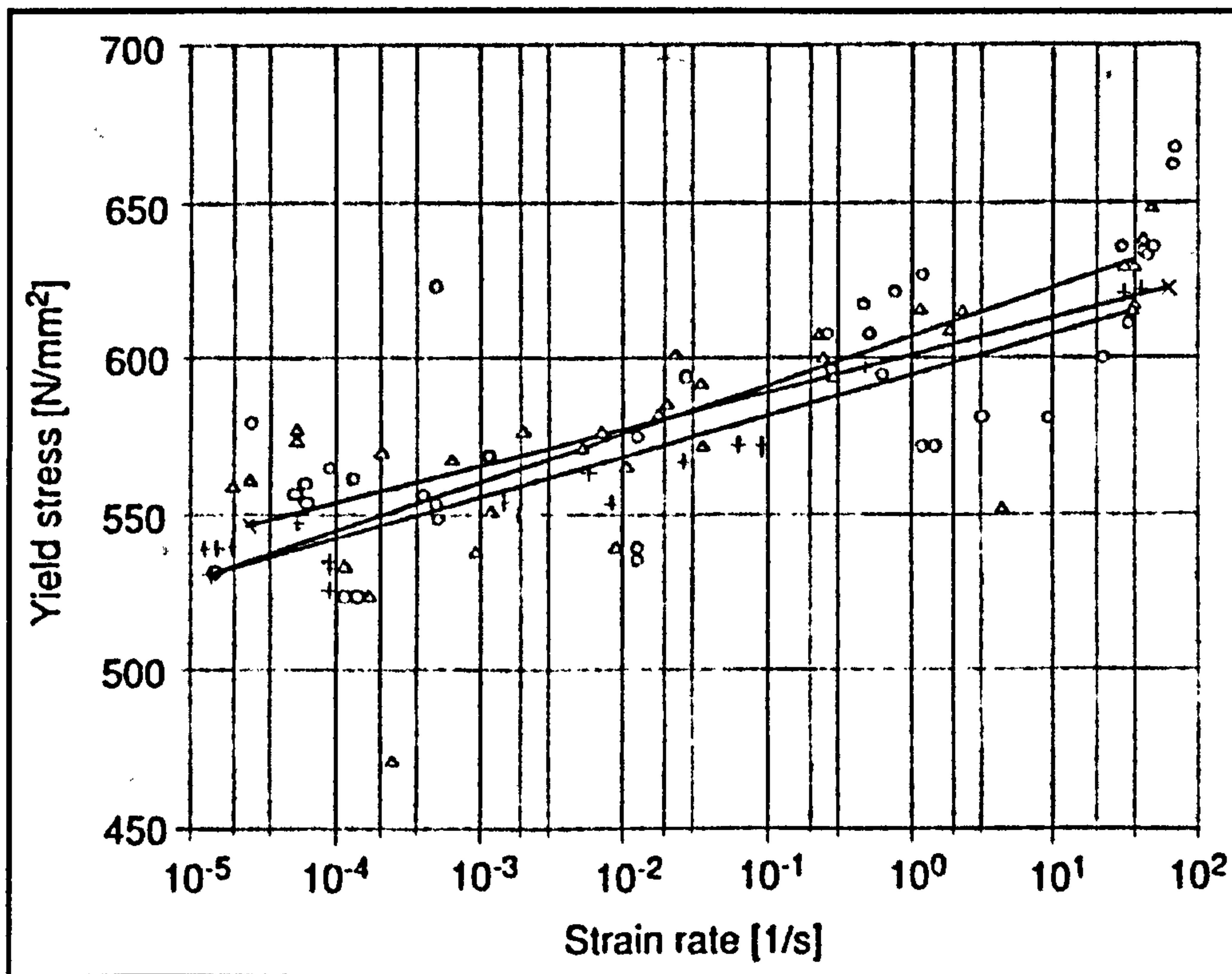


**Figure 2.4** Influence of strain rate on yield stress of hot rolled reinforcing steel bars  
[The regression lines indicate some minor influence of the different bar diameters]  
(Bachmann...et al, ref. [7])

### 2.1.1.1 Elastic Behaviour

The idealized stress-strain relationships for concrete and reinforcing steel bars (Fig. 2.1, 2.2) which has been considered for work in this research, show that the material properties behave in both an elastic & plastic manner depending on the magnitude of the load (it is divided into linear and non-linear parts). Therefore there are two methods which are used for analysis and design of reinforced concrete structures. The elastic theory, which depends on the characteristics of material through the linear portion of the idealized curves. The main assumption of this theory is that the stresses in the structure caused by the applied loads are within the elastic limit of the material used

and thus deflections (elastic deformation) are small. Also this theory is important to study the performance of structure, especially with regard to serviceability. As the stresses increase towards yield stress of the reinforced concrete material and exceed the elastic limit, the behaviour of the structure becomes plastic (inelastic deformation) and, on further increase, a fully plastic condition is reached until a sufficient number of plastic hinges are formed to transform the structure into a mechanism. This mechanism would collapse under any additional loading, Ghali and Neville, ref. [10], Moy, ref. [11]. This description for material characteristics through the non-linear part of curve is referred to as plastic theory, (see section 2.1.1.2.1). Plastic theory in analysis and design for structures and the study of collapse mechanisms is therefore important and the knowledge of the magnitude of the collapse load, which should be higher than service loading.

The analysis of reinforced concrete structures can be performed using elastic analysis (elastic theory) or inelastic analysis (plastic theory) but the design should be carried out using the ultimate limit state and serviceability limit state respectively. This will confirm the ability of the building to behave in a linear or nonlinear fashion under static loading (design loads) and resist the collapse when overloaded, perhaps during a dynamic earthquake event.

#### **2.1.1.1.1 Linear Analysis of Multi-Storey RC Buildings**

BS 8110 states that it is generally satisfactory to obtain the maximum design values of axial forces, shear forces and bending moments of multi storey reinforced concrete buildings (framed RC structures) from linear elastic analysis. The approach of linear elastic analysis depends on the assumption that the stress-strain relationship is linear and the deformation of material is elastic. Multi-storey reinforced concrete buildings are statically indeterminate structures and the linear elastic analysis of global structures is implemented using standard stiffness method based computer programs.

#### **2.1.1.1.2 Serviceability Limit State Design of Multi-Storey RC Buildings**

Serviceability limit state design is one of the two limit states (the other being ultimate limit state) that are considered in the design of reinforced concrete structures. The criterion for a safe design is that the structure should not become unfit for use, i.e.



that it should not reach a limit state during its design life. For reinforced concrete structures the normal practice is to design for the ultimate limit state and check for the serviceability limit state.

The serviceability limit state requires that the structure should not become unfit for use due to excessive deflection, cracking or vibration, concerned with structural behaviour under service loading (unfactored dead & live loads). The service loading is normally sufficiently low for results of an elastic analysis to be relevant. The calculations of deflections and cracking which satisfy the serviceability of reinforced concrete structures depend on the linear elastic analysis of reinforced concrete sections. Fig. 2.5 shows the linear elastic stress & strain distribution of beam section under service loading. For more details see ref. [3,5,6].

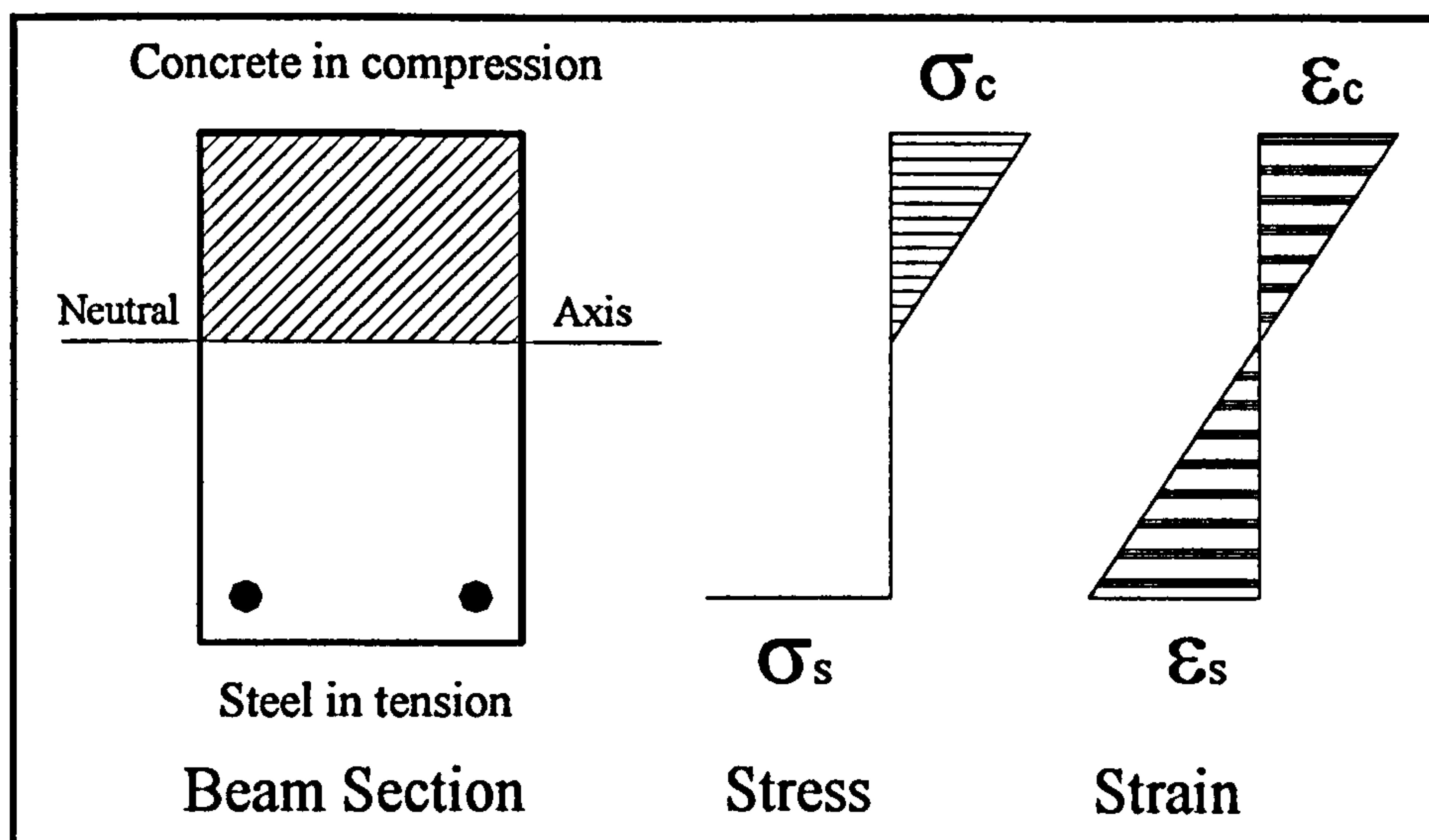


**Figure 2.5** Linear elastic stress & strain distribution of a beam section under service loading (ref. [3,5,6,11])

### 2.1.1.2 Inelastic Behaviour

In recent decades, the analysis and design of reinforced concrete structures based on the inelastic behaviour (plastic methods of analysis and design) are increasingly used and have become accepted by various codes of practice (such as normal & modern codes e.g., BS 8110 ref. [3] and Eurocode 8 ref. [4]). The inelastic behaviour (plastic deformation) of reinforced concrete is represented by the nonlinear part of the idealized stress-strain curve (refer to Fig. 2.1, 2.2). For static codes, the plastic methods of analysis and design are used for design of reinforced concrete



structures at ultimate limit state to guard against collapse, and also to obtain economy of design from the inherent nature of redundant structures to redistribute ultimate moments. For dynamic codes of practice, this plastic theory is used in a similar manner to incorporate deformation capacity (ductility) of structures under seismic loads.

#### **2.1.1.2.1 Plastic Analysis of Multi-Storey RC Buildings**

Plastic theory is used to determine the collapse mechanisms of multi-storey reinforced concrete models, which reveal the locations and number of plastic hinges at collapse assuming full ductility. Design of the plastic hinges and deformation capacity of the structure at collapse can help to control the collapse mechanism of the structure and increase the load carrying capacity. The conventional plastic method of analysis of three-dimensional multi-storey reinforced concrete building under seismic loads is a complicated process, one which is better carried out with the aid of a suitable FE computer package such as ANSYS. As will be discussed later on, the finite element models developed in this research will not directly incorporate nonlinear behaviour but judgement based on elastic code assessment progress will give insight into ductility requirements.

The plastic analysis of reinforced concrete sections (formation of a plastic hinge) shows clearly the ability of structural members of reinforced concrete structures to be ductile under static loads and this philosophy is important and applied for the ultimate limit state design. The section ductility of structural members and subsequently the full ductility of a global structure of the multi-storey reinforced concrete buildings are a major factor governing the improvement of resistance of these buildings against failure due to the earthquake (dynamic) loads. Review of the ductility of reinforced concrete will be presented in the next paragraphs.

#### **Ductility of Reinforced Concrete Concerning The Normal Design Codes**

Plain concrete is a brittle material and steel is ductile material. The degree of ductility of reinforced concrete material is related to the physical properties of each constituent material as well as the relative percentages of steel and concrete that are present. The reinforced concrete material consists of plain concrete and reinforcing steel bars that can exhibit elasto-plastic behaviour under the loading. The term ductility in structural

design is used to mean the ability of a structure to undergo large deformation in the post-elastic range without a substantial reduction in strength, Park, ref. [12].

The formation of a plastic hinge in the reinforced concrete section requires the structure to be ductile. The conventional plastic method defines the formation of plastic hinge by the moment of resistance that the section can carry. If this bending moment is the full plastic moment then the section must be fully ductile. Unfortunately, the analysis of the moment of resistance shows that reinforced concrete sections may have limited capacity for plastic rotation. It is that capacity which is essential to achieve the redistribution of moments required by the plastic method, Moy, ref. [11]. Fig. 2.6 shows the stress and strain distribution of a reinforced concrete beam section at first yield and ultimate stages (formation of the plastic hinge and variation of ductility), Moy, ref. [11] and Dowrick, ref. [13].

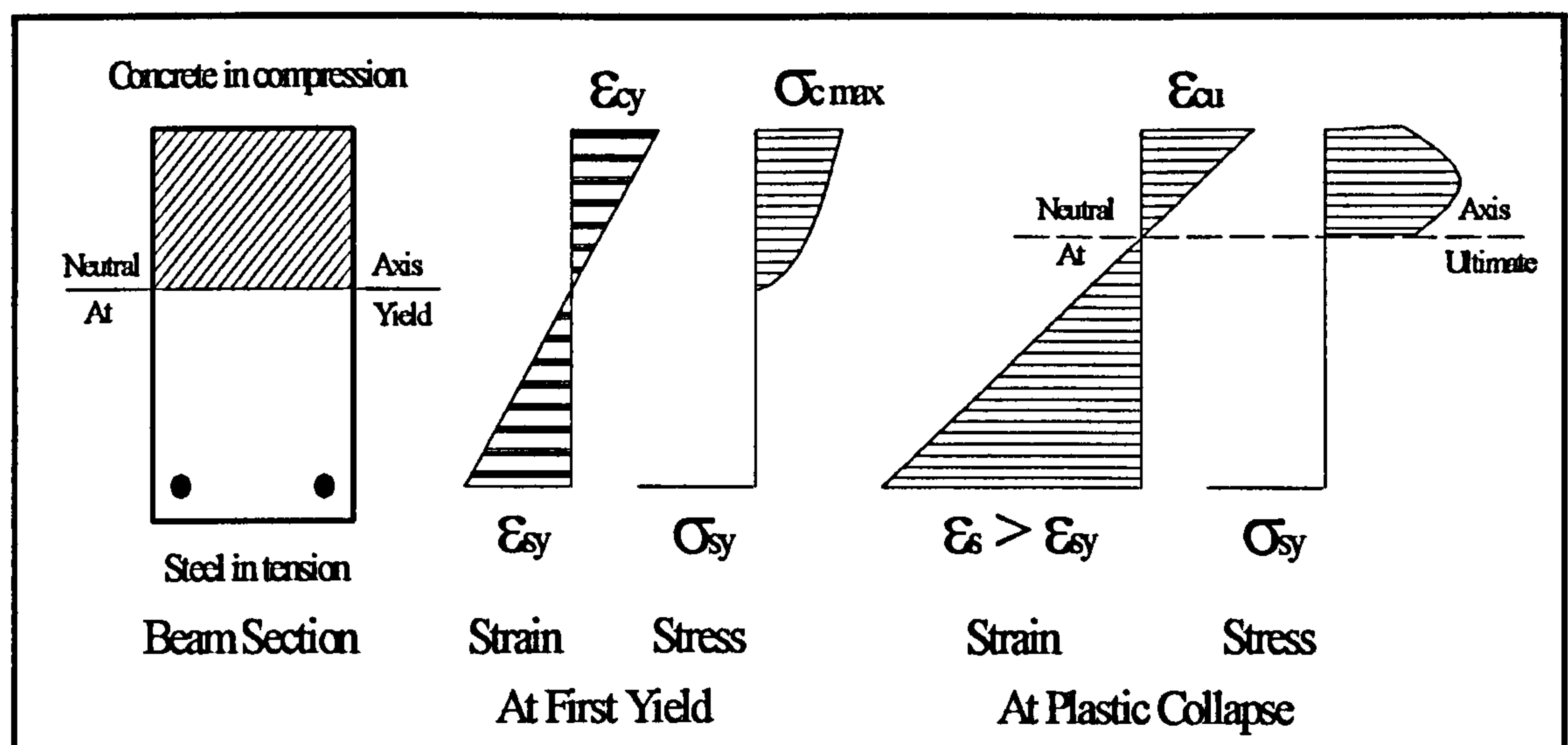


**Figure 2.6** Stress & strain distribution of a beam section at first yield and at RC failure (Moy, ref. [11] and Dowrick, ref. [13])

Ductility in reinforced concrete is influenced by the percentage of steel reinforcement within it. If the steel ratio is below a certain critical value (that is defined by design codes such as 0.13 % to 4 % of steel 460 N/mm<sup>2</sup> which is defined by BS 8110) it will be found that the steel yields before the concrete crushes in compression and the beam will continue to resist the increasing applied moment while the total compression force in the concrete remains relatively unchanged up to collapse. This case is called **under-reinforced** and is preferred by engineers in the design because the ductility of such a

member provides ample warning of impending failure, see Fig. 2.6. The other case occurs when the steel ratio is above this critical value, causing the concrete strain to reach its ultimate value before the steel strain reaches the yield value causing a brittle failure. This case is said to be **over-reinforced**, Kong & Evans, ref. [5].

### **Ductility of Reinforced Concrete Concerning The Modern Design Codes**

Many of the multi-storey reinforced concrete buildings which have collapsed during the earthquakes in many parts of the world were designed in compliance with the 'permissible stress' concept. This concept considers the state of a structure under service loading conditions, and completely ignores the ultimate limit state characteristic of the structure. As a result, the design method employed was incapable of securing ductile, and hence was incapable of safeguarding against brittle & types of failure, Kotsovos and Pavlovic, ref. [14].

The modern design code recognises the importance of ductility in design because if a structure is ductile then its ability to absorb energy without critical failure increases. In general, section ductility is increased by:

- 1- An increase in compression steel content.
- 2- An increase in concrete compressive strength.
- 3- An increase in ultimate concrete strain.

Section ductility is decreased by:

- 1- An increase in tension steel content.
- 2- An increase in steel yield strength.
- 3- An increase in axial load, ([http:// www.cen.bris.ac.uk/civil/students/eqteach97/](http://www.cen.bris.ac.uk/civil/students/eqteach97/)), ref. [15] and Mandal, ref. [16].

In 1987, the conventional definition of the ductility of reinforced concrete sections was presented by Dowrick, ref. [13]. The available section ductility of a reinforced concrete member is most conveniently expressed as the ratio of its curvature at ultimate moment  $\phi_u$  to its curvature at first yield  $\phi_y$ . The expression  $\phi_u / \phi_y$  may be evaluated from first principles, the answers varying with the geometry of the section, the reinforcement arrangement, the loading, and the stress-strain relationships of the steel and the concrete, Dowrick, ref. [13].



In 1992, Park, ref. [12] and 2002, Park, ref. [17] outlined the capacity design approach for ductile RC moment resisting frames developed in New Zealand, and also a comparison between the seismic design provisions of the New Zealand codes (seismic design codes of RC structures) and Eurocode 8 (modern codes). Park mentioned that the ductility of reinforced concrete structures required for earthquake resistance is best achieved by ensuring in design that it occurs by flexural yielding of plastic hinges. The most important design considerations for flexural ductility of members is the provision of adequate longitudinal compression reinforcement as well as tension reinforcement, and the provision of adequate transverse reinforcement in the form of rectangular stirrups or hoops and cross-ties or spirals. The transverse reinforcement is required to act as shear reinforcement, to confine and hence enhance the ductility of the compressed concrete, and to prevent premature buckling of the compressed longitudinal reinforcement. Also Park presented a good insight for the illustration of the ductile behaviour for the load / deflection relationship for a single degree of freedom system as shown in Fig. 2.7.

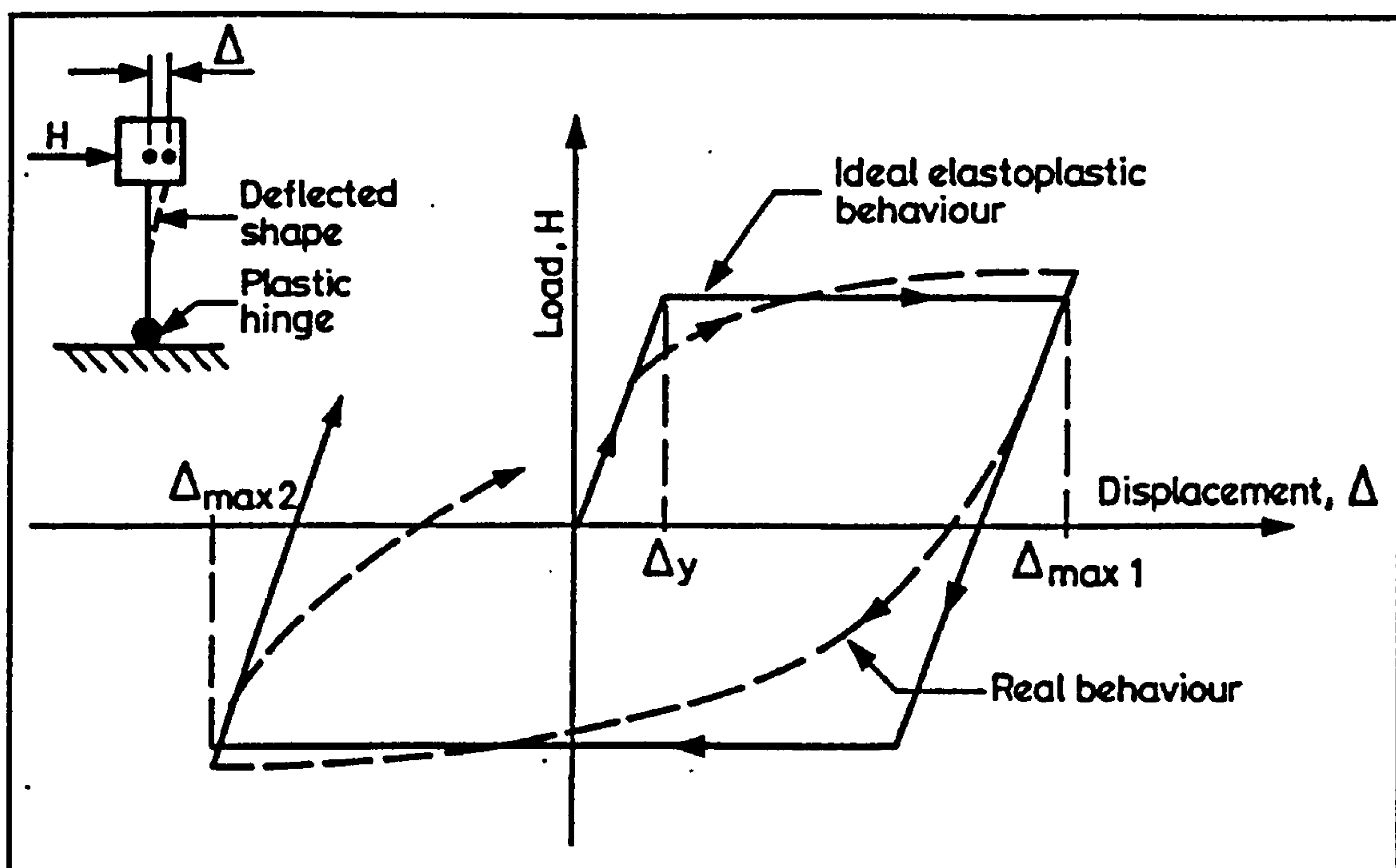


**Figure 2.7** Illustration of ductile behaviour during cyclic horizontal loading (Park, ref. [12])

#### 2.1.1.2.2 Collapse Mechanisms of Multi-Storey RC Buildings

The object of plastic theory (plastic analysis of RC structures) is to find the



possible collapse mechanisms of the structure at failure and the actual value of collapse loads directly. In many structures especially three-dimensional multi-storey structures, there are a number of alternative collapse mechanisms and the correct / actual mechanism is not immediately obvious. The number of plastic hinges at structure collapse is one in excess of the degree of redundancy. Hence as the degree of redundancy increases the number of plastic hinges that are required for formation of a collapse mechanism will increase, Moy, ref. [11] and Horne, ref. [18].

As the model portal frame in Fig. 2.8 shows, reinforced concrete frames can be designed to develop full collapse mechanisms. This model portal frame shows clearly the use of conventional plastic methods on reinforced concrete frames because it produces full ductility at collapse. If the plastic hinges of reinforced concrete sections have large deformation capacity, and have sufficient plastic rotation capacity for full redistribution of the bending moments, the structure will be able to withstand more loads before collapse. This occurs for plastic hinges when the steel ratio of a reinforced concrete section, especially in the tension zone is equal to (or below) the appropriate critical value (see section. 2.1.1.2.1).

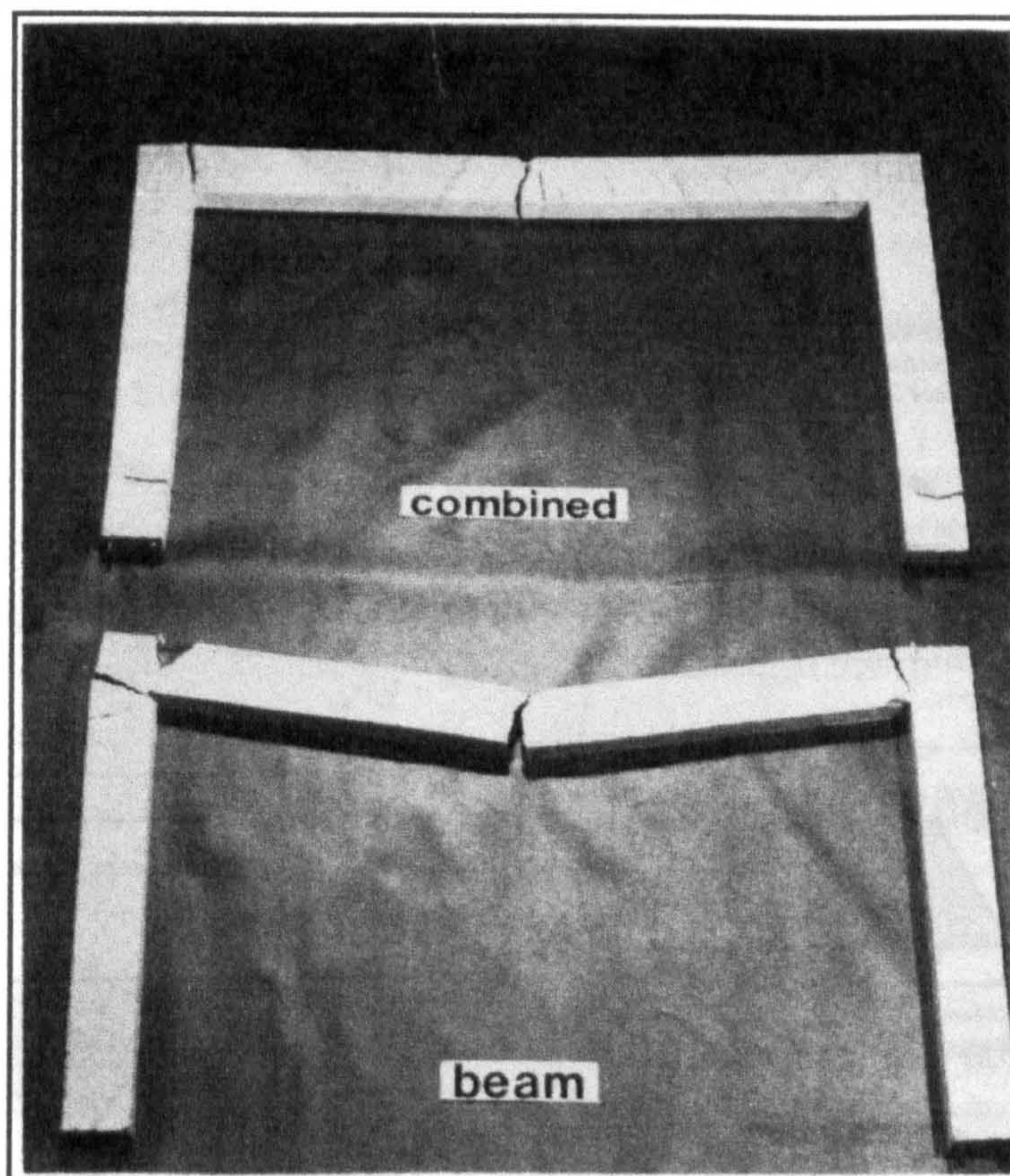


**Figure 2.8** Collapse beam mechanism and collapse combined mechanism for RC portal frame (Moy, ref. [11])



This portal frame illustrates the behaviour of a statically indeterminate elastic-plastic structure up to collapse. Analysis of a statically indeterminate structure using plastic methods reveals the benefits of this analysis in the design such as increasing the deformation capacity, load carrying capacity and economy of such a structure. This frame may collapse by being pushed sideways due to a horizontal force, or an individual beam may fail due to vertical loads and is called a partial collapse mechanism because its number of plastic hinges less than the required number for complete collapse by one, or there may be some combination of both. A plastic analysis is essential for the determination of the failure load to provide the correct collapse mechanism. The correct failure load is the least load of all available collapse mechanisms.

The principle of virtual work is a powerful analysis tool applied to frames is used to obtain the correct collapse load and collapse mechanism for this portal frame depending on the values of the plastic moment capacity ( $M_p$ ) of beam and columns which have been designed. At the connection between two members (joint) in the structure the plastic hinge forms at a bending moment equal to the plastic moment of the weaker member. This portal frame has three different types of collapse mechanisms depending on the loading applied. The sway mechanism is caused by the horizontal force alone, the beam mechanism is caused by the action of the vertical force alone and the horizontal and vertical force may cause the combined mechanism together. In the case of a combined mechanism the portal frame must exhibit full ductility under the applied loads and this mechanism is the actual collapse mechanism of this portal frame. Fig. 2.9 shows the details of these collapse mechanisms. In general, the types of collapse mechanisms, which include the realistic collapse mechanism of any structure, depend on the loading applied and the ductility provided by the structure sections.

In multi-storey reinforced concrete buildings distributing the inelastic deformation uniformly throughout the structure means mobilizing all storeys into the inelastic action. This can be achieved by investigating the types of collapse mechanisms for such structures under earthquake loads and obtaining a suitable design for the deformation capacity (full ductility). The plastic hinges are a useful part of earthquake design because when the structure degree of redundancy increases and the structure becomes more statically indeterminate, the number of plastic hinges required for collapse increases enhancing the load carrying capacity of structure (they also provide a means of energy absorption and warning for the failure).



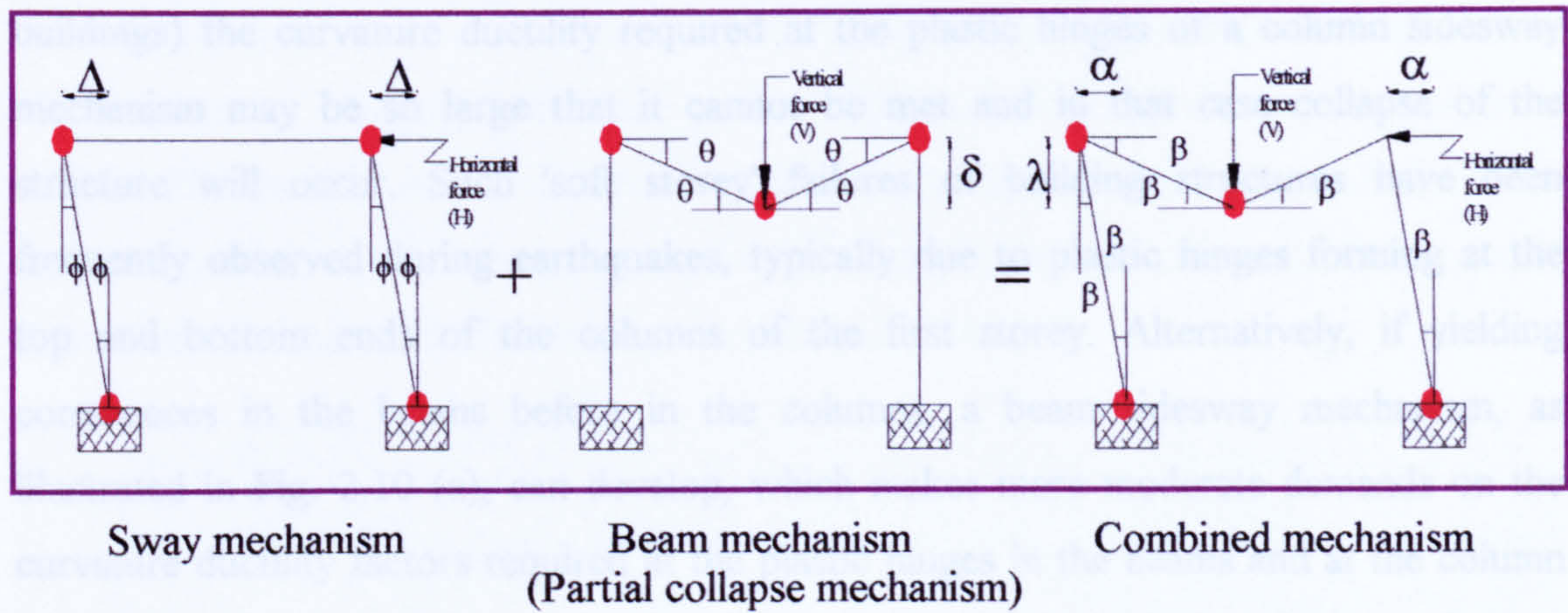


**Figure 2.9** Possible collapse mechanisms of reinforced concrete portal frame (Moy, ref. [11] and Horne, ref. [18])

The designed mode of failure for multi-storey reinforced concrete buildings during earthquakes involves the formation of sufficient plastic hinges at the joints to produce a mechanism. Structural collapse mechanisms depend mainly on the deformation capacity (ductility), location and number of plastic hinges in the structure. Plastic hinges may be formed at the end regions of nearly all beams in a high-rise building, causing a sway mechanism for whole building. At the other extreme, plastic hinges (ductility / inelastic deformation) may concentrate in a single storey at the two ends of all its columns, causing a 'soft-storey' or 'column-sway' mechanism. This mechanism accounts for numerous collapses of framed buildings in recent earthquakes. Modern codes strive to distribute ductility demands to all beams of the structure and to avoid formation of a soft-storey, by forcing vertical elements to remain elastic with the exception of their base region, Beskos & Anagnostopoulos, ref. [19] and Penelis & Kappos, ref. [8]. Fig. 2.10 illustrates the difference between a sway mechanism and soft-storey mechanism for similar buildings.

As shown in Fig. 2.10, it is evident that the position of plastic hinges which form in structures during the earthquake will influence the curvature ductility demand in the plastic hinge regions. This can be illustrated by examination of the sway mechanism and soft-storey mechanism. For moment resisting frames, if yielding commences in the columns before in the beams a column sidesway mechanism can form. In the worst case the plastic hinges may form in the columns of only one storey, as illustrated in Fig. 2.10 (b). Such a mechanism can make very large curvature ductility demands on the plastic hinges of the critical storey. For tall buildings (multi-storey reinforced concrete



buildings) the curvature ductility required at the plastic hinges of a column sidesway mechanism may be so large that it cannot be met and in that case collapse of the structure will occur. Such 'soft storey' failures of building structures have been frequently observed during earthquakes, typically due to plastic hinges forming at the top and bottom ends of the columns of the first storey. Alternatively, if yielding commences in the beams before in the columns, a beam sidesway mechanism, as illustrated in Fig. 2.10 (a), can develop, which makes more moderate demands on the curvature ductility factors required at the plastic hinges in the beams and at the column tops and bases. The curvature ductility demands at the plastic hinges of this mechanism can be met by careful detailing, Park, ref. [12].

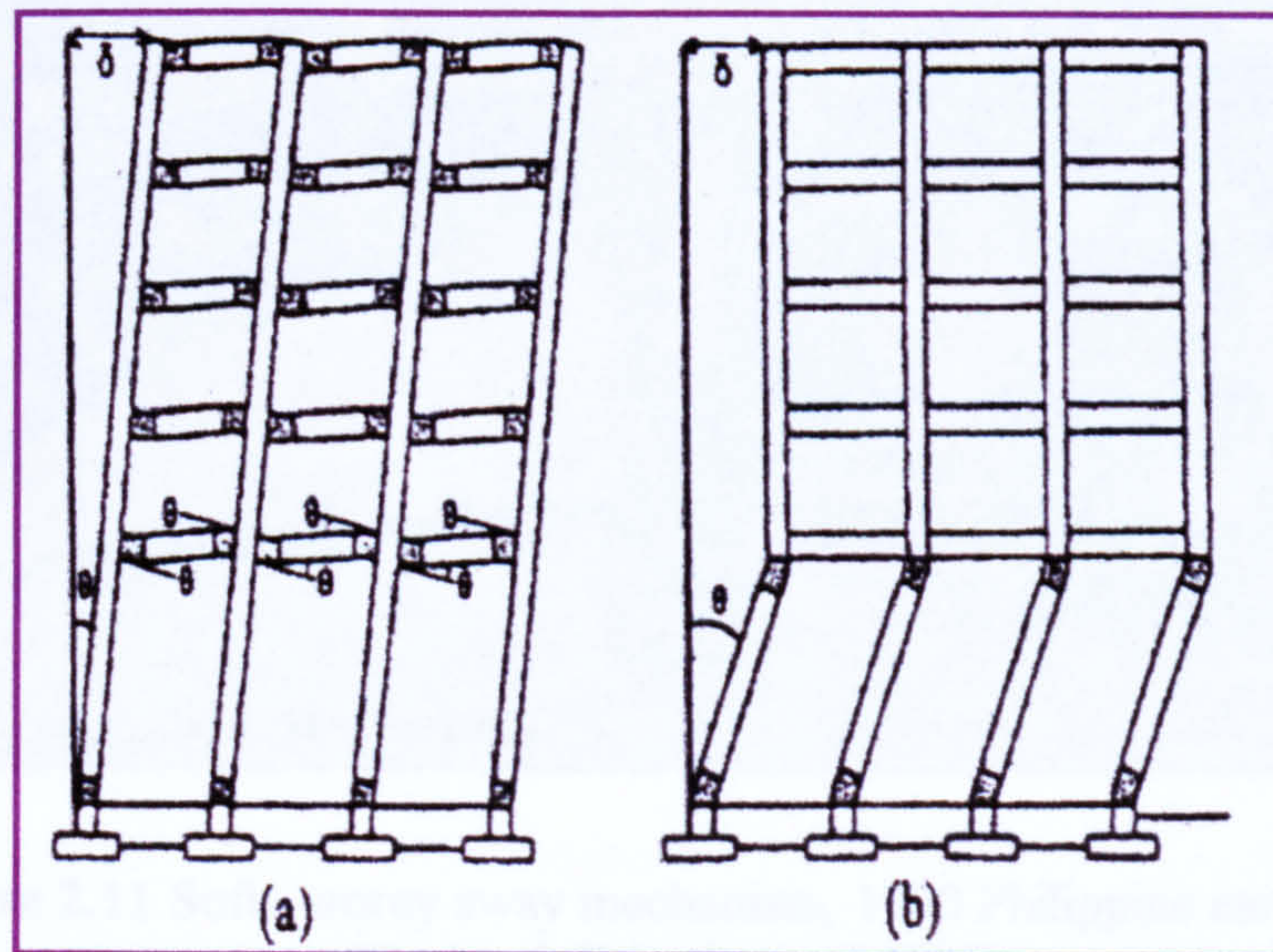


**Figure 2.10** Collapse mechanisms (ductility concentration) a- Beams and base of Columns (sway mechanism); b- Columns of a soft storey (column sway mechanism) (Beskos & Anagnostopoulos, ref. [19] and Penelis & Kappos, ref. [8])

Fig. 2.11 illustrates one of the most common causes of failure in earthquakes, the “soft story mechanism”. Where one level, typically the lowest, is weaker than upper levels, a column sway mechanism can develop with high local ductility demand. In taller buildings (multi-storey reinforced concrete buildings) than that depicted in Fig.2.11, this often results from a functional desire to open the lowest level to the maximum extent possible for retail shopping or parking requirements, Paulay & Priestley, ref. [20].

In 1997, Penelis & Kappos, ref. [8], outlined the formation causes of the soft-storey mechanism in the ground floor of multi-storey reinforced concrete buildings. The ground floor is used as a commercial area and this requires that the floor must be an



open (flexible) floor. In such a case, while the upper floors have high stiffness due to the presence of masonry infills, the ground floor has a drastically reduced stiffness because the vertical structural members contribute almost exclusively to it. In these buildings almost all the damage occurs in the vertical structural elements of the ground floor, while the rest of the building remains almost unaffected.



**Figure 2.11** Soft –storey sway mechanism, 1990 Philippine earthquake  
(Paulay & Priestley, ref. [20])

In 1999 Kocaeli, Turkey earthquake, the soft – storey mechanism was formed in the reinforced concrete building that have irregular placement of masonry infill walls. As shown in Fig.2.12, the moment frame is both flexible and weak in the first storey by comparison with the upper storeys. In the first storey of this building, masonry infill walls are present in the back face of the building and in the two faces perpendicular to the sidewalk. The front of the building was open in the first storey. The lateral stiffness of the building was considerably larger in the direction perpendicular to the sidewalk compared with parallel to the sidewalk. Deformations are concentrated in the first storey of this building parallel to the sidewalk, due to the weakness and flexibility of the moment frame because of lack of masonry infill walls in the front of the building. The first-storey columns in this building were severely damaged and likely close to failure due to gravity load instability, Sezen...et al, ref [21].





**Figure 2.12** Formation of a soft and weak storey, 1999 Turkey earthquake  
(Sezen...et al, ref [21])

The design requirements of the modern design codes (such as Eurocode 8) for tall reinforced concrete buildings to resist the formation of soft – storey mechanisms and subsequently the collapse under seismic events will be presented later in section 2.4. In this research, one of the main objectives is the behaviour analysis of the existing multi-storey reinforced concrete buildings (designed according to BS 8110; part1) containing a soft storey under seismic loads.

#### **2.1.1.2.3 Ultimate Limit State Design of Multi-Storey RC Buildings**

The ultimate limit state is reached when the structure (or part of it) collapses. Collapse may arise from the rupture of one or more critical sections, from the transformation of the structure into a mechanism, from elastic or inelastic instability, or from loss of equilibrium as a rigid body, and so on. Design of the structural concrete member to its ultimate limit state requires the assessment of the load – carrying capacity of the margin of safety against collapse. At the same time, the high internal stresses which develop at the ultimate limit state result in a reduction of both the size of the member cross-section and the amount of reinforcement required to sustain internal actions (BS 8110;part1 provides the design of RC structures using the ultimate limit state).



The structure must be designed to carry the most severe combination of loads to which it is subjected. The sections of the elements must be capable of resisting the axial loads, shears and moments derived from the analysis. The design is made for ultimate loads and design strengths of materials with partial safety factors applied to loads and material strengths. This permits uncertainties in the estimation of loads and in the performance of materials to be assessed separately. The section strength is determined using plastic analysis based on the short-term design stress-strain curves (see Fig. 2.1, 2.2) for concrete and reinforcing steel bars, for more details about requirements of ultimate limit state design of reinforced concrete structures refer to Fig. 2.6 and see ref. [3,5,6,11]. Nonlinear geometrical effects such as the 'p -  $\delta$ ' effect can also be a significant factor to consider in any nonlinear analysis.

Regarding the static analysis and design of reinforced concrete buildings, the major difference between low and tall buildings is the influence of the wind forces on the behaviour of the structural elements. The effects of wind forces on the analysis and design of tall reinforced concrete buildings will be ignored in this research. The gravity loads only are used for static analysis and design of reinforced concrete models according to BS 8110; part1, ref. [3]. Following on, earthquakes (dynamic) loads are subsequently used for dynamic analysis of these models. The structural analysis of the three dimensional tall reinforced concrete buildings is based on linear elastic behaviour of the structural elements. Non-linear behaviour of the tall reinforced concrete buildings makes the problem extremely and unnecessarily complex. Hence the statically designed building is assessed under earthquake loading to estimate its seismic performance.

## **2.2 Earthquake Engineering**

The subject of earthquake engineering has become advocated for research in the last few decades due to the severe effects of earthquakes on the human-made facilities such as reinforced concrete buildings. The development of earthquake engineering is very important for the countries that are at high risk due to the frequent occurrence of the earthquakes. As a result, many different seismic design codes (such as American codes – Eurocode 8 – Japanese code – New Zealand code, etc) were produced in these countries to regulate the design and construction of the buildings according to its seismic activity.

An effective approach to mitigate the destructive effects of earthquakes is the proper enforcement of the knowledge that is currently available for designing, constructing, and maintaining new earthquake-resistant structures and upgrading existing seismically hazardous structures. After the major seismic events which occurred during the past decade such as earthquakes of Northridge, California (1994), Kobe, Japan (1995), Turkey (1999), Taiwan (1999), and Central-Western India (2001), it was found that the seismic performance of reinforced concrete buildings especially the multi-storey needs improving against the sudden (earthquake) dynamic loads, Chandler & Lam, ref. [22].

Although structural damage may result from several basically different effects of an earthquake such as foundation failure due to loss of soil strength by liquefaction, foundation displacements associated with fault break or landslide movements, etc, the principal loading mechanism recognized by seismic design requirements in building codes (such as Eurocode 8) is the response to the earthquake ground motions applied at the base of the structure. The basic concept of theory of structural dynamics will be discussed in next section (2.2.1) as it applies to the calculation of such vibratory response (seismic response). The specific objective of this theory is to predict the stresses and deflections (forces e.g., axial loads, bending moments and shear forces) that will be developed in any given structural system as a result of any specified ground motion history applied at the base of the structure.

The dynamic problem is completely defined by the physical properties of the structural system, i.e., by its mass, stiffness, and damping characteristics, and by the time-varying displacements introduced at its foundation support points. Thus the evaluation of these structural properties and the selection of an appropriate earthquake input are the most critical factors in the earthquake response analysis. In the formulation of any dynamic response analysis, it must be recognized that the structure generally will be subjected to static loadings (e.g., gravitational forces) in addition to the dynamic excitation which is the subject of immediate interest. If the structure is linearly elastic, so that the principle of superposition is applicable, it is convenient to consider separately the static and dynamic loadings; then the total structural response is obtained by adding the static stresses and deflections to the results of the dynamic analysis. However, if the structure yields or is subject to some other nonlinear behaviour during the dynamic loading,



superposition is not valid and the static loads must be considered in the analysis concurrently with the dynamic effects.

### 2.2.1 General Theory of Structural Dynamic Analysis

The basic concept of the dynamic problem is that the forces are time-dependent and may cause vibration of the structure. In practice, dynamic loading is produced by seismic forces, nonsteady wind, blast, reciprocating machinery, or impact of moving loads.

The analysis and design of buildings and other structures to resist the effect produced by the dynamic loads requires conceptual idealizations and simplifying assumptions through which the physical system is represented by a new idealized system known as the mathematical model. In the mathematical model, the number of independent coordinates used to specify the position or configuration of the model at any time is referred to as the number of degrees of freedom. In principle, structures, being continuous systems, have an infinite number of degrees of freedom. However, the process of idealization or selection of an appropriate model permits the reduction of the number of degrees of freedom to a discrete number (multi-degree of freedom) and in some cases, to just a single degree of freedom.

Fig.2.13 shows a one-story building which may be modelled with one degree of freedom. The model represented in this figure contains the following elements: (1) the concentrated mass  $m$ , (2) the lateral stiffness indicated by the coefficient  $k$ , (3) the damping in the system represented by coefficient  $c$ , and (4) the external force  $F(t)$  (considered to be a function of time); the response (dynamic behaviour) is indicated by the lateral displacement  $y(t)$  of the mass  $m$ . The structural model shown in Fig.2.14 is assumed to be excited by a horizontal acceleration  $\ddot{y}_s(t)$  at its base. In this case, it is convenient to express the response by the relative motion  $u(t)$  between the displacement  $y(t)$  of the mass  $m$  and the displacement of the base  $y_s(t)$ , that is

$$u(t) = y(t) - y_s(t)$$

In general, the dynamic behaviour of the structure is defined by the equation of motion, which is the equation for equilibrium between the forces arising from inertia, damping and stiffness together with the externally applied force. The form of the equation of motion is:

$$m\ddot{y} + c\dot{y} + ky = F(t)$$

$y$  : displacement

$\dot{y}$  : velocity

$\ddot{y}$  : acceleration

$m$  : mass of structure

$k$  : stiffness of structure

$c$  : viscous damping

$F(t)$ : external force varying with time  $t$  (different excitation, force applied to the mass or an input ground motion in the case of seismic loading)

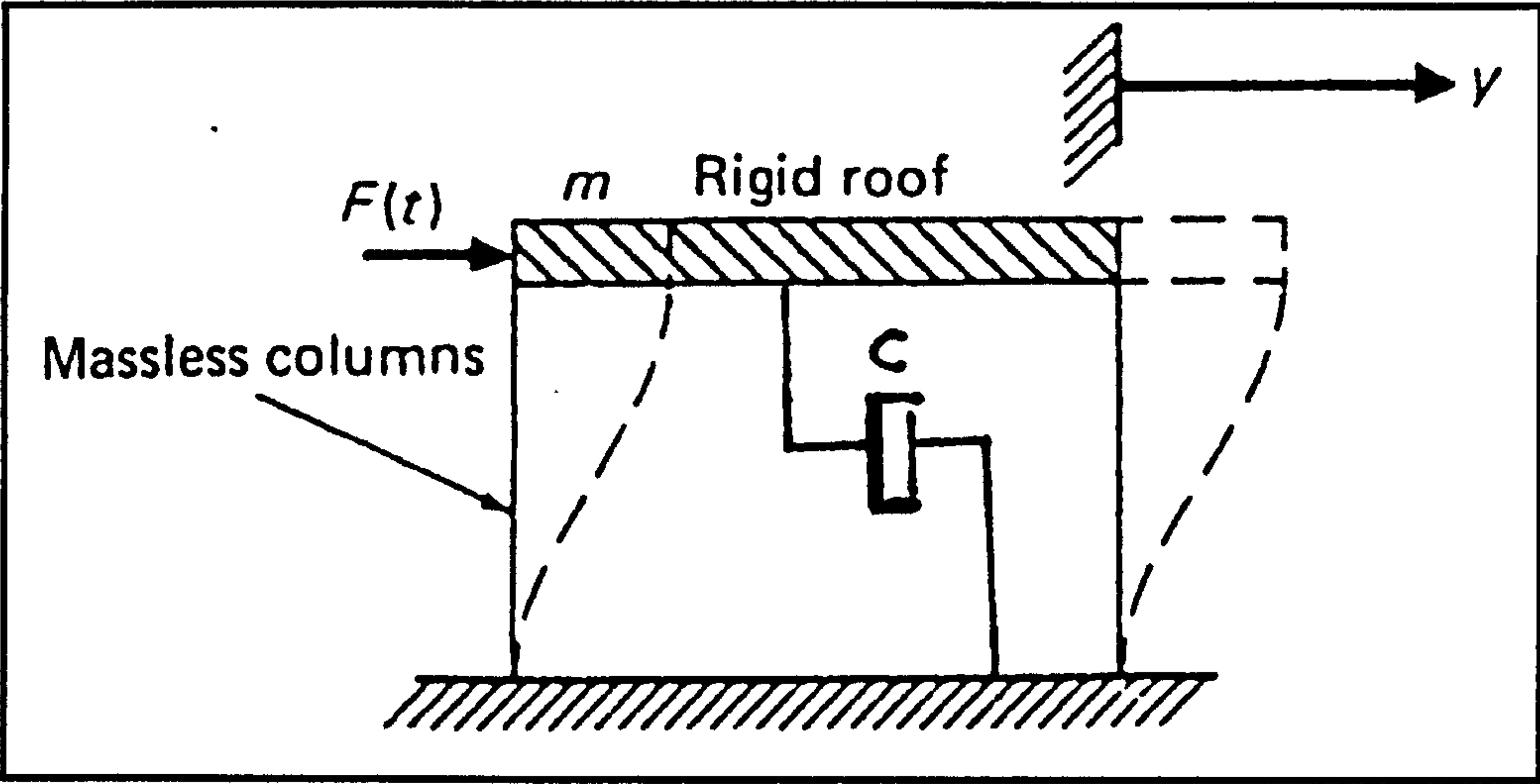


Figure 2.13 Mathematical model for one-storey structure excited by an external force (Paz, ref [23])

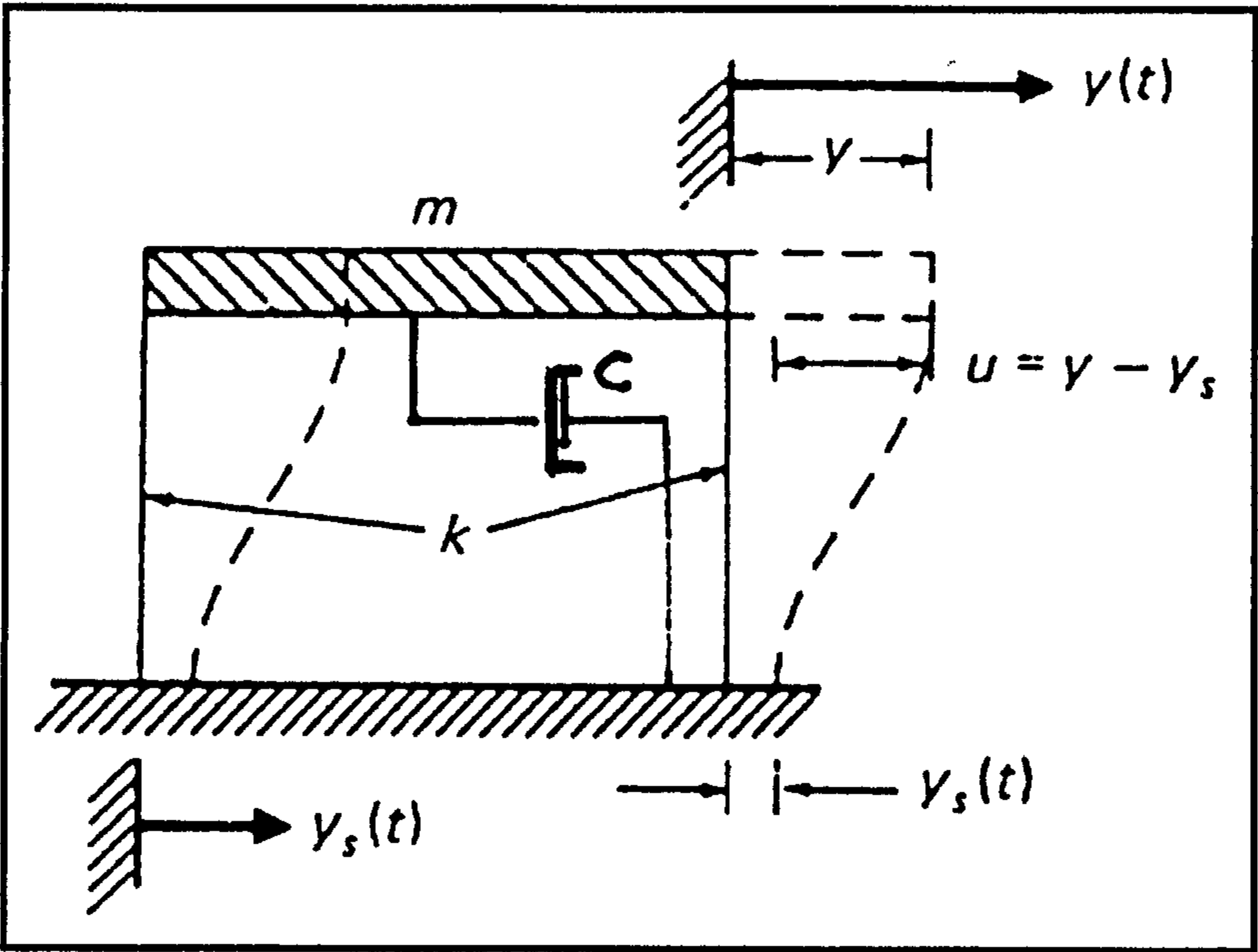


Figure 2.14 Mathematical model for a one-storey structure excited at its base (Paz, ref [23])



If the structure subjected to a force applied to the mass or a vibratory motion (such as earthquake) at the base, the mathematical formulation will be similar but the response of structure will be expressed in terms of the absolute displacement  $y(t)$  for case of a force applied to the mass and in terms of the relative motion  $u(t)$  for case of seismic loads. By solving the equation of motion the dynamic response (behaviour) of the structure can be defined, Paz, ref. [23], ICE, ref. [24], Paz, ref. [25].

The dynamic response of the structures is dependent on its modal characteristics. Modal analysis method is one of the dynamic analysis techniques used to calculate the dynamic response of the structures in absence of the applied external force and this analysis is carried out prior the actual seismic analysis of the structures as a preliminary analysis. This dynamic problem of structures can be illustrated and analysed as damped or undamped free vibration, it will be discussed in the next section.

**2.2.1.1 Undamped Analysis of Multi-Degree of Freedom System (Modal Analysis of Buildings)**

The dynamic analysis of reinforced concrete structures to determine its response to a seismic event has various techniques such as frequency domain techniques and time domain techniques. Modal analysis method is one of the frequency domain techniques and is an essential part of the dynamic analysis process that gives valuable insight into the dynamic characteristics of the building. This analysis yielded the natural frequencies, mode shapes of free structure vibration and the effective mass ( $m^{eff}$ ) for each mode, which are important for the subsequent analysis of the dynamic response of structure under earthquake loads.

For free vibration there is no externally applied force where modal analysis is satisfied by solving the equation of motion. The solution of this second order differential equation (equation of motion) provides the natural frequencies and mode shapes of the system. In most cases this equation will be solved with  $c$  (damping) = 0, and the equation of motion will be as follows:

$$m\ddot{y} + ky = 0$$

- |                         |                              |
|-------------------------|------------------------------|
| $m$ : mass of structure | $k$ : stiffness of structure |
| $y$ : displacement      | $\ddot{y}$ : acceleration    |

The modal damping ratios ( $\zeta$ ) that are applied for the structures in the dynamic analysis range from 2 % to 7 %. When these ratios are applied as a parameter in the relation between the damped natural frequency ( $\omega_d$ ) and undamped natural frequency ( $\omega_n$ ) as follows:

$$\omega_d = \omega_n (1 - \zeta)$$

$\omega_d$  : damped natural frequency

$\omega_n$  : undamped natural frequency

$\zeta$  : damping ratio

It can be seen that the  $(\omega_d) = (\omega_n)$  since the damping ratio is small except where heavy dampers have been added, Paz, ref. [25], ASCE standard, ref. [26].

The mode shapes, which result from the modal analysis show the local & global dynamic response of the structures and also show the natural frequencies. When the frequency of the excitation force (seismic force) equal to the natural frequency of structure, the resonance phenomenon occurs. This phenomenon is a problem for buildings since it increases the dynamic response of the structure which can result in failure and should be minimized in the seismic design of reinforced concrete buildings.

The single degree of freedom system is generalized for the multi-degree of freedom system. The equation of motion of any mode of the multi-degree of freedom system is exactly equivalent to the equation for a single degree of freedom system. Thus, the normal coordinates (mode shapes) of a multi-degree of freedom structure reduce its equations of motion to a set of independent equations, one for each mode of vibration. It also is of interest to note that the expressions for the generalized properties of any mode are equivalent to the expressions for a single degree of freedom system, Barbat and Canet, ref. [27]. Fig.2.15 shows a free antisymmetric vibration (mode shapes) of a multi-storey frame (multi-degree of freedom system).

In 1984, Blevins, ref. [29], listed formulas for calculating the natural frequencies and mode shapes of a single degree of freedom system and a multi degree of freedom system using the behaviour of spring and pendulum systems to illustrate more complex structures.

In 2001, Zalka, ref. [30], presented a simple hand method for calculating the natural frequencies of multi-storey buildings. Lateral vibration of buildings braced by



frameworks is characterised by three types of deformation: the full-height 'local' bending of the individual columns/wall sections, the full-height 'global' bending of the frameworks, which is associated with the axial deformations of the columns/wall sections, and the shear deformation of the frameworks, see Fig.2.16. Based on the stiffnesses associated with these three types of deformation, a closed formula is derived for calculation of the lateral frequencies. An analogy between bending and torsion is used to carry out the pure torsional frequency analysis. The coupling of the lateral and pure torsional modes is taken into account. The results of a comprehensive accuracy analysis covering 144 multi-storey structures demonstrate good agreement with the finite element solution, the maximum difference being 7%.

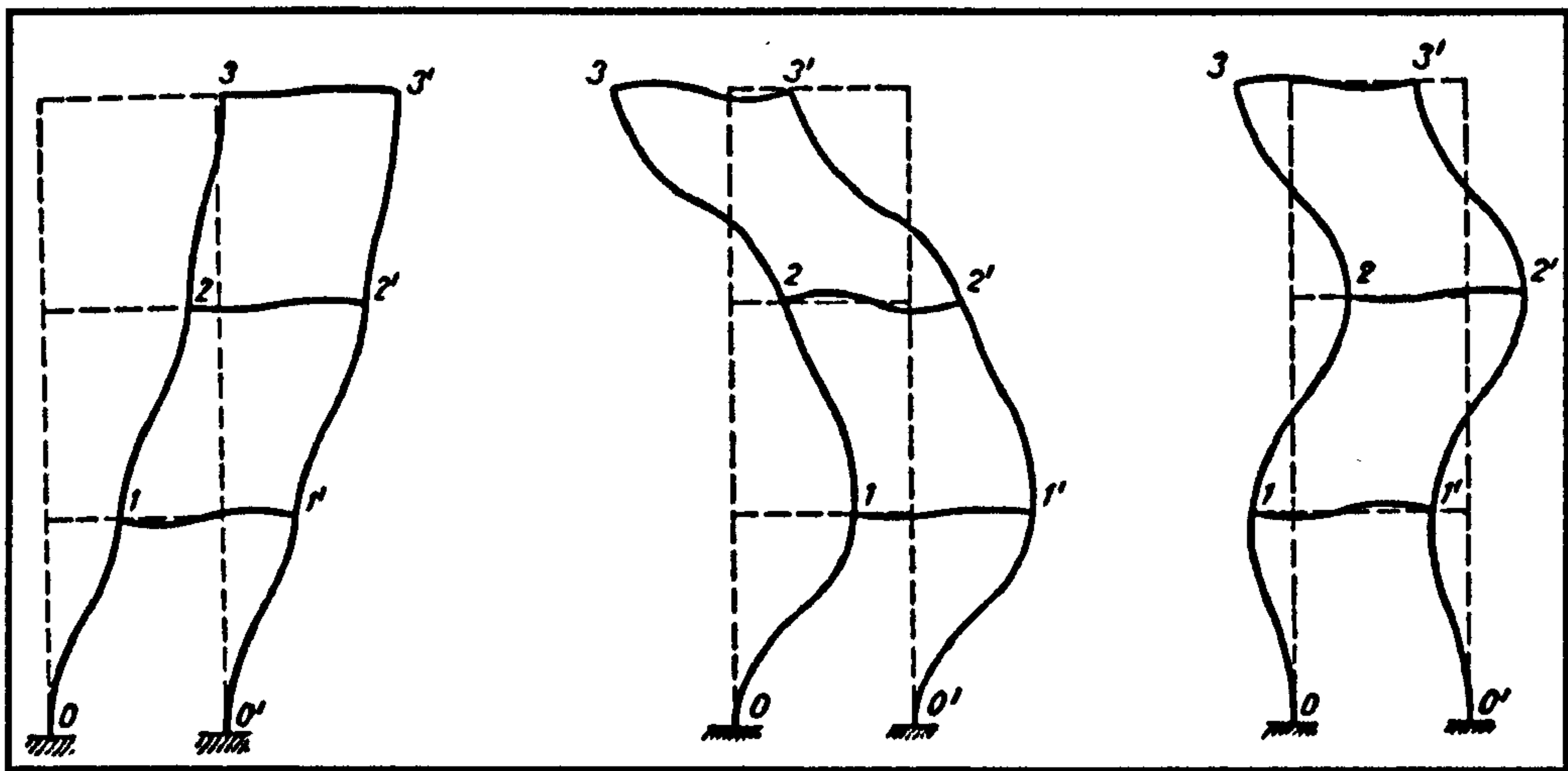


**Figure 2.15** Mode shapes of a free vibration three-storey frame  
(*koloušek*, ref [28])

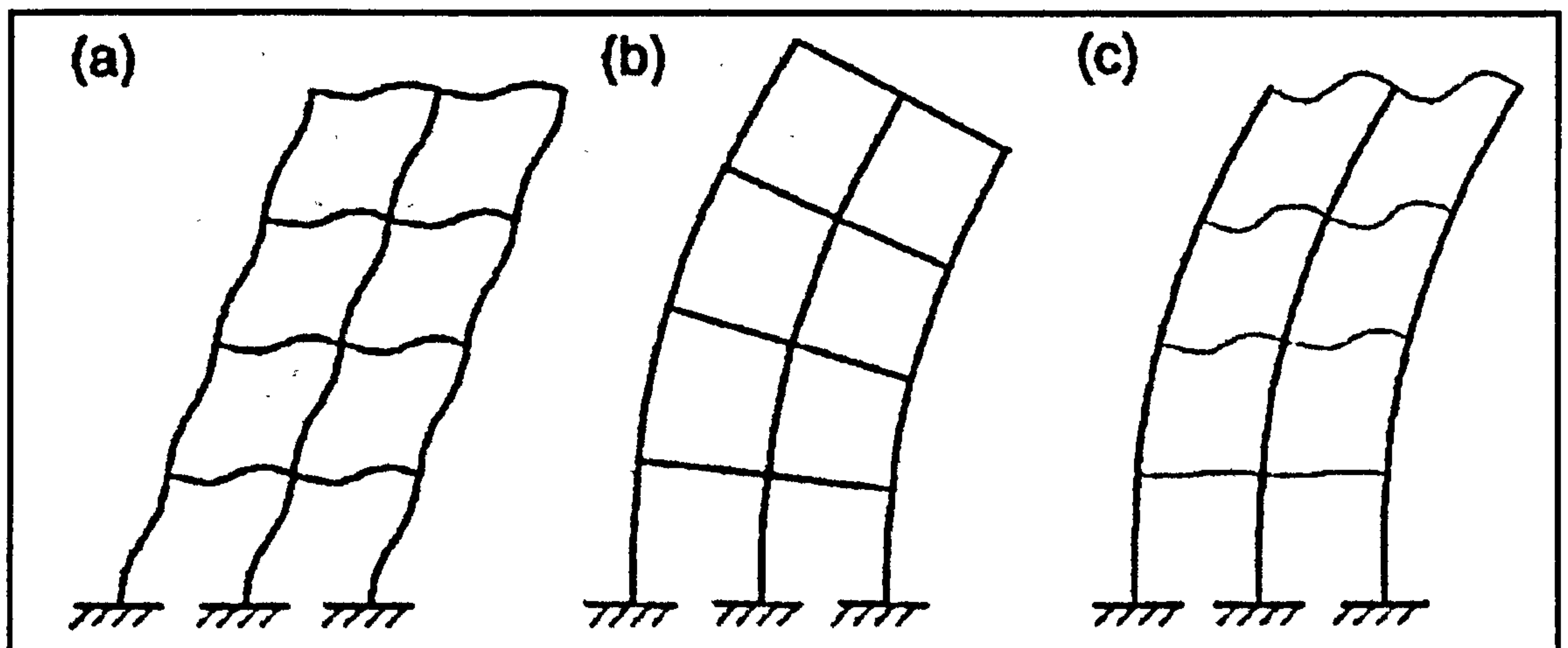


**Figure 2.16** Characteristic deformation: (a) shear; (b) full-height bending of the framework as a whole; (c) full-height bending of the individual columns  
(Zalka, ref. [30])

nature of the excitation and the dynamic characteristics of the structures, i.e. the manner in which it stores and dissipates vibrational energy. The dynamic response of structures is determined using the equation of motion and may be described in terms of displacement, velocity, or acceleration varying with time. When this excitation is applied to the base of the structure such as earthquake loads, it produces a time-dependent response in each element of the structure which may be described in terms of motions or forces to be used in the assessment of structures.

The response of the three-dimensional multi-storey reinforced concrete buildings under transient excitation of the earthquakes can be computed by representation of the buildings as multi-degree of freedom structures, with one degree of freedom for each storey in each spatial co-ordinate direction, and one natural mode and period of vibration ( $T$ : time or frequency  $\omega$ ) for each storey in each spatial co-ordinate direction, see Fig.2.15. The response history of any element of such structures is a function of all the modes of vibration, as well as its position within the overall structural configuration.

For multi-storey reinforced concrete buildings there are two types of response, firstly the seismic linear elastic response which can be computed with a high degree of mathematical accuracy, secondly the non-linear seismic response. Fig.2.17 shows the linear elastic response described in terms of the maximum horizontal shears at each floor level of a thirty-storey building subjected to a ground motion (earthquake loading). Also this figure shows the considerable difference in response between the elastic case assuming 2 percent damping (curve 1) and that for 5 percent damping (curve 3). For economical resistance against strong earthquakes most structures must behave inelastically (non-linear seismic response). It is evident that the computation of non-linear seismic response of the three-dimensional multi-storey reinforced concrete buildings under the earthquakes has obviously much complexity, Dowrick, ref. [13].

In 1987, Dowrick, ref. [13] mentioned that testing on beams and columns to determine the non-linear seismic response had not included floors or lateral beams, so that the response characteristics of complete buildings have not been properly described, and the strength of complete buildings may significantly exceed that predicted by codes. The



US-Japan Co-operative Research Program has addressed these problems and interim reports at the 8th World Conference on Earthquake Engineering confirm that floors and lateral beams have significant effects. In addition, the structural interaction of the frame and infill panels (bricks or concrete blocks walls) has a considerable effect on the overall linear elastic or non-linear seismic response of the structures and on the response of the individual members.

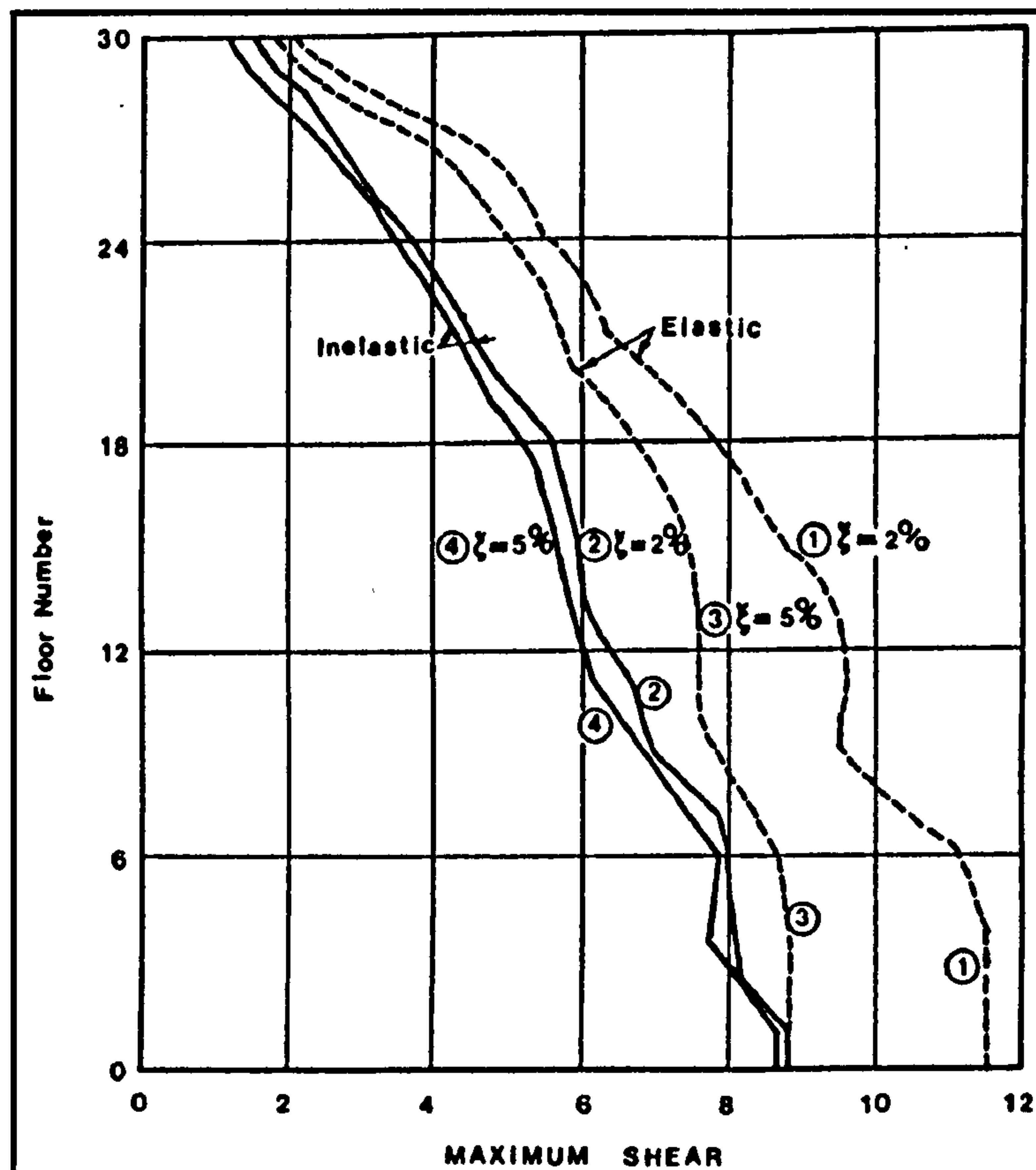


**Figure 2.17** Maximum horizontal shear response for Bank of New Zealand building (Dowrick, ref. [13])

The infill panels affects the overall linear elastic seismic response of the three-dimensional multi-storey reinforced concrete buildings and is included in this research (its review in previous works will be presented later in sections 2.3 & 2.4). As the dynamic response of the structures depends on the nature of the excitation at the bases, the earthquake loads will be discussed in the next section.

### 2.2.3 Earthquake Loads

Most earthquakes are caused by energy release at a dislocation or rupture in

crustal plates generated at a point in the interior of the earth known as the focus or hypocenter. The point on the earth's surface directly above the focus is the epicenter. The magnitude of an earthquake is commonly measured by the Richter magnitude ( $M$ ), which is commonly defined as the reading registered by an instrument called a Wood-Anderson seismograph at a specified distance of 100 km from the epicenter of the earthquake. Although the Richter magnitude provides a measure of the total energy released by an earthquake, it does not describe the damaging effects caused by an earthquake at a particular location. Such a description is required for structural engineers to analyse and design structures in seismic regions.

Graphical records or time histories of earthquakes are obtained with instruments called accelerographs. These instruments are installed on the ground in basements or in other locations of buildings or other structures. They are commonly designed to register the three orthogonal components of the ground acceleration. Fig.2.18 shows the component of the accelerogram of the El Centro earthquake, which occurred in 1940. The figure also shows, for this earthquake, the velocity and displacement obtained by integration of the accelerogram. The earthquake accelerogram also can be analysed to obtain direct estimates of peak ground motion, duration of the strong portion of ground shaking, and the frequency content of the earthquake, Paz, ref. [25], Ebeling, ref. [31].

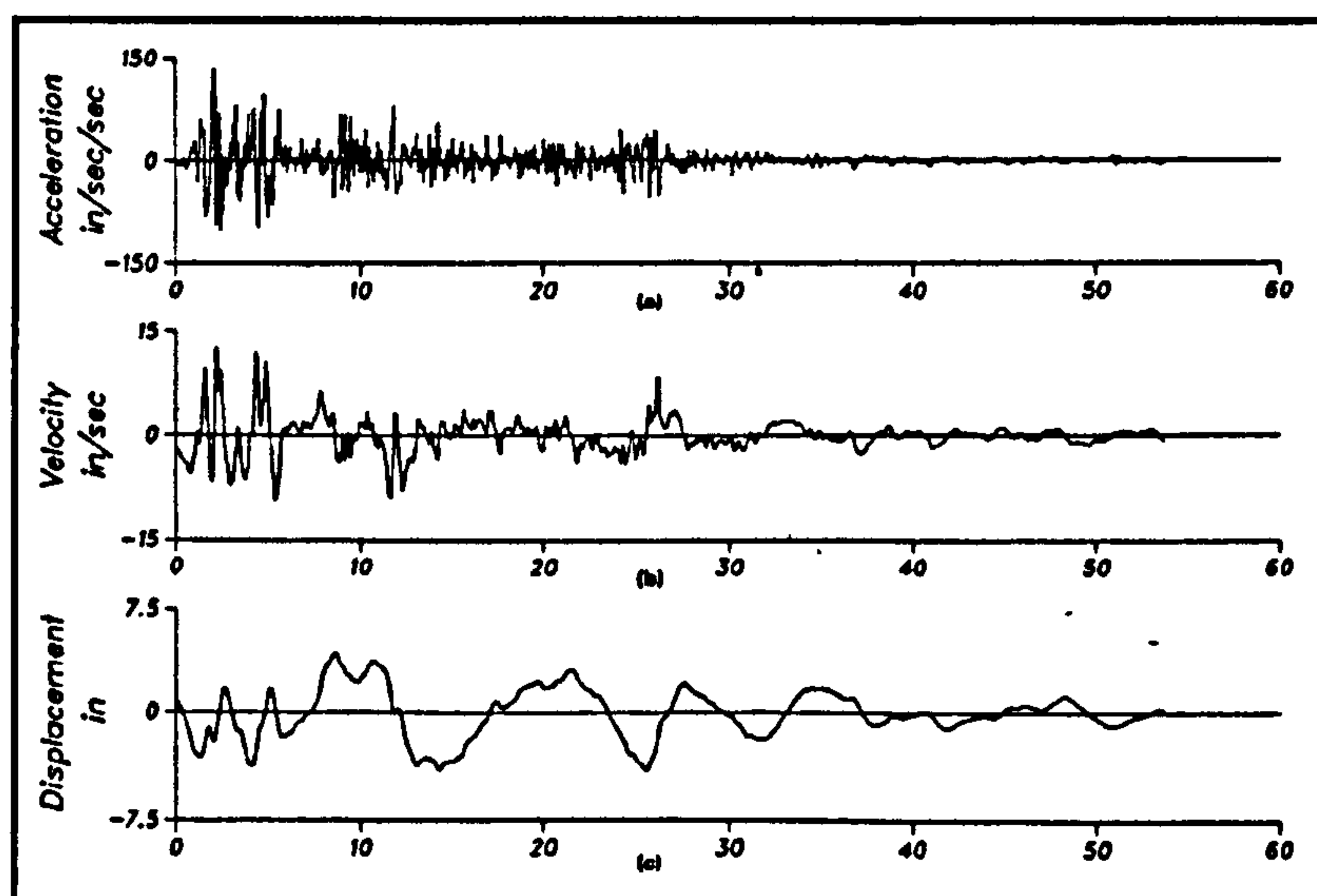


**Figure 2.18** North-south component of the El Centro earthquake, California, 1940 (Paz, ref. [25], Ebeling, ref. [31])



### 2.2.3.1 Forms of Earthquake Loads in Analysis and Design of Structures

A design earthquake is a specification of the seismic ground motion at a site, used for the earthquake resistant design of a structure. The ground motions may be specified in a number of ways, i.e. by peak accelerations, velocities, and displacements, by accelerograms, and by response spectra. The earthquake loads (seismic loads) are originally obtained in the form of an acceleration time history without information about some factors which may affect the dynamic response of structures such as the frequency content of the loading, which is critical for the dynamic response. Therefore the input ground motion is commonly defined in the form of a response spectrum.

The specification of design earthquakes requires information on seismic activity and on the site especially the influence of the soil type & properties (soil-structure interaction) on the intensity of the earthquake which is not included in this research. It is then necessary to establish the acceptable risk so that the appropriate rarity of event may be chosen. In general, establishing design earthquakes involves both deterministic and probabilistic considerations of various aspects contributing to the hazard assessment.

A response spectra represents the maximum response of a SDOF system (within a frequency or period range of interest) excited at its base by an input motion in form of an acceleration time history. The excitation is known only from experimentally recorded data and the response is evaluated by a numerical method. The response spectra which are graphs of the maximum values of acceleration, velocity, and/or displacement response for various damping levels versus undamped natural periods ( $T$ : units of seconds) or undamped natural frequency ( $\omega_n$ : units of hertz or cycles/sec), can be obtained directly from Duhamel's integral.

The response spectra can be generated from the input motion (acceleration time history) by repeated use of the Duhamel's integral. For each frequency of SDOF system in the range of interest the Duhamel's integral is used to calculate the response throughout the time (maximum response is recorded), thus a relationship between response & frequency is obtained ( $S_D$ : Displacement response spectra). A spectral pseudo velocity ( $S_V$ ) & acceleration ( $S_A$ ) can be calculated and obtained directly using the displacement response spectra as follows:

$$S_V = \omega_n S_D$$

$$S_A = \omega_n^2 S_D$$

$S_D$ : Displacement response spectra

$S_V$ : Spectral pseudo velocity

$S_A$ : Spectral pseudo acceleration

$\omega_n$ : Undamped natural frequency

As shown in Fig.2.19 it can be seen that the graph tends toward the maximum ground acceleration as the frequency  $> 33$  Hz and this is termed the ZPA (Zero Period Acceleration). For this figure the ZPA is equal to 0.2g, Dowrick, ref. [13], Paz, ref. [23], ASCE standard, ref. [26], Ebeling, ref. [31], Principia Mechanica Limited, ref. [32].

There are two types of response spectra that can be used for seismic analysis of structures according to their behaviour during an earthquake, the elastic response spectra (elastic structural behaviour) and inelastic response spectra (inelastic structural behaviour). Most of the seismic codes such as Eurocode 8 provide requirements for the seismic ground motions used in seismic analysis. For seismic input motions there are two orthogonal horizontal components and a vertical component must be considered. The vertical component of the design spectra can be obtained by scaling the corresponding ordinates of the horizontal component by two-thirds throughout the entire frequency range (it is expected that the vertical component has less energy than the horizontal component). The time-histories that are used and applied at the bases of structures for purpose of seismic analysis should be reasonably represented the ground motion expected for the site. Also the mean of the zero-period acceleration (ZPA) values calculated from the individual time histories must equal or exceed the design ground acceleration, for more details see ref. [4,8,13,23,26,31,32].

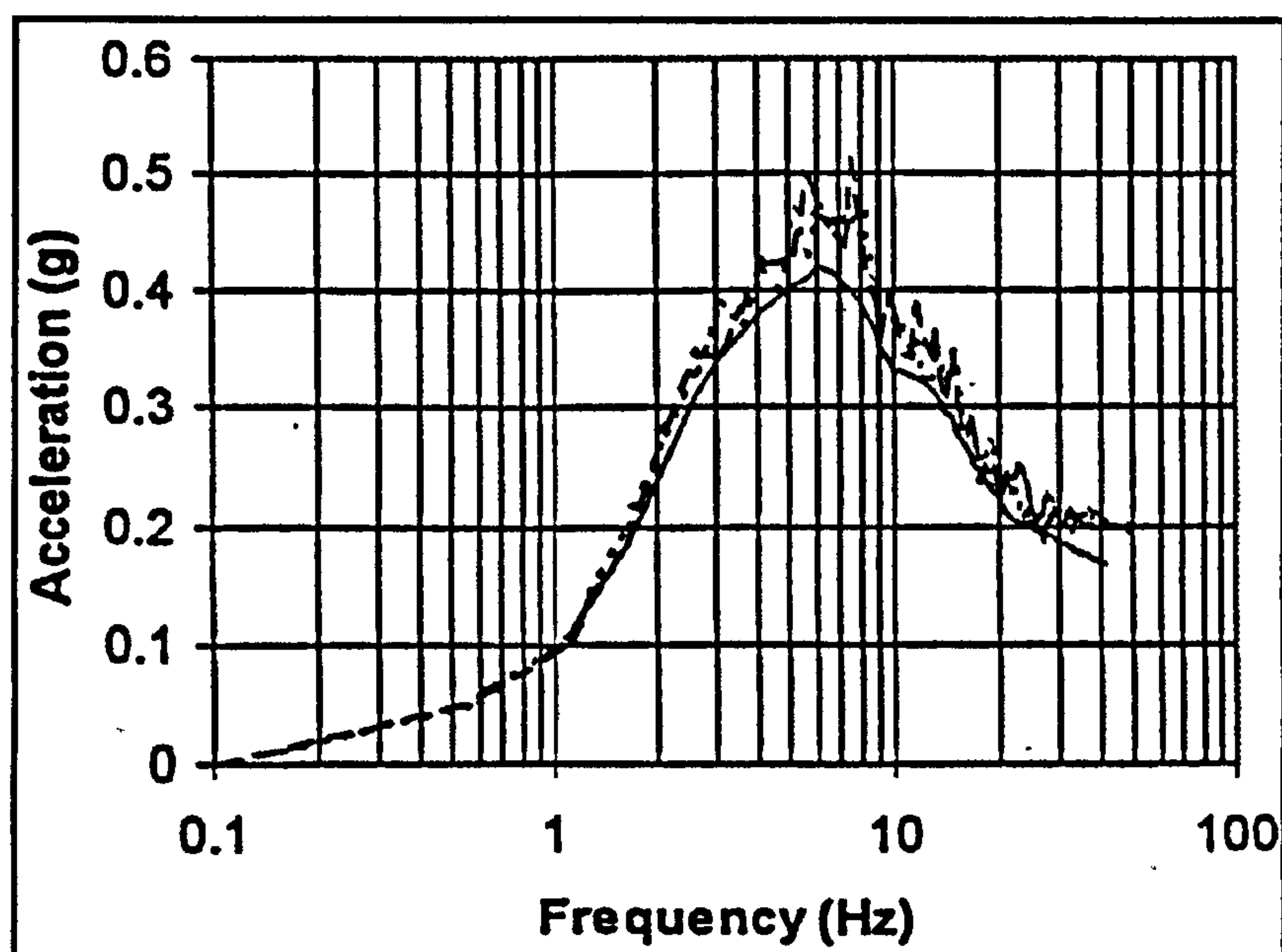


**Figure 2.19** Typical UK design response spectra (URS: Uniform Risk Spectra)  
(Principia Mechanica Limited, ref. [32])



$S_D$ : Displacement response spectra

$S_V$ : Spectral pseudo velocity

$S_A$ : Spectral pseudo acceleration

$\omega_n$ : Undamped natural frequency

As shown in Fig.2.19 it can be seen that the graph tends toward the maximum ground acceleration as the frequency  $> 33$  Hz and this is termed the ZPA (Zero Period Acceleration). For this figure the ZPA is equal to 0.2g, Dowrick, ref. [13], Paz, ref. [23], ASCE standard, ref. [26], Ebeling, ref. [31], Principia Mechanics Limited, ref. [32].

There are two types of response spectra that can be used for seismic analysis of structures according to their behaviour during an earthquake, the elastic response spectra (elastic structural behaviour) and inelastic response spectra (inelastic structural behaviour). Most of the seismic codes such as Eurocode 8 provide requirements for the seismic ground motions used in seismic analysis. For seismic input motions there are two orthogonal horizontal components and a vertical component must be considered. The vertical component of the design spectra can be obtained by scaling the corresponding ordinates of the horizontal component by two-thirds throughout the entire frequency range (it is expected that the vertical component has less energy than the horizontal component). The time-histories that are used and applied at the bases of structures for purpose of seismic analysis should be reasonably represented the ground motion expected for the site. Also the mean of the zero-period acceleration (ZPA) values calculated from the individual time histories must equal or exceed the design ground acceleration, for more details see ref. [4,8,13,23,26,31,32].

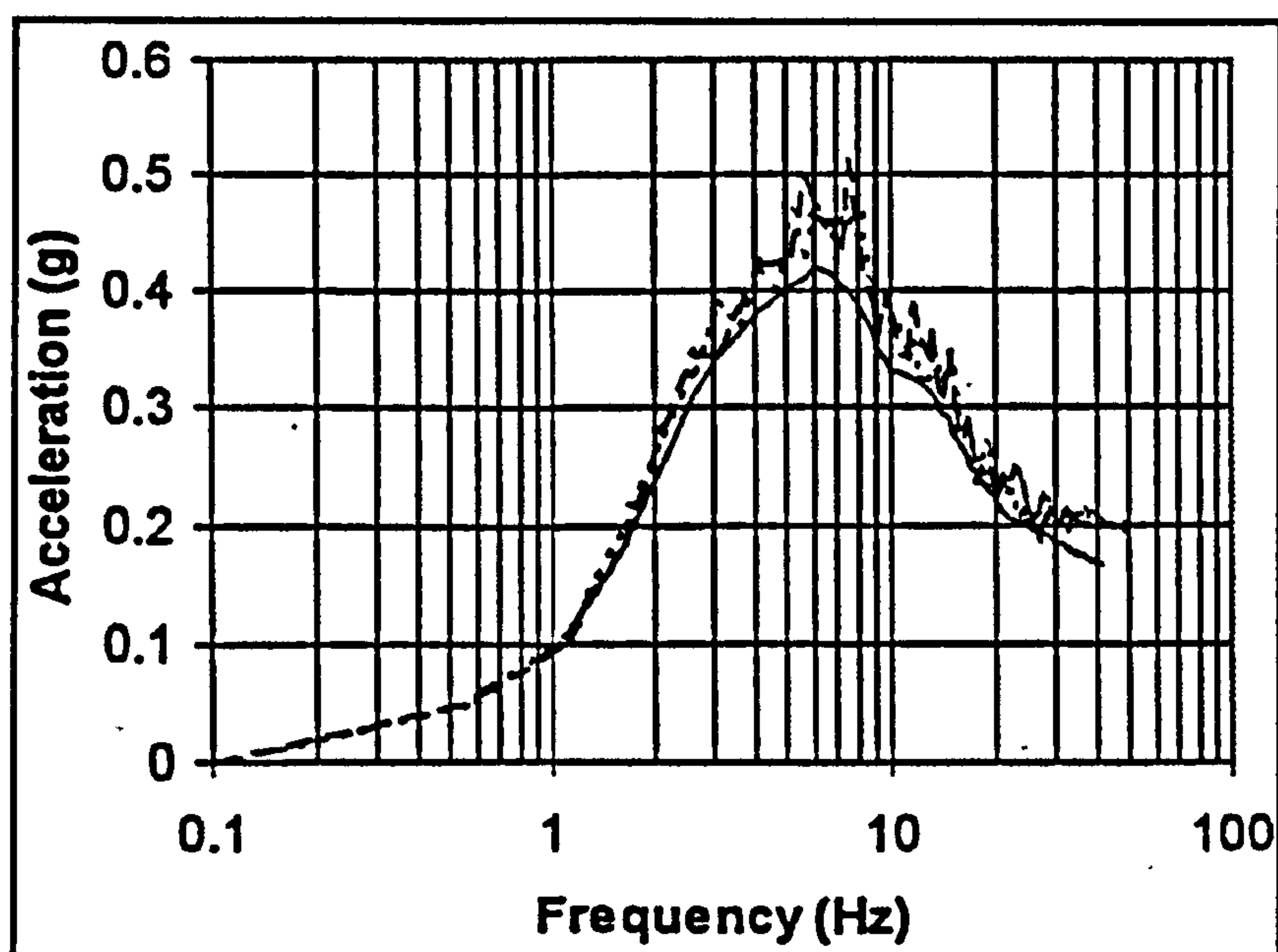


Figure 2.19 Typical UK design response spectra (URS: Uniform Risk Spectra) (Principia Mechanics Limited, ref. [32])

### 2.2.3.2 Effects of Earthquake Loads on RC Buildings

The potential destructiveness of an earthquake, although partly related to its magnitude, is also a function of other equally important factors, such as the focal depth of the earthquake, the distance from the epicentre, the soil conditions and the mechanical properties of the RC structures (strength, geometrical shape, natural period, ductility and so on). The term intensity of the earthquake is a measure of the consequences that this earthquake has on the people and the structures of a certain area. It is obvious that it is impossible to measure the damage due to an earthquake using a single quantity system. Therefore, the damage is usually qualitatively estimated using empirical intensity scales. The most common macroseismic scales that are used today are the modified Mercalli (MM) scale and the Medvedev, Sponheur, Karnik (MSK) scale (see table 2.2), both of which have 12 intensity grades.

Degree	Intensity	Effect		
		on people	on structures	on the environment
1	Insignificant	Not felt		
2	Very light	Slightly felt		
3	Light	Felt mainly by people at rest		
4	Somewhat strong	Felt by people indoors	Trembling of glass windows	
5	Almost strong	Felt indoors and outdoors, awakening of sleeping people	Oscillation of suspended objects, displacement of pictures on walls	
6	Strong	Many people are frightened	Light damage to structures, fine cracks in plaster	Very few cracks on wet soil
7	Very strong	Many people run outdoors	Considerable damage to structures, cracks in plaster, walls and chimneys	Landslides of steep slopes
8	Damaging	Everybody is frightened	Damage to buildings, large cracks in masonry, collapse of parapets and pediments	Changes in well-water, Landslips of road Embankments
9	Very damaging	Panic	General damage to buildings, collapse of walls and roofs	Cracks on the ground, landslides
10	Extremely damaging	General panic	General destruction of buildings, collapse of many buildings	Changes on the surface of the ground, appearance of new water wells
11	Destructive	General panic	Serious damage to well-built structures	
12	General destruction	General panic	Total collapse of buildings and other civil engineering structures	Changes on the surface of the ground, appearance of new water wells

**Table 2.2** The MSK intensity scale  
(Penelis & Kappos, ref. [8], Dowrick, ref. [13])



Due to the seismic regions having extended to new parts of the world in recent years, the Global Seismic Hazard Assessment Program which was launched in 1992 by support of the United Nations, produced a global seismic hazard map for all parts of the world in 1999 (see Fig. 2.20). This map shows the distribution of seismic regions in the world according to the intensity of earthquakes. Also it shows the peak ground acceleration (PGA) that any area can expect during the next 50 years depending on the seismic history of this area with 10 percent probability, <http://seismo.ethz.ch/gshap/Gshap98-stc.html>, ref. [33].

Reinforced concrete buildings often suffer major damage during the seismic event especially if the building has bad concrete quality, improper reinforcement detailing and so on. The damage classification is referred to the individual structural members of the building during the earthquake. In 1988 Key, ref. [9], summarized the effects of earthquakes on framed structures as follows:

- Corner columns often behave badly in comparison with other exterior and interior columns. This suggests that the effects of earthquake forces in orthogonal directions are not adequately dealt with in design.
- Complete failure in members detailed for ductility is rare. Where members with low ductility have failed it is clear that deterioration is swift. This is particularly marked in reinforced concrete members.
- The maximum practicable redundancy is shown to be desirable. The failure mechanism should involve as many members as possible.

and mentioned that the Typical damage to elements of the tall reinforced concrete buildings includes

- Cracking in the tension zone
- Diagonal cracking in the core
- Loss of concrete cover
- The concrete core breaking into lumps by reversing diagonal cracking
- Stirrups bursting outwards
- Buckling of the main reinforcement



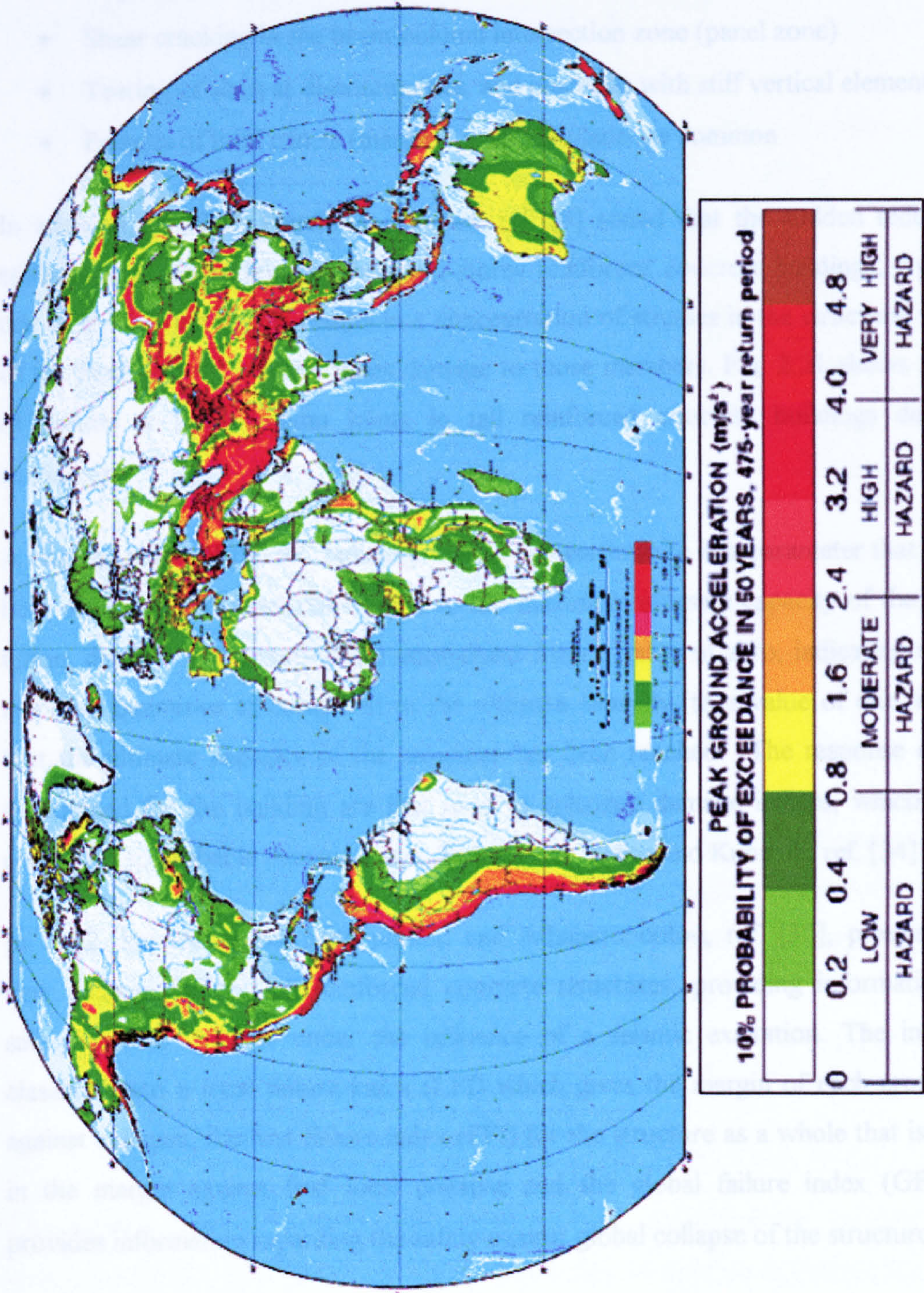


Figure 2.20 Global seismic hazard map of the world  
(<http://seismo.ethz.ch/gshap/Gshap98-stc.html>, ref. [33])

2.3 Seismic Analysis of Multi-Storey RC Buildings Using the FEM

The response of a structure to an earthquake may refer to stress, displacement,



- Bond failure, particularly in zones where there are high cyclic stresses in the concrete
- Direct shear failure of short elements, or those constrained so that only a short length is effectively free
- Shear cracking in the beam-column intersection zone (panel zone)
- Tearing of slabs at discontinuities, and junctions with stiff vertical elements
- Failures of infill panels (masonry walls) in plane are common

In addition, in 1997, Penelis & Kappos, ref. [8] stated that the sudden reduction of stiffness at a certain level of the multi-storey reinforced concrete buildings, typically at one of the bottom floors, results in a concentration of stresses in the structural members of the flexible floor, which causes damage to those members. Fig. 2.21 shows the types of failure at beam-column joints in tall reinforced concrete buildings during the earthquake.

A damage index of the RC buildings during the earthquake is a parameter that indicates how close the maximum response is to the maximum ultimate capacity of the building. Often, damage index models are normalized from a value of zero, indicating negligible response quantities as compared to the ultimate capacity, to a value of one, indicating that the ultimate capacity of the structure has been reached. The response quantities determined for the building are first used to calculate damage indices, which are then correlated to probable damage states, Reinhorn & Valles and Kunnath, ref. [34].

In 2002, Papadopoulos, Mitsopoulou and Athanatopoulou, ref. [35], presented three new damage indices for reinforced concrete structures, providing information about safety against collapse under the influence of a seismic excitation. The indices are classified into a local failure index (LFI) which gives the margin of each cross-section against collapse, the first failure index (FFI) for the structure as a whole that is accurate in the margin against first local collapse and the global failure index (GFI) which provides information regarding the safety against global collapse of the structure.

### **2.3 Seismic Analysis of Multi-Storey RC Buildings Using the FEM**

The response of a structure to an earthquake may refer to stress, displacement,

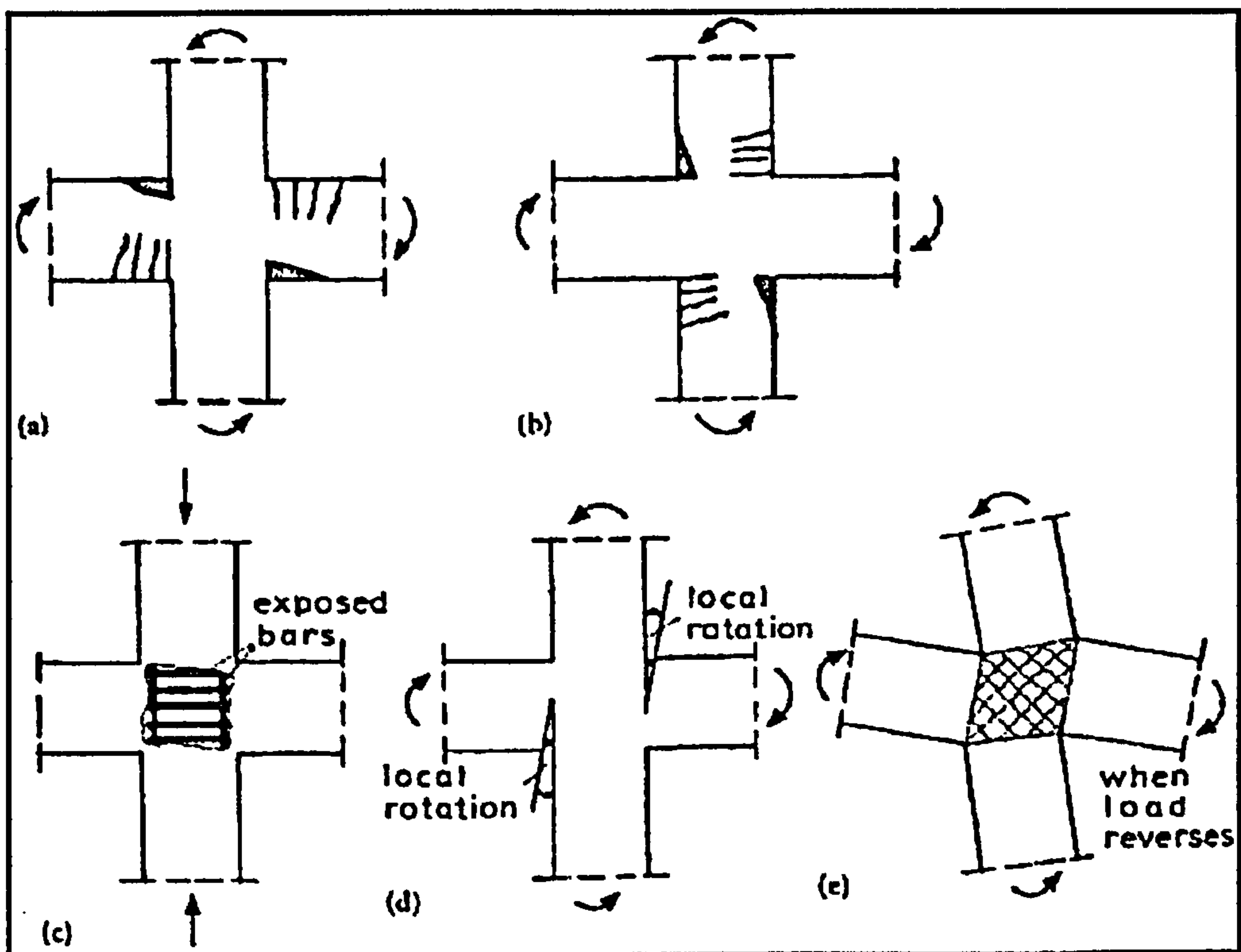


**Figure 2.21** Types of failure at beam-column joints during the earthquake  
(Penelis & Kappos, ref. [8])

- (a) Attainment of deformational capacity of the beam.
- (b) Attainment of deformational capacity of the column.
- (c) Spalling of joint core.
- (d) Anchorage failure of beam bars.
- (e) Shear failure of the joint core.

acceleration, velocity, shear or any other parameter affected by ground motion. Response may be defined in time, but it is customary to refer to the response as the peak value of the particular parameter caused by the earthquake. In general, the objectives of the dynamic analysis of a structure responding to dynamic forces can be, (a) to establish strength and ductility requirements, (b) to calculate the forces for design, (c) to calculate displacements, (d) to establish the nature of dynamic design input to equipment mounted on the structure-machinery, pipework, storage tanks etc.

The various dynamic analysis techniques used to determine the seismic forces in structures fall into two distinct categories depending on the type of domain (frequency or time) in which the equation of motion is solved. The first category contains the frequency domain techniques such the input motion is defined as response spectra or time history, and the second category contains the time domain techniques that the input motion is defined as a time-history.



The effects of vibration on a structure can be calculated if a numerical model of both the forcing function (earthquake loads) and the structure can be arrived at. This is the basic concept of any seismic analysis technique used for reinforced concrete structures. The reference method according to Eurocode 8, ref. [4], for determining the seismic effects on reinforced concrete buildings is modal response spectrum (frequency domain techniques) analysis using a linear-elastic model of the structure and the design response spectra of the input motion. Also depending on the structural characteristics of the building, one of the following two types of analysis is used:

1. Simplified modal response spectrum analysis where a static simulation of the seismic action is adopted
2. Multi-modal response spectrum analysis which is applicable to all types of buildings

EC8 gives alternative methods for seismic analysis such as direct integration method (time domain techniques) but these methods are allowed under conditions specified in the code.

Dowrick, ref. [13] and ASCE standard, ref. [26], determined the common seismic analysis methods which is used for three dimensional multi-storey reinforced concrete buildings as follows:

1. Modal analysis method (frequency domain techniques), which its results are required prior carrying out any one of the next two other methods. This method is limited to linear material behaviour. It was discussed in section 2.2.1.1.
2. Response spectrum analysis method (frequency domain techniques), which is strictly limited to linear analysis. In recent years there are attempts to use this method for nonlinear behaviour.
3. Direct integration or time-history analysis method (time domain techniques) that provides the most powerful and information analysis for any given earthquake motion. This method is used for both linear elastic and nonlinear inelastic material behaviour. It is used in this research as the main analysis tool for the seismic analysis of tall reinforced concrete buildings, and will be discussed later in section 2.3.1.1.

Frequency domain analysis techniques such as the response spectra method are easy and quick to implement both by hand or computer analysis. They are however limited to a linear analysis (as the spectra are representative of the linear response of a single degree of freedom system), and have a degree of conservatism associated with them. Time domain techniques such as the direct integration of the equations of motion requires more computer solution time, (as a series of analyses are carried out at small time intervals throughout the applied seismic event), but has the benefit of allowing nonlinear behaviour to be incorporated, and reducing the conservatism associated with frequency domain techniques.

In 1992, Paulay & Priestley, ref. [20], mentioned that the study of Seismic response of reinforced concrete structures is divided into two types of analysis, elastic seismic response of structures / non-linear seismic response of structures. It is generally uneconomic, often unnecessarily, and arguably undesirable to design structures to respond to design-level earthquakes in the elastic range. In regions of high seismicity, elastic response may imply resistance to lateral accelerations as high as 1.0g. The cost of providing the elastic strength necessary to resist forces associated with this level of response is often prohibitive, and the choice of structural system capable of resisting it may be severely restricted.

For tall buildings, the task of providing stability against the overturning moments generated would become extremely difficult. If the strength of the building's lateral force resisting structural system is developed at a level of seismic response less than that corresponding to the design earthquake, inelastic deformation must result, involving yield of reinforcement and possibly crushing of concrete or masonry. Provided that the strength does not degrade as a result of inelastic action, an acceptable response can be obtained. Displacements and damage must, however, be controlled at acceptable levels.

An advantage of inelastic response, in addition to the obvious one of reduced cost, is that the lower level of peak response acceleration results in reduced damage potential for building contents. Since these contents (including mechanical and electrical services) are frequently much more valuable than the structural framework, it is advisable to consider the effect of the level of seismic response not only on the structure but also on the building contents.



The matrix form of stiffness and force methods of elastic seismic analysis, programmed for digital computation, present a systematic approach to the study of rigid jointed multi-storey reinforced concrete buildings. Standard programs such as ANSYS are readily available. These require only the specification of material properties, stiffnesses, structural geometry, and the loading. In seismic design the advantages of such analyses is speed rather than accuracy. Analyses for any load or for any combination of (factored) loads can readily be carried out for the elastic structure. By superposition or directly, the desired combinations of load effects can be determined.

A more accurate and realistic prediction of the behaviour of strength of reinforced concrete structures may be achieved by various methods of nonlinear analysis. Some of these are rather complex and time consuming. With current available techniques, the computational effort involved in the total nonlinear analysis of a multi-storey reinforced concrete building is often prohibitive. A separate analysis would need to be carried out for each of the load combinations. Nonlinear analysis techniques have no particular advantage when earthquake forces, in combination with gravity loads, control the strength of the structure.

In 2002, Elnashai, ref. [36], carried out a comparison between the requirements for inelastic static and dynamic analysis applied for structures under seismic action. It is mentioned that whereas inelastic static analysis has become almost routine in the design office environment, its dynamic counterpart remains a challenge. This may be attributed to the complexity of time-integration algorithms, difficulties in damping representation and the effect of both of the above on the results, especially in terms of acceleration and force-related quantities. Although there is a presence of complexity and difficulties for the inelastic seismic analysis of structures, it is concluded that the inelastic seismic analysis is necessary but future developments should aim at reducing the instances where inelastic seismic analysis is needed.

Elastic behaviour during the design earthquake obviously has the advantage of making linear analysis entirely appropriate. It may arise because the designer chooses to keep a ductile material such as reinforced concrete within the elastic range where greater stiffness is required for functional reasons or greater safety

is desired. The stiffness of High-rise concrete structures can be used to advantage by minimizing seismic deformations and hence reduce the damage especially to non-structural components. This concept of seismic analysis of structures is used in this research for the applied models of multi-storey reinforced concrete buildings.

In general, the elastic or inelastic seismic analysis of tall reinforced concrete buildings is a complex task involving many parameters; therefore research into the response characteristics of complete buildings is still ongoing. Most previous testing has been carried out on beams and columns separately although the strength of complete buildings may significantly exceed that predicted by codes. The elastic and inelastic seismic analysis of multi-storey reinforced concrete buildings will be discussed later in sections 2.3.1 & 2.3.2 respectively.

The seismic response of tall reinforced concrete buildings is influenced by many parameters such as the geometric properties of the building. For example if the building is eccentric on plan, i.e. the centres of mass and stiffness are substantially separated, the effect of torsion may be sufficiently large to cause significant increases in lateral displacements. This effect is greatest on the outer elements of the structure. The coupling of response to torsional and lateral components may be high when the natural frequencies of the two modes are close. These parameters may be required to be included in the seismic analysis of buildings in order to obtaining a realistic seismic response. The influence of some parameters on the seismic response of reinforced concrete buildings will be presented in the following sections.

### **The effect of infill panels on overall seismic response**

Walls are often created in buildings by infilling parts of the frame with stiff construction such as bricks or concrete blocks. Unless adequately separated from the frame, the structural interaction of the frame and infill panels must be allowed for in the design. This interaction has a considerable effect on the overall seismic response of the structure and on the response of the individual members. In 1987, Dowrick, ref. [13], discussed briefly the principal effects of infill panels on the overall seismic response of structural frames as follows:



1. Increasing the stiffness and hence increasing the base shear response in most earthquakes
2. Increasing the overall energy absorption capacity of the building
3. To alter the shear distribution throughout the structure

The more flexible the basic structural frame, the greater will be the above-mentioned effects. As infill is often made of brittle and relatively weak materials, in strong earthquakes the response of such a structure will be strongly influenced by the damage sustained by the infill and its stiffness-degradation characteristics.

From the experimental and theoretical tests results on infilled reinforced concrete frames, it has already been clarified that the presence of infills modifies the basic global structural behaviour of infilled frames, stiffening the frame and creating new potential failure mechanisms, Comité Euro-International du Béton, ref. [37].

In 1996, Durrani & Haider, ref. [38], mentioned that the Infilling reinforced concrete frames with unreinforced masonry infills results in significant increases in the strength, stiffness and energy dissipation capacity of the frames under in-plane lateral loading. However, the unreinforced masonry infill is susceptible to out-of-plane fall-out after separation from the bounding frame. If this fall-out is effectively prevented, masonry infills may be used to improve the lateral strength and stiffness of multi-storey framed structures. Due to the introduction of the infill, the lateral strength of the reinforced concrete frames is increased up to 2.5 times the value for bare frame (without infill panels). Infills with stiffer bounding frames develop higher ultimate strengths and exhibit smaller stiffness degradation and better energy dissipation characteristics compared to those with relatively flexible confining frames. The common damage in panels is controlled by diagonal cracking, with an extension into the interface mortar-brick.

In 2002, Decanini & Liberatore and Mollaioli, ref. [39], carried out a dynamic analysis for reinforced concrete bare and infilled frames to investigate the effect of horizontal and vertical seismic excitation. It is concluded that if the infills are present in all storeys, it gives a significant contribution to the energy dissipation capacity, reducing the dissipation energy demands in columns and beams and decreasing significantly the maximum displacements. The presence of vertical motion does not significantly influence the horizontal displacements of bare frames, but can produce some effects



for the infilled ones. For what regards the influence of vertical component on dissipated energy, there is not a clear trend but it is possible to note that greater variations can occur for infilled frames.

### **The influence of high strength concrete on seismic response**

Use of high strength materials in construction is on the increase, mainly due to pressure on land use in urban centres. However, insufficient information exists on the deformational characteristics of members with high strength concrete and high yield steel in the inelastic range, relevant to seismic response. Since the constituent materials respond in a manner clearly distinct from their normal strength counterparts, it follows that existing seismic design guidelines are probably inadequate for design of high strength structures.

In 1998, Elnashai, ref. [40], presented briefly the effect of high strength concrete on the seismic response of tall reinforced concrete buildings. The preliminary information that was presented about these effects is:

- Increasing the compressive strength of concrete results in a decrease in ductility. This may be attributed mainly to the reduction in passive confinement effects and the increase in the applied axial load to represent a constant percentage of axial capacity. The rate of reduction in ductility increases for higher steel grades.
- The plastic hinge length in a high strength member is significantly shorter than for a normal strength member. This has the consequence of lower displacement ductility supply for a given curvature ductility.
- Spalling in high strength members is sudden and substantial. Thus, buckling of longitudinal bars for large hoop spacing in such members is more critical than for normal strength members.
- Under practical levels of axial force, the use of high yield steel for confining reinforcement is unnecessary. Use of lower grade steel at smaller spacing is recommended.



- The behaviour of high strength buildings under moderate earthquakes is superior to that of normal strength structures, due to their higher stiffness. Hence, serviceability limit states would be easier to satisfy.
- The redistribution potential of high strength buildings is significantly less than that of their normal strength counterparts, with behaviour factors close to unity in some cases. The number of plastic hinges developed at ultimate limit state almost invariably drops with higher strength (especially steel yield), thus reducing the energy absorption capacity.

Fig. 2.22 shows that the ductility of reinforced concrete decreases with an increase in the concrete compressive strength.

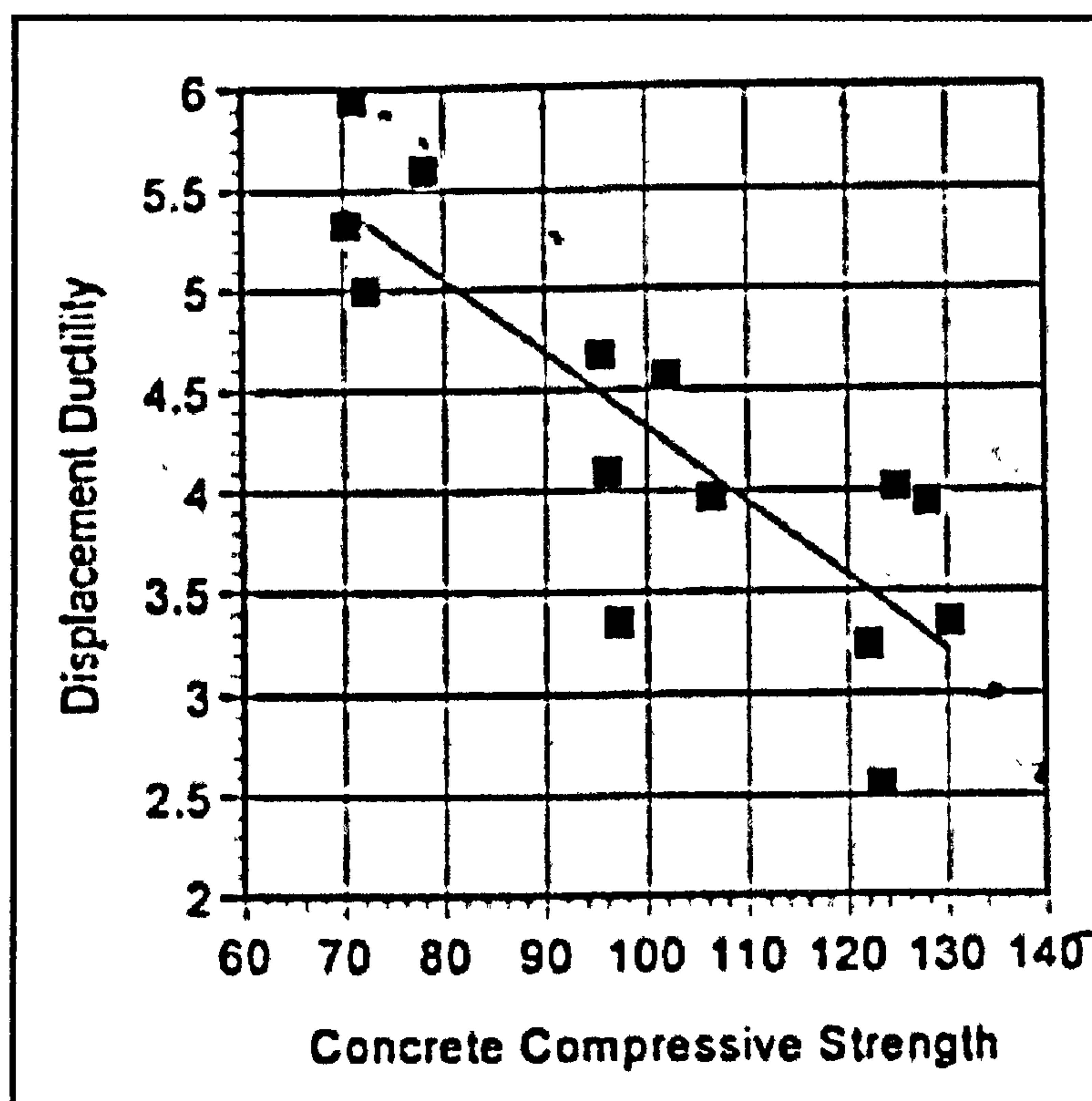


**Figure 2.22** Relationship between the ductility and concrete compressive strength (Elnashai, ref. [40])

In 2002, Petrusevska & Cvetanovska, ref. [41], stated that the modern trends impose design of high-rises and structures with large spans whose realization is impossible by use of traditional materials. So that use of high-strength concrete is necessary in construction of high-rise reinforced concrete buildings. In general, high-strength concrete is characterized by high strength and low deformability. The experimental investigations that have been performed throughout the world show that the high strength RC



elements having sufficient strength and deformability can be obtained by special construction of elements (i.e., confinement of concrete). There are many current researches throughout the world to define the behaviour of high strength concrete in the nonlinear range, as well as to develop a methodology and criteria for application of these materials in seismically prone areas.

### **2.3.1 Elastic Analysis of Multi-Storey RC Buildings Under Earthquake Loading**

The practical structural engineering problems associated with complicated geometry, boundary conditions, material behaviour and dynamic input can only be solved by numerical methods. Thus, a mathematical model of the real structure is constructed and a numerical method, such as the finite element method (FEM) is used to analyse that model and determine its response to prescribed applied loads and subsequently design the structure through a repetition of analyses. When the applied loads are dynamic, the behaviour of the structural model is governed by its equation of motion. In seismic analysis and design of structures, the applied dynamic loads are actually inertial forces and the task of the engineer is to numerically solve the equation of motion of the structure and determine its seismic response to these inertial forces.

When the material behaviour is linear elastic and the strains as well as the deformations are small, the equations of motion are linear. Then for the transient dynamic loads such as earthquake, these equations are usually solved by modal analysis or by stepwise time integration (time-history analysis). For tall RC buildings, the free vibration problem is solved first in order to obtain the natural frequencies and modal shapes of the structure (modal analysis). Subsequently, the dynamic response of the structure is computed using the direct integration method which will be presented in the next section, Beskos & Anagnostopoulos, ref. [19].

#### **2.3.1.1 Time–History Analysis of Three Dimensional Multi-Storey RC Buildings (Direct Integration Method)**

Time–history analysis or sometimes-called direct integration analysis is a technique used to determine the dynamic response of a structure under the action of any general time-dependent loads (seismic loads). The actual displacements and stresses



developed in a structure are time dependent, i.e. they are functions of time (t). This technique involves the step-by-step direct integration of the coupled equations of motion in order to derive the dynamic response of the structure at each increment of time. This method of analysis is only suitable for use on a computer that the model of the structure is solved on the basis of the finite element method. It is relatively expensive to run using the computer. Although the direct integration method can perform a close-to-reality analysis, this approach is justified and can be employed effectively only for large and complex structures (multi-storey RC buildings). It is used where no previous experience of the structural behaviour exists, or for detailed evaluation of the response of existing structures under specific earthquakes.

In the direct integration method the linear elastic response of multi-storey RC building subjected to an acceleration time-history is obtained by solving the following differential equation of motion in this form.

$$[M]\{\ddot{Y}\} + [C]\{\dot{Y}\} + [K]\{Y\} = -[M]\{U_b\}\ddot{u}_g$$

$[M]$  : mass matrix (n x n)                       $\{\ddot{Y}\}$  : column vector of relative accelerations (n x 1)

$[C]$  : damping matrix (n x n)                       $\{\dot{Y}\}$  : column vector of relative velocities (n x 1)

$[K]$  : stiffness matrix (n x n)                       $\{Y\}$  : column vector of relative displacement (n x 1)

$\{U_b\}$  : influence vector; displacement vector of the structural system when the support undergoes a unit displacement in the direction of the earthquake motion (n x 1)

n : number of dynamic degrees of freedom                       $\ddot{u}_g$  : ground acceleration

In direct integration technique, as the name implies, no transformation of the equation above into a different basis is performed and, thus, the equation of motion is integrated using a time step-by-step numerical procedure. There are two main methods for the integration of the equation above, explicit and implicit. Both methods use finite difference expressions involving values of the displacements, velocities, and accelerations at discrete time stations  $\Delta t$  apart, and in either case the equation above is not satisfied at any time t but at those discrete time stations. The variation of displacements, velocities, and accelerations within each time interval  $\Delta t$  is always assumed and, of course, depends on the particular solution procedure used.



In explicit methods, the differential equations of motion are converted to a set of linear algebraic equations with unknown state variables (at the present time), which are independent of one another. The displacements at any time station are computed using the equilibrium conditions of equation above at the previous time station. These methods do not require a factorisation of the stiffness matrix and in most practical cases they do not involve the solution of a system of equations, are easy to program, and present specific advantages in the handling of complex material & geometric models (material and geometric nonlinearities). However, the stability of the obtained solution depends exclusively on the size of the chosen time interval which in many cases can be prohibitively small.

There are a number of numerical techniques available to solve these equations. Acceptable schemes include Runge-Kutta method, predictor-corrector method and central difference method. These methods are conditionally stable so have a disadvantage of requiring very small time step sizes. The explicit integration tends to be used where the response is predominantly nonlinear.

In implicit methods, the differential equations of motion are converted to a set of linear simultaneous algebraic equations. The chosen difference expressions are of such form that permit the computation of displacements at any time station using the equilibrium conditions of the equation of motion at the same time station. Such methods require factorisation of the (effective) stiffness matrix. For this reason, when compared to explicit methods, the implicit methods usually require substantially more computational effort per time step. This technique allows non-linearities to be included in the analysis. The maximum values provided for the time step based on the integration constants and the natural period of vibration of the structure, but generally smaller values are used in order to represent effectively the variations in the ground motion accelerogram. Customary values of time step are 0.02 or 0.01 sec for building structures. If the analysis remains linear then the same time step is used throughout. However, as the response becomes non-linear it is usually necessary to significantly reduce the time step size.

There are a number of numerical techniques available to carry out this procedure. The most popular are the Newmark Beta method, the Houbolt method and the Wilson  $\theta$



method. This technique tends to be used where the response is predominantly linear. The finite element computer package (ANSYS Program) that is used in this research for seismic analysis (direct integration method) of RC buildings uses the implicit technique, Eurocode 8, ref. [4], Key, ref. [9], Beskos & Anagnostopoulos, ref. [19], Paz, ref. [25], ASCE standard, ref. [26], ANSYS, ref. [42].

### **2.3.2 Inelastic Analysis of Multi-Storey RC Buildings Under Earthquake Loading**

The inelastic seismic analysis of RC buildings is normally required due to presence of the geometric nonlinearities that significantly alter the effective system geometry and / or material nonlinearities such as plasticity under earthquake loads. Realistic earthquake engineering problems involve material and geometric nonlinearities. Material nonlinearities are due to the inelastic constitutive material behaviour of the structure while geometric nonlinearities are usually due to unilateral contact conditions between the structure and its foundation or excessive lateral displacement of the building. Analysis of these nonlinear dynamic structural systems is usually carried out using the time domain techniques available with the finite element method (FEM).

Actually the FEM discretizes the systems in space (semi-discretization) and time integration techniques are usually employed to solve the resulting nonlinear matrix equations of motion. There are some frequency and time domain techniques other than direct integration method which are stated above in section 2.3.1.1 for the nonlinear seismic analysis of RC buildings. These other techniques are also used for solving these nonlinear equations approximately but more efficiently.

In 1999, Ghobarah & Biddah, ref. [43], performed a nonlinear seismic analysis for existing reinforced concrete frames using the FEM. Lack of adequate confinement and shear reinforcement in the beam-column joints of existing reinforced concrete frames may be the cause of brittle failure during a seismic event. Difficulties of analysis and assessment of these frames arise due to reinforcement congestion when trying to achieve high ductilities in framed structures, and the problem of detailing beam-column joints. Therefore most of the nonlinear dynamic analysis programs assume infinitely rigid beam-column joints in concrete frames regardless of the reinforcement detail.



In 2001, Mwafy & Elnashai, ref. [44], mentioned that the inelastic time-history analysis (direct integration method) is a powerful tool for the study of structural seismic response. A set of carefully selected ground motion records can give an accurate evaluation of the anticipated seismic performance of structures. Despite the fact that the accuracy and efficiency of the computational tools have increased substantially, there are still some reservations about the dynamic inelastic analysis, which are mainly related to its complexity and suitability for practical design applications. Moreover, the calculated inelastic dynamic response is quite sensitive to the characteristics of the input motions, thus the selection of a suite of representative acceleration time-histories is mandatory. This increases the computational effort significantly. The inelastic static pushover analysis technique (frequency domain techniques) was used for the inelastic seismic analysis of two-dimensional RC buildings. It was concluded that this method is more appropriate analysis technique for low rise and short period frame structures.

### **2.3.3 Modelling and Analysis of Structures Using the Finite Element Method**

The seismic response of a structure must be determined by preparing a mathematical model of the structure and calculating the response of the model to the prescribed seismic input motion. The selection of the appropriate mathematical model of the physical structure for the purposes of analysis depends on the type of analysis to be applied, on the action to which the analysis refers and to the intended use of the analysis results. So the idealisation of a RC structure for a seismic response analysis has to capture all important features of the structural behaviour under the design seismic action. The mathematical model requires information on structural stiffness, derived from the geometric and material properties. In addition to this, because dynamic forces derive from the inertia of the structural masses, information on the mass distribution is required, and this can be either in the form of lumped masses at the structural nodes or as distributed mass.

Depending on the type of seismic analysis applied, RC buildings as well as other structures may be idealized as an assembly of elements connected at joints or nodal points. These elements can be unidirectional such as beams or rod elements, two dimensional like plates and shell elements, and three dimensional such as solid



elements. The structure may be modelled as a shear building when the horizontal diaphragms at the floor levels of a multi-storey RC building are assumed to be rigid. In such a model, it is assumed that: (1) the total mass of the structure is concentrated at the levels of the floors, (2) the horizontal diaphragms at the floor levels are plane rigid, and (3) the deformation of the structure is independent of the axial force present in the columns. These assumptions transform the problem from a system with an infinite number of degrees of freedom (due to the distributed mass) to a system that has only as many degrees of freedom as it has lumped masses at the floor levels. At the other extreme, the RC buildings may be modelled and analysed using the FEM, which is providing very accurate predictions of the dynamic response under the seismic action. This modelling method is commonly used for analysis of multi-storey RC buildings.

In the past there has generally been little choice in the method of seismic analysis for tall reinforced concrete buildings, mainly because suitable and economical finite element computer programs (such as ANSYS, ref. [42]) have not been readily available. An increasing number of efficient and economical dynamic analysis programs based on the finite element method are being written for faster computers, and many design offices have access to such programs, especially since the advent of microcomputers. Dynamic analyses are demanded now by some owners, and by the regulations of more countries. Therefore the finite element method for structural analysis is used widely nowadays – both in practice and research, where it is the most powerful modern method for analysis of the complex structural problems (such as seismic analysis of multi-storey reinforced concrete buildings). The FEM will be described in further detail in the next section.

### **2.3.3.1 Review of Finite Element Method (FEM)**

The finite element method represents the extension of stiffness (displacement) method for analysis of structures. Many engineering structures are composed of a series of individual members, which are connected together at a number of points being referred to as “node points”. The analysis of these structures can be carried out by first considering the behaviour of each individual element independently and by then assembling the elements together in such a way that equilibrium of forces and



compatibility of displacements are satisfied at each nodal point. This method of analysis is called the stiffness method of analysis. It is of limited use in hand analysis of large structures because this method is implemented by using an analytical solution which becomes very laborious due to the large number of the simultaneous equations involved. With the advance of the computer capabilities, this method has been programmed based on the fundamental methods of analysis to satisfy the analysis of large structures.

In the finite element method, the structure is divided into a discrete number of “finite” elements, the properties of each element is described by a simple mathematical representation, the elements are jointed at “nodes” forming the whole structure, and the loading conditions are applied. The finite element method is extremely powerful since it is used for any type of structural analysis and can solve very complex structural engineering problems such as structural static analyses, non-linear analysis, and transient dynamic analysis (seismic analysis) of two or three dimensional RC buildings, Rockey & Evans & Griffiths and Nethercot, ref. [45].

The use of a computer is essential in the finite element method especially, when applied to complex structural problems (such as seismic analysis of multi-storey RC buildings) due to the large number of computational processes for producing the required element matrices (such as  $[M]$ ,  $[C]$ ,  $[K]$ ) where the computer time and memory can be large. The finite elements can have many shapes with nodes at the corners or on the sides and different degrees of freedom for each node according to the dimensionality as shown in Fig. 2.23.

#### **2.3.4 Assessment of Seismic Performance of Existing Multi-Storey RC Buildings Designed to Normal Design Codes**

Seismic risk mitigation is an essential requirement of contemporary structural design and assessment of existing structures. Seismic ground motions are a major cause for concern when considering their damaging effects on existing multi-storey reinforced concrete buildings. Therefore mitigation of seismic risk implies improvement of seismic performance of these buildings. In recent years research has been carried out to investigate the seismic behaviour of RC structures designed to normal design codes (static codes such as BS8110, ref. [3]) but this research has commonly been limited to the seismic analysis of two-dimensional RC frames.



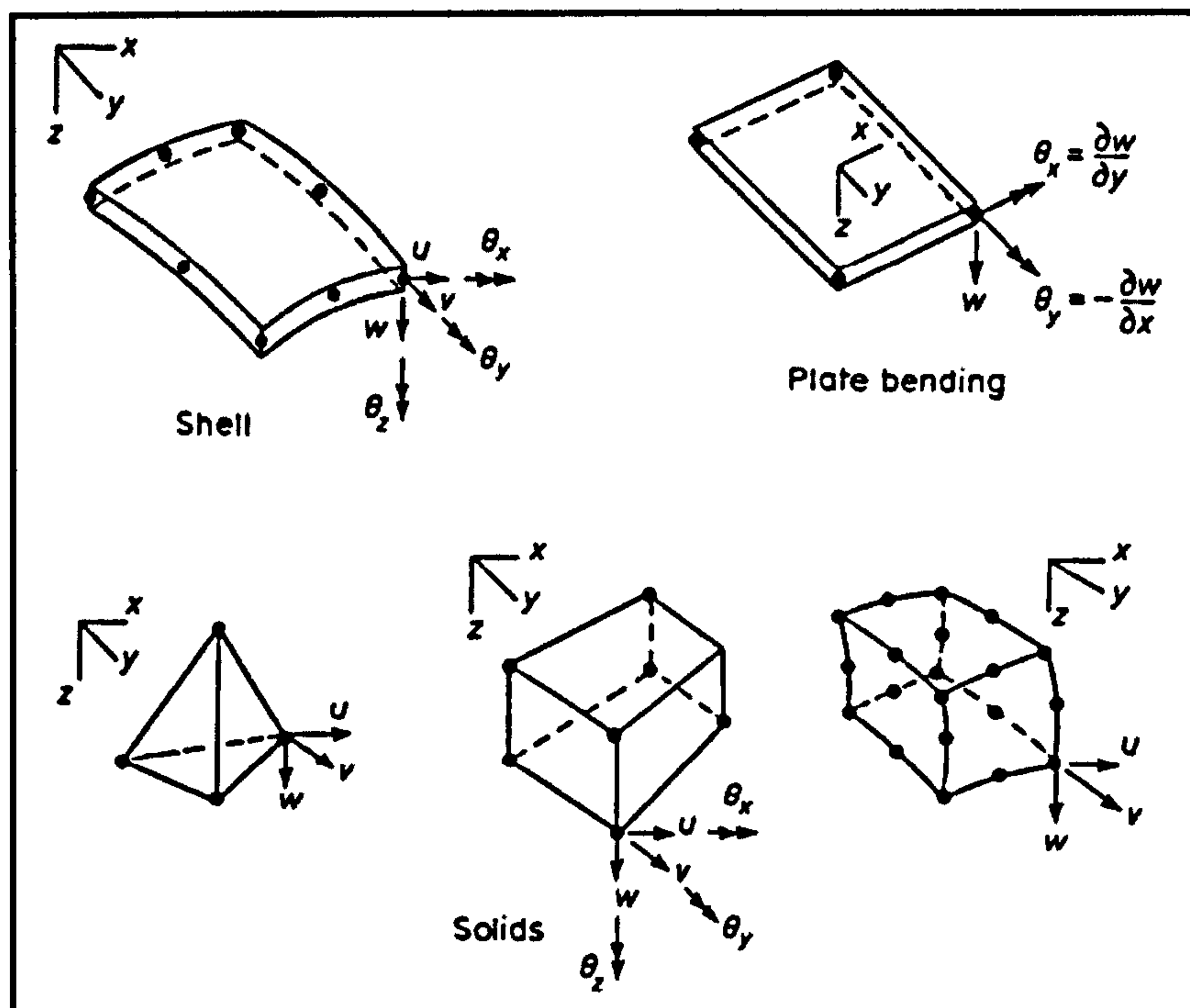


**Figure 2.23** Different types of finite element with nodal degrees of freedom shown at a typical node only (Ghali & Neville, ref. [10])

Due to the expected deficiency in the seismic performance of existing reinforced concrete buildings, it is necessary to define specific methods for the assessment and strengthening of these buildings. In this research, the seismic analyses are carried out for a typical three-dimensional multi-storey reinforced concrete building designed to a normal static design code (BS8110, ref. [3]). Also a retrofit suggestion for these buildings to improve seismic performance may be presented and analysed.

In 2002, Cosenza, Manfredi and Verderame, ref. [46], mentioned that the RC frames designed without seismic provisions have in many cases a structural behaviour characterised by low available ductility and lack of strength hierarchy inducing undesirable failure mechanisms. The lack of horizontal and vertical regularity and the high torsional deformation are also problems resulting in an unsatisfactory global behaviour. Details such as low confinement levels or insufficient anchorage of rebars can also represent potential critical zones, characterized by brittle mechanisms and low available ductility. A summary of models that permit the analysis of the non-linear behaviour of RC structures was presented (such as beam or column model). The seismic analysis of these models allows to outline some characteristics that a numerical model should provide in order to achieve a reliable assessment of the seismic capacity of underdesigned buildings.



It was concluded that the details are often poor (i.e. low percentage of transverse reinforcement, poor bond conditions); this determines that the critical zones (i.e. beam-column joints, footing zone of column) do not behave in a ductile manner and show brittle mechanisms of failure (i.e. pull out or buckling of the rebars, shear failure, etc.). The assessment of the seismic capacity of global existing RC building structures is a hard challenge in comparison to new RC structures. The reliability of the numerical outcomes is strictly related to the capacity of simulating the cracked flexibility at service and the brittle failure modes at ultimate. Both aspects require refined and very powerful numerical models.

Also in 2002, Calvi, Magenes and Pampanin, ref. [47], mentioned that the particular emphasis has been recently put on the problem of the seismic vulnerability of existing reinforced concrete buildings, with primary attention to underdesigned or designed-for-gravity-loads-only frame systems, as typically found in major seismic-prone countries before the introduction of adequate seismic-oriented design codes in the mid 1970s. The role of joint damage and collapse in the seismic response assessment of existing reinforced concrete frame buildings was investigated for some models of multi-storey RC frames. It was concluded that there is a relevance of considering the beam-column joint response to evaluate the global expected performance of a reinforced concrete frame. In general, columns were designed for gravity only, dimensioning the required concrete section and providing nominal reinforcement according to a reasonable geometrical percentage. The obvious consequence is that columns are in most cases considerably weaker than beams, even considering the contribution of gravity load flexural stresses. A soft storey mechanism is then usually predicted, but the relatively low reinforcement percentage and axial force in the columns may assure a considerable deformation capacity in the critical section.

## 2.1 Seismic Design

The design of a structure is a process of synthesis, as contrasted with the analysis for given loadings or environmental conditions. Buildings constitute the majority of RC structures designed for earthquake resistance. Moreover, although individually they may be less important than special structures such as bridges, tanks, etc., they are geometrically more complex and their codified seismic design is



more demanding. In general, the design of a building to resist earthquake motions requires that the designer works within certain constraints such as: the architectural configuration of the building, the foundation conditions, the nature and extent of the hazard should failure or collapse occur, the possibility of an earthquake, the possible intensity of earthquakes in the region, the cost or available capital for construction, and similar factors.

The problem of designing earthquake-resistant reinforced concrete buildings, like the design of structures (whether of concrete, steel, or other material) for other loading conditions, is basically one of defining the anticipated forces and/or deformations in a preliminary design and providing for these by proper proportioning and detailing of members and their connections. Designing a structure to resist the expected loading is generally aimed at satisfying established or prescribed safety and serviceability criteria. This is the general approach to engineering design. The process thus consists of determining the expected demands and providing the necessary capacity to meet these demands for a specific structure. Adjustments to the preliminary design may likely be indicated on the basis of results of the analysis-design evaluation sequence characterizing the iterative process that eventually converges to the final design. Successful experience with similar structures should increase the efficiency of the design process.

In earthquake-resistant design, the problem is complicated somewhat by the greater uncertainty surrounding the estimation of the appropriate design loadings as well as the capacities of structural elements and connections. However, information accumulated during the last three decades from analytical and experimental studies, as well as evaluations of structural behaviour during recent earthquakes, has provided a strong basis for dealing with this particular problem in a more rational manner. As with other developing fields of knowledge, refinements in design approach can be expected as more information is accumulated on earthquakes and on the response of particular structural configurations to earthquake-type loadings. As in design for other loading conditions, attention in design is generally focused on those areas in a structure which analysis and experience indicate are or will likely be subjected to the most severe demands. Special emphasis is placed on those regions whose failure can affect the integrity and stability of a significant portion of the structure.



The general concept of seismic design provision of RC buildings which are included in most of the modern design codes (such as Eurocode 8, ref. [4]) is:

- The provision of seismic resistance has an important influence on structural form. A building planned without considering the special needs of seismic design is unlikely to perform efficiently. Special attention has to be paid to the location of major lateral force resisting elements such as shear walls and service cores both of which can be effective in resisting lateral forces and controlling displacements.
- Desirable aspects of building form are simplicity, regularity and symmetry in both plan and elevation. These properties all contribute to a more even and predictable distribution of earthquake forces. Irregularities in stiffness, mass and strength can lead to increased dynamic response. In planning the framing system the need for a high degree of redundancy and for providing ductility must be kept in mind.
- Horizontal torsional forces from ground motion are not usually of concern unless the structure has an inherently low torsional strength. However torsion forces also arise from eccentricity in the disposition of mass and resistance and can cause substantial bending forces on the columns particularly those located at the corner of the building.
- Buildings which are tall in relation to their base width will generate high forces at the base due to the overturning moment. In this case reinforced concrete columns in tall buildings may fail in tension. It is probably in the range of buildings with height to width ratios of more than four that overturning forces become critical.
- The separation of complex structures into simpler regular forms by the use of joints can create more manageable systems. At major discontinuities stresses are caused by the connecting elements each trying to respond at their own natural frequency. Even where the frequencies are close the elements are unlikely to be responding in phase. Structures should not be located so that their foundations cross divisions between markedly different soil types for the same reason.



According to the complex interrelationships existing among the capacity design parameters (such as the strength, stiffness and ductility) that govern the seismic response of RC buildings, the design philosophy of national or regional codes dealing with seismic design is different. In the next section, a summary of the common regional codes of seismic design of RC buildings will be presented.

#### **2.4.1 Philosophy of Seismic Design of RC Buildings According to Modern Design Codes**

Reinforced concrete buildings have significant advantages and disadvantages as suitable building structures for earthquake resistance. These disadvantages (such as adequate ductility) have been treated in recent advances of design concepts and subsequently the modern codes of seismic design. In 1998, Comite Euro-International du Beton, ref. [48], presented the philosophy of seismic design of RC buildings for the following four regional codes.

##### **New Zealand seismic code (NZS 3101)**

The New Zealand capacity design principles for ductile moment-resisting RC frames aim primarily at

- Establishing a strong column - weak beam structure, i.e. eliminating the possibility of a column sway mechanism (soft storey) even during the most severe seismic motions
- Avoiding shear failures in columns and beams.

In order to avoid the formation of column plastic hinges (except at the base of the column and at roof level), inelastic dynamic effects, causing the bending moment diagrams in the columns to differ substantially from those derived from an elastic analysis based primarily on first mode response, must be taken into account. Consequently, the capacity design procedures are mainly concerned with deriving column design actions consistent with large inelastic deformations that cause plastic hinges in the beams to develop overstrength moments, and considering inelastic dynamic effects. The beams are designed for shear forces consistent with the beam hinges at both ends developing overstrength moments. In general, the intent is to spread plasticity to the largest possible number of hinges, and to minimize plastic rotations. For ductile structural walls and coupled walls, similar principles are



involved with a requirement for a dependable inelastic mechanism based on wall base flexural hinges and coupling-beam hinges, together with a capacity design approach to avoid shear failures.

### **American seismic codes**

There are a number of codes dealing with seismic resistance in the USA alongside documents that may be viewed as providing source material for code-drafting. There are four codes dealing with seismic provisions for buildings. These are the Council for American Building Officials (CABO) code for dwellings, the Building Officials and Code Administrators (BOCA) National Building Code, the Southern Building Code Congress International (SBCCI) Standard Building Code and the International Conference of Building Officials (ICBO) Uniform Building Code. The latter code is traditionally linked to the guidelines by the Structural Engineers Association of California (SEAOC). Therefore, reviewing the Uniform Building Code would provide a reasonable representation of existing seismic design practice in the USA.

Moment frames are classified and detailed according to the selected seismic performance category (A, B, C, D or E). There are three classes of moment frames as follows:

- (a) Ordinary moment frames - frames designed and detailed with no seismic provisions
- (b) Intermediate moment frames - frames designed and detailed for structures in areas of moderate seismic hazard, in addition to all requirements of ordinary moment frames
- (c) Special moment frames - frames designed and detailed to the full special seismic provisions in addition to the requirements of (a) above.

In these seismic codes, no explicit capacity design requirements are imposed on frames according to the target seismic performance level. Capacity design is implicit in prescribing that certain performance categories dictate the use of certain types of frame. Category A frames may be ordinary moment frames. Category B frames, which form part of the seismic load resistance system, should be intermediate frames.



Category C frames may be either intermediate or special moment frames, while for categories D and E only special moment frames are allowed.

There are five aspects in the code that may be classified strictly under capacity design requirements. These are as follows:

- The probable flexural strength, used to evaluate design shear forces in the cases below, is evaluated using a steel yield stress of 1.25 times the specified yield stress and no strength reduction factors.
- For structures in high seismic risk areas, the design shear force is evaluated not from applied design loads but from the probable flexural strength (defined above) of the member under consideration. In areas of moderate risk, the design shear force is the largest of (1) that corresponding to nominal flexural strength and (2) from analysis under factored loads. Walls and diaphragms are exempt even in high seismic risk areas.
- When the axial load on frame members is less than specific value, the contribution of axial load to concrete shear resisting mechanism is ignored.
- The sum of column design flexural strength at a joint should be equal to or greater than 1.2 times the sum of moments corresponding to flexural strength of the beams. This may be violated if any positive effect of the columns is neglected, all negative effects are catered for and additional confinement reinforcement is placed up the full column height.

### **Eurocode 8 (EC8)**

The requirements of capacity design contain three limit states as follows:

- (a) Serviceability limit state: Structures must resist low-intensity earthquakes without any structural damage. Thus, during small and frequent earthquakes all structural components forming the structure should remain in the elastic range.
- (b) Ultimate limit state: Structures should withstand an earthquake of moderate intensity ('design earthquake' having a peak ground acceleration (PGA) based on a return period of 475 years) with very



light and repairable damage in the structural elements, as well as in the infill elements.

- (c) Collapse limit state: Structures should withstand high-intensity earthquakes with a return period much longer than their design life without collapsing.

The code is applied for all categories of RC buildings in seismic regions according to the intensity (low-moderate-high) of earthquakes. For frame buildings, the code aims at a well-defined global mechanism, i.e. the so-called beams-sway mechanism, in which all beams at all storeys form plastic hinges, while all columns remain elastic for their entire height, with the exception of their base section at the ground storey. In this mechanism, the global inelastic drift (plastic displacement at the top divided by the height of the frame) equals the plastic rotation at the end regions of all the beams, which corresponds to the most uniform possible spreading of inelasticity throughout the building.

### **Japanese seismic code (AIJ)**

A complete procedure incorporating capacity design concepts and provisions for the design of reinforced concrete frame and wall-frame structures has been developed by the Architectural Institute of Japan (1990). The scope of this procedure is limited to regular building structures with a height not exceeding 45 m. As yet, the AIJ procedure does not have official status in Japan. The seismic action used for the design at the ultimate limit state is taken from the Building Standard Law Enforcement Order (1981), and it is not qualified in terms of average return period and implied amount of structural ductility. The suitability of this action to provide a satisfactory degree of protection is supported by the good overall behaviour exhibited by the building structures in the course of past disastrous events.

The AIJ procedure states that the preferred yield mechanism for frame structures is the optimum mechanism involving the formation of hinges at all beam ends and, at a later stage, at the base sections of the ground-storey columns. Hinges are allowed in columns at the top sections of the upper storey and in exterior columns when subjected to tension at the ultimate stage. When walls are also present, ductile flexural hinges and



uplifting rotation are admitted at their base and yielding in columns is permitted in mid-storeys.

Also in 1998, Booth, Kappos and Park, ref. [49], carried out a comparison between the provisions of the earthquake-resistant design of RC buildings in EC8, New Zealand seismic code (NZS 3101), American seismic code (ICBO: uniform building code) and Japanese seismic code (AIJ). It was concluded that there is a wide divergence in many of the detailed requirements of the four current seismic Codes. Changes in seismic design philosophy are currently under consideration in the countries where these Codes were developed. In particular, performance and displacement-based methods of design are already being considered to replace existing methods. The authors in principle support these broad changes, which have the potential for producing more rational and economic designs. However, the details of Code requirements can also have a profound impact on the outcome of practical designs, and therefore also on their safety and economics. The specification of design ground motions and detailing rules will clearly continue to be important, whatever the fundamental approach. Reliable methods of determining element strength are crucial for capacity design, even in displacement-based methods, while drift limitations are likely to assume even greater importance.

#### **2.4.2 Conceptual Design of Tall RC Buildings**

The governing consideration in conceptual design of tall RC buildings controlled by normal actions, is the minimization of cost and the maximization of the functionality of the facility. Safety is seldom a major concern in this phase of the design of such structures, as it is essentially guaranteed by the subsequent design phases, i.e. by the application of State-of-the-Art analysis methods and by conformance to Codes during member proportioning and detailing. On the contrary, structural configuration is a key factor for the safety of seismic-controlled structures, as it limits deviations of the actual response to the design seismic action from that assumed in design and used as the basis of member proportioning. A key postulate of codified seismic design is that peak structural displacements and deformations due to the design seismic action are approximated reasonably well, at the local and global level, by the results of an elastic analysis, even though members are not proportioned but for a small fraction of the internal forces resulting from it.



Aspects of structural configuration of tall RC buildings such as symmetry, mass distribution, and vertical regularity must be considered, and the importance of strength, stiffness and ductility in relation to acceptable response appreciated. Irregularities, often unavoidable, contribute to the complexity of structural behaviour. When not recognized, they may result in unexpected damage and even collapse. There are many sources of structural irregularities. Drastic changes in geometry, interruptions in load paths, discontinuities in both strength and stiffness, disruptions in critical regions by openings, unusual proportions of members, re-entrant corners, lack of redundancy, and interference with intended or assumed structural deformations are only a few of the possibilities, Paulay & Priestley, ref. [20].

The primary purpose of all structures used for building is to support gravity loads. However, buildings may also be subjected to lateral forces due to wind or earthquakes. The taller a building, the more significant the effects of lateral forces will be. Therefore in seismic design, as the seismic criteria governs the design of lateral resistance of buildings, the structural systems of tall RC buildings must provide sufficient resistance against lateral forces. The common types of structural systems that are used for tall RC buildings will be discussed in the next sections.

### **2.4.3 Structural Systems of Tall RC Buildings Against Earthquakes**

In multi-storey RC buildings, the structural system should preferably be composed of frames, either alone or coupled with shear walls in two directions, so that a clearly defined flow of lateral forces is achieved. Also the ductility for plastic hinges and beam-column joints should be specified without losing a large percentage of its strength. The three types of structures, most commonly used for tall RC buildings, will be presented in the following sections.

#### **2.4.3.1 Ductility System of Buildings**

Structures of multi-storey reinforced concrete buildings often consist of frames. Beams, supporting floors, and columns are continuous and meet at nodes, often called "rigid" joints. Such frames can readily carry gravity loads



while providing adequate resistance to horizontal forces, acting in any direction. The conventional approach to the seismic design of such structures, which relies on the ductile behaviour of the structural system to dissipate the seismic energy, may have a disadvantage that the structure, during high-intensity earthquakes, suffers damage requiring costly repair. This damage can sometimes be so severe that the building may need to be demolished.

The main aim of the capacity design procedure of ductile multi-storey reinforced concrete buildings is the ability of these structures to dissipate seismic energy. Dissipation of seismic energy requires designing the buildings to allow the formation of plastic hinges, see Fig. 2.10 (a). When designing these hinges into the system it is important that these are formed in the beams of the building rather than the columns. This is the opposite to static design but is necessary because if hinges form in the columns under seismic loading it will cause global collapse of the structure, also requiring fewer hinges to form. Also plastic hinges are a useful part of earthquake design because when the structure degree of redundancy increases and the structure becomes more statically indeterminate, the number of plastic hinges required for collapse increases enhancing the load carrying capacity of the structure (also providing warning for the impending failure).

The ductility of the structural members may be the most important factor which governs the global ductility of multi-storey RC buildings. The members and joints of structures must have appropriate levels of strength in flexure, shear and bond, so that appropriate detailing of longitudinal and transverse reinforcement will lead to structures with sufficient ductility in a flexural yielding mode to survive earthquakes.

According to the aim of capacity design procedure which requires dissipating the seismic energy, in recent years there have been many alternative approaches for earthquake resistant design. The important types of these approaches are isolation systems and energy absorbers. It should be noted that EC8 guidance on base isolated buildings is not given, but there special studies have been undertaken. Moreover, part 5 of EC8 (Draft) contains special provisions for base-isolated bridges. The basic concept of the isolation systems design is the separation of the structural system from the input ground motion. In contrast to conventional design philosophy, according to which the whole structure dissipates the seismic energy through plastic deformation cycles, the



superstructure and the foundation are separated by a seismic isolation system. This can be accomplished with some special kind of pads (rollers-layers of sand-bearing, etc) with elastoplastic response, which are placed between the foundations and the superstructure. The yield shear of the pads is set to be slightly higher than the seismic action corresponding to the serviceability limit state. When the structure is subjected to an earthquake loading, the pads absorb and dissipate the seismic energy. In case of a high intensity earthquake the pads will absorb the seismic energy and yield, the yield shear of the pads will be transferred from it to the superstructure. Fig. 2.24 shows isolated building structures supported on laminated rubber springs.

Energy absorbers work in a similar way to shock absorbers on a car. In their simplest form they are oil filled pistons connected to a brace on the structure and often set up between points having large relative displacement in response to ground motion, and the energy is dissipated as heat. The use of isolation or energy absorption on a building is rarely justified by a substantial saving in first cost. Justification is likely to come from increased levels of safety, lower levels of structural damage in extreme events or from lower damage levels for building contents. In the nuclear industry isolation has been used to achieve standard designs for the superstructure in areas of differing seismicity.

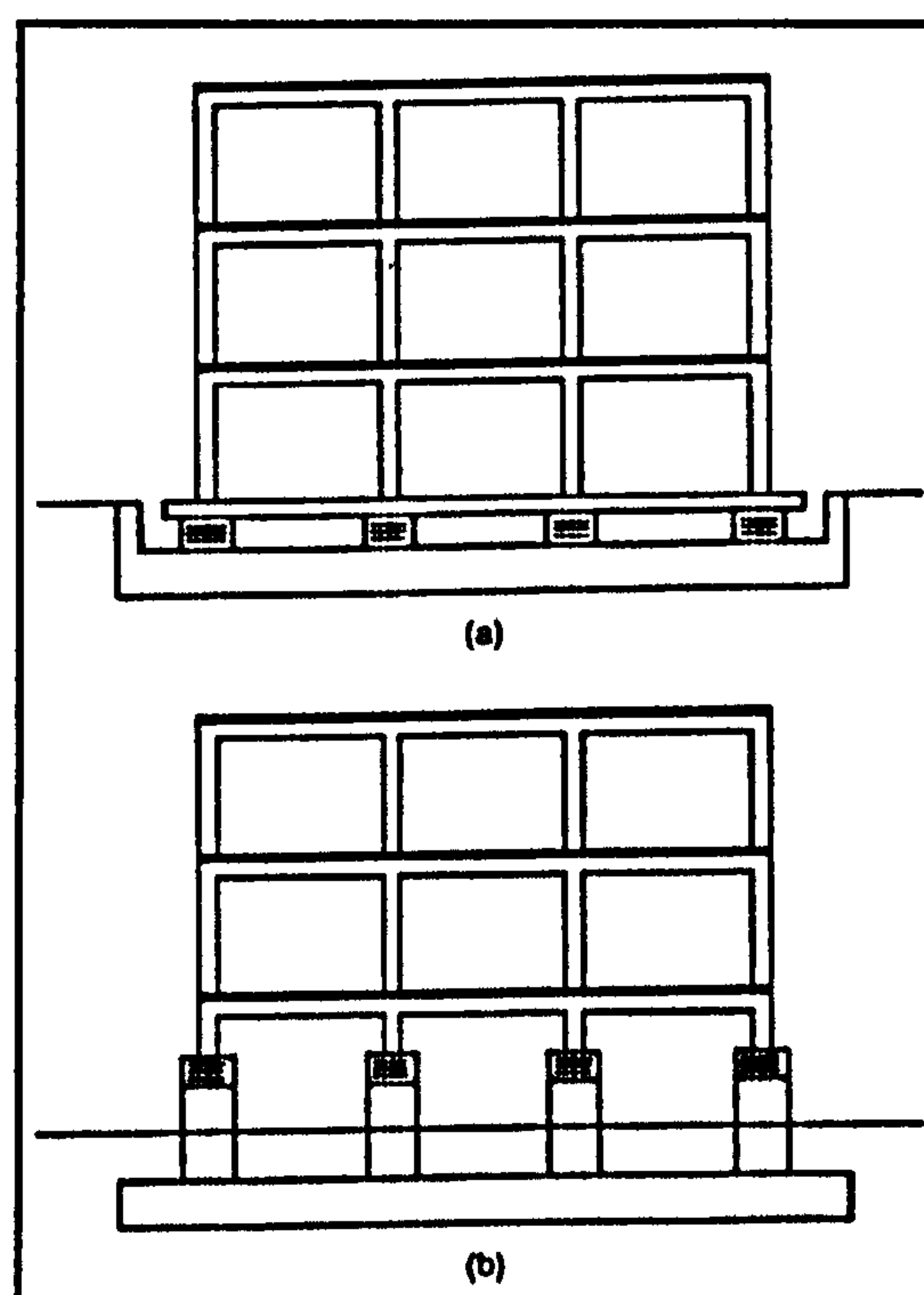


**Figure 2.24** Isolated building structures supported on laminated rubber springs: (a) double foundation with crawl space; (b) springs at mid-height of the lower storey columns (Key, ref. [9])



### 2.4.3.2 Structural Wall System

Structural wall systems consisting of flat slabs, small columns designed for gravity loads only, and a few relatively slender structural walls of rectangular cross-section, can easily be designed for ductile behaviour under moderate earthquake actions. The structural walls have to carry the horizontal earthquake forces and should exhibit a well-defined ductile behaviour. For the conceptual design of structural wall buildings the following general rules should be considered.

- In both main directions of the ground plan of the building at least 2 structural walls in each direction and must extend over the whole height of the building
- If possible the structural walls must be placed in plan at the periphery and more or less symmetrically. If the walls are located inside of the building they should be at a distance from the periphery measured in the direction of the strong axis of the wall cross-section of not more than  $1/4$  of the building plan dimension. With this arrangement torsional effects can be counteracted
- In general a simple rectangular cross-section is to be preferred. The horizontal wall length must be chosen in the range of about 3 m to 6 m or  $H/6$  to  $H/4$  (where  $H$  is the building height). Instead of a longer wall two walls with the same total stiffness but with a higher total bending strength (if the same reinforcement ratio as in the replaced longer wall is used) can be more favourable. The wall thickness can be chosen in the range of 260 to 340 mm; a well-proven dimension is 300 mm.

In general, individual walls may be subjected to axial, translational, and torsional displacements. The extent to which a wall will contribute to the resistance of overturning moments, story shear forces, and story torsion depends on its geometric configuration, orientation, and location within the plane of the building. The positions of the structural walls within a building are usually dictated by functional requirements. These may or may not suit structural planning. The purpose of a building and the consequent allocation of floor space may dictate arrangements of walls that can often be readily utilized for lateral force resistance, Paulay & Priestley, ref. [20].



### 2.4.3.3 Dual Systems

In many RC buildings, the ductile frames and ductile structural walls appear together. When lateral force resistance is provided by the combined contribution of frames and structural walls, it is customary to refer to them as a dual system or a hybrid structure. Dual systems may combine the advantages of their constituent elements. Ductile frames, interacting with walls, can provide a significant amount of energy dissipation, when required, particularly in the upper stories of a building. On the other hand, as a result of the large stiffness of walls, good story drift control during an earthquake can be achieved, and the development of story mechanisms involving column hinges (i.e., soft stories) can readily be avoided.

Despite the attractiveness and prevalence of dual systems, it is only recently that research effort has been directed toward developing relevant seismic design methodologies. This research has indicated a potential for excellent inelastic seismic response of this type of structural system. Under the action of lateral forces, a frame will deform primarily in a shear mode, whereas a wall will behave like a vertical cantilever with primary flexural deformations. Compatibility of deformations requires that frames and walls sustain at each level essentially identical lateral displacements. Because the preferred displacement mode of the two elements is modified, it is found that the walls and frames share in the resistance of story shear forces in the lower stories, but tend to oppose each other at higher levels. The mode of sharing the resistance to lateral forces between walls and frames of a dual system is also strongly influenced by the dynamic response characteristics and development of plastic hinges during a major seismic event, and it may be quite different from that predicted by an elastic analysis. Consequently, in the case of dual systems, simplified elastic analyses are likely to be misleading.

The preferred form of both frames and structural walls together in a building is the connection of structural walls by continuous beams in their plane to adjacent frames, Penelis & Kappos, ref. [8], Beskos & Anagnostopoulos, ref. [19] and Paulay & Priestley, ref. [20].



## CHAPTER 3 VERIFICATION OF ANSYS (Preliminary Analysis)

### 3.1 ANSYS Overview

The software package ANSYS, ref. [42], was produced by Swanson Analysis Systems Incorporated (SAS IP, Inc) in 1970. The program is a computer program for finite element analysis and design. It is one of the leading general-purpose finite element programs available to both educational and commercial establishments. It has a comprehensive menu driven system with general and time-history pre-processors for model creation, solution phase, and general or time-history postprocessors for viewing analysis and manipulation of the model solution data. The software of this computer program is normally updated and upgraded to provide the latest finite element analysis and design technology that can solve complicated structural problems (such as the seismic analysis of three-dimensional large structures). In this research, ANSYS version 5.7, ref. [42], is used. This version was released in 2000 including advanced modelling features allowing engineers to perform the following tasks:

- Build computer models for the three-dimensional large structures
- Apply operating loads or other design performance conditions
- Study physical responses, such as the seismic response of structures
- Optimise a design early in the development process to reduce production costs
- Do prototype testing in environments where it otherwise would be undesirable or impossible

Also this version has a comprehensive graphical user interface (GUI) that gives users easy, interactive access to program functions, commands, documentation, and reference material. An intuitive menu system helps users navigate through the ANSYS program.

#### 3.1.1 Basic Analysis Procedures of ANSYS

For performing an analysis using ANSYS, there are general steps which are common. A typical ANSYS analysis has the following three distinct steps:

1. Build the model (preprocessor stage)



2. Apply loads and obtain the solution (solution phase)
3. Review the results (postprocessor stage)

In the first step stated above for performing the analysis (generation of the model), the type of analysis is first selected, i.e. structural, thermal, static or dynamic etc. A large element library becomes available with general 1, 2, and 3 dimensional elements, and elements designed for specific purposes, each element having an individual reference number, features and characteristics. The next step is to select all the element types to be used in the model. During their selection, a number of key options are specified for each element type to define certain properties specific to the element in question, such as control of solution printout, or control of element physical properties. Real constant sets are then created, each with their own reference number, for use with these elements to define additional information about their geometric characteristics. Linear material properties are defined with reference numbers for each material, specifying each property, (such as elastic modulus) for a particular material. When a nonlinear stress-strain relationship is required, the form and hysteresis characteristics of the stress-strain graph are defined in a nonlinear table for the material, entering coordinates of points on the curve in the appropriate location in the table.

Having already planned out the desired finite element mesh, the nodes are generated first. Cartesian, cylindrical polar and spherical polar co-ordinates systems are available for input of these nodes, with facilities for defining local and global systems. The first 'set' of nodes are normally created such that subsequent node creation can be carried out by a generation procedure of the primary set, assuming the mesh has been well constructed in such a manner as to allow for this. Automatic meshing for more complicated models is also available. With all the nodes created, an element type, an associated real constants set, and a set of material properties are selected for the subsequent assembly. The elements are formed by assigning them to the correct nodes in a predetermined order. Again, as with the nodes, elements may be generated from an initial pattern and the complete one, two or three-dimensional model is formed. To change an element type or any of its properties, the selection of the appropriate reference number of a real constant set, material property set, or element type will facilitate this.



In the second step stated above for performing the analysis, once the model has been created, boundary conditions and applied loads must be defined. Boundary conditions may be entered as set displacements in the active co-ordinate system, or as constraint equations, thereby allowing an analysis by the specification of a prescribed displacement rather than by direct loading. A variety of external load application is available. Pressures over element faces, point loads at nodal locations, and accelerations coupled with specific material densities provide several means of direct loading. After that the solution is initiated using different options according to the analysis type.

In the third (final) step of analysis, the general and/or time history postprocessor menu (according to analysis type such as static or dynamic) are used to read and review the results. There are a number of advanced techniques for visualising the data graphically, i.e. stresses may be plotted as raster or vector contours superimposed upon element plots, which can be viewed from any desired angle. Comprehensive lists of data may be compiled for viewing graphically or in its raw form, and a certain amount of data manipulation can be performed within the postprocessor, such as summation of forces or moments about specified positions in the model. All data associated with each element has a specific postdata number allocated to each data item, which may be specified and labelled for analysis. The results data can be stored on an individual text file to be used with other computer programs (such as Microsoft office software to create specific graphs), Weekes, ref. [50].

### **3.1.2 Structural Analyses of ANSYS**

Structural analysis is probably the most common application of the finite element method. The term structural (or structure) implies not only civil engineering structures such as bridges and buildings, but also naval, aeronautical, and mechanical structures such as ship hulls, aircraft bodies, and machine housings, as well as mechanical components such as pistons, machine parts, and tools. The primary unknowns (nodal degrees of freedom) calculated in a structural analysis are displacements. Other quantities, such as strains, stresses, and reaction forces, are then derived from the nodal displacements. The available types of structural analyses that can be performed using the capabilities of the ANSYS program are as follows:



- Static analysis which is used to determine the displacements, stresses, etc, under static loading conditions. Both linear and nonlinear static analyses are included. Nonlinearities can include plasticity, stress stiffening, large deflection, large strain, hyperelasticity, contact surfaces, and creep.
- Modal analysis which is used to calculate the natural frequencies and mode shapes of a structure. Different mode extraction methods are available.
- Harmonic analysis which is used to determine the response of a structure to harmonically time-varying loads.
- Transient dynamic analysis which is used to determine the response of a structure to arbitrarily time-varying loads. All nonlinearities mentioned under static analysis above are allowed.
- Spectrum analysis that is performed as an extension of the modal analysis, and used to calculate stresses and strains due to a response spectrum or random vibrations.
- Buckling analysis which is used to calculate the buckling loads and determine the buckling mode shape. Both linear buckling and nonlinear buckling analyses are possible.
- Explicit dynamics analysis that is performed through an interface to the LS-DYNA (explicit finite element program), and is used to calculate fast solutions for large deformation dynamics and complex contact problems.

In this research, some types of analyses stated above are used such as static linear and nonlinear analyses, modal analysis and transient dynamic analysis. Therefore these types of analyses will be presented in more detail in the next sections.

### **3.1.2.1 Nonlinear Analysis**

In linear analysis, the behaviour of the structure is assumed to be completely reversible, i.e. the body returns to its original un-deformed state upon the removal of the applied loads, and solutions for various load cases can be superimposed. Many engineered structural systems are designed to remain linear (or nearly so) within their normal range of service loads. Standard linear equation solvers



such as are found in the ANSYS program and other finite element programs were initially developed to enable engineers to analyse complex linear structures. However, there are significant classes of engineering applications for which the relationship between force and displacement is not constant. A plot of force versus displacement for such systems is not a straight line; hence, such systems are said to be nonlinear and the solutions from several load cases cannot be superimposed. The behaviour of such systems cannot be represented directly with a set of linear equations.

Nonlinear structural behaviour arises from a number of causes, which can be grouped into these principal categories:

- **Changing status:** many common structural features exhibit nonlinear behaviour that is status-dependent. For example, a tension-only cable is either slack or taut; a roller support is either in contact or not in contact. Status changes might be directly related to load, or they might be determined by some external cause.
- **Geometric nonlinearities:** if a structure experiences large deformations, its changing geometric configuration can cause the structure to respond nonlinearly. Geometric nonlinearity is characterized by "large" displacements and/or rotations.
- **Material nonlinearities:** nonlinear stress-strain relationships are a common cause of nonlinear structural behaviour. Many factors can influence a material's stress-strain properties, including load history (as in elasto-plastic response), environmental conditions (such as temperature), and the amount of time that a load is applied (as in creep response). In general, nonlinear stress-strain relationships are the common cause of nonlinear structural behaviour. In this research, material nonlinearities are used for the static nonlinear analysis of steel fixed beam and one storey steel portal frame to check the capabilities of ANSYS program to perform the nonlinear analyses. This will be discussed later in section 3.2.

Before attempting the solution of nonlinear problems, accurate and reliable material data must be adequately defined, often requiring the utilisation of experimental data. A nonlinear system cannot be analysed directly with a linear equation solver. However, it can be analysed by using a series of linear approximations, with corrections. The



application of the finite element method to nonlinear problems usually requires the use of small load increments and/or an iterative procedure. Iterations are usually performed to ensure that the solution is convergent, i.e. the error in approximating the equilibrium state is acceptably small. A several well established numerical techniques (such as Newton-Raphson) already exist for using iterations to solve nonlinear equations.

ANSYS program employs the “Newton-Raphson” approach to solve nonlinear problems. In this approach, the load is subdivided into a series of load increments. The load increments can be applied over several load steps. Before each solution, the Newton-Raphson method evaluates the out-of-balance load vector, which is the difference between the restoring forces (the loads corresponding to the element stresses) and the applied loads. The program then performs a linear solution, using the out-of-balance loads, and checks for convergence. If convergence criteria are not satisfied, the out-of-balance load vector is re-evaluated, the stiffness matrix is updated, and a new solution is obtained. This iterative procedure continues until the problem converges. A number of convergence-enhancement and recovery features, such as line search, automatic load stepping, and bisection, can be activated to help the problem to converge. If convergence cannot be achieved, then the program attempts to solve with a smaller load increment.

In some nonlinear static analyses, if the Newton-Raphson method is used alone, the tangent stiffness matrix may become singular (or non-unique), causing severe convergence difficulties. Such occurrences include nonlinear buckling analyses in which the structure either collapses completely or "snaps through" to another stable configuration. For such situations, an alternative iteration scheme can be activated, the arc-length method, to help avoid bifurcation points and track unloading. The arc-length method causes the Newton-Raphson equilibrium iterations to converge along an arc, thereby often preventing divergence, even when the slope of the load versus deflection curve becomes zero or negative.

The procedure for analysing nonlinear transient behaviour is similar to that used for nonlinear static behaviour stated above. The load is applied in incremental steps, and the program performs equilibrium iterations at each step. The main difference between the static and transient procedures is that time-integration effects can be activated in the



transient analysis. Thus, "time" always represents actual chronology in a transient analysis. The automatic time stepping and bisection feature is also applicable for transient analyses.

### 3.1.2.2 Static Analysis

A static analysis calculates the effects of steady loading conditions on a structure, while ignoring inertia and damping effects, such as those caused by time-varying loads. A static analysis can, however, include steady inertia loads (such as gravity and rotational velocity), and time-varying loads that can be approximated as static equivalent loads (such as the static equivalent wind and seismic loads commonly defined in many building codes). Static analysis is used to determine the displacements, stresses, strains, and forces in structures or components caused by loads that do not induce significant inertia and damping effects. Steady loading and response conditions are assumed; that is, the loads and the structure's response are assumed to vary slowly with respect to time. The kinds of loading that can be applied in a static analysis include:

- Steady-state applied forces and pressures
- Steady-state inertial forces (such as gravity or rotational velocity)
- Imposed (non-zero) displacements

The procedure for a static linear or nonlinear analysis consists of these tasks:

1. Build the model (finite element model, material properties, etc)
2. Set solution controls (analysis type, etc)
3. Set additional solution options (such as the numerical technique)
4. Apply the loads
5. Solve the analysis
6. Review the results



### 3.1.2.3 Modal Analysis

Modal analysis is used to determine the natural frequencies and mode shapes of a structure. The natural frequencies and mode shapes are important parameters in the design of a structure for dynamic loading conditions. They are also required if a spectrum analysis or a mode superposition harmonic or transient analysis is performed. Modal analysis in the ANSYS program is a linear analysis. Any nonlinearities, such as plasticity and contact (gap) elements, are ignored even if they are defined. However, ANSYS will allow the application of damping in the structure. The procedure for a modal analysis consists of four main steps:

1. Build the model (finite element model, material properties can be linear, isotropic or orthotropic)
2. Apply loads and obtain the solution (analysis type, damping, number of modes, etc)
3. Expand the modes (writing mode shapes to the results file)
4. Review the results

### 3.1.2.4 Transient Dynamic Analysis

Transient dynamic analysis (sometimes called time-history analysis or direct integration analysis technique) is a technique used to determine the dynamic response of a structure under the action of any general time-dependent loads. This type of analysis is used to determine the time-varying displacements, strains, stresses, and forces in a structure as it responds to any combination of static, transient, and harmonic loads. The time scale of the loading is such that the inertia or damping effects are considered to be important. In transient dynamic analysis, the basic equation of motion (see chapter 2) is solved so that at any given time,  $t$ , these equations can be thought of as a set of "static" equilibrium equations that also take into account inertia forces and damping forces. The ANSYS program uses the Newmark time integration method to solve these equations at discrete timepoints. The time increment between successive timepoints is called the integration time step.

A transient dynamic analysis is more involved than a static analysis because it generally



requires more computer resources and more of any body resources, in terms of the “engineering” time involved. A significant amount of these resources can be saved by carrying out some preliminary analyses for simple models before analysis of the main structural problem. Three methods are available for performing the transient dynamic analysis: full, mode superposition, and reduced. The full method uses the full system matrices to calculate the transient response (no matrix reduction). It is the most general of the three methods because it allows all types of nonlinearities to be included (plasticity, large deflections, large strain, and so on). The advantages of the full method are, (1) it is easy to use, because no worry about choosing master degrees of freedom or mode shapes, (2) it allows all types of nonlinearities, (3) it uses full matrices, so no mass matrix approximation is involved, (4) all displacements and stresses are calculated in a single pass, (5) it accepts all types of loads: nodal forces, imposed (non-zero) displacements, element loads (pressures and temperatures), (6) it allows effective use of solid-model loads. The main disadvantage of the full method is that it is more expensive than either of the other methods. This method is used in this research for carrying out the transient dynamic analysis using ANSYS.

The procedure for a transient dynamic analysis consists of these tasks:

1. Build the model
2. Establish Initial Conditions (number of load steps)
3. Set solution controls (analysis type, etc)
4. Set additional solution options
5. Apply the loads
6. Save the Load Configuration for the Current Load Step
7. Repeat Steps 3-6 for Each Load Step
8. Save a Back-up Copy of the Database (database file)
9. Start the Transient Solution
10. Exit the Solution Processor
11. Review the results



The accuracy of the transient dynamic solution depends on the integration time step: the smaller the time step, the higher the accuracy. A time step that is too large will introduce error that affects the response of the higher modes (and hence the overall response). A time step that is too small will waste computer resources. As damping must be specified in a dynamic analysis, the ANSYS program has the following forms of damping.

- Alpha and Beta Damping (Rayleigh Damping)
- Material-Dependent Damping
- Constant Damping Ratio
- Modal Damping
- Element Damping

Rayleigh damping was chosen as a proven accurate method of incorporating damping in mathematical models. Mass proportional damping and stiffness proportional damping are used to define Rayleigh damping constants  $\alpha$  and  $\beta$ . The damping matrix  $[C]$  is calculated by using these constants to multiply the mass matrix  $[M]$  and stiffness matrix  $[K]$ :  $[C] = \alpha [M] + \beta [K]$ . This form of damping (Rayleigh Damping) in ANSYS program is used in this research for transient dynamic analyses.

### 3.2 Capability Check of ANSYS to Perform Nonlinear Analysis

The ANSYS program is commercial software for the finite element method and is widely used by the engineers around the world for analysis and design. It is used in the educational and industrial fields as a highly verified & validated finite element code. ANSYS 5.7, ref. [42], mentioned that the accuracy of results must be verified for any type of analysis prior performing the main analysis for solving the structural problem. Verification of nonlinear results which is carried out as a general criterion of the accuracy of finite element code (ANSYS program) is generally more difficult than verification of linear results. Verification can become more complicated for a nonlinear analysis, because by their nature nonlinear results tend to be harder to predict. Also verification through sensitivity studies (i.e., running the dynamic analysis for a three dimensional large structures, smaller load increments, etc.) becomes more complex, expensive and time-consuming for the linear analyses.



The structural engineering problem of this research (analysis of three dimensional multi-storey reinforced concrete buildings under seismic actions) presents a complex problem. The ANSYS program has the capability to solve complex structural engineering problems and has been used in this research due to the nature of the subject. For this reason the program results are verified before use in the seismic analysis. In this section the accuracy of ANSYS results are verified for static linear & nonlinear analysis of steel fixed beam and one storey steel portal frame. Also the capabilities of ANSYS to predict collapse mechanisms of these structures are checked (it should be noted that although nonlinear material verification analyses have been performed, due to the size of the global models of multi-storey RC buildings the decision not to involve nonlinearity was taken).

A simple steel fixed beam and one storey steel portal frame were modelled and applied using the ANSYS program through all stages of loading up to collapse to verify that the correct representation of the non-linear behaviour was achieved. At the same time these two models were solved analytically (free hand calculation) using the basic theories of elasticity and plasticity. A comparison between ANSYS program results and the analytical results is presented to verify the correct representation of the ANSYS program and the details of the formation of plastic hinges in structural elements. All details about these static linear & nonlinear analyses which were applied for steel fixed beam and one storey steel portal frame to verify the ANSYS program are included in the **Appendix I**.

In the next sections of this chapter, the capability of the ANSYS program for solving structural problems such as seismic analysis of three-dimensional large RC buildings will be verified and validated. The simulation of a three dimensional five-storey reinforced concrete building under seismic action (UK design response spectra) will be presented and discussed.

### **3.3 ANSYS Analysis of an unbraced 5-storey RC Building**

In this research the major objective is the investigation of the seismic behaviour (seismic performance) of existing multi-storey reinforced concrete buildings under seismic loads (earthquakes) using the finite element method (ANSYS Program). Seismic analysis of multi-storey reinforced concrete buildings using the finite element



method so far has been based on individual elements of the building or two-dimensional building for verification purposes. The analysis of the real seismic behaviour of multi-storey reinforced concrete buildings using the finite element method can be satisfied if the structure is simulated as a three-dimensional global structure consisting of a reinforced concrete material. This model has many complexities because firstly, the reinforced concrete material consists of two main components, the concrete and steel reinforcement, making generation of the model very complicated and excessively time-consuming, secondly, to analyse reinforced concrete structures in non-linear stage, the yield strength of the reinforced concrete material is required. This value is not constant for this material and is subjected to variation.

In this research to estimate the realistic seismic behaviour of existing reinforced concrete buildings, two 3-dimensional models were constructed as an initial models for the representation of multi-storey reinforced concrete buildings under seismic action. The first model is an unbraced 5-storey RC building (is presented and discussed in this section) and the second model is a braced 5-storey RC building (is presented and discussed in the section 3.4). These models are analysed statically and under seismic action using the ANSYS program (preliminary analyses prior the main analyses of the major research model, a braced 10-storey RC building). Seismic time-history analyses of these models using ANSYS were also carried out to verify its capability in simulating the realistic seismic behaviour of the global structure of a multi-storey RC building.

The model of unbraced 5-storey RC building (this model will be called UFS) was designed using an approximate design method (according to the design rules of BS 8110, ref. [3], BS 6399, ref. [51], BS 648, ref. [52]) to be safe against collapse under its own weight and live loads (the effect of structural walls of this model was omitted). The aim of this model was not to produce a building which would necessarily be used in real life, but to verify ANSYS for transient & modal analysis, and verify its behaviour with simple hand calculations. Figures 3.1, 3.2 show the three-dimensional finite element model of the UFS (as generated using ANSYS) and the floor plan of storeys. Also these figures show the geometric characteristics of this model. The details of this model are listed in table 3.1 (it must be noted that the reinforcement details of the global structure of RC buildings were omitted in this research due to the size of used models and analyses types as stated above).



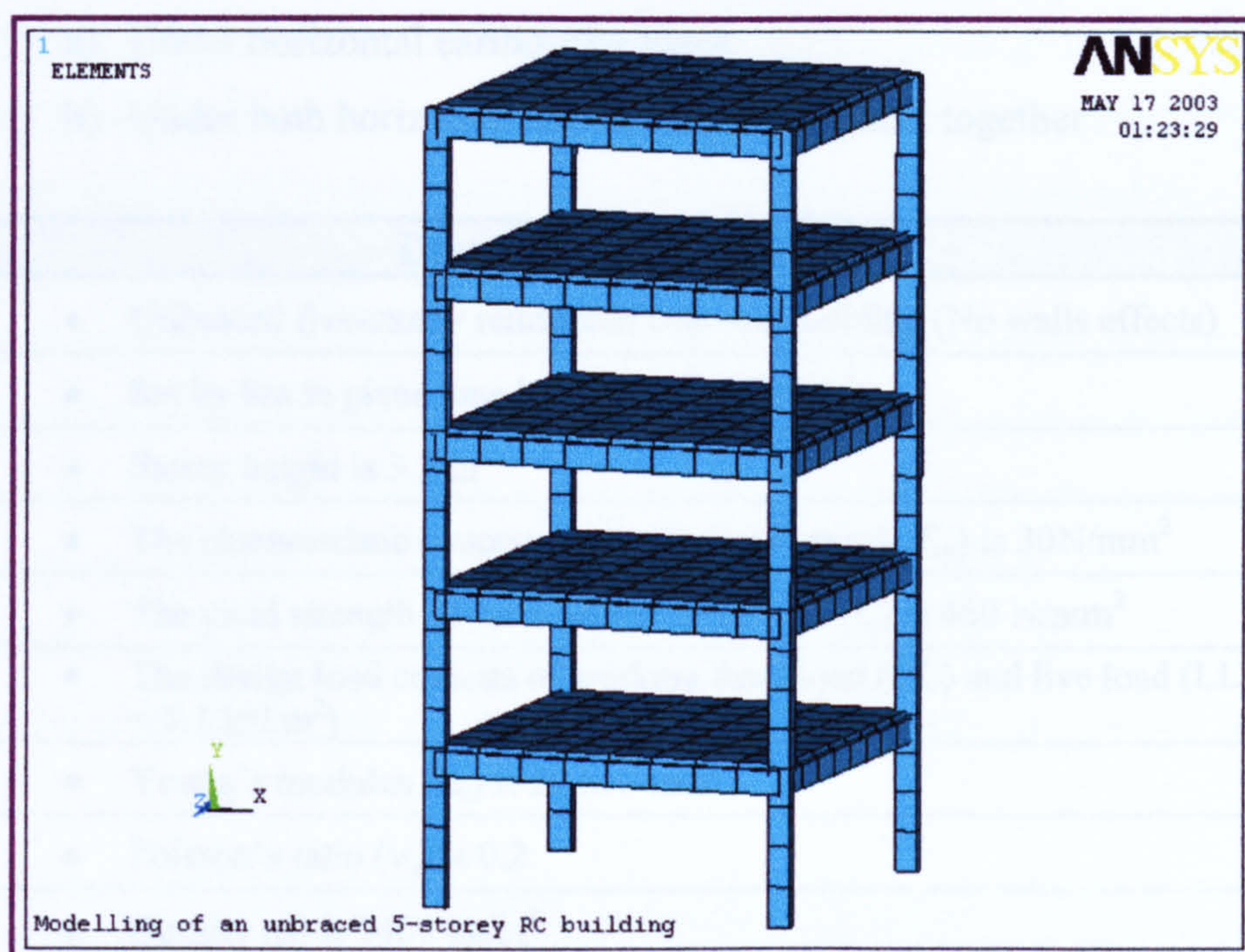


**Figure 3.1** The finite element model of unbraced five-storey RC building (UFS)

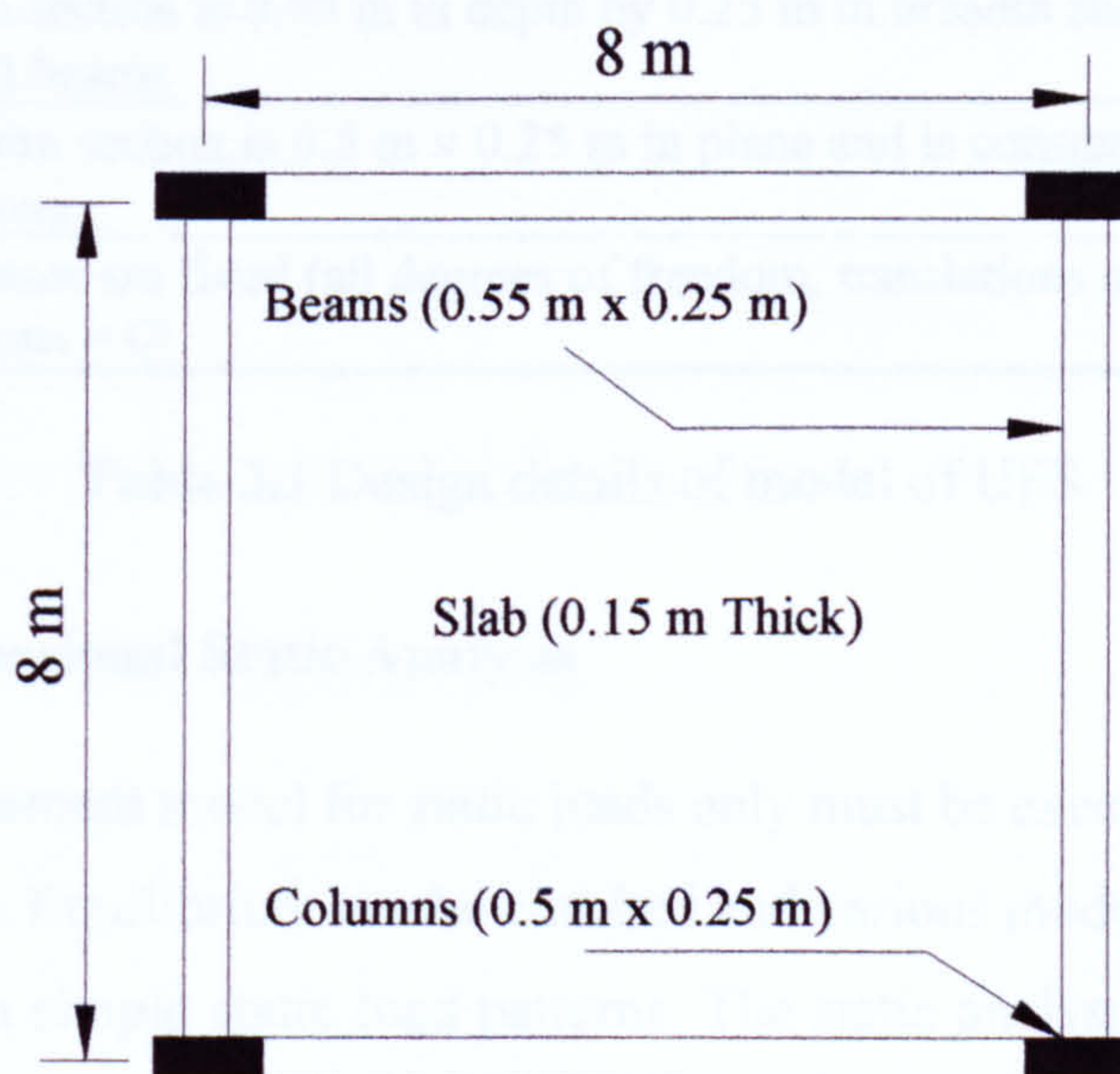


**Figure 3.2** The floor plan of storeys of UFS

Three types of analysis were conducted using ANSYS for this model (UFS) as follows:

1. Three-dimensional static linear analysis
2. Three-dimensional modal analysis
3. Three-dimensional transient linear dynamic analysis:



- a) Under horizontal earthquake alone
- b) Under both horizontal and vertical earthquake together

Description of UFS Model
• Unbraced five-storey reinforced concrete building (No walls effects)
• 8m by 8m in plane, one bay, 17.5 m in height
• Storey height is 3.5 m
• The characteristic concrete compressive strength ( $f_{cu}$ ) is 30N/mm <sup>2</sup>
• The yield strength of the steel reinforcement ( $f_y$ ) is 460 N/mm <sup>2</sup>
• The design load consists of working dead load (DL) and live load (LL = 3.5 kN/m <sup>2</sup> )
• Young's modulus ( $E_c$ ) is 20 kN/ mm <sup>2</sup>
• Poisson's ratio ( $\nu_c$ ) is 0.2
• Density ( $\rho$ ) is 2400 kg/m <sup>3</sup>
• Modified density accounting for live load ( $\rho_m$ ) is 4778.5 kg/m <sup>3</sup>
• Slab thickness is constant for all floors 0.15 m
• Beam section is 0.55 m in depth by 0.25 m in breadth and is constant for all beams
• Column section is 0.5 m $\times$ 0.25 m in plane and is constant for all columns
• All bases are fixed (all degrees of freedom, translations and rotations = 0)

**Table 3.1** Design details of model of UFS

### 3.3.1 Three Dimensional Static Analysis

The finite element model for static loads only must be executed prior conducting the seismic analysis. Equilibrium can be checked and various modelling approximations can be verified with simple static load patterns. The static analysis of UFS was carried out to check the safety of building against collapse under its own weight and live load and to verify forces in the static case. This model was generated using the finite element computer program ANSYS as shown in Fig. 3.1 in accordance with the design details listed in table 3.1. The static load (gravity loads that included specified dead and live loads) was applied using the gravitational constant of 9.81m/s<sup>2</sup> acting on the appropriate density (mass) of the model.

The results of static linear analysis of the UFS using ANSYS are in good agreement with the hand calculations results (the mass of building and its vertical reaction forces



were estimated with a high degree of accuracy). Also investigation of the ANSYS results of the model shows that the maximum degree of freedom value in y-direction (maximum deflection UY) is acceptable in accordance with the serviceability limit state requirements of BS 8110, ref. [3]. In accordance with the stress-strain curve of concrete presented in BS8110 (see Fig. 2.1), the maximum stress of concrete grade 30 N/mm<sup>2</sup> is equal to 13.4 N/mm<sup>2</sup>. A check of the maximum stress of this model under gravity loads (based on the static analysis results using ANSYS) revealed that the maximum value was equal to 5.95 N/mm<sup>2</sup>, less than the BS8110 limit. These checks were made to show that the UFS is safe against collapse under the gravity loads. Table 3.2 presents a comparison between the analytical and ANSYS results of the static linear analysis of UFS.

Static Linear Analysis Results of UFS			
Description	Analytical Analysis	ANSYS Analysis	Remarks
Mass of model (kg)	314577.5	303170	Good agreement (3.7 % difference)
Vertical reaction force of each base (kN)	771.5	743.5	Good agreement (3.7 % difference)
Maximum deflection UY (mm)	N/A	19	Acceptable value (BS8110, ref. [3])
Maximum stress of concrete (N/mm <sup>2</sup> )	13.4 (designed)	5.95 (applied)	Columns safe against stresses

**Table 3.2** Analytical and ANSYS results of static linear analysis of UFS

### 3.3.2 Three Dimensional Modal Analysis

Modal analysis is an essential part of the dynamic analysis process that gives valuable insight into the dynamic characteristics of the structure, and was carried out for the UFS model for this purpose in addition to the verification of ANSYS. This analysis of structures must be performed for a three-dimensional model due to the presence of torsional effects (especially for structures having irregularity in geometrical shape in plan or elevation). The first step in the dynamic (seismic) analysis of a structural model is the calculation of the three dimensional mode shapes and natural frequencies of vibration. A careful examination of the torsional effects of the three dimensional mode shapes at the early stages of a preliminary design (depending on the preliminary analysis) can give a structural engineer additional information which can be used to improve the earthquake resistant design of a structure. EC8, ref. [4], defines an



"irregular structure" as one which has a certain geometric shape or in which stiffness and mass discontinuities exist. Determination of the torsional effects may allow converting a "geometrically irregular" structure to a "dynamically regular" structure from an earthquake-resistant design standpoint. Modal analysis of UFS model (three-dimensional finite element model that is shown in Fig.3.1) was carried out using ANSYS in the absence of damping ( $C = 0$ , see section 2.2.1.1). Also up to 30 mode shapes were extracted. This analysis yielded the natural frequencies (undamped), mode shapes of free vibration, the mass participation factor ( $\Gamma$ ), and the effective mass ( $m^{\text{eff}}$ ) for each mode, which are important for carrying out the transient dynamic analysis, and simple hand calculations.

Both mass participation factor ( $\Gamma$ ) and effective mass ( $m^{\text{eff}}$ ) of each mode are significant that they represent a measure of how strongly motions in the degrees of freedom are represented. When the value of these two parameters of a mode shape is high (as a percentage of the total mass) then the mode can be considered to be significant. In general terms, if this 'major' mode is excited by an input motion (i.e. resonance is set up) then high accelerations, velocities and displacements would be expected to occur, as the dynamic amplification is significant. Modes in the frequency range 0 – 33 Hz (earthquake range) are extracted and the modes contributing up to 80 % of the total mass are considered (major modes are normally above 1 % mass acting). As the mass participation factor ( $\Gamma$ ) increases, the generalized force acting at the bases of building (earthquake loads) increases so that for a time-dependent base acceleration  $[\ddot{Y}(t)]$  the generalized force becomes  $F(t) = \Gamma \ddot{Y}(t)$ . Also effective masses can be used to calculate the real value of damping coefficients for subsequent use in the transient dynamic analysis (Rayleigh damping coefficients) and this will be discussed later in the section 3.4.2.1.

Assuming orthogonal modes, the sum of effective masses of all modes in any direction should give the total mass of the model (excluding mass at restrained degrees of freedom). Table 3.3 lists the sum of effective masses of all modes in each direction. When conducting a modal analysis as a prelude to a transient dynamic analysis (time-history analysis) it is important that the majority of the mass is captured i.e. no less than 80%. For this model (UFS), thirty modes up to 11.4 Hz were extracted and this proved sufficient to capture the majority of the mass and consequently the major modes of



response, see table 3.3. In practice, the interest is focused on the modes at which most mass is 'captured' as these represent the dominant modes of vibration. The seismic effects on the structure are likely to be amplified through resonance effects if any of these 'major' modes coincide with frequencies of ground motion within the dominant earthquake range (normally up to 33Hz) so that the determination of natural frequencies of structures are important to identify resonance. Table 3.4 summarizes the frequency, mass participation factors, captured masses, and description for the major modes of vibration of the UFS model.

Description	Mass (kg)	Percent of Mass (%)
Actual total mass of UFS	303170	100
Sum of effective masses of all modes in x-direction	301495	99.44
Sum of effective masses of all modes in y-direction	213617	70.5
Sum of effective masses of all modes in z-direction	301565	99.5

Table 3.3 Sum of effective masses of all modes in each direction for UFS

“Major” Modes (% Mass captured)						Description of Mode
Mode No.	Frequency (Hz)	Mass Partic. (Γ)	X - Direction	Y - Direction	Z - Direction	
1	0.6	509.99	N/A	N/A	86 %	Sway Mode
2	1.0	501.55	83 %	N/A	N/A	Sway Mode
9	4.7	392.27	N/A	51 %	N/A	Floors bounce up and down

Table 3.4 Modal analysis results of UFS (major modes of vibration)

The major modes in x–direction and z–direction show that the larger mass captured of those modes resulted from the sway modes (see table 3.4), which mean that these are the major modes. The behaviour of the model in case of sway-mode in x-direction and z-direction is representative of what we would expect in real life when a horizontal earthquake occurs as shown in Fig. 3.3. It must be noted that the absence of walls (bracing) in this building increases the effects of sway modes, such as the lateral displacements and shear forces, see Fig.3.3. The major modes in y-direction show that the captured mass of the model in this direction may be concentrated in one mode of



vibration. In this mode, the floors bounce up and down which show that the vertical earthquake may have a significant effect on the structure floors.

As each three-dimensional mode shape of the UFS model has displacement components in all directions, there are other results of the modal analysis which can give valuable additional information. Table 3.5 summarizes the modal base reactions and modal overturning moments for the major modes of vibration listed in table 3.4 and a torsional mode of the UFS model. Although these quantities are not strictly useful in terms of their application, qualitatively they provide insight into the effects of the major modes concerned. These results show that the change in translational and rotational motions of the structure with the change of mode shapes depends mainly on the frequency and type of mode shape of structure (see and note the coloured values in table 3.5). Also the results of mode shape in y-direction (floors bounce up and down) reveal that the vertical earthquakes are having a significant effect on the axial forces of columns (see the coloured value in table 3.5). The results in table 3.5 highlights the importance of the three-dimensional nature of the model due to the effects of torisional modes on the structure. Fig. 3.4 shows the typical torsional mode shape of the UFS model.

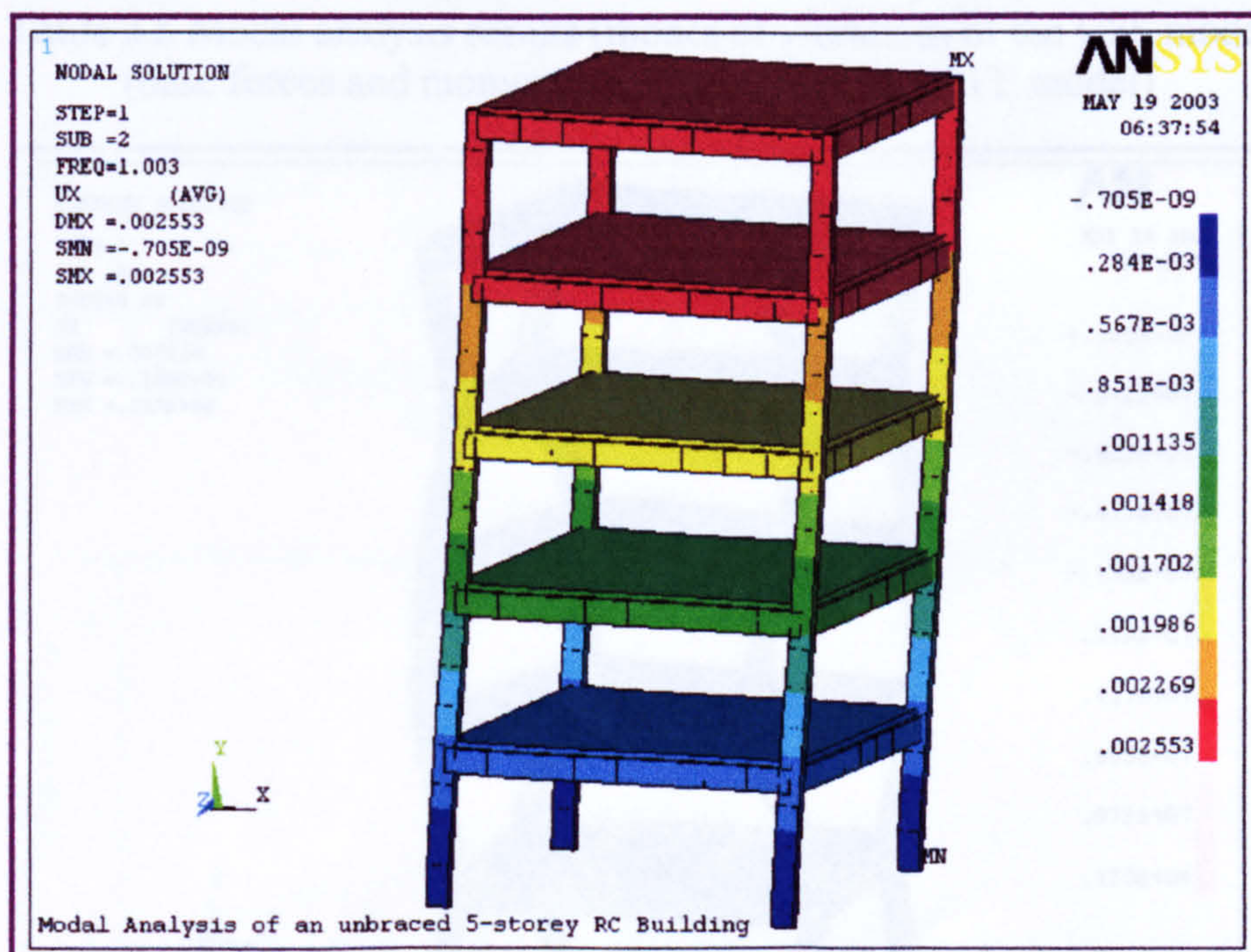


**Figure 3.3** Sway mode (major mode of vibration) of UFS model in x-direction (various colours indicate to the values of displacement in meter for storeys)

The three-dimensional analysis of this model (UFS) reveals that the torsional modes must be taken account of in the design of earthquake resistant concrete structures. This



building revealed a limitation against torsional mode due to a lack of links between the building joints. Results of torsional modes from modal analysis of this model (see table 3.5) show that the bracing is essential to decrease the translation and rotation of the frames joints (see Fig.3.4) of structure under earthquake loads. In essence the bracing will join between locations of maximum relative displacement & increase the overall stiffness of the building, increasing the natural frequencies.

Mode No. and Description	Frequency (Hz)	Total Modal Reactions of Model Bases			Total Modal Overturning Moments of Model Bases		
		X-dir	Y-dir	Z-dir	X-axis	Y-axis	Z-axis
(1) Sway mode	0.6	-0.5500	-3.0844	-8032.6	-14739	-0.01732	0.99004
(2) Sway mode	1.0	-19904	-0.3456	0.1170	0.19379	-0.03255	41254
(9) Floors bounce up and down	4.7	-2.2988	-340010	3.1230	5.6141	2.1823	3.4058
(20) Torsional mode	9.4	24.866	-72.903	-2.2394	-2.7960	-13945	-41.806

**Table 3.5** Modal analysis results (modes of vibration) of the UFS model (base forces and moments of three-dimensional FE model)

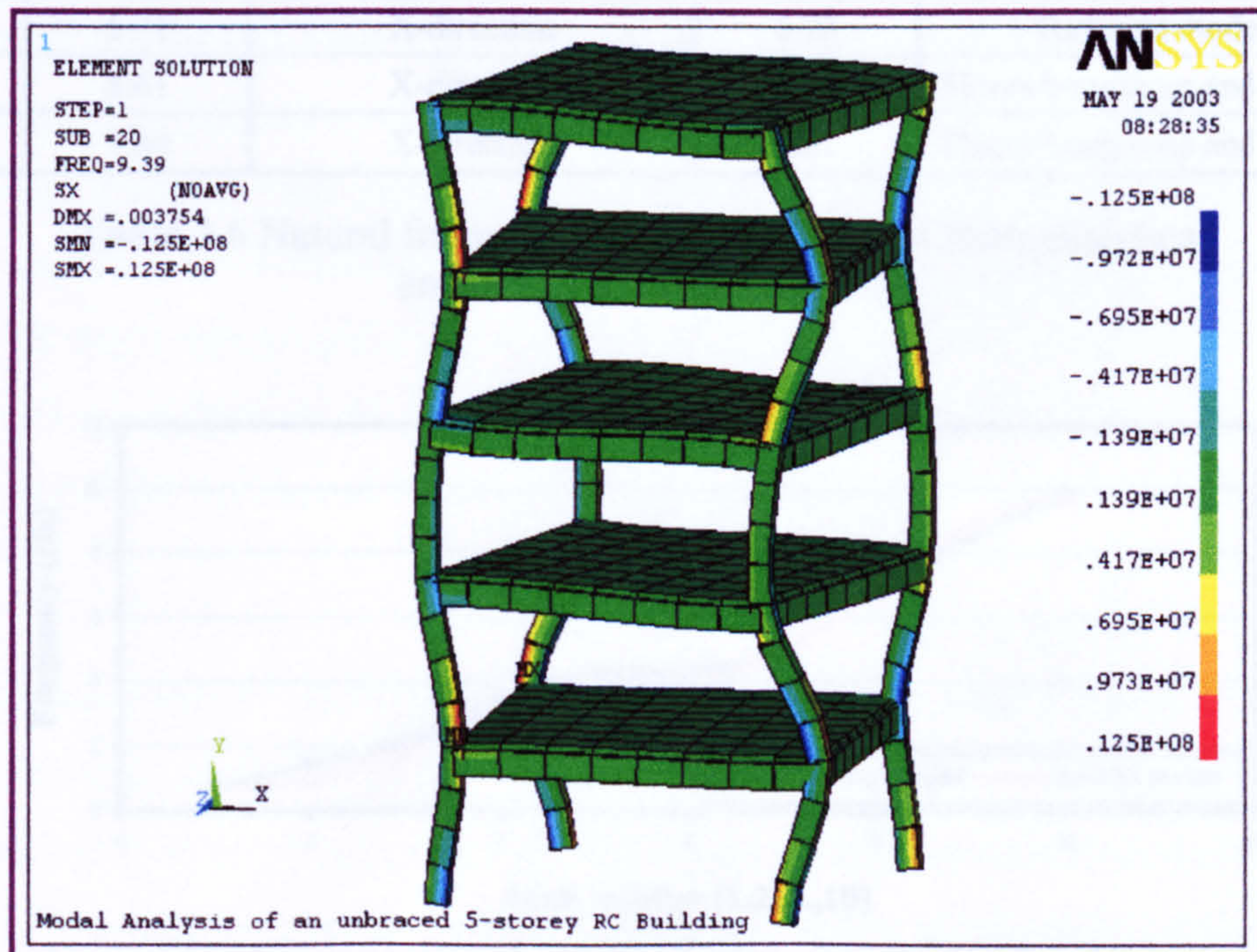


**Figure 3.4** Torsional mode shape of UFS model and its longitudinal stresses (various colours indicate to the values of stresses in x-direction)



3.3.2.1 Analytical Calculations of Natural Frequencies

An analytical modal analysis was carried out to obtain some natural frequencies of the UFS model in the x-direction and z-direction using the formulas of the theoretical modal analysis of multi degree of freedom system, Blevins, ref. [29]. The results of natural frequencies of the ANSYS modal analysis are in good agreement with the results of the analytical modal analysis of the UFS model. This verification confirms that the ANSYS program can predict the response of the structure under the dynamic (seismic) load. Table 3.6 lists the natural frequencies of the model that resulted from analytical and ANSYS analysis. Fig. 3.5 shows the comparison of natural frequencies between the theoretical and ANSYS modal analysis of the UFS model.

No.	Analytical Modal Analysis		ANSYS Modal Analysis	
	Frequency (Hz)	Direction of Modes	Frequency (Hz)	Direction and Description of Modes
1	0.73	Z-direction	0.63	Z-direction (Sway mode)
2	1.46	X-direction	1.0	X-direction (Sway mode)
3	2.13	Z-direction	1.88	Z-direction (Sway mode)
4	3.36	Z-direction	3.09	X-direction (Sway mode)
5	4.26	X-direction	4.06	Z-direction (Sway mode)
6	4.3	Z-direction	4.06	Z-direction (Sway mode)
7	4.92	Z-direction	4.93	Floors bounce up and down
8	6.71	X-direction	6.76	Torsional mode
9	8.61	X-direction	8.89	Floors bounce up and down
10	9.84	X-direction	9.81	Floors bounce up and down

Table 3.6 Natural frequencies of the UFS model from analytical and ANSYS modal analysis

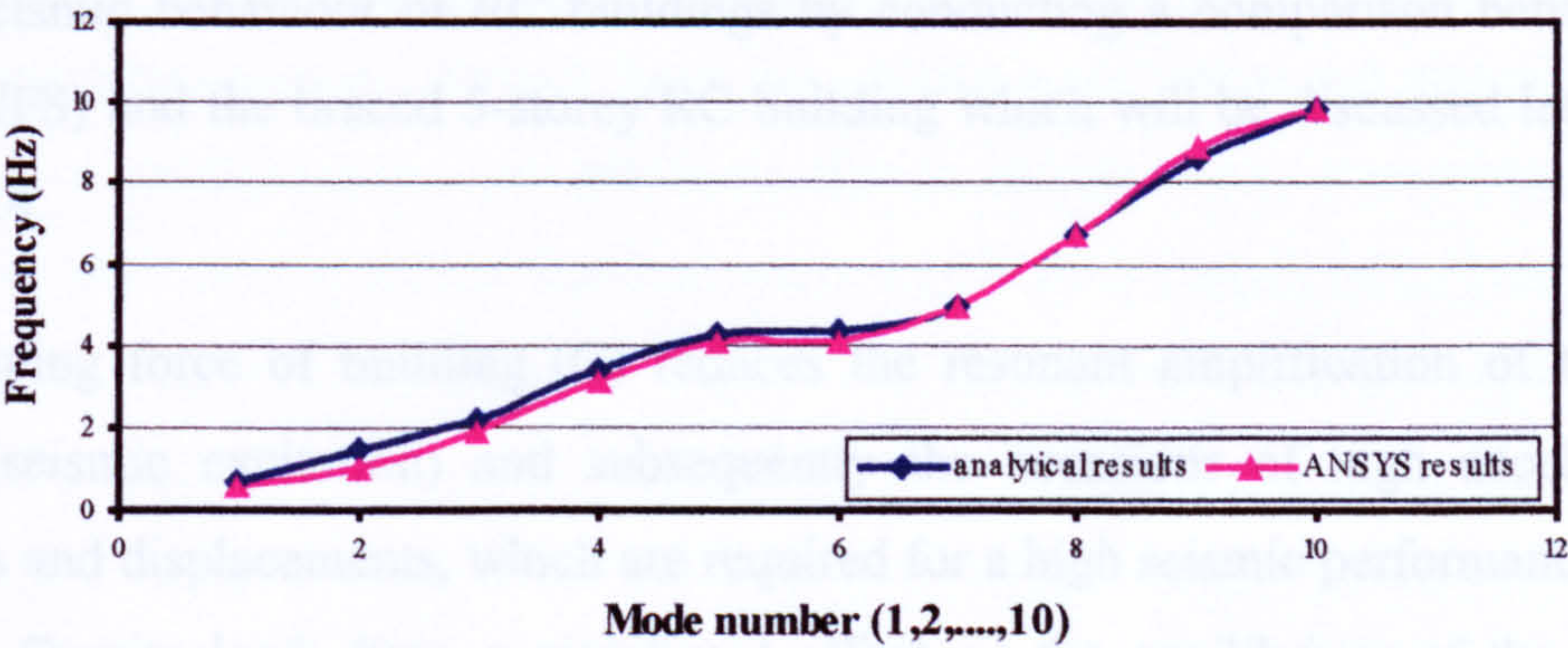


Figure 3.5 Comparison between theoretical and ANSYS modal analysis results (natural frequencies) of the UFS model



### 3.3.3 Three Dimensional Transient Dynamic Analysis

The three-dimensional transient linear dynamic analysis was conducted for the UFS model using ANSYS to determine the seismic response parameters such as displacements, strains, stresses, and forces. In general, this analysis was carried out in accordance with the following main steps.

1. Creation of the three dimensional finite element model as shown in Fig. 3.1 in the absence of walls (bracing)
2. Determination of the analysis type (transient linear dynamic analysis) and some solution options such as damping effects ( $C = 0$ ), the total time of earthquake applied loads ( $t = 10.19$  sec) and the time intervals of loading which is commonly constant (time step = 0.01 sec)
3. Applying the seismic loads (earthquake loads) as a displacement time-history at the fixed bases of the model and afterward the analysis solution is carried out (it must be noted that the effects of gravity loads were omitted and not applied for this model)

The transient dynamic analysis of this model (UFS) was applied under two types of time-history, horizontal time-history alone that contains two orthogonal components (two dimensional seismic action in the directions x, z), and both horizontal & vertical time-history together that contain three orthogonal components (three dimensional seismic action in the directions x, z, y). The UFS model was seismically analysed in the absence of walls, damping and gravity loads in order to study the effects of these factors on the seismic behaviour of RC buildings by conducting a comparison between this model (UFS) and the braced 5-storey RC building which will be discussed later in the section 3.4.

The damping force of building ( $C$ ) reduces the resonant amplification of the input motion (seismic excitation) and subsequently the occasions of high accelerations, velocities and displacements, which are required for a high seismic performance for the building. Gravity loads have a significant effect on the equilibrium of the building during the earthquake. It may stabilize the building vertically depending on the directions (positive or negative direction) of the horizontal and/or vertical earthquake i.e. depending on the value of generated overturning moment of the building. Also the



axial forces of columns that are in compression due to the gravity loads may be increased or even altered to tension under the horizontal and/or vertical earthquake.

### 3.3.3.1 Input Ground Motion

The earthquake for the purpose of seismic analysis and/or design of structures is usually characterised by a spectral shape (response spectra). The input ground motions (earthquakes) which are used for the transient dynamic analysis (time-history analysis) must be in the form of an acceleration, velocity or displacement time-history. This time-history is generated from the response spectra of the earthquake as acceleration, velocity or displacement versus time (see sections 2.2.3, 2.2.3.1). The input ground motions which were used in this research for all transient dynamic analysis of RC building models, are classified to horizontal and vertical input ground motions.

The horizontal input ground motions, which were in the form of an acceleration time-history, are representative of 10.19 second 0.2g ZPA (zero period acceleration) United Kingdom ground motion. This acceleration time-history ( $PGA = 0.2g$ ) was generated from a typical UK design response spectra of a hard site (Uniform Risk Spectra (URS), Principia Mechanica Limited, ref. [32]), refer to section 2.2.3.1. The vertical input ground motion was reduced by 2/3 of that of the horizontal motions to account for a typical reduction normally observed for vertical motion (for vibration periods  $T \leq 0.15$  sec, reduction factor is equal to 0.70), Eurocode 8, ref. [4], Penelis & Kappos, ref. [8].

Due to the displacement time-history being the only available option for applying input ground motion in a transient dynamic analysis using ANSYS, the horizontal and vertical acceleration time-histories derived from the spectra were integrated numerically and converted to displacement time-histories. These displacement time-histories were applied as 10.19 second with a digitized interval (vibration period) of 0.01 second (see Fig.3.6). This size of time increment is typical to allow the effect of frequencies within the normal earthquake range to be captured in the model. Soil properties and effects of soil structure interaction were ignored in this research, (but were recommended for future work). Hence the translational ground motion was applied in the three spatial co-ordinate directions directly to the bases of the model.



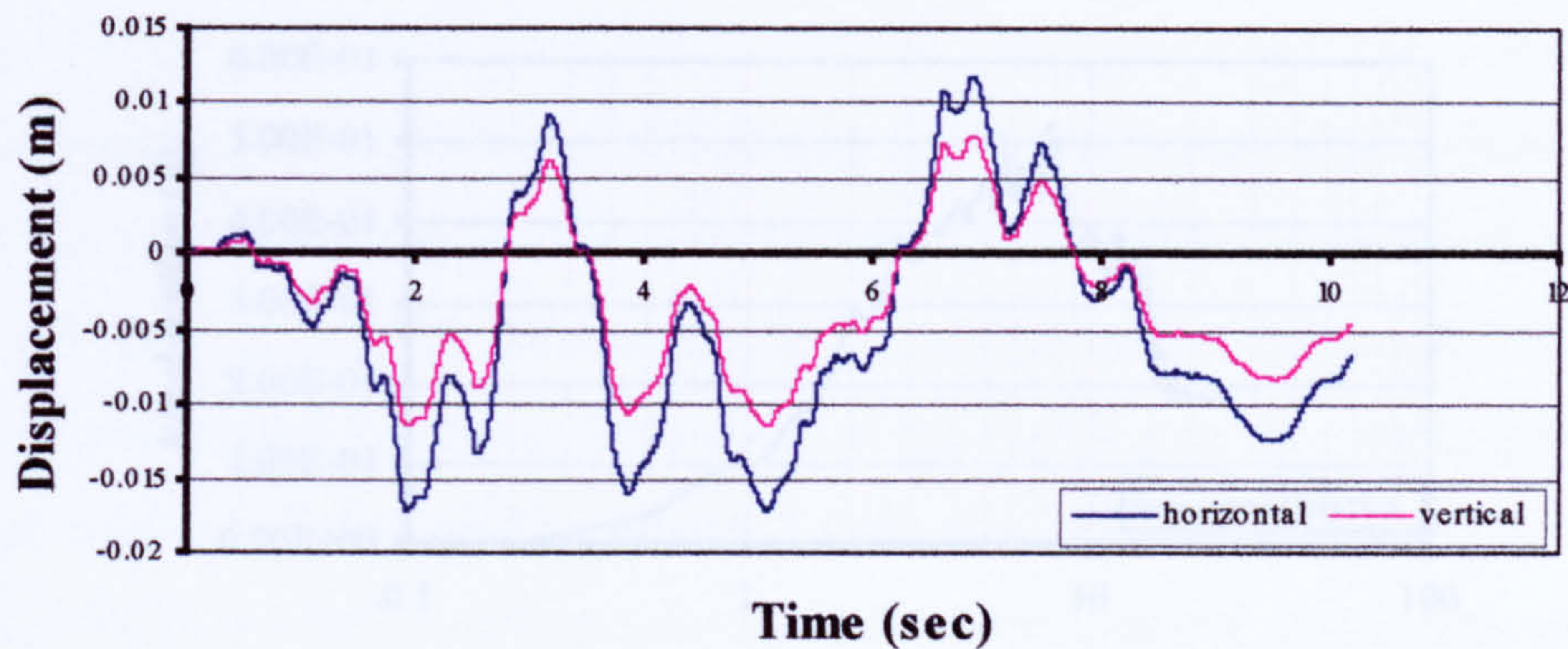


**Figure 3.6** Typical displacement (horizontal - vertical) time-history input motion

The ANSYS program has the capability to generate a response spectra from a displacement time-history for any selected node of the building model. The response spectra generator uses the displacements from the transient dynamic analysis results. Calculations are based on a numerical integration scheme with the displacement time-history data from the file as the input forcing function. The response spectra can be calculated and produced as a displacement, velocity, or acceleration response spectra. ANSYS was used to generate the acceleration response spectra (0.2g ZPA Typical UK URS) of the horizontal displacement time-history input motion used in this research (see Fig.3.6).

Many earthquake engineering research organizations throughout the world have computer programs for generating response spectra of earthquakes. A purpose written spectra generation program written in Fortran (based on the normal procedure using the 'Duhamel Integral') was used to generate the acceleration response spectra (0.2g ZPA Typical UK URS) of the horizontal acceleration time-history input motion (0.2g PGA) to verify the ANSYS program. Figures 3.7, 3.8 show the acceleration response spectra (0.2g ZPA Typical UK URS) that were generated using ANSYS and the computer program. The comparison between these figures confirms the capability of ANSYS in producing the response spectra and using it as an accurate seismic analysis tool.

### 3.3.3.2 Analysis under Horizontal Earthquake

A transient dynamic analysis (time – history analysis) was carried out for the



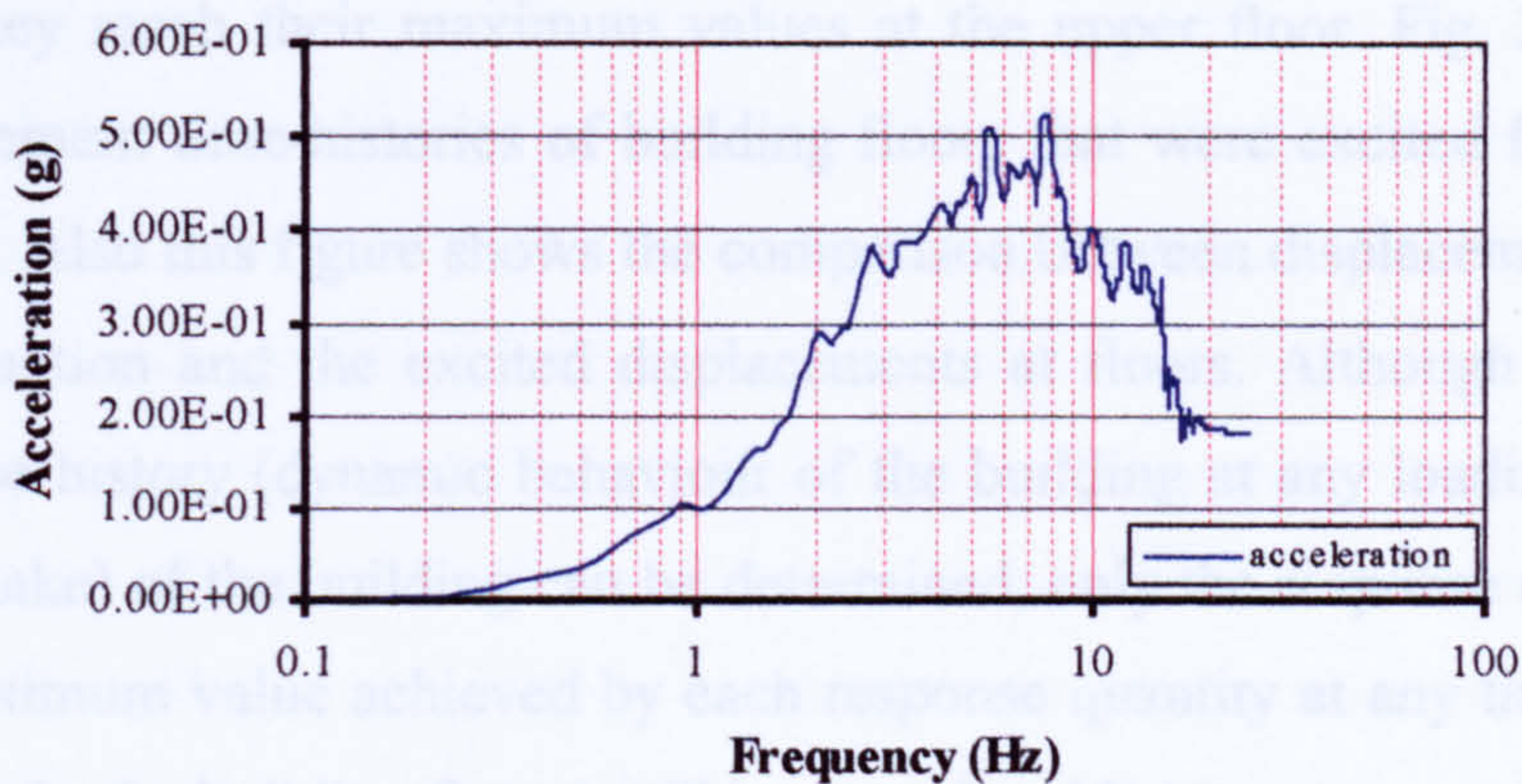


**Figure 3.7** Acceleration response spectra of horizontal input motion (displacement time-history) using ANSYS

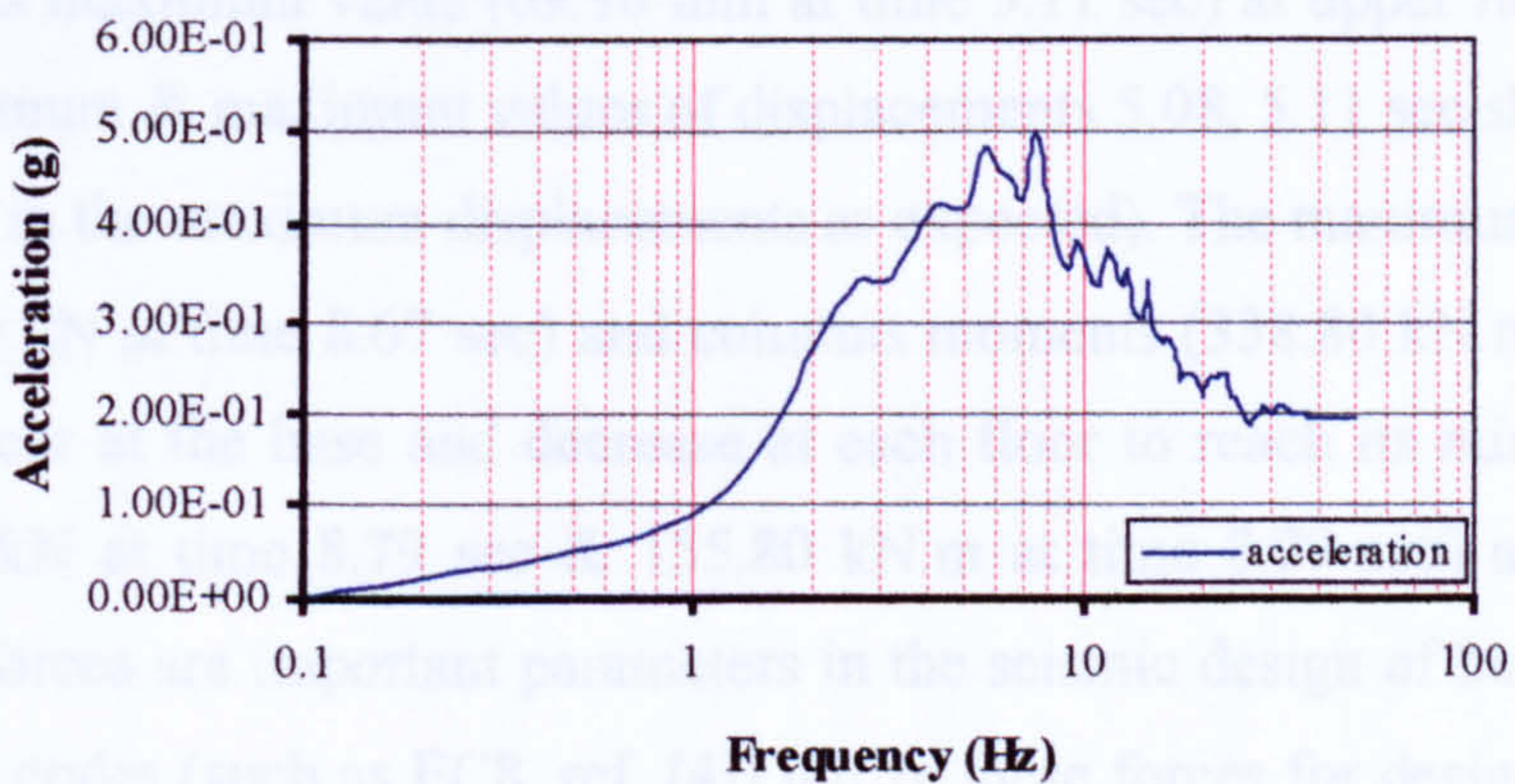


**Figure 3.8** Acceleration response spectra of horizontal input motion (acceleration time-history) using the computer program

UFS model under the horizontal displacement time – history input motion alone (see Fig.3.6). The displacement time-history was applied directly to the fixed bases of the model in x, z directions as a two-dimensional input motion. The complete response history (seismic behaviour) of the building was evaluated by the response parameters such as maximum amplitude of the relative displacement, the relative velocity and the absolute acceleration developed during a seismic excitation. Also the resulting forces (such as maximum stresses, strains, moments and shear & axial loads) were used to determine the dynamic response of the building. Investigation of the transient dynamic analysis results of the UFS model under horizontal input motion shows that:



1. In general, the lateral displacements ( $u_x$ ,  $u_z$ ) increase with the height of building until they reach their maximum values at the upper floor. Fig. 3.9 shows the displacement time-histories of building floors that were excited from the input motion. Also this figure shows the comparison between displacements values of input motion and the excited displacements at floors. Although the complete response history (dynamic behaviour of the building at any loading step of the earthquake) of the building can be determined, only the response envelope (i.e., the maximum value achieved by each response quantity at any time during the earthquake for building floors) will be considered here.

Figures 3.10, 3.11, 3.12 show the envelopes of lateral displacements, shear forces (lateral forces) and columns moments of the UFS model under the earthquake. From these figures it can be noted that the minimum displacements (17.20 mm at time 5.08 sec) occur at the base and increases at each floor to reach its maximum value (69.90 mm at time 5.11 sec) at upper floor (the times of minimum & maximum values of displacements 5.08, 5.11 sec show that there is a lag in the maximum displacements as expected). The maximum shear forces (167.30 kN at time 8.67 sec) and columns moments (338.80 kN.m at time 8.66 sec) occur at the base and decrease at each floor to reach its minimum values (79.90 kN at time 8.79 sec & 155.80 kN.m at time 8.79 sec) at upper floor. These forces are important parameters in the seismic design of buildings. Many seismic codes (such as EC8, ref. [4]) utilize these forces for design of buildings in accordance with the requirements of seismic analysis and design. Also the assessment technique of these forces for the complete response history of building allows us to determine the realistic seismic behaviour and identify the vulnerable areas of the building during the seismic excitation.

2. Axial forces in building columns is one of the important factors which affects the ductility (section rotation capacity) of columns during the earthquake. In general a reduction in the compressive axial load will increase the ductility of the section, but may compromise the ultimate strength. Fig. 3.13 shows the envelopes of moments and axial compressive loads of the UFS columns during the earthquake. As the gravity loads are not applied in this model (UFS), the axial forces of the columns are completely due to the earthquake. Fig. 3.13 exhibits the relationship between the moments and axial loads during the



earthquake. A number of important points with regard to the formation of collapse mechanisms are raised at this stage. In general terms it can be seen and assumed that the columns in the ground and lower floors have the greater compressive axial load within them, both under earthquake loading only, and earthquake plus gravity loading. It can be seen from Fig 3.13 that the applied moments are greater in the lower floors also, as expected. Hence in relation to the natural design state of the majority of reinforced concrete columns, the increased axial load will help in resisting the larger moments applied (within a reasonable axial load increase limit) at ground and lower floor levels. However the ductility may be compromised as a result, which may affect the global collapse mechanisms. Also the compressive effect within the concrete columns can affect their relative stiffnesses throughout the various stages of loading, which may in turn affect the distribution of loading throughout the structure. All of these points will be examined further, later on in the work.

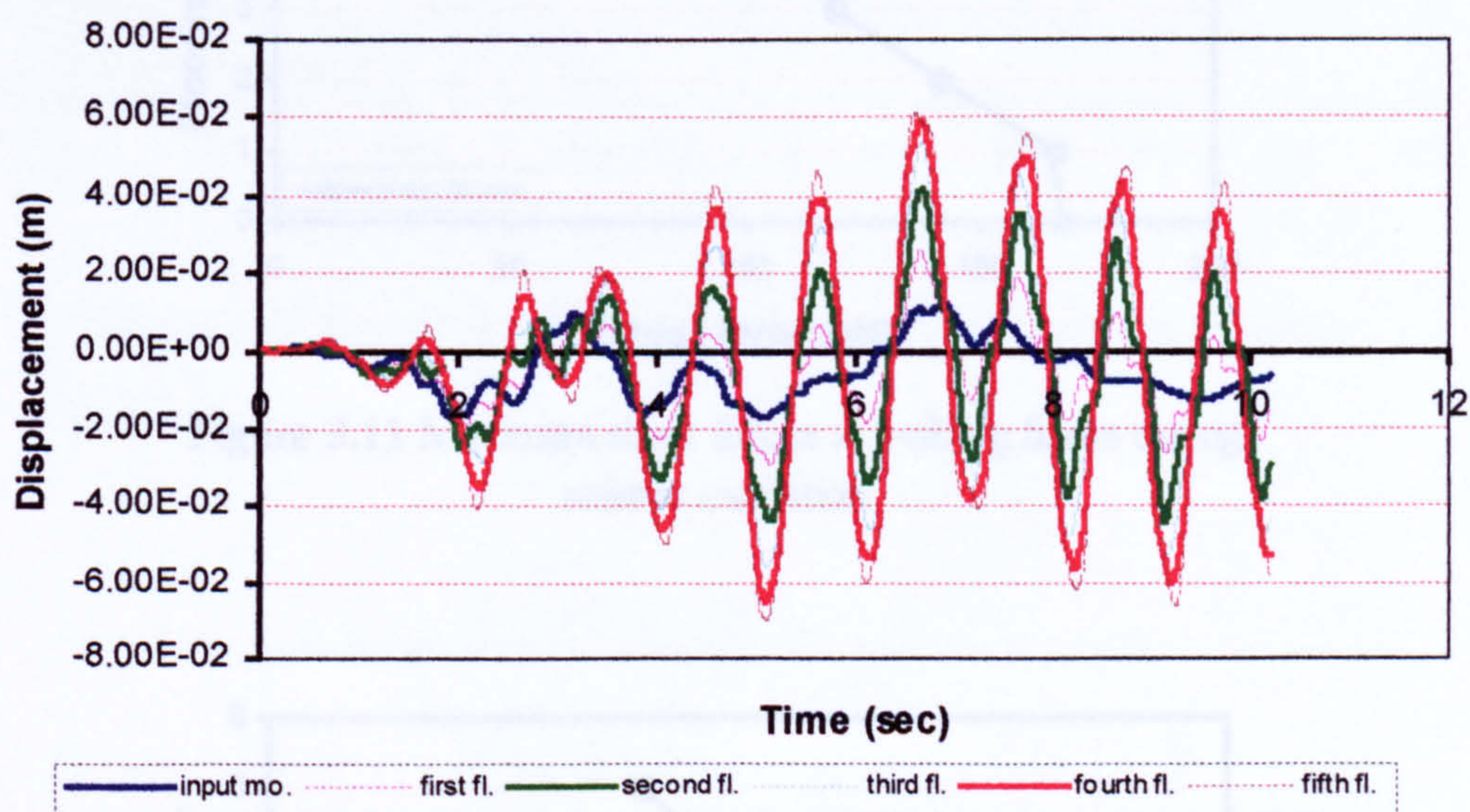


**Figure 3.9** Displacement time-histories of building floors and input motion

3. Fig. 3.14 shows the interstorey drift for the UFS model at the time step 5.11 sec since the maximum lateral displacement of the upper floor during the earthquake occurred. These types of plots are commonly used to compare between global seismic behaviour of RC frames including different types of joints (flexible or rigid) and/or under different types of earthquake (peak ground acceleration).



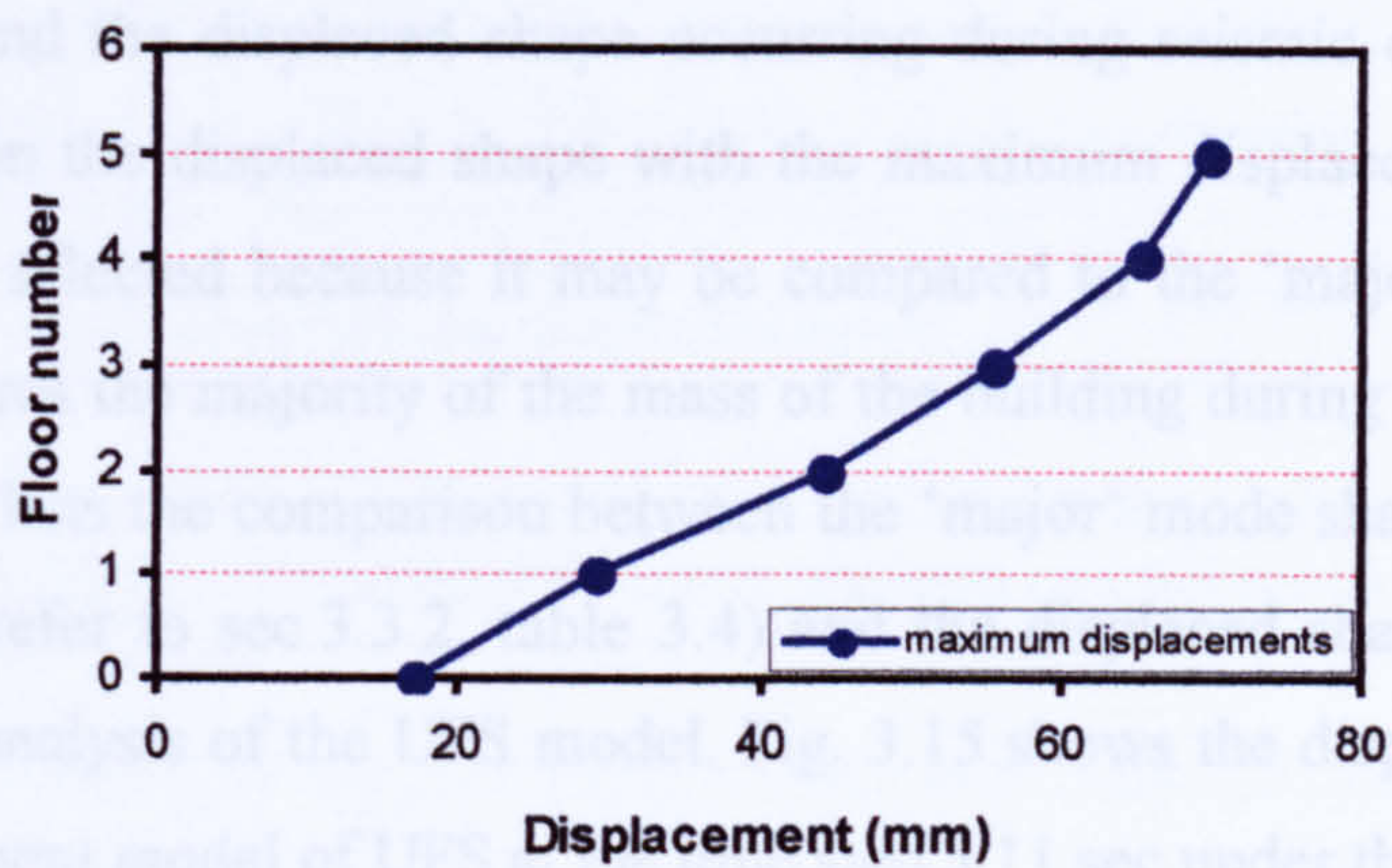


Figure 3.10 Maximum displacements of building floors during seismic excitation

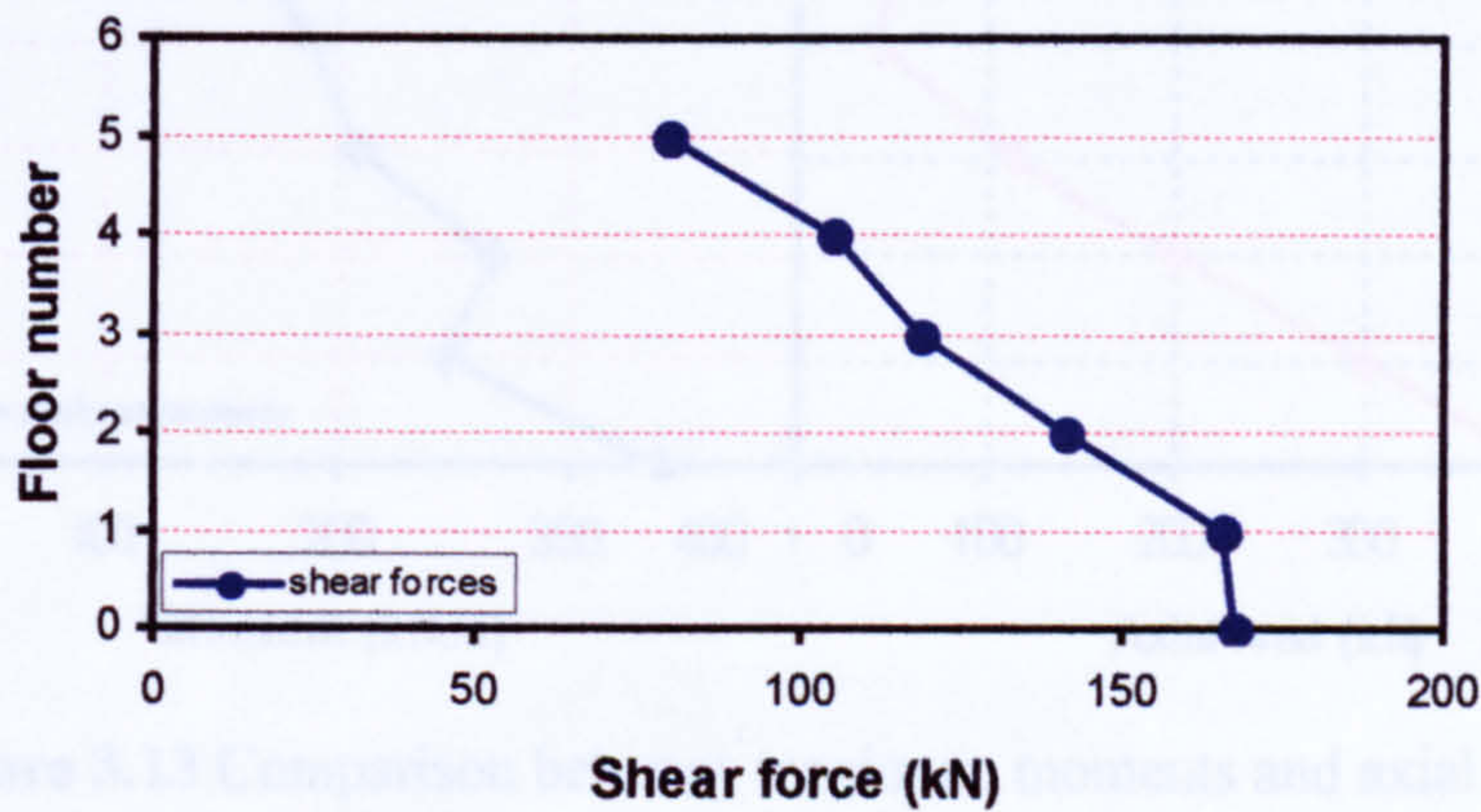


Figure 3.11 Maximum shear forces at building floors during seismic excitation

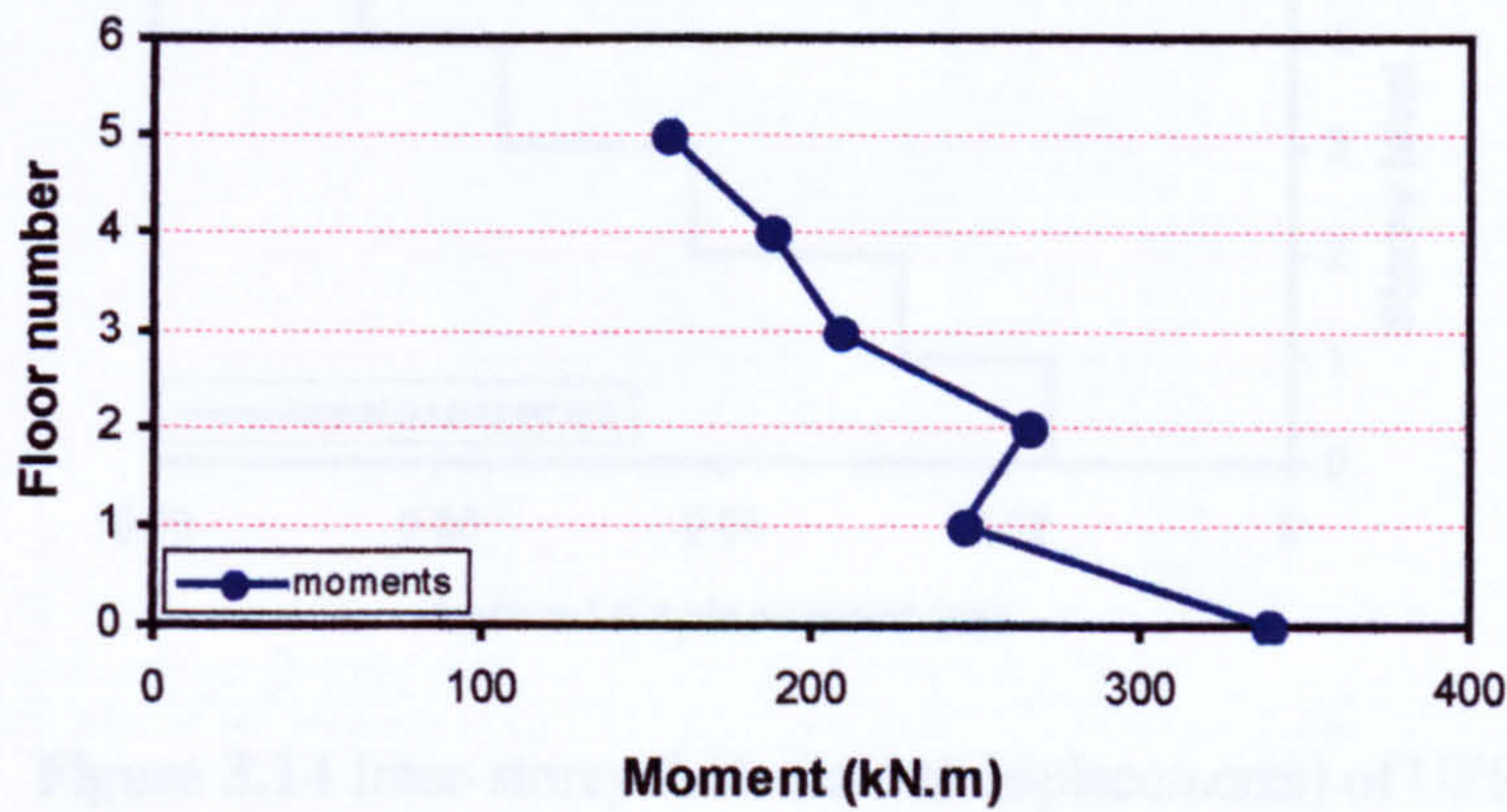
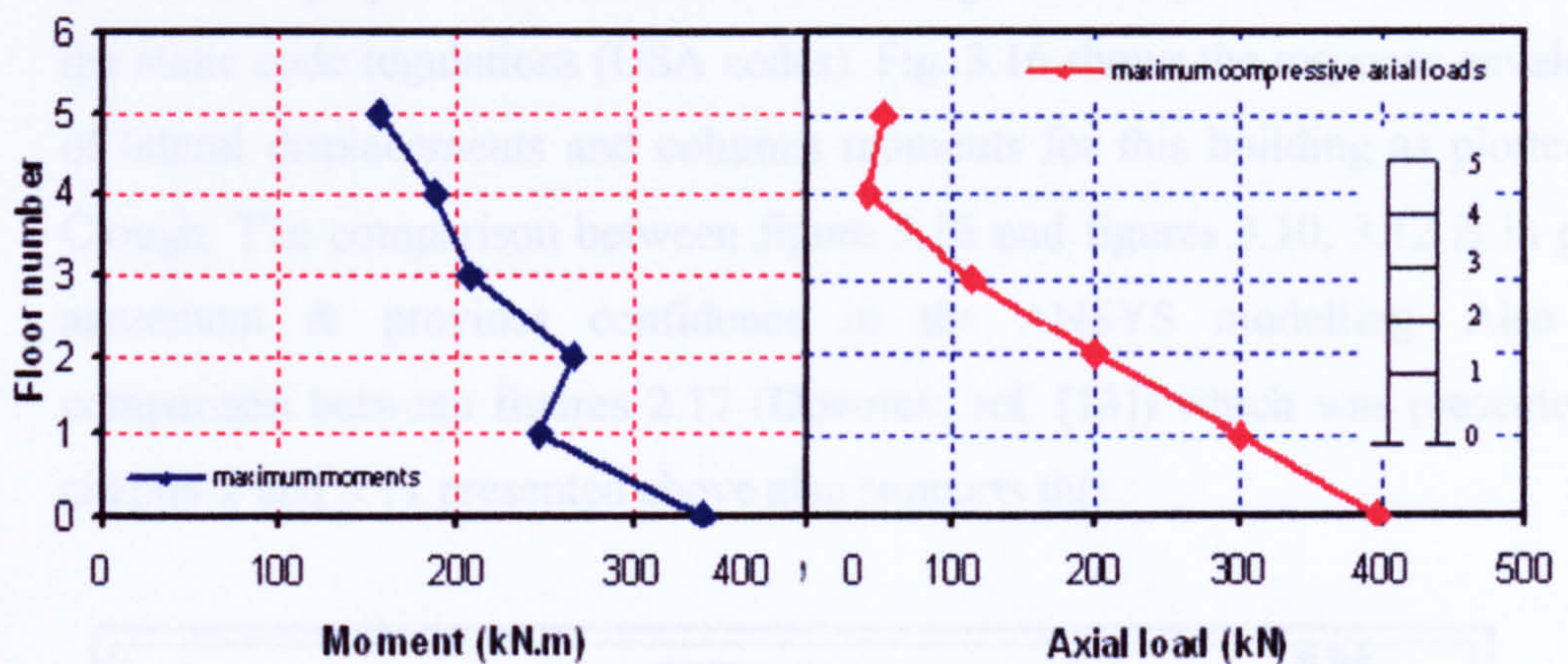


Figure 3.12 Maximum moments of columns at joints during seismic excitation



Here we will compare the mode shapes which were produced from the modal analysis and the displaced shape occurring during seismic excitation. For this comparison the displaced shape with the maximum displacement of the upper floor was selected because it may be compared to the 'major' mode of model that captures the majority of the mass of the building during seismic excitation. Table 3.7 lists the comparison between the 'major' mode shape from the modal analysis (refer to sec.3.3.2, table 3.4) and the displaced shape of the transient dynamic analysis of the UFS model. Fig. 3.15 shows the displaced shape of the finite element model of UFS at the time step 5.11 sec under the earthquake.



**Figure 3.13** Comparison between maximum moments and axial loads of building columns under earthquake

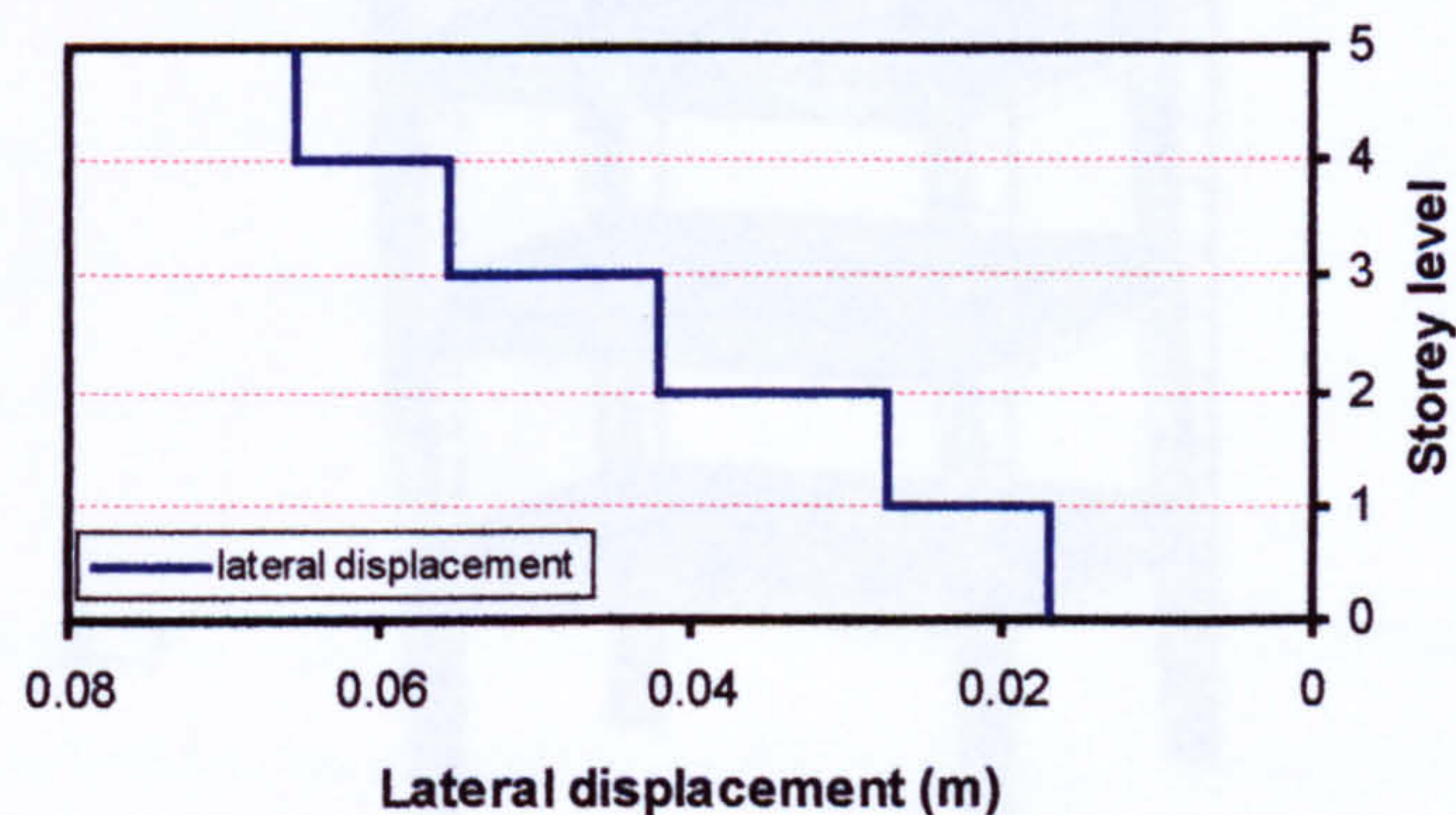


**Figure 3.14** Inter-storey drifts (lateral displacements) of UFS model at maximum displacement of upper floor under earthquake



Analysis type	Frequency (Hz)	Direction	Description of Mode
Modal analysis	1.0 (‘Major’ modal frequency)	X - direction	Sway Mode
Transient dynamic analysis	2.5 (Average global response frequencies)	X - direction	Sway Mode

**Table 3.7** Comparison between mode shapes from modal analysis and displaced shapes of transient dynamic analysis of UFS model

4. In 1970, Clough (Wiegel, ref. [53]), carried out an elastic dynamic analysis for a two-dimensional 20-storey RC building under an earthquake (0.3g PGA) using the mode superposition method. This building was designed in accordance with the static code regulations (USA codes). Fig. 3.16 shows the response envelopes of lateral displacements and columns moments for this building as plotted by Clough. The comparison between figure 3.16 and figures 3.10, 3.12 is in good agreement & provides confidence in the ANSYS modelling. Also the comparison between figures 2.17 (Dowrick, ref. [13]) which was presented in chapter 2 and 3.11 presented above also supports this.

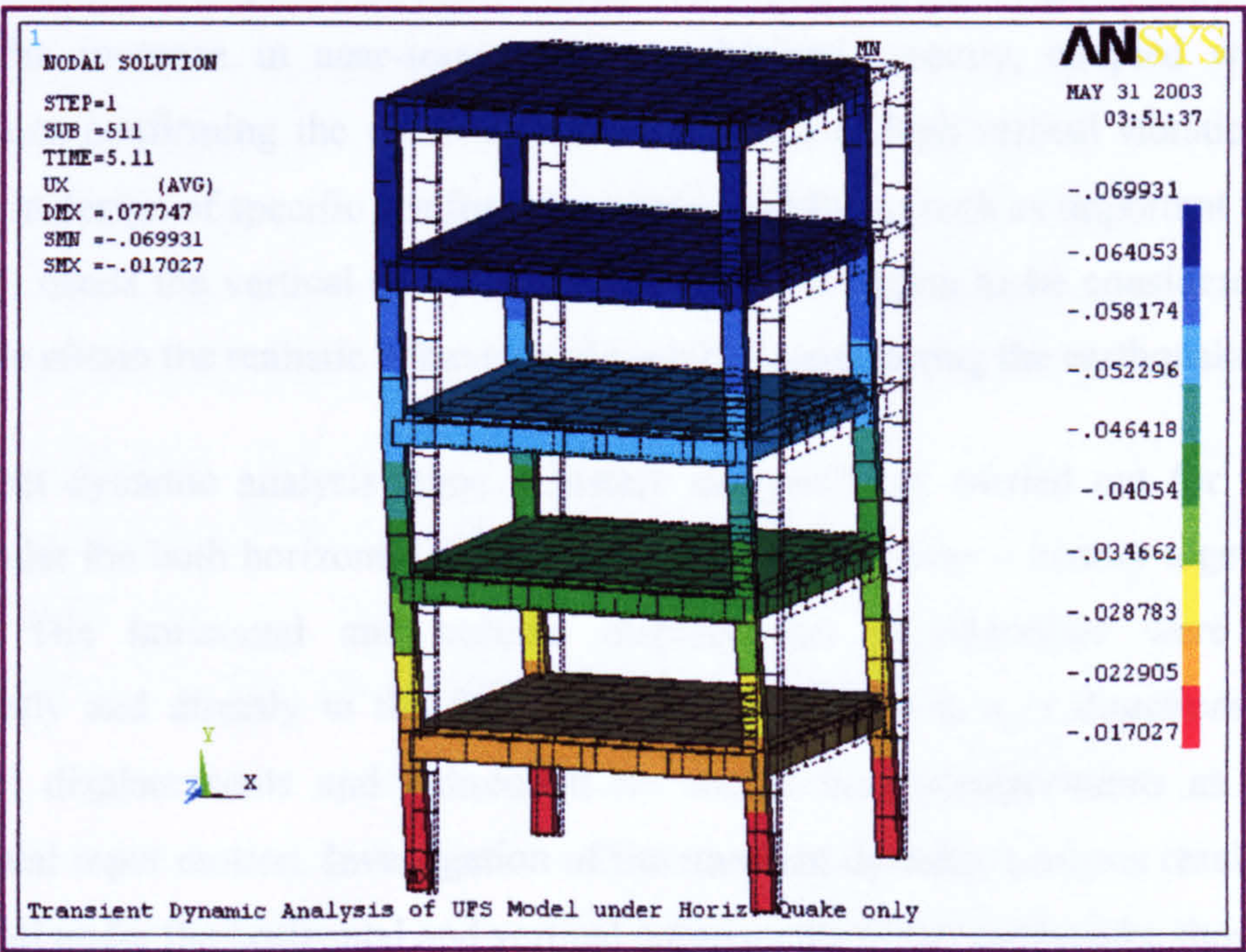


**Figure 3.15** Deformed and undeformed shape of UFS model at maximum displacement of upper floor under earthquake [time step 5.11 sec & various colours indicate to the values of lateral displacements in x-direction]



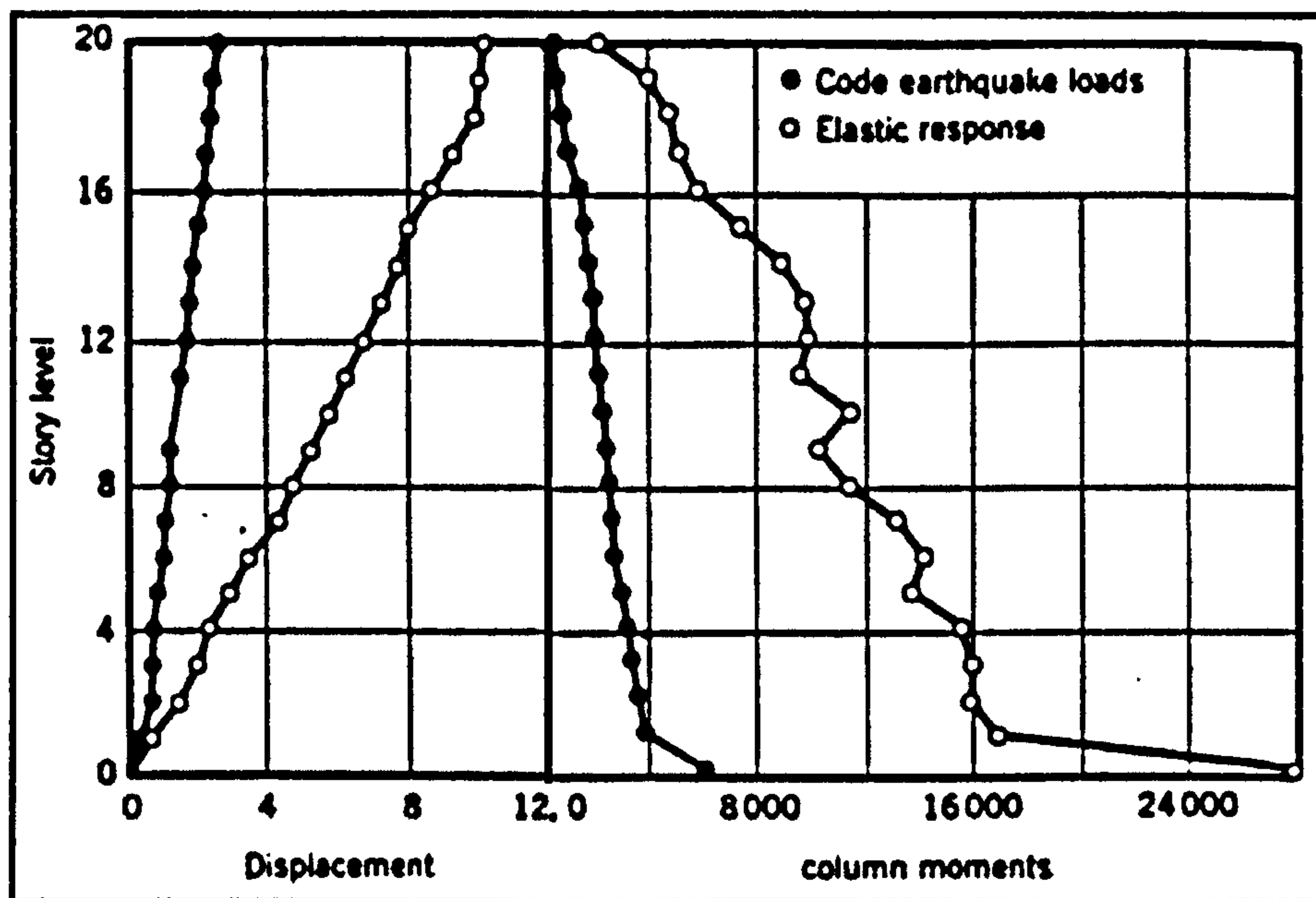


Figure 3.16 Response envelopes of elastic lateral displacements and columns moments of 20-storey RC building under an earthquake [Clough (Wiegel, ref. [53])]

### 3.3.3.3 Analysis under both Horizontal and Vertical Earthquake Together

The vertical component of earthquake ground motion has generally been neglected in the earthquake-resistant design of structures. This is gradually changing due to the increase in near-source records obtained recently, coupled with field observations confirming the possible destructive effect of high vertical vibrations. Also the seismic design of specific reinforced concrete buildings (such as important high rise buildings) needs the vertical component of the seismic action to be considered in the analysis to obtain the realistic behaviour of such buildings during the earthquake.

A transient dynamic analysis (time – history analysis) was carried out for the UFS model under the both horizontal and vertical displacement time – history together (see Fig.3.6). The horizontal and vertical displacement time-histories were applied concurrently and directly to the fixed bases of the model in x, z directions for the horizontal displacements and y-direction for the vertical displacements as a three-dimensional input motion. Investigation of the transient dynamic analysis results of the UFS model under the horizontal and vertical components of the earthquake shows that:

2. The vertical displacements ( $u_y$ ) increase with the height of building until they reach their maximum values at the upper floor. Fig. 3.17 shows the envelope of vertical displacements of the UFS model under the both horizontal and vertical



earthquake together. This figure shows that the minimum displacements (11.5 mm at time 5.08 sec) occur at the base and increases at each floor to reach its maximum value (12.70 mm at time 4.99 sec) at upper floor. This is expected due to the amplification effects through the higher elevation of the building.

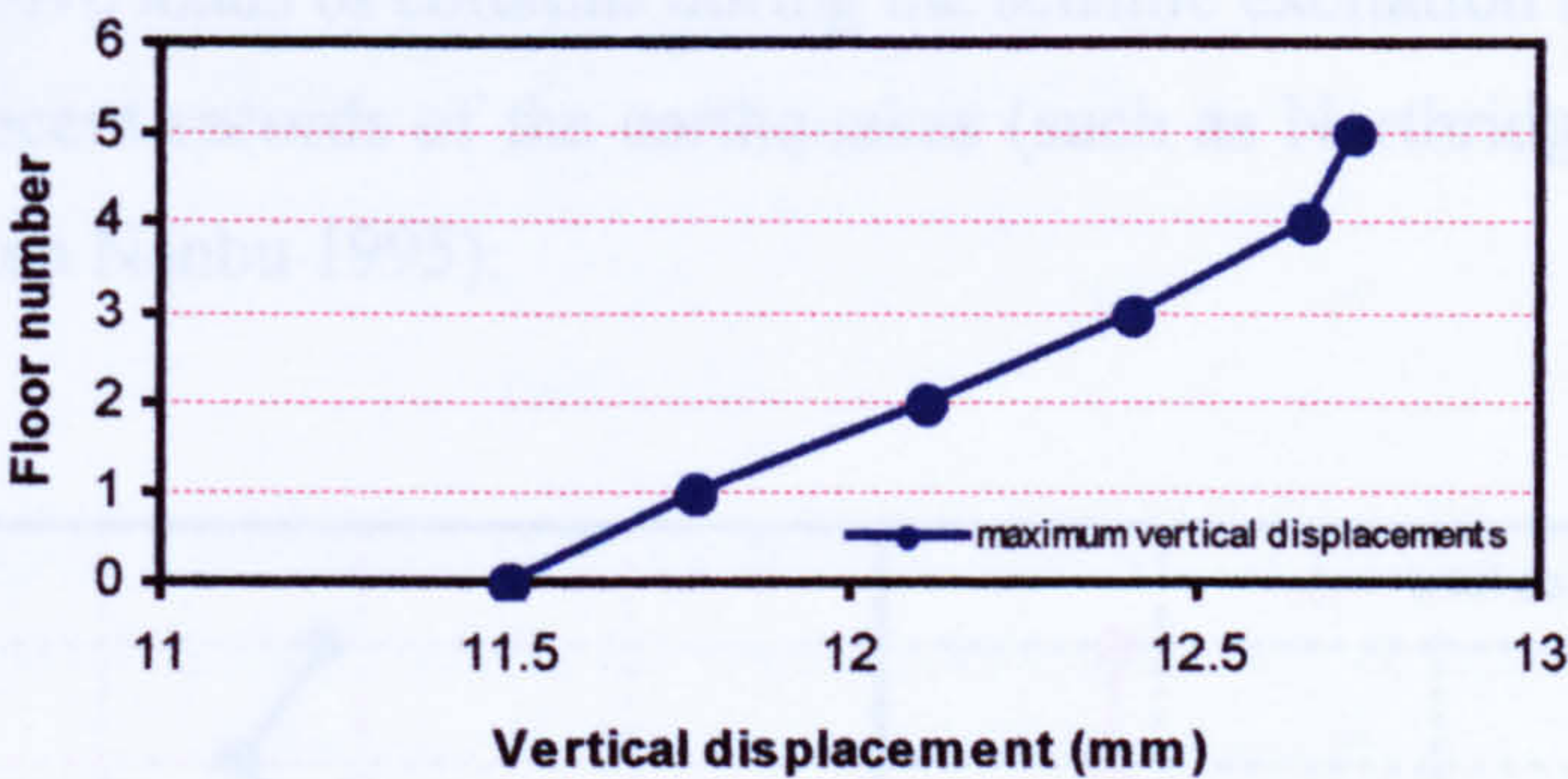


**Figure 3.17** Maximum vertical displacement of building floors during concurrent components (vertical & horizontal) of earthquake

3. In 2001, Collier & Elnashai, ref. [54], mentioned that a damage consistent with a high level of vertical acceleration was observed in the 1994 Northridge earthquake. The investigation report for the consequences of high vertical accelerations of this earthquake on RC buildings highlighted cases of brittle failure induced by direct compression, or by reduction in shear strength and ductility due to variation in axial forces arising from the vertical motion. Also for first mode vertical response, the reduction in axial force in columns is more significant for higher storeys, since it represents a larger relative change in the pre-existing static axial load (reduction of the columns strength). Interior columns were shown to be more vulnerable, and vertical oscillations of slabs at their natural period caused considerable damage. These points will be discussed later on through the next different models applied in this work.

Fig. 3.18 shows the envelopes of moments and axial compressive loads of the UFS columns during the concurrent horizontal and vertical earthquake. As the gravity loads are not applied in this model (UFS), the axial forces of the columns are completely due to the horizontal and vertical earthquake. Fig. 3.18 exhibits the relationship between the moments and axial loads during the earthquake. The comparison between figures 3.18 (under both horizontal & vertical



earthquake together) and 3.13 (under horizontal earthquake only) shows that the values of moments remained approximately unchanged and the axial compressive loads increased with a value range from 100 kN to 200 kN. This comparison shows clearly the effects of vertical vibrations on the axial compressive loads of columns during the seismic excitation as that was observed by the recent records of the earthquakes (such as Northridge earthquake 1994, Hyogo-ken Nanbu 1995).

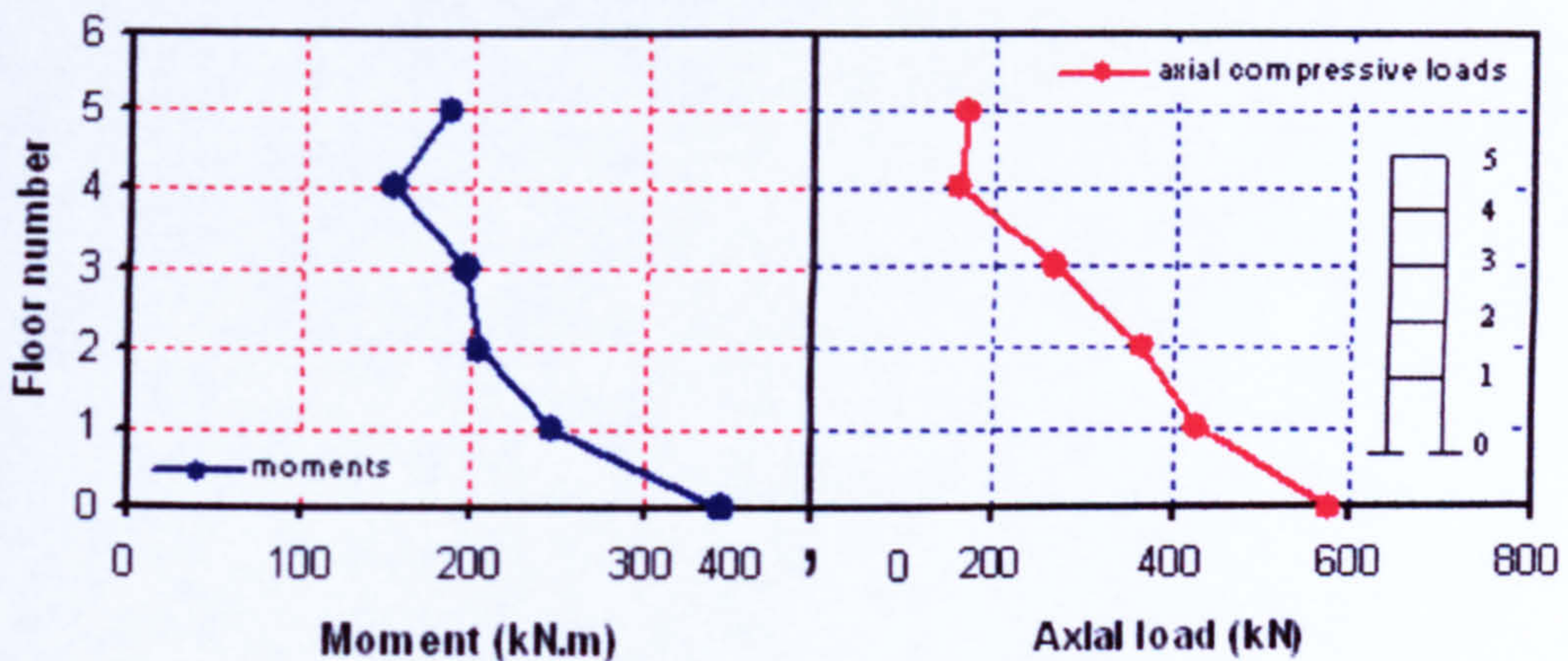


**Figure 3.18** Comparison between maximum moments and axial loads of building columns under horizontal & vertical earthquake

4. A decrease in the stiffness of some elements of the building during the seismic excitation will result in a decrease in the global stiffness of the building which will become more flexible (i.e. its global response fundamental period  $T$  will increase in accordance with the global response frequency  $F$  since  $T = 1/F$ ). Fig. 3.19 shows the difference of average response period for the UFS model under the horizontal earthquake only (maximum period is 1.70 sec at time 6.21 sec) & under the both horizontal and vertical earthquake together (maximum period is 0.80 sec at time 3.77 sec). As the global response period of the flexible building is always longer than that of the rigid building, the UFS model under the concurrent horizontal & vertical earthquake exhibited more rigidity than that under horizontal earthquake only. This rigidity may refer to the effects of vertical vibrations on the axial compressive loads of building columns. Hence the building columns will be vulnerable to the brittle failure during the seismic excitation as mentioned in Collier & Elnashai, ref. [54].



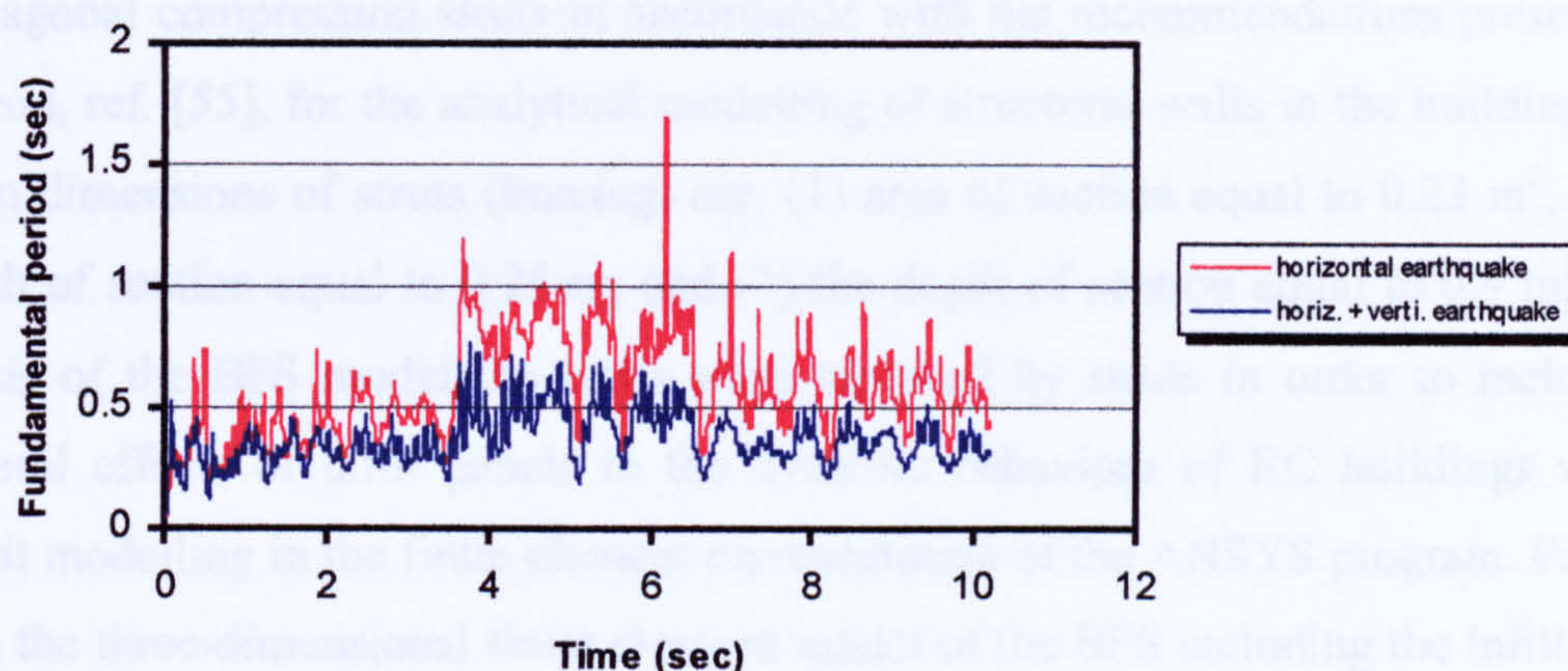


**Figure 3.19** Variation of the fundamental period with time step for the UFS model under horizontal earthquake only & under both horizontal and vertical earthquake together

### 3.4 ANSYS Analysis of a braced 5-storey RC Building

The model of braced 5-storey RC building (**this model will be called BFS**) has the geometric characteristics and design details that previously mentioned for the UFS model and are listed in the table 3.1. But the BFS model differs concerning the effects of walls. The BFS is braced model i.e. the effects of walls were involved in the design and analysis.

The idea of modelling an infill panel (wall) with a single element (strut) able to simulate the global effect of the panel on the response of the structure, has always been attractive because of the obvious advantages in terms of computation simplicity and efficiency. In 1990, Macleod, ref. [55], mentioned that the brickwork or blockwork which ‘infills’ the area between beams and columns in a frame makes a major contribution to behaviour. Under lateral load the normal model for the infill is a diagonal compression strut. Stafford Smith & Riddington (1978) recommend that the area of such a strut should be equal to one tenth of the diagonal length of the panel times the wall thickness. Also in 2002, Cameron & Pankaj, ref. [56], concluded that the infill panels (masonry walls) of the frame under the horizontal or/and vertical earthquake behave more likely as a diagonal strut.

For the design of BFS model the walls were chosen as blockwork panels having a 0.25 m thickness and 8.70 m diagonal length. For purpose of carrying out the static and dynamic analysis of the BFS model using ANSYS, these infill panels were replaced by



RC diagonal compression struts in accordance with the recommendations presented in Macleod, ref. [55], for the analytical modelling of structural walls in the buildings. The section dimensions of struts (bracing) are, (1) area of section equal to  $0.23 \text{ m}^2$ , (2) the breadth of section equal to  $0.25 \text{ m}$ , and (3) the depth of section equal to  $0.9 \text{ m}$ . In the analysis of the BFS model the walls were replaced by struts in order to include the structural effects of infill panels in the dynamic behaviour of RC buildings without explicit modelling in the finite element representation of the ANSYS program. Fig.3. 20 shows the three-dimensional finite element model of the BFS including the infill panels (as generated using ANSYS).

Three types of analysis were conducted (including gravity loads, damping) using ANSYS for this model (BFS) as follows:

1. Three-dimensional static linear analysis
2. Three-dimensional modal analysis
3. Three-dimensional transient linear dynamic analysis:
  - a) Under horizontal earthquake alone
  - b) Under both horizontal and vertical earthquake together

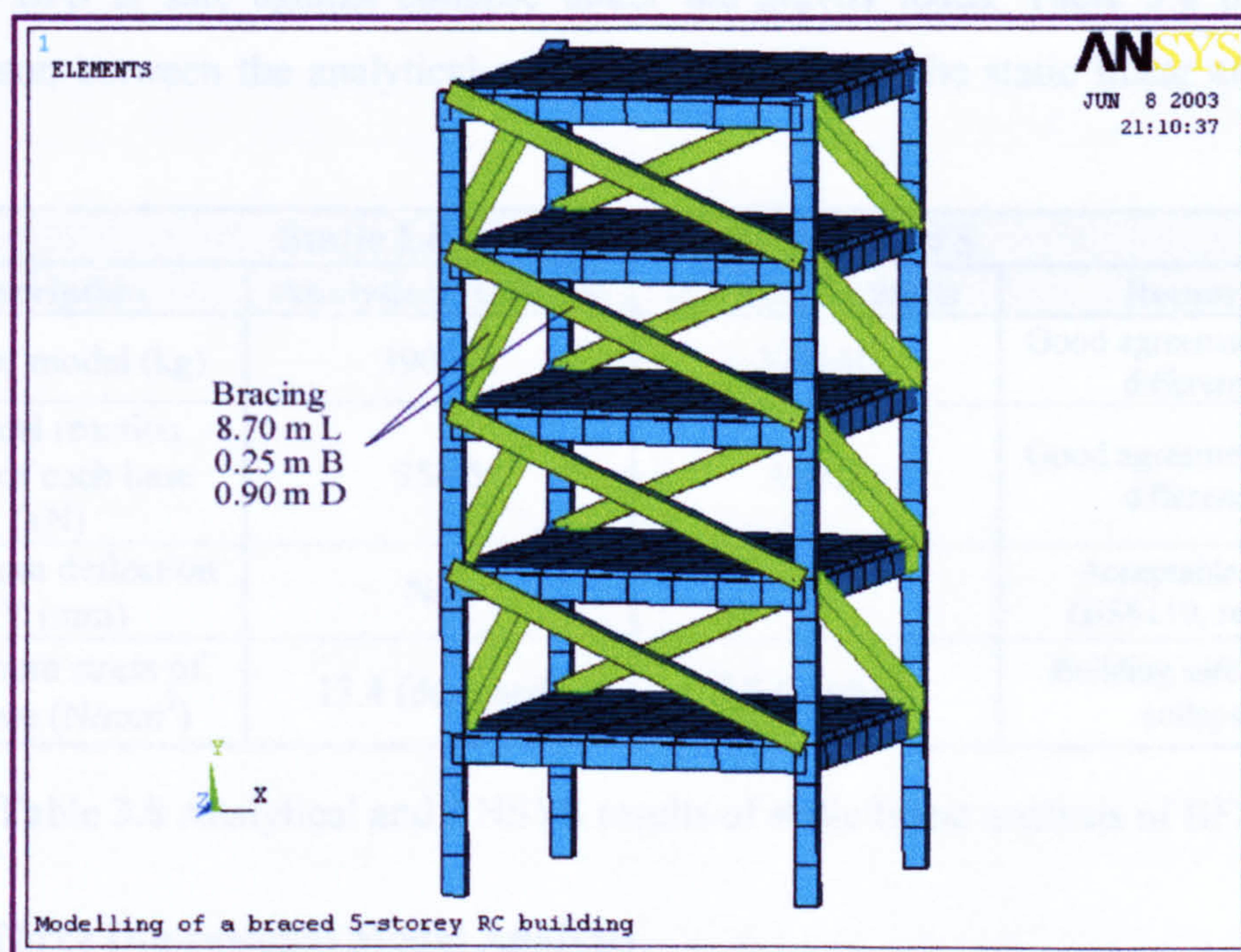


**Figure 3.20** The finite element model of braced five-storey RC building (BFS)



3.4.1 Three Dimensional Static Analysis

The static analysis of BFS was carried out to check the safety of building against collapse under its own weight and live load and to verify forces in the static case. This model was generated using the finite element computer program ANSYS as shown in Fig. 3.20 in accordance with the design details listed in table 3.1 and the details stated above. The static load (gravity loads that included specified dead and live loads) was applied using the gravitational constant of  $9.81\text{m/s}^2$  acting on the appropriate density (mass) of the model.

The results of static linear analysis of the BFS using ANSYS are in good agreement with the hand calculations results (the mass of building and its vertical reaction forces were estimated with a high degree of accuracy). Also investigation of the ANSYS results of the model shows that the maximum degree of freedom value in y-direction (maximum deflection UY) is acceptable in accordance with the serviceability limit state requirements of BS 8110, ref. [3]. In accordance with the stress-strain curve of concrete presented in BS8110 (see Fig. 2.1), the maximum stress of concrete grade  $30\text{ N/mm}^2$  is equal to  $13.4\text{ N/mm}^2$ . A check of the maximum stress of this model under gravity loads (based on the static analysis results using ANSYS) revealed that the maximum value was equal to  $7.80\text{ N/mm}^2$ , less than the BS8110 limit. These checks were made to show that the BFS is safe against collapse under the gravity loads. Table 3.8 presents a comparison between the analytical and ANSYS results of the static linear analysis of BFS.

Static Linear Analysis Results of BFS			
Description	Analytical Analysis	ANSYS Analysis	Remarks
Mass of model (kg)	390022	378610	Good agreement (2.9 % difference)
Vertical reaction force of each base (kN)	956.5	928.5	Good agreement (2.9 % difference)
Maximum deflection UY (mm)	N/A	20	Acceptable value (BS8110, ref. [3])
Maximum stress of concrete ( $\text{N/mm}^2$ )	13.4 (designed)	7.8 (applied)	Building safe against collapse

Table 3.8 Analytical and ANSYS results of static linear analysis of BFS

3.4.2 Three Dimensional Modal Analysis

Modal analysis of BFS model (three-dimensional finite element model that is



shown in Fig.3.20) was carried out using ANSYS in the absence of damping ( $C = 0$ , see section 2.2.1.1). Also up to 30 mode shapes were extracted. This analysis yielded the natural frequencies (undamped), mode shapes of free vibration, the mass participation factor ( $\Gamma$ ), and the effective mass ( $m^{eff}$ ) for each mode, which are important for carrying out the transient dynamic analysis, and simple hand calculations. For this model (BFS) the resulting effective masses were used particularly to calculate the real value of damping coefficients (Rayleigh damping coefficients) that were applied in the transient dynamic analyses. This will be presented later in the section 3.4.2.1.

Table 3.9 lists the sum of effective masses of all modes in each direction. When conducting a modal analysis as a prelude to a transient dynamic analysis (time-history analysis) it is important that the majority of the mass is captured i.e. no less than 80%. For this model (BFS), thirty modes up to 16.1 Hz were extracted and this proved sufficient to capture the majority of the mass and consequently the major modes of response, see table 3.9. As the investigation for the modal analysis results is focused on the modes at which most mass is 'captured' (the 'major' modes of vibration) in order to identify the resonance phenomenon of building under the earthquake, table 3.10 summarizes the frequency, mass participation factors, captured masses, and description for the major modes of vibration of the BFS model.

Description	Mass (kg)	Percent of Mass (%)
Actual total mass of BFS	378610	100
Sum of effective masses of all modes in x-direction	376827	99.51
Sum of effective masses of all modes in y-direction	349073	92.20
Sum of effective masses of all modes in z-direction	376997	99.57

**Table 3.9** Sum of effective masses of all modes in each direction for BFS

The major modes in the x-direction and the z-direction show that the majority of mass of the building was captured for these modes (see table 3.10). The behaviour of the model in case of the sway-mode in the x-direction and the z-direction for the major modes is representative for an occurrence of stressed storey (such as soft storey) under the horizontal earthquake when the model has irregularities in the infill panels (walls) as



shown in Fig. 3.21. The major modes in y-direction show that the captured mass of the model in this direction may be concentrated in several modes of vibration. In these modes, the floors bounce up and down in addition to a presence of torsion, which show that the vertical earthquake may have a significant effect on the structure.

“Major” Modes (% Mass captured)						Description of Mode
Mode No.	Frequency (Hz)	Mass Partic. (Γ)	X - Direction	Y - Direction	Z - Direction	
1	0.9	613.3	N/A	N/A	99.3 %	Sway Mode
2	1.6	607.9	97.6 %	N/A	N/A	Sway Mode
4	4.7	421.3	N/A	46.9 %	N/A	Floors bounce up and down
21	11.3	270.6	N/A	19.3 %	N/A	Floors bounce up and down plus torsion

Table 3.10 Modal analysis results of BFS (major modes of vibration)

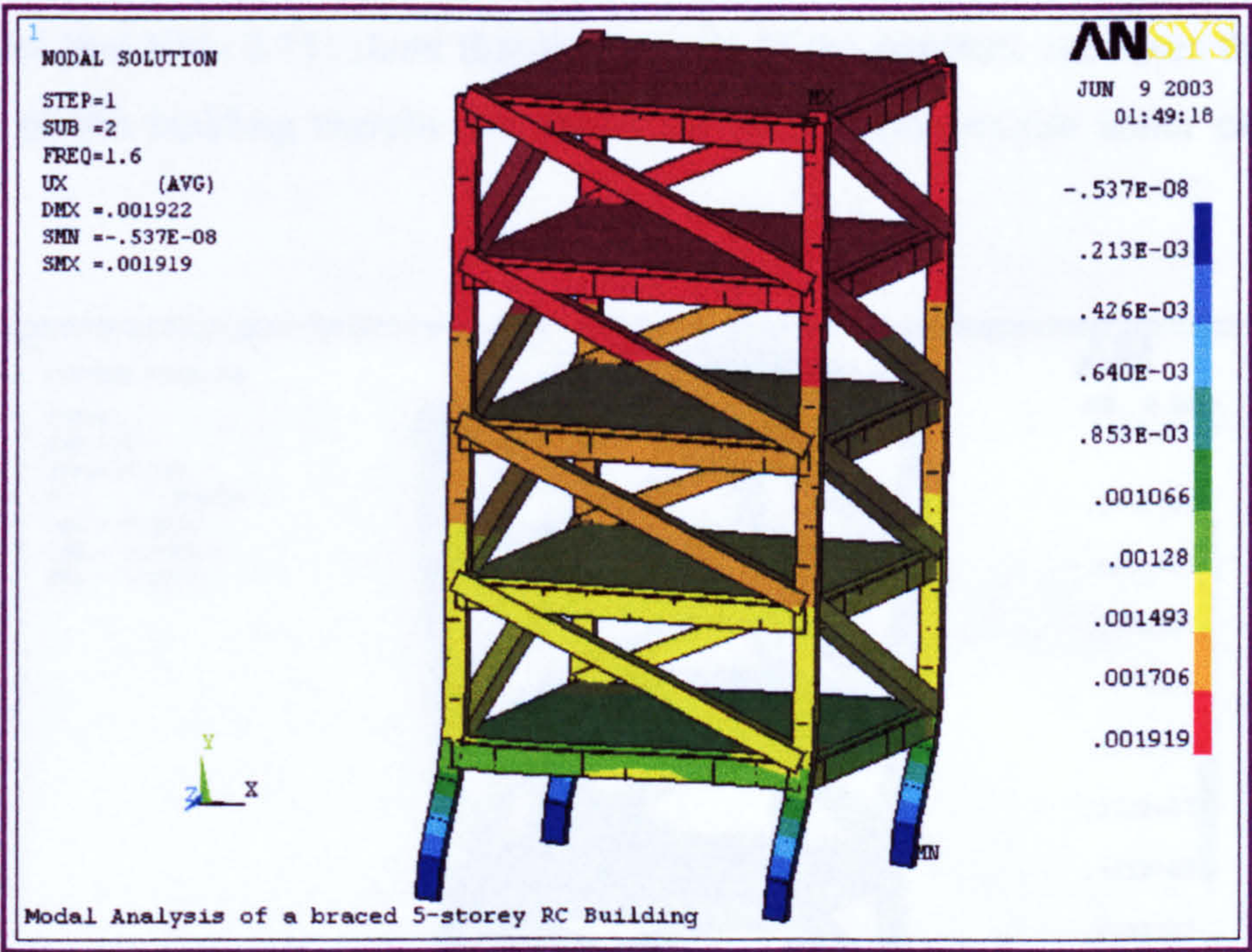


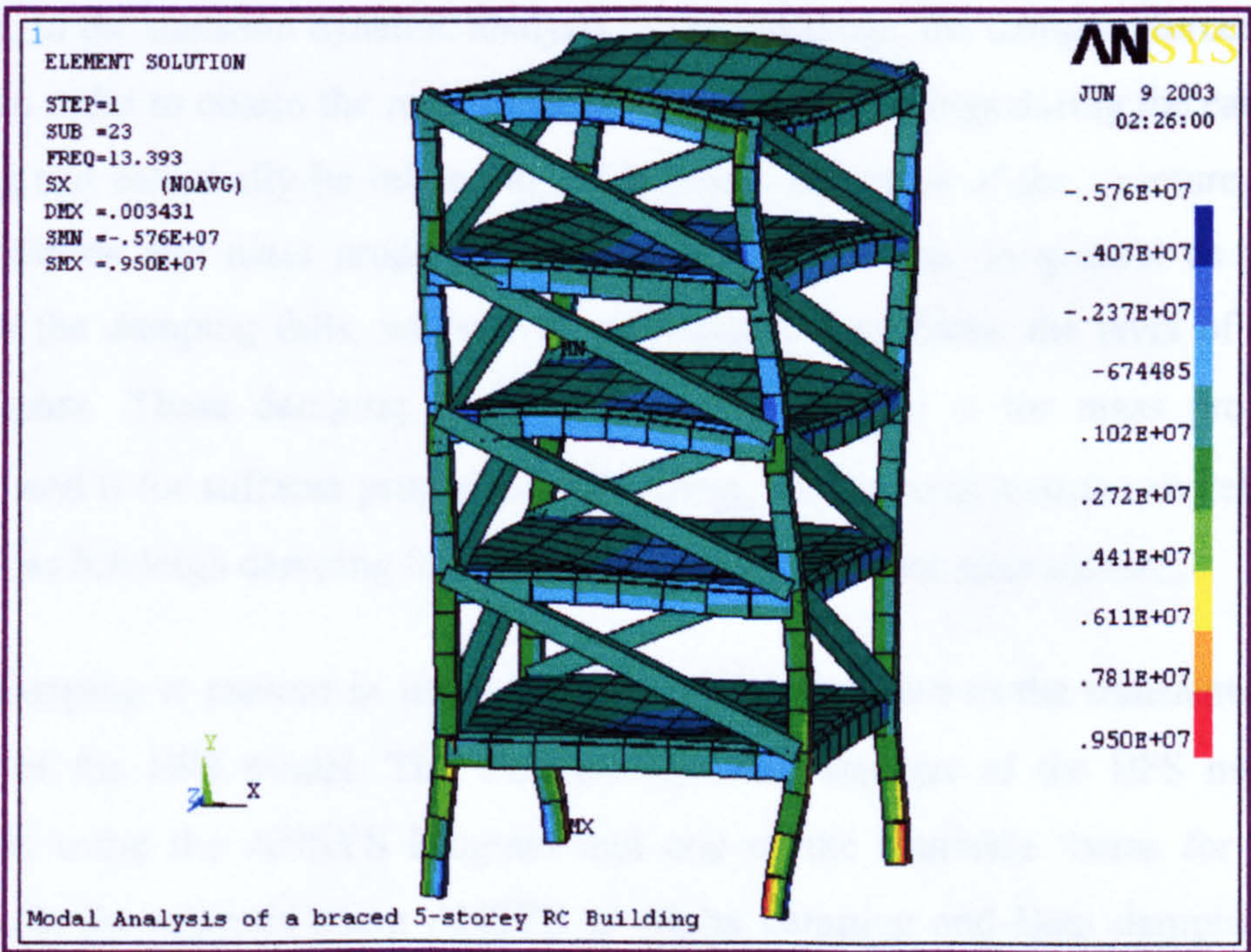
Figure 3.21 Sway mode (major mode of vibration) of BFS model in x-direction (various colours indicate to the values of displacement in meter for storeys)

Table 3.11 summarizes the modal base reactions and modal overturning moments for the major modes of vibration listed in table 3.10 and a torsional mode of the BFS model. Although these quantities are not strictly useful in terms of their application, qualitatively they provide insight into the effects of the major modes concerned. These



results show that the change in translational and rotational motions of the structure with the change of mode shapes depends mainly on the frequency and type of mode shape of the structure (see and note the coloured values in table 3.11). Also the results of the mode shape in the y-direction (floors bounce up and down) reveal that the vertical earthquakes are having a significant effect on the axial forces of columns (see the coloured value in table 3.11). The results in table 3.11 highlights the importance of the three-dimensional nature of the model due to the effects of torsional modes on the structure. Fig. 3.22 shows the typical torsional mode shape of the BFS model at a high natural frequency equal to 13.4 Hz.

The three-dimensional analysis of this model (BFS) reveals that the torsional modes must be taken account of in the design of earthquake resistant concrete structures especially in the seismic regions have severe earthquakes. This building exhibited a high natural frequency at the occurrence of torsional mode due to the presence of infill panels (links between joints). Results of the torsional modes from the modal analysis of this model (see table 3.11) show that the bracing of the structure increases the overall stiffness of the building thereby increasing the natural frequencies under earthquake loads.



**Figure 3.22** Torsional mode shape of BFS model and its longitudinal stresses (various colours indicate to the values of stresses in x-direction)



Mode No. and Description	Frequency (Hz)	Total Modal Reactions of Model Bases			Total Modal Overturning Moments of Model Bases		
		X-dir	Y-dir	Z-dir	X-axis	Y-axis	Z-axis
(1) Sway mode	0.9	5.65	0.10	-20789	-37234	-0.0005	28.41
(2) Sway mode	1.6	-61427	0.28831	-12.40	42.30	0.003	116020
(4) Floors bounce up and down	4.7	0.08	-362240	-0.004	-0.004	991.97	-0.15
(23) Torsional mode	13.4	1.55	-1297900	3.79	5.05	-10605	-2.20

**Table 3.11** Modal analysis results (modes of vibration) of the BFS model  
(base forces and moments of three-dimensional FE model)

**3.4.2.1 Rayleigh Damping Coefficients**

The seismic behaviour of building is defined by solving the equation of motion, which is the equation for equilibrium between the forces arising from inertia, damping and stiffness together with the externally applied force (earthquake). Therefore the damping force (C) of building is a significant factor influencing its seismic response. In the transient dynamic analysis of the buildings, the damping forces must be applied in order to obtain the realistic behaviour of the buildings during the earthquake. Damping can essentially be related to the stiffness and mass of the structure i.e. their exists stiffness and mass proportional damping coefficients. In general as the mass increases the damping falls, whilst with an increasing stiffness, the level of damping will increase. These damping coefficients are defined as  $\alpha$  for mass proportional damping and  $\beta$  for stiffness proportional damping, and in combination can define what is known as Rayleigh damping for the model (discussed in the next section).

As the damping is present in most systems, it was specified in the transient dynamic analysis of the BFS model. The transient dynamic analysis of the BFS model was conducted using the ANSYS Program and one of the available forms for applying damping in the analysis using ANSYS is Alpha damping and Beta damping. Alpha damping and Beta damping are used to define Rayleigh Damping constants  $\alpha$  and  $\beta$ . The damping matrix [C] is calculated by using these constants to multiply the mass



matrix  $[M]$  and stiffness matrix  $[K]$ :  $[C] = \alpha [M] + \beta [K]$ . The values of  $\alpha$  and  $\beta$  are not generally known directly, but are calculated from modal damping ratios,  $\xi_i$ .  $\xi_i$  is the ratio of actual damping to critical damping for a 'major' mode of vibration, (i). If  $\omega_i$  is the natural circular frequency of mode i,  $\alpha$  and  $\beta$  satisfy the relation  $\xi_i = (\alpha / 2 \omega_i) + (\beta \omega_i / 2)$ . To specify both Rayleigh damping coefficients  $\alpha$  and  $\beta$  which are applied in ANSYS for a given modal damping ratio  $\xi_i$ , it is commonly assumed that the sum of the  $\alpha$  and  $\beta$  terms is nearly constant over a range of frequencies. For the BFS model the Rayleigh damping coefficients  $\alpha$  and  $\beta$  were calculated as follows:

1. The modal analysis of the BFS model revealed that 99.3 % of mass of the building was captured for the sway ('major') mode in the z-direction in range of frequencies from 0.9 Hz to 1.6 Hz. Therefore the selected range of circular natural frequencies ( $\omega_i$ ) which contribute to the response of the BFS model was 5.5, 5.1, 5.2, 5.3, ..., 11 rad/sec depending on the frequency (Hz) =  $(\omega_i) / 2\pi$ .
2. In accordance with the ASCE standard, ref. [26], the damping ratio  $\xi_i$  of the reinforced concrete structures is equal to 0.07. Hence the approximate Rayleigh damping coefficients  $\alpha$  and  $\beta$  were computed numerically according to the following ASCE standard formulas (the resulting values of  $\alpha$  and  $\beta$  are 0.481 and 0.0088 respectively)

$$\alpha := \frac{2 \cdot \xi_i \cdot \omega_{\max} \cdot \omega_{\min}}{\omega_{\max} + \omega_{\min}}$$

$$\beta := \frac{2 \cdot \xi_i}{(\omega_{\max} + \omega_{\min})}$$

3. Afterward the values of  $\alpha$  and  $\beta$  were corrected and computed for every mode natural circular frequency  $\omega_i$  in the selected range of frequencies according to the formula of modal damping ratio  $\xi_i = (\alpha / 2 \omega_i) + (\beta \omega_i / 2)$  that  $\xi_{im} = (\alpha / 2 \omega_i)$  for mass proportional damping only ( $\beta = 0$ ) and  $\xi_{is} = (\beta \omega_i / 2)$  for stiffness proportional damping only ( $\alpha = 0$ ). Then the sum ( $\xi_{it}$ ) of  $\xi_{im}$  and  $\xi_{is}$  values for every mode natural circular frequency  $\omega_i$  was computed.
4. The values of  $\xi_{it}$ ,  $\xi_{im}$  and  $\xi_{is}$  were plotted versus the frequencies and from graphs the values of Rayleigh damping coefficients  $\alpha$  and  $\beta$  (values applied in the transient dynamic analysis) were computed as shown in the Fig. 3.23.



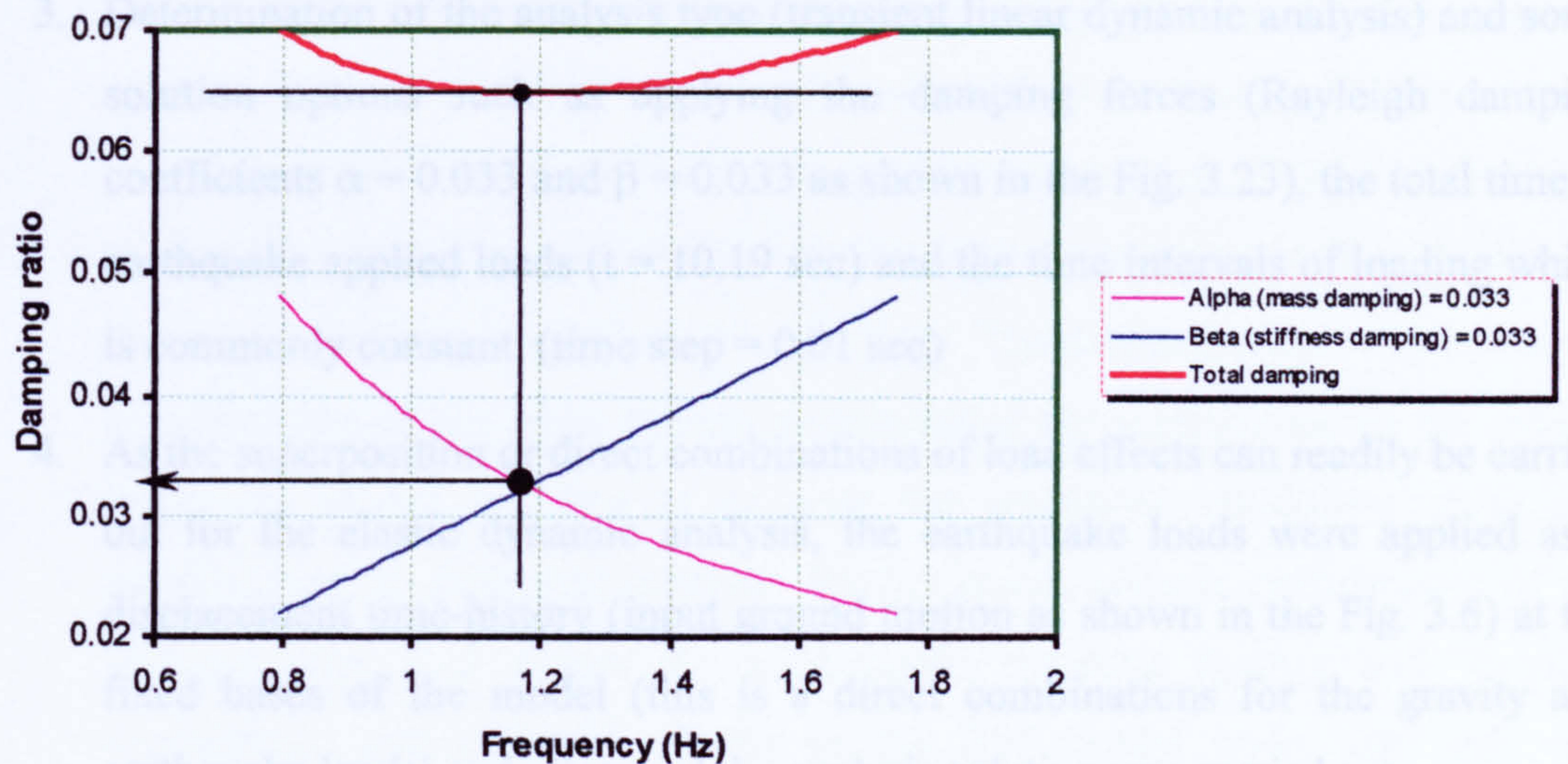


**Figure 3.23** Rayleigh damping coefficients (Alpha & Beta) of the UFS model

### 3.4.3 Three Dimensional Transient Dynamic Analysis

The three-dimensional transient linear dynamic analysis was carried out for the BFS model using ANSYS to determine the seismic response parameters (such as displacements, strains, stresses, and forces). Unlike the UFS model, the transient dynamic analysis of the BFS model was conducted in the presence of walls, damping forces and gravity loads in order to examine and determine the realistic seismic behaviour of existing RC buildings which are designed according to the normal design codes (such as BS-8110, ref. [3]). Also the effects of these factors (walls, damping forces and gravity loads) on the seismic behaviour of RC buildings through the comparison between the UFS model & this model (BFS) were studied and that will be presented later in the section 3.5.

In general, the analysis of the BFS model was carried out in accordance with the following main steps.

1. Creation of the three dimensional finite element model as shown in Fig. 3.20
2. Determination of the analysis type (transient linear dynamic analysis) and applying the gravity loads by using the gravitational constant  $9.81 \text{ m/s}^2$  acting on the appropriate density (mass) of the model



3. Determination of the analysis type (transient linear dynamic analysis) and some solution options such as applying the damping forces (Rayleigh damping coefficients  $\alpha = 0.033$  and  $\beta = 0.033$  as shown in the Fig. 3.23), the total time of earthquake applied loads ( $t = 10.19$  sec) and the time intervals of loading which is commonly constant (time step = 0.01 sec)
4. As the superposition or direct combinations of load effects can readily be carried out for the elastic dynamic analysis, the earthquake loads were applied as a displacement time-history (input ground motion as shown in the Fig. 3.6) at the fixed bases of the model (this is a direct combinations for the gravity and earthquake loads) and afterward the analysis solution was carried out

The transient dynamic analysis of this model (BFS) was applied under two types of time-history, horizontal time-history alone that contains two orthogonal components (two dimensional seismic action in the directions x, z), and both horizontal & vertical time-history together that contain three orthogonal components (three dimensional seismic action in the directions x, z, y).

#### 3.4.3.1 Analysis under Horizontal Earthquake

A transient dynamic analysis (time – history analysis) was carried out for the BFS model under the horizontal displacement time – history input motion alone (see Fig.3.6). The displacement time-history was applied directly to the fixed bases of the model in x, z directions as a two-dimensional input motion. The complete response history (seismic behaviour) of the building was evaluated by the response parameters such as maximum amplitude of the relative displacement, the relative velocity and the absolute acceleration developed during a seismic excitation. Also the resulting forces (such as maximum stresses, strains, moments and shear & axial loads) were used to determine the dynamic response of the building. Investigation of the transient dynamic analysis results of the BFS model under horizontal input motion shows that:

1. The lateral displacements ( $u_x, u_z$ ) increase with the height of building until they reach their maximum values at the upper floor. Fig. 3.24 shows the displacement time-histories of building floors that were excited from the input motion. Also this figure shows the comparison between displacements values of input motion



and the excited displacements at floors. By generating the acceleration response spectra of the excited displacement time histories of the building floors in the x-direction, it was noted that the peak ground acceleration (PGA) of the input motion (0.2g) was amplified through the higher elevation of the building at natural frequencies range from 1.5 to 2.5 Hz. The determination of the resonant amplification of the input motion demonstrates the significance of the natural frequency of the building at or near the resonance conditions. Also this amplification is important criterion for the global seismic performance of the building. Fig. 3.25 shows the acceleration response spectra and its peak acceleration values for the floors of the BFS model under the horizontal earthquake.

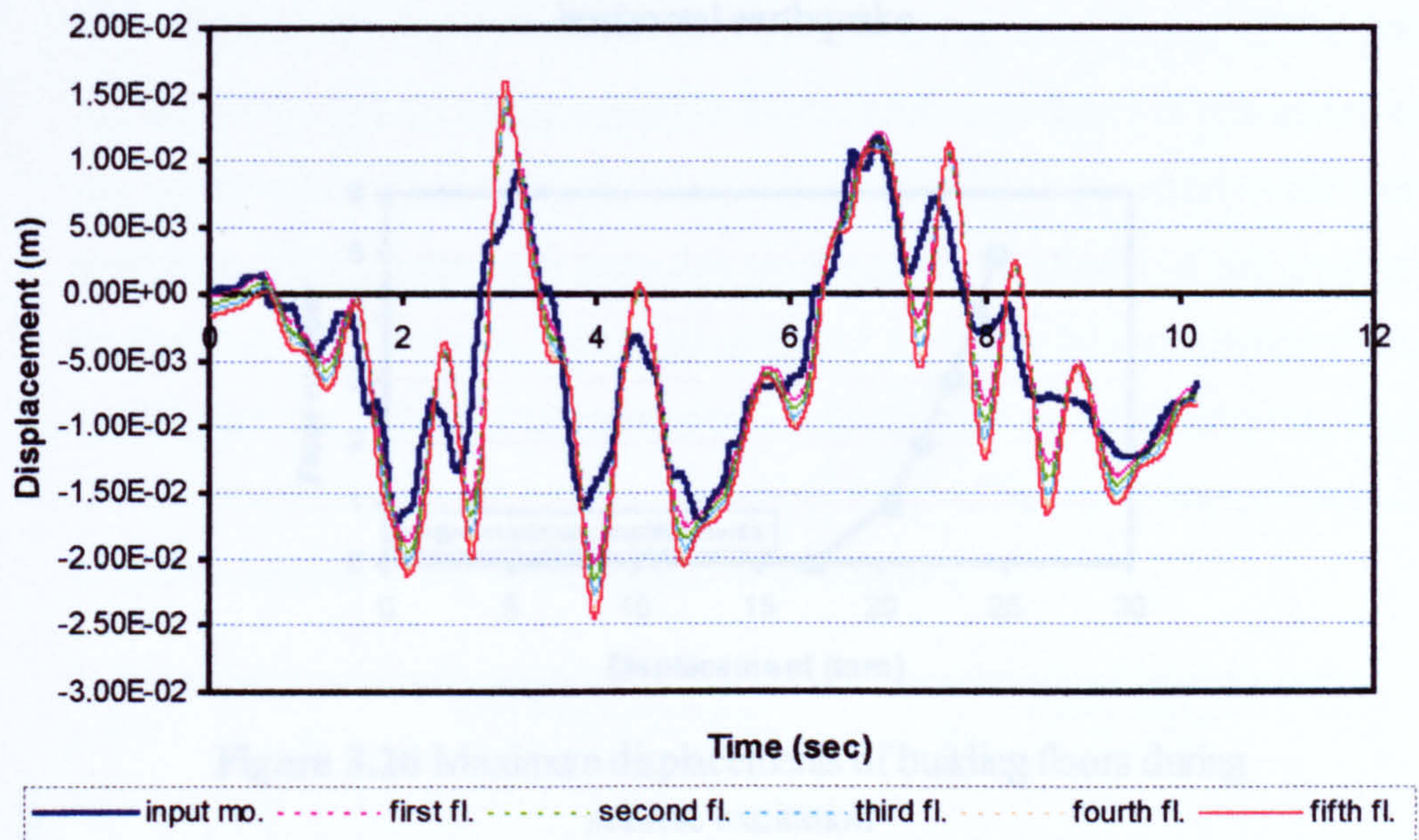


**Figure 3.24** Displacement time-histories of building floors and input motion

Figures 3.26, 3.27, 3.28 show the envelopes of lateral displacements, shear forces (lateral forces) and columns moments of the BFS model under the earthquake. From these figures it can be noted that the minimum displacements occur at the base and increases at each floor to reach its maximum value at upper floor. The maximum shear forces and columns moments occur at the base of the building. The distribution of shear forces and column moments is particularly dramatic due to the effects of walls and the stiffness discontinuities in the building.



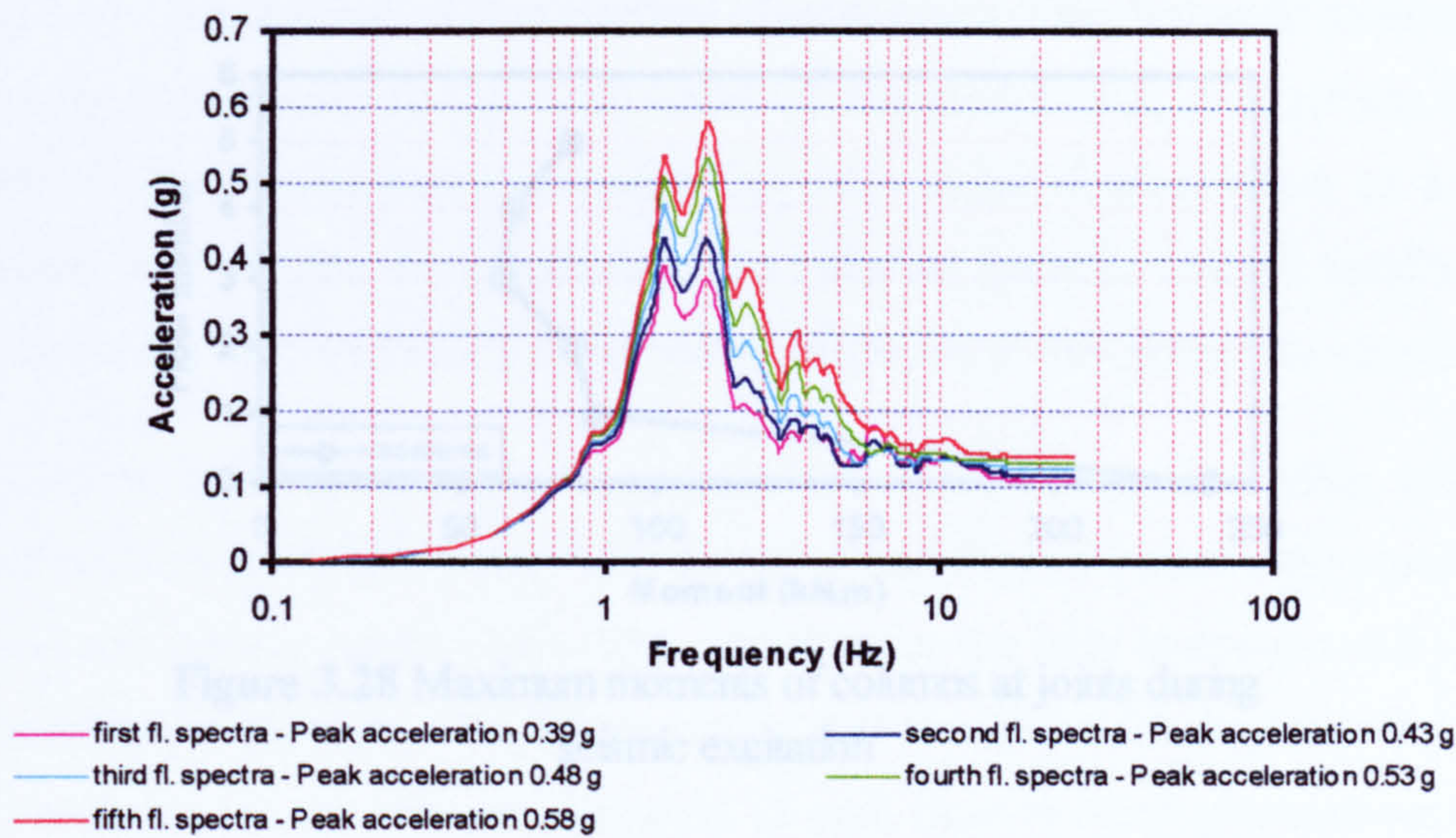


Figure 3.25 Acceleration response spectra of BFS floors under horizontal earthquake

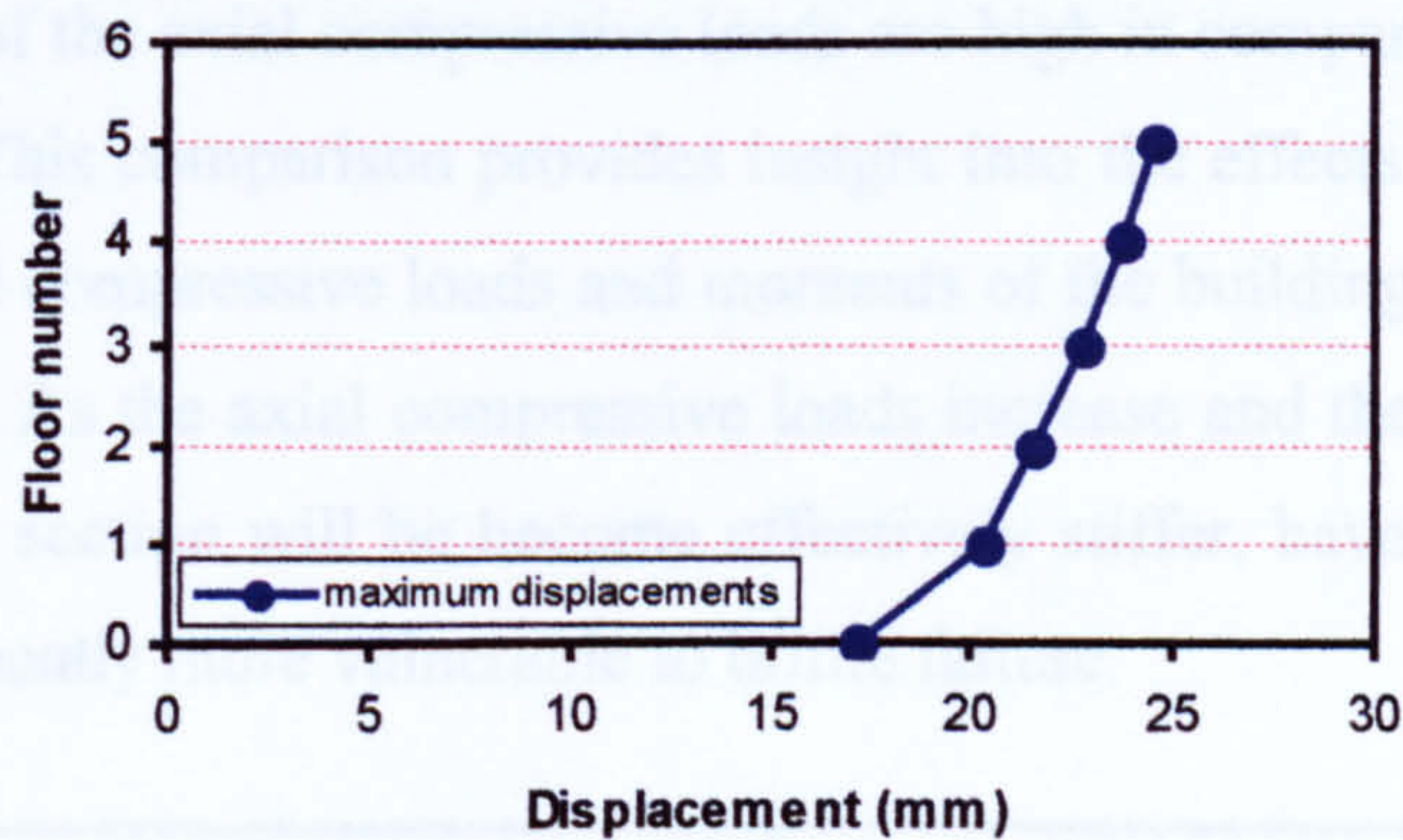


Figure 3.26 Maximum displacements of building floors during seismic excitation

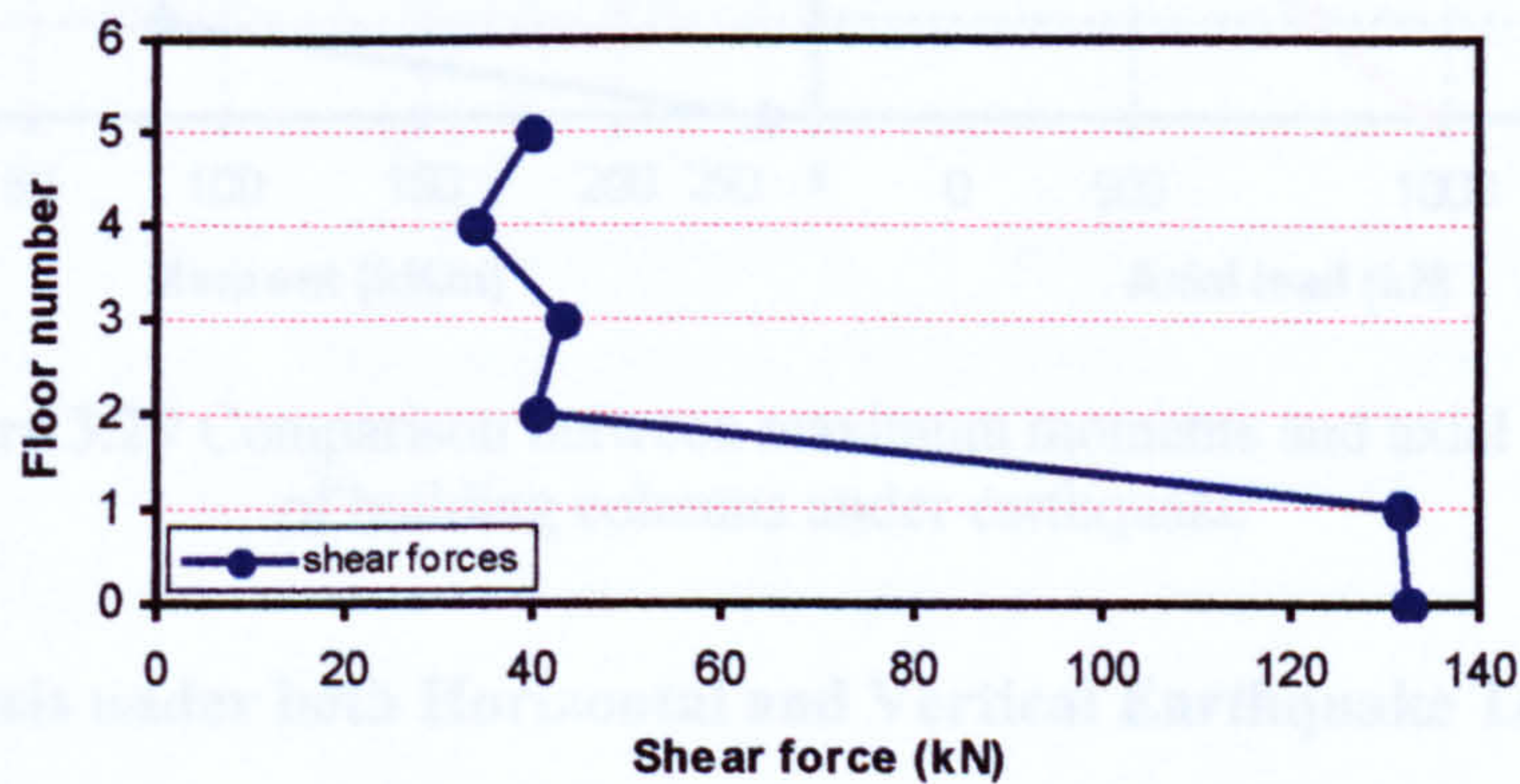


Figure 3.27 Maximum shear forces at building floors during seismic excitation



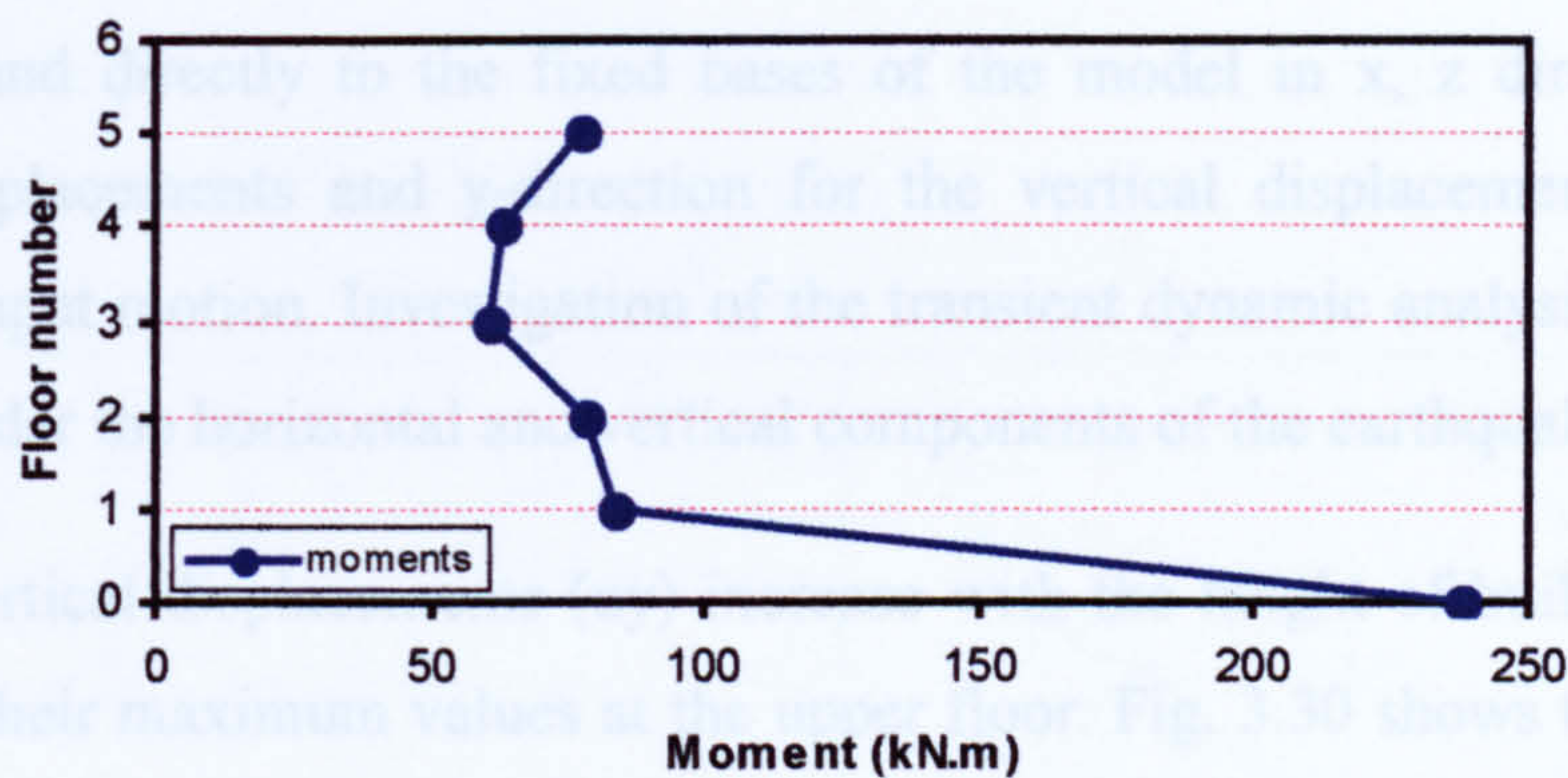


Figure 3.28 Maximum moments of columns at joints during seismic excitation

2. Fig. 3.29 shows the envelopes of moments and axial compressive loads of the BFS columns during the earthquake. The resulting axial forces of the columns are due to the gravity and earthquake loads. From this figure it was observed that the values of the axial compressive loads are high in comparison to the values of moments. This comparison provides insight into the effects of the gravity loads on the axial compressive loads and moments of the building columns during the earthquake. As the axial compressive loads increase and the moments decrease, the column section will be become effectively stiffer, have lower ductility and are consequently more vulnerable to brittle failure.

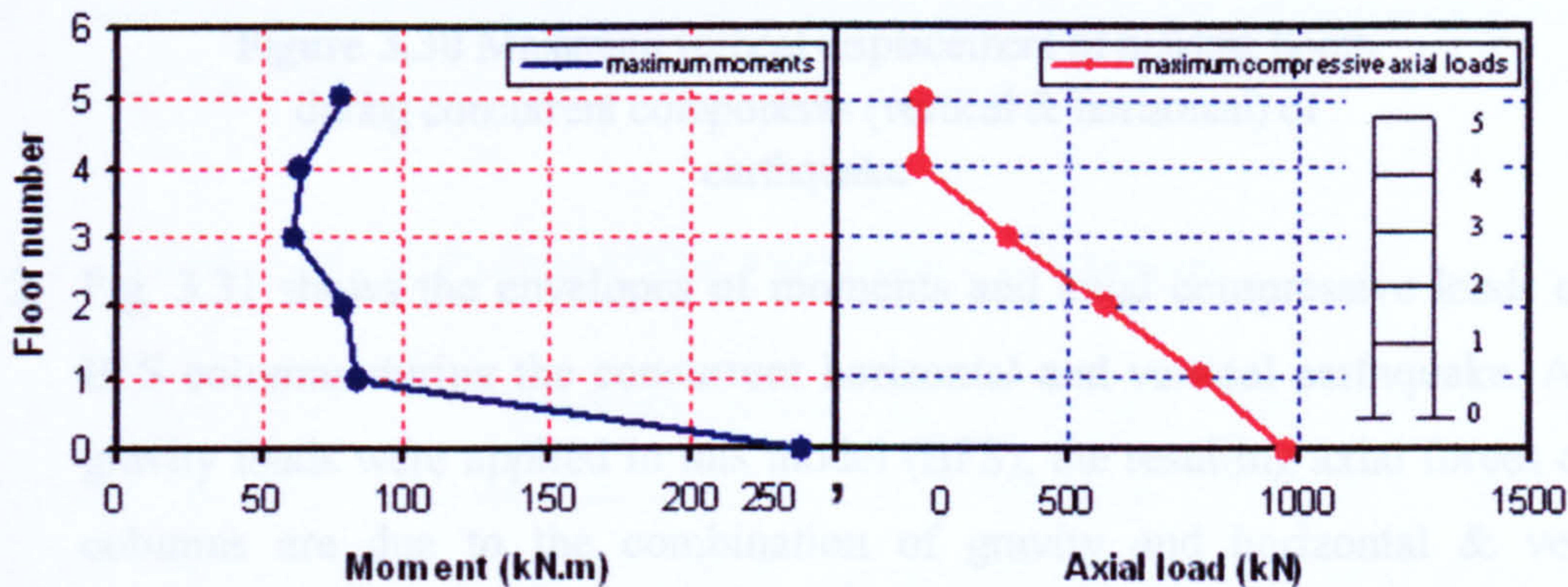


Figure 3.29 Comparison between maximum moments and axial loads of building columns under earthquake

3.4.3.2 Analysis under both Horizontal and Vertical Earthquake Together

The transient dynamic analysis (time – history analysis) was carried out for the BFS model under both horizontal and vertical displacement time – histories together



(see Fig.3.6). The horizontal and vertical displacement time-histories were applied concurrently and directly to the fixed bases of the model in x, z directions for the horizontal displacements and y-direction for the vertical displacements as a three-dimensional input motion. Investigation of the transient dynamic analysis results of the BFS model under the horizontal and vertical components of the earthquake shows that:

1. The vertical displacements ( $u_y$ ) increase with the height of building until they reach their maximum values at the upper floor. Fig. 3.30 shows the envelope of vertical displacements of the BFS model under the both horizontal and vertical earthquake together. This figure shows that the minimum displacements (11.5 mm) occur at the base and increases at each floor to reach its maximum value (15.75 mm) at upper floor. This is expected due to the amplification effects through the higher elevations of the building.

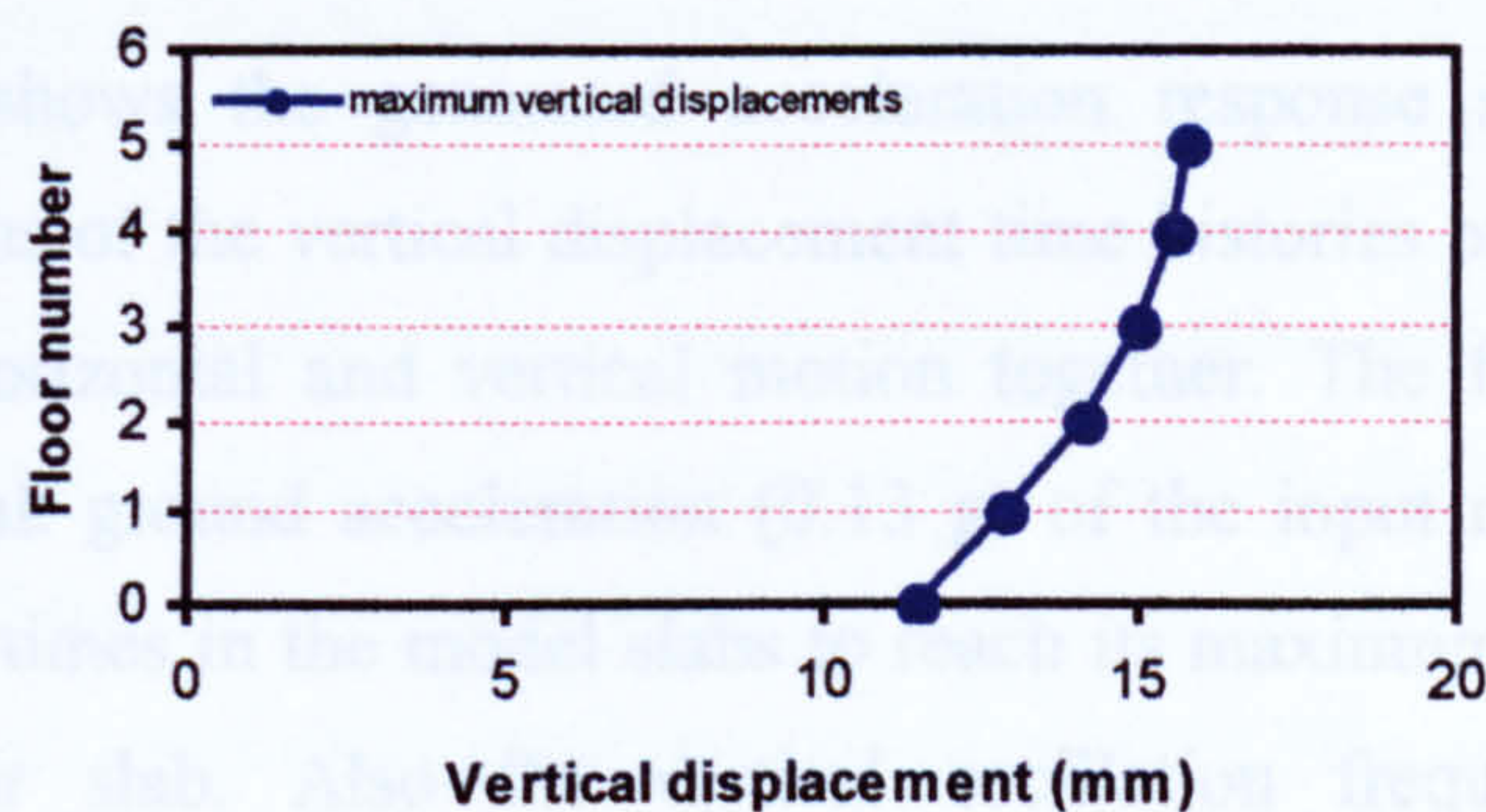


**Figure 3.30** Maximum vertical displacement of building floors during concurrent components (vertical & horizontal) of earthquake

2. Fig. 3.31 shows the envelopes of moments and axial compressive loads of the BFS columns during the concurrent horizontal and vertical earthquake. As the gravity loads were applied in this model (BFS), the resulting axial forces of the columns are due to the combination of gravity and horizontal & vertical earthquake loads. The comparison between figures 3.31 (under both horizontal & vertical earthquake together) and 3.29 (under horizontal earthquake only) shows that the values of moments and axial compressive loads remained generally unchanged.
3. In several recent earthquakes (such as Northridge earthquake 1994, Hyogo-ken Nanbu 1995), it was observed that the vertical earthquake ground motion caused



considerable damage to the slabs of the RC buildings due to the resonant amplification of the vertical earthquake that result in high frequencies larger than the natural frequencies of the slabs.

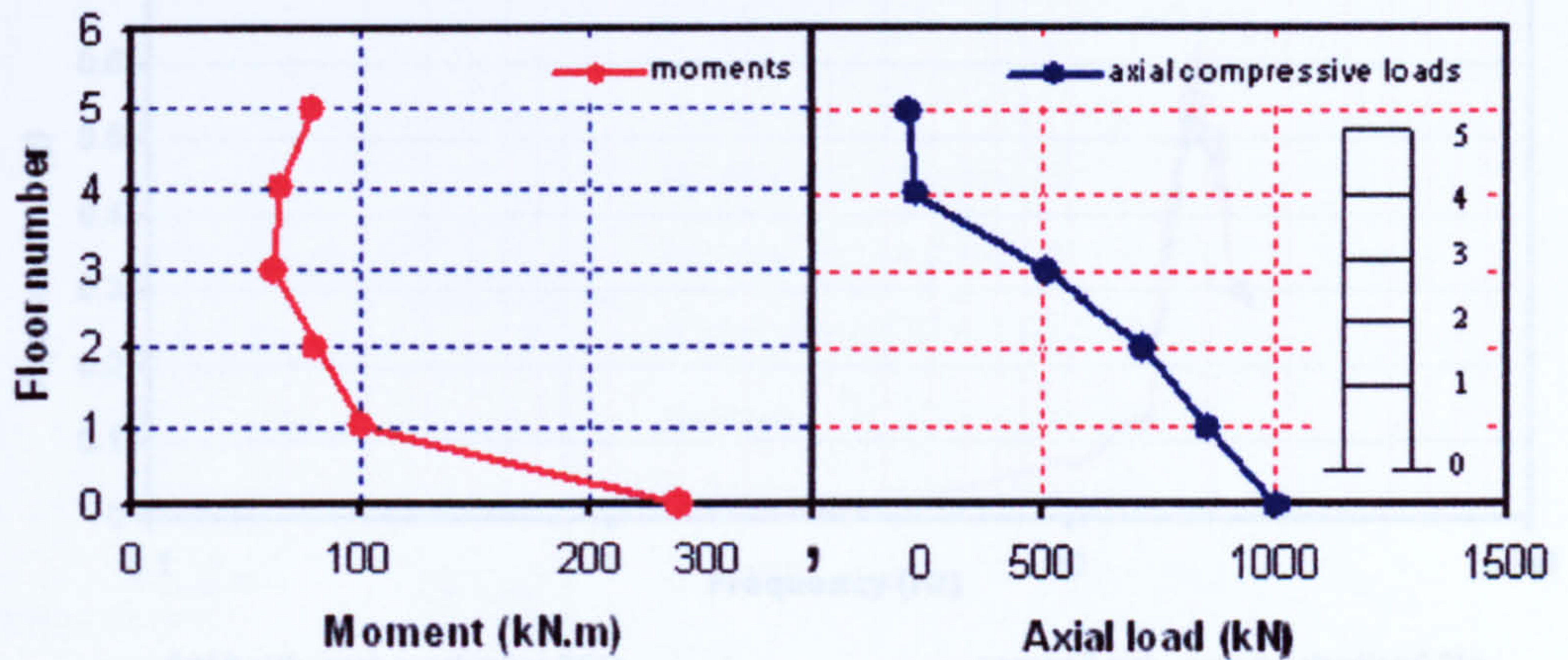


**Figure 3.31** Comparison between maximum moments and axial loads of building columns under horizontal & vertical earthquake

Fig. 3.32 shows the generated acceleration response spectra and its peak accelerations of the vertical displacement time histories of the BFS slabs under the both horizontal and vertical motion together. The figure shows that the vertical peak ground acceleration (0.13 g) of the input motion was amplified nearly five times in the model slabs to reach its maximum value (0.63 g) at the upper floor slab. Also the vertical oscillation frequencies at the peak accelerations of the slabs response spectra are very high (approximately ranging from 18 to 25 Hz).

### 3.4.3.3 Verification of Results Using Analytical Calculations

An analytical calculation was carried out for the BFS model in order to obtain the maximum limit value for the peak ground acceleration (PGA) of the horizontal earthquake that the building can withstand. The comparison between the analytical peak ground acceleration and the actual PGA of the horizontal input motion (0.2 g) that was applied in the transient dynamic analysis using ANSYS will verify the stabilization of the BFS model during the seismic action in addition to the dynamic analysis results of ANSYS. Also the peak acceleration values (analytically & ANSYS) of seismic response of the first floor can be compared. The peak ground acceleration that the building can withstand and also the value at the first floor was calculated with respect to the gravity



loads plus the overturning moment which is developed from the horizontal earthquake as shown in the Fig.3.33.

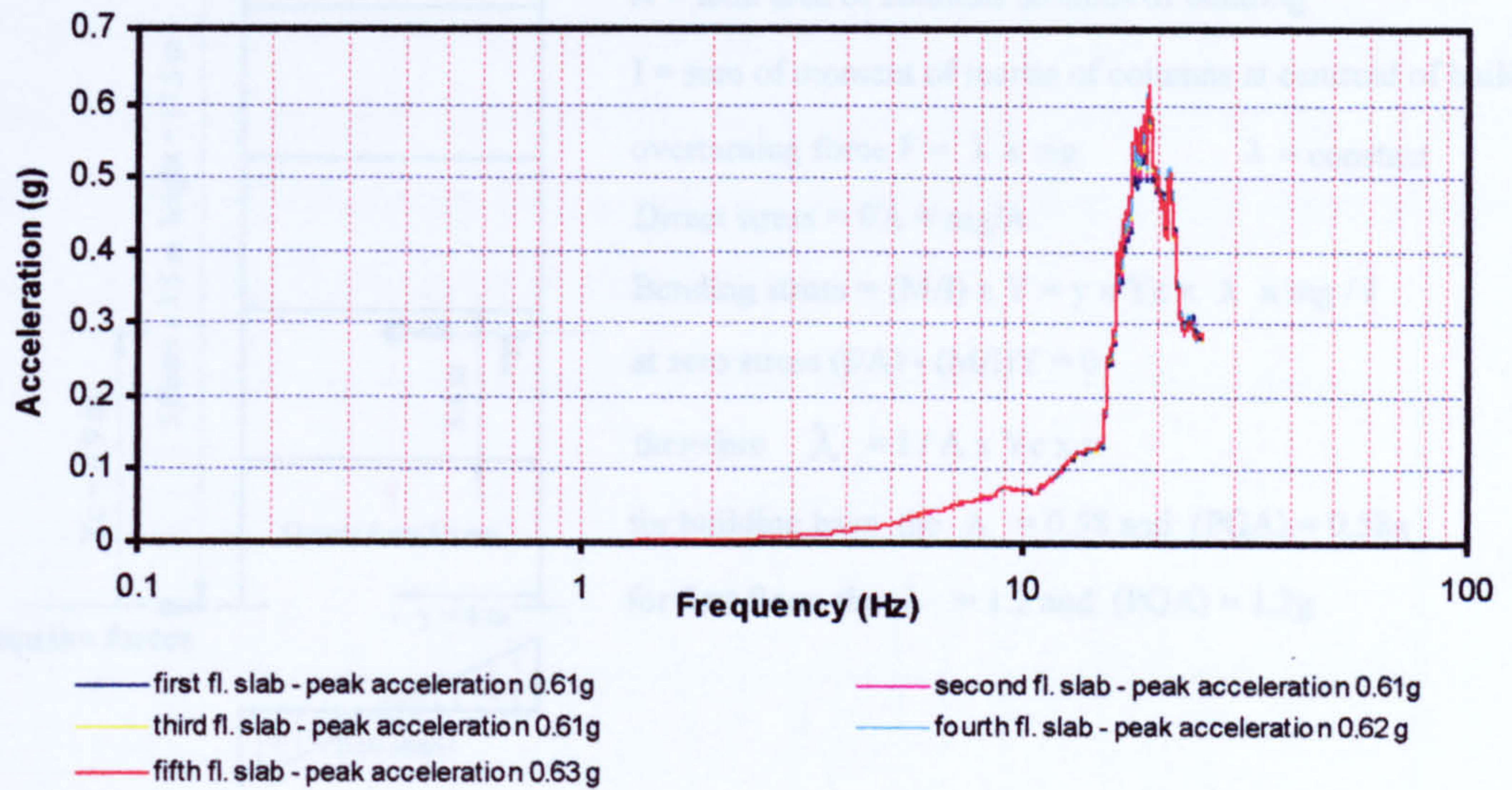


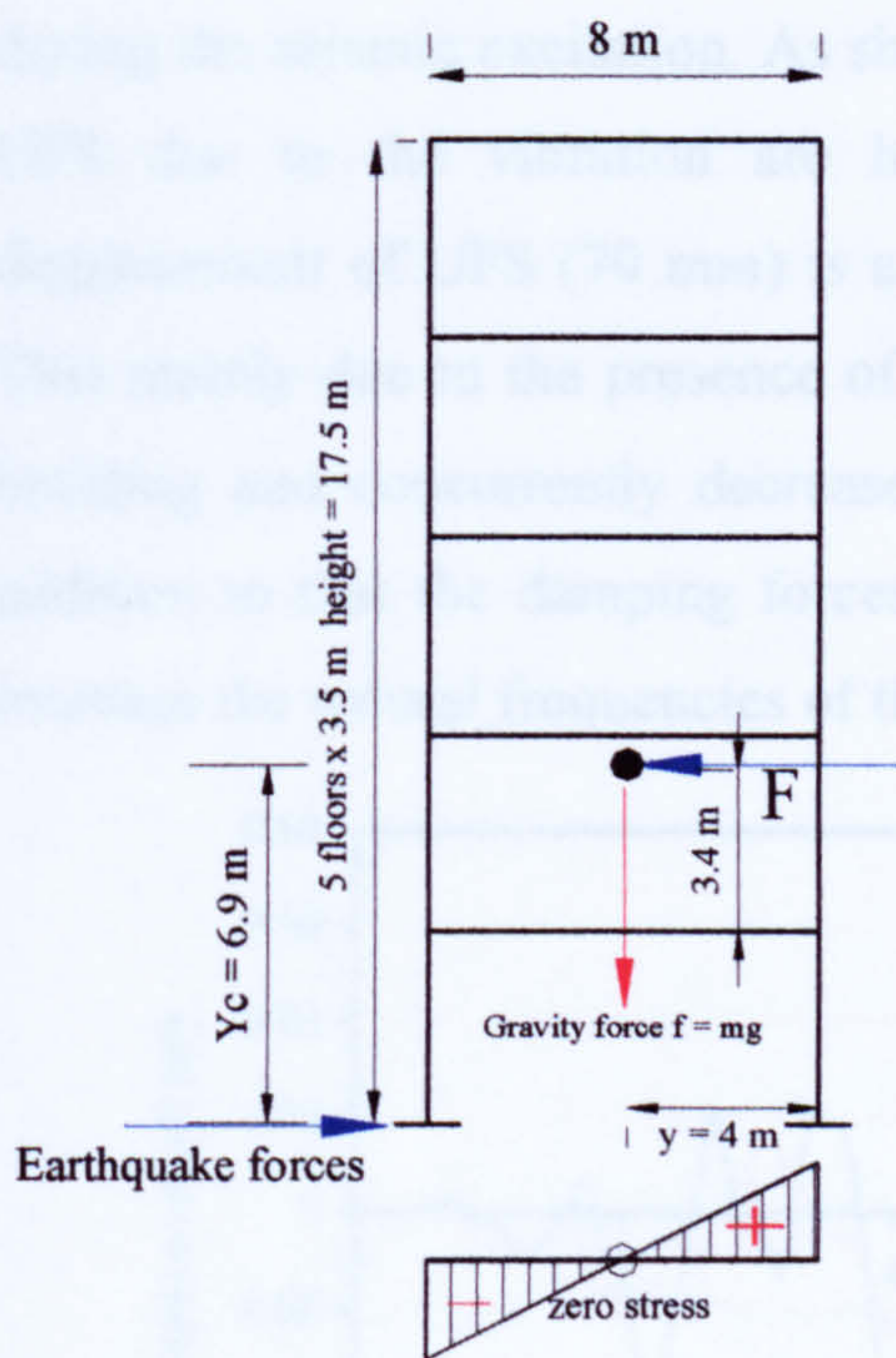
**Figure 3.32** Acceleration response spectra of slabs of building floors under both horizontal and vertical earthquake together

From the analytical calculation, it was found that the maximum limit value of the PGA that the building can stabilize against the overturning is equal to 0.58g. Also the analytical value of the first floor is equal to 1.2g. The ANSYS analysis of the BFS model under the horizontal earthquake only produced 0.2g PGA for the base of building and 0.39g PGA for the first floor (refer to Fig 3.25). The analytical PGA values are three times the ANSYS values and satisfy the amplification of the input motion through the higher elevation of the building. Therefore the comparison between the analytical & ANSYS results is in good agreement & provides confidence in the ANSYS transient dynamic analysis. Also as the analytical PGA values (0.58g, 1.2g) are larger than the applied values (0.2g, 0.39g), it is concluded that the building may have sufficient resistance against collapse during the earthquake.

### 3.5 Discussion of Seismic Response of the unbraced and braced 5-storey RC Building

A study of the disparity in the seismic response of the unbraced and braced 5-storey RC building will demonstrate the effects arising from the gravity loads, damping forces and bracing (walls) on the response of such buildings under the earthquake.





$m$  = total mass of building  
 $g$  = acceleration of gravity  $9.81 \text{ m/s}^2$   
 $A$  = total area of columns sections of building  
 $I$  = sum of moment of inertia of columns at centroid of building  
 overturning force  $F = \lambda \times mg$        $\lambda$  = constant  
 Direct stress  $= f/A = mg/A$   
 Bending stress  $= (M/I) \times Y = y \times Y_c \times \lambda \times mg / I$   
 at zero stress  $(f/A) - (M/I)Y = 0$   
 therefore  $\lambda = I / A \times Y_c \times y$   
 for building base, the  $\lambda = 0.58$  and  $(\text{PGA}) = 0.58g$   
 for first floor, the  $\lambda = 1.2$  and  $(\text{PGA}) = 1.2g$

**Figure 3.33** Analytical calculations of PGA for the BFS model under horizontal earthquake only

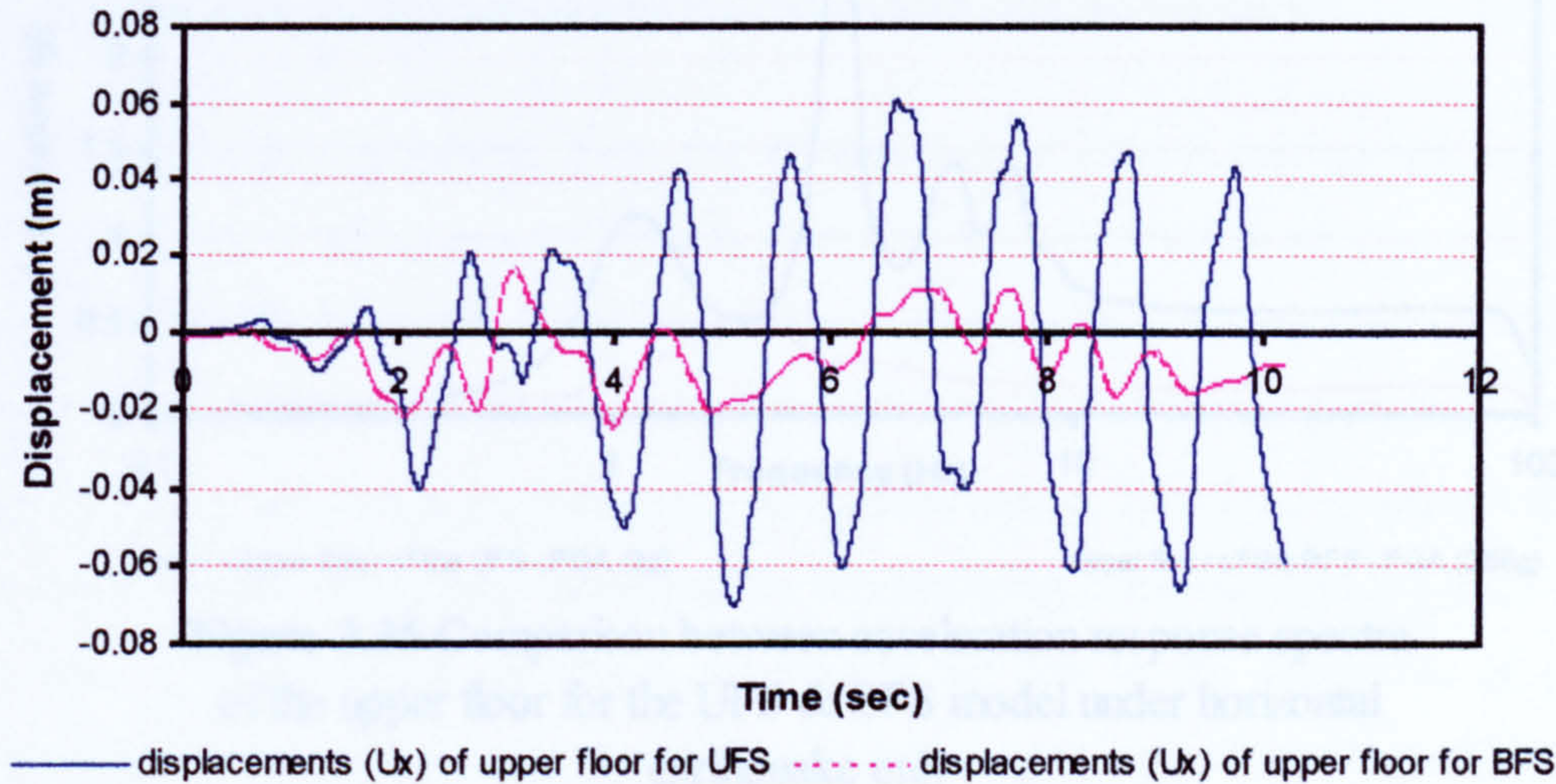
In general, an appropriate value of the gravity loads and damping forces reduces the resonant amplification of the input motion and consequently the applied seismic forces on the building will be decreased. Also the structural walls (brick or block walls) increase the stiffness of the building and subsequently the global seismic resistance against collapse (the formation of soft storey must be avoided due to the irregularities of walls). In the next section a study for the effects of these factors on the seismic response of the RC buildings will be presented through the comparison between the unbraced and braced 5-storey RC building.

### 3.5.1 Effects Study of Gravity Loads, Damping Ratio, and Infill Walls

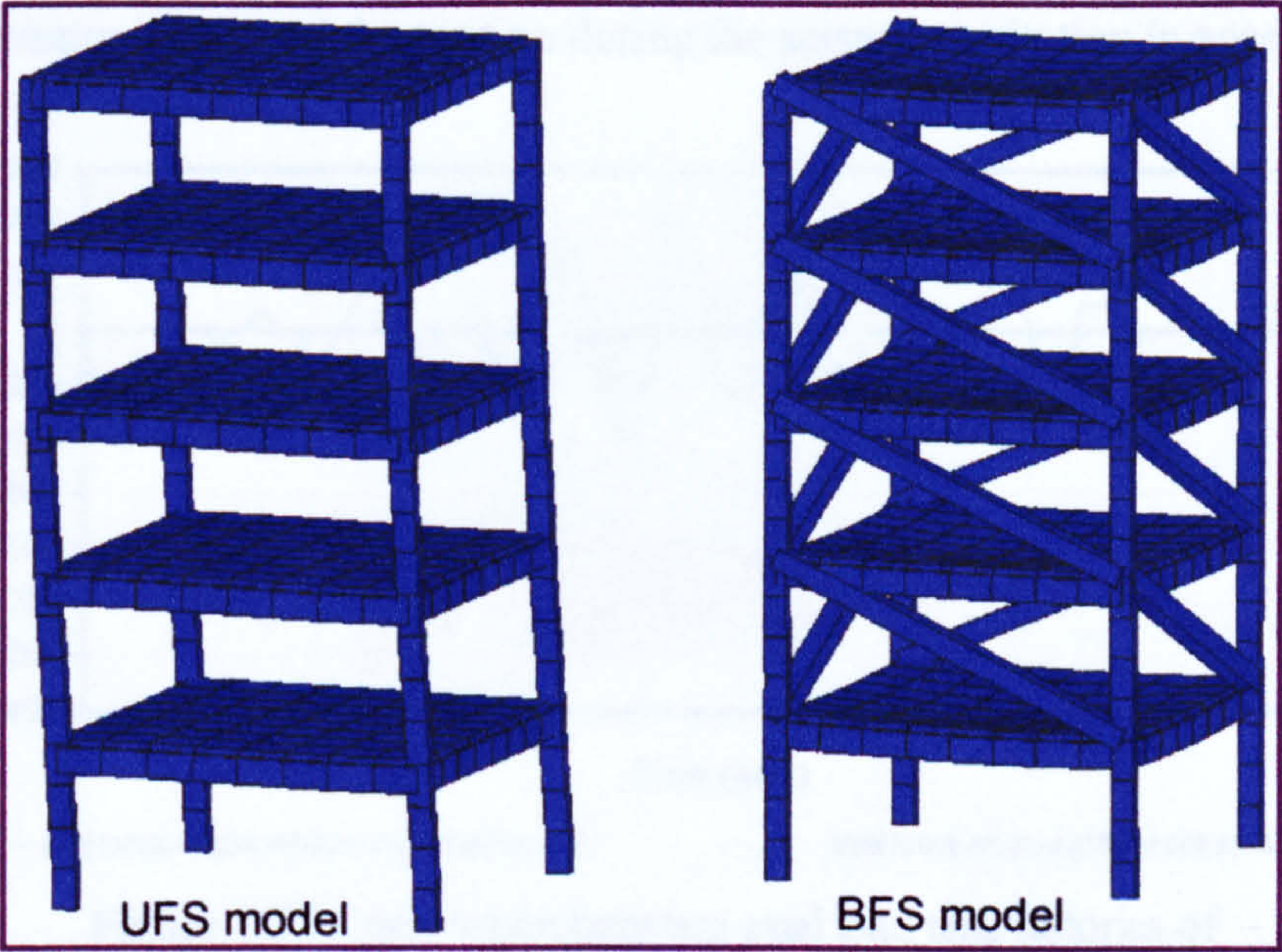
In order to study the effects of gravity loads, damping ratio and infill panels, a comparison was made between the seismic responses of the UFS & BFS model under the horizontal earthquake only. This comparison highlighted the difference in displacements, axial forces of columns and the amplification of the input ground motion. Fig. 3.34 shows the displacement time histories ( $u_x$ ) of the upper floor for the UFS & BFS model during the seismic excitation. Also Fig.3.35 shows the displaced shapes of the UFS & BFS finite element model at the maximum drift of the upper floor



during the seismic excitation. As shown in these figures, the resulting displacements of UFS due to the vibration are high in comparison to the BFS. The maximum displacement of UFS (70 mm) is approximately three times the BFS model (25 mm). This mainly due to the presence of bracing (walls) which increase the stiffness of the building and concurrently decrease the horizontal displacements of the columns. In addition to that the damping forces reduce the amplification of the input motion and increase the natural frequencies of the building.



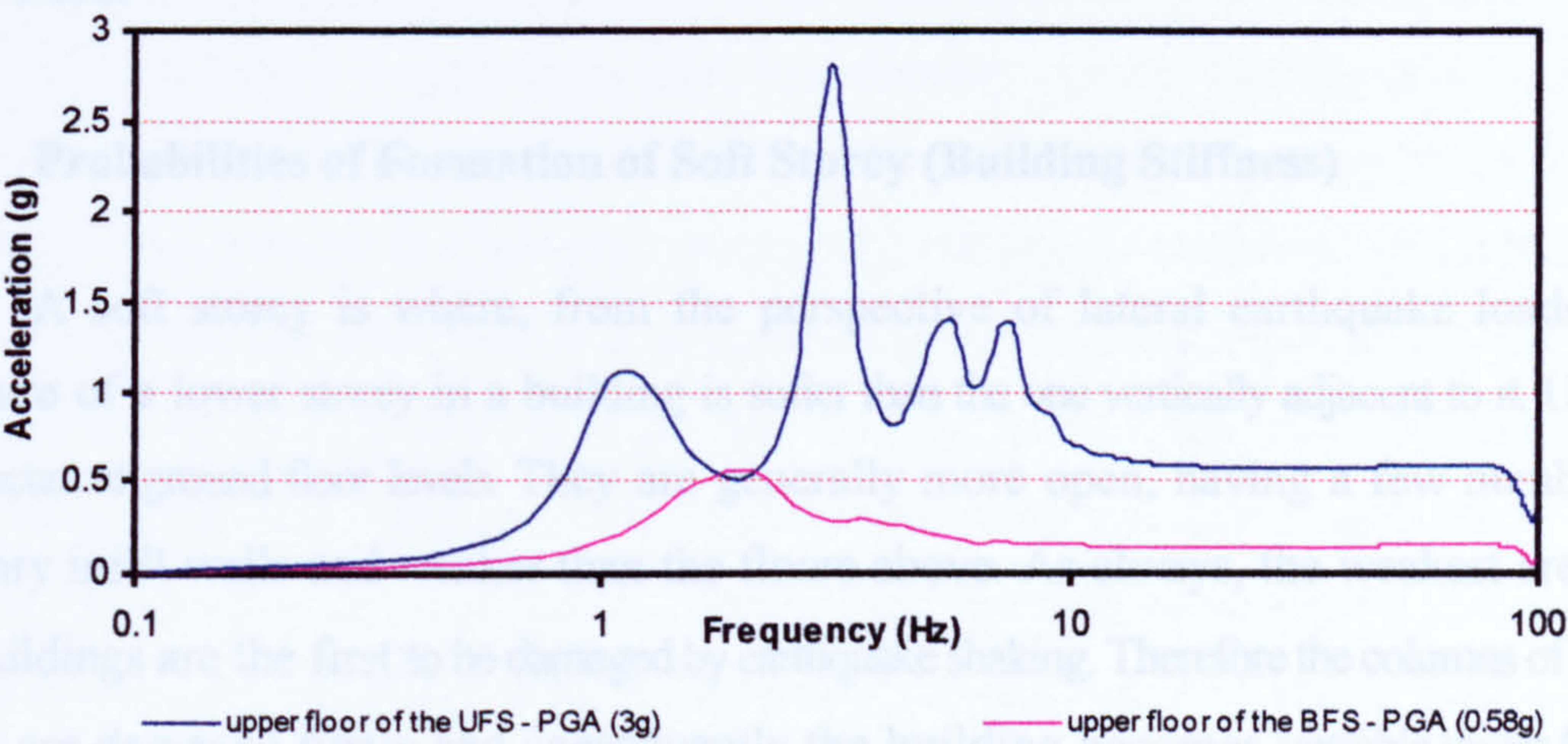
**Figure 3.34** comparison between excited displacement time histories of upper floor for the UFS & BFS model under horizontal earthquake only



**Figure 3.35** Deformed shape of the UFS & BFS model at maximum drift of the upper floor under horizontal earthquake only

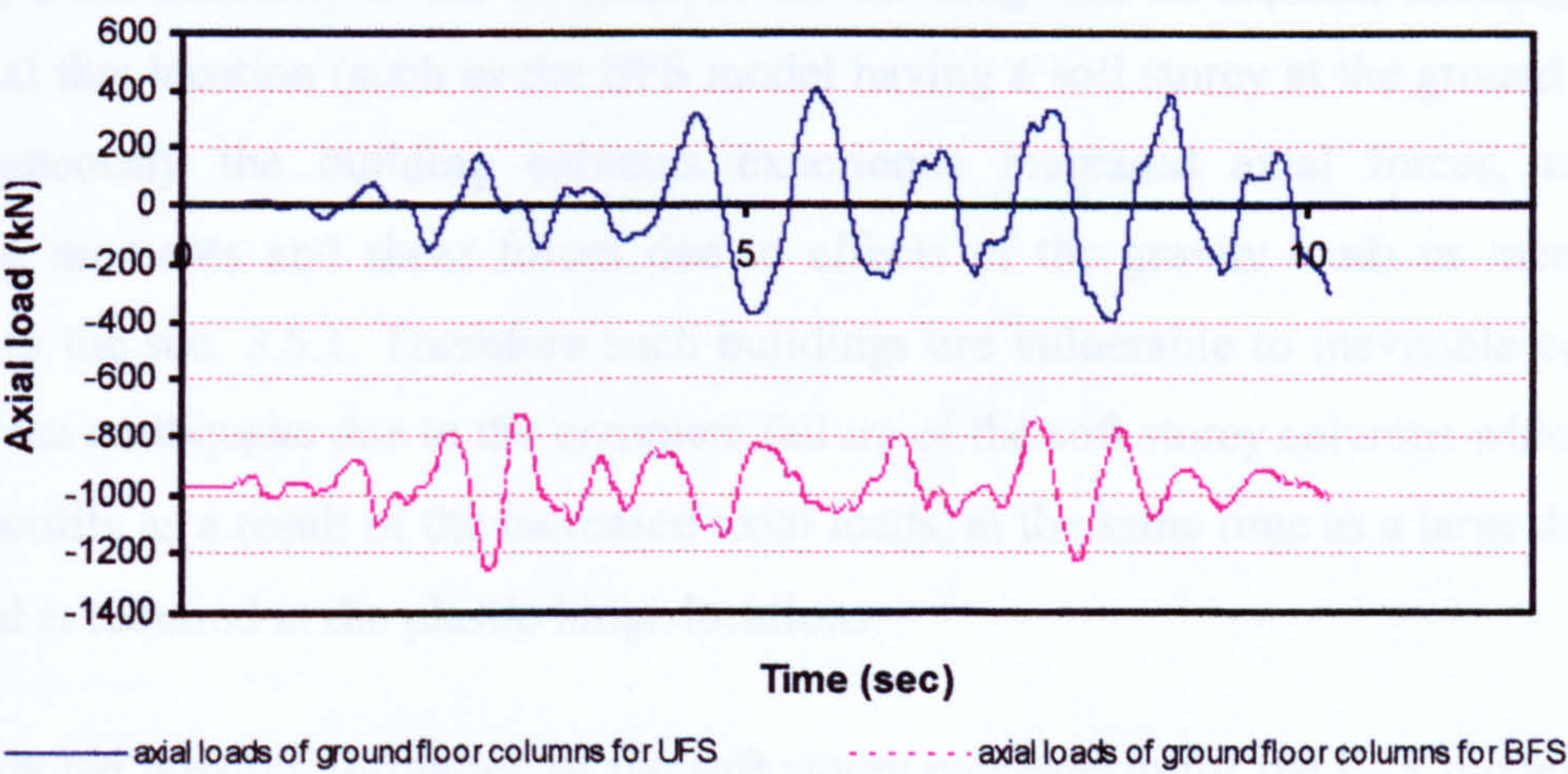


Fig. 3.36 shows the acceleration response spectra of the upper floor (which were generated from the displacement time histories in the Fig.3.34) of the UFS & BFS model under the horizontal earthquake. This figure demonstrates the significance of damping forces in reducing the resonant amplification of the earthquake that the PGA of UFS is nearly six times the BFS model at a higher frequency.



**Figure 3.36** Comparison between acceleration response spectra of the upper floor for the UFS & BFS model under horizontal earthquake only

Fig. 3.37 shows the axial load time-history of ground floor columns of the UFS & BFS model under the horizontal earthquake. This figure exhibits the effects of gravity loads on the axial loads of the columns. For the UFS model the axial loads of columns change among the compression and the tension during the seismic excitation in accordance with



**Figure 3.37** Comparison between axial load time histories of ground floor columns for the UFS & BFS model under the horizontal earthquake only



the values and directions of the resulting forces especially the generated overturning moments. For the BFS model, due to the presence of gravity loads the axial loads of columns are completely in compression having high values. This figure reveals thoroughly the role of the gravity loads in the structural integrity of the building during the earthquake. This point will be discussed in detail later on through the major model of the work.

### **3.5.2 Probabilities of Formation of Soft Storey (Building Stiffness)**

A soft storey is where, from the perspective of lateral earthquake loads, the structure of a lower storey in a building is softer than the one vertically adjacent to it. Usually this occurs at ground floor levels. They are generally more open, having a few number of masonry infill walls and weaker than the floors above. As always, the weakest areas of the buildings are the first to be damaged by earthquake shaking. Therefore the columns of a soft storey are damaged firstly and consequently the building becomes unstable under further lateral loads. Columns of the soft storey commonly fail due to the formation of plastic hinges at their tops and bottoms thereby only requiring a limited number of hinges to form before a global sway collapse occurs. Soft storey failure is a major cause of building collapse during damaging earthquakes.

Although the presence of the infill walls for the RC buildings increases the global stiffness of these buildings, when infills are not placed in a storey similar to the other stories, a discontinuity in the stiffness of the building will be created, forming a soft storey at this location (such as the BFS model having a soft storey at the ground floor). Simultaneously the building columns experience increased axial forces, reduced bending moments and shear forces due to effects of the gravity loads as mentioned above in the sec. 3.5.1. Therefore such buildings are vulnerable to inevitable collapse during the earthquake due to the complete failure of the soft storey columns which have low ductility as a result of the increased axial loads, at the same time as a large ductility demand is required at the plastic hinge locations.

To study the possible formation of the soft storey mechanism for the BFS model under the horizontal earthquake only, it was referred to in figures 3.26, 3.28, 3.29 to investigate the resulting forces (horizontal displacements, bending moments and axial loads) during the earthquake at the first floor (the possible soft storey and is commonly



called ground floor). These resulting forces were examined for the soft storey forces as mentioned above. It was found that the maximum bending moments of the first floor and second floor columns were equal to 238 kN.m & 83 kN.m respectively i.e. the first floor has an applied moment larger than second floor by 65 % and consequently larger ductility demand than other stories. Along with the maximum axial force of the first floor columns equal to 971 kN i.e. the value of axial force is four times the bending moment therefore the columns may have low ductility. As the ductility demand at any column section during the earthquake can be measured by the percentage of the relative horizontal displacement at this section to the total relative displacement of the building, it was found that the total relative displacement of the BFS was equal to 7.4 mm ( $\Delta$  as shown in the Fig.3.38) and at top of the first floor 3.2 mm i.e. the relative displacement at top of the first floor was equal to 42 % of the total relative displacement that confirms the large ductility demand at the first floor. Then it could be concluded that the soft storey mechanism was likely to form for the BFS model. Fig. 3.38 shows the displaced shape of the BFS model at the maximum moment for the first floor columns (238 kN.m) during the earthquake.

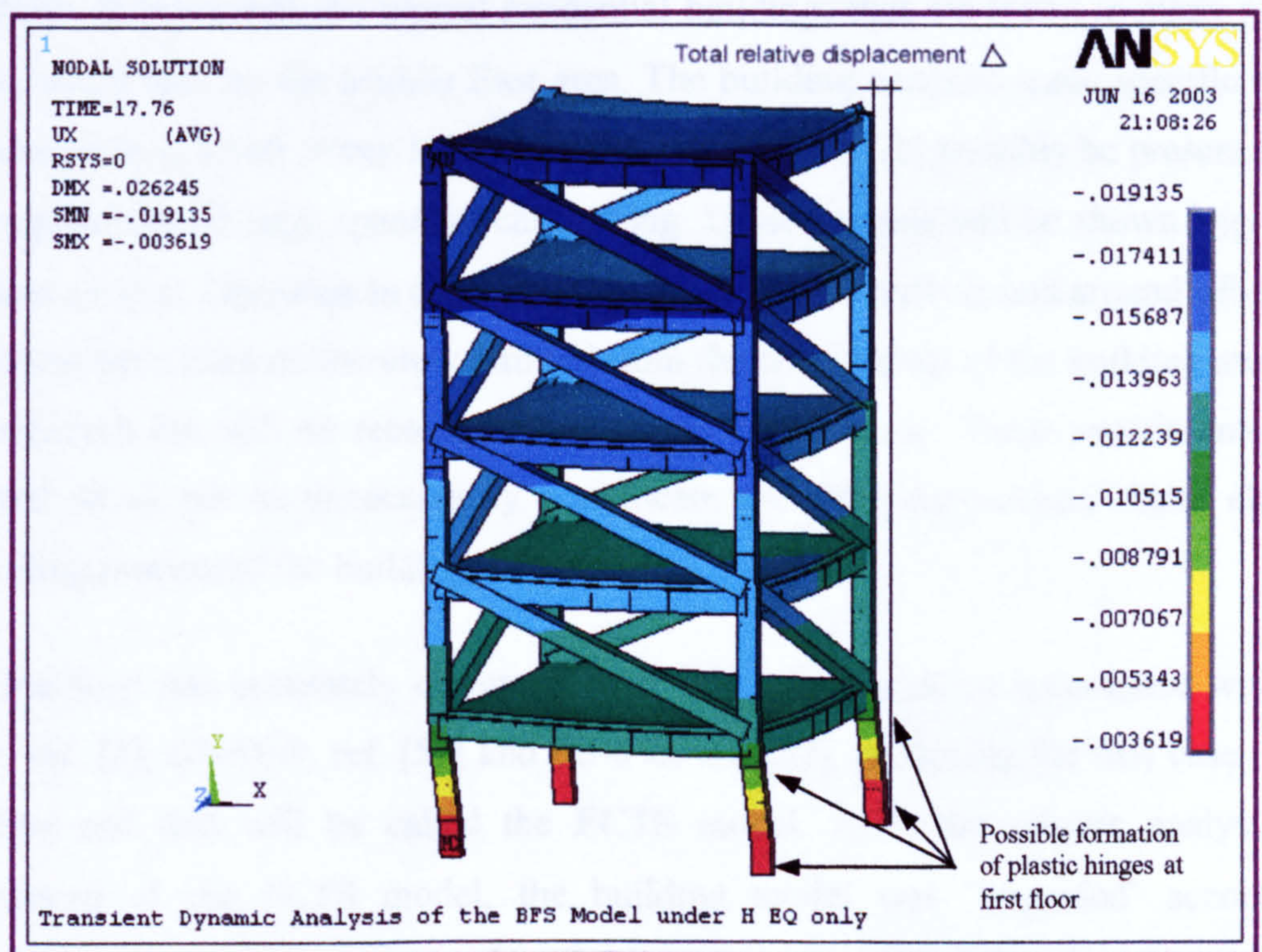


**Figure 3.38** Displaced shape of the BFS model at maximum moment of the first floor columns during the horizontal earthquake (various colours indicate to the horizontal displacements  $u_x$  in meter)



## **CHAPTER 4 THREE DIMENSIONAL MODELLING AND ANALYSIS**

### **4.1 Static Design Of The Ten-Storey RC Building**

Multi-storey framed RC buildings designed according to early seismic codes or without any seismic provision, have usually low resistance against earthquakes, and especially the buildings that contain a soft storey (which in most cases show a complete failure due to the formation of the soft-storey collapse mechanism). Because of these problems, the analysis and assessment of existing multi-storey RC buildings is required and necessitates a refined procedure. Hence the analysis and assessment of the seismic response of an existing ten-storey framed RC building is herein applied and examined.

In the absence of any available plans of existing multi-storey RC buildings, an accurate design in accordance with the BS-8110, ref. [3], of a 10 storey RC two-way frame building was produced. This building was selected as the main model of this research in order to examine the realistic seismic response of the existing multi-storey RC buildings. It represents the typical residential buildings that are found in many regions of the world such as the Middle East area. The building contains some specific design features such as a soft storey in the ground floor which could possibly be present due to the requirement of large spans for car parking. These features will be shown later on in the next section. Openings in the floor and non-structural walls at and around lift-shafts, and stairs have been deliberately omitted from the constituents of the building model in this research but will be recommended for any future work. These constituents were omitted so as not to unnecessarily complicate the three-dimensional finite element modelling process of the building.

The building was accurately designed under its gravity loads in accordance with BS-8110, ref. [3], BS-6399, ref. [51] and BS-648, ref. [52], producing the first case of this building and that will be called the FCTS model. After the seismic analysis and assessment of the FCTS model, the building model was ‘upgraded’ accordingly depending on the assessment results of this model to produce the second case of the building and that will be called the SCTS model. In the SCTS model the section dimensions of the all ground floor columns were increased to 1m x 1m in comparison to the FCTS model in which its ground floor columns have dimensions 0.8m x 0.8m &



0.6m x 0.8m (this only the disparity between the FCTS & SCTS model). The purpose of this upgrade is to study the effect of the stiffness factors on the soft storey and consequently the collapse of building. These points will be discussed in detail later on in the next chapters. The sequence and details of the design (calculation sheet of design) for the building models (FCTS & SCTS) according to the static design regulations, and the difference between them is included in **Appendix II**.

In the first instance after implementation of the static design of the FCTS model, all columns of the building were assessed with regard to the design capacity (ultimate limit state design) under the gravity loads using a column assessment computer program (this will be presented later on in the chapter 5). The results of the assessment revealed that some columns sections of the ninth floor have insufficient design capacity due to the absence of significant axial load (which can affect the moment carrying capacity of a column). Therefore the design of these columns was modified and the assessment program was reapplied to ensure that the building is safe under the gravity loads before running the seismic analysis. Also this examination was applied for the SCTS model prior the seismic analysis. All details of this modification are shown in the **Appendix II**.

In addition to this examination mentioned above, the FCTS & SCTS model were investigated with regard to the requirements of the serviceability limit state design. This investigation was carried out using the results of the linear static analysis of these models (safety checks which will be discussed later on in the section 4.3). The investigation exhibited that the design satisfied these requirements for both models.

#### **4.1.1 Description Of The Building**

The building was designed with the relevant general data which is included in the table 4.1. All design details are mentioned in the **Appendix II**. The inertia effects of walls were also included in the design, i.e. the self-weight. For analysis purposes these walls were modelled as bracing as recommended in chapter 3, section 3.4. The type of used walls is blockwork partitions with load  $2.5 \text{ kN/m}^2$  and was applied for the outer beams of the building. The inner partitions are lightweight partitions with load  $1 \text{ kN/m}^2$  and applied in the design as live loads. Fig. 4.1 shows the details of this building.



Description Of The Ten-Storey RC Building
• Building – 24m by 24m in plan, 36.5m in height
• Ground floor – 2 bay, 5m in height, 12m spans
• First floor to ninth floor – 3 bay, 3.5m in height, 8m spans
• All floors in other direction – 3 bay, 8m spans
• The characteristic concrete compressive strength ( $f_{cu}$ ) is 30 N/mm <sup>2</sup> for whole building except ground floor columns & transfer beams is 40 N/mm <sup>2</sup>
• The yield strength of the steel reinforcement ( $f_y$ ) is 460 N/mm <sup>2</sup>
• The design load consists of ultimate dead load and live load
• Density of the reinforced concrete material ( $\rho$ ) is 2400 Kg / m <sup>3</sup>

Table 4.1 General details of the ten-storey RC building

The frame span of ground floor was selected larger than other storey to satisfy firstly, current architectural design requirements, which state that, for multi-storey buildings the ground floor should be designed to service the residents for car parking, and secondly, to provide multi-storey building which contains a potential 'soft-storey' (in this case the ground floor storey).

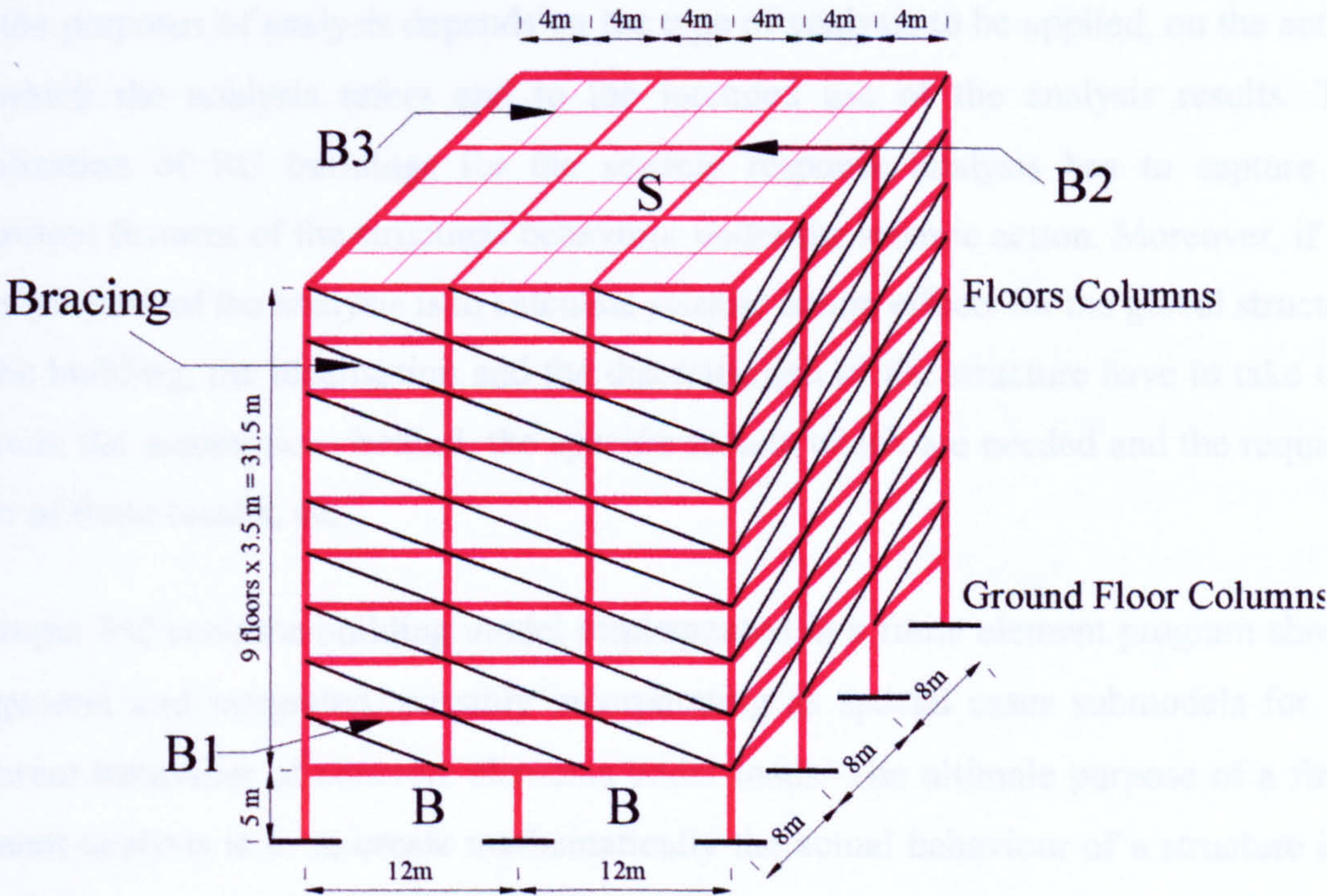


Figure 4.1 The ten-storey RC building



## **4.2 Three Dimensional Finite Element Modelling Of The Global Building Structure**

Three-dimensional structural modelling in the past was time consuming and required large computational resources. Previously the earthquake records indicated that the seismic excitations are primarily two-dimensional, and recently these records exhibited significance of the vertical component of the earthquakes. Therefore the seismic excitations must be considered as three-dimensional. These excitations occur generally in three orthogonal directions. Furthermore, they are inherently random and their orthogonality and independence promote the importance of the seismic modelling and analysis to be subject to the two or three orthogonal components concurrently. These concurrent components 'biaxial or triaxial' interaction provides the means to investigate the real seismic response of existing structures. Consequently, three-dimensional modelling presents the appropriate method to capture the effects of these two or three degree of freedom orthogonal excitations. Moreover, three-dimensional structural modelling incorporating concurrent orthogonal seismic excitations can provide insight into secondary effects, such as torsional modes of behaviour.

In general, the selection of the appropriate mathematical model of the physical structure for the purposes of analysis depends on the type of analysis to be applied, on the action to which the analysis refers and to the intended use of the analysis results. The idealization of RC buildings for the seismic response analysis has to capture all important features of the structural behaviour under the seismic action. Moreover, if the main purpose of the analysis is to calculate seismic action effects for the global structure of the building, the idealisation and the discretisation of the structure have to take into account the assumptions behind, the specific results which are needed and the required form of these results, etc.

A proper RC concrete building model implemented in a finite element program should be general and integrated, possibly incorporating as special cases submodels for the different behaviour of concrete elements under loads. The ultimate purpose of a finite element analysis is to re-create mathematically the actual behaviour of a structure i.e., the analysis must be an accurate mathematical model of a physical prototype. In the broadest sense, this model comprises all the nodes, elements, material properties, real



constants, boundary conditions, and other features that are used to represent the physical structure. Hence, the type of model appropriate for an analysis of RC buildings is a member-by-member type of model (direct generation), in which every beam or column, and every part of a wall between successive floors is represented as a 3D beam element, and the only degrees of freedom considered are the 3 translations and the 3 rotations at each joint of these elements. This requires nodes with 6 degrees of freedom at these points, regardless of whether other elements frame into them there, or not.

#### **4.2.1 Modelling Approach**

For the three-dimensional finite element modelling of the building structures, ANSYS has three different techniques (approaches) for the model generation (process of defining the geometric configuration of the model's nodes and elements). These techniques allow generating the model which represent the spatial volume and connectivity of the actual building. Generation of the 3D finite element model of the FCTS & SCTS was carried out using the direct generation approach. The direct generation technique is convenient for small or simple models and provides the modeller with complete control over the geometry and numbering of every node and every element. But it is too time consuming, the volume of data can become overwhelming, the design optimization less convenient and it is difficult to modify the mesh which was selected. Also this technique requires more attention to every detail of the mesh and can sometimes cause the modeller to become more prone to committing errors.

Nevertheless direct generation approach was selected and applied for 3D finite element modelling of the ten-storey RC building (FCTS & SCTS) as the building contains a variety of structural members and complicated geometrical properties. The approach of ANSYS, and other computer analysis packages (such as ABAQUS) exclusively allow the generating of the realistic 3D finite element modelling for such buildings. Due to the nature of the ten-storey RC building being rather large & complex, all types of performed analyses are linear. The type of mesh (number and shapes of elements) is not significant factor and is commonly used for the solid model approach which allows the automatic mesh (control the mesh type and size according to the element shape). The



mesh type (fine or condensed) is a significant factor which may affect the accuracy of analysis results using the solid model approach.

The sequence of generating the 3D finite element model of the ten-storey RC building was implemented as follows:

1. Selection of the finite element type for every structural member to represent the major characteristics of the building structure. The properties of each element type satisfies the requirements of modelling (such as the three dimensional) and analysis type (such as linear analysis)
2. Set the element attributes for the selected finite elements such as the geometrical properties (cross-sectional area, etc) and the material properties (Young's modulus, etc)
3. Definition of the nodes for the global building structure and the number of nodes required for each element in the building
4. Definition of the all elements of the building to form the global 3D finite element model that every element in the building is defined by identifying its nodes

The above steps of generating the model of the FCTS & SCTS model will be presented in detail in the next section.

#### **4.2.2 Generation Of The Finite Element Model**

As the three-dimensional finite element model of the ten-storey RC building (FCTS & SCTS) was generated using the finite element computer package ANSYS, The first step in generating the model was the pre-processing stage, including:

##### **Definition Of Element Types**

Within the framework of linear elasticity, 3D beam elements are typically Beam elements which must be used for columns and beams. For modelling columns, the **Beam 4** element type (3D elastic beam) was used. Beam 4 is a uniaxial element with tension, compression, torsion, and bending capabilities. This element has six degrees of freedom at each node, translations in the nodal x, y, and z directions and rotations about



the nodal x, y, and z-axes. This element is defined by two or three nodes as shown in Fig. 4.2. For modelling the beams, **Beam 44** (3D elastic tapered unsymmetrical beam) element type was used. Beam 44 is a uniaxial element with tension, compression, torsion, and bending capabilities. The element has six degrees of freedom at each node, translations in the nodal x, y, and z directions and rotations about the nodal x, y, and z-axes. This element allows a different unsymmetrical geometry at each end and permits the end nodes to be offset from the centroidal axis of the beam (at connection between beams and slabs the modelling nodes are in the centre of slabs therefore the type of finite element of beams must permit the offset). This element is defined originally by two nodes but there is a third node used for identifying the offset as shown in Fig. 4.3.

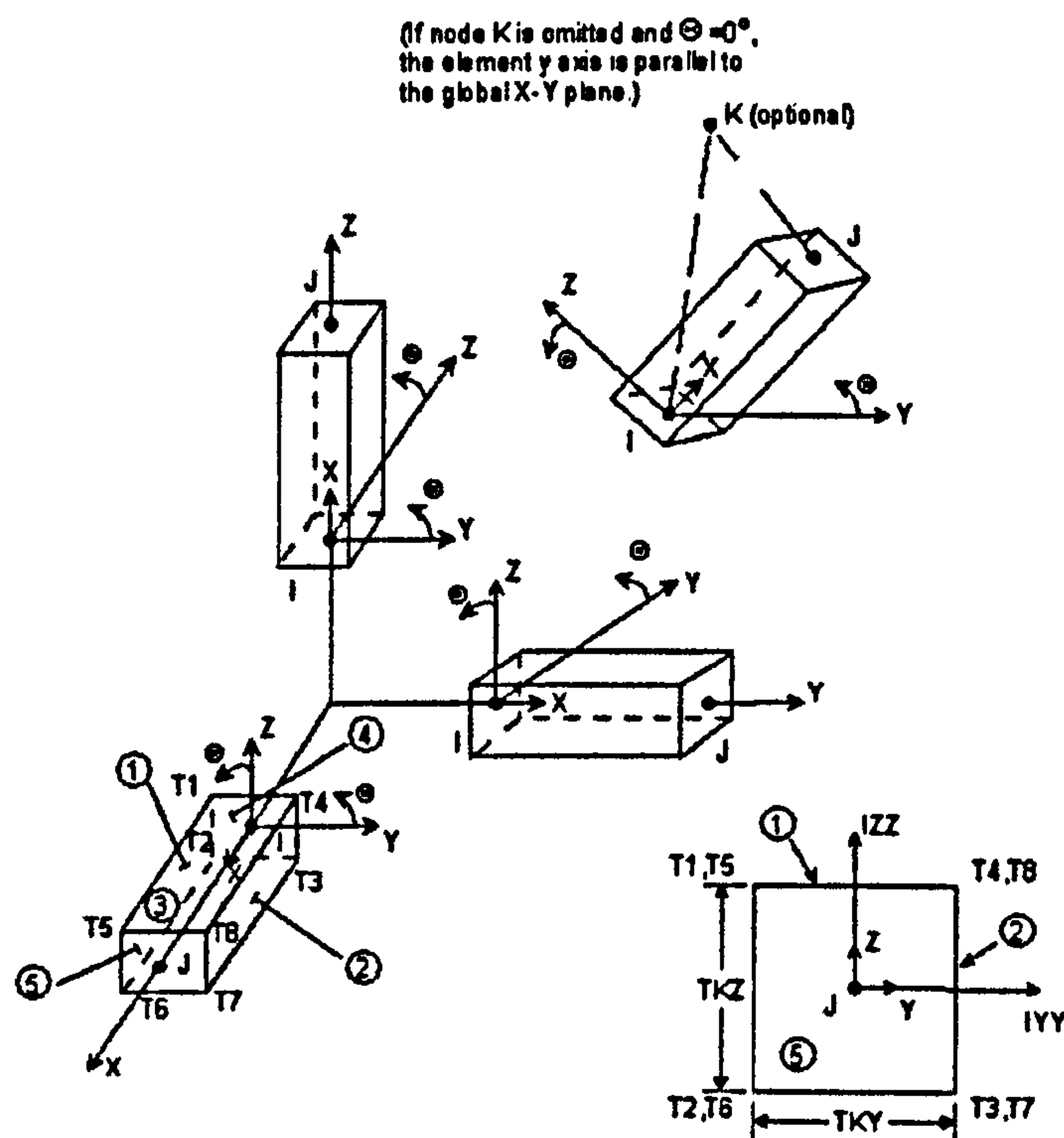


**Figure 4.2** The ANSYS finite element type Beam 4 (3D elastic beam)

Typically slabs are considered on rigid supports and analysed and designed for gravity actions separately from the frame and/or wall system that resists lateral actions and carries the gravity loads to the ground. They should be present, though, in the geometric 3D model of the structure, so that their dead and live loads are computed and appropriately distributed as reactions to their supporting beams, walls and/or columns. Under seismic actions floor slabs play the important role of transmitting the inertial loads to the lateral-force-resisting system, and of tying



together the elements of the latter into a 3D entity. To perform these roles slabs should be monolithically connected with their supporting beams, walls and columns. To satisfy these requirements of slab modelling, the **Shell 63** (elastic shell) element type was used. Shell 63 has both bending and membrane capabilities. Both in-plane and normal loads are permitted. The element has six degrees of freedom at each node, translations in the nodal x, y, and z directions and rotations about the nodal x, y, and z-axes. This element is defined by four nodes as shown in Fig. 4.4.

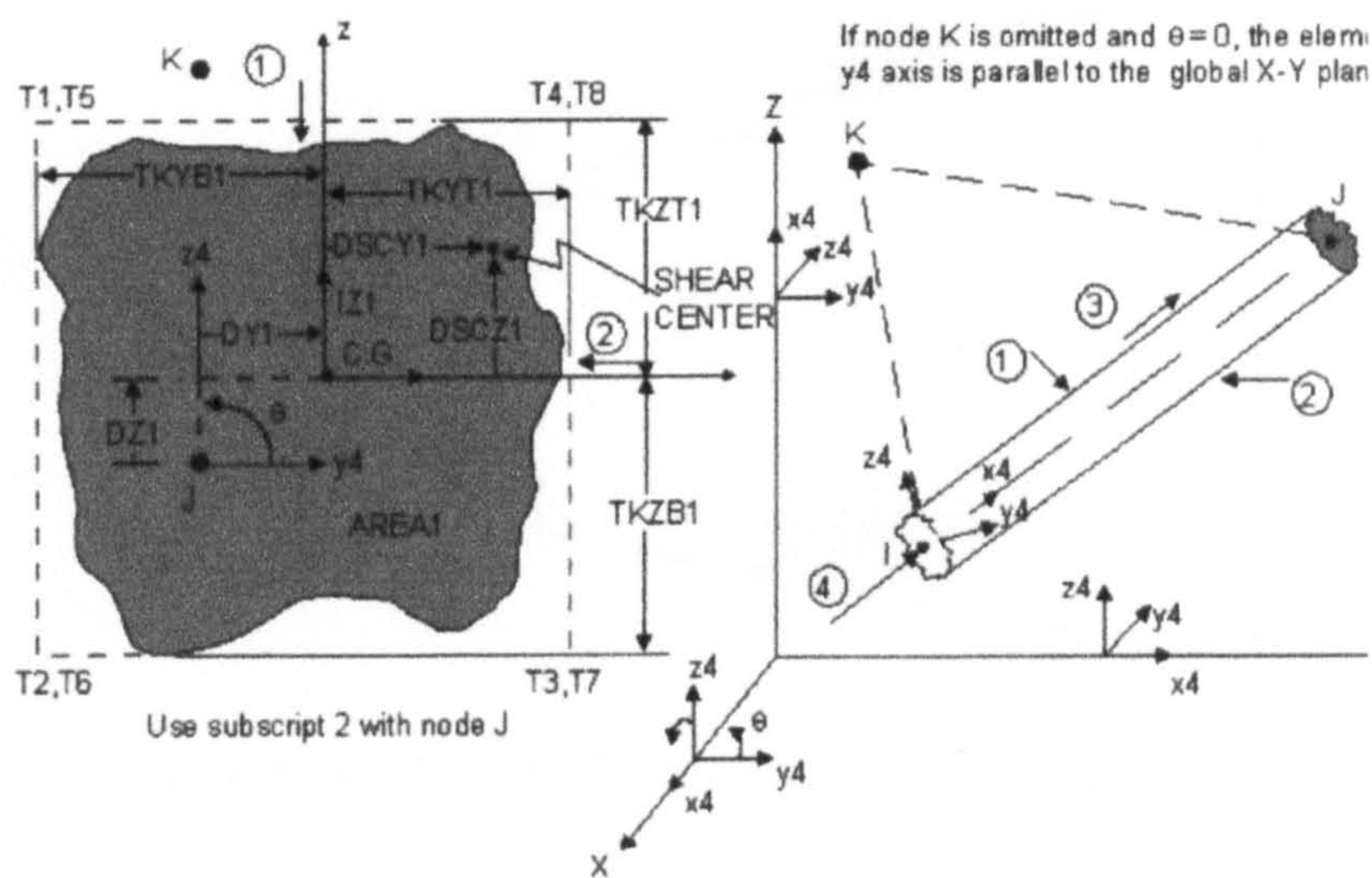


**Figure 4.3** The ANSYS finite element type Beam 44  
(3D elastic tapered unsymmetrical beam)

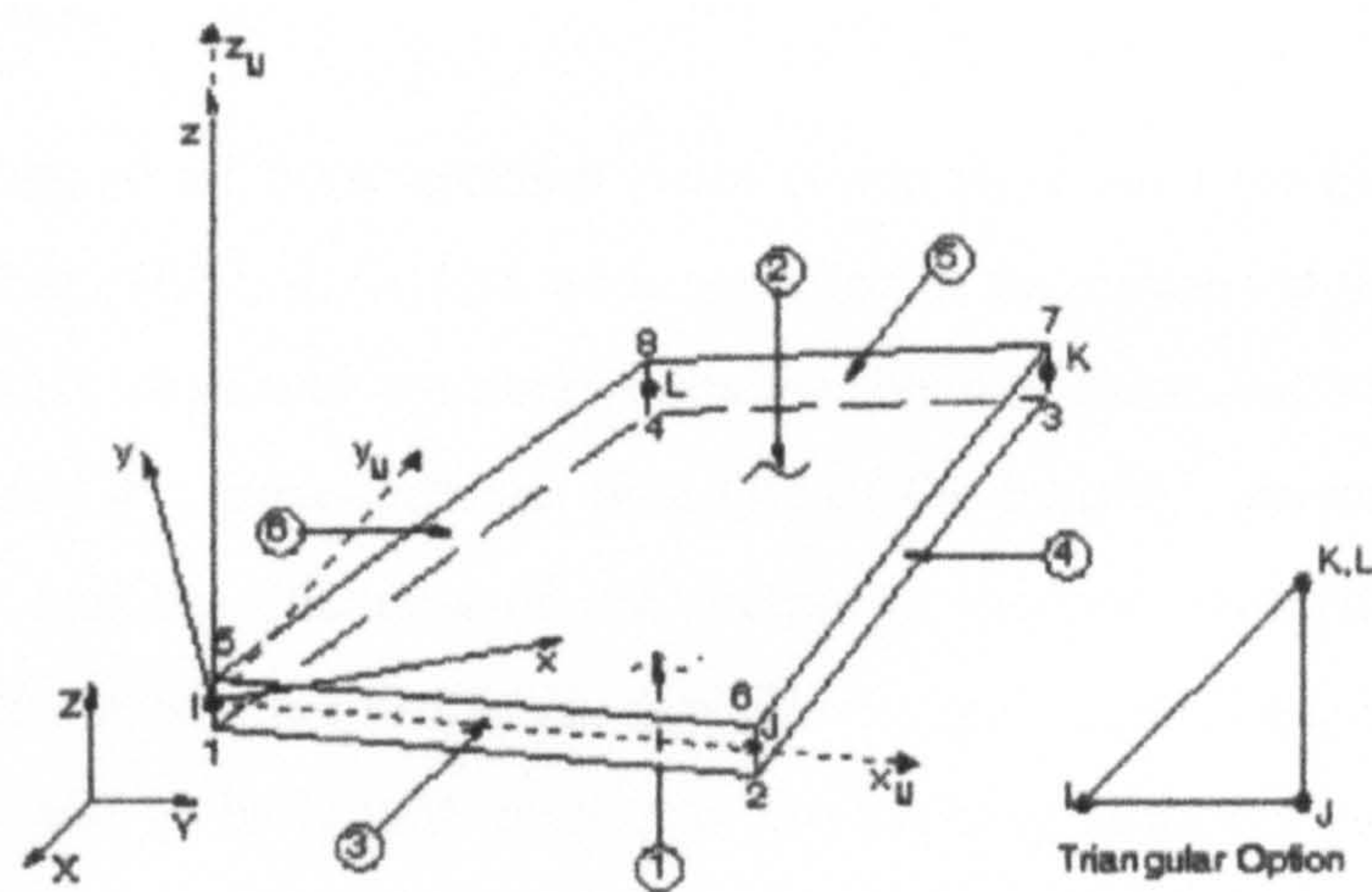


**Figure 4.4** The ANSYS finite element type Shell 63 (elastic shell)



**Link 8 (3D Spar or Truss)** element type was used as the typical finite element modelling of the bracing (walls). This element type may be used in a variety of engineering applications. Link 8 can be used to model trusses, sagging cables, links, springs, etc. The three-dimensional spar element is a uniaxial tension-compression element with three degrees of freedom at each node, translations in the nodal  $x$ ,  $y$ , and  $z$  directions. As in a pin-jointed structure, no bending of the element is considered. This element is defined by two nodes as shown in Fig. 4.5.

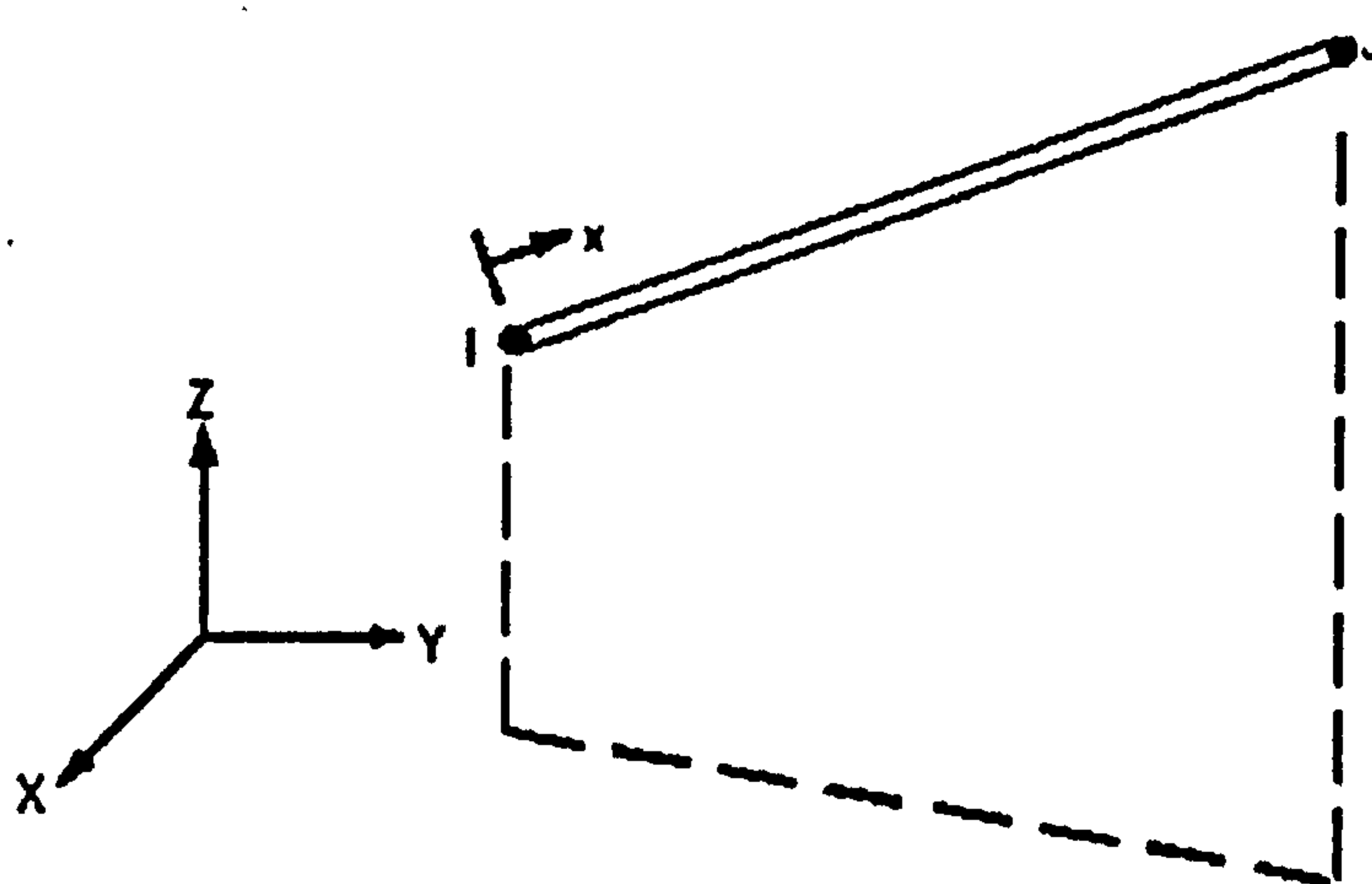


**Figure 4.5** The ANSYS finite element type Link 8 (3D spar)

### Definition Of Element Real Constants

Element real constants are geometrical properties that depend on the element type, such as cross-sectional area of the structural member, moment of inertia, etc. Not all element types require real constants, and different elements of the same type may have different real constant values.

The real constants of all finite element types which were used for modelling the ten-storey RC building (FCTS & SCTS), were specified in accordance with the geometrical properties of every structural member (columns, beams, slabs and walls). These real constants included the cross-sectional area ( $A$ ) of the member, moment of inertia ( $I$ ) around its axes and the thickness of the section in the two perpendicular directions (depth & breadth). Also other properties describe the geometrical shape of the structural member locally and globally with respect to the building structure (such as the offset distance of the element type Beam 44). For example, real constants for the finite element type Beam 4 of the ground floor columns Cgii (refer to section 9, Appendix II)



of the FCTS model, have a cross-sectional area ( $A = 0.64 \text{ m}$ ), moment of inertia ( $0.034 \text{ m}^4$  around the two axes) and thickness ( $0.8 \text{ m}$  in the two directions).

### **Definition Of Element Material Properties**

Most element types require material properties such as Young's modulus ( $E$ ), Poisson's ratio ( $\nu$ ), density ( $\rho$ ), etc. Depending on the desired type of the structural analysis, the material properties can be linear or nonlinear. Concerning the linear analysis, material properties can be isotropic or orthotropic.

As the three-dimensional finite element model of the ten-storey RC building herein (FCTS & SCTS) has considered a model constructed of linear elements only, the linear material properties for all element types of the structural members were implemented. These material properties were applied similarly to those used in the static design of the building according to BS8110 provisions (see Appendix II).

Also due to the applied analysis types for the building (FCTS & SCTS) being linear, the overall global building model was not created as a composite material i.e., created as concrete only, with only linear isotropic behaviour being considered for the material properties. The material properties of all element types of the structural members of the ten storey RC building (FCTS & SCTS) were constant except the density of the Shell 63 elements. The RC density of the Shell 63 elements was modified due to the presence of the live loads, inner partitions loads and floor covering loads which were distributed over the slabs (see Appendix II). The applied linear material properties for the building (FCTS & SCTS) were, Young's modulus ( $E = 20 \times 10^9 \text{ N/m}^2$ ), Poisson's ratio ( $\nu = 0.2$ ), and the density ( $\rho = 2400 \text{ Kg / m}^3$ ). For the element type Shell 63, the density used was  $4778.5 \text{ Kg / m}^3$ .

The second step in generating the model was to build the model in the three-dimensions. The building of this model was carried out using the direct generation technique (modelling approach) which was mentioned above in section 4.2.1. This 3D model was generated manually 'floor by floor' by defining firstly all nodes which simulate the global building structure in the three spatial co-ordinate directions. Then the different element types of the structural members for each floor were generated using the nodes defined previously. The model meshing was carried out using the free mesh technique (an ANSYS mesh technique) which allows the modeller to choose the appropriate finite



element size. The mesh size is constant for every type of the structural members of the building. Each member except the bracing (Link 8 element type) was equally divided to a number of finite elements having an appropriate size compatible with the global size of the building structure. Nevertheless, this mesh size was demanding of the available physical & computer resources. In addition the number of elements used is dependent on the post-processing requirement i.e., a column modelled with a number of beam elements will give insight into the behaviour at local areas of the column, rather than using one element which can only indicate acceptability or failure. All building beams (Beam 44 element type) and ground floor columns (Beam 4 element type) were divided to 1m length finite elements. Also all other building columns (Beam 4 element type) and the floor slabs (Shell 63 element type) were divided to 0.875m length & 1m length x 1m width finite elements respectively. In general, the building of the model was time consuming and the complete 3D model included approximately 10000 elements & 6600 nodes.

The third step was the application of the appropriate boundary conditions for column bases, which were assigned equal to zero for all degrees of freedom (creating fixed ends and simultaneously the modelling of the soil structure interaction was omitted in this research and will be recommended for the future works). The Three-dimensional finite element model of the ten storey RC building (FCTS) that was generated using ANSYS is shown in Fig. 4.6.

### **4.3 Linear Static Analysis Of The FCTS And SCTS Model**

After transformation of the geometrical model of the ten-storey RC building into a realistically simulated three-dimensional finite element model comprising all the designed static gravity loads, the linear static analysis using ANSYS was performed for the building models (FCTS & SCTS) under these gravity loads. The linear static analysis was executed prior the dynamic analyses in order to verify generally the equilibrium of the building models under the static gravity loads and also the various modelling approximations that have been assumed.

As the main aim of a finite element analysis is to examine how a structure responds to certain loading conditions, specification of the proper loading conditions is the key step in the analysis. The ANSYS program is provided with a variety of ways for applying



the loads on the model. These ways contain a variety of options that can control how the loads are actually used during solution. In a linear static analysis, the gravity forces of a structure are calculated and applied using the mass of the structure model (that is commonly supplied by a density specification) and the gravitational acceleration ( $g$ ).

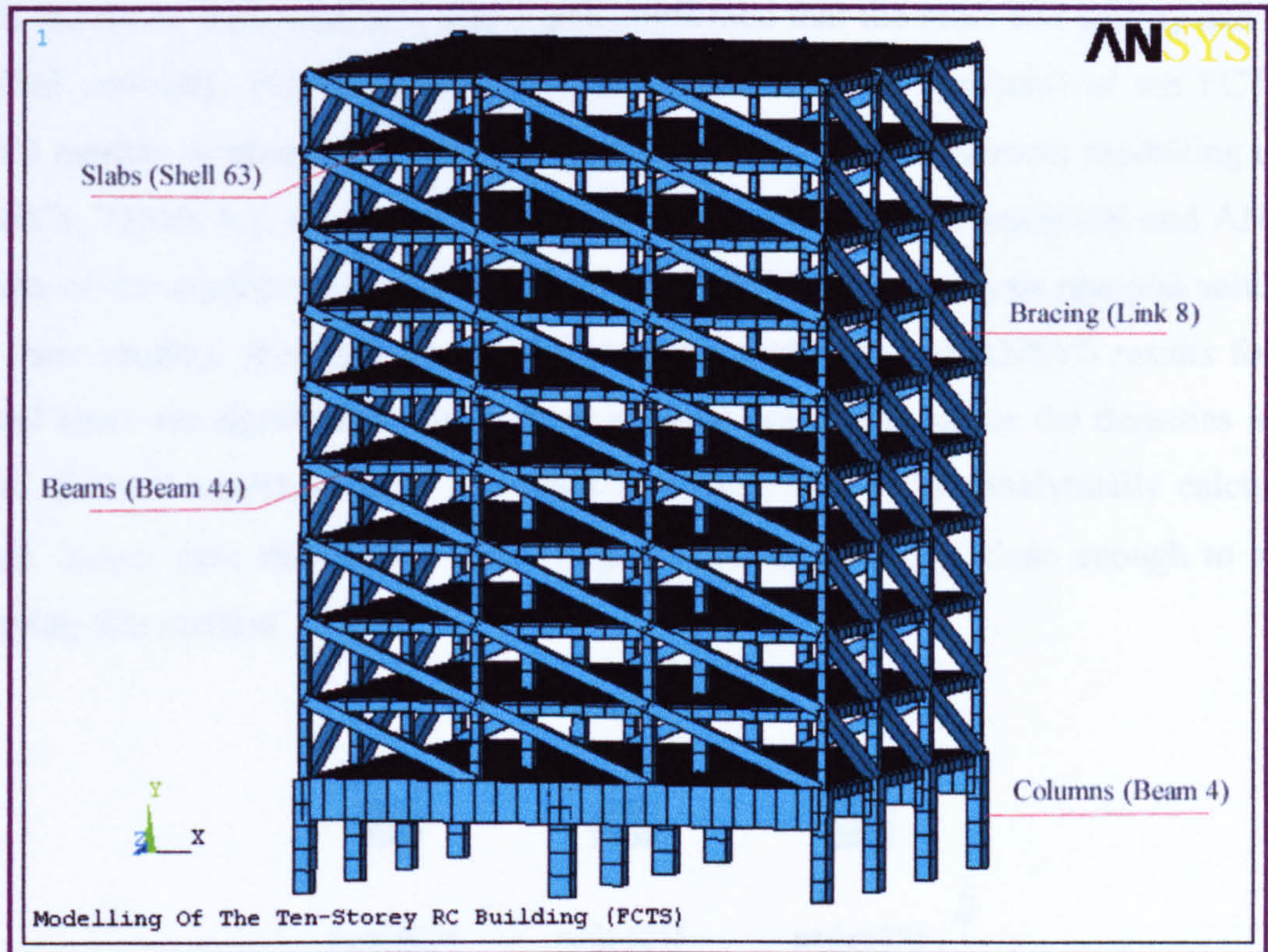


**Figure 4.6** The 3D finite element model of the ten-storey RC building (FCTS)

The 3D finite element models of the FCTS & SCTS (as shown in Fig. 4.6) were analysed statically under the gravity loads only prior conducting the modal and seismic analysis. The static analysis of these models were carried out to check the safety of building against collapse under its own weight and live load and to verify forces in the static case. After generation of the finite element models of the ten-storey RC building (FCTS & SCTS) as shown in Fig. 4.6, the linear static analysis was performed for them by applying the static load (gravity loads that included specified dead and live loads) using the gravitational constant of  $9.81\text{m/s}^2$  acting on the appropriate density (mass) of the models.

As mentioned above in the section 4.1, the static analysis results for all columns of the FCTS & SCTS models were assessed with regard to the design capacity of BS 8110 using a column assessment computer program to ensure the structural integrity of the



building against collapse under the gravity loads. The assessment results demonstrated that the building (FCTS & SCTS) is safe against collapse under the gravity loads.

The mass of the building models (FCTS & SCTS) was checked by comparing the analytical calculation of the building mass and results (mass & reaction forces at bases) from the linear static analysis. The check confirmed that the mass and gravity had been applied correctly. Fig. 4.7 shows the base numbers (node numbers) of the FCTS & SCTS models in accordance with the numbering of the finite element modelling using ANSYS. Tables 4.2, 4.3, 4.4 present a comparison between the analytical and ANSYS results of the models mass and also show the ANSYS static analysis reaction solutions for these models. It should be noted that if the analytical and ANSYS results for the model mass are significantly different it is usual practice to factor the densities in the finite element model to ‘tune’ the mass to exactly that of the analytically calculated value. In our case the masses were judged to be significantly close enough to avoid applying this method.

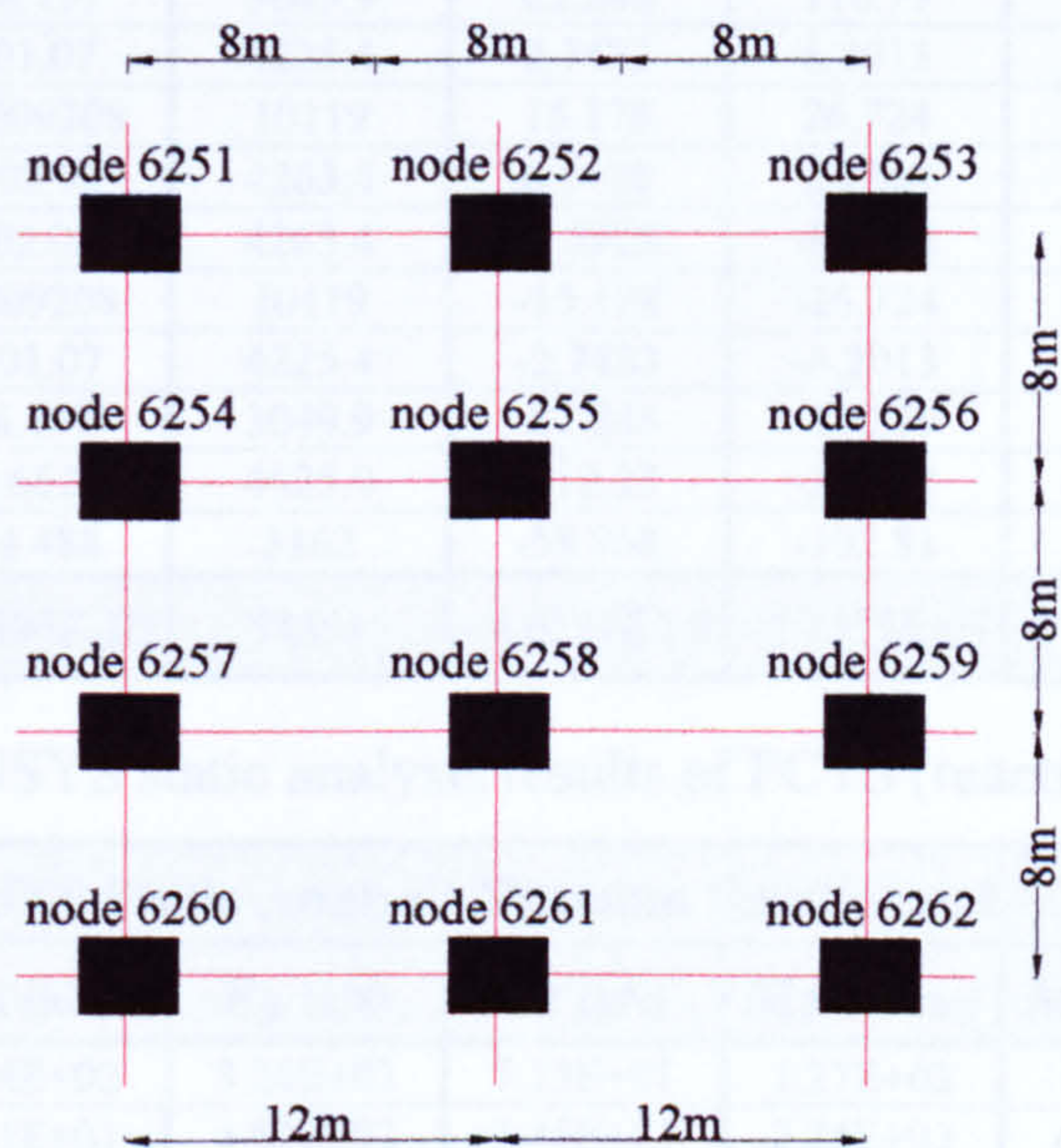


Figure 4.7 Base numbers of the FCTS & SCTS models

Mass Of Building Models				
Description	Building	Analytical	ANSYS	Remarks
Mass of model (kg)	FCTS	6037224	6003200	0.6 % difference
	SCTS	6084552	6070400	0.3 % difference

Table 4.2 Analytical and ANSYS results for mass of FCTS & SCTS



The FCTS & SCTS model were investigated with regard to the requirements of the serviceability limit state of BS 8110. This investigation was carried out using the ANSYS results of the linear static analysis of these models. The investigation consequence revealed that the maximum degree of freedom value in y-direction (maximum deflection UY) for the FCTS & SCTS occurred at the transfer beams (structural member beam B, refer to Fig. 4.1) of the ground floor under the columns of the floors above. The resulting maximum deflection for FCTS & SCTS was 10.49 mm and 8.75 mm respectively. These values demonstrate that the serviceability limit state requirements of BS 8110 were satisfied for both models. (It is noted that concrete is normally cracked at serviceable levels of loading, hence reduced stiffnesses may be considered – which should improve the response characteristic in any case).

ANSYS Static Analysis Reaction Solutions of FCTS						
Node Number	Fx (kN)	Fy (kN)	Fz (kN)	Mx (kN.m)	My (kN.m)	Mz (kN.m)
6251	44.488	3162	58.968	102.81	-2.6865	-65.073
6252	4.6624	4625.9	112.23	200.92	0.74925	-3.76
6253	-56.197	3049.9	62.246	110.79	-1.9397	78.089
6254	101.07	4225.4	2.7433	6.2013	-1.42	-147.27
6255	-0.009208	10119	15.178	26.724	0.58877	0.85396
6256	-102.03	4263.4	6.5928	8.7558	1.7411	149.49
6257	102.03	4263.4	-6.5928	-8.7558	1.7411	-149.49
6258	0.009208	10119	-15.178	-26.724	0.58877	-0.85396
6259	-101.07	4225.4	-2.7433	-6.2013	-1.42	147.27
6260	56.197	3049.9	-62.246	-110.79	-1.9397	-78.089
6261	-4.6624	4625.9	-112.23	-200.92	0.74925	3.76
6262	-44.488	3162	-58.968	-102.81	-2.6865	65.073
Total	-2.7494E-10	58891	- 4.0397E-09	- 1.2575E-08	-5.9344	7.0495E-10

Table 4.3 ANSYS static analysis results of FCTS (reaction solutions)

ANSYS Static Analysis Reaction Solutions of SCTS						
Node Number	Fx (kN)	Fy (kN)	Fz (kN)	Mx (kN.m)	My (kN.m)	Mz (kN.m)
6251	2.04E+02	3.24E+03	7.13E+01	1.27E+02	-1.39E+01	-3.02E+02
6252	1.31E+01	4.52E+03	1.45E+02	2.74E+02	6.66E-01	-1.84E+01
6253	-2.40E+02	3.14E+03	8.15E+01	1.57E+02	6.29E-01	3.20E+02
6254	4.48E+02	4.43E+03	1.62E+00	7.50E-01	-6.14E+00	-6.45E+02
6255	1.89E+00	9.96E+03	2.25E+01	4.06E+01	4.94E-01	-3.04E+00
6256	-4.49E+02	4.48E+03	1.25E+01	1.91E+01	5.07E+00	6.46E+02
6257	4.49E+02	4.48E+03	-1.25E+01	-1.91E+01	5.07E+00	-6.46E+02
6258	-1.89E+00	9.96E+03	-2.25E+01	-4.06E+01	4.94E-01	3.04E+00
6259	-4.48E+02	4.43E+03	-1.62E+00	-7.50E-01	-6.14E+00	6.45E+02
6260	2.40E+02	3.14E+03	-8.15E+01	-1.57E+02	6.29E-01	-3.20E+02
6261	-1.31E+01	4.52E+03	-1.45E+02	-2.74E+02	6.66E-01	1.84E+01
6262	-2.04E+02	3.24E+03	-7.13E+01	-1.27E+02	-1.39E+01	3.02E+02
Total	-7.94E-10	5.96E+04	- 3.96E-09	- 1.48E-08	-2.64E+01	2.24E-09

Table 4.4 ANSYS static analysis results of SCTS (reaction solutions)



The transfer beams (structural member beam B, refer to Fig. 4.1) of the ground floor of the FCTS & SCTS models perform a main role in the structural integrity of the ten storey RC building rather than columns under the gravity loads. These beams as shown in Fig. 4.1 have large spans, carry the columns of the above floors and are located in the ground floor (in essence these beams form a soft storey with the ground floor columns). Due to these reasons, the resulting forces (ANSYS static analysis) of these beams were examined in comparison to the used design forces (refer to section 7.1.2, Appendix II) in accordance with the design capacity of BS 8110. This safety check was conducted in order to ensure the overall structural integrity of the buildings (FCTS & SCTS) against collapse under the gravity loads. Table 4.5 lists the comparison between the maximum design & analysis forces of the transfer beams (B) of the buildings ground floor. The comparison shows that the design forces are larger than the analysis forces i.e. the buildings are safe against collapse with regard to the transfer beams.

Design And Analysis Forces Of Transfer Beams (B)						
Building	Max. Shear Force kN		Max. Positive Moment (under columns above) kN.m		Max. Negative Moment (at support) kN.m	
	Design	Analysis	Design	Analysis	Design	Analysis
FCTS	5547.5	5353.3	8460.8	6998.1	13214	11933
SCTS	5547.5	5382.8	8460.8	6807.2	13214	11747

Table 4.5 Comparison between design and analysis forces of transfer beams (B)

4.4 Modal Analysis Of The FCTS And SCTS Model

As mentioned previously in chapter 3, sections 3.3.2 & 3.4.2, the modal analysis for a structure must be performed prior the seismic analysis due to the significance of this analysis in identifying the dynamic response of structures. Modal analysis is a linear analysis providing the structural engineer with a valuable insight into the dynamic characteristics of the structure (expected dynamic behaviour during the earthquake) and also with a necessary data for the seismic analysis (such as Rayleigh damping coefficients), as follows:

- Modal analysis presents the 3D modes of vibration & natural frequencies of the structure. By examination the effective masses of these modes, the ‘major’



modes of vibration for the structure can be determined. The characteristics of the major modes of vibration (such as frequency and type of mode) have to be taken into account due to its possible presence and onerous effects on the structure during the earthquake (resonance phenomenon).

- Also the three-dimensional modal analysis of the structure demonstrates the torsional effects through the examination of the 3D mode shapes. These effects arise when the structure has irregular geometric shape or stiffnesses discontinuity.
- The frequencies of major modes of the structure are used to calculate the real value of damping coefficients (Rayleigh damping coefficients) which must be applied in the transient dynamic analysis to obtain a realistic dynamic response during the earthquake.

ANSYS has several mode extraction methods such as subspace, power dynamics, reduced, unsymmetric, damped, etc. Selection of the proper method for modal analysis of the required structure based on the involving of damping effects, geometrical shape of structure, the desired results, etc. The subspace method is used for large symmetric eigenvalue problems (3D large structures), and contains various solution controls that govern the subspace iteration process. In addition to that, the subspace method is available for solving the modal analysis of structures in the absence of the damping effects (i.e. the damping matrix of the equation of motion is equal to zero,  $[C] = [0]$ ).

Modal analysis of the FCTS & SCTS model (three-dimensional finite element model that is shown in Fig. 4.6) was carried out using the ANSYS subspace method in the absence of damping ( $C = 0$ ). This analysis was performed in several steps, 1- definition of the analysis type as modal, 2- selection of the subspace method as the solution method, 3- specifying the number of modes to extract, and 4- running the 3D finite element modal analysis. For the FCTS & SCTS model, a thirty modes up to 6.22 Hz & 6.23 Hz respectively were extracted. Tables 4.6, 4.7 list the modal analysis results of the FCTS & SCTS models including the frequencies of the all extracted modes, the effective mass for each mode in the three orthogonal directions (X, Y, Z), the sum and percent of effective masses of all modes in each direction. Also the coloured rows in these tables indicate to those modes which have large effective masses in any direction



(X or Y or Z) in comparison to the other modes (the major modes). These tables show that the number of extracted modes was sufficient to capture the majority of the mass in any direction for both models (the captured mass must not be less than 80 % of the building mass), and the modal analysis was applied correctly.

Modal Analysis Results of FCTS				
Mode No.	Frequency (Hz)	Effective Masses (Kg)		
		X - Direction	Y - Direction	Z - Direction
1	0.89	1031.79	0.00	5271320
2	0.94	5178970	0.00	802.18
3	1.45	0.00	12111.3	0.00
4	2.41	8968.08	0.00	592418
5	2.49	680976	0.00	5697.82
6	3.08	0.00	4193900	0.00
7	3.91	14789.3	0.00	5439.73
8	3.98	8103.8	0.00	12304.5
9	4.33	0.00	157141	0.00
10	4.78	0.00	138.13	0.00
11	4.95	4083.42	0.12	47481.2
12	4.97	55721.5	0.00799	2555.37
13	5.26	0.00	362260	0.00
14	5.73	0.00	3244.97	0.00
15	5.76	1261.29	0.69	2138.35
16	5.78	0.00	208639	0.00
17	5.80	1598.58	1.36	1377.36
18	5.91	0.00	46481.5	0.00
19	5.91	0.01	43168.7	0.01
20	5.92	142.46	0.00	181.23
21	5.93	257.81	0.04	61.02
22	6.00	1.85	0.02	706.76
23	6.01	0.00	47761.7	0.00
24	6.01	757.77	0.10	0.00
25	6.09	8.09	0.25	135.56
26	6.10	225.96	0.00	30.72
27	6.13	0.00	68791.7	0.00
28	6.20	4.58	0.02	4.98
29	6.21	21.93	0.25	36.87
30	6.22	0.00	211.32	0.00
Sum of effective masses (In each orthogonal direction) (Kg)		5956930	5143850	5942690
Actual total mass of building (Kg)		6003200		
Percent of mass for each direction (%)		99.2	85.7	98.9

Table 4.6 ANSYS modal analysis of the FCTS model



As the examination for the modal analysis results is focused on the modes at which most mass is 'captured' (the 'major' modes of vibration), in order to identify the resonance phenomenon of building under the earthquake, table 4.8 summarizes the frequency, captured masses, and description for the major modes of vibration of the FCTS & SCTS model.

Modal Analysis Results of SCTS				
Mode No.	Frequency (Hz)	Effective Masses (Kg)		
		X - Direction	Y - Direction	Z - Direction
1	1.03	26.53	0.00	4803500
2	1.12	4414920	0.00	8.67
3	1.96	0.00	64447.20	0.00
4	2.75	505.81	0.01	907100
5	3.04	989573	0.00	1.88
6	3.17	0.00	3996910	0.01
7	4.02	24607.60	0.00	31778.90
8	4.09	69418.90	0.01	11703.70
9	4.49	0.00	286324	0.04
10	4.81	0.01	134.81	0.03
11	5.21	312.23	0.17	134872
12	5.49	191395	0.06	406.07
13	5.69	0.00	453656	0.00
14	5.74	0.06	51503.70	0.00
15	5.82	1476.36	0.06	16171.30
16	5.86	0.10	6701.71	0.00
17	5.89	56950.70	0.00	39.39
18	5.93	0.00	575.90	0.00
19	5.95	1757.48	0.00	779.46
20	5.96	4519.83	0.01	37.97
21	5.97	0.04	2965.18	0.27
22	6.02	42.21	0.01	4179.34
23	6.05	23245.90	0.51	13.60
24	6.05	0.02	29752.30	0.02
25	6.10	319.20	0.01	1206.16
26	6.12	15666.90	0.01	10.99
27	6.16	0.02	83225.70	0.02
28	6.21	983.55	0.04	84.52
29	6.23	1254.57	0.02	142.25
30	6.23	0.04	1.59	0.00
Sum of effective masses (In each orthogonal direction) (Kg)		5796970	4976200	5912040
Actual total mass of building (Kg)		6070400		
Percent of mass for each direction (%)		95.5	81.9	97.4

Table 4.7 ANSYS modal analysis of the SCTS model



Investigation of the major modes of the FCTS & SCTS model (see table 4.8) presents significant information with regard to the expected dynamic response of these buildings during the earthquakes. There are some important points derived from the consequences of this investigation as follows:

“Major” Modes (% Mass captured)						Description of Mode
Building	Mode No.	Frequency (Hz)	X - Direction	Y - Direction	Z - Direction	
FCTS	1	0.89	N/A	N/A	87.8 %	Sway Mode for complete building
	2	0.94	86.3 %	N/A	N/A	Sway Mode for complete building
	4	2.41	N/A	N/A	9.9 %	Sway Mode for building except ground floor
	5	2.49	11.3 %	N/A	N/A	Sway Mode for building except ground floor
	6	3.08	N/A	69.9 %	N/A	Floors bounce up
	13	5.26	N/A	6 %	N/A	Torsional mode plus Floors bounce up
SCTS	1	1.03	N/A	N/A	79.2 %	Sway Mode for complete building
	2	1.12	72.7 %	N/A	N/A	Sway Mode for complete building
	4	2.75	N/A	N/A	14.9 %	Sway Mode for building except ground floor
	5	3.04	16.3 %	N/A	N/A	Sway Mode for building except ground floor
	6	3.17	N/A	65.8 %	N/A	Floors bounce up
	13	5.69	N/A	7.5 %	N/A	Torsional mode plus Floors bounce up

Table 4.8 Modal analysis results of the FCTS & SCTS model  
(Major modes of vibration)

- As the major modes are concentrated in the sway behaviour in the x-direction and z-direction, the importance of carrying out seismic analysis for the buildings in the three dimensions arises for the input ground motion (must be concurrent two-dimensional horizontal earthquake) and the building (must be a three dimensional model). In addition to that, the sway behaviour may be in the resultant direction of these two horizontal directions and in this case the three-dimensional modelling of building and two-dimensional of input motion is imperative to obtain the global realistic behaviour under seismic loading.
- The major modes in the y-direction highlight the significance of the three dimensional modelling of the building and also the input ground motion due to the possible torsional effects on the building as a result for the presence of the



vertical component of the earthquake. Also as these buildings have stiffnesses discontinuity at the ground floor, the major modes in the y-direction included a torsional mode.

- The natural frequencies of the buildings (FCTS & SCTS) at the major modes must be compared with the resonant frequencies which can be obtained from the response spectra of these buildings under the earthquakes in order to identify the resonant frequencies correctly.

Figures 4.8, 4.9 show the major modes of vibration of the three dimensional finite element model for FCTS (sway mode in x-direction at frequency 0.94 Hz & torsional mode in y-direction at frequency 5.26 Hz).

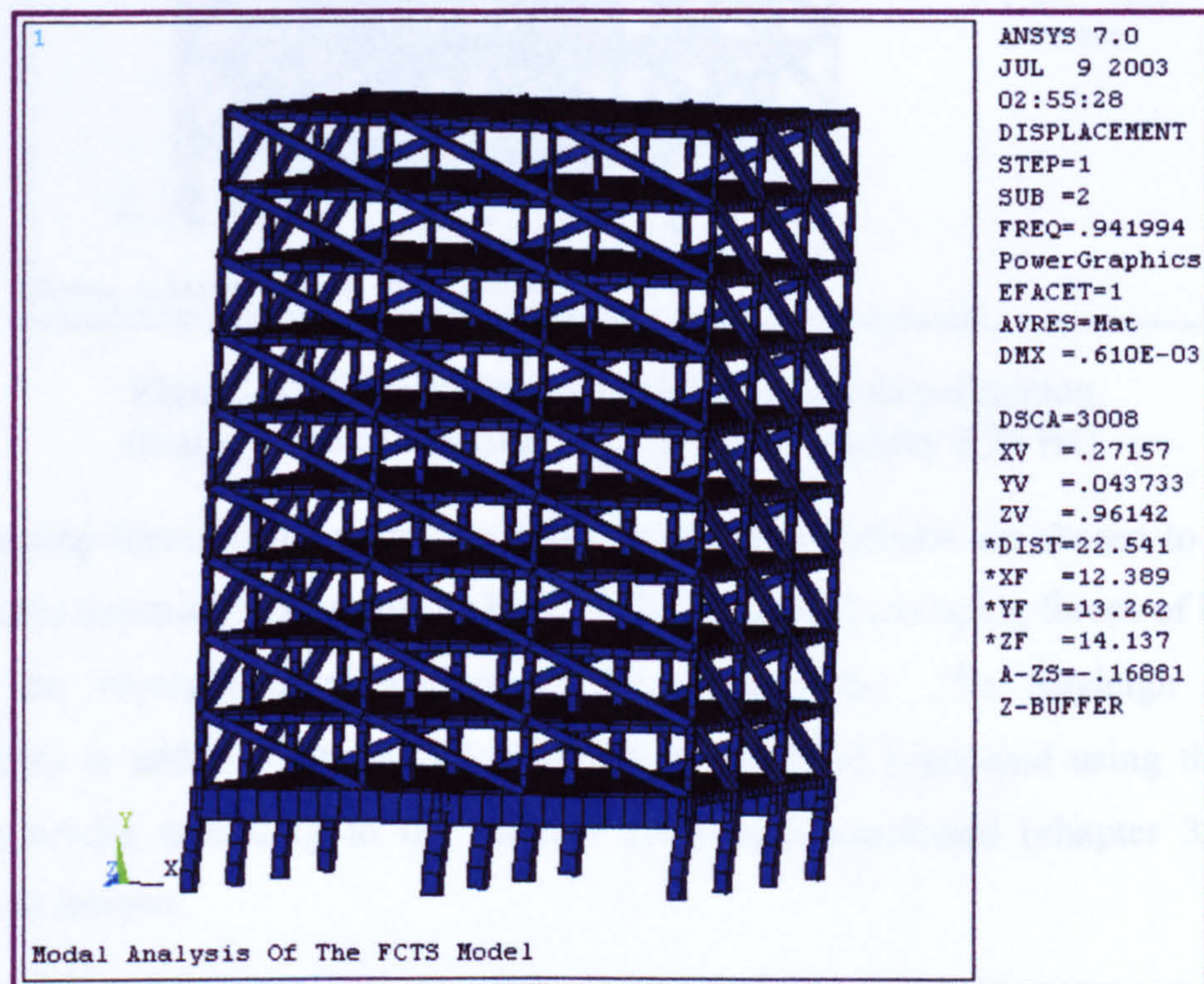


**Figure 4.8** Sway mode of FCTS model in x-direction  
(major mode of vibration with natural frequency 0.94 Hz)

### Rayleigh Damping Coefficients

It has been mentioned previously in chapter 3, section 3.4.2.1, that the damping forces must be applied in the seismic analysis of buildings. These forces influence the dynamic response of the buildings during the earthquakes, and consequently it constitutes one of the significant parameters in the equation of motion which is used to describe the realistic seismic behaviour of structures. Also it was mentioned in detail how the damping forces are calculated using the modal analysis results and applied in the



transient dynamic analysis of the buildings using the Rayleigh damping coefficients method.

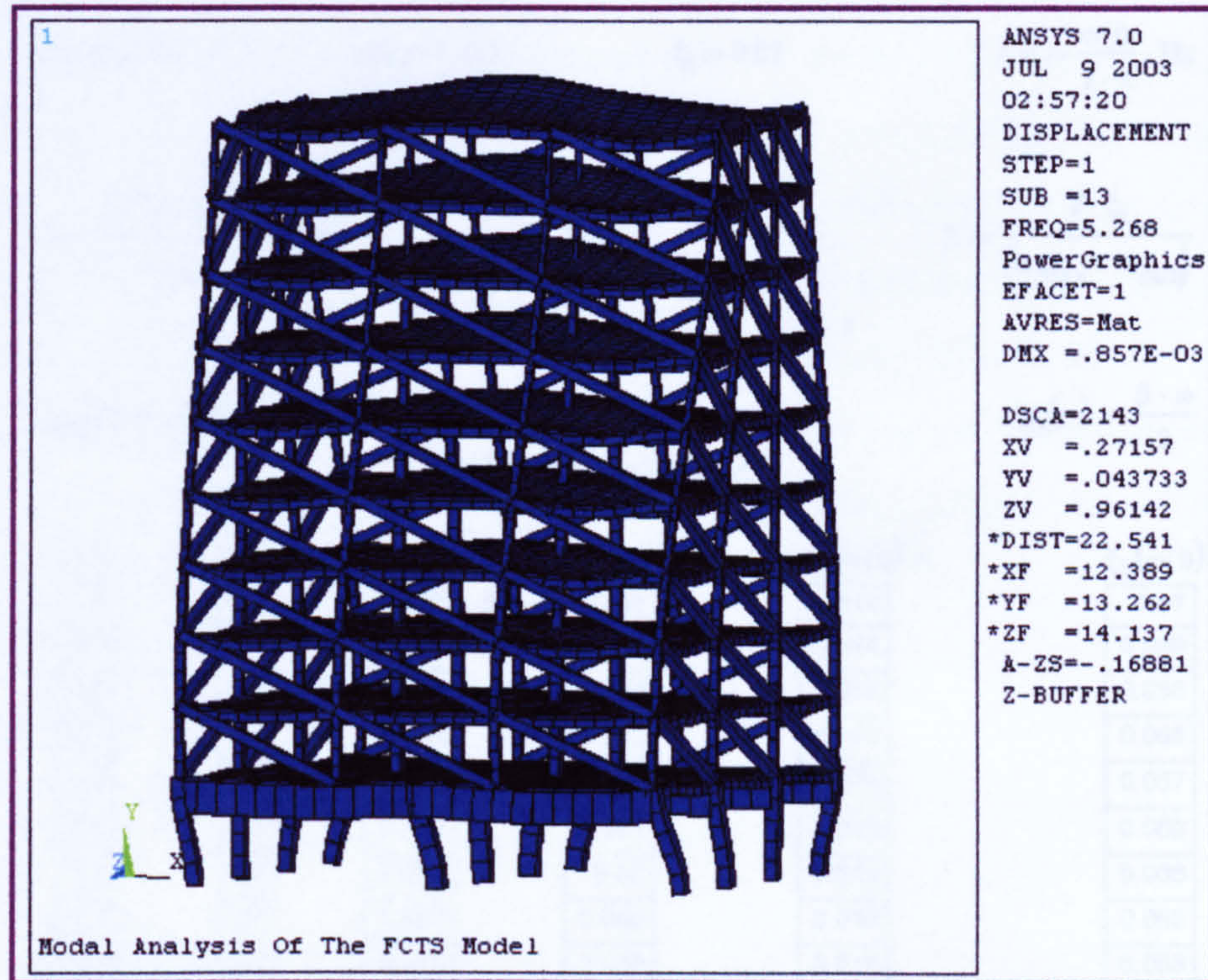


**Figure 4.9** Torsional mode of FCTS model in y-direction (major mode of vibration with natural frequency 5.26 Hz)

The damping forces involved in the transient dynamic analysis are chosen to simulate the realistic seismic response of the FCTS & SCTS model (damping forces of buildings reduce the resonant amplification of the earthquakes). The Rayleigh damping coefficients  $\alpha$  and  $\beta$  of the FCTS & SCTS model were computed using the modal analysis results according to the method previously mentioned (chapter 3, section 3.4.2.1) as follows:

### The FCTS Model

The modal analysis results (refer to tables 4.6, 4.8) of the FCTS model revealed that 97.5 % of the building mass was captured for the sway ('major') modes in the two transverse directions (X, Z) in frequencies ranging from 0.9 Hz to 2.5 Hz.  $\alpha$  and  $\beta$  are chosen such that the required material damping is set at frequencies corresponding to the lowest mode and the mode at which 90 % of the response of the structure has been captured. According to the ASCE standard, ref. [26], the damping ratio  $\xi_i$  of the reinforced concrete structures is typically equal to 0.07. Computation of the Rayleigh



damping coefficients of the FCTS model is shown in the following section. Also the resulting values of these coefficients were  $\alpha = 0.029$  and  $\beta = 0.028$ .

$i := 50..200$  $\omega(i) := i \cdot 0.1$  $\xi_i := 0.07$  $f(i) := \frac{\omega(i)}{2 \cdot \pi} \cdot \text{Hz}$

$\omega_{\min} := 5$  $\omega_{\max} := 20$

$\alpha := \frac{2 \cdot \xi_i \cdot \omega_{\max} \cdot \omega_{\min}}{\omega_{\max} + \omega_{\min}}$  $\beta := \frac{2 \cdot \xi_i}{(\omega_{\max} + \omega_{\min})}$

$\alpha = 0.56$  $\beta = 5.6 \times 10^{-3}$

$\xi_{im}(\omega) := \frac{\alpha}{2 \cdot \omega}$  $\xi_{is}(\omega) := \frac{\beta \cdot \omega}{2}$

$\xi_{it}(\omega) := \xi_{im}(\omega) + \xi_{is}(\omega)$

$\omega(i) =$	$i =$	$f(i) =$	$\xi_{im}(\omega(i)) =$	$\xi_{is}(\omega(i)) =$	$\xi_{it}(\omega(i)) =$
5	50	0.796 Hz	0.056	0.014	0.07
5.1	51	0.812	0.055	0.014	0.069
5.2	52	0.828	0.054	0.015	0.068
5.3	53	0.844	0.053	0.015	0.068
5.4	54	0.859	0.052	0.015	0.067
5.5	55	0.875	0.051	0.015	0.066
5.6	56	0.891	0.05	0.016	0.066
5.7	57	0.907	0.049	0.016	0.065
5.8	58	0.923	0.048	0.016	0.065
5.9	59	0.939	0.047	0.017	0.064
6	60	0.955	0.047	0.017	0.063
6.1	61	0.971	0.046	0.017	0.063
6.2	62	0.987	0.045	0.017	0.063
6.3	63	1.003	0.044	0.018	0.062
6.4	64	1.019	0.044	0.018	0.062
6.5	65	1.035	0.043	0.018	0.061

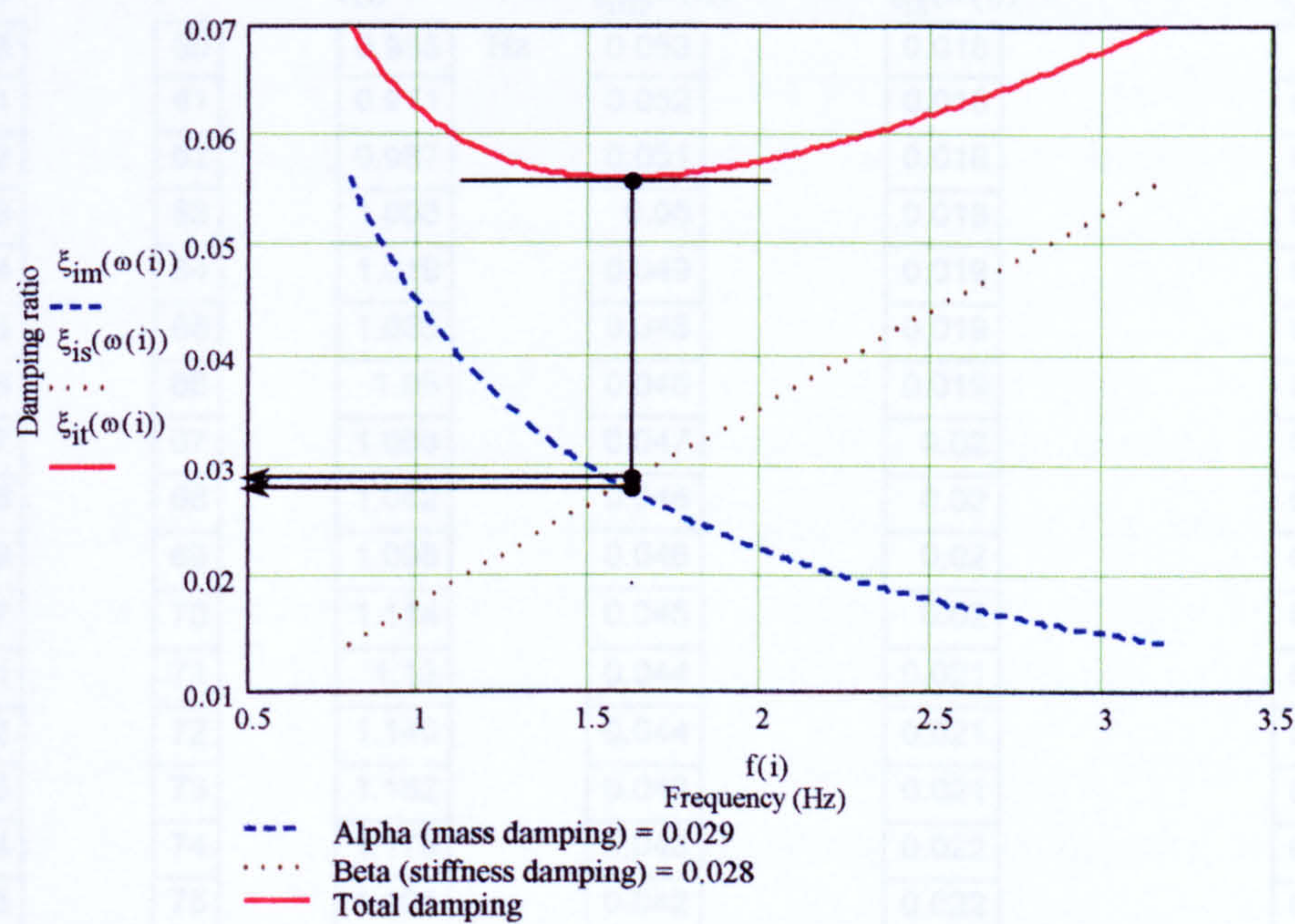


Figure 4.10 Rayleigh damping coefficients (Alpha & Beta) of the FCTS model



The SCTS Model

The modal analysis results (refer to tables 4.7, 4.8) of the SCTS model revealed that 94.1 % of the building mass was captured for the sway ('major') modes in the z-directions in frequencies ranging from 1.03 Hz to 2.75 Hz ( $\alpha$  and  $\beta$  are chosen such that the required material damping is set at frequencies corresponding to the lowest mode and the mode at which 90 % of the response of the structure has been captured). According to the ASCE standard, ref. [26], the damping ratio  $\xi_i$  of the reinforced concrete structures is typically equal to 0.07. Computation of the Rayleigh damping coefficients of the SCTS model is shown in the following section. Also the resulting values of these coefficients were  $\alpha = 0.032$  and  $\beta = 0.029$ .

$i := 60..180$  $\omega(i) := i \cdot 0.1$  $\xi_i := 0.07$  $f(i) := \frac{\omega(i)}{2 \cdot \pi} \cdot \text{Hz}$

$\omega_{\min} := 6$  $\omega_{\max} := 18$

$\alpha := \frac{2 \cdot \xi_i \cdot \omega_{\max} \cdot \omega_{\min}}{\omega_{\max} + \omega_{\min}}$  $\beta := \frac{2 \cdot \xi_i}{(\omega_{\max} + \omega_{\min})}$

$\alpha = 0.63$  $\beta = 5.833 \times 10^{-3}$

$\xi_{im}(\omega) := \frac{\alpha}{2 \cdot \omega}$  $\xi_{is}(\omega) := \frac{\beta \cdot \omega}{2}$

$\xi_{it}(\omega) := \xi_{im}(\omega) + \xi_{is}(\omega)$

$\omega(i) =$	$i =$	$f(i) =$		$\xi_{im}(\omega(i)) =$	$\xi_{is}(\omega(i)) =$	$\xi_{it}(\omega(i)) =$
6	60	0.955	Hz	0.053	0.018	0.07
6.1	61	0.971		0.052	0.018	0.069
6.2	62	0.987		0.051	0.018	0.069
6.3	63	1.003		0.05	0.018	0.068
6.4	64	1.019		0.049	0.019	0.068
6.5	65	1.035		0.048	0.019	0.067
6.6	66	1.05		0.048	0.019	0.067
6.7	67	1.066		0.047	0.02	0.067
6.8	68	1.082		0.046	0.02	0.066
6.9	69	1.098		0.046	0.02	0.066
7	70	1.114		0.045	0.02	0.065
7.1	71	1.13		0.044	0.021	0.065
7.2	72	1.146		0.044	0.021	0.065
7.3	73	1.162		0.043	0.021	0.064
7.4	74	1.178		0.043	0.022	0.064
7.5	75	1.194		0.042	0.022	0.064



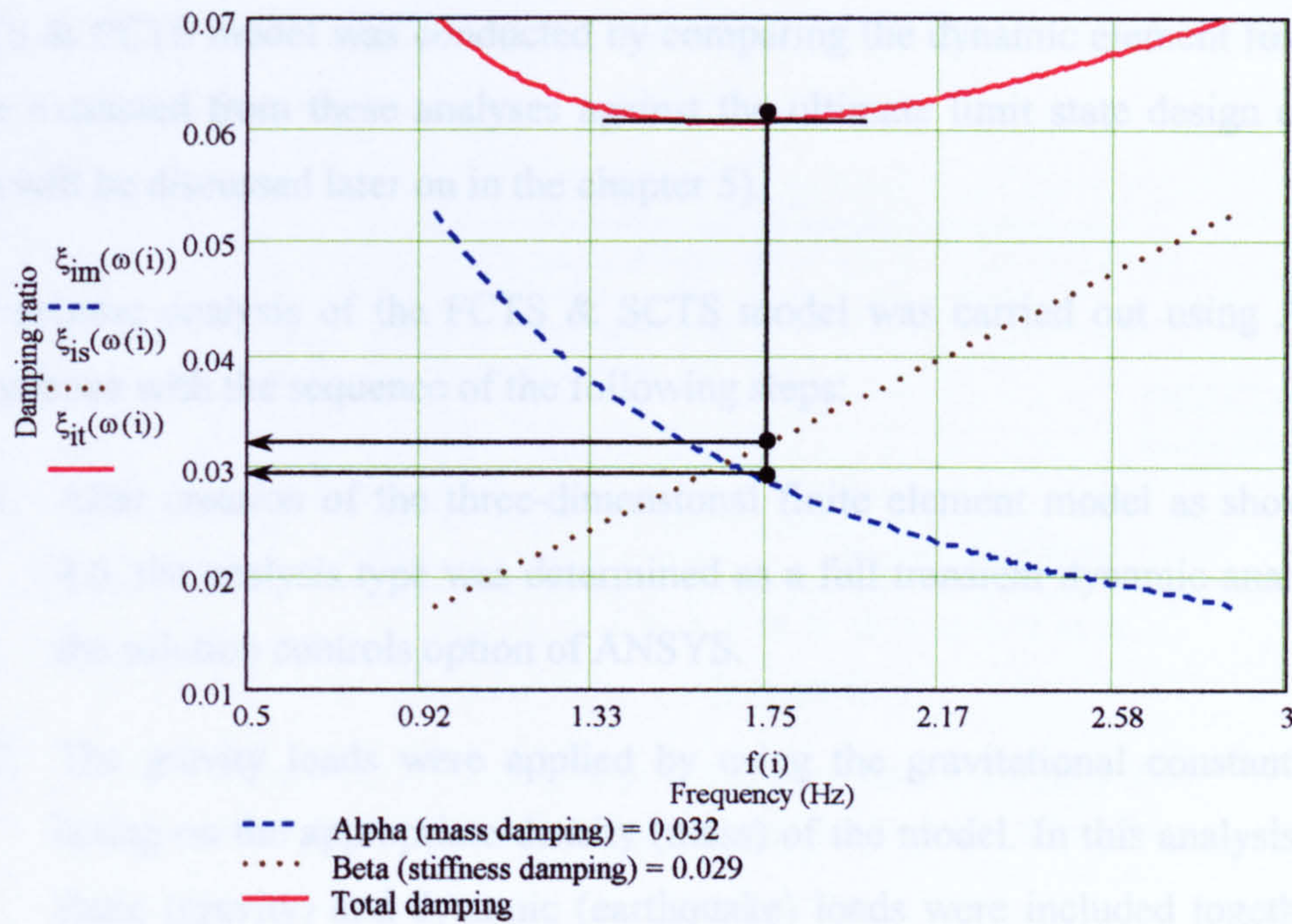


Figure 4.11 Rayleigh damping coefficients (Alpha & Beta) of the SCTS model

4.5 Transient Linear Dynamic Analysis Of The FCTS And SCTS Model

Transient dynamic analysis (direct integration time-history analysis) of the buildings using real or designed acceleration time-history (according to the earthquake records such as UK design response spectra) presents a reliable technique to obtain the realistic seismic response of the buildings. The ANSYS program is provided with three different methods full, mode superposition and reduced method for carrying out the time-history analysis of the buildings. The full method (refer to chapter 3, section 3.1.2.4) is a comprehensive method for calculating the transient seismic response of the structures accurately. Therefore this method is commonly used although it is the most expensive method.

As the main objective of this research is to assess the performance of the existing multi-storey RC buildings (statically designed RC buildings) under the prescribed seismic event, the three-dimensional finite element models (as shown in Fig. 4.6) of the FCTS & SCTS building were analysed seismically (time-history analysis) using the full method of the ANSYS program. The three-dimensional seismic (time-history) analysis for these models was performed under the horizontal earthquake alone & both horizontal and vertical earthquake together. The assessment of seismic response of the



FCTS & SCTS model was conducted by comparing the dynamic element forces which were extracted from these analyses against the ultimate limit state design of BS8110 (this will be discussed later on in the chapter 5).

The seismic analysis of the FCTS & SCTS model was carried out using ANSYS in accordance with the sequence of the following steps:

1. After creation of the three-dimensional finite element model as shown in Fig. 4.6, the analysis type was determined as a full transient dynamic analysis using the solution controls option of ANSYS.
2. The gravity loads were applied by using the gravitational constant  $9.81\text{m/s}^2$  acting on the appropriate density (mass) of the model. In this analysis, both the static (gravity) and dynamic (earthquake) loads were included together (direct combinations). When the gravity load is applied directly with the dynamic loads, ANSYS will include the effects of these loads in the modelling of dynamic behaviour of the building in the vertical direction (i.e. ANSYS will define the gravity loads as a vertical dynamic load at every time step of the seismic loading). Consequently, to avoid these effects, the gravity loads were applied as dynamic loads (gravity loads are defined as a function of time).

The gravitational constant  $9.81\text{ m/s}^2$  was applied gradually (0.98, 1.96, 2.94,....., 8.83, 9.81) as shown in Fig. 4.12 using the load step option of ANSYS. Ten load steps were performed for applying the gravitational constant  $9.81\text{ m/s}^2$  progressively. The first nine load steps were specified for a time interval 0.1 sec & total time of loading was 1.0 sec and also the tenth load step for a time interval 0.1 sec. A total time of loading of 14 sec was applied to ensure that the building has been damped completely under the total gravity loads.

For every load step, some solution options were defined such as the end time of every load step (the time at end of the tenth load step was 15 sec), the time intervals of loading (time step size was constant equal to 0.1 sec), the type of desired results (the running of each analysis was divided into two individual times according to the type of results) and the Rayleigh damping coefficients which were chosen to be equal to artificial high values of 0.09, 0.09 to



contribute in damping of the vertical dynamic characteristics of the building under the gravity loads.

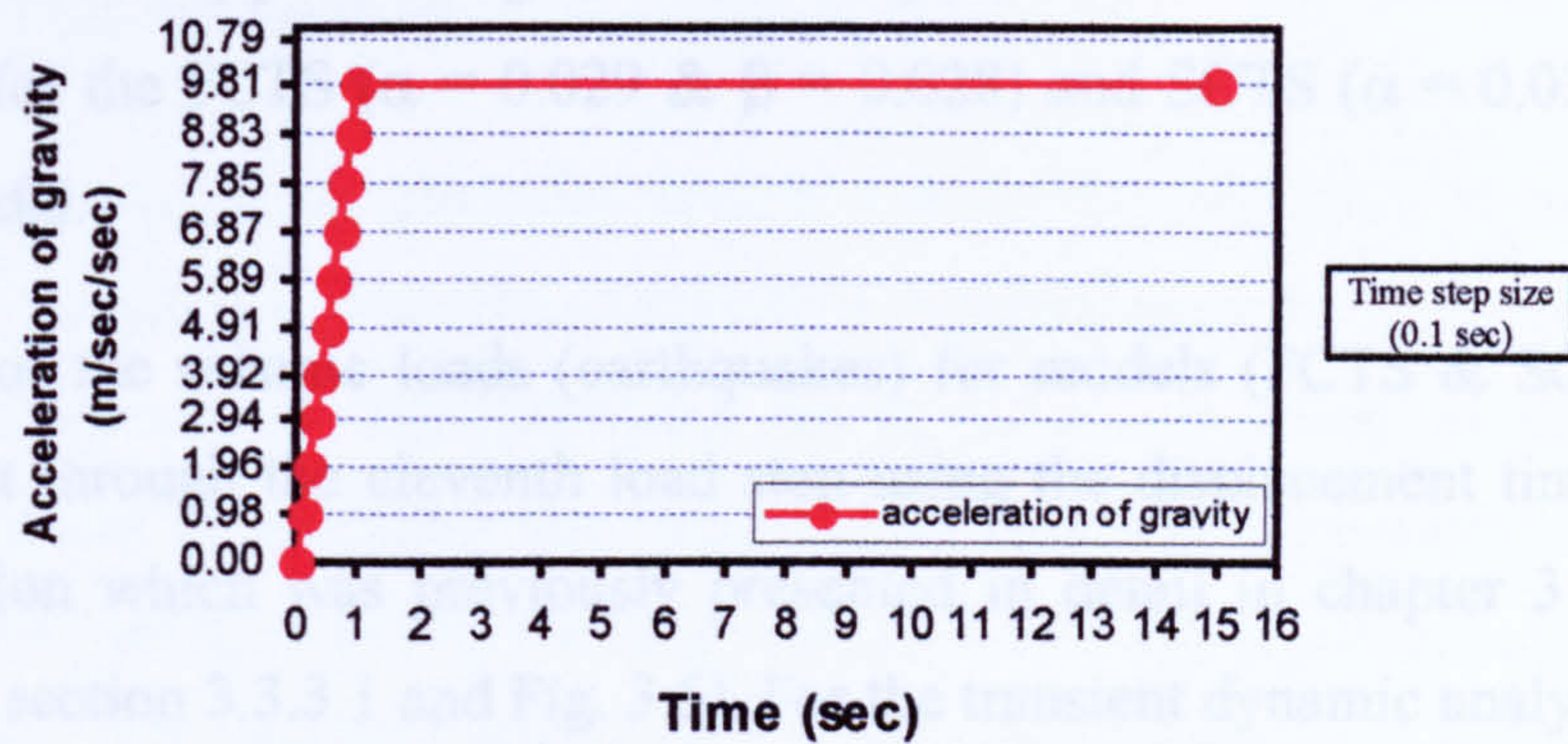


**Figure 4.12** Loading steps of the gravitational constant 9.81 m/s/s in ANSYS for applying the gravity loads of model

- After the building has become static under the effects of gravity loads, ANSYS then automatically established the static case of the building as the initial conditions for the analysis under the earthquake i.e., the initial dynamic loads were equal to zero at time 15 sec.
- Then the eleventh load step was created and configured for applying the dynamic loads (earthquakes) of the building analysis. This load step was performed by setting some solution options which must be specified before applying the time-history loads. As the prescribed total time of the earthquake was 10.19 sec, the end time of this load step was defined at 25.19 sec. Also the time step size (the time intervals of loading) of this load step was constant and equal to 0.01 sec (i.e. the earthquake was applied through 1019 load cases). The type of the desired results and the Rayleigh damping coefficients were specified also using the solution options of ANSYS.

Due to the large number of the nodes & elements of the building model, and the maximum storage capacity for any file of an NTFS operating system being 8GB, the complete seismic analysis for every model was carried out in two individual times of running in accordance with the maximum result file size of the analysis.

As the damping forces influence the realistic seismic response of the buildings, the Rayleigh damping coefficients (refer to section 4.4) were applied for the



transient dynamic analysis of the FCTS & SCTS model according to the calculated values using the modal analysis results of these models. These coefficients were applied using the solution options of the eleventh load step and specified for the FCTS ( $\alpha = 0.029$  &  $\beta = 0.028$ ) and SCTS ( $\alpha = 0.032$  &  $\beta = 0.029$ ) model.

5. Applying of the seismic loads (earthquakes) for models (FCTS & SCTS) was carried out through the eleventh load step using the displacement time-history input motion which was previously presented in detail in chapter 3 (refer to chapter 3, section 3.3.3.1 and Fig. 3.6). For the transient dynamic analysis of the ten-storey RC buildings under the horizontal earthquake alone, the horizontal displacement time-history was applied directly to the fixed bases of the models in x, z directions as a two-dimensional input motion. For the models under both horizontal and vertical earthquake together, the horizontal and vertical displacement time-histories were applied concurrently and directly to the fixed bases of the model in x, z directions for the horizontal displacements and y-direction for the vertical displacements as a three-dimensional input motion.
6. After completion of the eleven load steps of the analysis, the transient dynamic analysis solution was carried out according to these load steps. Then the post elastic results were reviewed and extracted using the time-history postprocessor of ANSYS.

Due to the seismic analysis of the ten-storey RC building using the finite element method (the ANSYS program) included some complicated processes (such as modelling and analysis), all ANSYS commands which were used for executing the transient dynamic analysis of the FCTS model under the both horizontal and vertical earthquake together are shown in the ANSYS input data batch file in **Appendix III**. It can be referred to this file for more additional information about the used modelling and analysis technique.



## CHAPTER 5 SEISMIC ASSESSMENT

### 5.1 Philosophy Of Assessment

The developments in seismic design standards through the years have brought about the realisation that many structures designed prior to the modern design codes (such as Eurocode 8, ref. [4]) may be deficient according to the seismic requirements of current design standards. This deficiency in seismic performance of the structures has been emphasised by the observation of the damage effects of the recent earthquakes on the 'old' building structures (existing multi-storey RC buildings). For example, the earthquake with Richter magnitude 7.2 which struck Kobe, Japan, in 1995 badly damaged many buildings and bridges. However, the damage to reinforced concrete buildings in that earthquake was much more severe for buildings built before the current Japanese seismic code came into effect in 1981. Most buildings built after 1981 suffered only minor damage. As a consequence for this recent observation concerning the deficient RC buildings under the earthquakes, the need for the seismic assessment arises in many countries in order to upgrade (retrofit) these buildings if necessary.

The structural deficiencies of many existing reinforced concrete buildings designed to normal design codes (such as BS8110) are generally not just a result of inadequate strength. The longitudinal reinforcement present in some existing structures results in a horizontal load strength which may approach or exceed that required by current seismic design standards for structures of limited ductility or even ductile structures. However, poor structural response during earthquakes is normally due to a lack of a static design approach to ensure the formation of an appropriate global mechanism of post-elastic deformation and/or to poor detailing of reinforcement, which means that the available ductility of the structure may be inadequate to withstand the earthquake without collapse.

Due to the expected deficiency in the seismic performance of existing reinforced concrete buildings, it is necessary to define specific methods for the seismic assessment of these buildings. In 2002, Park, ref. [17], mentioned that a detailed assessment procedure for the seismic assessment of existing reinforced concrete frames has been



suggested by Priestley and Calvi and by Park. The suggested procedure is based on determining the horizontal load strength and ductility of the critical post-elastic mechanism of structural deformation. Once the available horizontal load strength and ductility of the structure has been established, reference to the current code seismic acceleration response spectra for earthquake loading then enables the designer to assess the seismic risk. The procedure uses recent analytical and experimental evidence of the behaviour of elements and joints subjected to simulated seismic loading. The experimental information obtained included the interactions between the shear strength of members or joints and flexural ductility, and the performance of lap-splices and anchorages.

Retrofit when necessary to enhance the strength and/or ductility of the structure has been achieved in some countries (such as New Zealand, United States, Japan and other earthquake countries) by adding

- New structural steel bracing
- New structural concrete walls, either sprayed on to existing walls or as infills within existing frames, or as new walls placed vertically up the structure
- By jacketing (enclosing) existing elements using jackets of reinforced concrete or steel or fibre glass or carbon fibre
- By adding seismic isolation

Also it was mentioned that currently a Study Group of the New Zealand Earthquake Society is preparing a seismic assessment document. It is anticipated that it will be nominated by the New Zealand Building Code Handbook as a means of compliance.

In this research, the assessment of seismic response of the existing multi-storey RC buildings was conducted depending on the three-dimensional transient linear dynamic (time-history) analysis of these buildings. As the solution of the time-history analysis of the FCTS & SCTS model under the horizontal earthquake & under the horizontal and vertical earthquake together was carried out, the post elastic time-history forces (such as moments and axial loads) of these building analyses were extracted to be used in the assessment of these models in accordance with the applied assessment technique. The concept and procedure of the assessment technique which was applied for the FCTS &



SCTS model in order to obtain the realistic seismic response of these models, is presented in the following sections.

### **Methodology Of The Assessment Technique**

The global RC building structure is composed of various structural members such as columns, beams and slabs. These members are 'linked' structurally, and the forces they experience are distributed according to their relative stiffnesses. It is standard practice with seismic design to ensure that plastic hinges form in beam before columns to avoid soft storey global collapse and to realise the maximum benefit of post-elastic load redistribution. Due to the linear nature of the model, the post elastic yielding behaviour is not captured, and assessment must be based on the integrity of the structure for the elastic case only. Assessment of all beams, slabs & columns would provide a thorough examination of the building model. However, the columns provide the main vertical load supporting members & it is imperative that these remain in-tact to maintain global structural integrity. Due to these reasons the seismic assessment of the FCTS & SCTS model was focussed only on the buildings columns. Nevertheless the assessment for buildings columns only was still onerous due to the number of finite elements the columns were comprised of (636), the types of resulting seismic forces used (moments & axial loads) and the number of load cases (1019) according to the acceleration time-history input motion.

The concept of the columns assessment is based on the assessment of the combined axial load and biaxial bending moments ( $f_y$ ,  $m_x$ ,  $m_z$ ) of a column section against the requirements of BS8110 (ultimate limit state design). The assessment of the columns of the FCTS & SCTS model under the earthquakes was performed as follows:

1. The post elastic forces of columns from the time-history analysis were obtained. These forces consist of extreme values (maximum and minimum value) of the axial load ( $f_y$ ) & bending moments ( $m_x$ ,  $m_z$ ) throughout the time-history for bottom & top node of every 3D finite element of the columns. At each node of the column finite element the total number of the output axial load or any bending moment of all building columns were 636 maximum and 636 minimum values. Due to the axial load of columns during the earthquakes being either compressive or tensile forces, the assessment was performed for the maximum and minimum values of axial load



separately according to its resulting sign. In the other extreme, the maximum (absolute) bending moment value ( $m_x$  or  $m_z$ ) of the maximum or minimum values of bending moments only was assessed.

2. The applied seismic forces which were obtained (stated above in step No.1) for all finite elements of the building columns for every dynamic analysis type according to the model type (FCTS or SCTS) and the seismic action (horizontal alone or both horizontal & vertical together) were organized using a computer data file (maximum  $f_y$ , maximum absolute  $m_x$ , maximum absolute  $m_z$  & minimum  $f_y$ , maximum absolute  $m_x$ , maximum absolute  $m_z$ ). Subsequent to that these forces, dimensions of the columns sections, the reinforcement details of the columns according to the static design (see appendix II) and other information (such as identification of the column finite elements) were compiled into a computer data file (spreadsheet) as required by the input format for the assessment computer program.
3. The assessment of the combined axial load and biaxial bending moments of building columns was carried out using a fortran computer program. The complete program running for every data file was carried out twice in accordance with the design concrete compressive strength ( $f_{cu}$ ) of ground floor 40 N/mm<sup>2</sup> and the above floors 30 N/mm<sup>2</sup> (see Appendix II).

The fortran computer program was written primarily to assess the ability of a reinforced concrete column to withstand axial load and biaxial bending moments. It reads in a database of columns with corresponding section properties, together with an applied axial load and bending moments about section axes  $x$  and  $z$ . Using strain compatibility and equilibrium checks, the ultimate bending moment capacities about both section axes are computed for the applied load. The procedures set out in BS8110 are then used to 'assess' the applied bending moments against the ultimate moments computed for the section, producing a margin of safety. Failure surface theory is also included as an additional check in the program, as used in older codes of practice.

4. For every analysis type according to the model type (FCTS or SCTS) and input motion components included (horizontal alone or concurrent horizontal & vertical), the number of the assessment results files was 4 according to the bottom & top nodes and maximum & minimum axial load at each node. Each



file contained 636 assessment results according to the total number of the column finite elements. The files of all assessment results were imported into spreadsheets and formatted & summarized in tables. Appendix IV includes the spreadsheet of the assessment results file of the FCTS model under the horizontal earthquake only (bottom node & minimum axial loads). This Appendix shows clearly some of the input data of the columns and the results of assessment for every column finite element during the earthquake. Also it demonstrates the conservatism of the assessment technique used for the seismic analysis results.

5. As the assessment results were formatted into spreadsheets as shown in Appendix IV, the margins and acceptability of columns were examined accurately by hand for every spreadsheet to summarize the case of building columns under the earthquakes for every type of analysis. The resulting margins at every column node (top or bottom) from the two spreadsheets of maximum & minimum axial loads at this node were studied to get the worst case under the earthquakes. The columns were registered as passing the assessment if the margins were greater than 1, and failed if the column margins fall below the acceptable limit, less than 1. Margins less than 1 were reviewed regarding overload capacity or complete failure occurrence for a column and/or the columns having snapped due to the axial tensile forces. Hence the worst-case scenario of the global seismic response (realistic collapse mechanism) was evaluated for the building models (FCTS & SCTS).

As the main collapse mechanisms of the FCTS & SCTS model were drawn in accordance with the columns assessment, the transfer beams (B) of the buildings under the earthquakes were assessed against the design values of the maximum shear forces and bending moments of these beams (see Appendix II, section 7.1.2). This assessment was conducted in order to confirm the realistic seismic response of the buildings that was obtained from the columns assessment. This was also done to give insight into the seismic behaviour of the transfer beams of the RC building soft storey under the vertical component of the earthquakes.



## 5.2 Assessment Of The FCTS Model

Investigation of the global seismic behaviour of the first case ten-storey RC building (FCTS) determined by the seismic margins study of the columns gives significant insight into the vulnerable local areas of the building. The description of the global collapse mechanism of the FCTS model will be shown in the next sections.

The procedure of the seismic assessment technique which has been utilized has two distinct areas of conservatism, from the loading applied and those inherent in the applied design code. The conservatism of this seismic assessment technique will be discussed later on in the section 5.2.2.

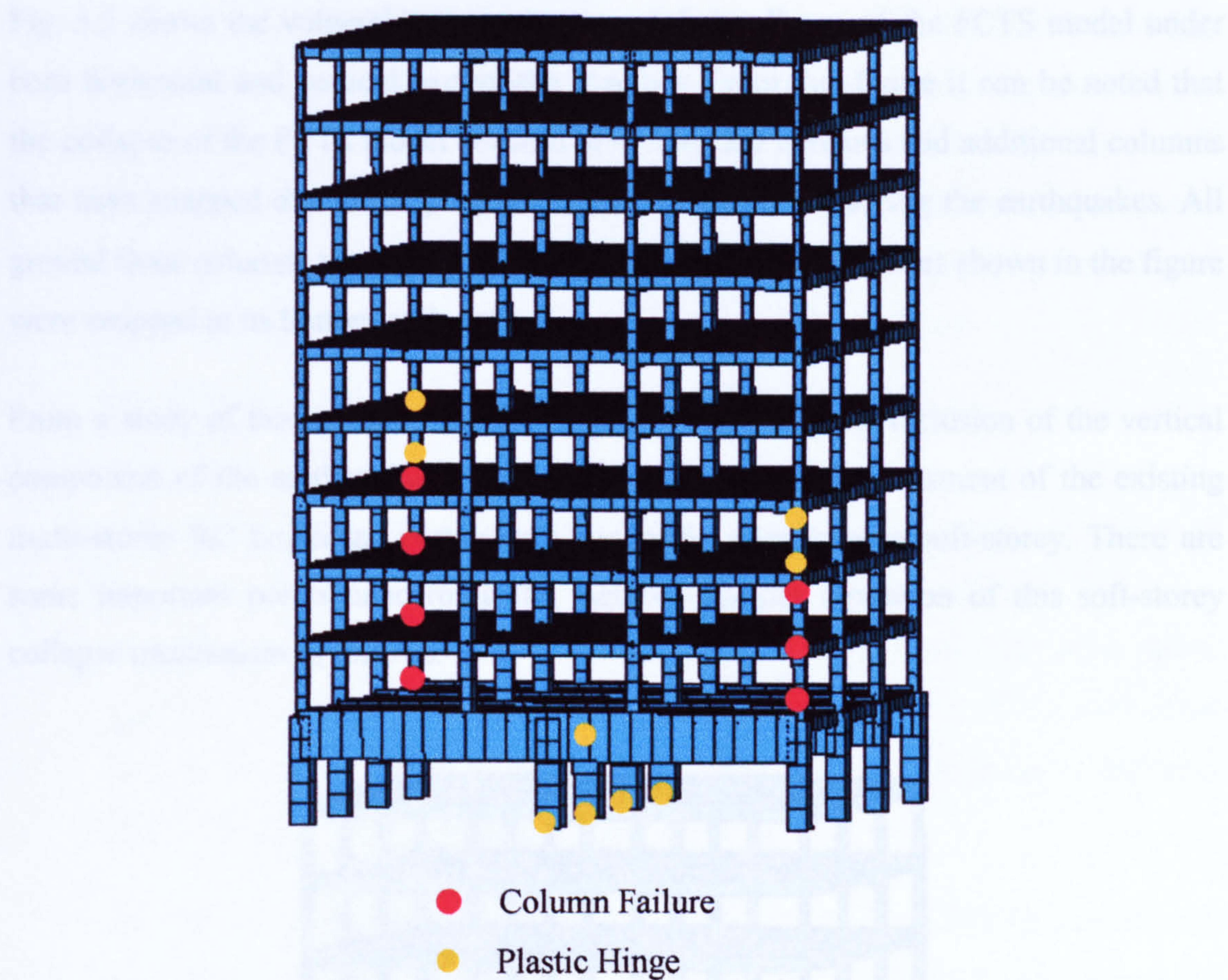
### 5.2.1 Discussion And Evaluation Of Assessment Results (Collapse Mechanism)

Fig. 5.1 shows the realistic global collapse mechanism of the FCTS model under the horizontal earthquake only. This collapse mechanism is the worst-case scenario which was produced from the seismic assessment of the building in accordance with the requirements of BS8110. From this figure it can be noted that the formation of collapse mechanism of the FCTS model consists of failed and overloaded columns (requiring the presence of plastic hinges). Plastic hinges must form at the bottom end of the internal columns of the ground floor. In addition to that a plastic hinge must form at the top end of one of these internal columns. The back corner columns of the building were failed at the first, second and third floor. Also the fourth floor column requires plastic hinges at both its ends. The front corner columns were failed in the first & second floor and plastic hinges must develop at both ends of the third floor column.

The description of the collapse mechanism stated above (see Fig. 5.1) indicates the particular areas in the building that are structurally vulnerable. Examination of this collapse mechanism gives insight into the factors affecting the resulting seismic response of the FCTS model as follows:

- The failure is concentrated in two corner columns of the building as shown in Fig. 5.1, and there is reserve capacity of the surrounding structure. Hence there is vast potential for overload due to redistribution of forces to the stronger sections.





**Figure 5.1** Realistic seismic response of the FCTS model under horizontal earthquake only (global collapse mechanism)

- The failure occurs in the corner columns in the direction of the resultant of the 2D horizontal input motion (in the two orthogonal directions  $x$  &  $z$ ). As the time-histories are identical the peaks in each direction occur simultaneously putting the onus on the two diagonally opposing corners.
- Although the building contained a soft-storey in the ground floor, the failure and some of the required plastic hinges are occurring in the above floors commencing with the first floor. Due to the stiffness discontinuity at the connection points between the ground and first floor, the failure occurred at these particular points and extended toward the floors that have less stiffnesses. The columns stiffnesses of the ground and first floor were calculated analytically to determine which floor is less stiff. The stiffness of the ground floor is larger than the first floor, hence the failure and plastic hinges extended to the above floors not the ground floor.



Fig. 5.2 shows the vulnerable areas causing global collapse of the FCTS model under both horizontal and vertical earthquake together. From this figure it can be noted that the collapse of the FCTS model consists of overloaded columns and additional columns that have snapped due to the presence of the tensile forces during the earthquakes. All ground floor columns were snapped except two internal columns as shown in the figure were snapped at its bottom ends only.

From a study of this collapse, the first significant point is the inclusion of the vertical component of the earthquakes for the seismic analysis and assessment of the existing multi-storey RC buildings, particularly our model containing a soft-storey. There are some important points concerning the factors affecting formation of this soft-storey collapse mechanism as follows:

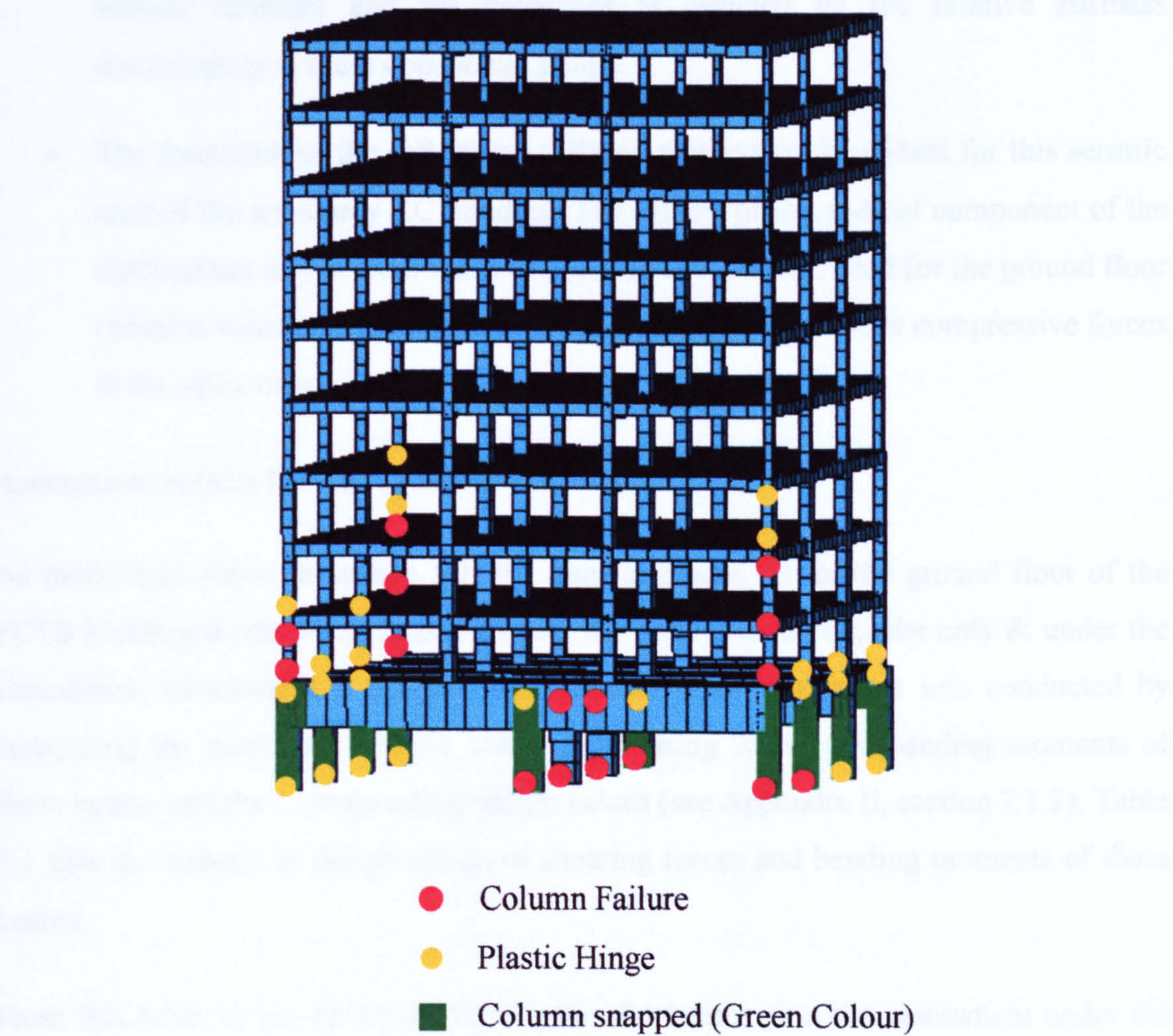


**Figure 5.2** Realistic seismic response of the FCTS model under both horizontal & vertical earthquake together (global collapse mechanism)



- When compared with the results from the horizontal earthquake only (see Fig. 5.1), the effects of the vertical component can be revealed through the collapse of the soft-storey (ground floor) as predicted. The collapse of the soft-storey will lead to the complete failure of the building. Also investigation of the soft-storey regarding the required plastic hinge formation shows that there is practically no benefit from redistribution of load and global collapse is likely.
- Examination of the top ends of the ground floor corner columns (back left & front right column) and bottom ends of the first floor corner columns (back left & front right column) suggests that there is no requirement for the formation of plastic hinges at the top ends of ground floor corner columns. Failure is occurring at the bottom ends of first floor corner columns. This observation confirms that the building is vibrating in the direction of the horizontal input motion resultant and the behaviour is affected by the relative stiffness discontinuity at these connection points.
- The formation of the soft storey collapse mechanism is evident for this seismic case of the ten-storey RC building. The effects of the vertical component of the earthquakes on the axial loads of columns are demonstrated for the ground floor columns which were snapped although their axial loads were compressive forces in the static case.

### **Assessment results Of The Transfer Beam (B)**

As mentioned above in section 5.1, the transfer beams (B) of the ground floor of the FCTS building model were assessed under the horizontal earthquake only & under the concurrent horizontal and vertical input motion. This assessment was conducted by comparing the maximum seismic values of shearing forces and bending moments of these beams and the corresponding design values (see Appendix II, section 7.1.2). Table 5.1 lists the seismic & design values of shearing forces and bending moments of these beams.

From this table, it can be noted that the transfer beams pass the assessment under the horizontal earthquake that emphasizes the satisfactory seismic performance of the soft storey (ground floor) of the building through the realistic collapse mechanism shown in



Fig. 5.1. Also the comparison for the building under the concurrent horizontal & vertical earthquake confirm this. The seismic performance of the transfer beams under the vertical component of the earthquakes is mainly dependent on the shearing performance of these beams. The shear forces of the transfer beams listed in table 4.1 under the both horizontal and vertical earthquake together show that the shearing is a problem and the beams may fail due to this reason. The mode of shearing failure is non-ductile and therefore this presents an additional hazard to the collapse mode, however there is much conservatism in shear design according to the codes of practice.

Seismic Assessment Of The FCTS Transfer Beam (B)			
Applied Forces	Maximum Design Values	Under Horizontal Earthquake Only	Under Concurrent Horizontal & Vertical Earthquake
Shear Force (kN)	5547.5	4985	7146
Bending Moment (kN.m)	13214	12750	16370

Table 5.1 Seismic response of the transfer beam (B) of the FCTS model

5.2.2 Conservatism Of The Assessment Technique For The Seismic Analysis Results

The assessment procedure which was mentioned above in section 5.1, was applied for the seismic analysis results with an approach leading to the worst-case predicted for the collapse mechanism of the ten-storey RC building. To satisfy this purpose from the assessment procedure, the conservatism was inherent as a consequence for the type of loading used (time-history loading) and also in the assessment results from the static design code (BS8110).

Due to the input ground motion (earthquake) used in this research being discretised into 0.01 sec time intervals (with the total time of the earthquake of 10.19 sec) the number of load cases that were applied for the elements (636) of the models columns was 1019. This large number of load cases and column elements increases the data manipulation required for the assessment. As a result the extreme values of loading throughout the total time were extracted (regardless of time of occurrence) and applied as a single load case which demonstrates the presence of the conservatism using this assessment technique. To reduce this conservatism, the ‘100-40-40’ rule of ASCE standard, ref. [26], can be used.



By using this rule the three orthogonal spatial seismic components of the load case are applied in the ratios of 100% - 40% - 40% therefore the load case would have to be applied three times, as the reduction ratio in the seismic components must be cycled through all three orthogonal directions, and the most onerous case will be applied.

This conservatism was also evident in summarizing the seismic margins of every case of loading for the models. For every analysis type (according to the applied directions of the input motion & the model type), there were 4 spreadsheets and every spreadsheet contains a large number of the results (636) as shown in Appendix IV.

To estimate the benefit (level of the present conservatism) using this assessment technique, a single column element was chosen to be assessed under the full time-history of 1019 load cases. Figures 5.3, 5.4 shows the drawings of the columns axes for the ground & above floors of the building models. According to these drawings the 636 elements of columns were identified in the assessment process. Regarding the spreadsheet included in Appendix IV, every column element was identified according to the axis character, number and additional number relates to the element order in the height of column (the columns were divided to 1m elements). The column element B31 in the ground floor was selected for this purpose as the desired margin of the selected column was less than 1. This column had a margin 0.87 from the global assessment of the FCTS model columns under the horizontal earthquake only as shown in Appendix IV (see coloured row in this spreadsheet). From the assessment of this column under the horizontal time-history loading, it was found that the worst margin less than 1 was equal to 0.89 (spreadsheet of the assessment of this column under the time-history loading is included in Appendix IV). The approximate benefit was calculated using the above margins of this column from the global and actual assessment under the time-history loading as shown in the following section.

$$\text{Approximate Benefit (level of the conservatism)} = (0.89 - 0.87) / 0.87 = 2.3 \%$$

The conservatism arises also from the assessment procedures of static design codes (BS8110). As any design code contains a number of factors which inherently (and purposefully) produce a margin of safety, and the assessment may be examined according to the required values of these factors. Material safety factors of 1.5 and 1.05 are prescribed for the concrete and steel in accordance with the BS8110 and these values were used for this assessment. Part 2 of the BS8110 mentioned that it can be



used a material safety factor 1.2 for the concrete in certain circumstances as a worst credible value. Therefore the conservatism due to the material safety factors is evident.

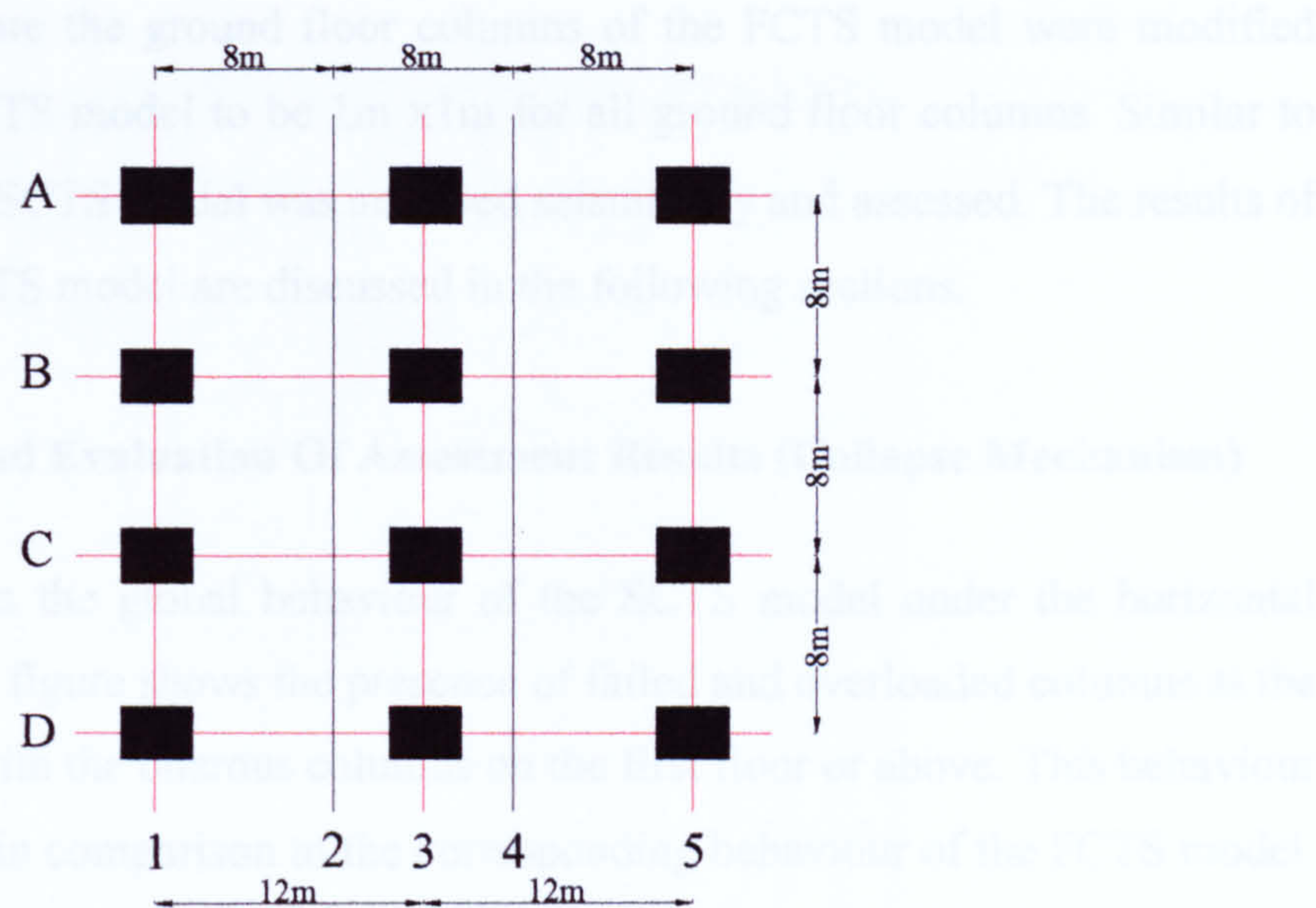


**Figure 5.3** Columns axes of the ground floor of the FCTS & SCTS model

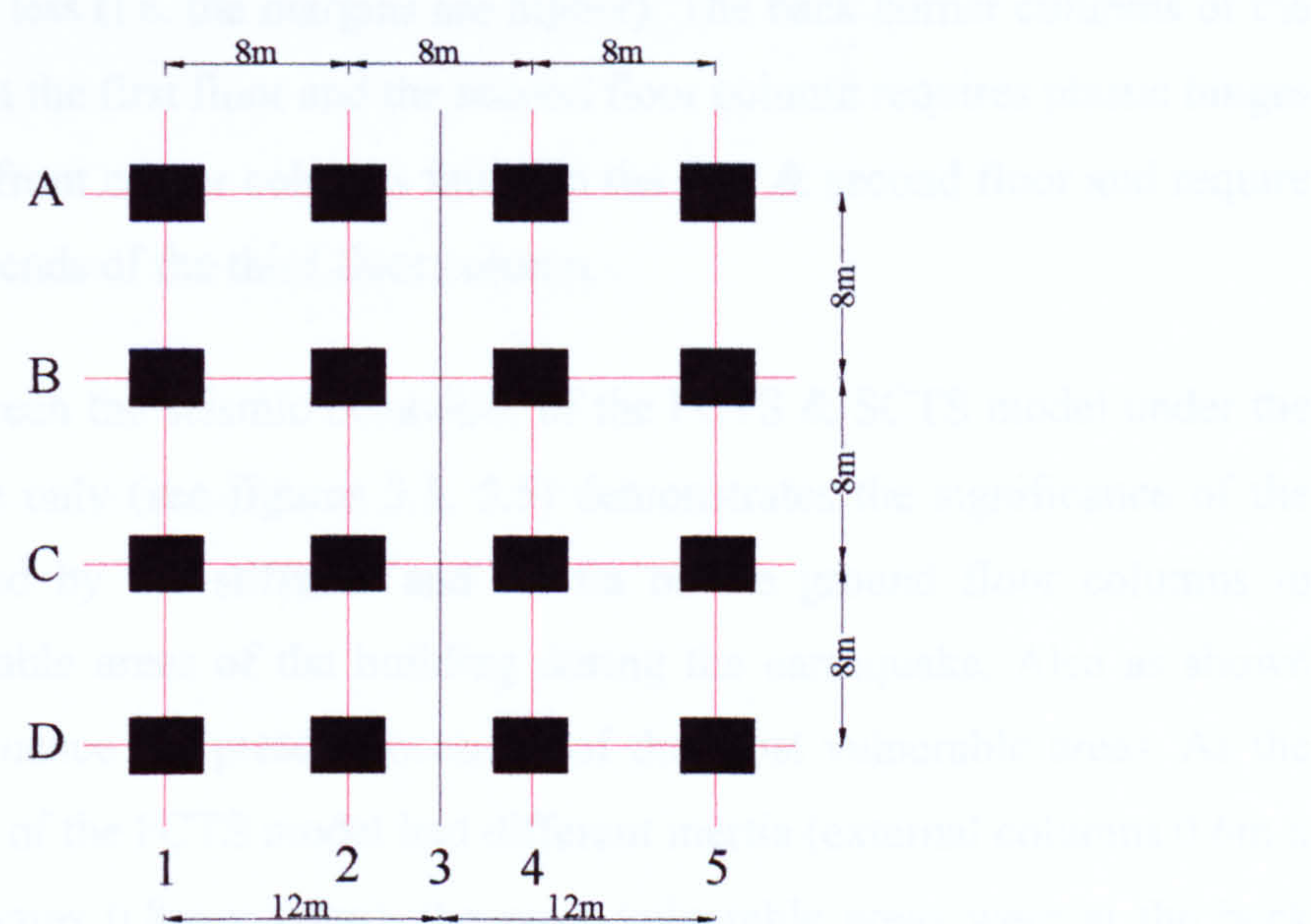


**Figure 5.4** Columns axes of the above floors of the FCTS & SCTS model

**5.3 Assessment Of The SCTS Model**

Due to the formation of the soft-storey collapse mechanism for the FCTS model under the both horizontal and vertical earthquake together (see Fig. 5.2), the SCTS model was produced as an upgraded model to present a more desirable seismic



performance against this collapse mechanism. The main aim of this model was to alter the ground floor stiffness (the soft storey) in an attempt to improve the seismic performance. Therefore the ground floor columns of the FCTS model were modified (increased) in the SCTS model to be 1m x 1m for all ground floor columns. Similar to the FCTS model, the SCTS model was analysed seismically and assessed. The results of assessment of the SCTS model are discussed in the following sections.

### 5.3.1 Discussion And Evaluation Of Assessment Results (Collapse Mechanism)

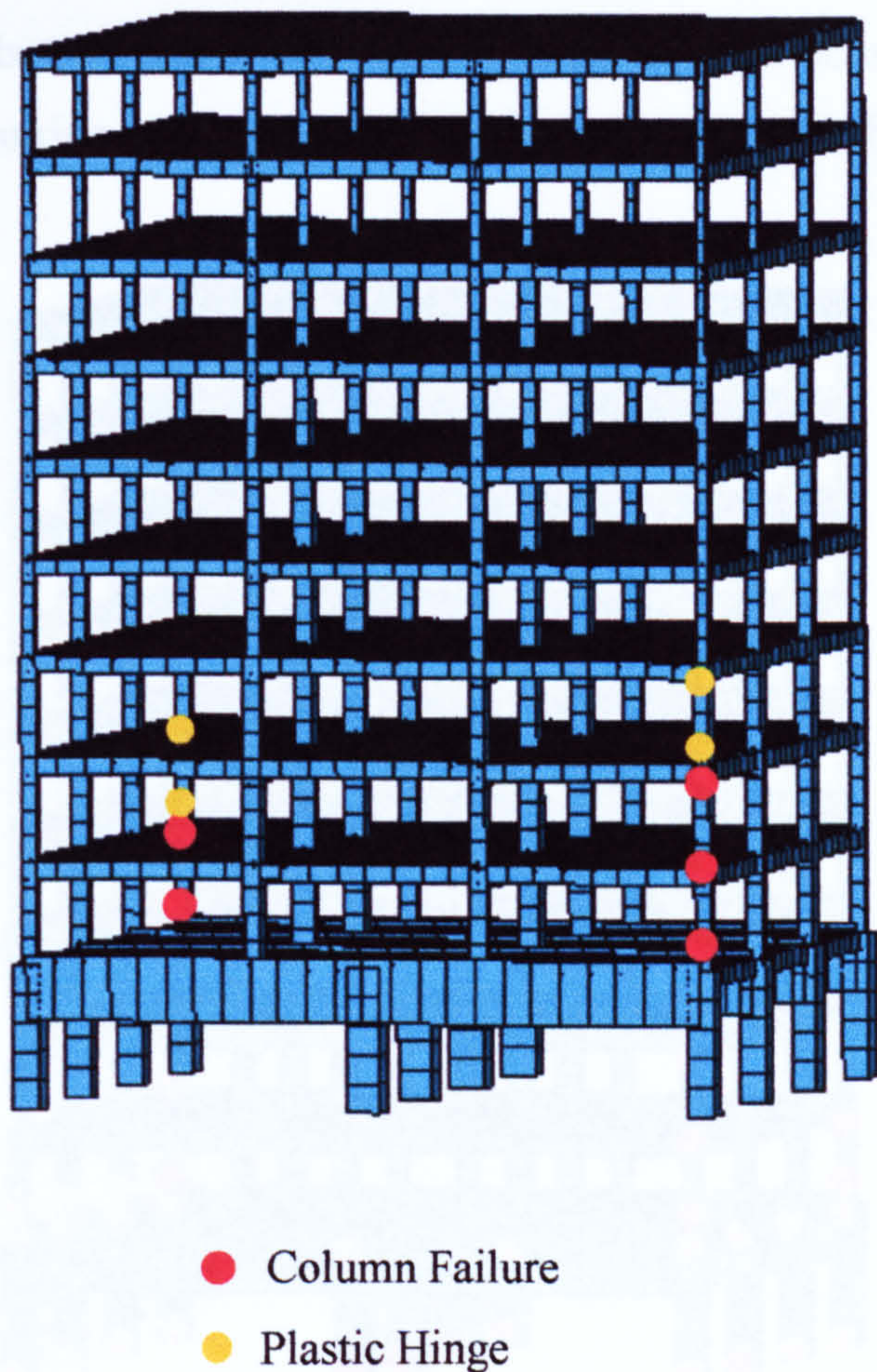
Fig. 5.5 shows the global behaviour of the SCTS model under the horizontal earthquake only. This figure shows the presence of failed and overloaded columns at the corners once again, with the onerous columns on the first floor or above. This behaviour exhibits less damage in comparison to the corresponding behaviour of the FCTS model. Unlike the FCTS model, there is no plastic hinges required to form at the ground floor columns of this model. Also the ductility requirement or failure for the corner columns of the above floors is less (i.e. the margins are higher). The back corner columns of the building were failed at the first floor and the second floor column requires plastic hinges at both its ends. The front corner columns failed in the first & second floor and require plastic hinges at both ends of the third floor column.

The comparison between the seismic behaviour of the FCTS & SCTS model under the horizontal earthquake only (see figures 5.1, 5.5) demonstrates the significance of the role that is performed by the stiffness and inertia of the ground floor columns in mitigating the vulnerable areas of the building during the earthquake. Also as shown these two factors influence the present locations of the most vulnerable areas. As the ground floor columns of the FCTS model had different inertia (external columns 0.6m x 0.8m & internal columns 0.8m x 0.8m), the most vulnerable areas were at the back corner columns hence the building is predominantly bending clockwise i.e. the back corner columns are experiencing the greater tensile forces. For the SCTS model due to the all ground floor columns having similar inertia rather than increasing the stiffnesses, the most vulnerable areas were at the front corner columns hence the building is predominantly bending anti-clockwise i.e. the front corner columns are experiencing the greater tensile forces. In general increasing the size of the ground floor columns of the



ten-storey RC building decreased the onerous effects of the horizontal earthquake i.e. the seismic performance of the ten-storey RC building was enhanced.

Plastic hinges formed at the top ends of the back & front corner columns of the SCTS model. Also a failure at the base of the back corner column of the FCTS model was converted to failure at the base of the front corner column of the SCTS model.



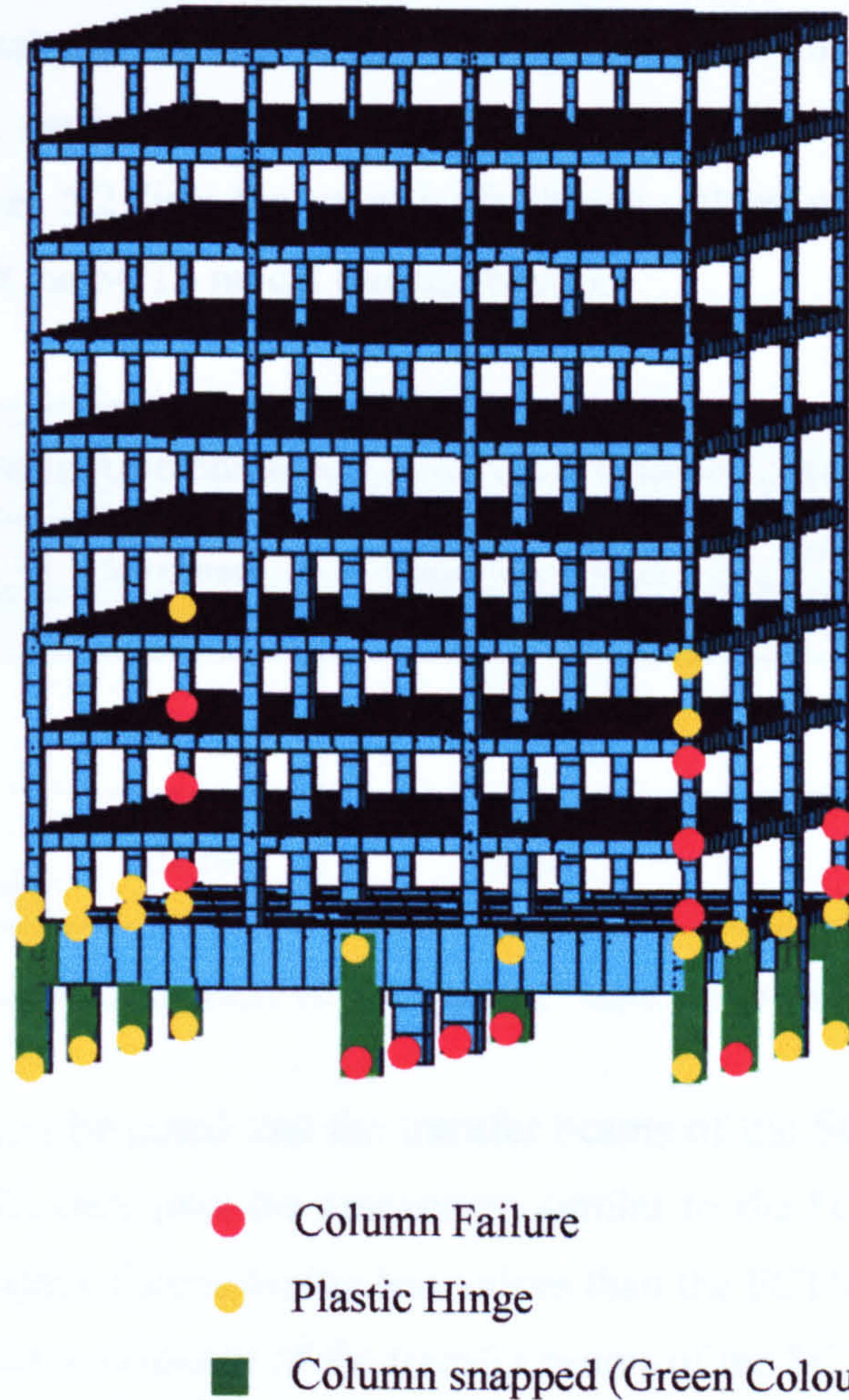
**Figure 5.5** Realistic seismic response of the SCTS model under horizontal earthquake only (global collapse mechanism)

Fig. 5.6 shows the vulnerable areas causing global collapse of the SCTS model under both horizontal and vertical earthquake together. Similar to the FCTS model under the concurrent horizontal & vertical earthquake (see Fig. 5.2), the collapse of the SCTS model consists of overloaded columns and additional columns that have snapped due to the presence of the tensile forces during the earthquakes. Also all ground floor columns were snapped (except two internal columns had snapped at their bottom ends only as shown in Fig. 5.6).

The seismic behaviour of the SCTS model as shown in Fig. 5.6 shows that the formation of the soft-storey collapse is similar (the margins are approximately the same) to the FCTS model (see Fig. 5.2) including some slight changes. These changes are



summarized in the conversion and reallocation of the failure at the top ends of two of the internal columns of the FCTS model (the columns not snapped) to requiring plastic hinges to form at the top ends of the back & front corner columns of the SCTS model. Also a failure at the bottom end of one of the right external columns of the FCTS model was converted to requiring a plastic hinge at the same location for the SCTS model.



**Figure 5.6** Realistic seismic response of the SCTS model under both horizontal & vertical earthquake together (global collapse mechanism)

The seismic behaviour of the SCTS model as shown in Fig. 5.6 regarding the above floors exhibits a slightly improved performance above the corresponding FCTS model (see Fig. 5.2) as predicted. In general as the soft storey collapse of the SCTS model was formed similar to the FCTS model, the complete collapse of the building is likely to occur and consequently the increase of the ground floor stiffness which was suggested



for improving the seismic performance is not significant under both horizontal and vertical earthquake together.

**Assessment results Of The Transfer Beam (B)**

Similar to the FCTS model the transfer beams (B) of the ground floor of the SCTS building model were assessed under the horizontal earthquake only & under the concurrent horizontal and vertical input motion. This assessment was conducted to confirm the seismic performance of the upgraded model of the FCTS building (i.e. the SCTS model). Table 5.2 lists the seismic & design values of shearing forces and bending moments of the SCTS model transfer beams.

Seismic Assessment Of The SCTS Transfer Beam (B)			
Applied Forces	Maximum Design Values	Under Horizontal Earthquake Only	Under Concurrent Horizontal & Vertical Earthquake
Shear Force (kN)	5547.5	4917	7636
Bending Moment (kN.m)	13214	12220	16610

**Table 5.2** Seismic response of the transfer beam (B) of the SCTS model

From this table, it can be noted that the transfer beams of the SCTS model under the horizontal earthquake only pass the assessment similar to the FCTS model (see table 5.1) with applied seismic forces having less values than the FCTS model. Also like the FCTS model the seismic response of the transfer beams of the SCTS building under the concurrent horizontal & vertical earthquake revealed insufficient structural integrity to withstand the seismic event.

The comparison between the applied seismic forces of the transfer beams of the SCTS model under concurrent horizontal & vertical earthquake and the corresponding FCTS model exhibits the effects of the stiffnesses of the ground floor columns on the seismic behaviour of the transfer beams. From this comparison it can be noted that the seismic forces of the SCTS model transfer beams are larger than the FCTS model. This confirms that when the columns are stronger than beams the required plastic hinges at column-beam joint will be formed in the weaker member (beams).



## 5.4 Response Spectra Of The FCTS And SCTS model

The seismic behaviour of the buildings can be evaluated by the response parameters such as maximum amplitude of the relative displacement, the relative velocity and the absolute acceleration developed during a seismic excitation. The generation of secondary response spectra of the building provides significant information regarding the seismic behaviour of the buildings. For a defined level of input ground motion response spectra are commonly used to define peak structural response in terms of peak acceleration, maximum velocity, and maximum displacement. Also the secondary response spectrum defines confidently the natural frequencies of the buildings at which the resonance phenomenon can occur i.e. the frequencies at peak responses of the buildings under a seismic event.

The value of the peak response of the buildings under the earthquakes at various levels of damping is often required for seismic analysis and design. The seismic performance of the buildings and equipment within it can be evaluated using the peak acceleration, velocity and displacement of the buildings seismic response. Analytically the peak accelerations of the buildings against the overturning moments can be computed. Consequently, by comparing the values result from the response spectra of the buildings and the analytical calculations, the seismic performance of the buildings can be determined. This approach for defining the seismic performance of the buildings was used for the FCTS & SCTS model and will be discussed in the next sections.

### 5.4.1 Under Horizontal Earthquake Only

The acceleration secondary response spectra of the FCTS & SCTS model under the horizontal earthquake only were generated using the extracted displacement time-histories of the building floors in the x-direction. It should be mentioned that the peak ground acceleration (PGA) of the horizontal input motion which was used for the seismic analysis of these models is equal to 0.2g. Figures 5.7, 5.8 shows the horizontal response spectra of the FCTS & SCTS model respectively under the horizontal earthquake only. From these figures it can be noted that the PGA (0.2g) of the input ground motion was amplified through the higher elevation of the buildings to reach its maximum value at the upper floor. The peak value at the upper floor for the FCTS & SCTS model is equal to 0.68g & 0.53g respectively as shown in the figures. Also the



figures demonstrate the resonant natural frequencies of the buildings (FCTS & SCTS) at the peak acceleration values of their seismic response. The shapes indicate that peak accelerations are irregularly distributed over the frequency range but decrease very significantly at the high frequencies. The resonant natural frequency content of the FCTS & SCTS model is ranging from 0.95 to 2.8 Hz and 1.3 to 5.5 Hz respectively.

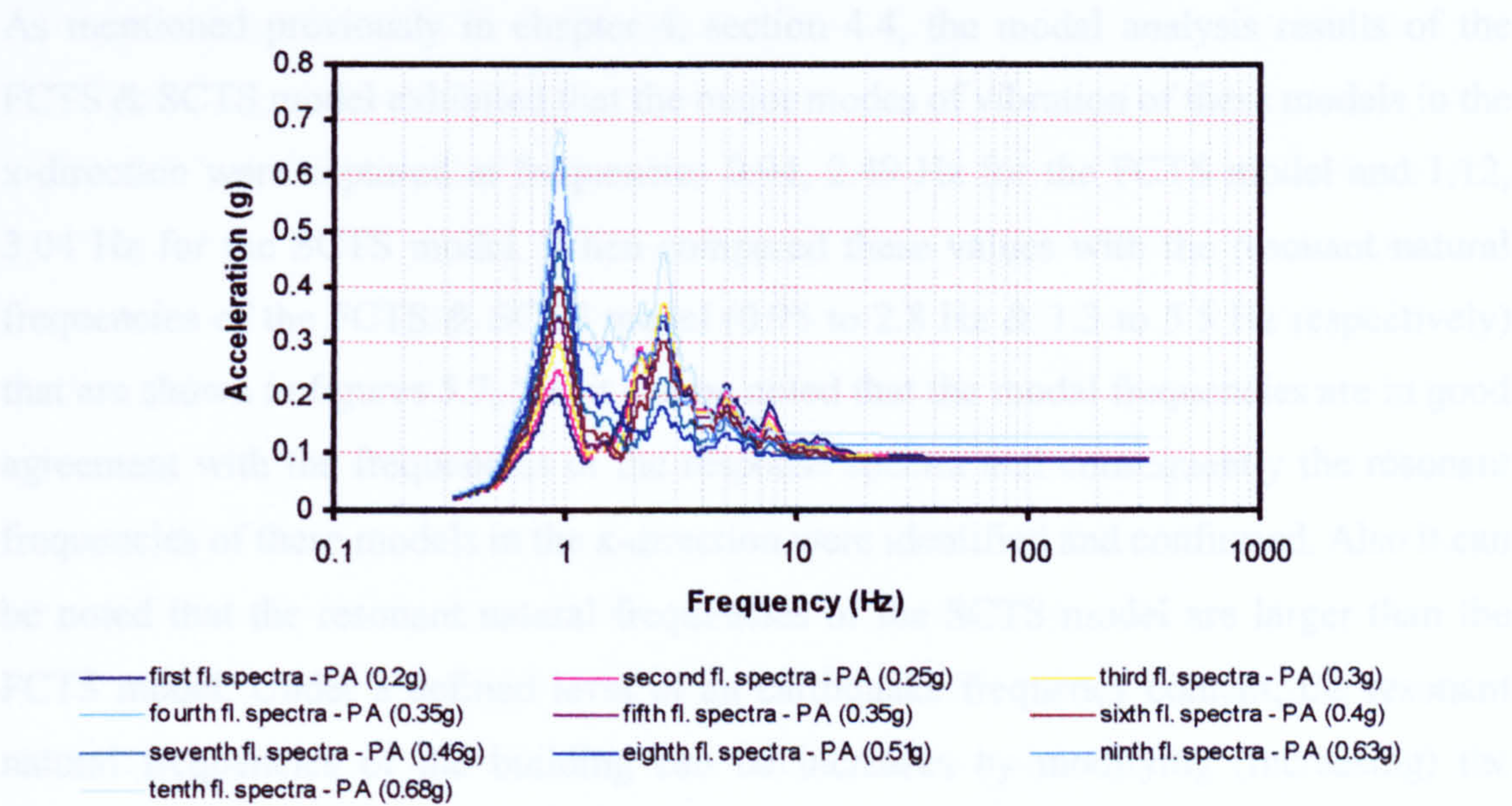


**Figure 5.7** Horizontal acceleration secondary response spectra of FCTS floors under horizontal earthquake

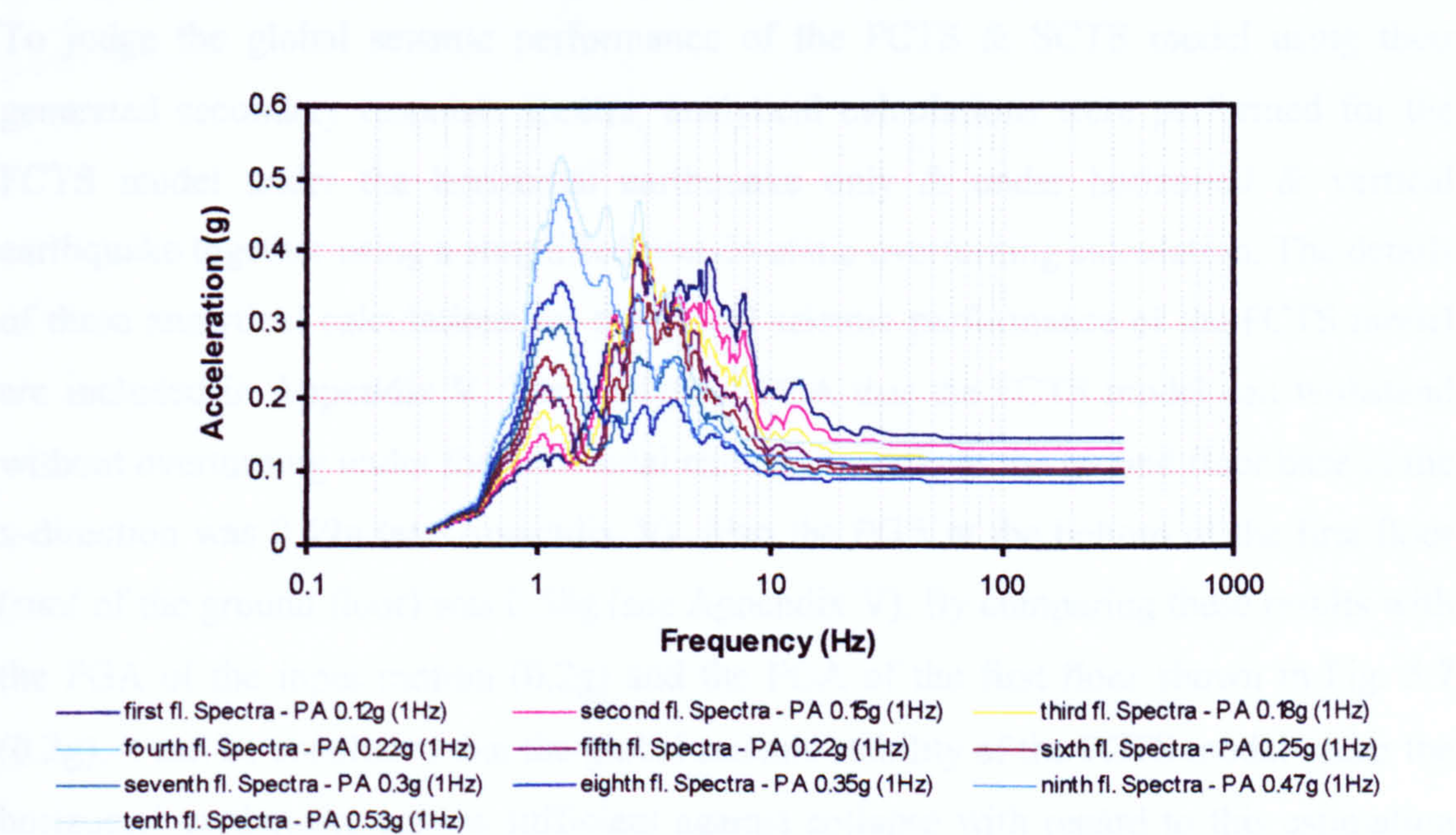


**Figure 5.8** Horizontal acceleration secondary response spectra of SCTS floors under horizontal earthquake



As shown in the figures 5.7, 5.8 the peak accelerations of the seismic response of the FCTS model are larger than the SCTS model. This disparity in the peak accelerations between the FCTS & SCTS model arises due to the effects of the stiffnesses of the ground floor. As the stiffnesses of the ground floor columns were increased, then the damping forces increased reducing the resonant amplification of the input motion.

As mentioned previously in chapter 4, section 4.4, the modal analysis results of the FCTS & SCTS model exhibited that the major modes of vibration of these models in the x-direction were captured at frequencies 0.94, 2.49 Hz for the FCTS model and 1.12, 3.04 Hz for the SCTS model. When compared these values with the resonant natural frequencies of the FCTS & SCTS model (0.95 to 2.8 Hz & 1.3 to 5.5 Hz respectively) that are shown in figures 5.7, 5.8, it can be noted that the modal frequencies are in good agreement with the frequencies of the response spectra and consequently the resonant frequencies of these models in the x-direction were identified and confirmed. Also it can be noted that the resonant natural frequencies of the SCTS model are larger than the FCTS model. Under a defined level of an earthquake frequency content, the resonant natural frequencies of the building can be increases by modifying (increasing) the building stiffnesses to reduce the onerous effects of resonant amplification of the input motion.

To judge the global seismic performance of the FCTS & SCTS model using their generated secondary response spectra, analytical calculations were performed for the FCTS model under the horizontal earthquake only & under horizontal & vertical earthquake together using a simplified pseudo-static overturning calculation. The details of these analytical calculations for the global seismic performance of the FCTS model are included in Appendix V. The analytical PGA that the FCTS model can withstand without overturning under the horizontal earthquake only at the ground floor base in the x-direction was 0.49g (see Appendix V). Also the PGA at the bottom of the first floor (roof of the ground floor) was 0.58g (see Appendix V). By comparing these results with the PGA of the input motion (0.2g) and the PGA of the first floor shown in Fig. 5.7 (0.2g), it can be concluded that the global seismic stability of the FCTS model under the horizontal earthquake only is sufficient against collapse with regard to this estimation method. Also this comparison confirms the global collapse mechanism of the FCTS model is that shown in Fig. 5.1.



5.4.2 Under Both Horizontal And Vertical Earthquake Together

The acceleration secondary response spectra of the FCTS & SCTS model under both horizontal and vertical earthquake together were generated using the excited displacement time histories of the building floors in the x-direction & the y-direction. It should be mentioned that the peak ground acceleration (PGA) of the horizontal and vertical input motion which were used for the seismic analysis of these models are equal to 0.2g & 0.13g respectively. By generating the horizontal secondary response spectra of the FCTS & SCTS model under the concurrent horizontal & vertical earthquake in the x-direction, it was found that these spectra are similar to those mentioned above under horizontal earthquake only (see figures 5.7, 5.8). Figures 5.9, 5.10 shows the vertical secondary response spectra of the FCTS & SCTS model respectively under the concurrent horizontal & vertical earthquake. From these figures it can be noted that the vertical PGA (0.13g) of the input ground motion was amplified through the higher elevation of the buildings to reach its maximum value at the upper floor. The peak value at the upper floor for the FCTS & SCTS model is equal to 0.71g and 0.81g as shown in the figures. Also these figures show that the resonant natural frequencies of the FCTS & SCTS model in y-direction are equal to 2.8 Hz. From these figures it can be noted that the vertical input ground motion (0.13g) was significantly amplified for both models (0.71g, 0.81g) and that exhibits the onerous effects of the vertical component of the earthquakes.

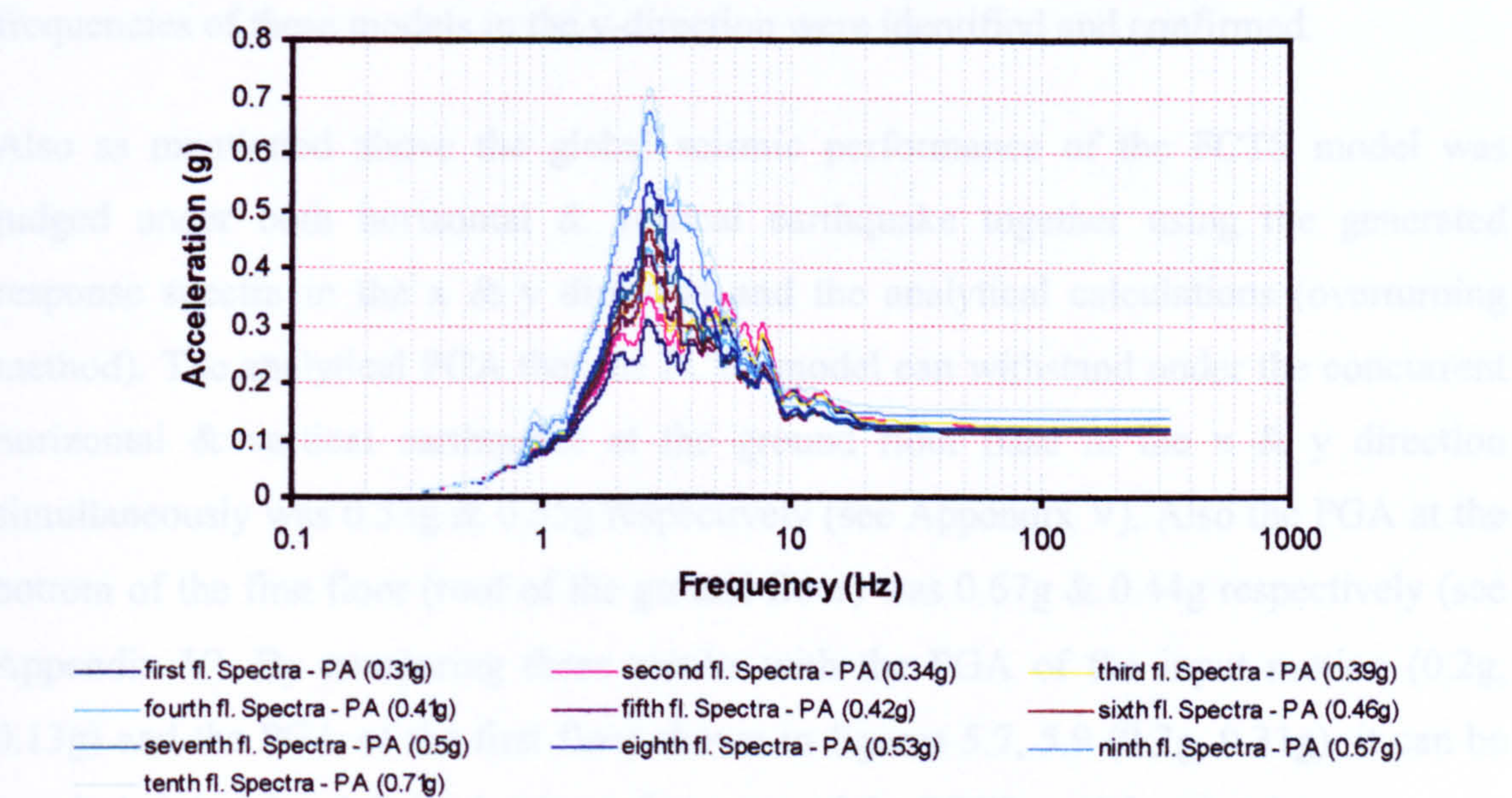
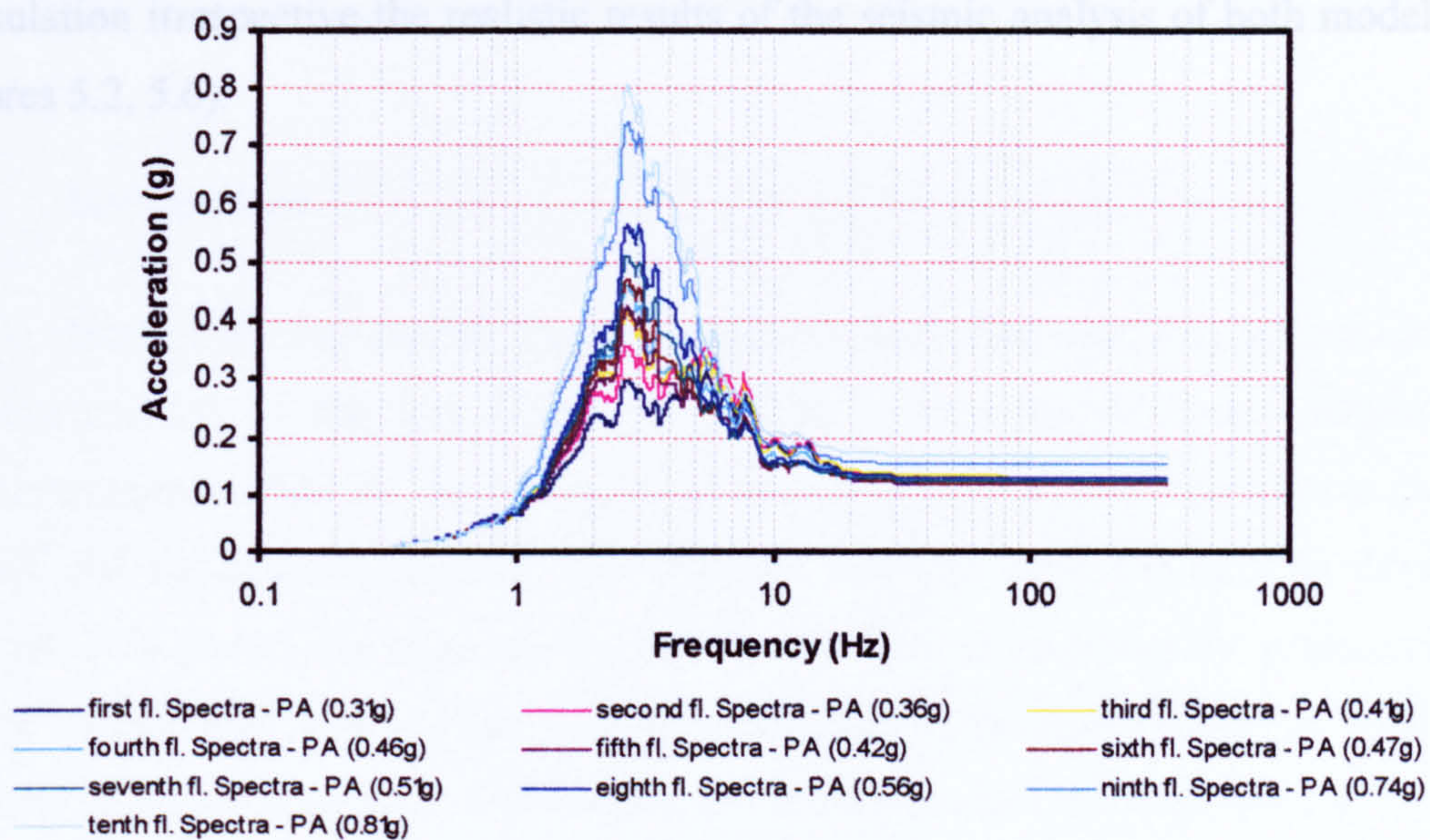


Figure 5.9 Vertical acceleration secondary response spectra of FCTS floors under concurrent horizontal & vertical earthquake





**Figure 5.10** Vertical acceleration secondary response spectra of SCTS floors under concurrent horizontal & vertical earthquake

As mentioned previously in chapter 4, section 4.4, the modal analysis results of the FCTS & SCTS model exhibited that the major modes of vibration of these models in the y-direction were captured at frequencies 3.08, 5.26 Hz for the FCTS model and 3.17, 5.69 Hz for the SCTS model. When comparing these values with the resonant natural frequencies of the FCTS & SCTS model (2.8 Hz) that are shown in figures 5.9, 5.10, it can be noted that the modal frequencies in the y-direction are in good agreement with the vertical frequencies of the response spectra and consequently the resonant frequencies of these models in the y-direction were identified and confirmed.

Also as mentioned above the global seismic performance of the FCTS model was judged under both horizontal & vertical earthquake together using the generated response spectra in the x & y direction and the analytical calculations (overturning method). The analytical PGA that the FCTS model can withstand under the concurrent horizontal & vertical earthquake at the ground floor base in the x & y direction simultaneously was 0.53g & 0.35g respectively (see Appendix V). Also the PGA at the bottom of the first floor (roof of the ground floor) was 0.67g & 0.44g respectively (see Appendix V). By comparing these results with the PGA of the input motion (0.2g, 0.13g) and the PGA of the first floor shown in figures 5.7, 5.9 (0.2g, 0.31g), it can be concluded that the global seismic performance of the FCTS model under the concurrent horizontal & vertical earthquake is sufficient against collapse with regard to this



calculation irrespective the realistic results of the seismic analysis of both models (see figures 5.2, 5.6).



## CHAPTER 6 DISCUSSION OF RESULTS

### 6.1 Introduction

Earthquake engineering, as an independent field of science, may be considered as a development of the last 40-50 years. The installation of dense networks of accelerograms worldwide, the feasibility of analysing complicated structures in both the elastic and the inelastic stage of their dynamic response using the recently developed powerful computers, the experimental testing of structural members and subassemblages under inelastic load reversals including inelastic response, the development of earthquake simulators for studying structural models, the refinement and the extensive use of in situ measuring techniques, and finally the broadening of the knowledge regarding the behaviour of soil, either in free-field conditions or in interaction with the structures, constitute significant steps towards the development of this relatively new field of engineering.

As knowledge was accumulating, it became clear that the problem of the seismic behaviour of structures is primarily an energy-related one. In order for a structure to avoid collapse, it should be in a position to absorb and dissipate the kinetic energy imparted in it during the seismic excitation. To satisfy this aim, it must be understood how the building structures behave during the seismic event i.e. how the building structures dissipate this energy globally during the seismic excitation. Subsequent to that the local vulnerable areas must be investigated and the building structures seismically upgraded specifically the existing building structures. In general the modern design codes attempt to balance between the energy dissipation capacity & demand of the building structures under the earthquakes in order to reduce the disasters.

As shown above when dealing with a subject such as seismic engineering it is appreciated that there are many variables and factors involved which make it a far from precise branch of science. Although a thorough understanding of the effects of each variable is required, it cannot be investigated these effects completely through one research or more. Therefore in this chapter we attempt to discuss few of these variables (such as soft storey, vertical earthquake, building response and 3D simulation) with regard to the finite element model studied in this research.



## **6.2 Investigation Of The Affecting Factors On Collapse Mechanisms Of The FCTS And SCTS Model**

From the examination of the behaviour of the FCTS & SCTS model under the horizontal motion only & under concurrent horizontal and vertical motion, a number of the significant factors that have influenced the behaviour of these mechanisms are highlighted.

The presence of the soft storey collapse of these models emphasized the seismic risk for such buildings particularly if they are statically designed such as these models. Although the effects of the vertical component of the earthquakes on the tall RC buildings were previously ignored and recently still have to be taken into account in narrow range, the significance of this component in judgement on the realistic seismic behaviour of the global RC building structures was demonstrated through its onerous effects on the FCTS & SCTS model. As we endeavoured to upgrade the FCTS model to be the SCTS model in order to improve the seismic performance of the ten-storey RC building and mitigate its seismic risk, the effects of this modification will be discussed in the next sections. In the seismic analysis for the global RC building structures the important function for the 3D simulation of these buildings that significantly influence the realistic seismic response will be pointed out in the next sections.

### **6.2.1 Soft Storey**

Tall RC buildings often contain a storey having wider spans in accordance with architectural design. In essence this storey is often specified in residential or office buildings to satisfy the requirements of car parking, or in particular circumstances for retail shopping. Also this storey is commonly located in the lowest level of the building (i.e. the ground floor). Therefore this storey by its nature is ‘softer’ than those at the higher elevation, causing concern for its behaviour at ultimate load.

Under the seismic event, the soft-storey is detrimental for the building because of abrupt stiffness changes that act as a load ‘attractor’. As the soft-storey of the building is typically at the lowest level and weaker than upper levels, a column sway mechanism can develop with high local ductility demand. For the FCTS & SCTS model the soft-storey collapse mechanism occurs due to the vertical component of the earthquake as mentioned in chapter 5. As the finite element model of the ten-storey RC buildings



(FCTS & SCTS) was linear, the stiffness changes of the soft-storey columns due to the overload & axial load ‘confinement’ effects cannot be captured but the collapse mechanisms of the models under the vertical earthquake (see chapter 5) demonstrate the dramatic effect of the reduced vertical load on the soft-storey making it much weaker.

Formation of the soft-storey collapse mechanism of the FCTS & SCTS model due to the vertical earthquake can be examined using the margins of safety from the assessment (refer to chapter 5). For the soft-storey collapse mechanism of the FCTS model under the vertical earthquake (see Fig. 5.2), the margins of the front left corner column & the surrounding columns for the ground floor were examined. Also the margins of the front internal column & the surrounding columns for the ground floor were examined for the collapse mechanism of the FCTS model under the horizontal earthquake only. Figures 6.1, 6.2 show the margin values of the front left corner column & the surrounding columns under the vertical earthquake, and the front internal column & the surrounding columns under the horizontal earthquake only for the FCTS model.

**Figure 6.1** Margin values of the front left corner column and its surrounding columns of the FCTS model under the vertical earthquake

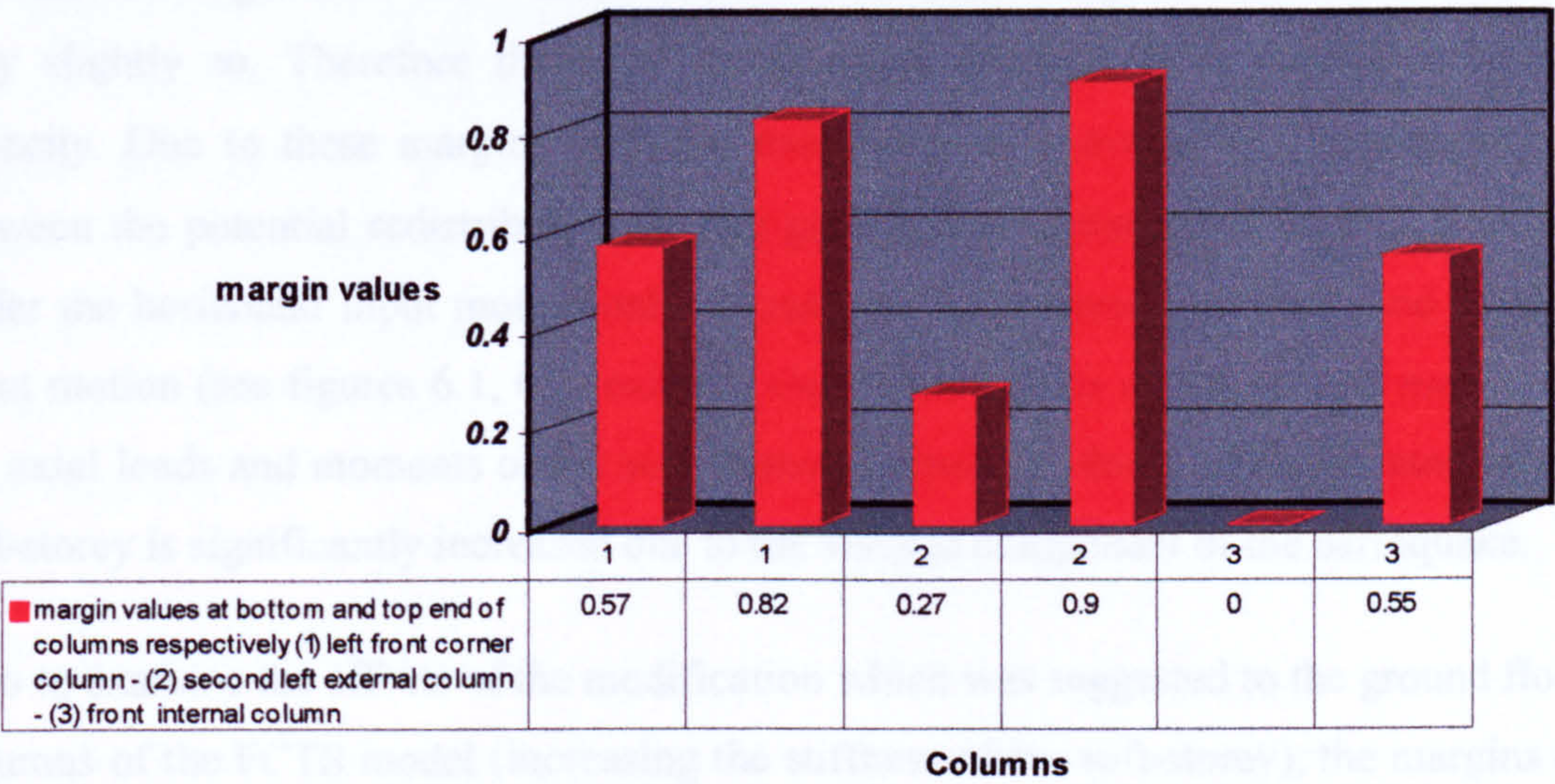
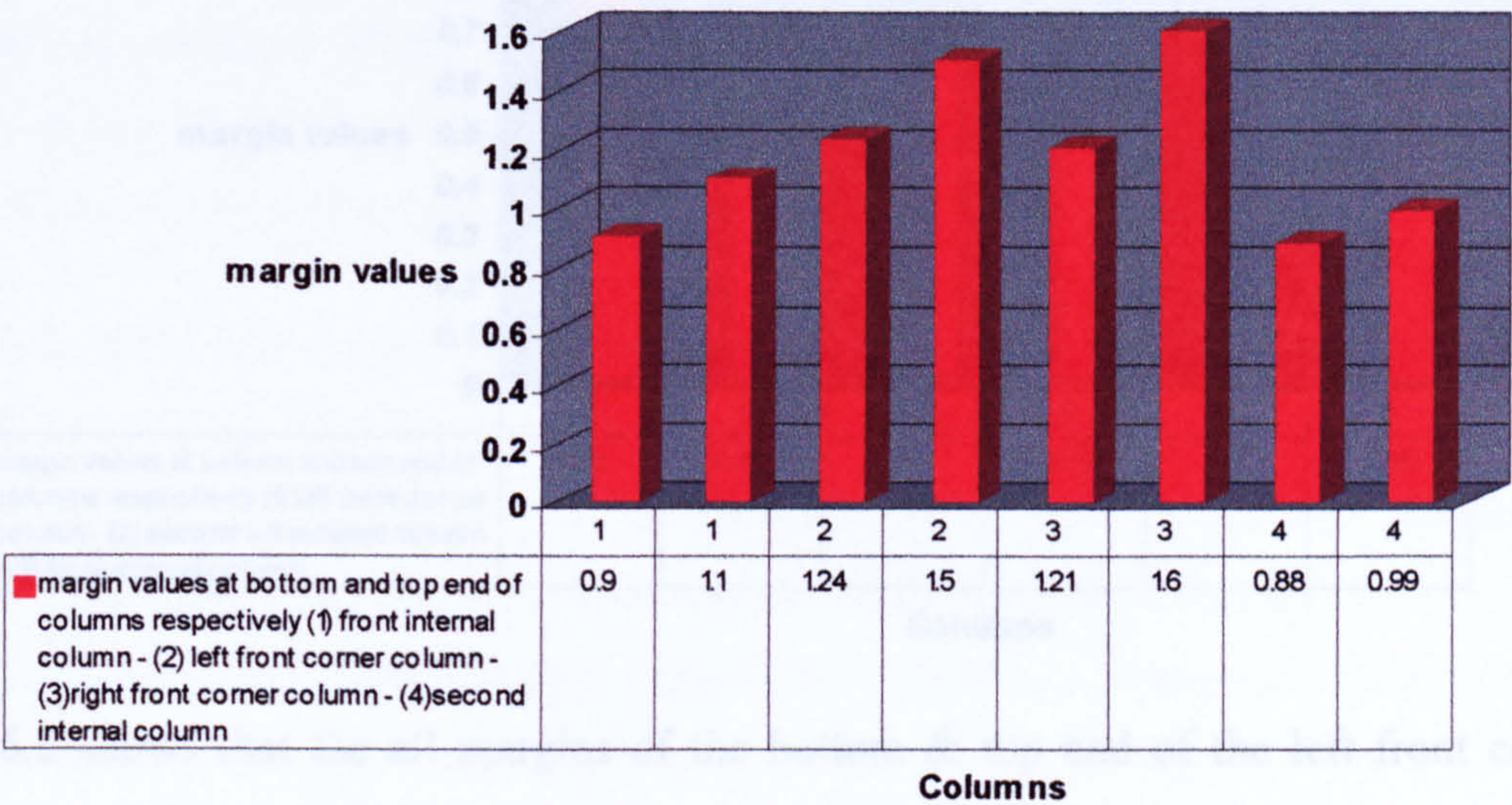


Fig. 6.1 shows that the all margins of the bottom & top end of the left front corner column and the surrounding columns are less than 1 i.e. no column has a reserve capacity. Therefore the applied moments for this column and also the surrounding columns cannot redistribute. By investigation of all margins of the ground floor



columns, it was found that the margins cannot allow for any potential redistribution and the soft-storey collapse mechanism of the FCTS model was formed.

**Figure 6.2** Margin values of the front internal column and its surrounding columns of the FCTS model under the horizontal earthquake only



For the FCTS model under horizontal earthquake only, Fig. 6.2 shows that the majority of margins of the bottom & top end of the front internal column and the surrounding columns are larger than 1. For those columns where the margin is less than 1 they are only slightly so. Therefore there are many columns which have reserve structural capacity. Due to these margins potential redistribution is available. The comparison between the potential redistribution for the ground floor columns of the FCTS model under the horizontal input motion only & under the concurrent horizontal and vertical input motion (see figures 6.1, 6.2) exhibits clearly the effects of the vertical motion on the axial loads and moments of the soft-storey columns i.e. the ductility demand of the soft-storey is significantly increased due to the vertical component of the earthquake.

Also to examine the effects of the modification which was suggested to the ground floor columns of the FCTS model (increasing the stiffness of the soft-storey), the margins of the front left corner column & the surrounding columns (the same column investigated for the FCTS model above, see Fig. 6.1) for the ground floor of the SCTS model were examined. Fig. 6.3 shows the margin values of the front left corner column & the surrounding columns under the vertical earthquake for the SCTS model.



**Figure 6.3** Margins values of the front left corner column and its surrounding columns of the SCTS model under the vertical earthquake

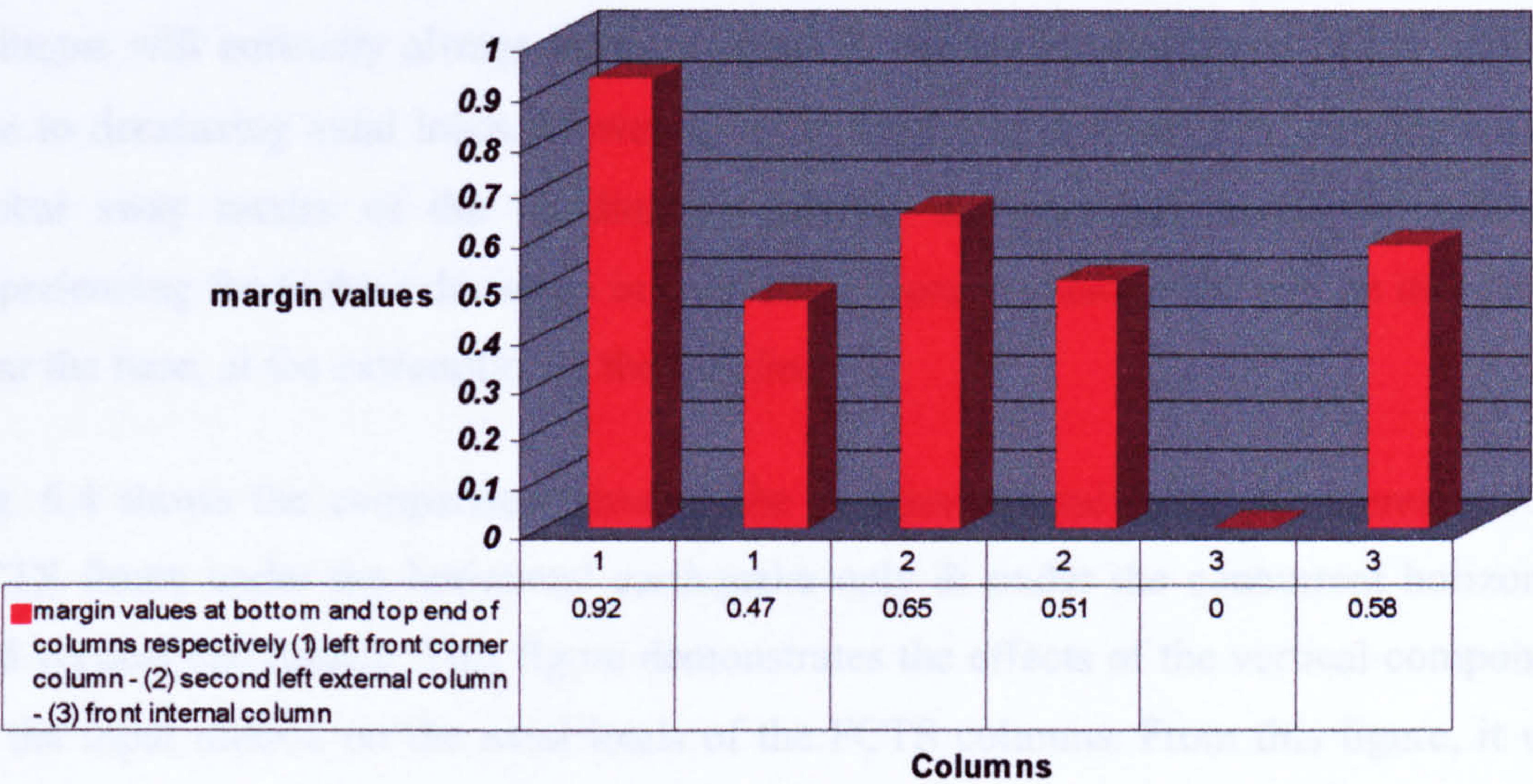


Fig. 6.3 shows that the all margins of the bottom & top end of the left front corner column and the surrounding columns are less than 1 similar to the FCTS model. By investigation the margins of this column & the surrounding columns for the FCTS above (see Fig. 6.1) and SCTS (see Fig. 6.3) model, it was found that the margins for this column and the second left external column the same in total for the bottom and top end for every column. Increasing the stiffness has redistributed the larger values of margins from top ends to bottom ends for every column. The margins of the front internal column are similar. From this comparison it can be concluded that the relative stiffness increase is disproportionate to the strength enhancement gained by increasing the column size. Other factors such as damping & building response will be altered but only marginally so.

**6.2.2 Vertical Earthquake**

In general the vertical component of the earthquake (motion) governs the seismic behaviour of the RC buildings columns. When columns are subjected to reduced compressive & possibly tensile forces, the corresponding bending capacities are reduced significantly. For the static design case it is likely that the margins of the columns are operating below the peak axial load required to resist maximum bending. Hence the most onerous case is when the compressive axial load decreases and possibly become tensile. On the other hand, reduced axial loading can have the benefit of



increasing the ductility of the columns. The interaction is complex especially under a transient event such as an earthquake, but it can be seen that there is a ‘trade-off’ between strength & ductility when concerned with axial load. Hence statically designed columns will normally always have problems at the higher elevations in the building due to decreasing axial loads. However in our case, the problem lies with the natural global sway modes of the building dominating the response, hence the columns experiencing the highest deviation in axial loads from the static case will be those at or near the base, at the extremities of the building.

Fig. 6.4 shows the comparison between the maximum axial loads of columns of the FCTS floors under the horizontal earthquake only & under the concurrent horizontal and vertical earthquake. This figure demonstrates the effects of the vertical component of the input motion on the axial loads of the FCTS columns. From this figure, it was noted that the ground floor columns experience a significant change in their axial loads due to the vertical earthquake.

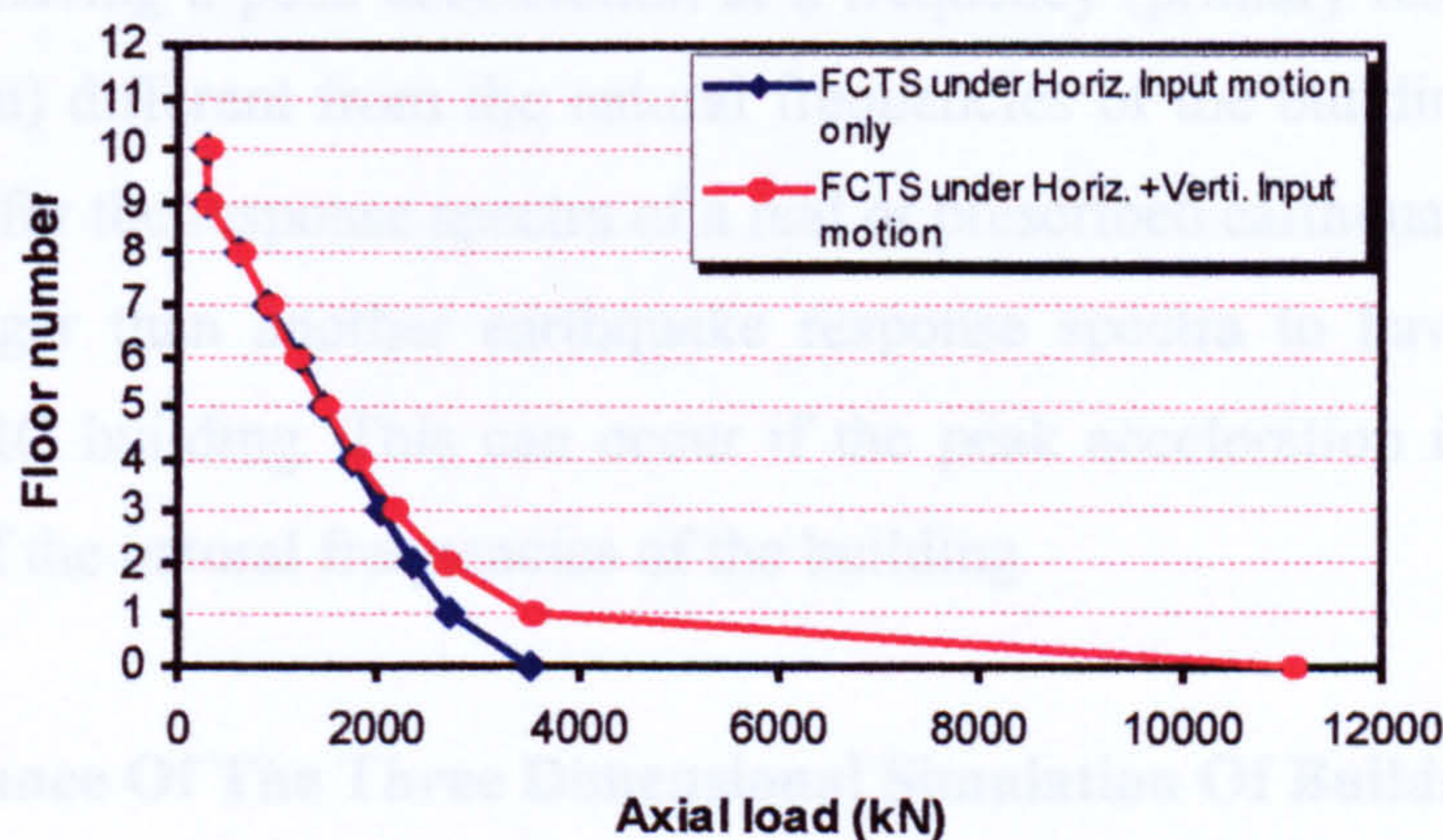


**Figure 6.4** Maximum axial loads of floor corner columns of the FCTS model under horizontal earthquake only & under concurrent horizontal and vertical earthquake

### 6.2.3 Building Response

As the RC building response under the earthquakes is significantly affected by the damping forces, the yielding of the RC material has a significant effect on the building damping during the seismic excitation. Although this effect has not been captured in the seismic response of the FCTS & SCTS model, the role which this effect perform in the seismic response of the RC building must be demonstrated. Besides the



viscoelastic behaviour of materials that generate the damping forces there is the hysteretic behaviour of materials. The hysteretic behaviour is the dissipated energy due to the plastic behaviour of the material. When the deformation level of the material increases the dissipated energy increases and therefore the damping increases. As the inelastic behaviour of the RC building increases the damping level under the earthquakes, the excited accelerations reduce and consequently the seismic mitigation of the building increases.

The secondary response spectra of the FCTS & SCTS model shown in chapter 5 were generated according to the viscous damping of 5 %. If these secondary response spectra are generated including the damping due to the plastic behaviour of the FCTS & SCTS model, the peak accelerations of the building floors will be significantly reduced and the seismic performance of the buildings may be improved. It should be mentioned that the damping forces increase the natural frequencies of the building and consequently the onerous effects of the resonance phenomenon may be reduced under a defined input ground motion having a peak acceleration at a frequency (primary response spectra of the input motion) different from the natural frequencies of the building. Also it is not always the case for the response spectra of a real or prescribed earthquake having a peak acceleration larger than another earthquake response spectra to have more onerous effects on the RC building. This can occur if the peak acceleration is at a frequency similar to one of the natural frequencies of the building.

### **6.3 Significance Of The Three Dimensional Simulation Of Buildings**

The seismic behaviour of the tall RC buildings is demonstrated realistically when the finite element simulation for the building is three-dimensional. Many buildings are commonly simulated as a two-dimensional finite element model normally, as a consequence of the increased complexity in simulation of tall RC buildings in three-dimensions (due to the complicated geometrical shape and material properties of the buildings). Hence the components of the input ground motion which is used for the seismic analysis are often a one-dimensional horizontal earthquake.

The resulting seismic responses of the FCTS & SCTS model as a three-dimensional model (with the input motion two or three dimensional) revealed the significance for the realistic seismic behaviour of high-rise RC buildings. The three-dimensional modelling



of these buildings and the horizontal concurrent two-dimensional earthquake simultaneously demonstrated that the global seismic response was produced identifying local vulnerable areas in two opposite corner columns i.e. the buildings were responding under the seismic event in the three-dimensions. Also the significance of the three-dimensional input ground motion (two horizontal and one vertical component) & three-dimensional modelling of the buildings simultaneously was demonstrated through the soft storey collapse mechanism. This has demonstrated the importance of incorporating all these spatial co-ordinate dimensions in a seismic simulation for the purposes of subsequent building assessment.



## CHAPTER 7 CONCLUSION AND FUTURE WORK

### 7.1 General Conclusion

In conclusion, a methodology for the seismic analysis and assessment of a detailed structure using a commercial finite element package has been presented in this work. Based upon a direct time-history integration technique, the behaviour of a statically designed ten-storey reinforced concrete building subject to a typical synthetic UK earthquake with a probable return period of 1 in 10000 years has been simulated. A logical conservative assessment to the appropriate British Standard code (BS8110) was performed to give insight into any available overload capacity, and probable modes of failure, both locally and globally.

When dealing with a subject such as seismic engineering it is appreciated that there are many variables and factors involved which make it a far from precise branch of science. Therefore when embarking on such a topic, a thorough understanding of the effects of each variable is required, and certain conservative approaches must be adopted to filter and narrow down the number of 'unknowns', providing a focus for the work. The level and consequences of the inherent conservatism can certainly be qualified (and quantified in some circumstances), which may provide mitigating arguments in the event of a collapse scenario. These conservatisms and factors which effect the analysis are discussed in more detail here.

#### 7.1.1 Choice Of The Earthquake Accelerogram

The earthquake accelerogram chosen for this project was generated from a typical 0.2g Uniform Risk spectrum commonly used within the UK Nuclear Industry. This presents one of many variables, as the choice of earthquake was somewhat arbitrary. Actual seismic time-history records could have been used from the growing databases that are now available, however many of these are long in duration and are associated with many site specific issues such as local soil conditions. Hence it was deemed reasonable to use a synthetic 'spectrum-compatible' accelerogram derived from an appropriate typical design response spectra. In this way a ten second earthquake was acceptable.



### 7.1.2 Consideration Of Soil Structure interaction

The model used in the research was assumed to have a fixed base, as the concern was for the building performance. However soil-structure interaction is rarely insignificant should be taken into account depending on the local soil conditions. For building founded on rock or 'hard-sites' the fixed base representation is fairly adequate. For softer soils, interaction between the structure and the ground is significant and has a direct effect on the loading that the building will experience.

Models for incorporating soil structure interaction have typically been represented by 'springs and dashpots' to model the relative stiffness and damping, depending on the foundation soil type. These soil compliances are usually obtained from complex purpose written programs for foundation-soil interaction such as CLASSI, which require substantial detail of the soil strata. The modeller can then use the results for damping and stiffness directly within the model.

However, a more accurate method, (and one which is becoming more common) is to model the soil explicitly with the structure. Any accurate model for the soil will need to incorporate complex plasticity models, something which explicit codes such as DYNA-3D lend themselves to well.

For the purposes of this research, as the focus is on the structure, soil-structure interaction was deemed a side issue which may be incorporated into any possible future iterations of the work.

## 7.2 Assessment

For the assessment of the structure, a logical approach has been adopted, whereby a conservative 'sweep' of the columns (deemed to be the main load-bearing structural members) is performed in the first instance against the static design code (BS8110). Obviously if all of the resulting margins of the columns pass the assessment ( $> 1$ ) then there is no need for any further action and the conclusion is that the structure has reserve load carrying capacity when subject to the prescribed earthquake. When the column margins fall below the acceptable limit ( $< 1$ ) then these columns may be reviewed for refinement in the assessment.



The conservatism is present in two distinct areas of the assessment procedure - from the loading applied and experienced by the structure and those inherent in the applied design code.

### 7.2.1 Conservatism In The loading

Firstly the conservatism in the loading is discussed. As the earthquake is discretised into 0.01 sec time intervals, in theory it is possible to obtain the loading at a particular instant in time on a particular element, thereby examining the actual loading. However for the duration of the 10 second earthquake, there would be 1000 load cases to apply to a large number of elements, increasing the effort required for assessment. In our case the maximum loading throughout time (irrespective of the instance of occurrence) has been extracted and applied as a single load case, hence the conservatism is evident.

For a single column (with a margin less than 1), the extraction of 1000 load cases throughout the time history was performed to give an estimation of the level of conservatism present, about 3% for the particular column chosen. Other methodology is allowed in various codes of practice for reducing the conservatism when using a load case which is the most onerous of a transient event. ASCE 4-86 presents what is commonly known as the '100-40-40' rule, whereby the three orthogonal spatial seismic components of the load case can be applied in the ratios of 100% - 40% - 40%, derived from a risk argument based on the unlikelihood of the simultaneous occurrence of the peak loading. Of course the load case will have to be applied three times, as the reduction ratio in the seismic components must be cycled through all three orthogonal directions, and the most onerous case will govern. An alternative is to use the square root of the sum of the squares (SRSS) of orthogonal load components and assess accordingly for the resultant loading.

Further conservatism in the loading originates from the material properties used. The finite element model was constructed of linear elements only, so judgements regarding the required and available ductility to form plastic hinges can only be formulated as mitigating arguments throughout the assessment process. It is possible however to incorporate nonlinear material properties within a time-history analysis. Any model of reinforced concrete which incorporates nonlinear material properties will need to



account for a number of factors. The material is composite, therefore the behaviour of each constituent material must be considered. If the materials are modelled explicitly, then the discretisation required is likely to effect the size of the model which can be produced, i.e. the number of elements required and local detail is increased. Alternatively some kind of pseudo stress-strain characteristics for the composite can be formulated which can minimise the discretisation needed. Whichever option is used, any nonlinearity will require the finite element program to iterate between time steps, increasing computer time, storage requirements, and ultimately stretching the limits of available computing power and expense.

In the real structure when a structural member is overloaded, yielding will occur, assuming it has been correctly designed and detailed. The onset of yielding then has a number of implications. As the material stress-strain characteristics are no longer linear, the response of the structure is altered, such that the accelerations are reduced. Also it is likely that the hysteretic damping will increase, serving to reduce the loading upon members even further. Assuming the yielded member in question has sufficient post-yield deformation characteristics (i.e. significant ductility), this will serve to redistribute loading to the stiffer un-yielded members, assuming there is sufficient redundancy available. This behaviour forms a significant part of the philosophy of seismic design, the provision of adequate redundancy and design of members to form as many plastic hinges (in the beams) as possible before collapse. Hence seismic design must incorporate the provision of adequate ductility (capacity) which must outweigh the ductility demand of the designed collapse mechanism.

The issue of strain rate has been addressed but judged not to be of significance within this analysis. When dealing with any transient dynamic problem, if inertia effects are significant then the rate of loading can possibly have an effect. In essence, if the rate of straining is high enough, and the time of load application is small, then the structure in question may exhibit an apparent 'overstrength'. The strain rates exhibited in the model were found not to be high enough to claim overstrength. Also the issue of low cycle fatigue, whereby the structural members undergo load reversal are not evident. The material properties will degrade under these conditions, so this would also present an issue when considering the use of non-linear material properties.



It should be noted that by their nature, analyses carried out in the frequency domain can only cope with linear material properties due to their dependence on the modal characteristics of the structure (properties which require a linear response). These methods allow simpler satisfactory analysis and assessment of structural models, but will have more inherent conservatism within them due to the simplifying assumptions they incorporate.

### **7.2.2 Conservatism In The Code Assessment**

The columns are initially assessed using an automated routine which compares the combined bending and axial loading to the requirements of BS8110. Within any design code there are a number of factors which are inherently (and purposefully) produce a margin of safety, hence it is necessary to examine the sources of this and their implication. Material safety factors of 1.5 and 1.05 are prescribed for the concrete and steel material. Part 2 of the code suggests that a worst credible value of 1.2 may be taken for the concrete in certain circumstances, and this may be judged appropriate for use in the assessment.

The combined axial load and biaxial bending design method used in BS8110 is essentially combines the biaxial moments into a modified uniaxial load. This is based on a modification of the previous superseded design code whereby a 'failure-surface' was used (this is an extension of the traditional reinforced concrete column axial load and bending capacity curves into three dimensions). Although not presented, the failure surface assessment model was also incorporated and generally produced less conservative results and is inherently more accurate.

### **7.3 Model Behaviour – Static vs Seismic Design**

The adopted approach gives insight into the seismic behaviour of the statically designed structure. It is evident that when subjected to horizontal earthquakes the structure exhibits a good seismic withstand capacity, having significant capacity above the normal static state, and it is likely that it will remain in-tact. However, the introduction of the vertical component is all important and can have dire consequences for the columns. For the model chosen, a soft-storey was deliberately incorporated in the ground floor, and it is at this elevation (where the stiffness changes abruptly) that



the problems occur. The dominant sway and bouncing modes of the structure concentrate loading in the ground floor, and the only outcome is global collapse. It is likely that if the structure were to have a uniform stiffness throughout its elevation, the non-compliant margins of the columns would be distributed more evenly around the structure. It is also likely that the columns at the higher elevations would exhibit the lower margins due to the decrease in static axial loading.

The response spectra show clearly the coupling of the structure with the input motion causing resonance at the major sway modes. The accelerations appear to increase with height, but it is the shear size and geometry of the structure (relatively high height to base width ratio) which cause a problem for the ground floor, generally in overturning. It should be noted that if nonlinear behaviour had been incorporated, this would have effected the building response, moving the frequency away from the peak of the input spectra, thereby reducing the accelerations, giving a 'better' result.

The structure is symmetrical, which is normally a feature of good seismic design, even though the building is statically designed only. The centre of mass and geometric centre are close together, minimizing torsion in plan, so this has had serious beneficial effect on the seismic performance on the model. No local detail has been included such as stairwells and lift shafts which may cause local stiffness changes. The details will also serve to add strength, stiffness and mass to the structure with the overall likelihood of beneficial action. Detailing of the reinforcement is a primary focus of seismic design. The model in question may only serve to show that certain level of ductility is required, something which may not be necessary for static design, although it is common to allow for a certain amount of moment redistribution. This is provided by the correct detailing of members. All members will be designed, regardless of the code followed, to fail in a ductile flexural manner rather than shear which is normally a sudden brittle failure. But to realise this failure mode, adequate anchorage must be provided at member junctions to ensure bond failure cannot influence the behaviour. Hence one of the major differences between seismic and static design is the provision of greater anchorage lengths and confinement (shear reinforcement). The assessment procedure does not presently incorporate this check.



One very important consideration which cannot be accounted for in any of the 'desk' work is workmanship. The desired behaviour of the real structure can only be attained if the workmanship on site meets or exceeds that required. Of the important variables, properties of the concrete should meet the specification and be correctly cast, and reinforcement provision (anchorage) must also be closely adhered to. The good intentions of the designer can be completely undone by the quality of the build and works on site, and this often seen as a major contributing factor to the collapse of RC buildings subject to a seismic event.

#### 7.4 Future Work

There are two distinct important areas of focus which future work should address. The provision of appropriate non-linear behaviour, and incorporation of soil structure interaction effects.

Non-linear material properties can easily be incorporated into finite element models using implicit time marching schemes (such as ANSYS), but explicit codes present an attractive option. Explicit finite element codes such as DYNA-3D are ideal for analysis with transient events where material nonlinearity is required and it is used extensively in the field of impact and crashworthiness. The finite difference time-marching scheme employed differs from the normal implicit codes of ANSYS and ABAQUS, requiring the load to be applied over a time period. The explicit solution will set a time-step size based on the element discretisation, and material nonlinearity is easily handled. As the code is developing and becoming used more for seismic work, the confidence is growing in its reliability, and may present the way forward for future work regarding the seismic analysis of buildings.

Soil structure interaction effects can be incorporated directly into the finite element model. Complex plasticity models are now readily available such as Mohr Coulomb or Drucker Prager, incorporating a 'cap' model to model dilatency effects properly. Modified shear and damping properties due to the motion of the prescribed earthquake can be obtained from simple soil column models using programs like 'Shake 2000'

The assessment could easily be extended to incorporate the other important structural members such as beams and slabs. In the assessment routines used, the influence of



material safety factors can be studied, and the 100-40-40 rule can be employed. If serious data handling routines are automated, it is not beyond the realms of possibility to assess the loading throughout the time period for each time increment. Modifications to the existing assessment would be possibly to run a series of models with modified (reduced)  $I$  values depending on the margins of the columns from previous runs. This would perhaps give insight into a progressive collapse state, however if material non-linearity is incorporated, this may not prove necessary. Effects of non-symmetry of the building geometry can be studied and incorporating actual structural features should also be considered. Detrimental workmanship also provides a possible path for parametric study concerning its influence.

Only a brief mention has been made regarding some of the parameters and features which may be studied, there are many more issues. The subject is too broad to cover in one project, but the approach presented can be adapted as required to focus on the studies in question.



## REFERENCES

1. Wang, C and Salmon, C.G, ' Reinforced Concrete Design ', Sixth Edition, Addison Wesley Educational Publishers, Inc 1998.
2. Ali, M.M., ' Evolution of Concrete Skyscrapers ', Electronic Journal of Structural Engineering, Volume 1, pp 2-14, 2001.
3. British Standard 8110-1 (1997), Structural Use of Concrete, Part 1: Code of Practice for Design and Construction.
4. Eurocode 8 (1998-1-1), Design Provisions for Earthquake Resistance of Structures, Part 1.1: Seismic Actions and General Requirements for Structures.
5. Kong & Evans, ' Reinforced and Prestressed Concrete ', Third Edition, 1987.
6. MACGinley, T.J and Choo, B.S, ' Reinforced Concrete ', Second Edition, E & FN Spon 1990.
7. Hugo Bachmann....(ET AL.) ' Vibration Problems in Structures ', Practical Guidelines, 1995.
8. Penelis, G.G and Kappos, A.J, ' Earthquake-Resistant Concrete Structures ', First Edition, E & FN Spon 1997.
9. Key, D, ' Earthquake Design Practice for Buildings ', Thomas Telford 1988.
10. Ghali, A and Neville, A.M, ' Structural Analysis ', Fourth Edition, E & FN Spon 1997.
11. S.S.J.Moy, ' Plastic Methods for Steel and Concrete Structures ', Macmillan 1989.
12. R. Park, ' Capacity Design of Ductile RC Building Structures for Earthquake Resistance', Journal of the Structural Engineer, Volume 70, No. 16, pp 279-289, August 1992.
13. D.J.Dowrick, ' Earthquake Resistant Design for Engineers and Architects ', Second Edition, Wiley & Sons 1997.
14. Kotsovos, M.D and Pavlovic, M.N, ' Ultimate Limit-State Design of Concrete Structures', Thomas Telford 1999.
15. [Http:// www.cen.bris.ac.uk/civil/students/eqteach97/](http://www.cen.bris.ac.uk/civil/students/eqteach97/), Internet website in 02 / 2003, Teaching pages of civil engineering department, Earthquake Engineering, University of Bristol, 2001.



16. P.Mandal,' Expressions of Curvature Ductility for RC sections ', 12<sup>th</sup> European Conference on Earthquake Engineering, Paper Reference 784, Elsevier Science Ltd 2002.
17. R. Park, ' New Zealand Innovations in the Design of Earthquake Resistant Structures', Journal of the Structural Engineer, pp 26-31, 15 January 2002.
18. M.R.Horne, ' Plastic Theory of Structures ', Second Edition, Pergamon Press 1979.
19. Beskos, D.E and Anagnostopoulos, S.A, Editors, ' Computer Analysis and Design of Earthquake Resistant Structures ', A Handbook, Computational Mechanics Publications, Southampton, UK, 1997.
20. Paulay, T and Priestley, M.J.N, ' Seismic Design of Reinforced Concrete and Masonry Buildings ', Wiley & Sons 1992.
21. H.Sezen, A.S. Whittaker, K.J. Elwood and K.M. Mosalam, ' Performance of Reinforced Concrete Buildings during the August 17, 1999 Kocaeli, Turkey Earthquake, and Seismic Design and Construction Practise in Turkey', Journal of Engineering Structures, Volume 25, pp 103-114, Elsevier 2003.
22. Chandler, A.M and Lam, N.T.K, ' Performance-Based Design in Earthquake Engineering ', Journal of Engineering Structures, Volume 23, pp 1525-1543, Elsevier 2001.
23. Mario Paz, ' International Handbook of Earthquake Engineering ', Chapman & Hall 1994.
24. Maguire, J.R and Wyatt, T.A, ' ICE Design and Practice Guide, Dynamics', The Institution of Civil Engineers, Thomas Telford 1999.
25. Mario Paz, ' Structural Dynamics, Theory and Computation ', Fourth Edition, Chapman & Hall 1997.
26. ASCE Standard 4-86, ' Seismic Analysis of Safety-Related Nuclear Structures and Commentary ', August 1995.
27. Barbat, A.H and Canet, J.M, ' Structural Response Computations in Earthquake Engineering ', 1989.
28. Vladimir Kolousek, ' Dynamics in Engineering Structures ', Butterworths, London, 1973.
29. Robert D.Blevins, ' Formulas for Natural Frequency and Mode Shape ', Krieger Publishing Co., INC. 1984.



30. K.A. Zalka, ' A Simplified Method for Calculation of the Natural Frequencies of Wall-Frame Buildings ', Journal of Engineering Structures, Volume 23, pp 1544-1555, Elsevier 2001.
31. Robert M. Ebeling, ' Introduction to the Computation of Response Spectrum for Earthquake Loading ', US Army Corps of Engineers, Washington, DC 1992.
32. Principia Mechanica Limited, ' UK Uniform Risk Spectra Report ', PML Report 498/88, Report produced for NNC, April 1981.
33. <http://seismo.ethz.ch/gshap/Gshap98-stc.html>, Internet website in 02 / 2003 for the global seismic hazard map of the world, Global Seismic Hazard Assessment Program, United Nations, 1999.
34. Reinhorn, A.M, Mattox, R.E and Kunnath, S.K, ' Seismic Damageability Evaluation of a Typical RC Building in the Central U.S. ', The Quarterly Publication of NCEER, Volume 10, No. 3, October 1996.
35. P. Papadopoulos, E. Mitsopoulou and A. Athanatopoulou' Failure Indices for RC Building Structures ', 12<sup>th</sup> European Conference on Earthquake Engineering, Paper Reference 616, Elsevier Science Ltd 2002.
36. Amr S. Elnashai,' Do We Really Need Inelastic Dynamic Analysis ', Journal of Earthquake Engineering, Vol. 6, Special Issue 1, pp 123-130, 2002.
37. Comite Euro-International DU Beton, ' RC frames Under Earthquake Loading ', Thomas Telford 1996.
38. A.J. Durrani and S. Haider,' Seismic Response of RC Frames With Unreinforced Masonry Infills', 11<sup>th</sup> World Conference on Earthquake Engineering, Paper Reference 165, Elsevier Science Ltd 1996.
39. L.D. Decanini, L. Liberatore and F. Mollaioli,' Response of Bare and Infilled RC Frames Under the Effect of Horizontal and Vertical Seismic Excitation ', 12<sup>th</sup> European Conference on Earthquake Engineering, Paper Reference 164, Elsevier Science Ltd 2002.
40. A.S. Elnashai,' Earthquake Resistance of High Strength Reinforced Concrete Buildings ', Seismic Design Practice into the Next Century, Booth (ed.), Balkema, Rotterdam, 1998.
41. Petrusevska, R, Cvetanovska, G.N,' Application of High Strength Concrete in Seismic Active Regions ', 12<sup>th</sup> European Conference on Earthquake Engineering, Paper Reference 109, Elsevier Science Ltd 2002.



42. ANSYS Program Release 5.7, Analysis User Manual, Swanson Analysis System Inc, 2002.
43. A. Ghobarah and Ashraf Biddah, ' Dynamic Analysis of Reinforced Concrete Frames Including Joint Shear Deformation ', Journal of Engineering Structures, Volume 21, pp 971-987, Elsevier 1999.
44. A.M. Mwafy and A.S. Elnashai, ' Static Pushover Versus Dynamic Collapse Analysis of RC Buildings ', Journal of Engineering Structures, Volume 23, pp 407-424, Elsevier 2001.
45. K.C. Rockey, H.R. Evans, D.W. Griffiths and D.A. Nethercot, The Finite Element Method, Second Edition, Granada Publishing Limited 1983.
46. Cosenza, E, Manfredi, G and Verderame, G,' Seismic Assessment of Gravity Load Designed RC Frames ', Journal of Earthquake Engineering, Vol. 6, Special Issue 1, pp 101-122, 2002.
47. Calvi, G, Magenes, G and Pampanin,' Relevance of Beam-Column Joint Damage and Collapse in RC Frame Assessment ', Journal of Earthquake Engineering, Vol. 6, Special Issue 1, pp 75-100, 2002.
48. Comité Euro-International DU Béton, ' Seismic Design of Reinforced Concrete Structures for Controlled Inelastic Response ', Thomas Telford 1998.
49. E.D. Booth, A.J. Kappos and R. Park, ' A Critical Review of International Practice on Seismic Design of Reinforced Concrete Buildings', Journal of the Structural Engineer, Volume 76, No. 11, pp 213-220, 2 June 1998.
50. L. Weekes, ' A Study of Secondary Moments and Moment Redistribution in Continuous Prestressed Concrete Beams ', PhD Thesis, 1994.
51. British Standard 6399-1 (1996), Loading for Buildings, Part 1: Code of Practice for Dead and Imposed Loads.
52. British Standard 648 (1964), Schedule of Weights of Building Materials.
53. Wiegel, R.L, ' Earthquake Engineering ', Prentice-Hall, Inc., 1970.
54. Collier, C.J and Elnashai, A.S,' A Procedure for Combining Vertical and Horizontal Seismic Action Effects ', Journal of Earthquake Engineering, Vol. 5, No. 4, pp 521-539, 2001.
55. Iain A.Macleod, ' Analytical Modelling of Structural Systems ', Ellis Horwood Limited, 1990.



56. N.J.K. Cameron and Pankaj,' Modelling Masonry Infills for Seismic Response Analysis of RC Frames ', 12<sup>th</sup> European Conference on Earthquake Engineering, Paper Reference 543, Elsevier Science Ltd 2002.
57. The Institution of Structural Engineers & The Institution of Civil Engineers, ' Manual for the Design of Reinforced Concrete Building Structures, October 1985.



**APPENDIX I**


**Static Linear and Nonlinear Analyses of Steel Fixed Beam & One-Storey Steel Portal Frame**

**Steel Fixed Beam**

A steel beam with fixed ends and carrying a point load (see Fig. I.1) was analysed using the basic theories of elasticity and plasticity (analytical solution), and the ANSYS program to verify the ANSYS program results in linear and non-linear analysis. Also the non-linear analysis of the beam shows the features of plastic theory by studying the formation of a collapse mechanism and plastic hinges in this beam at failure. This beam is a statically indeterminate structure with a degree of redundancy of two. It therefore needs three plastic hinges to form a collapse mechanism and it is considered a good case study for plasticity. The description of the beam geometry and material properties is shown in table I.1.

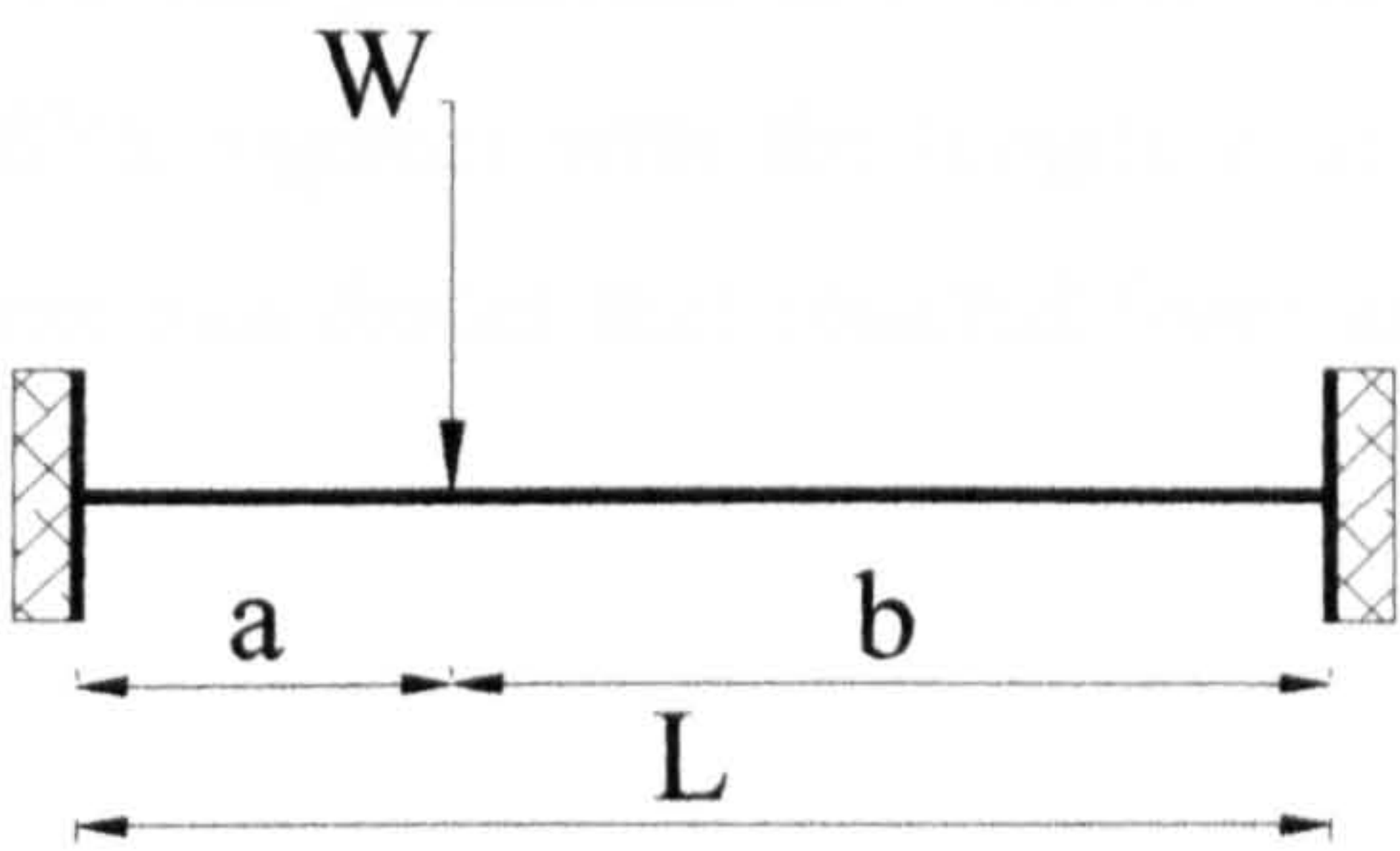


**Figure I.1** The steel fixed ended beam

Description of steel fixed beam		Remarks
Span (L)	1000 mm	
Dimensions of the section	100 × 100 mm	Solid square 
Yield stress ( $\sigma_y$ )	250 N/mm <sup>2</sup>	BS 8110 part1, ref. [3]
Poisson's ratio ( $\nu_s$ )	0.3	BS 8110 part1, ref. [3]
Young's modulus ( $E_s$ )	200 kN/mm <sup>2</sup>	BS 8110 part1, ref. [3]
(a)	3000 mm	
(b)	7000 mm	

**Table I.1** Description of steel fixed ended beam



Firstly, in accordance with the linear and non-linear stress-strain curve of steel and the properties of the beam section, the maximum moments and forces of the beam section were calculated analytically for four cases starting from the yielding of the outside edge of the section up to flow of yielding for whole section as shown in Fig. I.2. The fourth case illustrates the full plastic hinge producing the plastic moment and collapse load values for the beam. By drawing the general form of elastic bending moment diagram of the beam under the point load, the distribution of moment shows that the maximum moment is at the left hand support of the beam, see Fig. I.3. Hence the formation of the collapse mechanism begins by the formation of plastic hinges at the restrained ends of the beam and finally under the point load as shown in Fig. I.4.

Secondly, the beam was created in the ANSYS program with all geometry and material properties as stated in table I.1, and was loaded by the force values that have been obtained from the analytical analysis of the beam section. These values contain bending moment values for the first yield for the section and full plasticity also. For that reason a material non-linear analysis was performed in ANSYS. Fig. I.5 shows the deformed shape of beam from ANSYS together with the longitudinal stresses for the case (1). Table I.2 lists the moments and forces that resulted from analytical and the ANSYS program analysis.

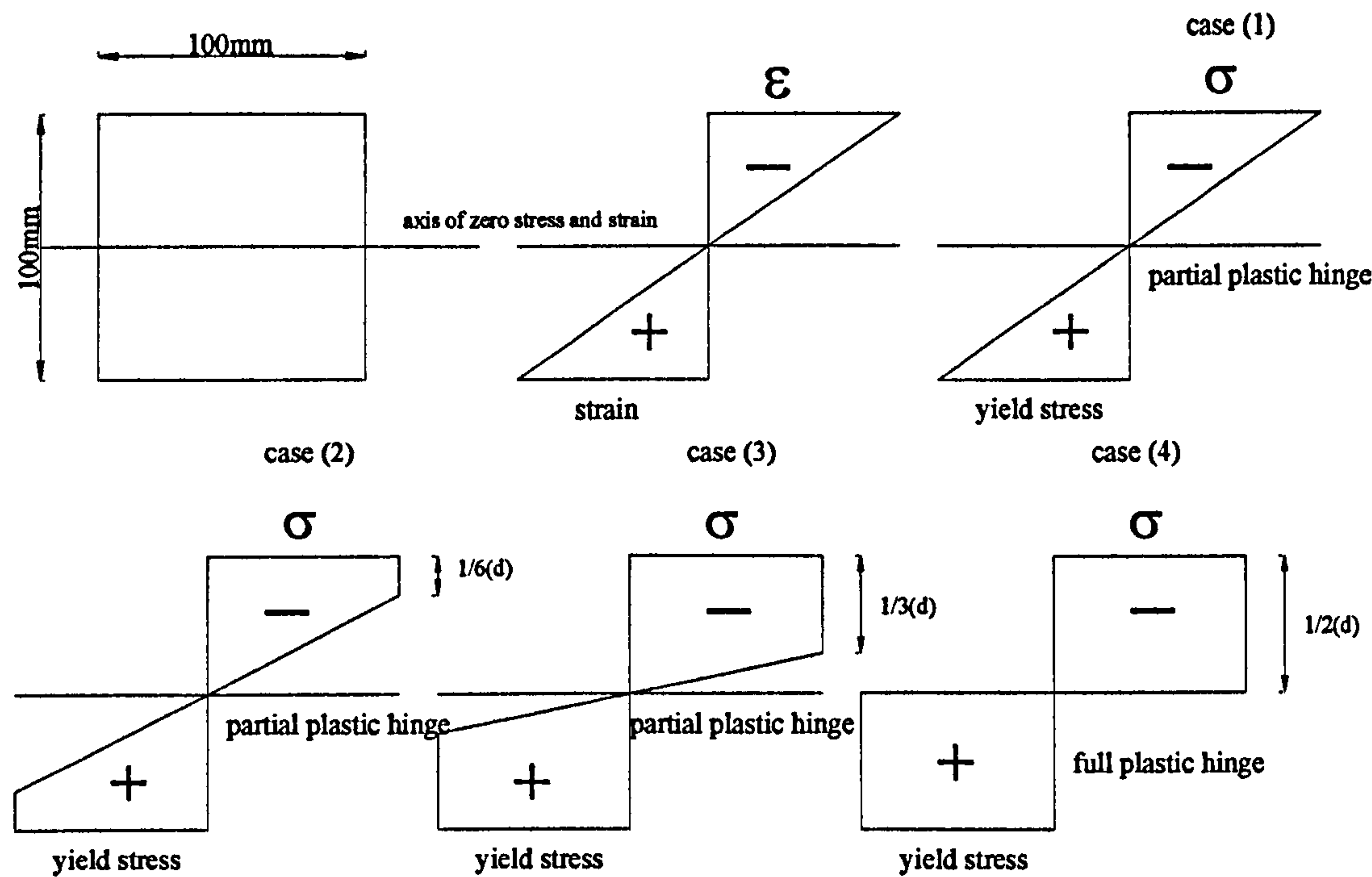


Figure I.2 The stress distribution of beam section of the studied cases



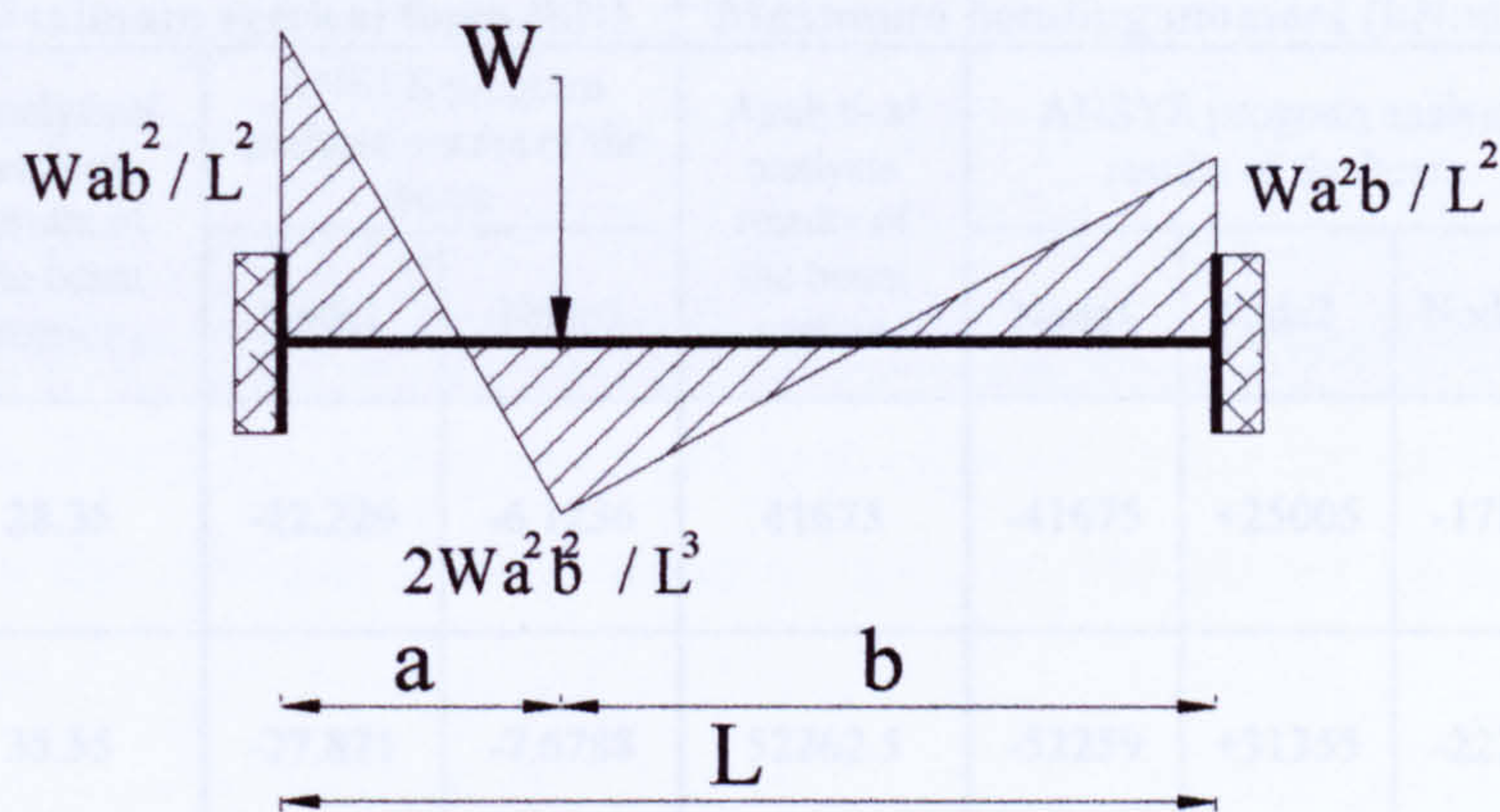


Figure I.3 The elastic bending moment distribution of the beam  
(Values of bending moments taken from Moy, ref. [11])

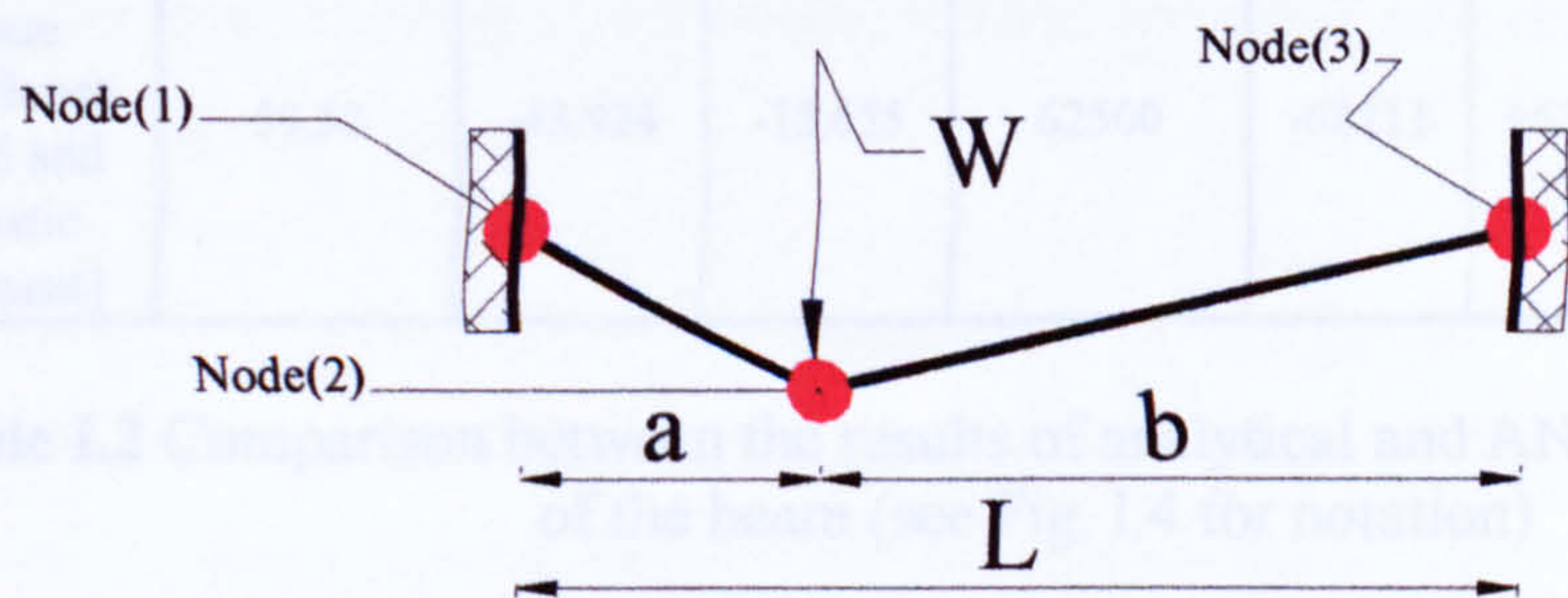


Figure I.4 The collapse mechanism of the beam

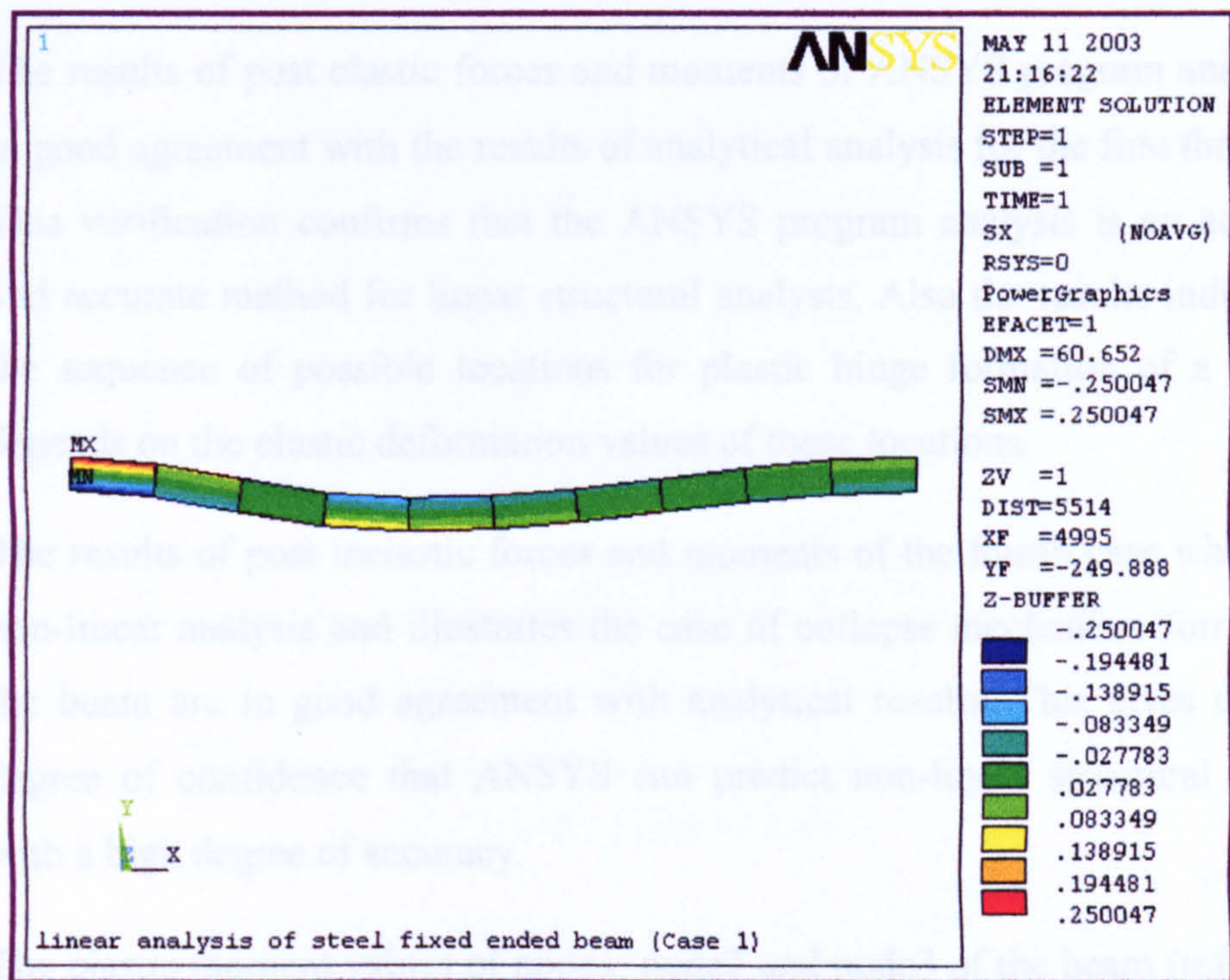


Figure I.5 The deformed shape of the beam under a vertical point load  
and its horizontal stresses



Cases	Maximum vertical force (kN)			Maximum bending moment (kN.mm)				Remarks
	Analytical analysis results of the beam section	ANSYS program analysis results of the beam		Analytical analysis results of the beam section	ANSYS program analysis results of the beam			
		Node1	Node3		Node1	Node2	Node3	
First case	28.35	-22.226	-6.1236	41675	-41675	+25005	-17861	First yielding case
Second case	35.55	-27.871	-7.6788	52262.5	-52259	+31355	-22397	Plastic hinge formation
Third case	40.25	-31.556	-8.6940	59170	-59168	+35501	-25358	Plastic hinge formation
Fourth case [Collapse load and plastic moment]	59.52	-43.924	-15.655	62500	-68211	+62467	-48337	Non-linear analysis case for $M_p$ and $W_c$ (Collapse mechanism)

**Table I.2** Comparison between the results of analytical and ANSYS program analyses of the beam (see Fig. I.4 for notation)

Investigation of the beam analysis results using the analytical and ANSYS program analyses shows that:

1. The results of post elastic forces and moments of ANSYS program analysis are in good agreement with the results of analytical analysis for the first three cases. This verification confirms that the ANSYS program analysis is an acceptable and accurate method for linear structural analysis. Also the results indicate that the sequence of possible locations for plastic hinge formation of a structure depends on the elastic deformation values of these locations.
2. The results of post inelastic forces and moments of the fourth case which has a non-linear analysis and illustrates the case of collapse mechanism formation of the beam are in good agreement with analytical results. This gives us a high degree of confidence that ANSYS can predict non-linear structural response with a high degree of accuracy.
3. The plastic moment values of node1, node2 and node3 of the beam (refer to Fig. I.4) that were resulted from ANSYS (refer to table I.2) show that the plastic hinges formed at node1 and node2 whereas the values are equal or more than the



analytically calculated plastic moment value. At the same time the plastic hinge was not formed at node3 that the value is less than the analytical plastic moment which means, the collapse mechanism of the beam was not formed completely. Clarification of that relates to the ANSYS program (see section 3.1.2.1, chapter 3). The ANSYS solution does not converge when the structure has collapsed because the stiffness matrix becomes singular and cannot be solved, ANSYS, ref. [42].

4. Further studies using a refined mesh indicate that the structure will attain a maximum load slightly under the theoretical collapse load due to the limitations of developing the full plastic behaviour toward the core of the beam at the imposed fixed ends. Hence the behaviour is structure oriented, and these results are as expected.

Figures (I.6, I.7, I.8) show the comparison of results between the theoretical and ANSYS analyses of the beam for node1, node2 and node3 that verify the capability of ANSYS. In these figures, the vertical forces (analytical and ANSYS program results) were plotted versus the bending moments (analytical and ANSYS program results) of the left hand support, under point load and right hand support of the beam for all of the studied cases.

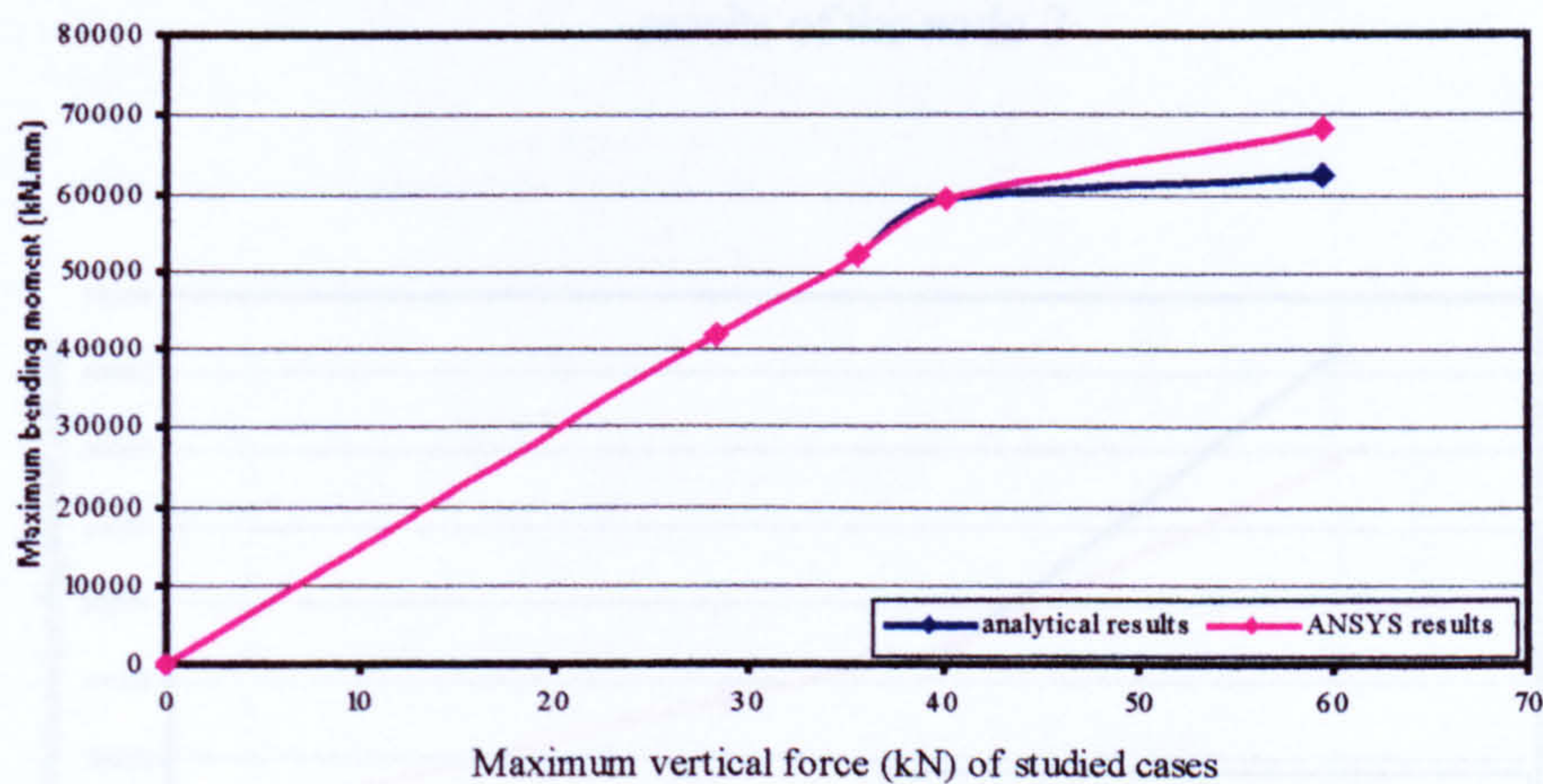


**Figure I.6** Comparison between analytical and ANSYS results of the node 1

### Steel portal frame

A steel portal frame with fixed bases was studied in this stage to verify the capability of



the ANSYS program in linear and non-linear analysis of the structures having a large number of members and joints. This steel portal frame illustrates the one-bay single storey structure which provides a more complex plastic analysis problem. The frame having the same section and material properties as the fixed beam before is described in the following sections, see table I.1. Fig. I.9 shows the geometry and the general case of loading of the steel portal frame. This frame is a statically indeterminate structure with a degree of redundancy of three. Hence it requires four plastic hinges to form a complete collapse mechanism. The static elastic and plastic behaviour of the portal frame was analysed using classical theory and the ANSYS program according to the load cases, which are shown in table I.3.

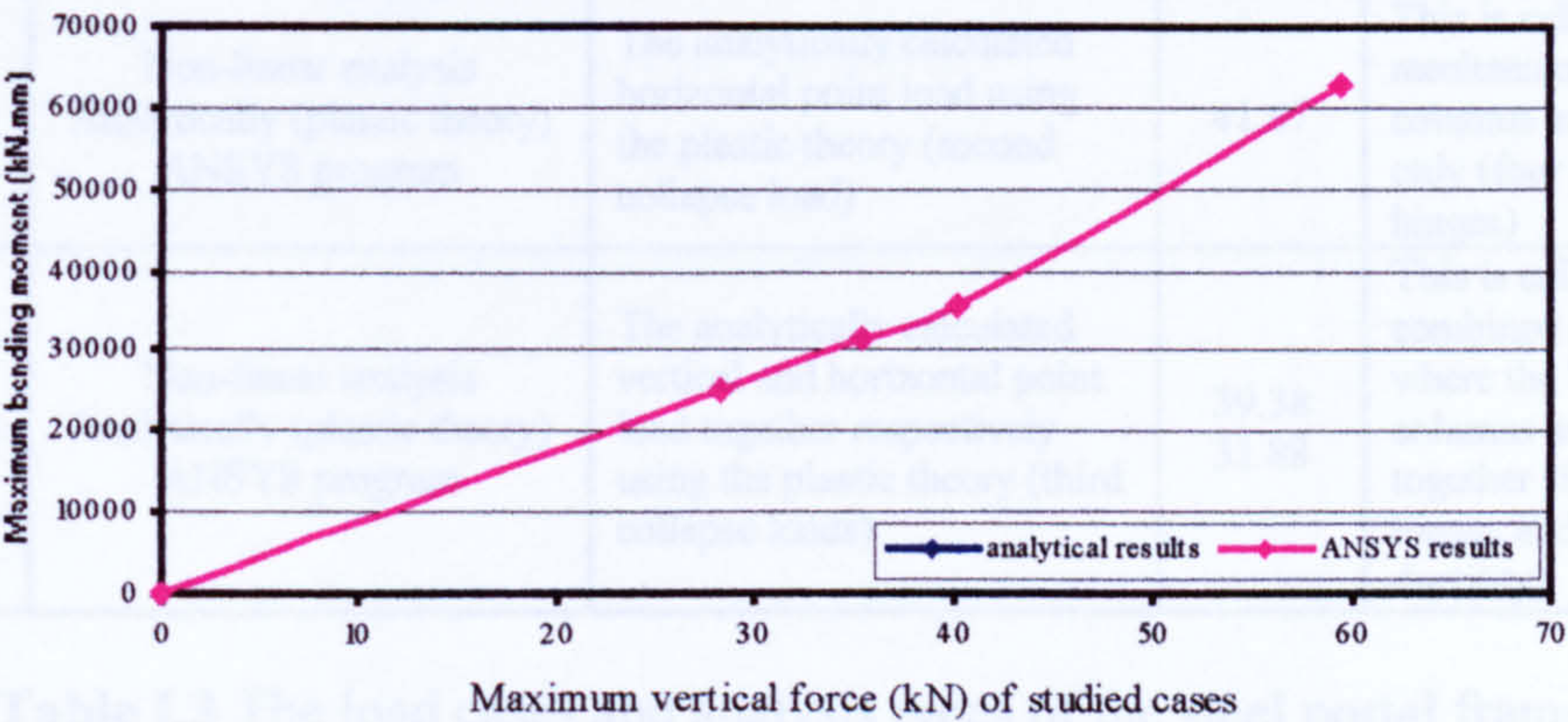


Figure I.7 Comparison between analytical and ANSYS results of the node 2

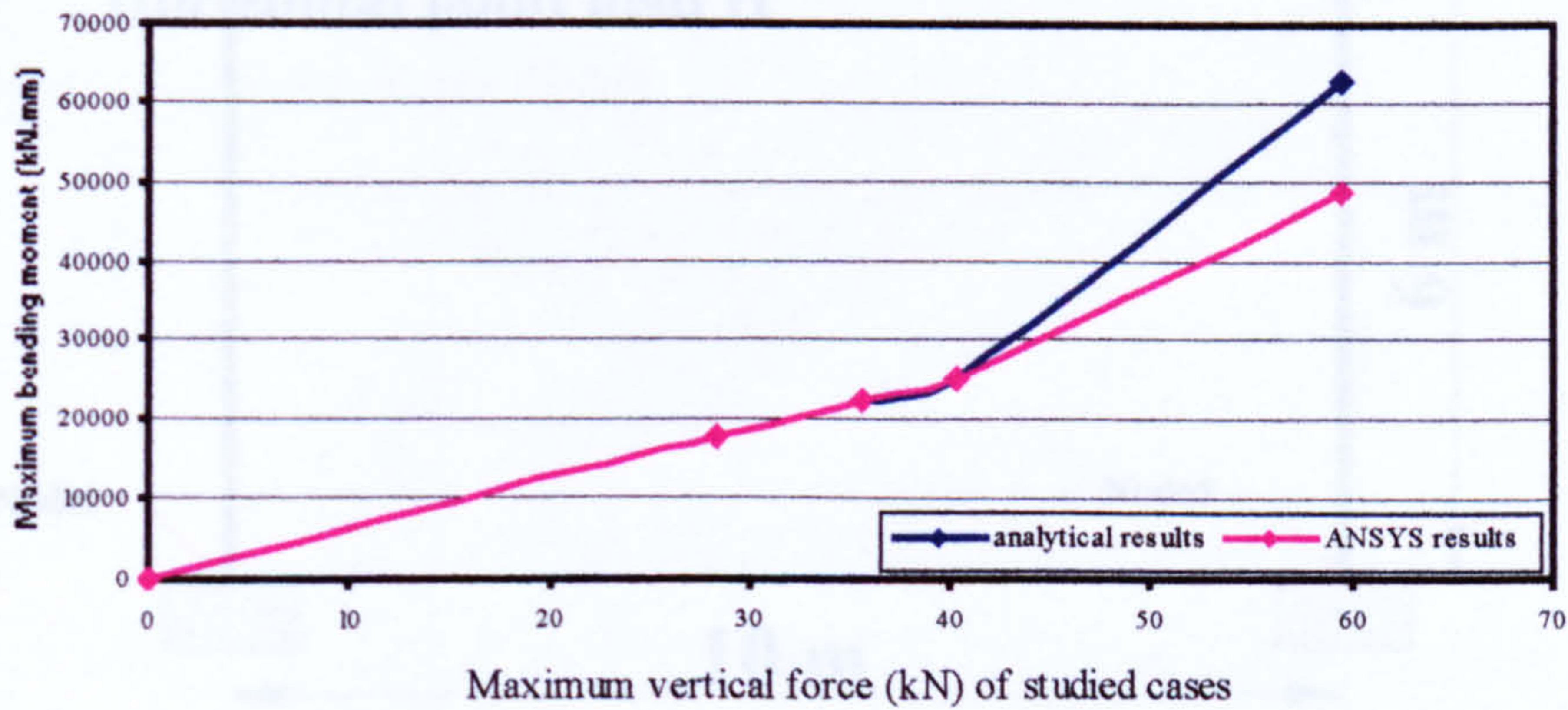


Figure I.8 Comparison between analytical and ANSYS results of the node 3

The static elastic analysis of this frame was implemented using the analytical method



and the ANSYS program to verify the ANSYS program as an accurate structural analysis tool and to achieve the ductile plastic hinge behaviour of this frame as predicted by theory.

Cases	Analysis types and tools	Loads (kN)		Remarks
		Type	Value	
First case	Linear analysis Analytically (elastic theory) ANSYS program	An assumed vertical point load	60	Elastic behaviour
Second case	Linear analysis Analytically (elastic theory) ANSYS program	An assumed horizontal point load	50	Elastic behaviour
Third case	Linear analysis Analytically (elastic theory) ANSYS program	The assumed vertical and horizontal point loads together	60 50	Elastic behaviour
Fourth case	Non-linear analysis Analytically (plastic theory) ANSYS program	The analytically calculated vertical point load using the plastic theory (first collapse load)	59.52	This is called beam mechanism where the beam is failed only (three plastic hinges)
Fifth case	Non-linear analysis Analytically (plastic theory) ANSYS program	The analytically calculated horizontal point load using the plastic theory (second collapse load)	41.67	This is called sway mechanism where the columns are failed only (four plastic hinges)
Sixth case	Non-linear analysis Analytically (plastic theory) ANSYS program	The analytically calculated vertical and horizontal point load together respectively using the plastic theory (third collapse loads)	39.38 31.88	This is called combined mechanism where the beam and columns are failed together (four plastic hinges and full ductility)

Table I.3 The load cases and analysis types of the steel portal frame

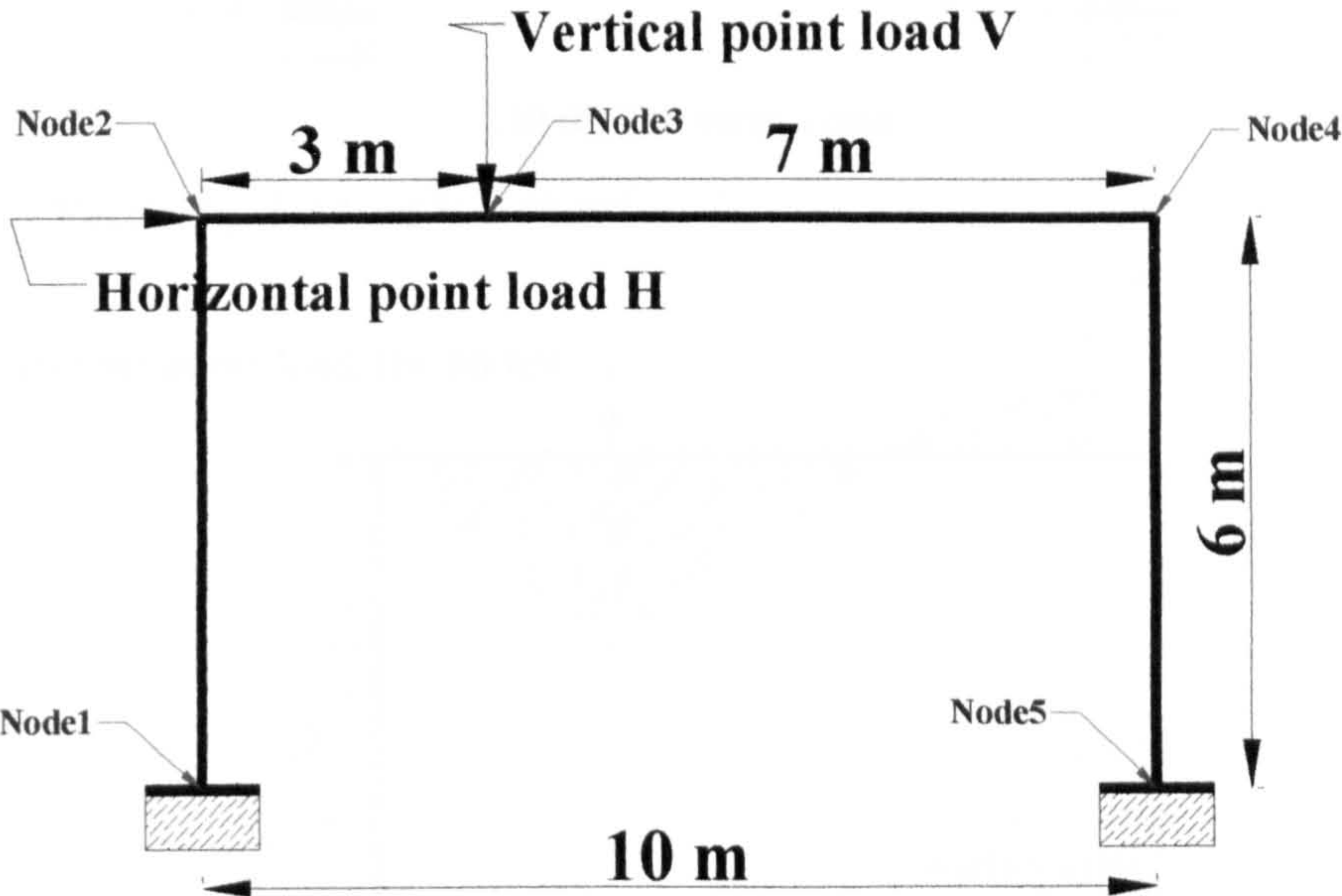
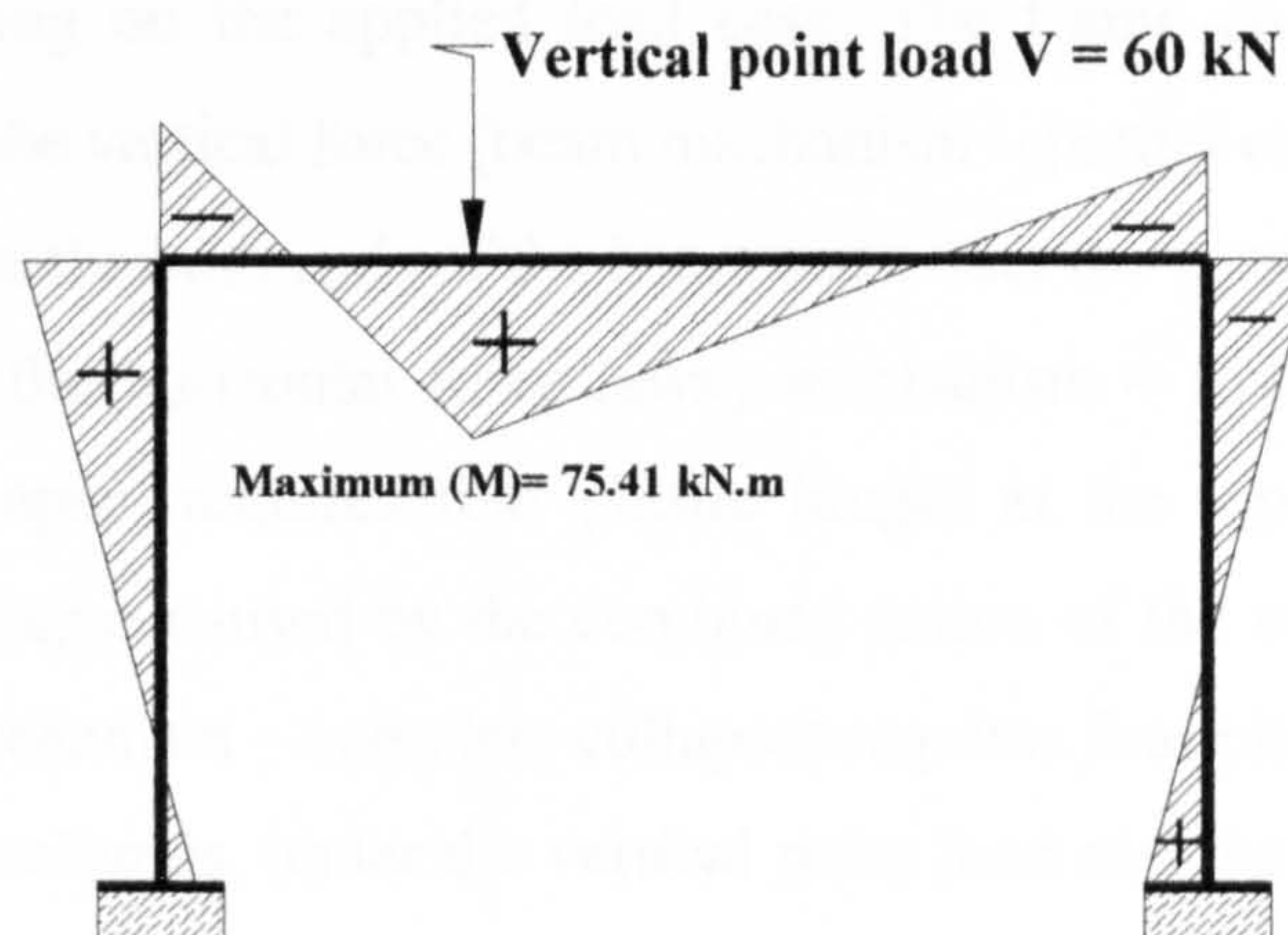


Figure I.9 The geometry and loads of the steel portal frame (general case)

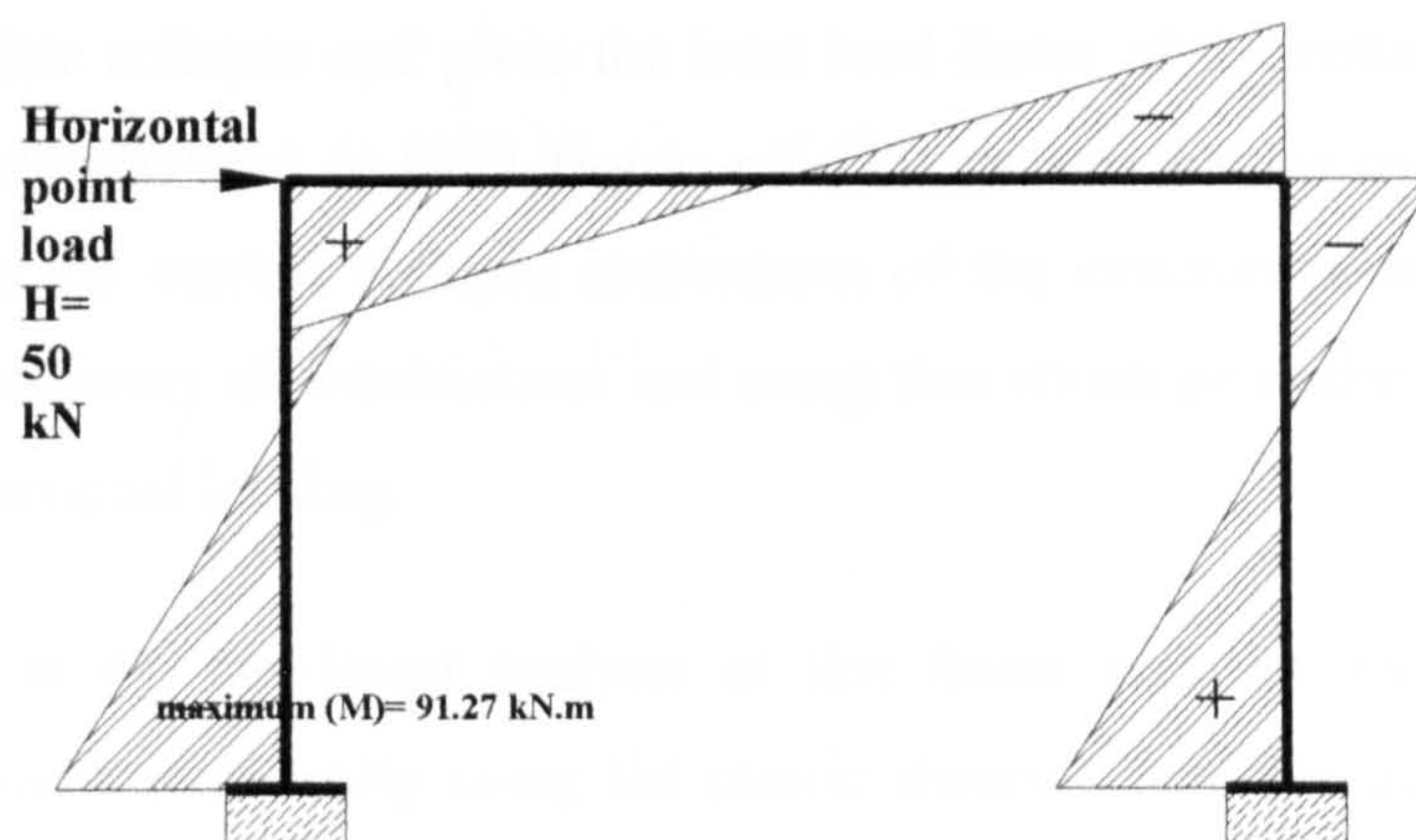
Because the frame is a statically indeterminate structure, it was solved analytically using the moment distribution method to obtain all its internal deformations against the



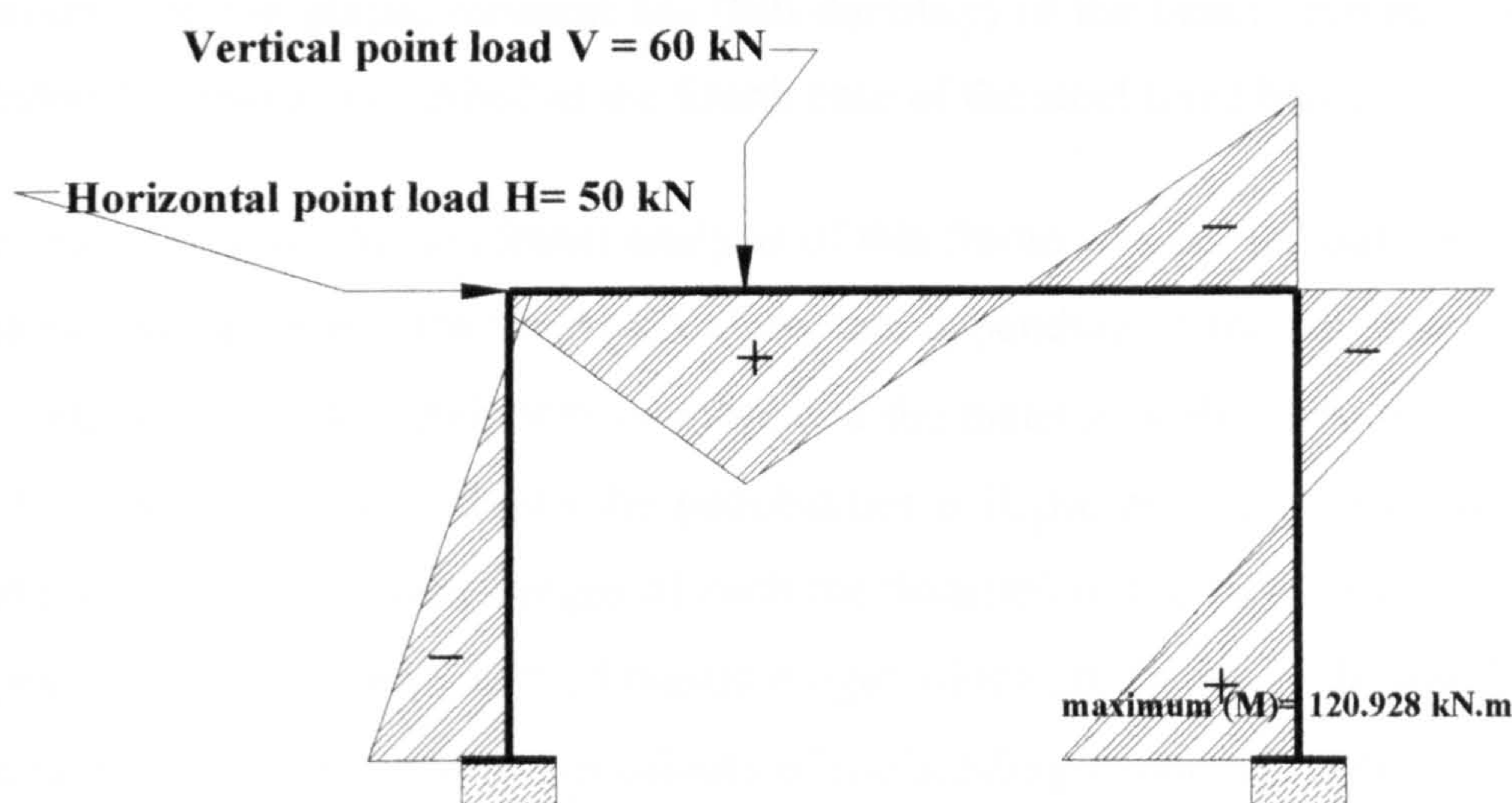
external forces for all cases of linear analysis, and subsequent to that the same cases were applied on ANSYS program (see table I.3). Fig. I.10 shows the moment distribution diagrams of all elastic behaviour cases.



I.10 (a) The first case



I.10 (b) The second case



I.10 (c) The third case

**Figure I.10** The moment distribution diagrams of the steel portal frame (linear analyses cases)



The static non-linear analysis of this frame was implemented using plastic theory and ANSYS to investigate inelastic behaviour. Determination of the correct collapse mechanism of this frame presents a problem because there are three possibilities for the mechanism depending on the applied load case. The frame collapse caused by the dominant action of the vertical force (beam mechanism – partial collapse) requires three plastic hinges only at the both ends of the beam and under the vertical point load. Frame collapse caused by the horizontal force (sway mechanism – structure is pushed sideways complete collapse) requires four plastic hinges at the top and bottom of both columns. Frame collapse caused by the combined action of the vertical and horizontal loads (combined mechanism – complete collapse) requires four plastic hinges to form at the bottom of both columns, under the vertical point load and the top of the right-hand column. The combined mechanism is the actual collapse mechanism of this frame. It presents complete collapse and gives the least load factor of the collapse loads of the three collapse mechanisms. In 1979, Horne, ref. [18], proved that the correct failure load which provides the correct collapse mechanism of the structure would appear to be derived by considering all mechanisms and using that which gives the least load factor assuming proportional loading.

The first step in the non-linear analysis of this frame was the investigation of its inelastic behaviour analytically using the plastic theory. Each relevant load case was solved to obtain the collapse loads  $W_C$  and the internal deformations at failure depending on the plastic moment  $M_P$  (full ductility) of the beam sections, (which was calculated before as described in the fourth case of the steel fixed beam).

The second step of the non-linear analysis of this frame was carried out for all possible collapse mechanisms using the ANSYS program depending on the collapse loads which was obtained from the analytical solution, and the material yield stress of the frame ( $\sigma_y = 250 \text{ N/mm}^2$ ). Fig. I.11 shows the possibilities collapse mechanisms (also shows the locations of formed plastic hinges of each mechanism) of the frame using the ANSYS program. The locations of formed plastic hinges which are shown in the Fig. I.11 can be determined using the variation in colours of the bending moment diagram of frame that these colours indicate to the values of bending moments. Table I.4 and I.5 lists the analytical and ANSYS results that describe the internal deformations (forces and moments) of the steel portal frame for all of the studied cases.



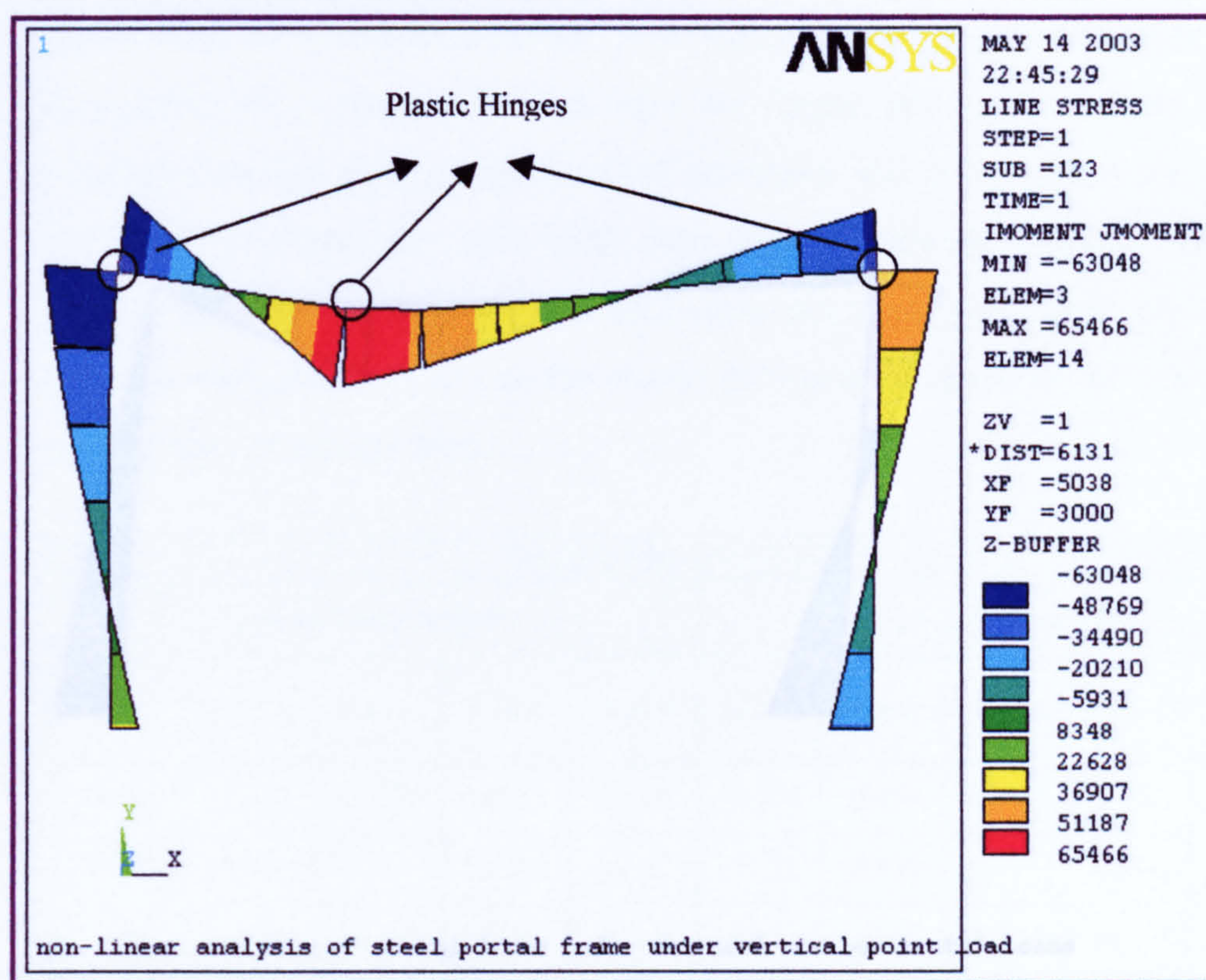


**Figure I.11 (a)** The beam mechanism of the steel portal frame and its bending moment diagram (The first non-linear analysis case)

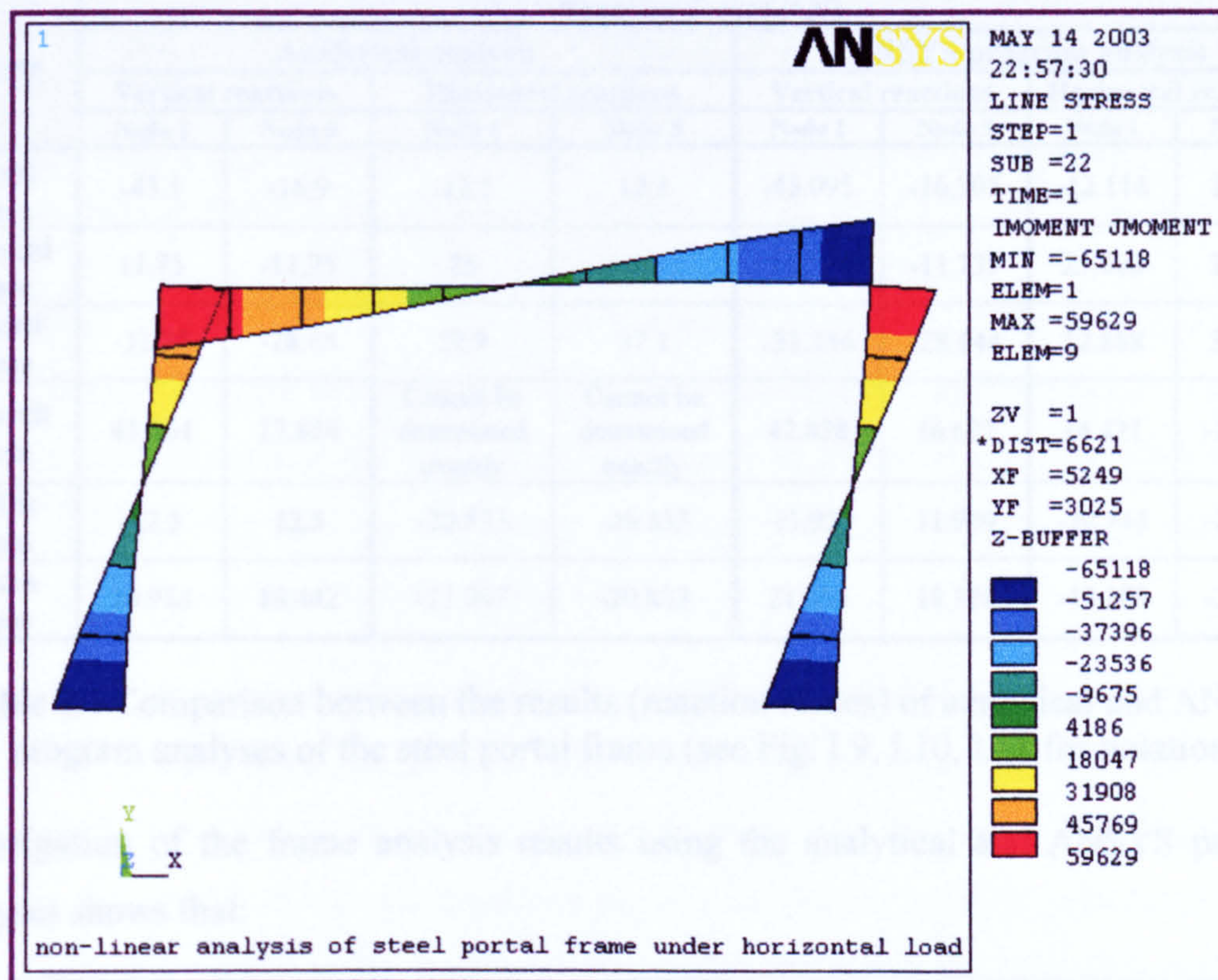


**Figure I.11 (b)** The sway mechanism of the steel portal frame and its bending moment diagram (The second non-linear analysis case)



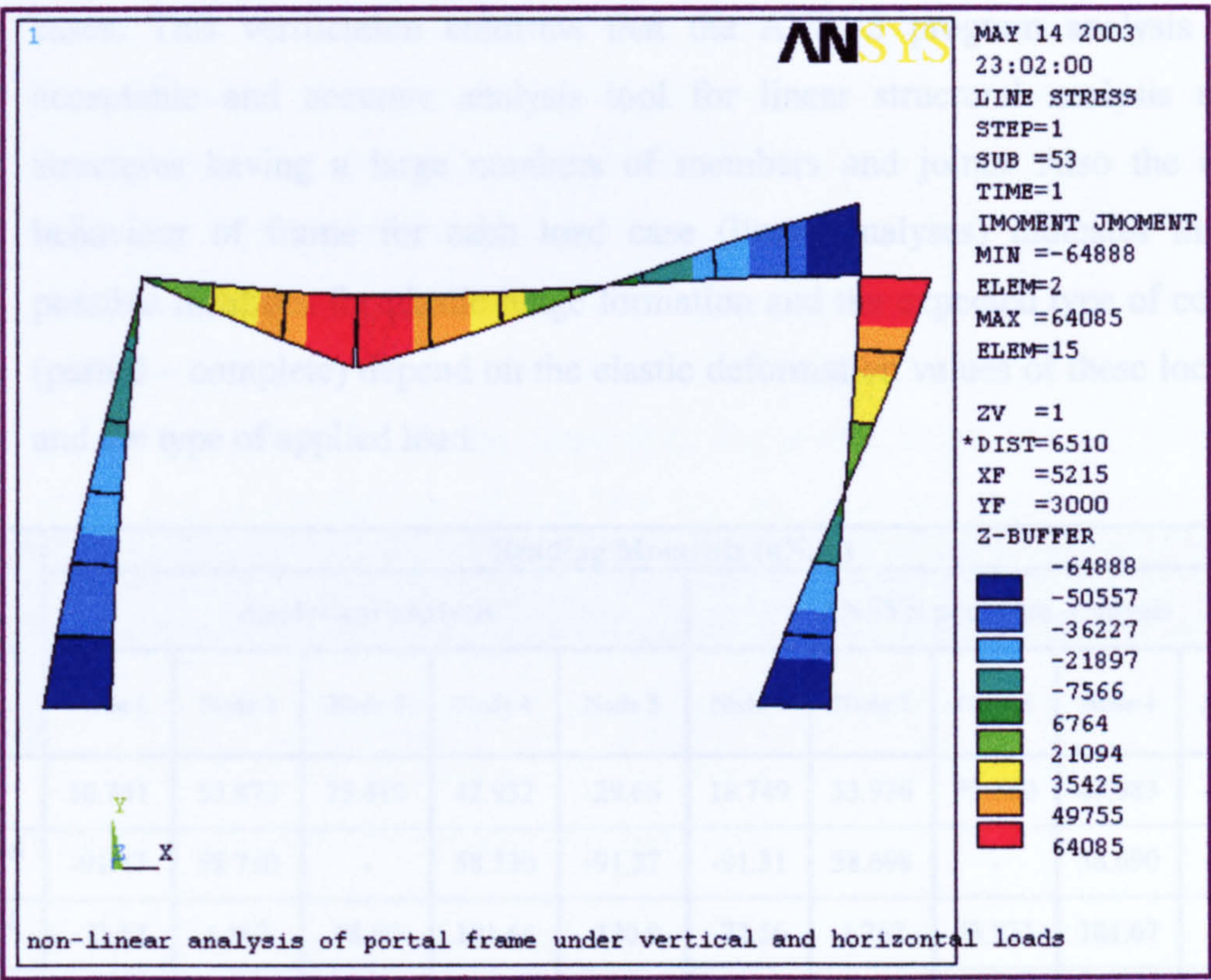


Figure I.11 (c) The combined mechanism of the steel portal frame and its bending moment diagram (The third non-linear analysis case)

Cases	Reaction forces (kN)							
	Analytical analysis				ANSYS program analysis			
	Vertical reactions		Horizontal reactions		Vertical reactions		Horizontal reactions	
	Node 1	Node 5	Node 1	Node 5	Node 1	Node 5	Node 1	Node 5
First case	-43.1	-16.9	-12.1	12.1	-43.095	-16.905	-12.114	12.114
Second case	11.75	-11.75	25	25	11.739	-11.739	25.002	24.998
Third case	-31.35	-28.65	12.9	37.1	-31.356	-28.644	12.888	37.112
Fourth case	41.664	17.856	Cannot be determined exactly	Cannot be determined exactly	42.838	16.682	14.421	-14.421
Fifth case	-12.5	12.5	-20.833	-20.833	-11.939	11.939	-20.743	-20.743
Sixth case	20.938	18.442	-11.047	-20.833	21.053	18.328	-10.209	-21.417

Table I.4 Comparison between the results (reaction forces) of analytical and ANSYS program analyses of the steel portal frame (see Fig. I.9, I.10, I.11 for notation)

Investigation of the frame analysis results using the analytical and ANSYS program analyses shows that:

1. The results of post elastic forces and moments of ANSYS program analysis are in good agreement with the results of analytical analysis for the linear analysis



cases. This verification confirms that the ANSYS program analysis is an acceptable and accurate analysis tool for linear structural analysis of the structures having a large numbers of members and joints. Also the elastic behaviour of frame for each load case (linear analyses) indicates that the possible locations for plastic hinge formation and the expected type of collapse (partial – complete) depend on the elastic deformation values of these locations and the type of applied load.

Cases	Bending Moments (kN.m)									
	Analytical analysis					ANSYS program analysis				
	Node 1	Node 2	Node 3	Node 4	Node 5	Node 1	Node 2	Node 3	Node 4	Node 5
First case	18.741	53.873	75.410	42.932	-29.66	18.749	53.936	75.350	42.983	-29.70
Second case	-91.27	58.730	-	58.730	-91.27	-91.31	58.698	-	58.690	-91.29
Third case	-72.52	4.862	98.90	101.66	-120.9	-72.56	4.762	98.831	101.67	-121.0
Fourth case	Cannot be determined exactly	62.5	62.5	62.5	Cannot be determined exactly	23.479	62.877	65.466	51.307	-35.21
Fifth case	-62.50	62.50	25.00	62.50	-62.50	-65.11	59.629	23.882	59.609	-65.11
Sixth case	-62.50	3.782	62.50	62.50	-62.50	-60.96	1.055	64.004	63.866	-64.89

**Table I.5** Comparison between the results (bending moments) of analytical and ANSYS program analyses of the steel portal frame (see Fig. I.9, I.10, I.11 for notation)

- The results of post inelastic forces and moments of the non-linear analysis cases, which illustrate the three types of collapse mechanism of the frame, are in good agreement with analytical results. This gives us a high degree of confidence that ANSYS can predict non-linear structural response with a high degree of accuracy for the complex plastic analysis problem.
- The plastic moment values of node2, node3 and node4 of the frame that required to form the beam mechanism (fourth case) and resulted from ANSYS program (refer to table I.5) show that the plastic hinge was formed at node2 and node3 whereas the values are equal or more than the analytically calculated plastic moment value. At the same time the plastic hinge was not formed at node4 that the value is less than the analytical plastic moment with small value which



means, the beam mechanism of the frame was not formed completely. Clarification of that relates to the ANSYS program (refer to the section of steel fixed beam). The plastic moment values of node1, node2, node4 and node5 of the frame that required to form the sway mechanism (fifth case) and resulted from ANSYS program (refer to table I.5) show that the plastic hinge was formed at node1 and node5 whereas the values are more than the analytically calculated plastic moment value. At the same time the plastic hinge was not formed at node2 and node4 that the value is less than the analytical plastic moment with very small value. The ANSYS program results of sixth case (combined mechanism) show a high degree of accuracy of the ANSYS analysis that the plastic moment values of node1, node3, node4 and node5 that required to form the actual collapse mechanism of this frame are approximately equal to the analytical plastic moment value (see table I.5).

Figures (I.12, I.13, I.14) show the comparison of results between the theoretical and ANSYS analyses of the frame for node1, node2, node3, node4 and node5 that verify the capability of ANSYS. In the figures I.12 & I.13, the vertical reactions of node1 (analytical and ANSYS program results) were plotted versus the bending moments (analytical and ANSYS program results) of the node 1 for all of the studied cases (static linear and nonlinear analyses). Fig. I.14 shows the capability of ANSYS program to perform the nonlinear analysis (formation of the combined collapse mechanism of frame). In this figure the node numbers (1,2,3,4,5) were plotted versus its moment values for the studied sixth case of frame (analytical and ANSYS program results).

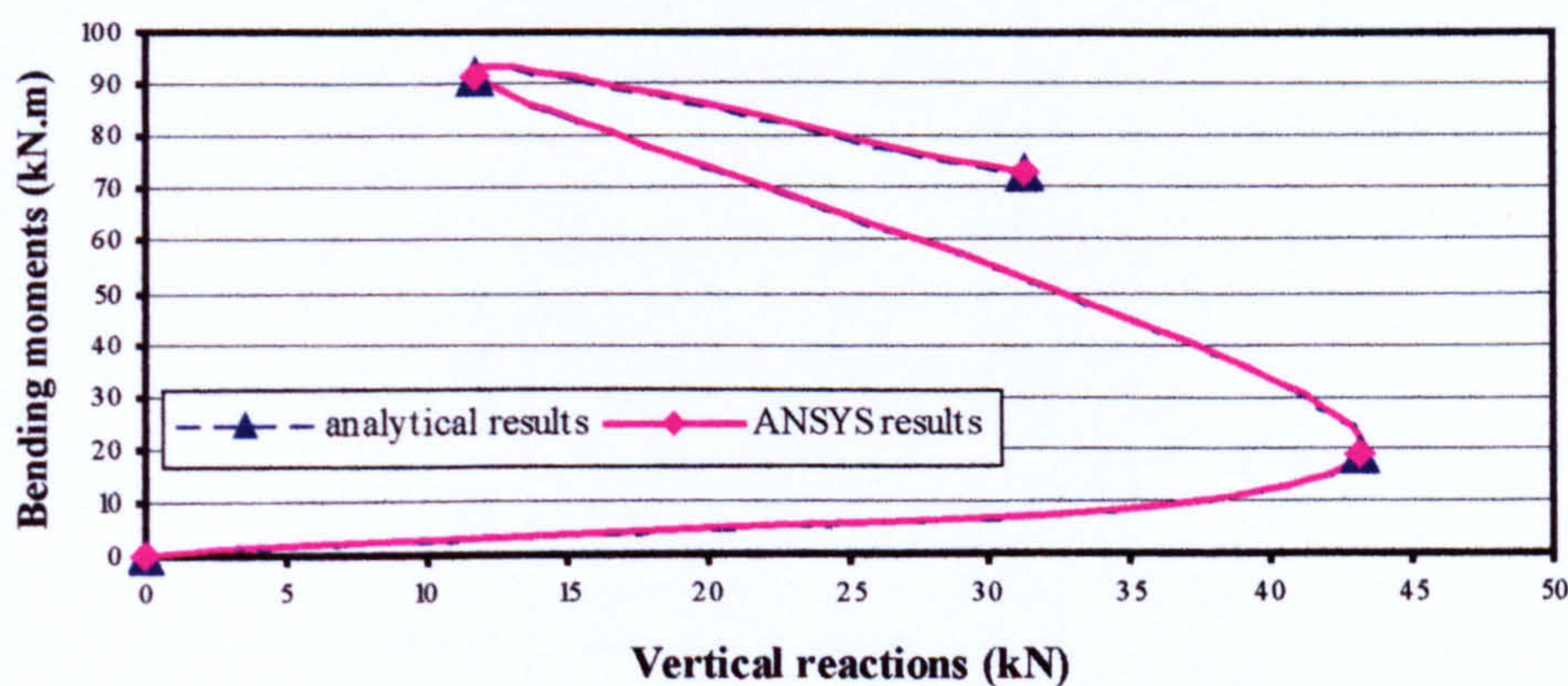


**Figure I.12** Comparison between analytical and ANSYS results of the node 1 for the linear analysis cases



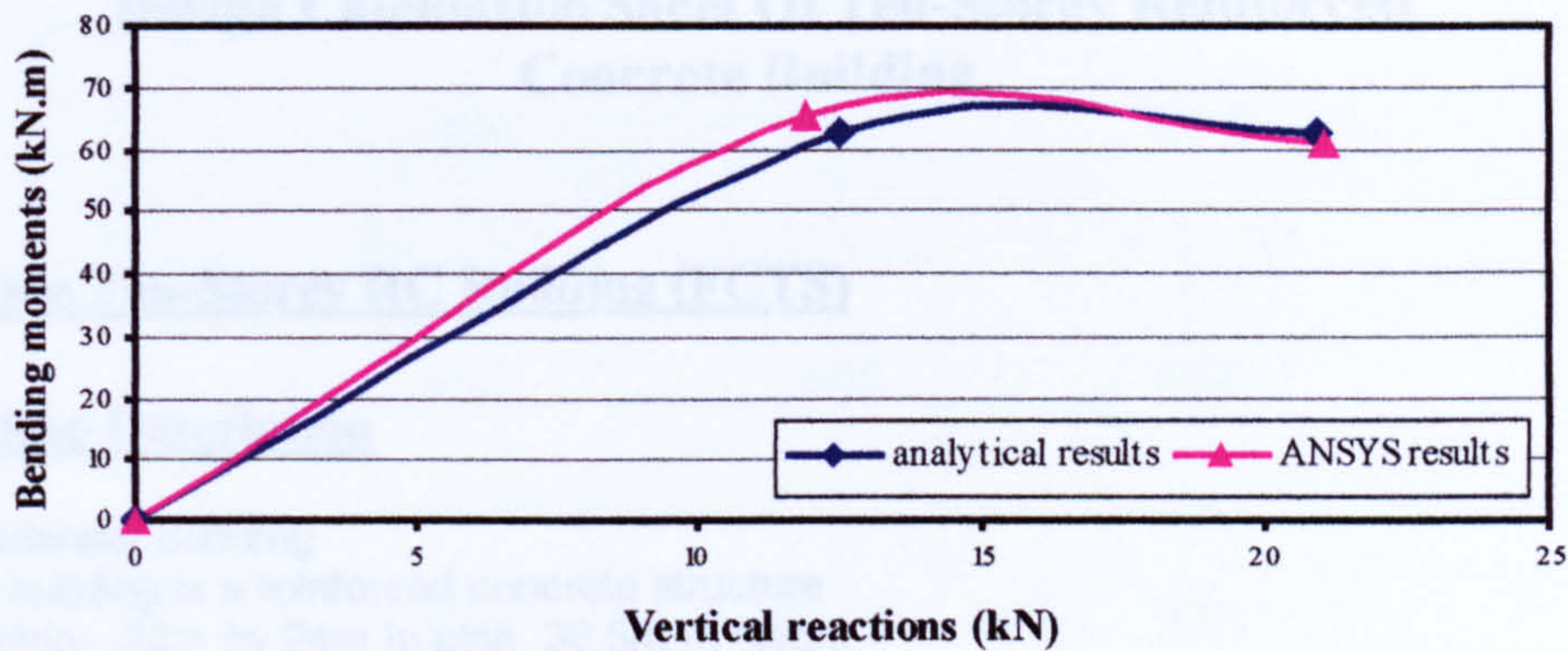


**Figure I.13** Comparison between analytical and ANSYS results of the node 1 for the nonlinear analysis cases

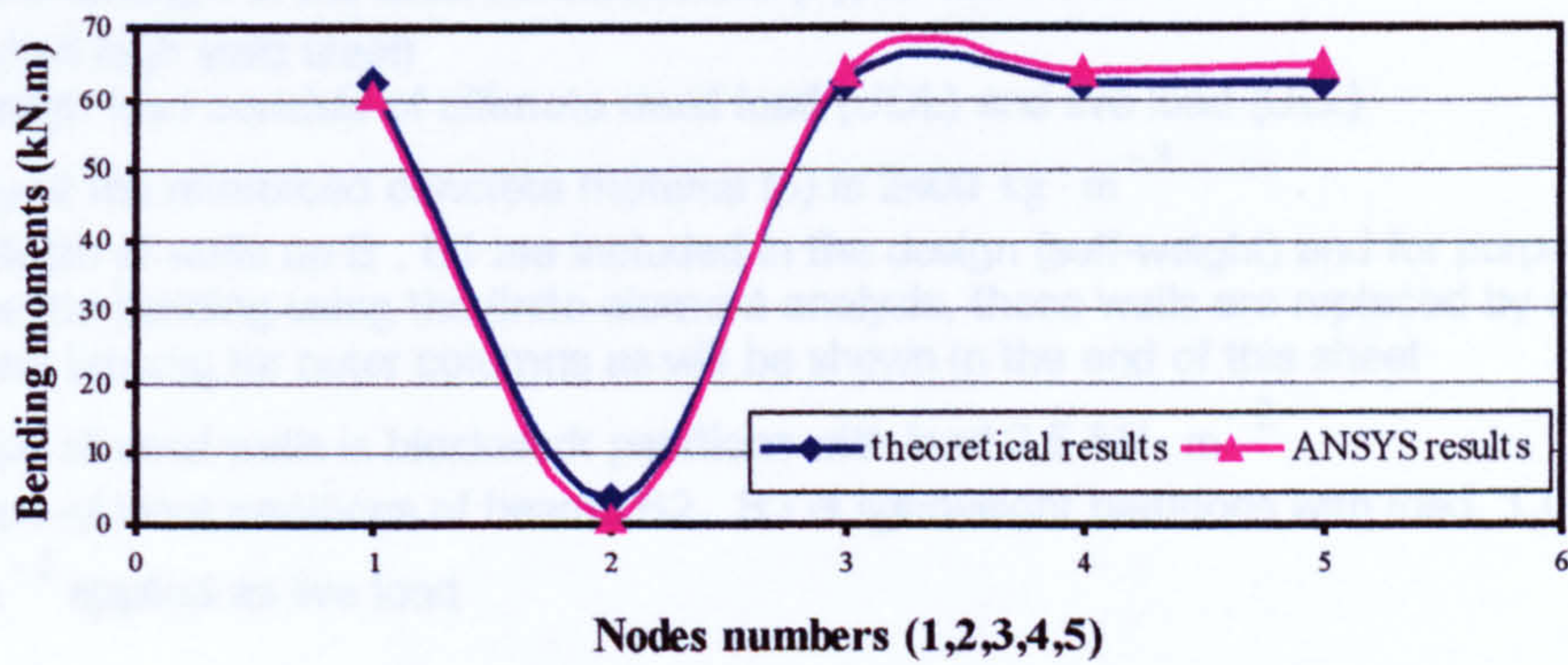


**Figure I.14** Comparison between theoretical and ANSYS results of the formation of combined collapse mechanism (moments at nodes 1,2,3,4,5)



## Design Calculation Sheet Of Ten-Storey Reinforced Concrete Building

### First Case Ten-Storey RC Building (FCTS)

#### 1. Building Description

- Residential Building
- The building is a reinforced concrete structure
- Building - 24m by 24m in plan, 36.5m in height
- Ground floor - 2 bay, 5m in height, 12m spans
- First floor to ninth floor - 3 bay, 3.5m in height, 8m spans
- All floors in other direction - 3 bay, 8m spans
- The characteristic concrete compressive strength ( $F_{cu}$ ) is  $30 \text{ N} \cdot \text{mm}^{-2}$  for all slabs & beams and columns of building except for transfer beams " B " and columns " C " of ground floor is Grade 40 ( $F_{cug}$  is  $40 \text{ N} \cdot \text{mm}^{-2}$ )
- The yield strength of the steel reinforcement ( $F_y$ ) is  $460 \text{ N} \cdot \text{mm}^{-2}$  (Hot rolled high yield steel)
- The design load consists of ultimate dead load (UDL) and live load (ULL)
- Density of the reinforced concrete material ( $\rho$ ) is  $2400 \text{ kg} \cdot \text{m}^{-3}$
- The effects of walls on B , B1 are included in the design (self-weight) and for purpose to analyse the building using the finite element analysis, these walls are replaced by a designed bracing for outer columns as will be shown in the end of this sheet
- The type of used walls is blockwork partitions with load  $2.5 \text{ kN} \cdot \text{m}^{-2}$
- The type of inner partitions of beams B2 , B3 is lightweight partitions with load  $1.0 \text{ kN} \cdot \text{m}^{-2}$  applied as live load

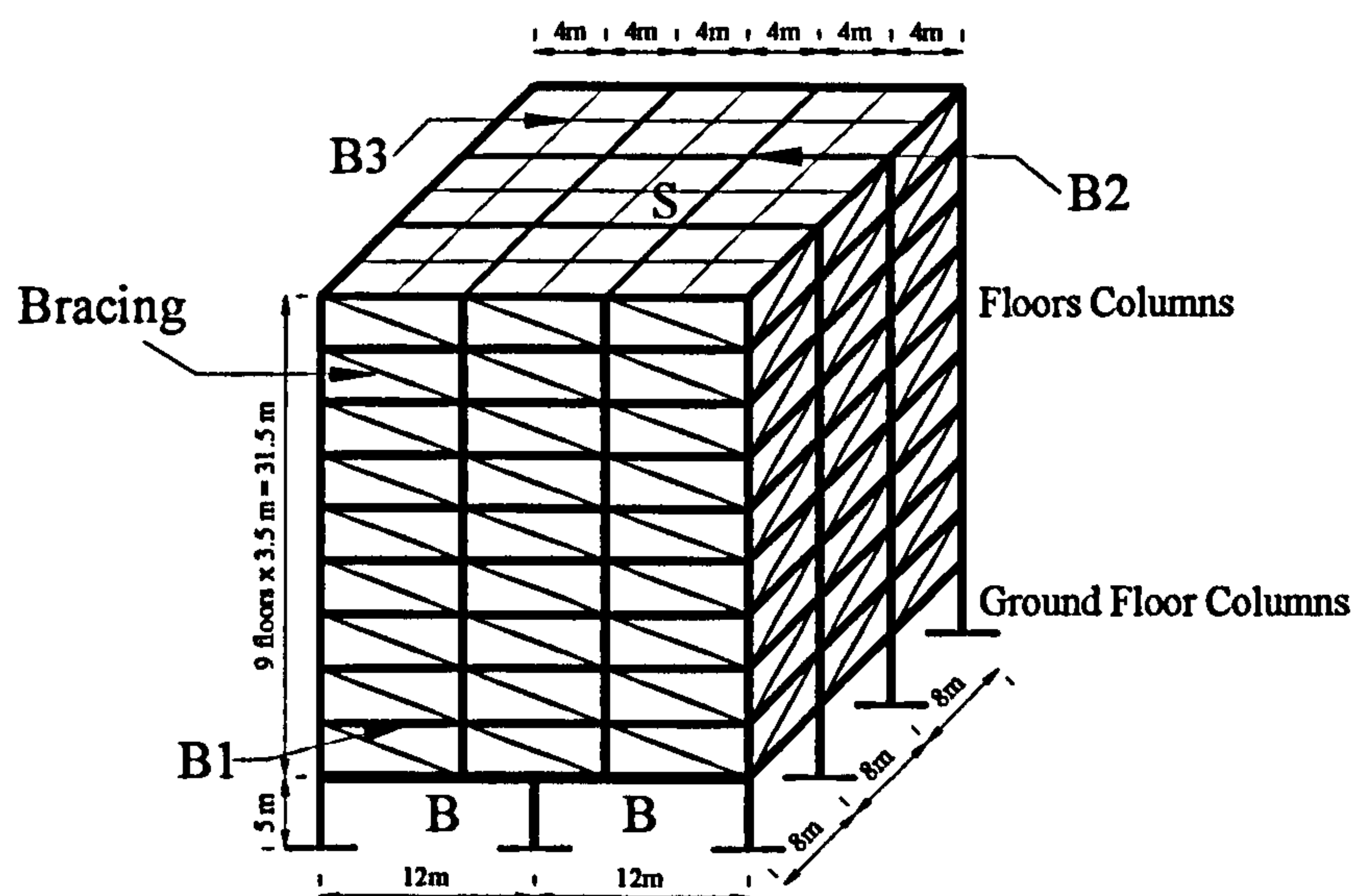


**Figure II.1 Details of the building**



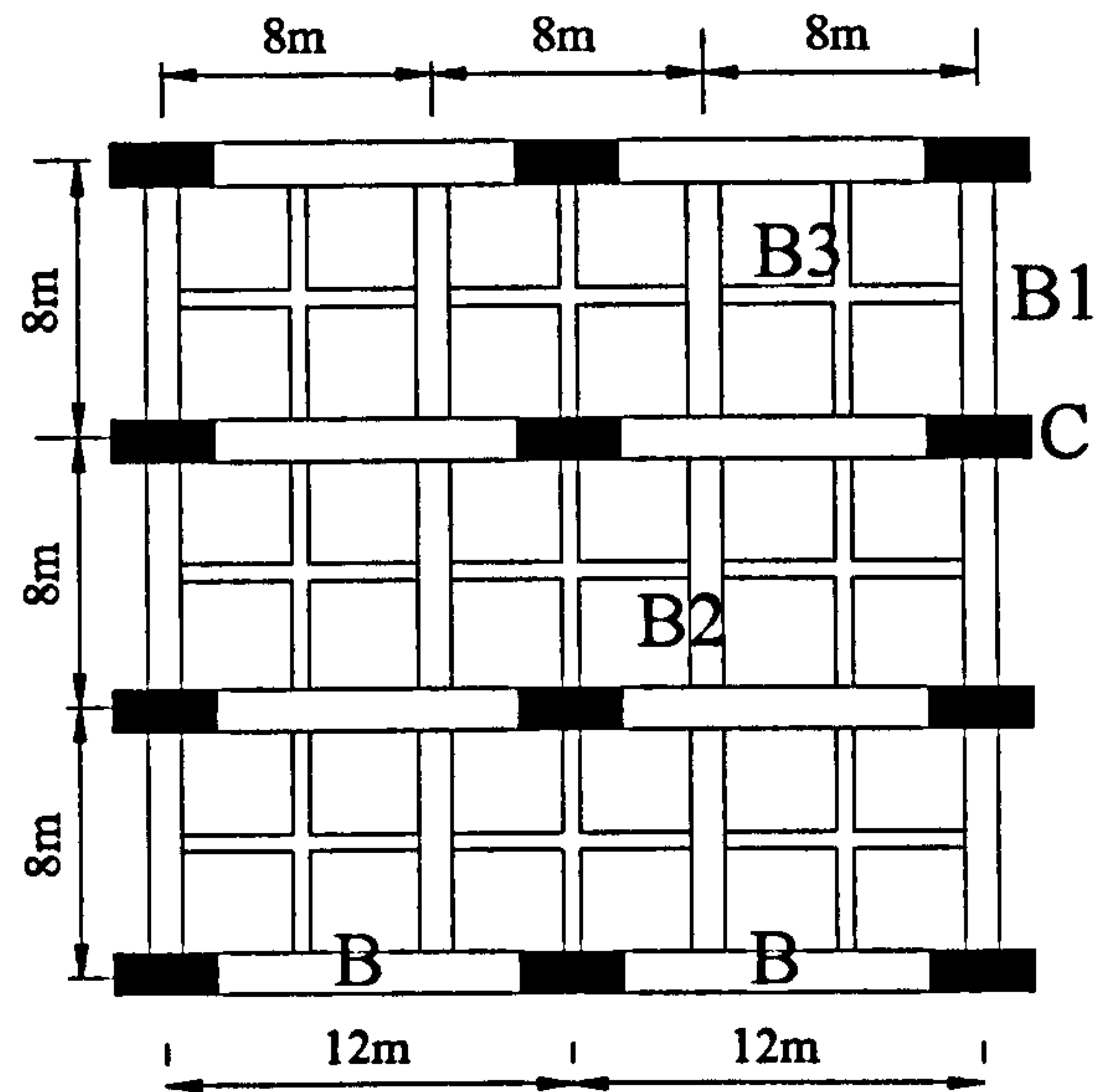


**Figure II.2 Plan of the ground floor slab**

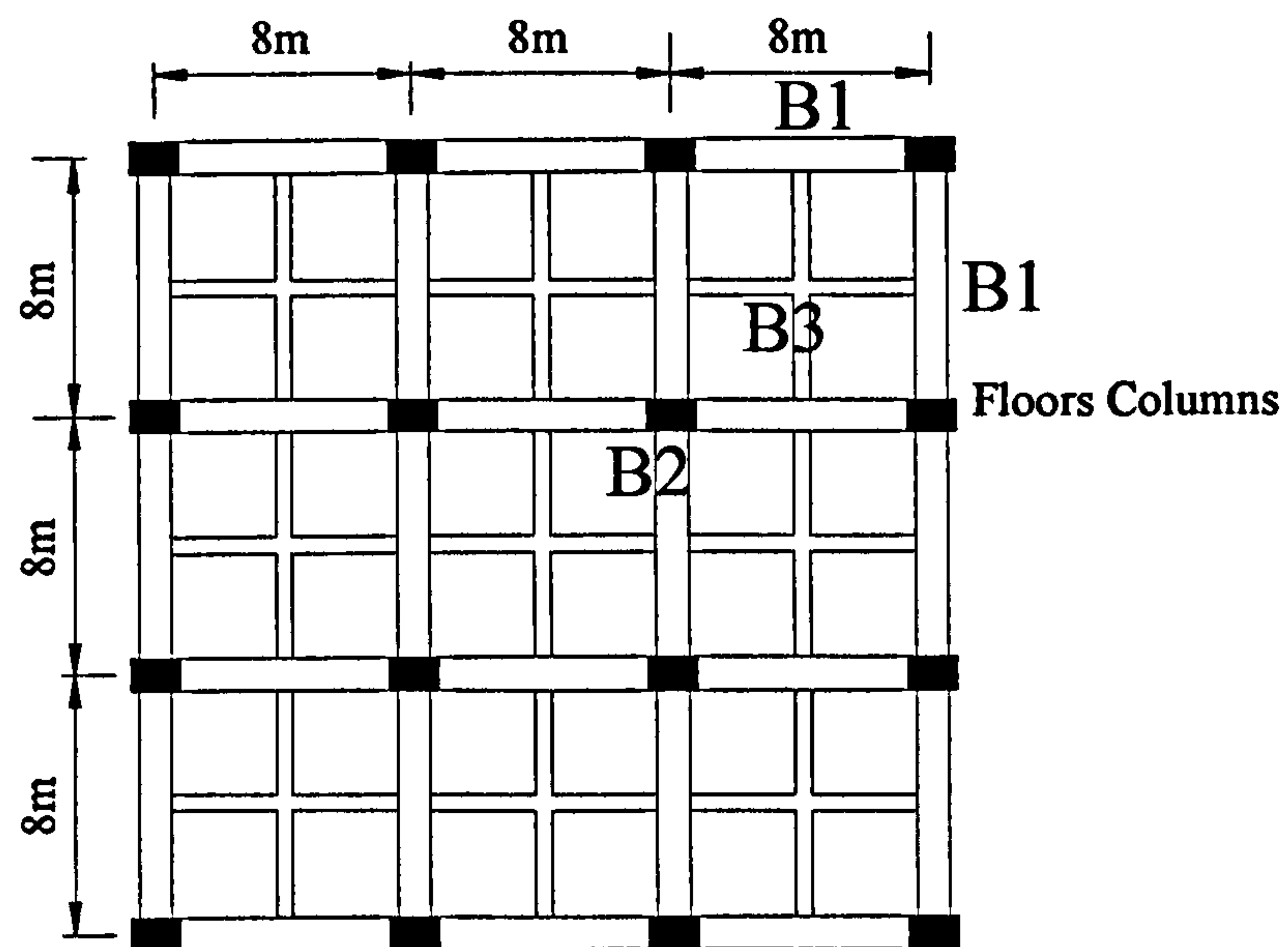


**Figure II.3 Plan of every floor slab for the floors from the first to ninth**



**2. Slab Design**

The structural system of the slab for all storeys is similar. Design of one floor slab is enough for this part of calculation as it will be the same for all floors slabs of the building. as the slab is square it is designed as two - way spanning.

**2.1 Initial Slab Thickness**

kN := 1000N

Long Span of slab  $l := 4000 \cdot \text{mm}$ 

The basic span to depth ratio for initial design of continuous slabs spanning in two directions gives the initial thickness of slab.

$$S_t := \frac{1}{35}$$

$$S_t := \text{if} \left( S_t < 150\text{mm}, 150\text{mm}, \frac{1}{35} \right)$$

$$S_t = 150 \text{ mm}$$



**2.2 Dimensions And Materials**Short Span  $L_x := 4000\text{mm}$ 

$$F_{cu} := 30 \cdot \text{N} \cdot \text{mm}^{-2}$$

Long Span  $L_y := 4000\text{mm}$ 

$$F_y := 460 \cdot \text{N} \cdot \text{mm}^{-2}$$

Density of reinforced concrete material  $\rho := 23.544 \cdot \text{kN} \cdot \text{m}^{-3}$ **2.3 Loading Characteristic**

All the following constant loads for imposed and dead loads are based on BS 648, BS 6399 and manual for the design of reinforced concrete building structures (The Institution of Structural Engineers - The Institution of Civil Engineers)

Load of blockwork walls for B , B1

$$L_w := 2.5 \cdot \text{kN} \cdot \text{m}^{-2}$$

Load of Partitions for B2 , B3

$$LL_p := 1 \cdot \text{kN} \cdot \text{m}^{-2}$$

Live (imposed) Load per unit area

$$LL := 1.5 \cdot \text{kN} \cdot \text{m}^{-2}$$

Floor Covering (dead load) per unit area

$$DL_{fc} := 1 \cdot \text{kN} \cdot \text{m}^{-2}$$

Volume of Slab  $\text{Vol} := L_x \cdot L_y \cdot S_t$ 

$$\text{Vol} = 2.4 \text{m}^3$$

Slab Load (dead load)  $DL_1 := \rho \cdot \text{Vol}$ 

$$DL_1 = 56.506 \text{kN}$$

Floor Covering (dead load)  $DL_2 := DL_{fc} \cdot L_x \cdot L_y$ 

$$DL_2 = 16 \text{kN}$$

Live (imposed) Load  $LL_1 := LL \cdot L_x \cdot L_y$ 

$$LL_1 = 24 \text{kN}$$

Live (partitions) Load  $LL_2 := LL_p \cdot L_x \cdot L_y$ 

$$LL_2 = 16 \text{kN}$$

Ultimate Dead Load  $UDL := (DL_1 + DL_2) \cdot 1.4$ 

$$UDL = 101.508 \text{kN}$$

Ultimate Live Load  $ULL := (LL_1 + LL_2) \cdot 1.6$ 

$$ULL = 64 \text{kN}$$

Total Design Load Per Unit Area  $n := \frac{(UDL + ULL)}{(L_x \cdot L_y)}$ 

$$n = 10.344 \text{kN} \cdot \text{m}^{-2}$$



**2.4 Maximum Design Moments**

The slab and supports are assumed to be monolithic, therefore equations 14 and 15 are applied (BS 8110 - 1). Also the slab has two short edges discontinuous which determines the coefficients values from table 3.14 depending on the  $L_y/L_x$  value.

$\frac{L_y}{L_x} = 1$  This means the moments are similar in the two directions X and Y and From table (3 -14)

Coefficients of Negative moment at continuous edge  $\beta_1 := 0.046$

Coefficients of Positive moment at mid - span  $\beta_2 := 0.034$

$$(-ve \text{ Cont.}) \quad M_{s1} := \beta_1 \cdot n \cdot L_x^2 \quad M_{s1} = 7.613 \text{ kN} \cdot \text{m} \cdot \text{m}^{-1}$$

$$(+ve \text{ mid.}) \quad M_{s2} := \beta_2 \cdot n \cdot L_x^2 \quad M_{s2} = 5.627 \text{ kN} \cdot \text{m} \cdot \text{m}^{-1}$$

**2.5 Effective Depths**

$$\text{cover}_s := 30 \text{ mm}$$

$$\phi_s := 12 \text{ mm}$$

$$\text{First direction - span bars in the bottom layer (effective depth)} \quad d_{s1} := S_t - \text{cover}_s - \frac{\phi_s}{2}$$

$$d_{s1} = 114 \text{ mm}$$

$$\text{Second direction - span bars in the top layer (effective depth)} \quad d_{s2} := S_t - \text{cover}_s - \phi_s - \frac{\phi_s}{2}$$

$$d_{s2} = 102 \text{ mm}$$

**2.6 Area Of Steel**

$$b := 1000 \text{ mm}$$

$$\text{Minimum area of steel of section} \quad A_{sm} := \frac{1}{100} \cdot 0.13 \cdot b \cdot S_t$$

$$A_{sm} = 195 \text{ mm}^2$$

$$k_{s1} := \frac{M_{s1}}{F_{cu} \cdot b \cdot d_{s1}^2} \cdot 1 \text{ m}$$

$$k_{s1} = 0.02$$



$$\text{Lever arm} \quad z_{s1} := d_{s1} \cdot \left[ 0.5 + \left( 0.25 - \frac{k_{s1}}{0.9} \right)^2 \right]^{\frac{1}{2}} \quad z_{s1} := \text{if}(z_{s1} > 0.95d_{s1}, 0.95d_{s1}, z_{s1})$$

$$z_{s1} = 108.3 \text{ mm}$$

**First direction - bars in the bottom layer for support**

$$A_{s1} := \frac{M_{s1}}{0.95 \cdot F_y \cdot z_{s1}} \cdot 1\text{m} \quad A_{s1} := \text{if}(A_{s1} < A_{sm}, A_{sm}, A_{s1})$$

$$A_{s1} = 195 \text{ mm}^2$$

For this area of steel use T12 bars at 500 mm centres ( area1 := 226.19mm<sup>2</sup> )

**First direction - bars in the bottom layer for mid - span**

$$A_{s2} := \frac{M_{s2}}{0.95 \cdot F_y \cdot z_{s1}} \cdot 1\text{m} \quad A_{s2} := \text{if}(A_{s2} < A_{sm}, A_{sm}, A_{s2})$$

$$A_{s2} = 195 \text{ mm}^2$$

For this area of steel use T12 bars at 500 mm centres ( area2 := 226.19mm<sup>2</sup> )

**Second direction - bars in the top layer for support**

$$k_{s2} := \frac{M_{s1}}{F_{cu} \cdot b \cdot d_{s2}^2} \cdot 1\text{m} \quad k_{s2} = 0.024$$

$$\text{Lever arm} \quad z_{s2} := d_{s2} \cdot \left[ 0.5 + \left( 0.25 - \frac{k_{s2}}{0.9} \right)^2 \right]^{\frac{1}{2}} \quad z_{s2} := \text{if}(z_{s2} > 0.95d_{s2}, 0.95d_{s2}, z_{s2})$$

$$z_{s2} = 96.9 \text{ mm}$$



$$A_{s3} := \frac{M_{s1}}{0.95 \cdot F_y \cdot z_{s2}} \cdot 1m$$

$$A_{s3} := \text{if}(A_{s3} < A_{sm}, A_{sm}, A_{s3})$$

$$A_{s3} = 195 \text{ mm}^2$$

For this area of steel use T12 bars at 500 mm centres ( area3 := 226.19mm<sup>2</sup> )

### Second direction - bars in the top layer for mid - span

$$A_{s4} := \frac{M_{s2}}{0.95 \cdot F_y \cdot z_{s2}} \cdot 1m$$

$$A_{s4} := \text{if}(A_{s4} < A_{sm}, A_{sm}, A_{s4})$$

$$A_{s4} = 195 \text{ mm}^2$$

For this area of steel use T12 bars at 500 mm centres ( area4 := 226.19mm<sup>2</sup> )

### 2.7 Deflection (serviceability check)

Service Stress  $f_s := \frac{2 \cdot F_y \cdot A_{s2}}{3 \cdot \text{area2}}$

$$f_s = 264.38 \text{ N} \cdot \text{mm}^{-2}$$

Modification Factor  $f_{ms} := 0.55 + \frac{477 \cdot \frac{\text{N}}{\text{mm}^2} - f_s}{120 \cdot \left( 0.9 \cdot \frac{\text{N}}{\text{mm}^2} + \frac{M_{s2}}{b \cdot d_{s2}^2} \cdot 1m \right)}$

$$f_{ms} = 1.78$$

Allowable Span to Depth Ratio  $SD_{rs} := 26 \cdot f_{ms}$

$$SD_{rs} = 46.272$$

Actual Span to Depth Ratio  $SD_{as} := \frac{1}{d_{s2}}$

$$SD_{as} = 39.216$$

**The slab is satisfactory with respect to deflections**

### 2.8 Shear Resistance

The shear coefficients are 1- at cont. edge  $B_{v1} := 0.4$

From table 3.15 and  $\frac{L_y}{L_x} = 1$

2- at discont. edge  $B_{v2} := 0.26$



Shear forces  $V_{s1} := B_{v1} \cdot n \cdot L_x$

$V_{s2} := B_{v2} \cdot n \cdot L_x$

$V_{s1} = 16.551 \text{ m}^{-1} \text{ kN}$

$V_{s2} = 10.758 \text{ m}^{-1} \text{ kN}$

Max shear stress  $v := \frac{V_{s1}}{b \cdot d_{s2}} \cdot 1\text{m}$

$v = 0.162 \text{ N} \cdot \text{mm}^{-2}$

Design concrete shear stress (BS 8110 - 1:1997, Table 3.8)

$$v_c := \frac{0.79 \cdot \frac{\text{N}}{\text{mm}^2} \cdot \left( \frac{100 \cdot \text{area1}}{b \cdot d_{s1}} \right)^{\frac{1}{3}} \cdot \left( \frac{400 \cdot \text{mm}}{d_{s1}} \right)^{\frac{1}{4}} \cdot \left( \frac{F_{cu}}{25 \cdot \frac{\text{N}}{\text{mm}^2}} \right)^{\frac{1}{3}}}{1.25}$$

$v_c = 0.536 \text{ N} \cdot \text{mm}^{-2}$

The slab is satisfactory with respect to shear and no shear reinforcement required

### 3. Design Of Beam B3

Span of Beam  $l_{B3} := 8000\text{mm}$

Height of Floor (1 - 9)  $h_f := 3500\text{mm}$

#### 3.1 Design Loading On Beam B3

##### Max Design Load

Patch load ( From slab, BS 8110 - 1:1997, Figure 3.10)  $L_{p3} := V_{s1} \cdot 0.75 \cdot l_{B3}$   $L_{p3} = 99.305 \text{ kN}$

Total patch load  $L_{tp3} := L_{p3} \cdot 2$   $L_{tp3} = 198.609 \text{ kN}$

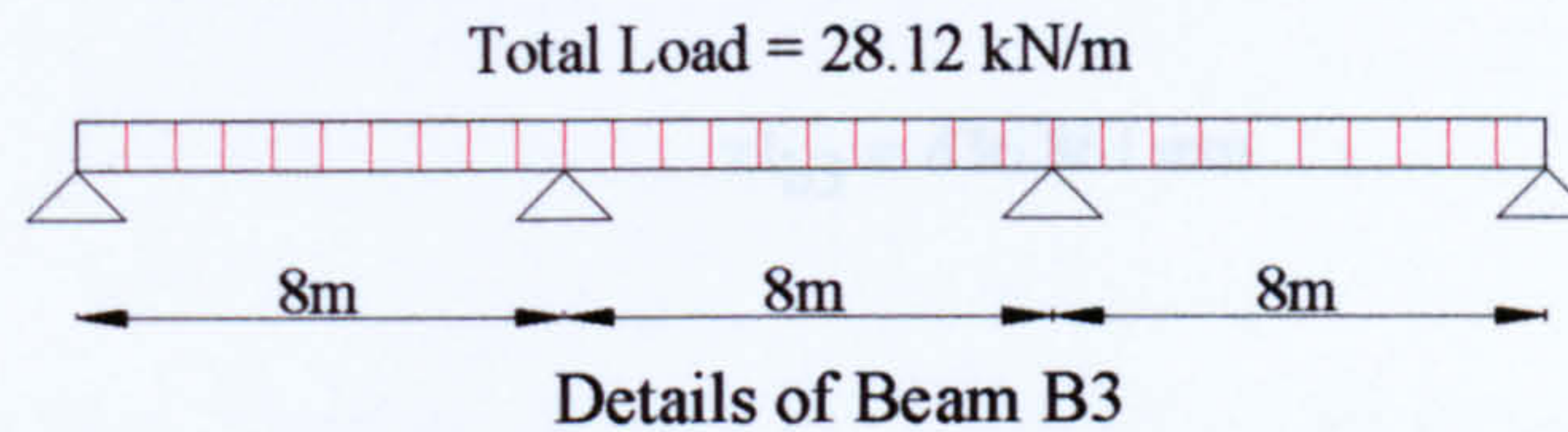
Assume the initial dimensions of beam are  $b_{B3} := 250\text{mm}$   $d_{B3} := 400\text{mm}$

Ultimate self weight of beam  $UL_{B3} := b_{B3} \cdot d_{B3} \cdot l_{B3} \cdot \rho \cdot 1.4$

$UL_{B3} = 26.369 \text{ kN}$

Total load on beam  $L_{tB3} := L_{tp3} + UL_{B3}$   $L_{tB3} = 224.979 \text{ kN}$





### 3.2 Section Properties Of Beam B3

The beams are treated as T - section at mid - span and rectangular section at supports  
the effective width of this flanged beam is

$$W_{\text{eff}} := \frac{0.7 \cdot l_{B3}}{5} + b_{B3}$$

$$W_{\text{eff}} = 1.37 \times 10^3 \text{ mm}$$

### 3.3 Ultimate Bending Moments And Shear Forces

From table 3.5 the max bending moments and shear forces are

max moment at support  $M1_{b3} := 0.11 \cdot L_{tB3} \cdot l_{B3}$

$$M1_{b3} = 197.981 \text{ m kN}$$

max moment at mid - span  $M2_{b3} := 0.09 \cdot L_{tB3} \cdot l_{B3}$

$$M2_{b3} = 161.985 \text{ m kN}$$

max shear force  $FS_{b3} := 0.6 \cdot L_{tB3}$

$$FS_{b3} = 134.987 \text{ kN}$$

### 3.4 Critical Section At Support

Assume the diameter of bars used is T16 and 2 layers of bars

$$\phi1_{b3} := 16 \text{ mm}$$

$$\text{cover}_{b3} := 30 \text{ mm}$$

$$d3_{\text{efl}} := (d_{B3} + S_t) - \text{cover}_{b3} - \phi1_{b3}$$

$$d3_{\text{efl}} = 504 \text{ mm}$$

$$k1_{b3} := \frac{M1_{b3}}{F_{cu} \cdot b_{B3} \cdot d3_{\text{efl}}^2}$$

$$k1_{b3} = 0.104$$

compression reinforcement is not required



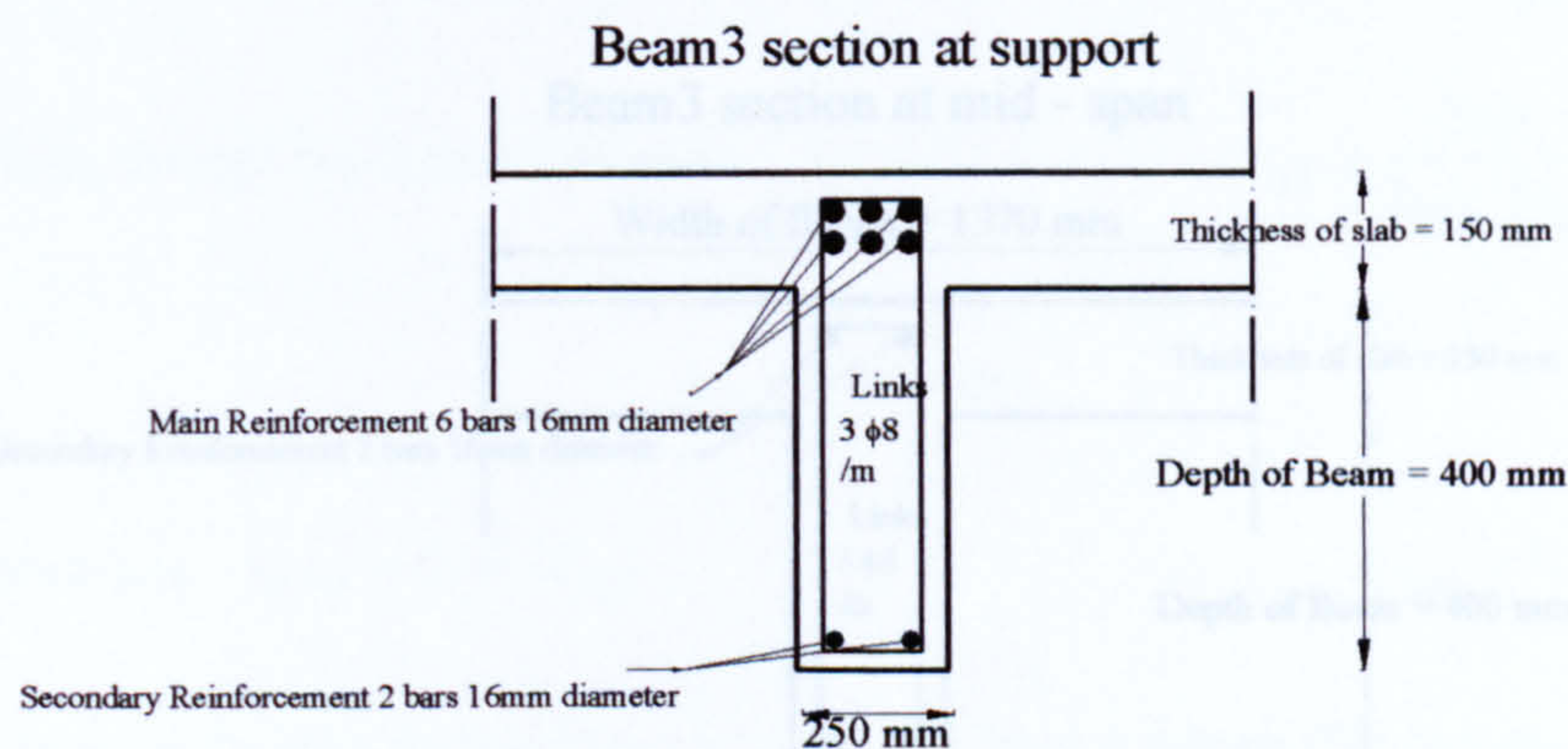
$$z_{l_{b3}} := d_{3_{efl}} \cdot \left[ 0.5 + \left( 0.25 - \frac{k_{l_{b3}}}{0.9} \right)^{\frac{1}{2}} \right] \quad z_{l_{b3}} := \text{if}(z_{l_{b3}} > 0.95d_{3_{efl}}, 0.95d_{3_{efl}}, z_{l_{b3}})$$

$$z_{l_{b3}} = 436.861 \text{ mm}$$

$$\text{Minimum area of steel of section } A_{sm1} := \frac{1}{100} \cdot 0.13 \cdot b_{B3} \cdot (d_{B3} + S_t) \quad A_{sm1} = 178.75 \text{ mm}^2$$

$$A_{s5} := \frac{M_{l_{b3}}}{0.95 \cdot F_y \cdot z_{l_{b3}}} \quad A_{s5} := \text{if}(A_{s5} < A_{sm1}, A_{sm1}, A_{s5}) \quad A_{s5} = 1.037 \times 10^3 \text{ mm}^2$$

6 bars of T16 are arranged in 2 layers with area5 := 1206.37mm<sup>2</sup>



### **3.5 Critical Section At Mid - Span**

$$\text{Check of neutral axis} \quad M_T := 0.45 \cdot F_{cu} \cdot W_{eff} \cdot S_t \cdot \left( d_{3_{efl}} - \frac{S_t}{2} \right) \quad M_T = 1.19 \times 10^3 \text{ m kN}$$

Because the  $M_T > M_{2_{b3}}$  the neutral axis lies in the flange and the section is treated as rectangular section

$$k_{2_{b3}} := \frac{M_{2_{b3}}}{F_{cu} \cdot W_{eff} \cdot d_{3_{efl}}^2} \quad k_{2_{b3}} = 0.016 \quad \text{No compression reinforcement is required}$$



$$z_{b3} := d_{3efl} \cdot \left[ 0.5 + \left( 0.25 - \frac{k_{2b3}}{0.9} \right)^2 \right] \quad z_{b3} := \text{if}(z_{b3} > 0.95d_{3efl}, 0.95d_{3efl}, z_{b3})$$

$$z_{b3} = 478.8 \text{ mm}$$

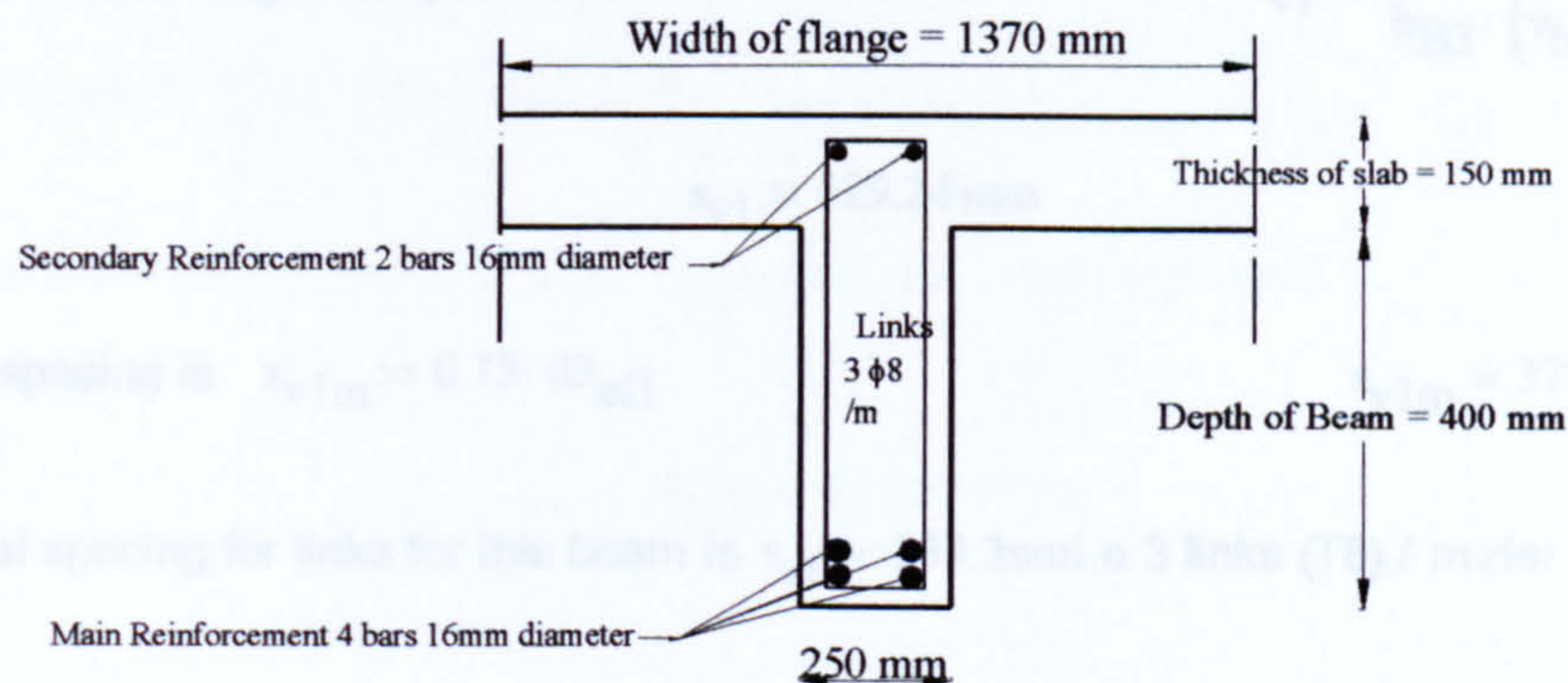
$$\text{Minimum area of steel of section } A_{sm2} := \frac{1}{100} \cdot 0.13 \cdot [(W_{eff} \cdot S_t) + (d_{B3} \cdot b_{B3})]$$

$$A_{sm2} = 397.15 \text{ mm}^2$$

$$A_{s6} := \frac{M_{2b3}}{0.95 \cdot F_y \cdot z_{b3}} \quad A_{s6} := \text{if}(A_{s6} < A_{sm2}, A_{sm2}, A_{s6}) \quad A_{s6} = 774.173 \text{ mm}^2$$

4 bars of T16 are arranged in two rows with area6 := 804.25mm<sup>2</sup>

#### Beam3 section at mid - span



### 3.6 Shear Reinforcement

$$\text{Ultimate shear stress } v_{b3} := \frac{FS_{b3}}{b_{B3} \cdot d_{3efl}} \quad v_{b3} = 1.071 \text{ N} \cdot \text{mm}^{-2}$$

$$eqterm := \frac{400 \cdot \text{mm}}{d_{3efl}} \quad eqterm := \text{if}(eqterm < 1, 1, eqterm) \quad eqterm = 1$$



Design concrete shear stress (BS 8110 - 1:1997, Table 3.8)

$$v_{cb3} := \frac{0.79 \cdot \frac{N}{mm^2} \cdot \left( \frac{100 \cdot area5}{b_{B3} \cdot d_{efl}^3} \right)^{\frac{1}{3}} \cdot (eqterm)^{\frac{1}{4}} \cdot \left( \frac{F_{cu}}{25 \cdot \frac{N}{mm^2}} \right)^{\frac{1}{3}}}{1.25} \quad v_{cb3} = 0.662 N \cdot mm^{-2}$$

From table 3.7 category 3 is required here and choose links only so that T8 is provided for this section

$$\phi_{b3} := 8mm$$

Total cross - section area of links at the neutral axis for 2 legs of T8 is  $A_{sv1} := 2 \cdot \frac{\pi \cdot \phi_{b3}^2}{4}$

$$A_{sv1} = 100.531 mm^2$$

Spacing of links through the span of beam is

$$s_{v1} := \frac{A_{sv1} \cdot 0.95 \cdot F_y}{b_{B3} \cdot (v_{b3} - v_{cb3})}$$

$$s_{v1} = 429.24 mm$$

Max links spacing is  $s_{v1m} := 0.75 \cdot d_{efl}$ 

$$s_{v1m} = 378 mm$$

So the final spacing for links for this beam is  $s_{vf} := 333.3mm$  i.e 3 links (T8) / meter

**Note:**

Due to the beam being singly reinforced secondary steel bars should be provided to stabilize shear links i.e 2 T16 for the beam section as secondary steel bars.

**3.7 Deflection Check**

Service Stress  $fs_{b3} := \frac{2 \cdot F_y \cdot A_{s6}}{3 \cdot area6}$

$$fs_{b3} = 295.198 N \cdot mm^{-2}$$

Modification Factor  $fm_{b3} := 0.55 + \frac{477 \cdot \frac{N}{mm^2} - fs_{b3}}{120 \cdot \left( 0.9 \cdot \frac{N}{mm^2} + \frac{M_{2b3}}{b_{B3} \cdot d_{efl}^2} \right)}$   $fm_{b3} = 0.989$



Allowable Span to Depth Ratio

$$SD_{r1} := 26 \cdot f_{m_{b3}}$$

$$SD_{r1} = 25.715$$

Actual Span to Depth Ratio

$$SD_{a1} := \frac{l_{B3}}{d_{3_{efl}}^3}$$

$$SD_{a1} = 15.873$$

The beam is satisfactory with respect to deflections

#### 4. Design OF Beam B2

$$l_{B2} := 8000\text{mm}$$

##### 4.1 Design Loading On Beam B2

##### Max Design Load

Patch load (From slab, BS 8110 - 1:1997, Figure 3.10)  $L_{p2} := V_{s1} \cdot 0.75 \cdot l_{B2}$   $L_{p2} = 99.305\text{ kN}$

Total patch load

$$L_{tp2} := L_{p2} \cdot 2$$

$$L_{tp2} = 198.609\text{ kN}$$

Assume the initial dimensions of beam are

$$b_{B2} := 250\text{mm}$$

$$d_{B2} := 550\text{mm}$$

Ultimate self weight of beam

$$UL_{B2} := b_{B2} \cdot d_{B2} \cdot l_{B2} \cdot \rho \cdot 1.4$$

$$UL_{B2} = 36.258\text{ kN}$$

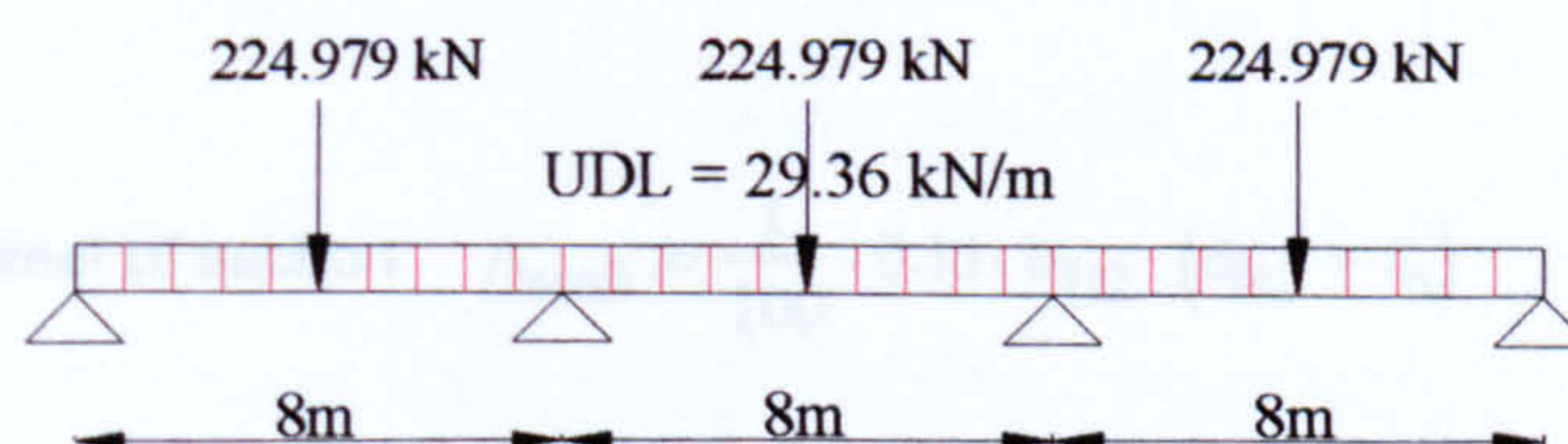
Total load of beam (From distributed load)

$$L_{tB2} := L_{tp2} + UL_{B2}$$

$$L_{tB2} = 234.867\text{ kN}$$

Also there is a concentrated load from beam B3 on beam B2 at every mid - span  $P_{tB2} := \frac{L_{tB3}}{2} \cdot 2$

$$P_{tB2} = 224.979\text{ kN}$$



Details of Beam B2



**4.2 Ultimate Bending Moments And Shear Forces**

The beam sections are treated as beam B3 above

$$W_{\text{eff}} = 1.37 \times 10^3 \text{ mm}$$

From computer program the Max moments and shear forces as follows

max moment at support

$$M1_{b2} := 379.1 \text{ kN} \cdot \text{m}$$

max moment at mid - span

$$M2_{b2} := 305.7 \text{ kN} \cdot \text{m}$$

max shear force

$$FS_{b2} := 229.9 \text{ kN}$$

**4.3 Critical Section At Support**

Assume the diameter of bars used is T16 and 2 layers of bars  $\phi1_{b2} := 16 \text{ mm}$   $\text{cover}_{b2} := 30 \text{ mm}$

$$d2_{ef1} := (d_{B2} + S_t) - \text{cover}_{b2} - \phi1_{b2}$$

$$d2_{ef1} = 654 \text{ mm}$$

$$k1_{b2} := \frac{M1_{b2}}{F_{cu} \cdot b_{B2} \cdot d2_{ef1}^2}$$

$$k1_{b2} = 0.118$$

compression reinforcement is not required

$$z1_{b2} := d2_{ef1} \cdot \left[ 0.5 + \left( 0.25 - \frac{k1_{b2}}{0.9} \right)^{\frac{1}{2}} \right]$$

$$z1_{b2} := \text{if}(z1_{b2} > 0.95d2_{ef1}, 0.95d2_{ef1}, z1_{b2})$$

$$z1_{b2} = 552.307 \text{ mm}$$

$$\text{Minimum area of steel of section } A_{sm3} := \frac{1}{100} \cdot 0.13 \cdot b_{B2} \cdot (d_{B2} + S_t) \quad A_{sm3} = 227.5 \text{ mm}^2$$

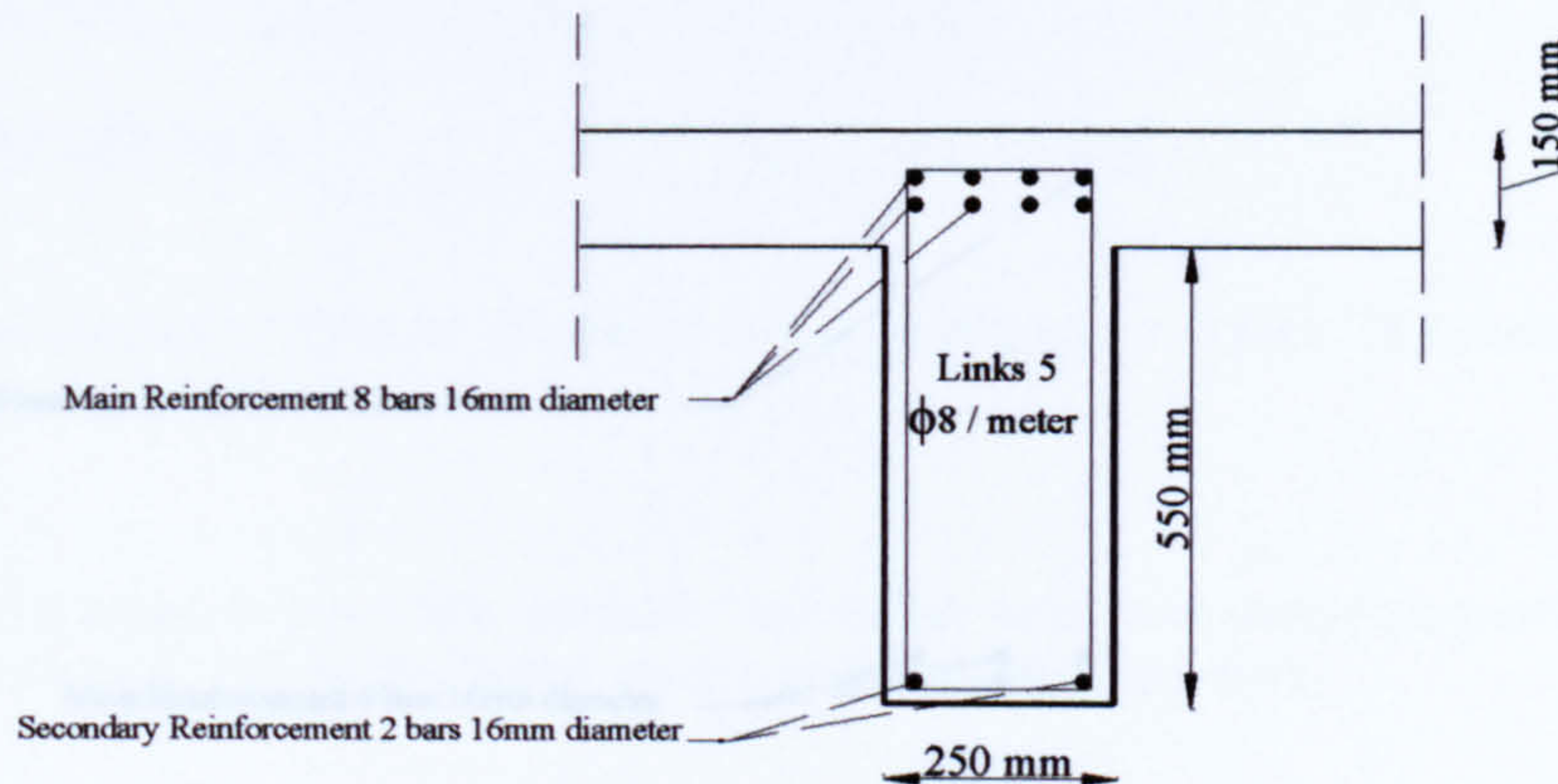
$$A_{s7} := \frac{M1_{b2}}{0.95 \cdot F_y \cdot z1_{b2}}$$

$$A_{s7} := \text{if}(A_{s7} < A_{sm3}, A_{sm3}, A_{s7})$$

$$A_{s7} = 1.571 \times 10^3 \text{ mm}^2$$

8 bars of T16 are arranged in 2 layers with  $\text{area7} := 1608.49 \text{ mm}^2$



**Beam2 section at support****4.4 Critical Section At Mid - Span**

Check of neutral axis  $M_{R1} := 0.45 \cdot F_{cu} \cdot W_{eff} \cdot S_t \cdot \left( d_{efl} - \frac{S_t}{2} \right)$   $M_{R1} = 1.606 \times 10^3 \text{ kN} \cdot \text{m}$

Because the  $M_{R1} > M_{2b2}$  the neutral axis lies in the flange and the section is treated as rectangular section

$k_{b2} := \frac{M_{2b2}}{F_{cu} \cdot W_{eff} \cdot d_{efl}^2}$   $k_{b2} = 0.017$  compression reinforcement is not required

$z_{b2} := d_{efl} \cdot \left[ 0.5 + \left( 0.25 - \frac{k_{b2}}{0.9} \right)^{\frac{1}{2}} \right]$   $z_{b2} := \text{if}(z_{b2} > 0.95d_{efl}, 0.95d_{efl}, z_{b2})$

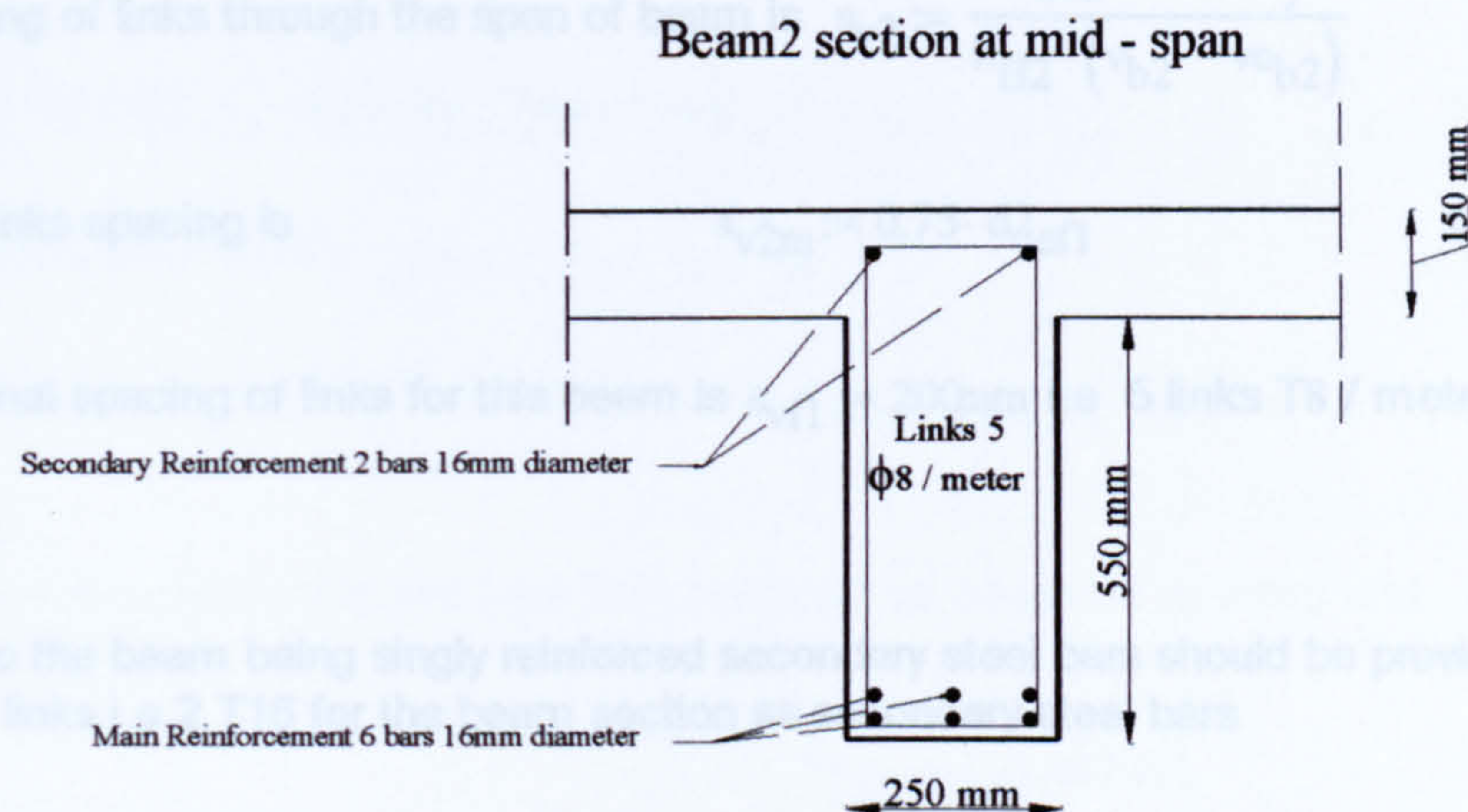
$z_{b2} = 621.3 \text{ mm}$

Minimum area of steel of section  $A_{sm4} := \frac{1}{100} \cdot 0.13 \cdot [(W_{eff} \cdot S_t) + (d_{B2} \cdot b_{B2})]$   $A_{sm4} = 445.9 \text{ mm}^2$

$A_{s8} := \frac{M_{2b2}}{0.95 \cdot F_y \cdot z_{b2}}$   $A_{s8} := \text{if}(A_{s8} < A_{sm4}, A_{sm4}, A_{s8})$   $A_{s8} = 1.126 \times 10^3 \text{ mm}^2$

6 bars of T16 are arranged in 2 layers with  $area8 := 1206.37 \cdot \text{mm}^2$



**4.5 Shear Reinforcement**

Ultimate shear stress  $v_{b2} := \frac{FS_{b2}}{b_{B2} \cdot d_{efl}^2}$   $v_{b2} = 1.406 \text{ N} \cdot \text{mm}^{-2}$

$eqterm1 := \frac{400 \cdot \text{mm}}{d_{efl}^2}$   $eqterm1 := \text{if}(eqterm1 < 1, 1, eqterm1)$   $eqterm1 = 1$

Design concrete shear stress (BS 8110 - 1:1997, Table 3.8)

$$v_{c_{b2}} := \frac{0.79 \cdot \frac{\text{N}}{\text{mm}^2} \cdot \left( \frac{100 \cdot \text{area7}}{b_{B2} \cdot d_{efl}} \right)^{\frac{1}{3}} \cdot (eqterm1)^{\frac{1}{4}} \cdot \left( \frac{F_{cu}}{25 \cdot \frac{\text{N}}{\text{mm}^2}} \right)^{\frac{1}{3}}}{1.25}$$

$v_{c_{b2}} = 0.668 \text{ N} \cdot \text{mm}^{-2}$

From table 3.7 category 3 is required here and choose links only so that T8 is provided for this section

$$\phi_{2_{b2}} := 8\text{mm}$$

Total cross - section area of links at the neutral axis for 2 legs of T8 is  $A_{sv2} := 2 \cdot \frac{\pi \cdot \phi_{2_{b2}}^2}{4}$

$$A_{sv2} = 100.531 \text{ mm}^2$$



Spacing of links through the span of beam is  $s_{v2} := \frac{A_{sv2} \cdot 0.95 \cdot F_y}{b_{B2} \cdot (v_{b2} - v_{c_{b2}})}$   $s_{v2} = 238.001 \text{ mm}$

Max links spacing is  $s_{v2m} := 0.75 \cdot d_{ef1}$   $s_{v2m} = 490.5 \text{ mm}$

The final spacing of links for this beam is  $s_{vf1} := 200 \text{ mm}$  i.e 5 links T8 / meter

**Note:**

Due to the beam being singly reinforced secondary steel bars should be provided to stabilize shear links i.e 2 T16 for the beam section as secondary steel bars.

**4.6 Deflection Check**

service stress  $f_{sb2} := \frac{2 \cdot F_y \cdot A_{s8}}{3 \cdot \text{area8}}$   $f_{sb2} = 286.238 \text{ N} \cdot \text{mm}^{-2}$

Modification Factor  $f_{mb2} := 0.55 + \frac{477 \cdot \frac{\text{N}}{\text{mm}^2} - f_{sb2}}{120 \cdot \left( 0.9 \cdot \frac{\text{N}}{\text{mm}^2} + \frac{M_{2b2}}{b_{B2} \cdot d_{ef1}^2} \right)}$   $f_{mb2} = 0.973$

Allowable span to depth ratio is  $SD_{r2} := 26 \cdot f_{mb2}$   $SD_{r2} = 25.295$

Actual span to depth ratio  $SD_{a2} := \frac{l_{B2}}{d_{ef1}}$   $SD_{a2} = 12.232$

**The beam is satisfactory with respect to deflections**

**5. Design Of Beam B1**

$l_{B1} := 8000 \text{ mm}$

**5.1 Design Loading On Beam B1**

This type of beams is exterior beams of building and carry blockwork wall and one panel of slab

**Max Design Load**

Total Patch load (From slab, BS 8110 - 1:1997, Figure 3.10)  $L_{tp1} := V_{s2} \cdot 0.75 \cdot l_{B1}$   $L_{tp1} = 64.548 \text{ kN}$

Assume the initial dimensions of beam are  $b_{B1} := 250 \text{ mm}$   $d_{B1} := 400 \text{ mm}$



Ultimate self weight of beam  $UL_{B1} := b_{B1} \cdot d_{B1} \cdot l_{B1} \cdot \rho \cdot 1.4$   $UL_{B1} = 26.369 \text{ kN}$

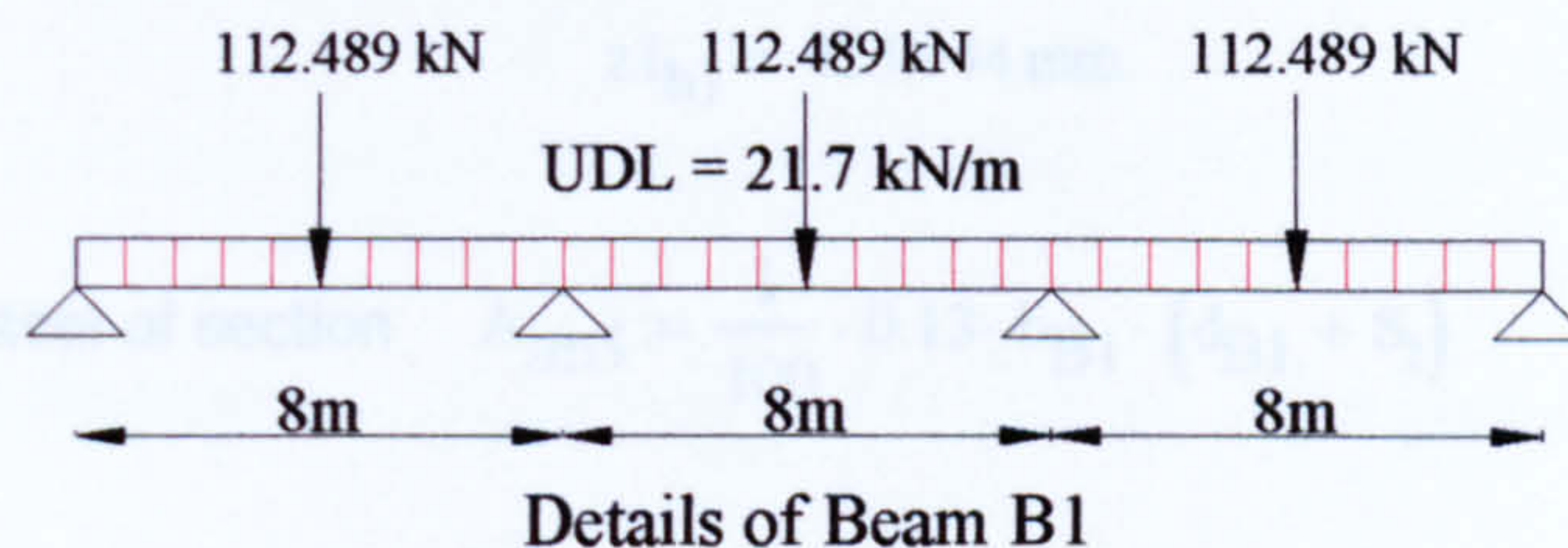
Height of wall  $h_w := h_f - (d_{B1} + S_t)$   $h_w = 2.95 \times 10^3 \text{ mm}$

Ultimate Load of Wall  $UL_w := h_w \cdot l_{B1} \cdot L_w \cdot 1.4$   $UL_w = 82.6 \text{ kN}$

Total load on beam (From distributed load)  $L_{tB1} := L_{tp1} + UL_{B1} + UL_w$   $L_{tB1} = 173.517 \text{ kN}$

Also there is a concentrated load from beam B3 on beam B1 at every mid - span  $P_{tB1} := \frac{L_{tB3}}{2}$

$P_{tB1} = 112.489 \text{ kN}$



## 5.2 Ultimate Bending Moments And Shear Forces

The beam sections are treated as L - beams  $W_{eff1} := 0.7 \cdot \frac{l_{B1}}{10} + b_{B1}$   $W_{eff1} = 810 \text{ mm}$

From computer program the Max moments and shear forces as follows

max moment at support  $M1_{b1} := 229.09 \text{ kN} \cdot \text{m}$

max moment at mid - span  $M2_{b1} := 173.5 \text{ kN} \cdot \text{m}$

max shear force  $FS_{b1} := 145.08 \text{ kN}$



### 5.3 Critical Section At Support

Assume the diameter of bars used is T16 and 2 layers of bars  $\phi_{b1} := 16\text{mm}$   $\text{cover}_{b1} := 30\text{mm}$

$$d_{l_{ef1}} := (d_{B1} + S_t) - \text{cover}_{b1} - \phi_{b1} \quad d_{l_{ef1}} = 504\text{mm}$$

$$k_{l_{b1}} := \frac{M_{l_{b1}}}{F_{cu} \cdot b_{B1} \cdot d_{l_{ef1}}^2} \quad k_{l_{b1}} = 0.12 \quad \text{compression reinforcement is not required}$$

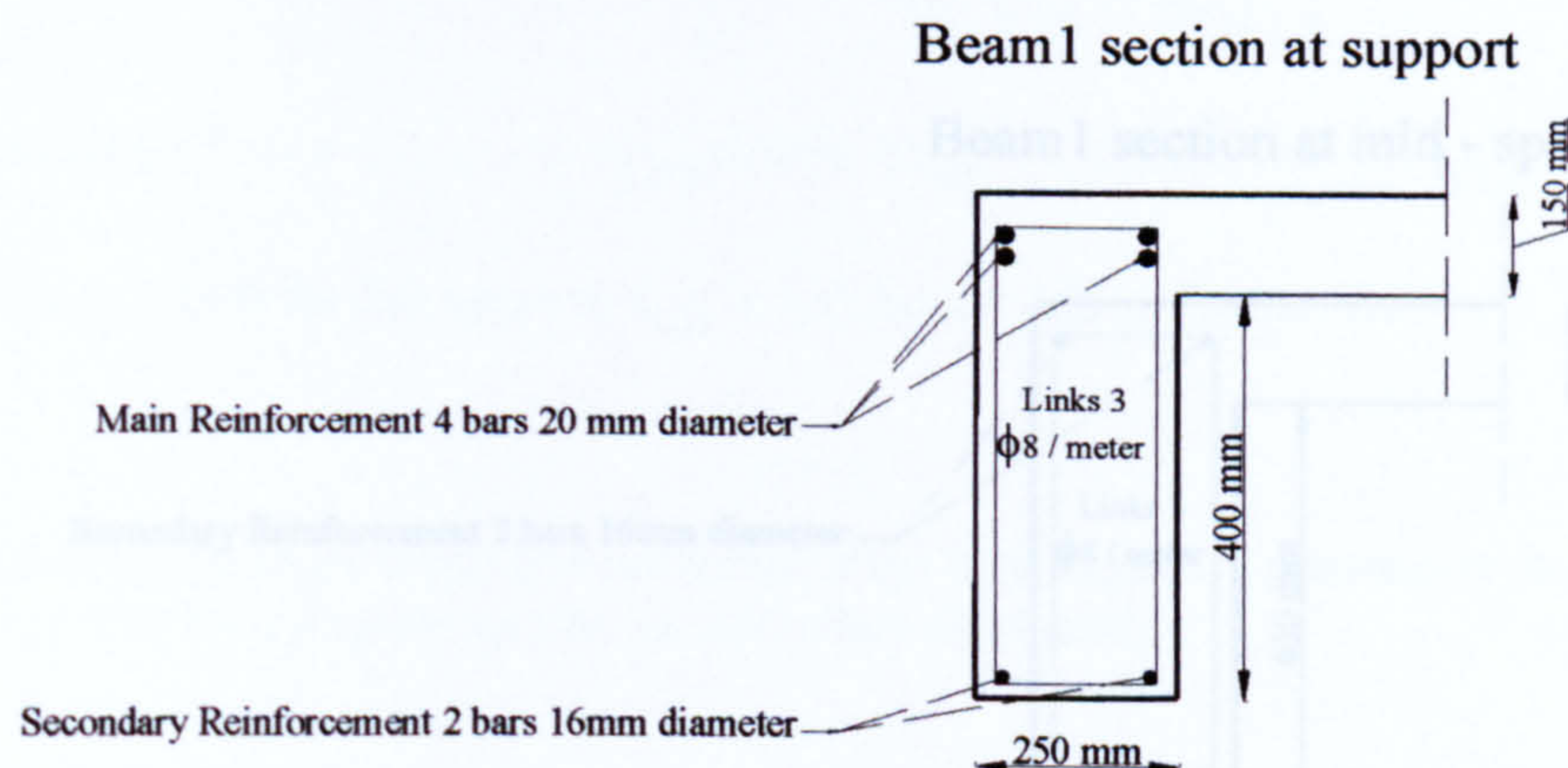
$$z_{l_{b1}} := d_{l_{ef1}} \cdot \left[ 0.5 + \left( 0.25 - \frac{k_{l_{b1}}}{0.9} \right)^{\frac{1}{2}} \right] \quad z_{l_{b1}} := \text{if}(z_{l_{b1}} > 0.95d_{l_{ef1}}, 0.95d_{l_{ef1}}, z_{l_{b1}})$$

$$z_{l_{b1}} = 423.944\text{mm}$$

Minimum area of steel of section  $A_{sm5} := \frac{1}{100} \cdot 0.13 \cdot b_{B1} \cdot (d_{B1} + S_t) \quad A_{sm5} = 178.75\text{mm}^2$

$$A_{s9} := \frac{M_{l_{b1}}}{0.95 \cdot F_y \cdot z_{l_{b1}}} \quad A_{s9} := \text{if}(A_{s9} < A_{sm5}, A_{sm5}, A_{s9}) \quad A_{s9} = 1.237 \times 10^3\text{mm}^2$$

4 bars of T20 are arranged in 2 layers with  $\text{area}_9 := 1256.64\text{mm}^2$





**5.4 Critical Section At Mid - Span**

Check of neutral axis  $M_{r2} := 0.45 \cdot F_{cu} \cdot W_{eff1} \cdot S_t \cdot \left( d_{1efl} - \frac{S_t}{2} \right)$   $M_{r2} = 703.667 \text{ kN} \cdot \text{m}$

Because the  $M_{r2} > M_{2b1}$  the neutral axis lies in the flange and the section is treated as rectangular section

$k_{2b1} := \frac{M_{2b1}}{F_{cu} \cdot W_{eff1} \cdot d_{1efl}^2}$   $k_{2b1} = 0.028$  compression reinforcement is not required

$z_{2b1} := d_{1efl} \cdot \left[ 0.5 + \left( 0.25 - \frac{k_{2b1}}{0.9} \right)^{\frac{1}{2}} \right]$   $z_{2b1} := \text{if}(z_{2b1} > 0.95d_{1efl}, 0.95d_{1efl}, z_{2b1})$

$z_{2b1} = 478.8 \text{ mm}$

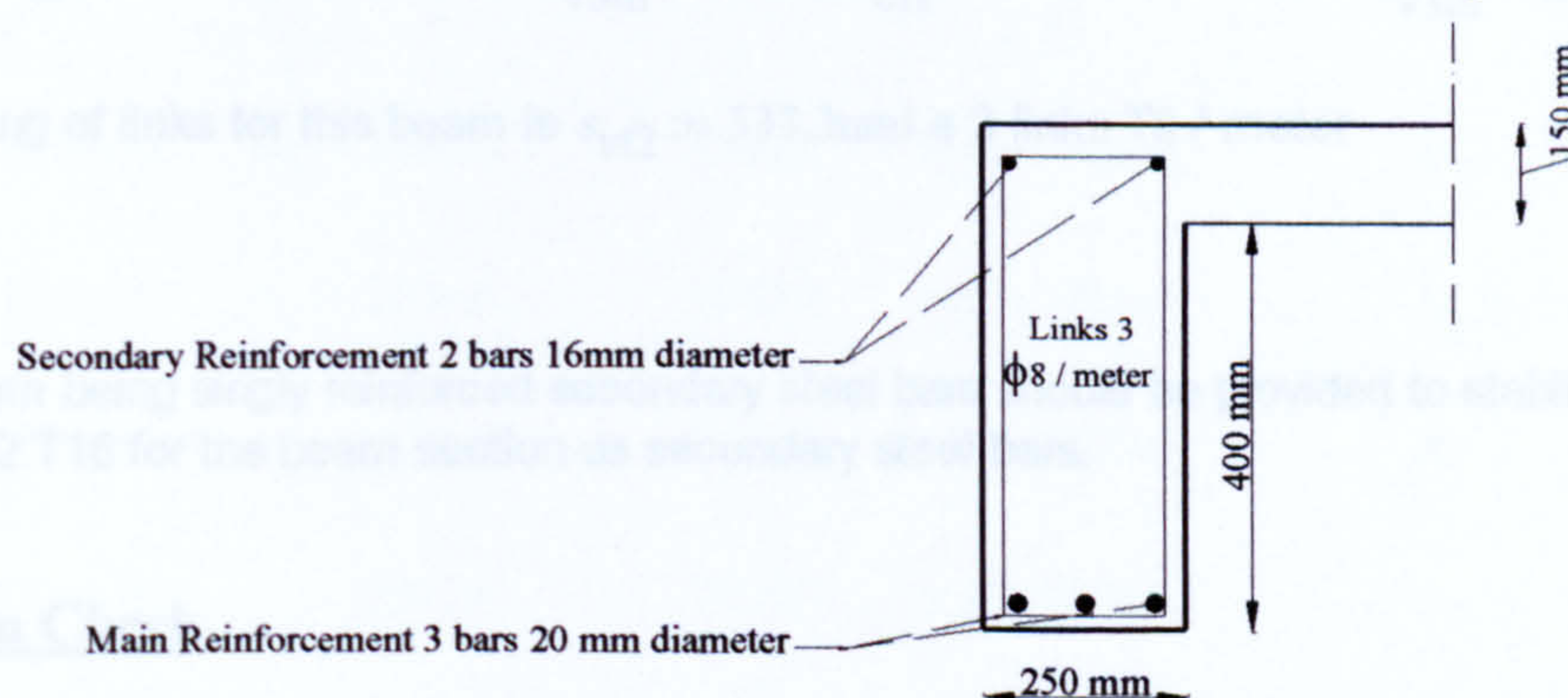
Minimum area of steel of section  $A_{sm6} := \frac{1}{100} \cdot 0.13 \cdot [(W_{eff1} \cdot S_t) + (d_{B1} \cdot b_{B1})]$

$A_{sm6} = 287.95 \text{ mm}^2$

$A_{s10} := \frac{M_{2b1}}{0.95 \cdot F_y \cdot z_{2b1}}$   $A_{s10} := \text{if}(A_{s10} < A_{sm6}, A_{sm6}, A_{s10})$   $A_{s10} = 829.543 \text{ mm}^2$

3 bars of T20 are arranged in 1 layer with  $\text{area}_{10} := 942.48 \cdot \text{mm}^2$

Beam1 section at mid - span





**5.5 Shear Reinforcement**

Ultimate shear stress  $v_{b1} := \frac{FS_{b1}}{b_{B1} \cdot d1_{efl}}$   $v_{b1} = 1.151 \text{ N} \cdot \text{mm}^{-2}$

$eqterm2 := \frac{400 \cdot \text{mm}}{d1_{efl}}$   $eqterm2 := \text{if}(eqterm2 < 1, 1, eqterm2)$   $eqterm2 = 1$

Design concrete shear stress (BS 8110 - 1:1997, Table 3.8)

$$v_{c_{b1}} := \frac{0.79 \cdot \frac{\text{N}}{\text{mm}^2} \cdot \left( \frac{100 \cdot \text{area9}}{b_{B1} \cdot d1_{efl}} \right)^{\frac{1}{3}} \cdot (eqterm2)^{\frac{1}{4}} \cdot \left( \frac{F_{cu}}{25 \cdot \frac{\text{N}}{\text{mm}^2}} \right)^{\frac{1}{3}}}{1.25}$$
 $v_{c_{b1}} = 0.671 \text{ N} \cdot \text{mm}^{-2}$

From table 3.7 category 3 is required here and choose links only so that T8 is provided for this section

$$\phi 2_{b1} := 8 \text{ mm}$$

Total cross - section area of links at the neutral axis for 2 legs of  $\phi 8$  is  $A_{sv3} := 2 \cdot \frac{\pi \cdot \phi 2_{b1}^2}{4}$

$$A_{sv3} = 100.531 \text{ mm}^2$$

Spacing of links through the span of beam is  $s_{v3} := \frac{A_{sv3} \cdot 0.95 \cdot F_y}{b_{B1} \cdot (v_{b1} - v_{c_{b1}})}$   $s_{v3} = 365.776 \text{ mm}$

Max links spacing is  $s_{v3m} := 0.75 \cdot d1_{efl}$   $s_{v3m} = 378 \text{ mm}$

The final spacing of links for this beam is  $s_{vf2} := 333.3 \text{ mm}$ . i.e 3 links T8 / meter

**Note:**

Due to the beam being singly reinforced secondary steel bars should be provided to stabilize shear links i.e 2 T16 for the beam section as secondary steel bars.

**5.6 Deflection Check**

service stress  $fs_{b1} := \frac{2 \cdot F_y \cdot A_{s10}}{3 \cdot \text{area10}}$   $fs_{b1} = 269.919 \text{ N} \cdot \text{mm}^{-2}$



Column 3    Breadth     $b_3 := 350\text{mm}$

$$f_{m_{b1}} := 0.55 + \frac{477 \cdot \frac{N}{\text{mm}^2} - f_{s_{b1}}}{120 \cdot \left( 0.9 \cdot \frac{N}{\text{mm}^2} + \frac{M_{2_{b1}}}{b_{B1} \cdot d_{1_{efl}}^2} \right)}$$

$f_{m_{b1}} = 1.025$

Allowable span to depth ratio is
  $SD_{r3} := 26 \cdot f_{m_{b1}}$ 
 $SD_{r3} = 26.649$

Actual span to depth ratio
  $SD_{a3} := \frac{l_{B1}}{d_{1_{efl}}}$ 
 $SD_{a3} = 15.873$

The beam is satisfactory with respect to deflections

### 6. Design Of Columns For Floors From First To Ninth Floor

From floors plan there are three types of columns: 1- corner columns , 2- facade columns, 3- interior columns. every column is designed according to its type.

#### 6.1 Corner Columns From First To Ninth Floor ( Braced columns)

Clear height of columns in each floor
  $l_0 := h_f - (d_{B1} + S_t)$ 
 $l_0 = 2.95 \times 10^3 \text{ mm}$

From BS8110 - 1(table 3.19), effective height coefficients of columns are
  $\beta := 0.75$

Effective height of columns
  $l_{ex} := l_0 \cdot \beta$ 
 $l_{ey} := l_0 \cdot \beta$

$l_{ex} = 2.213 \times 10^3 \text{ mm}$ 
 $l_{ey} = 2.213 \times 10^3 \text{ mm}$

The assumed dimensions and areas for floors from top to bottom (ninth to first floor) are as follows:

Column 9	Breadth	$b_9 := 250\text{mm}$	Width	$w_9 := 250\text{mm}$	$A_9 := b_9 \cdot w_9$
Column 8	Breadth	$b_8 := 250\text{mm}$	Width	$w_8 := 250\text{mm}$	$A_8 := b_8 \cdot w_8$
Column 7	Breadth	$b_7 := 250\text{mm}$	Width	$w_7 := 250\text{mm}$	$A_7 := b_7 \cdot w_7$
Column 6	Breadth	$b_6 := 300\text{mm}$	Width	$w_6 := 300\text{mm}$	$A_6 := b_6 \cdot w_6$
Column 5	Breadth	$b_5 := 300\text{mm}$	Width	$w_5 := 300\text{mm}$	$A_5 := b_5 \cdot w_5$
Column 4	Breadth	$b_4 := 300\text{mm}$	Width	$w_4 := 300\text{mm}$	$A_4 := b_4 \cdot w_4$



Column 3      Breadth       $b_3 := 350\text{mm}$       Width       $w_3 := 350\text{mm}$        $A_3 := b_3 \cdot w_3$

Column 2      Breadth       $b_2 := 350\text{mm}$       Width       $w_2 := 350\text{mm}$        $A_2 := b_2 \cdot w_2$

Column 1      Breadth       $b_1 := 350\text{mm}$       Width       $w_1 := 350\text{mm}$        $A_1 := b_1 \cdot w_1$

$$A_9 = 6.25 \times 10^4 \text{ mm}^2$$

$$A_8 = 6.25 \times 10^4 \text{ mm}^2$$

$$A_7 = 6.25 \times 10^4 \text{ mm}^2$$

$$A_6 = 9 \times 10^4 \text{ mm}^2$$

$$A_5 = 9 \times 10^4 \text{ mm}^2$$

$$A_4 = 9 \times 10^4 \text{ mm}^2$$

$$A_3 = 1.225 \times 10^5 \text{ mm}^2$$

$$A_2 = 1.225 \times 10^5 \text{ mm}^2$$

$$A_1 = 1.225 \times 10^5 \text{ mm}^2$$

#### Check of column type ( short - slender)

$$r_x := \frac{l_{ex}}{w_9}$$

$$r_y := \frac{l_{ey}}{b_9}$$

$$r_x = 8.85$$

$$r_y = 8.85$$

Then the columns are short columns because  $r_x$  and  $r_y < 15$  for these braced columns and this check for first column is enough for all columns which its dimensions increase.

#### Design Loading for Columns

From BS 6399 - 1, 1996 (Loading for buildings) there are reduction factors for distributed imposed floor loads (including partitions loads) differing in values according to number of floors in building. From that the ultimate load of floor per unit area should be recalculated as follows:

For ninth to forth floor       $ULL_{4.9} := ULL \cdot 0.6$

$$ULL_{4.9} = 38.4 \text{ kN}$$

$$n_{4.9} := \frac{UDL + ULL_{4.9}}{L_x \cdot L_y}$$

$$n_{4.9} = 8.744 \text{ kN} \cdot \text{m}^{-2}$$

For third floor       $ULL_3 := ULL \cdot 0.7$

$$ULL_3 = 44.8 \text{ kN}$$

$$n_3 := \frac{UDL + ULL_3}{L_x \cdot L_y}$$

$$n_3 = 9.144 \text{ kN} \cdot \text{m}^{-2}$$

For second floor       $ULL_2 := ULL \cdot 0.8$

$$ULL_2 = 51.2 \text{ kN}$$

$$n_2 := \frac{UDL + ULL_2}{L_x \cdot L_y}$$

$$n_2 = 9.544 \text{ kN} \cdot \text{m}^{-2}$$

For first floor       $ULL_1 := ULL \cdot 0.9$

$$ULL_1 = 57.6 \text{ kN}$$



$$n_1 := \frac{UDL + ULL_1}{L_x \cdot L_y}$$

$$n_1 = 9.944 \text{ kN} \cdot \text{m}^{-2}$$

The area of floor that this column type carries  $A_f := 4.125 \cdot \text{m} \cdot 4.125 \cdot \text{m}$

$$A_f = 1.702 \times 10^7 \text{ mm}^2$$

Load from slab on every column for ninth to forth floor  $LC_{s4.9} := n_{4.9} \cdot A_f$

$$LC_{s4.9} = 148.789 \text{ kN}$$

Load from slab on column of third floor

$$LC_{s3} := n_3 \cdot A_f$$

$$LC_{s3} = 155.595 \text{ kN}$$

Load from slab on column of second floor

$$LC_{s2} := n_2 \cdot A_f$$

$$LC_{s2} = 162.401 \text{ kN}$$

Load from slab on column of first floor

$$LC_{s1} := n_1 \cdot A_f$$

$$LC_{s1} = 169.207 \text{ kN}$$

Loads from beam B3 on every column for ninth to first floor

$$LC_{B3} = 12.773 \text{ kN}$$

$$LC_{B3} := d_{B3} \cdot b_{B3} \cdot \left( \frac{l_{B3}}{2} - \frac{b_{B1}}{2} \right) \cdot \rho \cdot 1.4$$

Loads from beam B1 on every column for ninth to first floor

$$LC_{B1} = 26.369 \text{ kN}$$

$$LC_{B1} := d_{B1} \cdot b_{B1} \cdot l_{B1} \cdot \rho \cdot 1.4$$

Loads from walls on every column for ninth to first floor  $LC_w := l_{B1} \cdot l_0 \cdot L_w \cdot 1.4$

$$LC_w = 82.6 \text{ kN}$$

Tota axial loads on every column except self weight for ninth to fourth floor  $LC_{4.9} := LC_{s4.9} + LC_{B3} + LC_{B1} + LC_w$

$$LC_{4.9} = 270.531 \text{ kN}$$

Tota axial loads on every column except self weight for third floor

$$LC_3 = 277.337 \text{ kN}$$

$$LC_3 := LC_{s3} + LC_{B3} + LC_{B1} + LC_w$$

Tota axial loads on every column except self weight for second floor

$$LC_2 = 284.143 \text{ kN}$$

$$LC_2 := LC_{s2} + LC_{B3} + LC_{B1} + LC_w$$

Tota axial loads on every column except self weight for first floor

$$LC_1 = 290.949 \text{ kN}$$

$$LC_1 := LC_{s1} + LC_{B3} + LC_{B1} + LC_w$$

**Self weight of each column from ninth to first floor**

$$L_{c9} := A_9 \cdot l_0 \cdot \rho \cdot 1.4$$

$$L_{c9} = 6.077 \text{ kN}$$

$$L_{c8} := A_8 \cdot l_0 \cdot \rho \cdot 1.4$$

$$L_{c8} = 6.077 \text{ kN}$$

$$L_{c7} := A_7 \cdot l_0 \cdot \rho \cdot 1.4$$

$$L_{c7} = 6.077 \text{ kN}$$

$$L_{c6} := A_6 \cdot l_0 \cdot \rho \cdot 1.4$$

$$L_{c6} = 8.751 \text{ kN}$$

$$L_{c5} := A_5 \cdot l_0 \cdot \rho \cdot 1.4$$

$$L_{c5} = 8.751 \text{ kN}$$



$$L_{c4} := A_4 \cdot l_0 \cdot \rho \cdot 1.4$$

$$L_{c4} = 8.751 \text{ kN}$$

$$L_{c3} := A_3 \cdot l_0 \cdot \rho \cdot 1.4$$

$$L_{c3} = 11.911 \text{ kN}$$

$$L_{c2} := A_2 \cdot l_0 \cdot \rho \cdot 1.4$$

$$L_{c2} = 11.911 \text{ kN}$$

$$L_{c1} := A_1 \cdot l_0 \cdot \rho \cdot 1.4$$

$$L_{c1} = 11.911 \text{ kN}$$

All columns are designed as axially loaded and to compensate for the effect of eccentricities, the ultimate load from the floor immediately above the column is multiplied by factor 2.0. (Manual for the design of reinforced concrete building structures, the institution of structural engineers).

### Design of column C9

Total axial load of column

$$N_9 := LC_{4.9} \cdot 2 + L_{c9}$$

$$N_9 = 547.139 \text{ kN}$$

Vertical steel bars of column

$$A_{sc9} := \frac{N_9 - 0.35 \cdot F_{cu} \cdot A_9}{0.7 \cdot F_y - 0.35 \cdot F_{cu}}$$

$$A_{sc9} = -350.278 \text{ mm}^2$$

The result means that the load is very small so that the area of steel will be the allowable minimum percentage of reinforcement for the column

$$\text{4 bars of T12 with area } area_{c9} := 452.39 \text{ mm}^2$$

Check of minimum and maximum steel bars area of column such that the minimum is  $r = 0.4\%$  and maximum =  $6\%$

$$r_{c9} := \frac{area_{c9}}{A_9} \cdot 100$$

$$r_{c9} = 0.724$$

(Acceptable ratio)

Links diameter for column less than 6mm and the links diameter for this column is

$$\phi_{c9} := 0.25 \cdot 12 \text{ mm}$$

$$\phi_{c9} = 3 \text{ mm}$$

So that the links diameter of this column is 6mm (T6)

Max spacing for links is

$$s_{c9} := 12 \cdot 12 \text{ mm}$$

$$s_{c9} = 144 \text{ mm}$$

So that the used spacing for this column links is 125 mm i.e 8 T6 / meter

### Design of column C8

Total axial load of column

$$N_8 := LC_{4.9} + L_{c9} + LC_{4.9} \cdot 2 + L_{c8}$$

$$N_8 = 823.746 \text{ kN}$$



Vertical steel bars of column  $A_{sc8} := \frac{N_8 - 0.35 \cdot F_{cu} \cdot A_8}{0.7 \cdot F_y - 0.35 \cdot F_{cu}}$   $A_{sc8} = 537.709 \text{ mm}^2$

4 bars of T16 with area  $area_{c8} := 804.28 \text{ mm}^2$

Check of minimum and maximum steel bars area of column such that the minimum is  $r = 0.4\%$  and maximum =  $6\%$

$r_{c8} := \frac{area_{c8}}{A_8} \cdot 100$   $r_{c8} = 1.287$  (Acceptable ratio)

Links diamete for column less than 6mm and the links diameter for this column is

$\phi_{c8} := 0.25 \cdot 16 \text{ mm}$   $\phi_{c8} = 4 \text{ mm}$

So that the links diameter of this column is 6mm (T6)

Max spacing for links is  $s_{c8} := 12 \cdot 16 \text{ mm}$   $s_{c8} = 192 \text{ mm}$

So that the used spacing for this column links is 175 mm i.e 5.5 T6 / meter

### Design of column C7

Total axial load of column  $N_7 := LC_{4.9} \cdot 2 + L_{c9} + L_{c8} + LC_{4.9} \cdot 2 + L_{c7}$   $N_7 = 1.1 \times 10^3 \text{ kN}$

Vertical steel bars of column  $A_{sc7} := \frac{N_7 - 0.35 \cdot F_{cu} \cdot A_7}{0.7 \cdot F_y - 0.35 \cdot F_{cu}}$   $A_{sc7} = 1.426 \times 10^3 \text{ mm}^2$

4 bars of T20 + 4 bars of T12 with area  $area_{c7} := 1709.03 \text{ mm}^2$

Check of minimum and maximum steel bars area of column such that the minimum is  $r = 0.4\%$  and maximum =  $6\%$

$r_{c7} := \frac{area_{c7}}{A_7} \cdot 100$   $r_{c7} = 2.734$  (Acceptable ratio)

Links diamete for column less than 6mm and the links diameter for this column is

$\phi_{c7} := 0.25 \cdot 20 \text{ mm}$   $\phi_{c7} = 5 \text{ mm}$

So that the links diameter of this column is 6mm (T6)



Max spacing for links is  $s_{c7} := 12 \cdot 12\text{mm}$ 

$s_{c7} = 144\text{mm}$

So that the used spacing for this column links is 125 mm i.e 8 T6 / meter

**Design of column C6**Total axial load of column  $N_6 := LC_{4.9} \cdot 3 + L_{c9} + L_{c8} + L_{c7} + LC_{4.9} \cdot 2 + L_{c6}$ 

$$N_6 = 1.38 \times 10^3 \text{ kN}$$

Vertical steel bars of column  $A_{sc6} := \frac{N_6 - 0.35 \cdot F_{cu} \cdot A_6}{0.7 \cdot F_y - 0.35 \cdot F_{cu}}$ 

$$A_{sc6} = 1.395 \times 10^3 \text{ mm}^2$$

8 bars T16 with area  $area_{c6} := 1608.49 \text{ mm}^2$ 

$$r_{c6} := \frac{area_{c6}}{A_6} \cdot 100$$

$$r_{c6} = 1.787$$

(Acceptable ratio)

$$\phi_{c6} := 0.25 \cdot 16\text{mm}$$

$$\phi_{c6} = 4\text{mm}$$

So that the links diameter of this column is 6mm (T6)

Max spacing for links is  $s_{c6} := 12 \cdot 16\text{mm}$ 

$s_{c6} = 192\text{mm}$

So that the used spacing for this column links is 175 mm i.e 5.5 T6 / meter

**Design of column C5**Total axial load of column  $N_5 := LC_{4.9} \cdot 4 + L_{c9} + L_{c8} + L_{c7} + L_{c6} + LC_{4.9} \cdot 2 + L_{c5}$ 

$$N_5 = 1.659 \times 10^3 \text{ kN}$$

Vertical steel bars of column  $A_{sc5} := \frac{N_5 - 0.35 \cdot F_{cu} \cdot A_5}{0.7 \cdot F_y - 0.35 \cdot F_{cu}}$ 

$$A_{sc5} = 2.292 \times 10^3 \text{ mm}^2$$

8 bars  $\phi 20$  with area  $area_{c5} := 2513.27 \text{ mm}^2$ 

$$r_{c5} := \frac{area_{c5}}{A_5} \cdot 100$$

$$r_{c5} = 2.793$$

(Acceptable ratio)



The links diameter of this column is 6mm (T6)

The used spacing for this column links is 200 mm i.e 5 T6 / meter

### Design of column C4

Total axial load of column  $N_4 := LC_{4.9} \cdot 5 + L_{c9} + L_{c8} + L_{c7} + L_{c6} + L_{c5} + LC_{4.9} \cdot 2 + L_{c4}$

$$N_4 = 1.938 \times 10^3 \text{ kN}$$

Vertical steel bars of column  $A_{sc4} := \frac{N_4 - 0.35 \cdot F_{cu} \cdot A_4}{0.7 \cdot F_y - 0.35 \cdot F_{cu}}$   $A_{sc4} = 3.188 \times 10^3 \text{ mm}^2$

4 bars T25 + 4 bars T20 with area  $area_{c4} := 3220.13 \text{ mm}^2$

$$r_{c4} := \frac{area_{c4}}{A_4} \cdot 100 \quad r_{c4} = 3.578 \quad (\text{Acceptable ratio})$$

The links diameter of this column is 8mm (T8)

The used spacing for this column links is 200 mm i.e 5 T8 / meter

### Design of column C3

Total axial load of column  $N_3 := LC_{4.9} \cdot 6 + L_{c9} + L_{c8} + L_{c7} + L_{c6} + L_{c5} + L_{c4} + LC_3 \cdot 2 + L_{c3}$

$$N_3 = 2.234 \times 10^3 \text{ kN}$$

Vertical steel bars of column  $A_{sc3} := \frac{N_3 - 0.35 \cdot F_{cu} \cdot A_3}{0.7 \cdot F_y - 0.35 \cdot F_{cu}}$   $A_{sc3} = 3.043 \times 10^3 \text{ mm}^2$

4 bars T25 + 4 bars T20 with area  $area_{c3} := 3220.13 \text{ mm}^2$

$$r_{c3} := \frac{area_{c3}}{A_3} \cdot 100 \quad r_{c3} = 2.629 \quad (\text{Acceptable ratio})$$

The links diameter of this column is 8mm (T8)

The used spacing for this column links is 250 mm i.e 4 T8 / meter



**Design of column C2**

Total axial load of column

$$N_2 := N_3 - LC_3 + LC_2 \cdot 2 + L_{c2}$$

$$N_2 = 2.537 \times 10^3 \text{ kN}$$

Vertical steel bars of column

$$A_{sc2} := \frac{N_2 - 0.35 \cdot F_{cu} \cdot A_2}{0.7 \cdot F_y - 0.35 \cdot F_{cu}}$$

$$A_{sc2} = 4.016 \times 10^3 \text{ mm}^2$$

4 bars T32 + 4 bars T16 with area

$$area_{c2} := 4021.24 \text{ mm}^2$$

$$r_{c2} := \frac{area_{c2}}{A_2} \cdot 100$$

$$r_{c2} = 3.283$$

(Acceptable ratio)

The links diameter of this column is 8mm (T8)

The used spacing for this column links is 175 mm i.e 5.5 T8 / meter

**Design of column C1**

Total axial load of column

$$N_1 := N_2 - LC_2 + LC_1 \cdot 2 + L_{c1}$$

$$N_1 = 2.847 \times 10^3 \text{ kN}$$

Vertical steel bars of column

$$A_{sc1} := \frac{N_1 - 0.35 \cdot F_{cu} \cdot A_1}{0.7 \cdot F_y - 0.35 \cdot F_{cu}}$$

$$A_{sc1} = 5.01 \times 10^3 \text{ mm}^2$$

4 bars T32 + 4 bars T25 with area

$$area_{c1} := 5180.48 \text{ mm}^2$$

$$r_{c1} := \frac{area_{c1}}{A_1} \cdot 100$$

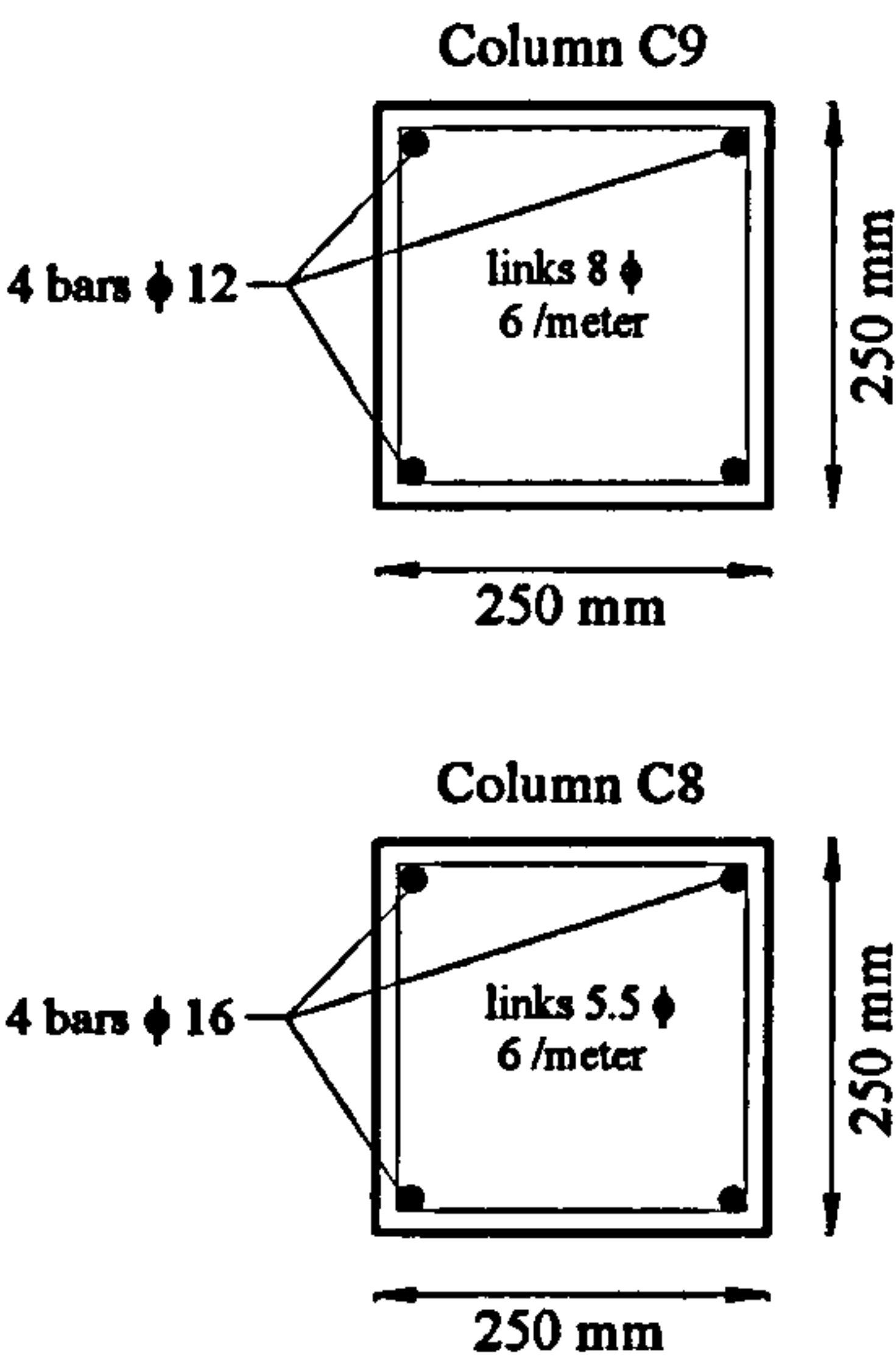
$$r_{c1} = 4.229$$

(Acceptable ratio)

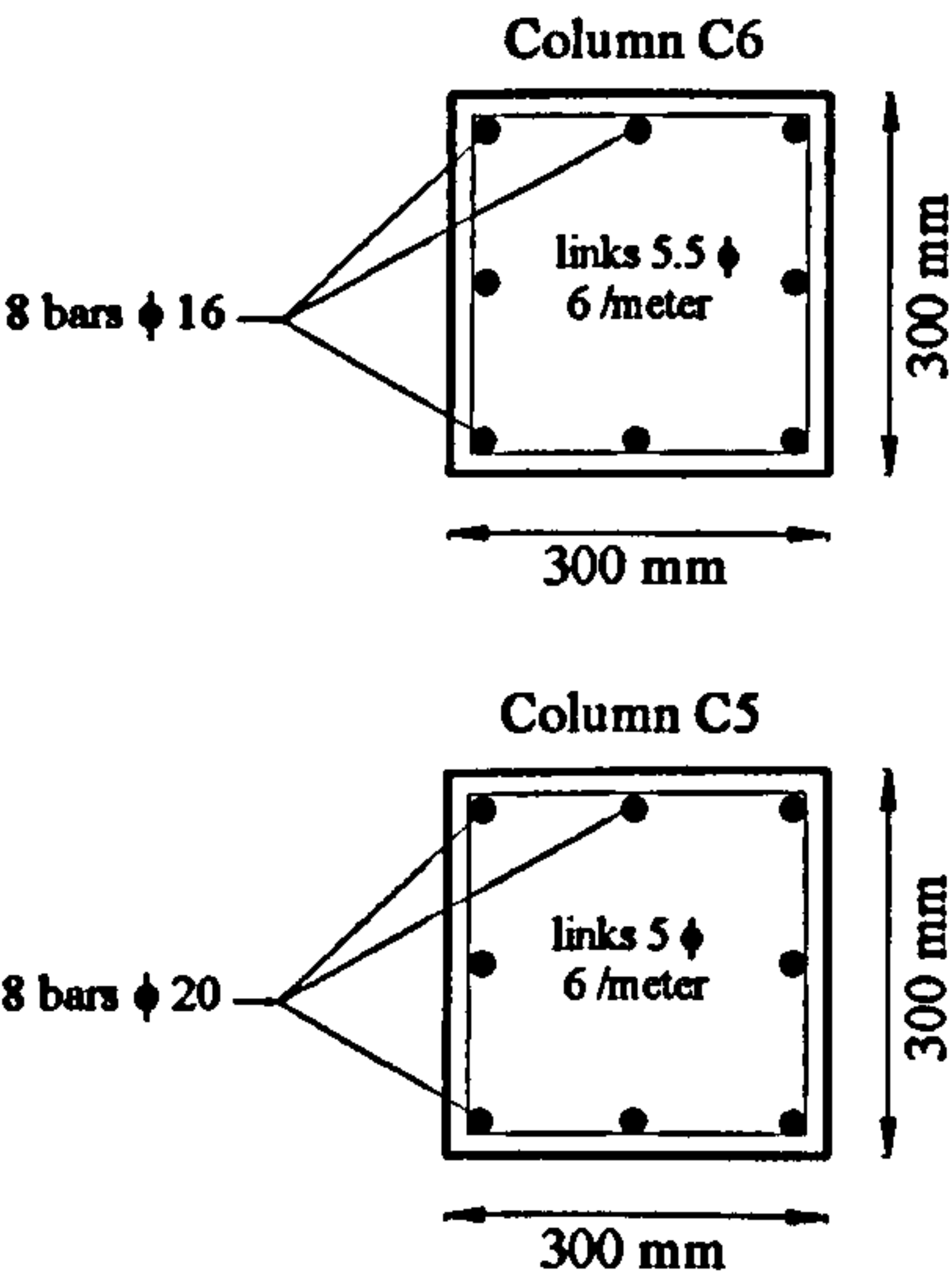
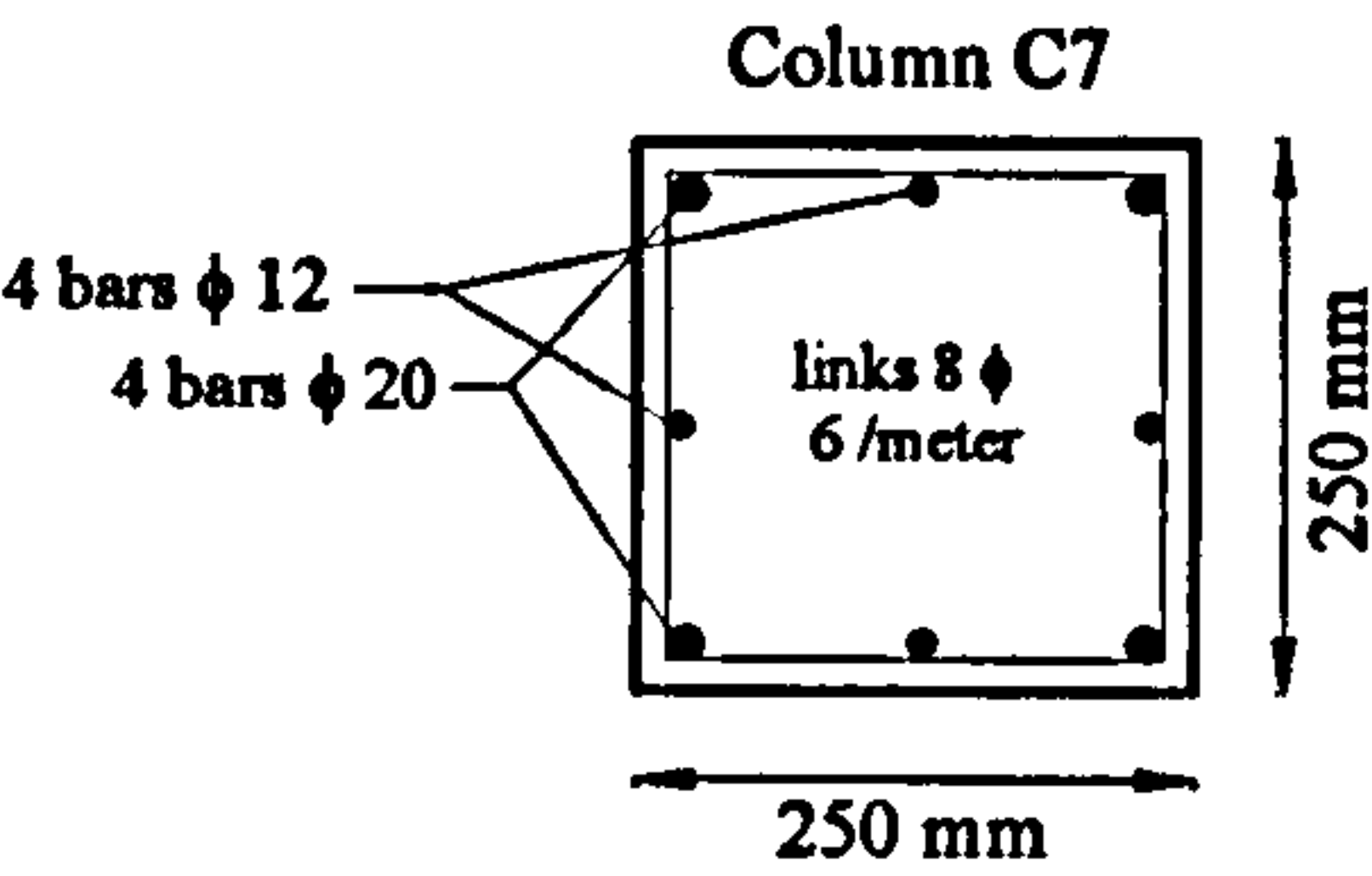
The links diameter of this column is 8mm (T8)

The used spacing for this column links is 250 mm i.e 4 T8 / meter

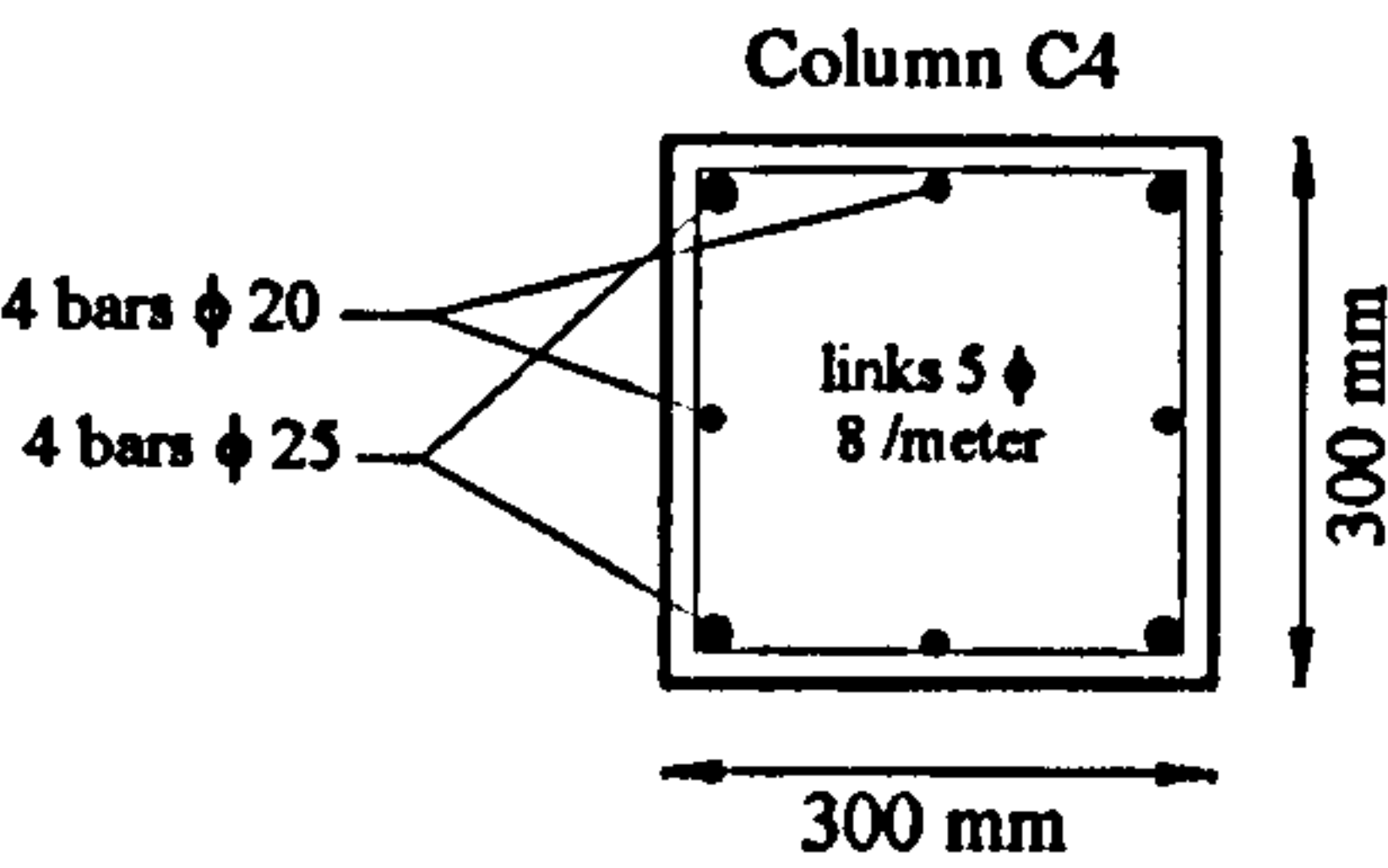




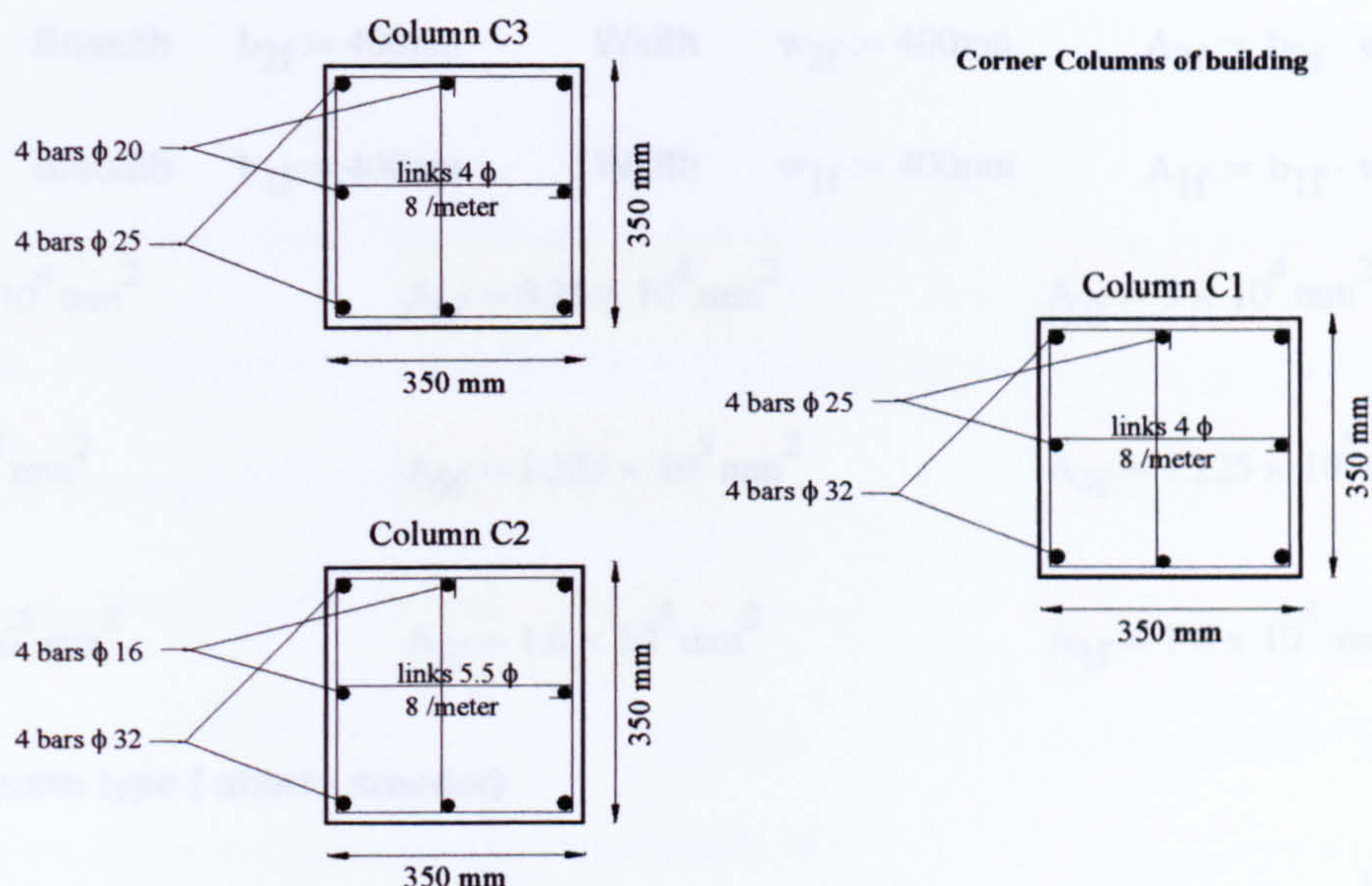
Corner Columns of building



Corner Columns of building







## 6.2 Facade Columns From First to Ninth Floor ( braced columns)

Clear height of columns in each floor  $l_0 := h_f - (d_{B1} + S_t)$   $l_0 = 2.95 \times 10^3 \text{ mm}$

From BS8110 - 1(table 3.19), effective height coefficients of columns are  $\beta := 0.75$

Effective height of columns  $l_{ex} := l_0 \cdot \beta$   $l_{ey} := l_0 \cdot \beta$

$$l_{ex} = 2.213 \times 10^3 \text{ mm}$$

$$l_{ey} = 2.213 \times 10^3 \text{ mm}$$

The assumed dimensions and areas for floors from top to bottom (ninth to first floor) are as follows:

Column 9f	Breadth	$b_{9f} := 250\text{mm}$	Width	$w_{9f} := 250\text{mm}$	$A_{9f} := b_{9f} \cdot w_{9f}$
Column 8f	Breadth	$b_{8f} := 250\text{mm}$	Width	$w_{8f} := 250\text{mm}$	$A_{8f} := b_{8f} \cdot w_{8f}$
Column 7f	Breadth	$b_{7f} := 300\text{mm}$	Width	$w_{7f} := 300\text{mm}$	$A_{7f} := b_{7f} \cdot w_{7f}$
Column 6f	Breadth	$b_{6f} := 300\text{mm}$	Width	$w_{6f} := 300\text{mm}$	$A_{6f} := b_{6f} \cdot w_{6f}$
Column 5f	Breadth	$b_{5f} := 350\text{mm}$	Width	$w_{5f} := 350\text{mm}$	$A_{5f} := b_{5f} \cdot w_{5f}$
Column 4f	Breadth	$b_{4f} := 350\text{mm}$	Width	$w_{4f} := 350\text{mm}$	$A_{4f} := b_{4f} \cdot w_{4f}$
Column 3f	Breadth	$b_{3f} := 400\text{mm}$	Width	$w_{3f} := 400\text{mm}$	$A_{3f} := b_{3f} \cdot w_{3f}$



Column 2f	Breadth	$b_{2f} := 400\text{mm}$	Width	$w_{2f} := 400\text{mm}$	$A_{2f} := b_{2f} \cdot w_{2f}$
-----------	---------	--------------------------	-------	--------------------------	---------------------------------

Column 1f	Breadth	$b_{1f} := 400\text{mm}$	Width	$w_{1f} := 400\text{mm}$	$A_{1f} := b_{1f} \cdot w_{1f}$
-----------	---------	--------------------------	-------	--------------------------	---------------------------------

$$A_{9f} = 6.25 \times 10^4 \text{ mm}^2$$

$$A_{8f} = 6.25 \times 10^4 \text{ mm}^2$$

$$A_{7f} = 9 \times 10^4 \text{ mm}^2$$

$$A_{6f} = 9 \times 10^4 \text{ mm}^2$$

$$A_{5f} = 1.225 \times 10^5 \text{ mm}^2$$

$$A_{4f} = 1.225 \times 10^5 \text{ mm}^2$$

$$A_{3f} = 1.6 \times 10^5 \text{ mm}^2$$

$$A_{2f} = 1.6 \times 10^5 \text{ mm}^2$$

$$A_{1f} = 1.6 \times 10^5 \text{ mm}^2$$

### Check of column type ( short - slender)

$$r_{xf} := \frac{l_{ex}}{w_{9f}}$$

$$r_{yf} := \frac{l_{ey}}{b_{9f}}$$

$$r_{xf} = 8.85$$

$$r_{yf} = 8.85$$

Then the columns are short columns because  $r_x$  and  $r_y < 15$  for these braced columns and this check for first column is enough for all columns which its dimensions increase.

### Design Loading for Columns

From BS 6399 - 1, 1996 (Loading for buildings) there are reduction factors for distributed imposed floor loads (including partitions loads) differ in values according to number of floors in building. from that the ultimate load of floor per unit area should be recalculated as follows:

For ninth to forth floor	$ULL_{4.9} := ULL \cdot 0.6$	$ULL_{4.9} = 38.4 \text{ kN}$
--------------------------	------------------------------	-------------------------------

$$n_{4.9} := \frac{UDL + ULL_{4.9}}{L_x \cdot L_y}$$

$$n_{4.9} = 8.744 \text{ kN} \cdot \text{m}^{-2}$$

For third floor	$ULL_3 := ULL \cdot 0.7$
-----------------	--------------------------

$$ULL_3 = 44.8 \text{ kN}$$

$$n_3 := \frac{UDL + ULL_3}{L_x \cdot L_y}$$

$$n_3 = 9.144 \text{ kN} \cdot \text{m}^{-2}$$

For second floor	$ULL_2 := ULL \cdot 0.8$
------------------	--------------------------

$$ULL_2 = 51.2 \text{ kN}$$

$$n_2 := \frac{UDL + ULL_2}{L_x \cdot L_y}$$

$$n_2 = 9.544 \text{ kN} \cdot \text{m}^{-2}$$

For first floor	$ULL_1 := ULL \cdot 0.9$
-----------------	--------------------------

$$ULL_1 = 57.6 \text{ kN}$$



$$n_1 := \frac{\text{UDL} + \text{ULL}_1}{L_x \cdot L_y}$$

$$n_1 = 9.944 \text{ kN} \cdot \text{m}^{-2}$$

The area of floor that this column type carries  $A_{ff} := 8 \cdot \text{m} \cdot 4.125 \cdot \text{m}$

$$A_{ff} = 3.3 \times 10^7 \text{ mm}^2$$

Load form slab on every column for ninth to forth floor  $LC_{s4.9f} := n_{4.9} \cdot A_{ff}$

$$LC_{s4.9f} = 288.56 \text{ kN}$$

Load form slab on column of third floor  $LC_{s3f} := n_3 \cdot A_{ff}$

$$LC_{s3f} = 301.76 \text{ kN}$$

Load form slab on column of second floor  $LC_{s2f} := n_2 \cdot A_{ff}$

$$LC_{s2f} = 314.96 \text{ kN}$$

Load form slab on column of first floor  $LC_{s1f} := n_1 \cdot A_{ff}$

$$LC_{s1f} = 328.16 \text{ kN}$$

Loads from beam B3 on every column for ninth to first floor

$$LC_{B3f} = 25.545 \text{ kN}$$

$$LC_{B3f} := d_{B3} \cdot b_{B3} \cdot (l_{B3} - b_{B1}) \cdot \rho \cdot 1.4$$

Loads from beam B2 on every column for ninth to first floor

$$LC_{B2f} = 17.562 \text{ kN}$$

$$LC_{B2f} := d_{B2} \cdot b_{B2} \cdot \left( \frac{l_{B2}}{2} - \frac{b_{B1}}{2} \right) \cdot \rho \cdot 1.4$$

Loads from beam B1 on every column for ninth to first floor

$$LC_{B1f} = 26.369 \text{ kN}$$

$$LC_{B1f} := d_{B1} \cdot b_{B1} \cdot l_{B1} \cdot \rho \cdot 1.4$$

Loads from walls on every column for ninth to first floor  $LC_{wf} := l_{B1} \cdot l_0 \cdot L_w \cdot 1.4$

$$LC_{wf} = 82.6 \text{ kN}$$

Tota axial loads on every column except self weight for ninth to fourth floor  $LC_{4.9f} := LC_{s4.9f} + LC_{B3f} + LC_{B2f} + LC_{B1f} + LC_{wf}$

$$LC_{4.9f} = 440.637 \text{ kN}$$

Tota axial loads on every column except self weight for third floor

$$LC_{3f} = 453.837 \text{ kN}$$

$$LC_{3f} := LC_{s3f} + LC_{B3f} + LC_{B2f} + LC_{B1f} + LC_{wf}$$

Tota axial loads on every column except self weight for second floor

$$LC_{2f} = 467.037 \text{ kN}$$

$$LC_{2f} := LC_{s2f} + LC_{B3f} + LC_{B2f} + LC_{B1f} + LC_{wf}$$

Tota axial loads on every column except self weight for first floor

$$LC_{1f} = 480.237 \text{ kN}$$

$$LC_{1f} := LC_{s1f} + LC_{B3f} + LC_{B2f} + LC_{B1f} + LC_{wf}$$

**Self weight of each column from ninth to first floor**

$$L_{c9f} := A_{9f} \cdot l_0 \cdot \rho \cdot 1.4$$

$$L_{c9f} = 6.077 \text{ kN}$$

$$L_{c8f} := A_{8f} \cdot l_0 \cdot \rho \cdot 1.4$$

$$L_{c8f} = 6.077 \text{ kN}$$

$$L_{c7f} := A_{7f} \cdot l_0 \cdot \rho \cdot 1.4$$

$$L_{c7f} = 8.751 \text{ kN}$$

$$L_{c6f} := A_{6f} \cdot l_0 \cdot \rho \cdot 1.4$$

$$L_{c6f} = 8.751 \text{ kN}$$



$$L_{c5f} := A_{5f} \cdot l_0 \cdot \rho \cdot 1.4$$

$$L_{c5f} = 11.911 \text{ kN}$$

$$L_{c4f} := A_{4f} \cdot l_0 \cdot \rho \cdot 1.4$$

$$L_{c4f} = 11.911 \text{ kN}$$

$$L_{c3f} := A_{3f} \cdot l_0 \cdot \rho \cdot 1.4$$

$$L_{c3f} = 15.558 \text{ kN}$$

$$L_{c2f} := A_{2f} \cdot l_0 \cdot \rho \cdot 1.4$$

$$L_{c2f} = 15.558 \text{ kN}$$

$$L_{c1f} := A_{1f} \cdot l_0 \cdot \rho \cdot 1.4$$

$$L_{c1f} = 15.558 \text{ kN}$$

All columns are designed as axially loaded and to compensate for the effect of eccentricities, the ultimate load from the floor immediately above the column is multiplied by factor 1.5. (Manual for the design of reinforced concrete building structures, the institution of structural engineers).

### Design of column C9f

Total axial load of column  $N_{9f} := LC_{4.9f} \cdot 1.5 + L_{c9f}$

$$N_{9f} = 667.032 \text{ kN}$$

Vertical steel bars of column  $A_{sc9f} := \frac{N_{9f} - 0.35 \cdot F_{cu} \cdot A_{9f}}{0.7 \cdot F_y - 0.35 \cdot F_{cu}}$

$$A_{sc9f} = 34.615 \text{ mm}^2$$

The result means that the load is very small so that the area of steel will be the allowable minimum percentage of reinforcement for the column.

4 bars of T12 with area  $area_{c9f} := 452.39 \text{ mm}^2$

Check of minimum and maximum steel bars area of column such that the minimum is  $r = 0.4\%$  and maximum =  $6\%$

$$r_{c9f} := \frac{area_{c9f}}{A_{9f}} \cdot 100$$

$$r_{c9f} = 0.724$$

(Acceptable ratio)

Links diameter for column less than 6mm and the links diameter for this column is

$$\phi_{c9f} := 0.25 \cdot 12 \text{ mm}$$

$$\phi_{c9f} = 3 \text{ mm}$$

So that the links diameter of this column is 6mm (T6)

Max spacing for links is  $s_{c9f} := 12 \cdot 12 \text{ mm}$

$$s_{c9f} = 144 \text{ mm}$$

So that the used spacing for this column links is 125 mm i.e 8 T6 / meter



**Design of column C8f**Total axial load of column  $N_{8f} := LC_{4.9f} + L_{c9f} + LC_{4.9f} \cdot 1.5 + L_{c8f}$ 

$$N_{8f} = 1.114 \times 10^3 \text{ kN}$$

Vertical steel bars of column  $A_{sc8f} := \frac{N_{8f} - 0.35 \cdot F_{cu} \cdot A_{8f}}{0.7 \cdot F_y - 0.35 \cdot F_{cu}}$ 

$$A_{sc8f} = 1.469 \times 10^3 \text{ mm}^2$$

8 bars of T16 with area  $area_{c8f} := 1608.49 \text{ mm}^2$ Check of minimum and maximum steel bars area of column such that the minimum is  $r = 0.4\%$  and maximum =  $6\%$ 

$$r_{c8f} := \frac{area_{c8f}}{A_{8f}} \cdot 100$$

$$r_{c8f} = 2.574$$

(Acceptable ratio)

Links diameter for column less than 6mm and the links diameter for this column is

$$\phi_{c8f} := 0.25 \cdot 16 \text{ mm}$$

$$\phi_{c8f} = 4 \text{ mm}$$

So that the links diameter of this column is 6mm (T6)

Max spacing for links is  $s_{c8f} := 12 \cdot 16 \text{ mm}$ 

$$s_{c8f} = 192 \text{ mm}$$

So that the used spacing for this column links is 175 mm i.e 5.5 T6 / meter

**Design of column C7f**Total axial load of column  $N_{7f} := LC_{4.9f} \cdot 2 + L_{c9f} + L_{c8f} + LC_{4.9f} \cdot 1.5 + L_{c7f}$ 

$$N_{7f} = 1.563 \times 10^3 \text{ kN}$$

Vertical steel bars of column  $A_{sc7f} := \frac{N_{7f} - 0.35 \cdot F_{cu} \cdot A_{7f}}{0.7 \cdot F_y - 0.35 \cdot F_{cu}}$ 

$$A_{sc7f} = 1.984 \times 10^3 \text{ mm}^2$$

4 bars of T20 + 4 bars of T16 with area  $area_{c7f} := 2060.89 \text{ mm}^2$ Check of minimum and maximum steel bars area of column such that the minimum is  $r = 0.4\%$  and maximum =  $6\%$ 

$$r_{c7f} := \frac{area_{c7f}}{A_{7f}} \cdot 100$$

$$r_{c7f} = 2.29$$

(Acceptable ratio)

Links diameter for column less than 6mm and the links diameter for this column is



$$\phi_{c7f} := 0.25 \cdot 20\text{mm}$$

$$\phi_{c7f} = 5\text{ mm}$$

So that the links diameter of this column is 6mm (T6)

Max spacing for links is  $s_{c7f} := 12 \cdot 16\text{mm}$

$$s_{c7f} = 192\text{ mm}$$

So that the used spacing for this column links is 175 mm i.e 5.5 T6 / meter

### Design of column C6f

Total axial load of column  $N_{6f} := LC_{4.9f} \cdot 3 + L_{c9f} + L_{c8f} + L_{c7f} + LC_{4.9f} \cdot 1.5 + L_{c6f}$

$$N_{6f} = 2.013 \times 10^3\text{ kN}$$

Vertical steel bars of column  $A_{sc6f} := \frac{N_{6f} - 0.35 \cdot F_{cu} \cdot A_{6f}}{0.7 \cdot F_y - 0.35 \cdot F_{cu}}$

$$A_{sc6f} = 3.427 \times 10^3\text{ mm}^2$$

4 bars T32 + 4 bars T12 with area  $area_{c6f} := 3669.38\text{mm}^2$

$$r_{c6f} := \frac{area_{c6f}}{A_{6f}} \cdot 100$$

$$r_{c6f} = 4.077$$

(Acceptable ratio)

$$\phi_{c6f} := 0.25 \cdot 32\text{mm}$$

$$\phi_{c6f} = 8\text{ mm}$$

So that the links diameter of this column is 8mm (T8)

Max spacing for links is  $s_{c6f} := 12 \cdot 12\text{mm}$

$$s_{c6f} = 144\text{ mm}$$

So that the used spacing for this column links is 125 mm i.e 8 T8 / meter

### Design of column C5f

Total axial load of column  $N_{5f} := LC_{4.9f} \cdot 4 + L_{c9f} + L_{c8f} + L_{c7f} + L_{c6f} + LC_{4.9f} \cdot 1.5 + L_{c5f}$

$$N_{5f} = 2.465 \times 10^3\text{ kN}$$

Vertical steel bars of column  $A_{sc5f} := \frac{N_{5f} - 0.35 \cdot F_{cu} \cdot A_{5f}}{0.7 \cdot F_y - 0.35 \cdot F_{cu}}$

$$A_{sc5f} = 3.784 \times 10^3\text{ mm}^2$$

8 bars T25 with area  $area_{c5f} := 3926.99\text{mm}^2$

$$r_{c5f} := \frac{area_{c5f}}{A_{5f}} \cdot 100$$

$$r_{c5f} = 3.206$$

(Acceptable ratio)



The links diameter of this column is 8mm (T8)

The used spacing for this column links is 250 mm i.e 4 T8 / meter

### Design of column C4f

Total axial load of column  $N_{4f} := LC_{4.9f} \cdot 5 + L_{c9f} + L_{c8f} + L_{c7f} + L_{c6f} + L_{c5f} + LC_{4.9f} \cdot 1.5 + L_{c4f}$

$$N_{4f} = 2.918 \times 10^3 \text{ kN}$$

Vertical steel bars of column  $A_{sc4f} := \frac{N_{4f} - 0.35 \cdot F_{cu} \cdot A_{4f}}{0.7 \cdot F_y - 0.35 \cdot F_{cu}}$   $A_{sc4f} = 5.237 \times 10^3 \text{ mm}^2$

4 bars T32 + 8 bars T20 with area  $area_{c4f} := 5730.26 \text{ mm}^2$

$r_{c4f} := \frac{area_{c4f}}{A_{4f}} \cdot 100$   $r_{c4f} = 4.678$  (Acceptable ratio)

The links diameter of this column is 8mm (T8)

The used spacing for this column links is 200 mm i.e 5 T8 / meter

### Design of column C3f

Total axial load of column  $N_{3f} := N_{4f} - 0.5 \cdot LC_{4.9f} + LC_{3f} \cdot 1.5 + L_{c3f}$   $N_{3f} = 3.394 \times 10^3 \text{ kN}$

Vertical steel bars of column  $A_{sc3f} := \frac{N_{3f} - 0.35 \cdot F_{cu} \cdot A_{3f}}{0.7 \cdot F_y - 0.35 \cdot F_{cu}}$   $A_{sc3f} = 5.501 \times 10^3 \text{ mm}^2$

4 bars T32 + 8 bars T20 with area  $area_{c3f} := 5730.26 \text{ mm}^2$

$r_{c3f} := \frac{area_{c3f}}{A_{3f}} \cdot 100$   $r_{c3f} = 3.581$  (Acceptable ratio)

The links diameter of this column is 8mm (T8)

The used spacing for this column links is 200 mm i.e 5 T8 / meter

### Design of column C2f

Total axial load of column  $N_{2f} := N_{3f} - 0.5 \cdot LC_{3f} + LC_{2f} \cdot 1.5 + L_{c2f}$   $N_{2f} = 3.883 \times 10^3 \text{ kN}$



Vertical steel bars of column

$$A_{sc2f} := \frac{N_{2f} - 0.35 \cdot F_{cu} \cdot A_{2f}}{0.7 \cdot F_y - 0.35 \cdot F_{cu}}$$

$$A_{sc2f} = 7.072 \times 10^3 \text{ mm}^2$$

4 bars T32 + 8 bars T25 with area  $area_{c2f} := 7143.98 \text{ mm}^2$

$$r_{c2f} := \frac{\text{area}_{c2f}}{A_{2f}} \cdot 100$$

$$r_{c2f} = 4.465$$

(Acceptable ratio)

**The links diameter of this column is 8mm (T8)**

The used spacing for this column links is 250 mm i.e 4 T8 / meter

### Design of column C1f

**Total axial load of column**  $N_{1f} := N_{2f} - 0.5 \cdot LC_{2f} + LC_{1f} \cdot 1.5 + L_{c1f}$

$$N_{lf} = 4.385 \times 10^3 \text{ kN}$$

Vertical steel bars of column  $A_{sc1f} := \frac{N_{1f} - 0.35 \cdot F_{cu} \cdot A_{1f}}{0.7 \cdot F_y - 0.35 \cdot F_{cu}}$

$$A_{sclf} = 8.684 \times 10^3 \text{ mm}^2$$

8 bars T32 + 8 bars T20 with area  $area_{clf} := 8947.25 \text{ mm}^2$

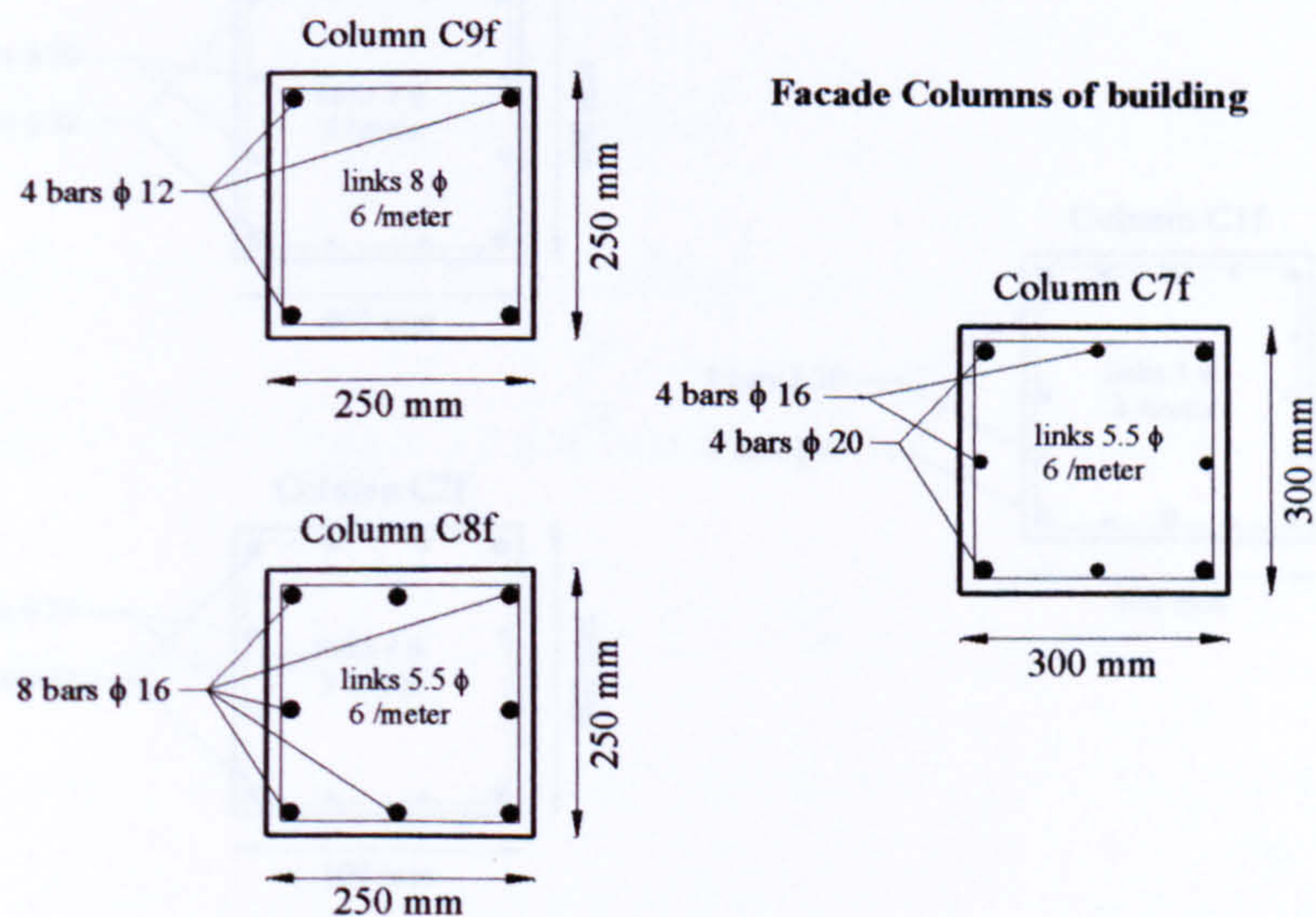
$$r_{\text{clf}} := \frac{\text{area}_{\text{clf}}}{A_{\text{lf}}} \cdot 100$$

$$r_{\text{clf}} = 5.592$$

(Acceptable ratio)

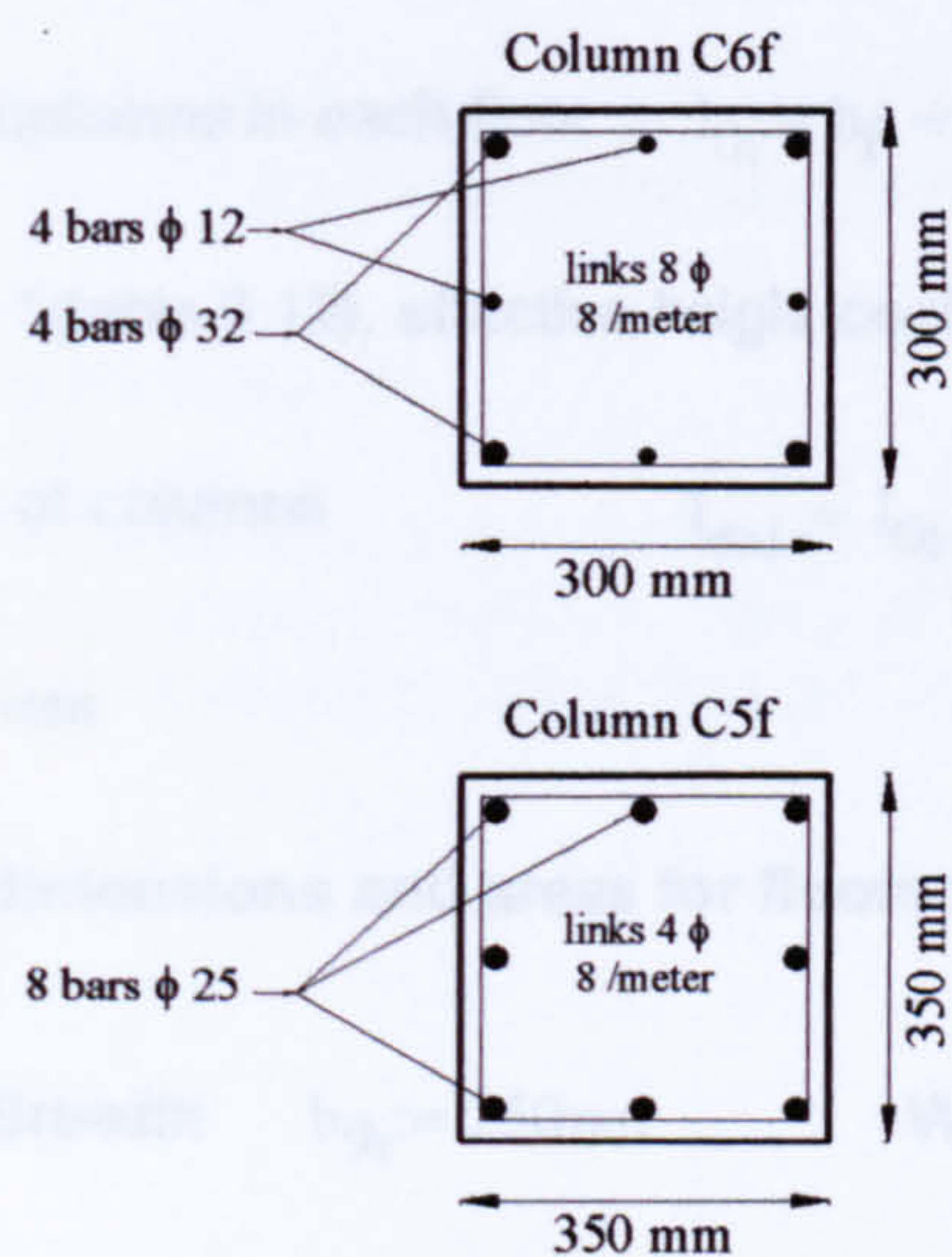
The links diameter of this column is 8mm (T8)

The used spacing for this column links is 200 mm i.e 5 T8 / meter

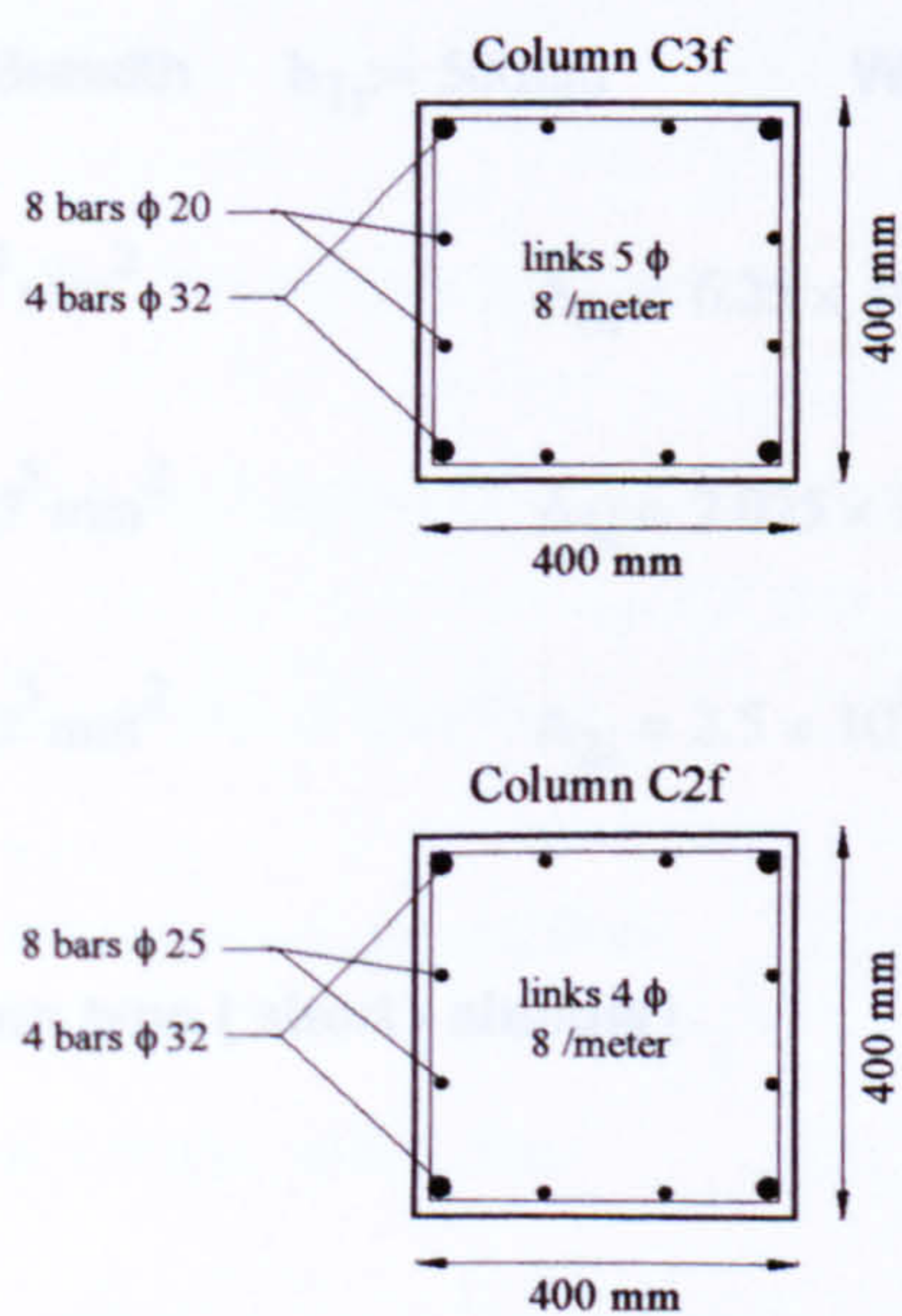
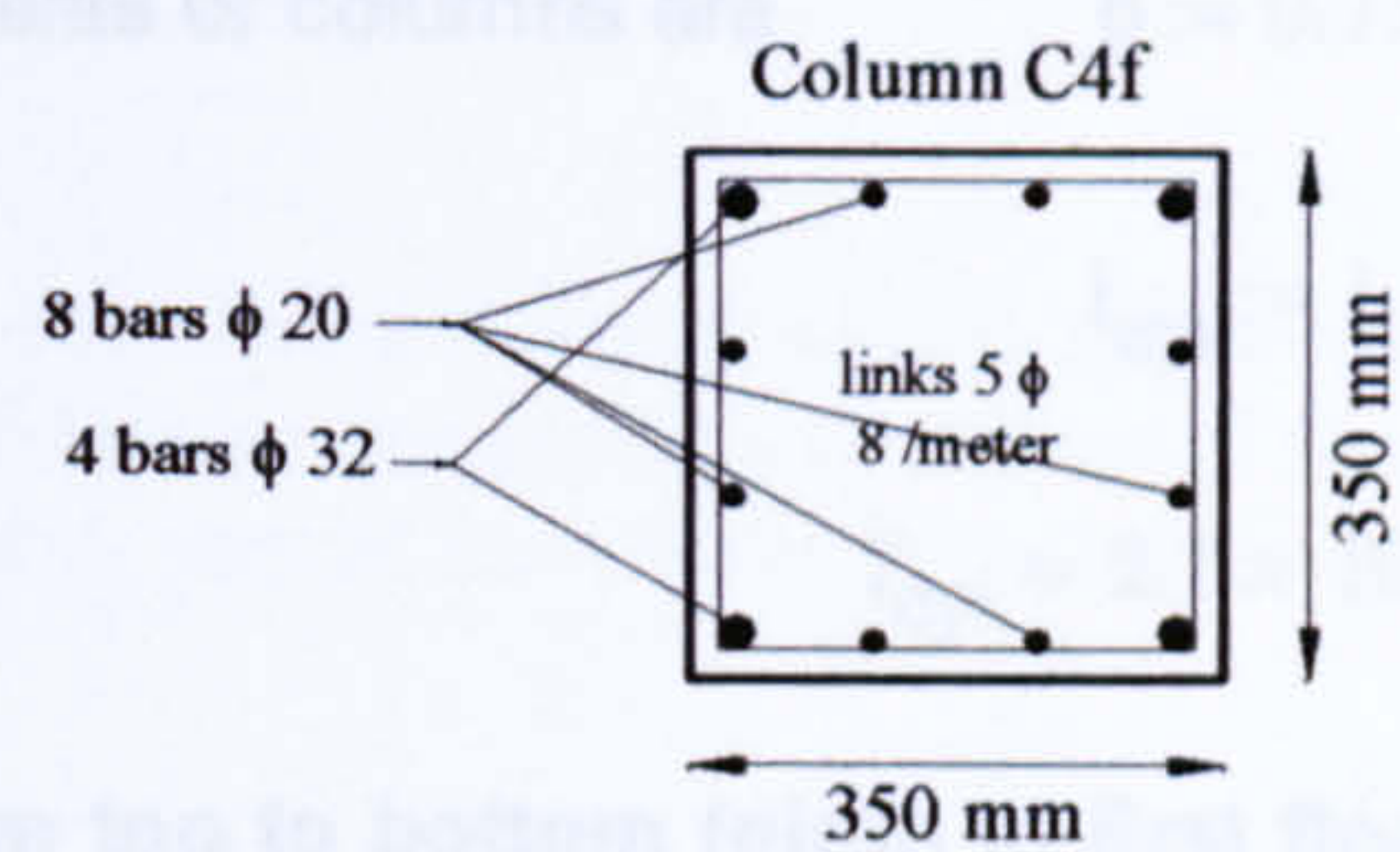




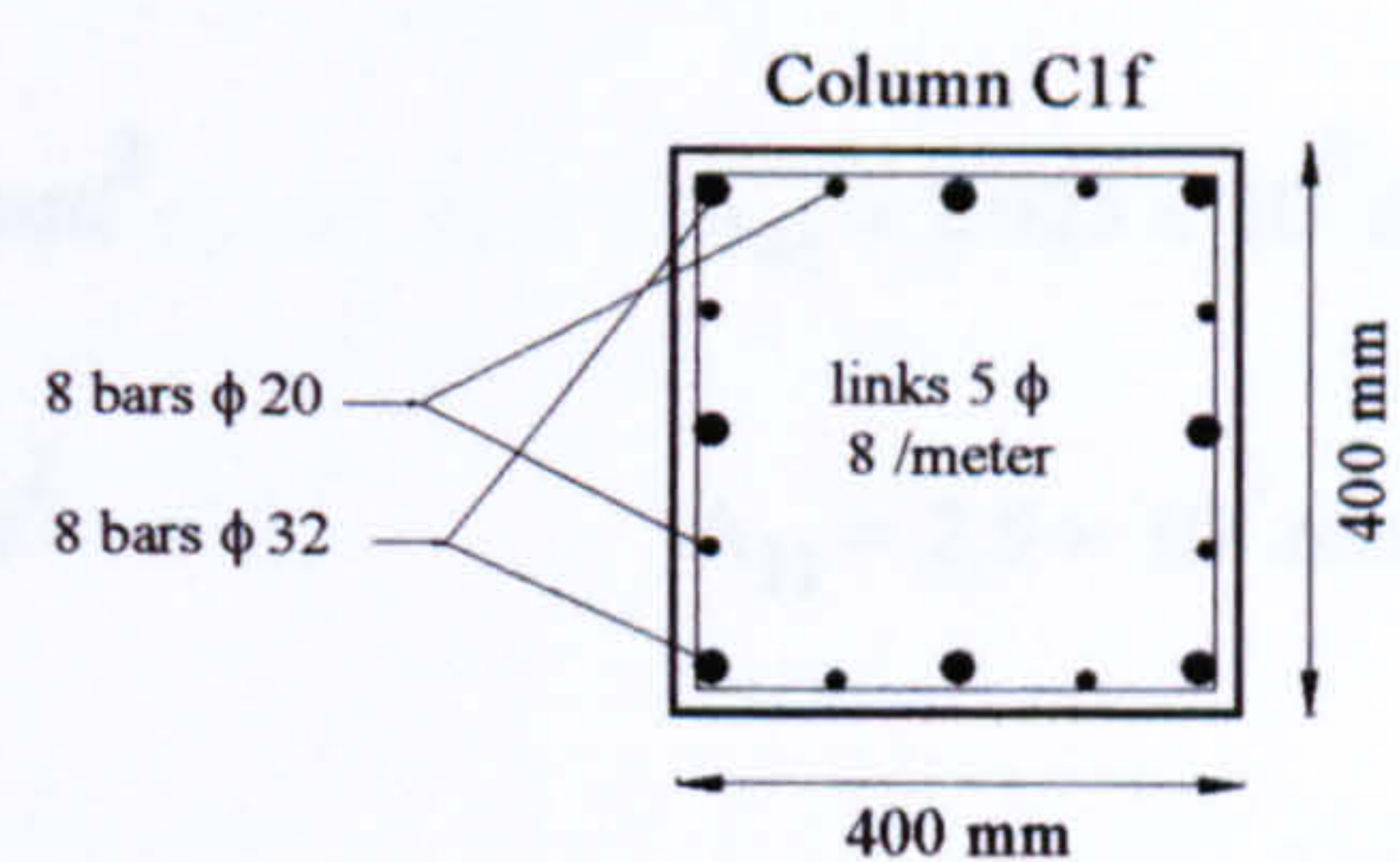
**6.3 Internal Columns From First To Ninth Floor (unbraced columns)**



**Facade Columns of building**



**Facade Columns of building**





**6.3 Internal Columns From First To Ninth Floor ( unbraced columns)**

Clear height of columns in each floor  $l_{0i} := h_f - (d_{B2} + S_t)$   $l_{0i} = 2.8 \times 10^3 \text{ mm}$

From BS8110 - 1(table 3.19), effective height coefficients of columns are  $\beta := 0.75$

Effective height of columns  $l_{exi} := l_{0i} \cdot \beta$   $l_{eyi} := l_{0i} \cdot \beta$

$l_{exi} = 2.1 \times 10^3 \text{ mm}$   $l_{eyi} = 2.1 \times 10^3 \text{ mm}$

**The assumed dimensions and areas for floors from top to bottom (ninth to first floor) are as follows:**

Column 9i	Breadth	$b_{9i} := 250\text{mm}$	Width	$w_{9i} := 250\text{mm}$	$A_{9i} := b_{9i} \cdot w_{9i}$
Column 8i	Breadth	$b_{8i} := 250\text{mm}$	Width	$w_{8i} := 250\text{mm}$	$A_{8i} := b_{8i} \cdot w_{8i}$
Column 7i	Breadth	$b_{7i} := 350\text{mm}$	Width	$w_{7i} := 350\text{mm}$	$A_{7i} := b_{7i} \cdot w_{7i}$
Column 6i	Breadth	$b_{6i} := 350\text{mm}$	Width	$w_{6i} := 350\text{mm}$	$A_{6i} := b_{6i} \cdot w_{6i}$
Column 5i	Breadth	$b_{5i} := 450\text{mm}$	Width	$w_{5i} := 450\text{mm}$	$A_{5i} := b_{5i} \cdot w_{5i}$
Column 4i	Breadth	$b_{4i} := 450\text{mm}$	Width	$w_{4i} := 450\text{mm}$	$A_{4i} := b_{4i} \cdot w_{4i}$
Column 3i	Breadth	$b_{3i} := 450\text{mm}$	Width	$w_{3i} := 450\text{mm}$	$A_{3i} := b_{3i} \cdot w_{3i}$
Column 2i	Breadth	$b_{2i} := 500\text{mm}$	Width	$w_{2i} := 500\text{mm}$	$A_{2i} := b_{2i} \cdot w_{2i}$
Column 1i	Breadth	$b_{1i} := 500\text{mm}$	Width	$w_{1i} := 500\text{mm}$	$A_{1i} := b_{1i} \cdot w_{1i}$

$$A_{9i} = 6.25 \times 10^4 \text{ mm}^2$$

$$A_{8i} = 6.25 \times 10^4 \text{ mm}^2$$

$$A_{7i} = 1.225 \times 10^5 \text{ mm}^2$$

$$A_{6i} = 1.225 \times 10^5 \text{ mm}^2$$

$$A_{5i} = 2.025 \times 10^5 \text{ mm}^2$$

$$A_{4i} = 2.025 \times 10^5 \text{ mm}^2$$

$$A_{3i} = 2.025 \times 10^5 \text{ mm}^2$$

$$A_{2i} = 2.5 \times 10^5 \text{ mm}^2$$

$$A_{1i} = 2.5 \times 10^5 \text{ mm}^2$$

**Check of column type ( short - slender)**

$$r_{xi} := \frac{l_{exi}}{w_{9i}}$$

$$r_{yi} := \frac{l_{eyi}}{b_{9i}}$$



$$r_{xi} = 8.4$$

$$r_{yi} = 8.4$$

Then the columns are short columns because  $r_x$  and  $r_y < 10$  for these unbraced columns and this check for first column is enough for all columns which its dimensions increase.

### Design Loading for Columns

From BS 6399 - 1, 1996 (Loading for buildings) there are reduction factors for distributed imposed floor loads (including partitions loads) differ in values according to number of floors in building. from that the ultimate load of floor per unit area should be recalculated as follows:

For ninth to forth floor  $ULL_{4.9} := ULL \cdot 0.6$   $ULL_{4.9} = 38.4 \text{ kN}$

$$n_{4.9} := \frac{UDL + ULL_{4.9}}{L_x \cdot L_y} \quad n_{4.9} = 8.744 \text{ kN} \cdot \text{m}^{-2}$$

For third floor  $ULL_3 := ULL \cdot 0.7$   $ULL_3 = 44.8 \text{ kN}$

$$n_3 := \frac{UDL + ULL_3}{L_x \cdot L_y} \quad n_3 = 9.144 \text{ kN} \cdot \text{m}^{-2}$$

For second floor  $ULL_2 := ULL \cdot 0.8$   $ULL_2 = 51.2 \text{ kN}$

$$n_2 := \frac{UDL + ULL_2}{L_x \cdot L_y} \quad n_2 = 9.544 \text{ kN} \cdot \text{m}^{-2}$$

For first floor  $ULL_1 := ULL \cdot 0.9$   $ULL_1 = 57.6 \text{ kN}$

$$n_1 := \frac{UDL + ULL_1}{L_x \cdot L_y} \quad n_1 = 9.944 \text{ kN} \cdot \text{m}^{-2}$$

The area of floor that this column type carries  $A_{fi} := 8 \cdot \text{m} \cdot 8 \cdot \text{m}$   $A_{fi} = 6.4 \times 10^7 \text{ mm}^2$

Load form slab on every column for ninth to forth floor  $LC_{s4.9i} := n_{4.9} \cdot A_{fi}$   $LC_{s4.9i} = 559.631 \text{ kN}$

Load form slab on column of third floor  $LC_{s3i} := n_3 \cdot A_{fi}$   $LC_{s3i} = 585.231 \text{ kN}$

Load form slab on column of second floor  $LC_{s2i} := n_2 \cdot A_{fi}$   $LC_{s2i} = 610.831 \text{ kN}$

Load form slab on column of first floor  $LC_{s1i} := n_1 \cdot A_{fi}$   $LC_{s1i} = 636.431 \text{ kN}$

Loads from beam B3 on every column for ninth to first floor  $LC_{B3i} = 51.09 \text{ kN}$   
 $LC_{B3i} := d_{B3} \cdot b_{B3} \cdot 2 \cdot (l_{B3} - b_{B2}) \cdot \rho \cdot 1.4$



Loads from beam B2 on every column for ninth to first floor

$$LC_{B2i} := d_{B2} \cdot b_{B2} \cdot (2 \cdot l_{B2} - b_{B2}) \cdot \rho \cdot 1.4$$

$$LC_{B2i} = 71.382 \text{ kN}$$

Tota axial loads on every column except self weight for ninth to fourth floor

$$LC_{4.9i} := LC_{s4.9i} + LC_{B3i} + LC_{B2i}$$

$$LC_{4.9i} = 682.104 \text{ kN}$$

Tota axial loads on every column except self weight for third floor

$$LC_{3i} := LC_{s3i} + LC_{B3i} + LC_{B2i}$$

$$LC_{3i} = 707.704 \text{ kN}$$

Tota axial loads on every column except self weight for second floor

$$LC_{2i} := LC_{s2i} + LC_{B3i} + LC_{B2i}$$

$$LC_{2i} = 733.304 \text{ kN}$$

Tota axial loads on every column except self weight for first floor

$$LC_{1i} := LC_{s1i} + LC_{B3i} + LC_{B2i}$$

$$LC_{1i} = 758.904 \text{ kN}$$

**Self weight of each column from ninth to first floor**

$$L_{c9i} := A_{9i} \cdot l_{0i} \cdot \rho \cdot 1.4$$

$$L_{c9i} = 5.768 \text{ kN}$$

$$L_{c8i} := A_{8i} \cdot l_{0i} \cdot \rho \cdot 1.4$$

$$L_{c8i} = 5.768 \text{ kN}$$

$$L_{c7i} := A_{7i} \cdot l_{0i} \cdot \rho \cdot 1.4$$

$$L_{c7i} = 11.306 \text{ kN}$$

$$L_{c6i} := A_{6i} \cdot l_{0i} \cdot \rho \cdot 1.4$$

$$L_{c6i} = 11.306 \text{ kN}$$

$$L_{c5i} := A_{5i} \cdot l_{0i} \cdot \rho \cdot 1.4$$

$$L_{c5i} = 18.689 \text{ kN}$$

$$L_{c4i} := A_{4i} \cdot l_{0i} \cdot \rho \cdot 1.4$$

$$L_{c4i} = 18.689 \text{ kN}$$

$$L_{c3i} := A_{3i} \cdot l_{0i} \cdot \rho \cdot 1.4$$

$$L_{c3i} = 18.689 \text{ kN}$$

$$L_{c2i} := A_{2i} \cdot l_{0i} \cdot \rho \cdot 1.4$$

$$L_{c2i} = 23.073 \text{ kN}$$

$$L_{c1i} := A_{1i} \cdot l_{0i} \cdot \rho \cdot 1.4$$

$$L_{c1i} = 23.073 \text{ kN}$$

All columns are designed as axially loaded and to compensate for the effect of eccentricities, the ultimate load from the floor immediately above the column is multiplied by factor 1.25. (Manual for the design of reinforced concrete building structures, the institution of structural engineers).

**Design of column C9i**

Total axial load of column

$$N_{9i} := LC_{4.9i} \cdot 1.25 + L_{c9i}$$

$$N_{9i} = 858.399 \text{ kN}$$

Vertical steel bars of column

$$A_{sc9i} := \frac{N_{9i} - 0.35 \cdot F_{cu} \cdot A_{9i}}{0.7 \cdot F_y - 0.35 \cdot F_{cu}}$$

$$A_{sc9i} = 648.952 \text{ mm}^2$$



4 bars T16 with area  $area_{c9i} := 804.25 \text{ mm}^2$

Check of minimum and maximum steel bars area of column such that the minimum is  $r = 0.4\%$  and maximum =  $6\%$

$$r_{c9i} := \frac{area_{c9i}}{A_{9i}} \cdot 100 \quad r_{c9i} = 1.287 \quad (\text{Acceptable ratio})$$

Links diameter for column less than 6mm and the links diameter for this column is

$$\phi_{c9i} := 0.25 \cdot 16 \text{ mm} \quad \phi_{c9i} = 4 \text{ mm}$$

So that the links diameter of this column is 6mm (T6)

$$\text{Max spacing for links is } s_{c9i} := 12 \cdot 16 \text{ mm} \quad s_{c9i} = 192 \text{ mm}$$

So that the used spacing for this column links is 150 mm i.e 5.5 T6 / meter

#### Design of column C8i

$$\text{Total axial load of column } N_{8i} := N_{9i} - 0.25 \cdot LC_{4.9i} + LC_{4.9i} \cdot 1.25 + L_{c8i} \quad N_{8i} = 1.546 \times 10^3 \text{ kN}$$

$$\text{Vertical steel bars of column } A_{sc8i} := \frac{N_{8i} - 0.35 \cdot F_{cu} \cdot A_{8i}}{0.7 \cdot F_y - 0.35 \cdot F_{cu}} \quad A_{sc8i} = 2.857 \times 10^3 \text{ mm}^2$$

4 bars T25 + 4 bars T20 with area  $area_{c8i} := 3220.13 \text{ mm}^2$

Check of minimum and maximum steel bars area of column such that the minimum is  $r = 0.4\%$  and maximum =  $6\%$

$$r_{c8i} := \frac{area_{c8i}}{A_{8i}} \cdot 100 \quad r_{c8i} = 5.152 \quad (\text{Acceptable ratio})$$

Links diameter for column not less than 6mm and the links diameter for this column is

$$\phi_{c8i} := 0.25 \cdot 25 \text{ mm} \quad \phi_{c8i} = 6.25 \text{ mm}$$

So that the links diameter of this column is 8mm (T8)

$$\text{Max spacing for links is } s_{c8i} := 12 \cdot 20 \text{ mm} \quad s_{c8i} = 240 \text{ mm}$$

So that the used spacing for this column links is 200 mm i.e 5 T8 / meter

#### Design of column C7i

$$\text{Total axial load of column } N_{7i} := N_{8i} - LC_{4.9i} \cdot 0.25 + LC_{4.9i} \cdot 1.25 + L_{c7i} \quad N_{7i} = 2.24 \times 10^3 \text{ kN}$$



Vertical steel bars of column  $A_{sc7i} := \frac{N_{7i} - 0.35 \cdot F_{cu} \cdot A_{7i}}{0.7 \cdot F_y - 0.35 \cdot F_{cu}}$   $A_{sc7i} = 3.061 \times 10^3 \text{ mm}^2$

4 bars of T32 with area  $area_{c7i} := 3216.99 \text{ mm}^2$

Check of minimum and maximum steel bars area of column such that the minimum is  $r = 0.4\%$  and maximum =  $6\%$

$r_{c7i} := \frac{area_{c7i}}{A_{7i}} \cdot 100$   $r_{c7i} = 2.626$  (Acceptable ratio)

Links diameter for column not less than 6mm and the links diameter for this column is

$\phi_{c7i} := 0.25 \cdot 32 \text{ mm}$   $\phi_{c7i} = 8 \text{ mm}$

So that the links diameter of this column is 8mm (T8)

Max spacing for links is  $s_{c7i} := 12 \cdot 32 \text{ mm}$   $s_{c7i} = 384 \text{ mm}$

So that the used spacing for this column links is 350 mm i.e 2.5 T8 / meter

#### Design of column C6i

Total axial load of column  $N_{6i} := N_{7i} - LC_{4.9i} \cdot 0.25 + LC_{4.9i} \cdot 1.25 + L_{c6i}$   $N_{6i} = 2.933 \times 10^3 \text{ kN}$

Vertical steel bars of column  $A_{sc6i} := \frac{N_{6i} - 0.35 \cdot F_{cu} \cdot A_{6i}}{0.7 \cdot F_y - 0.35 \cdot F_{cu}}$   $A_{sc6i} = 5.287 \times 10^3 \text{ mm}^2$

4 bars T32 + 8 bars T20 with area  $area_{c6i} := 5730.27 \text{ mm}^2$

$r_{c6i} := \frac{area_{c6i}}{A_{6i}} \cdot 100$   $r_{c6i} = 4.678$  (Acceptable ratio)

$\phi_{c6i} := 0.25 \cdot 32 \text{ mm}$   $\phi_{c6i} = 8 \text{ mm}$

So that the links diameter of this column is 8mm (T8)

Max spacing for links is  $s_{c6i} := 12 \cdot 20 \text{ mm}$   $s_{c6i} = 240 \text{ mm}$

So that the used spacing for this column links is 200 mm i.e 5 T8 / meter

#### Design of column C5i

Total axial load of column  $N_{5i} := N_{6i} - LC_{4.9i} \cdot 0.25 + LC_{4.9i} \cdot 1.25 + L_{c5i}$   $N_{5i} = 3.634 \times 10^3 \text{ kN}$



Vertical steel bars of column  $A_{sc5i} := \frac{N_{5i} - 0.35 \cdot F_{cu} \cdot A_{5i}}{0.7 \cdot F_y - 0.35 \cdot F_{cu}}$

$$A_{sc5i} = 4.84 \times 10^3 \text{ mm}^2$$

4 bars T32 + 4 bars T25 with area  $area_{c5i} := 5180.48 \text{ mm}^2$

$$r_{c5i} := \frac{area_{c5i}}{A_{5i}} \cdot 100$$

$$r_{c5i} = 2.558$$

(Acceptable ratio)

The links diameter of this column is 8mm (T8)

The used spacing for this column links is 250 mm i.e 4 T8 / meter

**Design of column C4i**

Total axial load of column  $N_{4i} := N_{5i} - LC_{4.9i} \cdot 0.25 + LC_{4.9i} \cdot 1.25 + L_{c4i}$

$$N_{4i} = 4.335 \times 10^3 \text{ kN}$$

Vertical steel bars of column  $A_{sc4i} := \frac{N_{4i} - 0.35 \cdot F_{cu} \cdot A_{4i}}{0.7 \cdot F_y - 0.35 \cdot F_{cu}}$

$$A_{sc4i} = 7.09 \times 10^3 \text{ mm}^2$$

4 bars T32 + 8 bars T25 with area  $area_{c4i} := 7143.97 \text{ mm}^2$

$$r_{c4i} := \frac{area_{c4i}}{A_{4i}} \cdot 100$$

$$r_{c4i} = 3.528$$

(Acceptable ratio)

The links diameter of this column is 8mm (T8)

The used spacing for this column links is 250 mm i.e 4 T8 / meter

**Design of column C3i**

Total axial load of column  $N_{3i} := N_{4i} - LC_{4.9i} \cdot 0.25 + LC_{3i} \cdot 1.25 + L_{c3i}$

$$N_{3i} = 5.067 \times 10^3 \text{ kN}$$

Vertical steel bars of column  $A_{sc3i} := \frac{N_{3i} - 0.35 \cdot F_{cu} \cdot A_{3i}}{0.7 \cdot F_y - 0.35 \cdot F_{cu}}$

$$A_{sc3i} = 9.442 \times 10^3 \text{ mm}^2$$

12 bars T32 with area  $area_{c3i} := 9650.97 \text{ mm}^2$

$$r_{c3i} := \frac{area_{c3i}}{A_{3i}} \cdot 100$$

$$r_{c3i} = 4.766$$

(Acceptable ratio)

The links diameter of this column is 8mm (T8)

The used spacing for this column links is 350 mm i.e 2.5 T8 / meter



**Design of column C2i**Total axial load of column  $N_{2i} := N_{3i} - LC_{3i} \cdot 0.25 + LC_{2i} \cdot 1.25 + L_{c2i}$ 

$$N_{2i} = 5.83 \times 10^3 \text{ kN}$$

Vertical steel bars of column  $A_{sc2i} := \frac{N_{2i} - 0.35 \cdot F_{cu} \cdot A_{2i}}{0.7 \cdot F_y - 0.35 \cdot F_{cu}}$ 

$$A_{sc2i} = 1.029 \times 10^4 \text{ mm}^2$$

8 bars T32 + 8 bars T25 with area  $area_{c2i} := 10360.96 \text{ mm}^2$ 

$$r_{c2i} := \frac{area_{c2i}}{A_{2i}} \cdot 100$$

$$r_{c2i} = 4.144$$

(Acceptable ratio)

The links diameter of this column is 8mm (T8)

The used spacing for this column links is 250 mm i.e 4 T8 / meter

**Design of column C1i**Total axial load of column  $N_{1i} := N_{2i} - LC_{2i} \cdot 0.25 + LC_{1i} \cdot 1.25 + L_{c1i}$ 

$$N_{1i} = 6.619 \times 10^3 \text{ kN}$$

Vertical steel bars of column  $A_{sc1i} := \frac{N_{1i} - 0.35 \cdot F_{cu} \cdot A_{1i}}{0.7 \cdot F_y - 0.35 \cdot F_{cu}}$ 

$$A_{sc1i} = 1.282 \times 10^4 \text{ mm}^2$$

16 bars T32 with area  $area_{c1i} := 12867.96 \text{ mm}^2$ 

$$r_{c1i} := \frac{area_{c1i}}{A_{1i}} \cdot 100$$

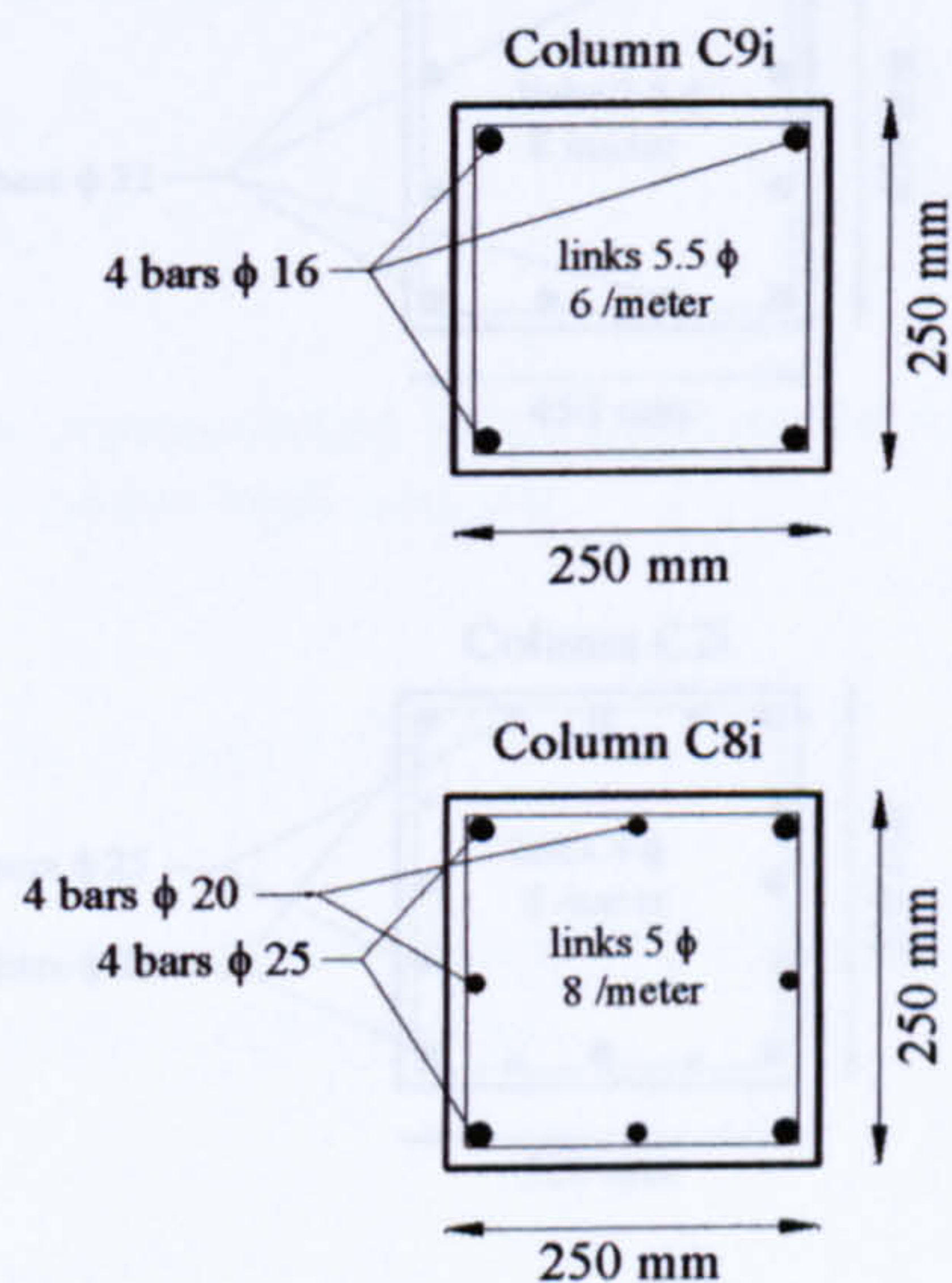
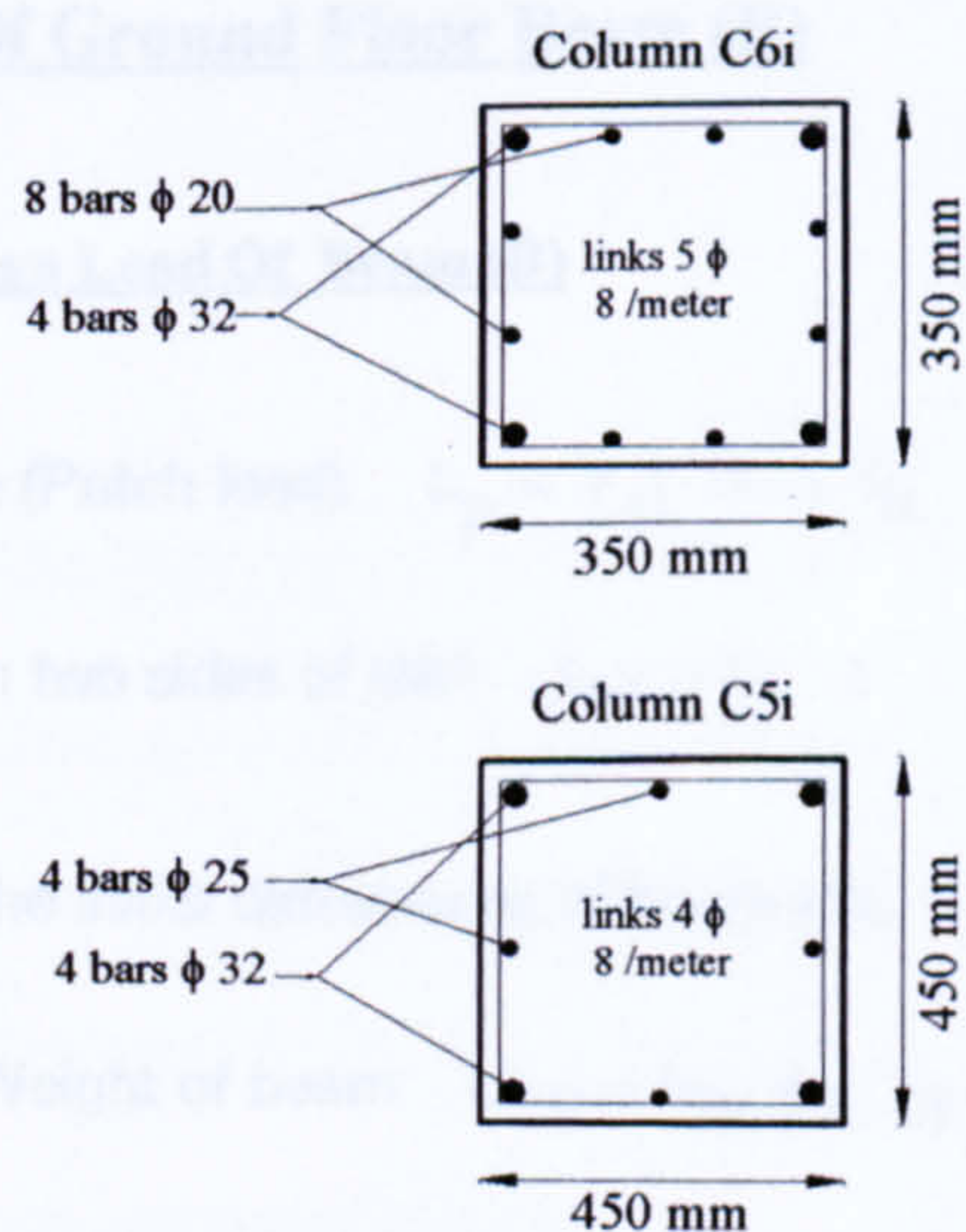
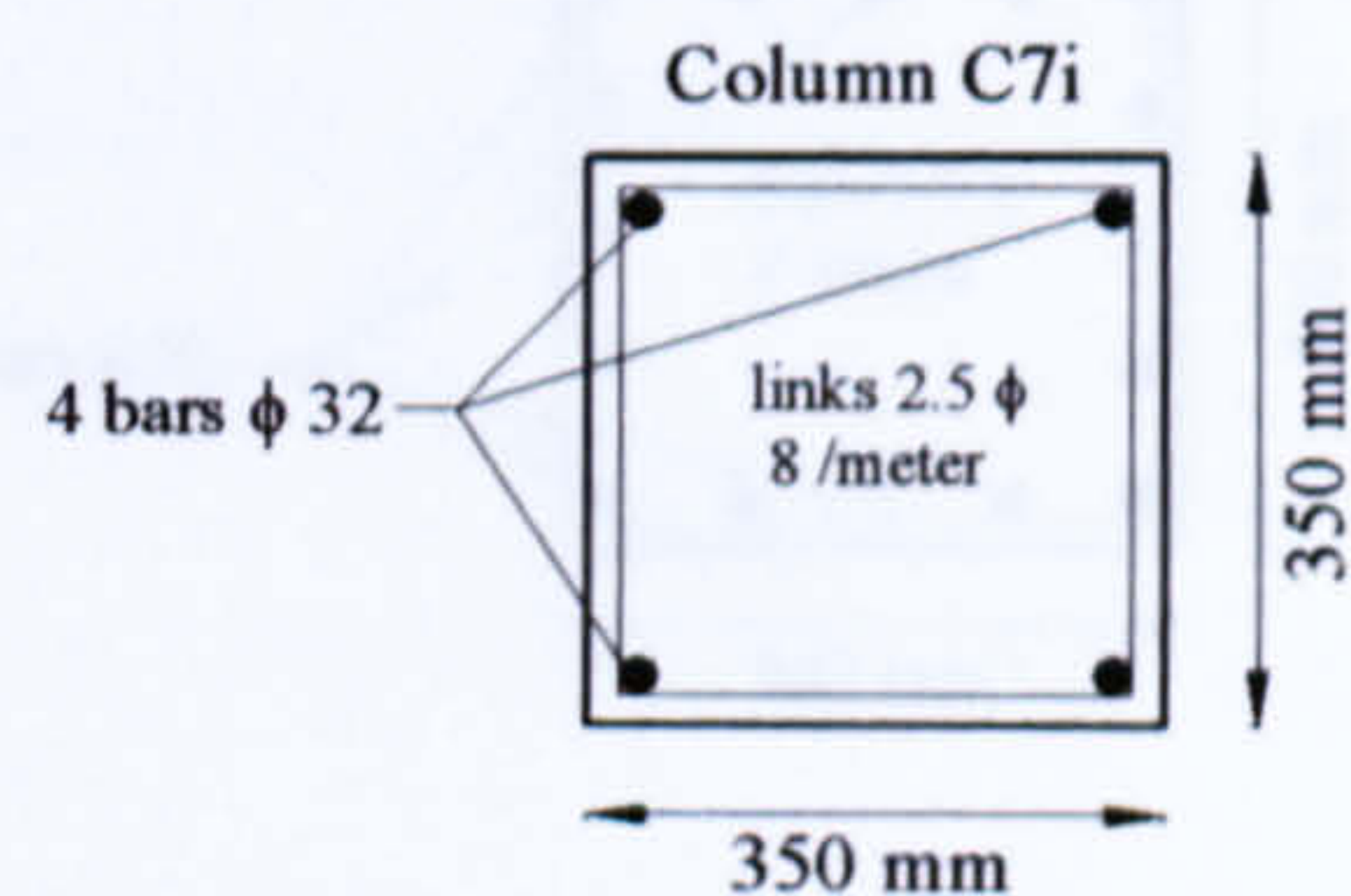
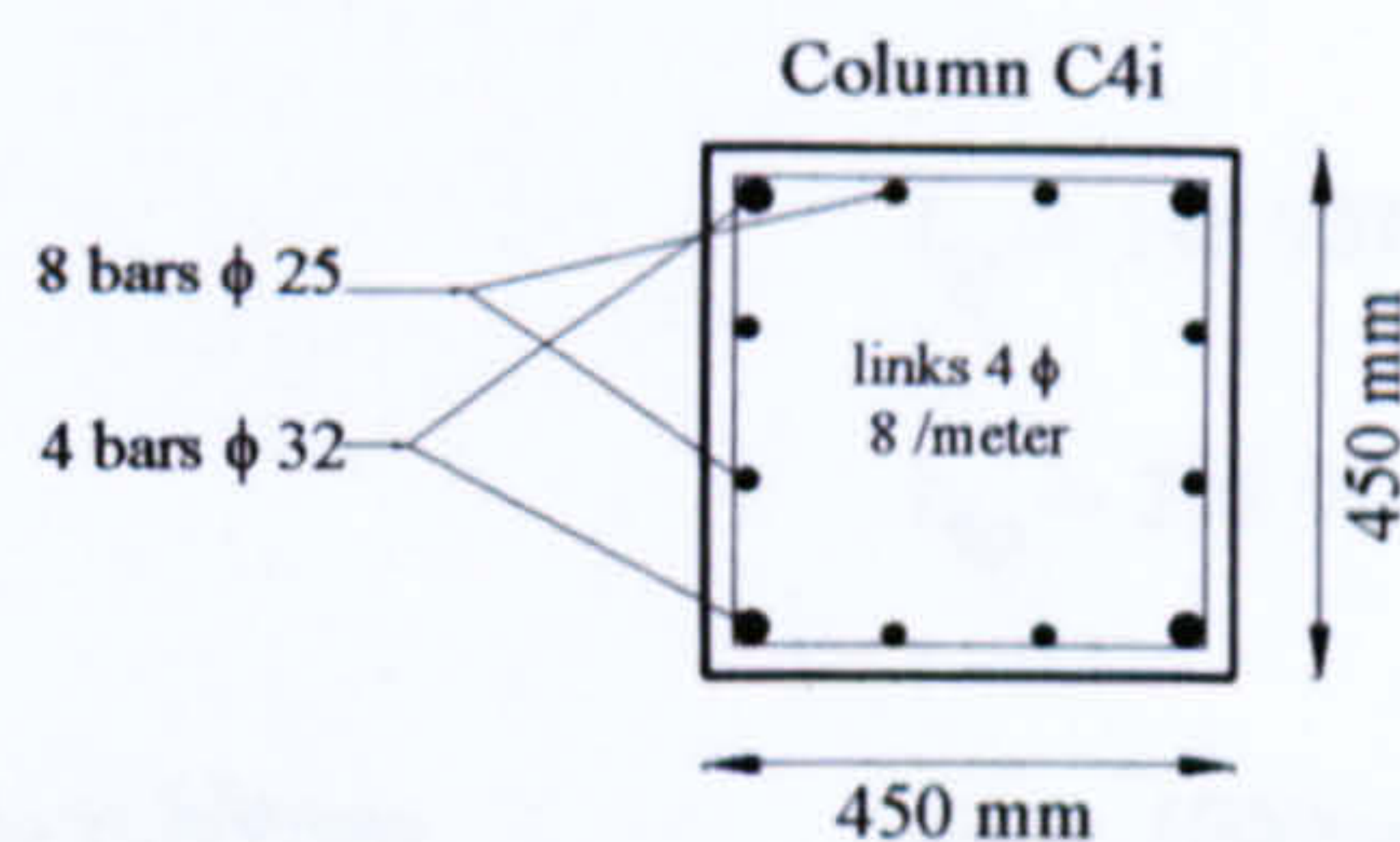
$$r_{c1i} = 5.147$$

(Acceptable ratio)

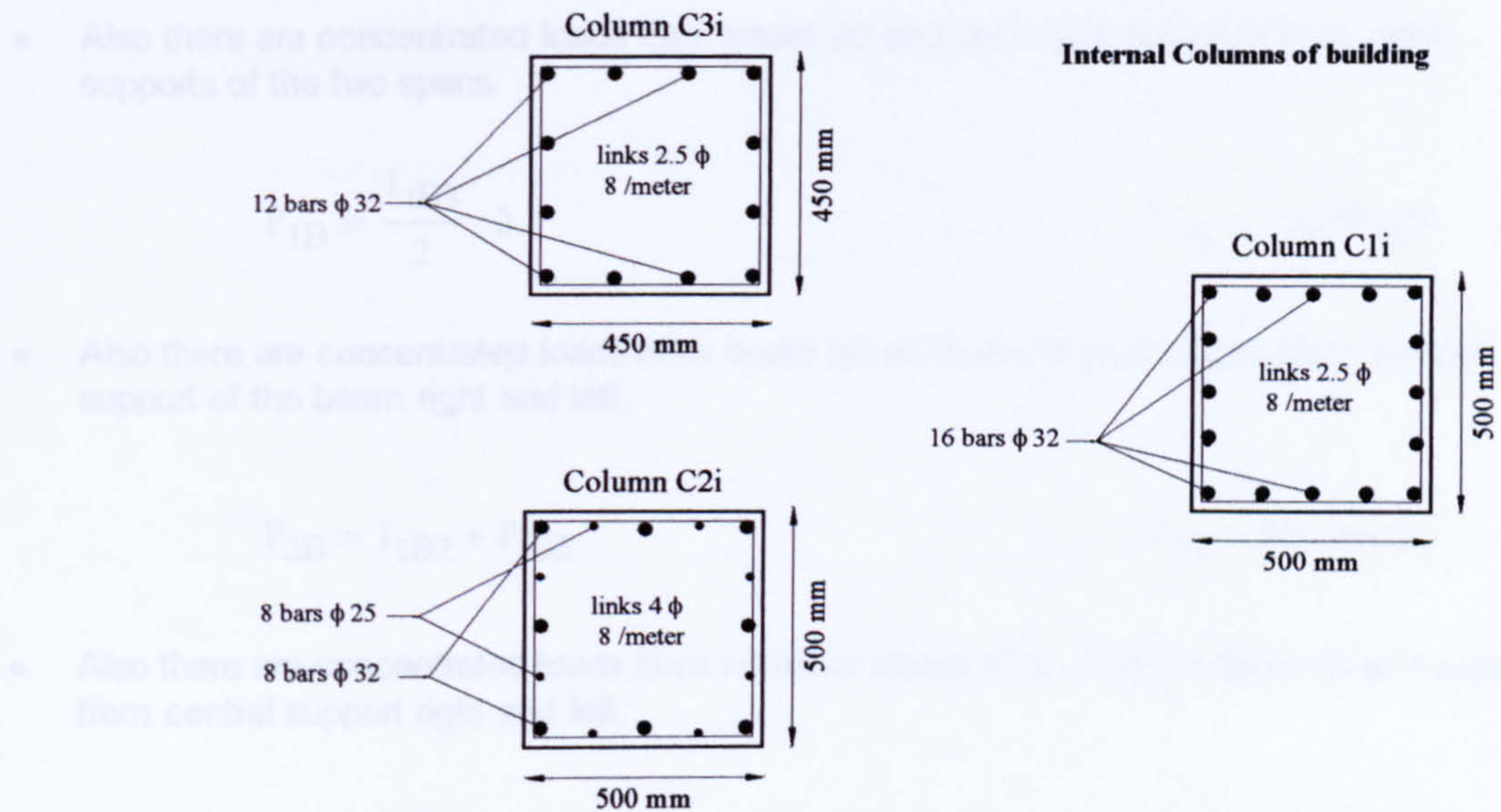
The links diameter of this column is 8mm (T8)

The used spacing for this column links is 350 mm i.e 2.5 T8 / meter



**Internal Columns of building****Internal Columns of building**





## 7. Design Of Beam (B) And Column (C) of Ground Floor

The concrete grade for the design of this structure increases to 40 N / mm<sup>2</sup>

The length of span is  $l_B := 12000 \text{ mm}$

The height of ground floor is  $h_c := 5000 \text{ mm}$

Concrete grade  $F_{cug} := 40 \cdot \text{N} \cdot \text{mm}^{-2}$

### 7.1 Design Of Ground Floor Beam (B)

#### 7.1.1 Max Design Load Of Beam (B)

• From Slab (Patch load)  $L_p := V_{s1} \cdot 0.75 \cdot l_B$   $L_p = 148.957 \text{ kN}$

Total load from two sides of slab  $L_{tp} := L_p \cdot 2$   $L_{tp} = 297.914 \text{ kN}$

• Assume the initial dimensions of beam are  $b_B := 800 \text{ mm}$   $d_B := 1500 \text{ mm}$

Ultimate self Weight of beam  $UL_B := b_B \cdot d_B \cdot l_B \cdot \rho \cdot 1.4$   $UL_B = 474.647 \text{ kN}$

Total load of beam (from distributed load)  $L_{tB} := L_{tp} + UL_B$   $L_{tB} = 772.561 \text{ kN}$



- Also there are concentrated loads from beam b3 on Beam B at 4 meters from outer supports of the two spans.

$$P_{1B} := \frac{L_{tB3}}{2} \cdot 2$$

$$P_{1B} = 224.979 \text{ kN}$$

- Also there are concentrated loads from beam b2 on Beam B at 4 meters from central support of the beam right and left.

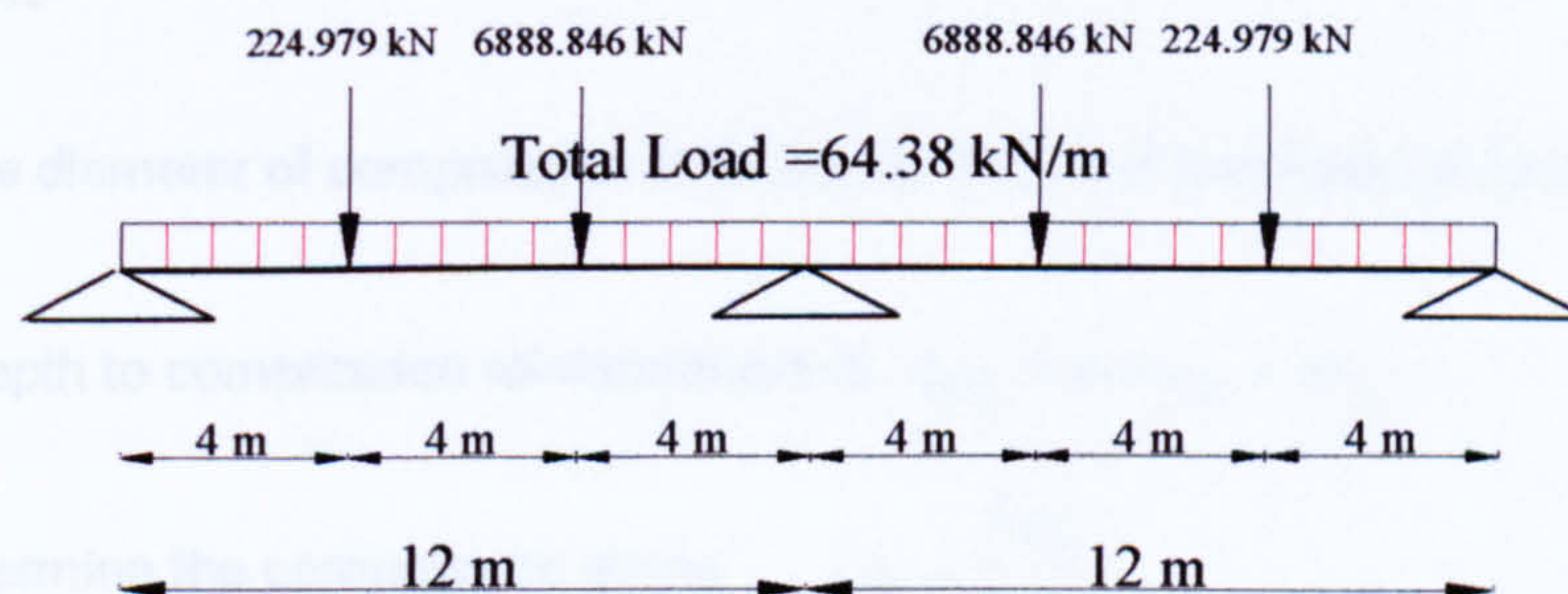
$$P_{2B} := L_{tB2} + P_{tB2}$$

$$P_{2B} = 459.846 \text{ kN}$$

- Also there are concentrated loads from columns above (C1i - C9i) on Beam B at 4 meters from central support right and left.

$$P_{3B} := N_{1i} - LC_{1i} \cdot 0.25$$

$$P_{3B} = 6.429 \times 10^3 \text{ kN}$$



Details of ground floor Beam B

### 7.1.2 Ultimate Bending Moments And Shear Forces Of Beam (B)

The beam sections are treated as rectangular sections

From computer program the max moments and shear forces as follows:

max negative moment at support

$$M_{1b} := 13214 \cdot \text{kN} \cdot \text{m}$$

max positive moment under column

$$M_{2b} := 8460.8 \cdot \text{kN} \cdot \text{m}$$

max shear force

$$FS_b := 5547.5 \cdot \text{kN}$$



**7.1.3 Critical Section At Support**

Assume the diameter of bars used is T40 and 3 layers of bars

$$\phi l_b := 40 \cdot \text{mm}$$

$$\text{cover}_b := 40 \text{mm}$$

$$d_{ef1} := (d_B + S_t) - \text{cover}_b - \phi l_b - \frac{\phi l_b}{2}$$

$$d_{ef1} = 1.55 \times 10^3 \text{ mm}$$

$$k l_b := \frac{M l_b}{F_{cug} \cdot b_B \cdot d_{ef1}^2}$$

$$k l_b = 0.172$$

compression reinforcement is required

$$k_0 := 0.156 \quad z l_b := d_{ef1} \cdot \left[ 0.5 + \left( 0.25 - \frac{k_0}{0.9} \right)^{\frac{1}{2}} \right]$$

$$z l_b = 1.204 \times 10^3 \text{ mm}$$

$$x_b := \frac{d_{ef1} - z l_b}{0.45}$$

$$x_b = 768.499 \text{ mm}$$

Assume the diameter of compression steel bars is T40 and two layers of bars

effective depth to compression reinforcement is  $d_{ef2} := \text{cover}_b + \phi l_b$ 

$$d_{ef2} = 80 \text{ mm}$$

ratio to determine the compression stress  $r_b := \frac{d_{ef2}}{x_b}$ 

$$r_b = 0.104$$

Then the compression stress is 0.95 Fy

$$\text{Area of compression reinforcement } A_{sb1} := \frac{(k l_b - k_0) \cdot F_{cug} \cdot b_B \cdot d_{ef1}^2}{0.95 \cdot F_y \cdot (d_{ef1} - d_{ef2})}$$

$$A_{sb1} = 1.9 \times 10^3 \text{ mm}^2$$

4 bars of T32 are arranged in 1 layer with  $\text{area}_{sb1} := 3216.99 \text{ mm}^2$ 

max percentage of compression or tension reinforcement should not exceed 4% of the area of beam section. min percentage of compression reinforcement should not less than 0.2 and of tension reinforcement should not less than 0.13.

$$r_{B1c} := \frac{\text{area}_{sb1}}{(S_t + d_B) \cdot b_B} \cdot 100$$

$$r_{B1c} = 0.244$$

acceptable ratio



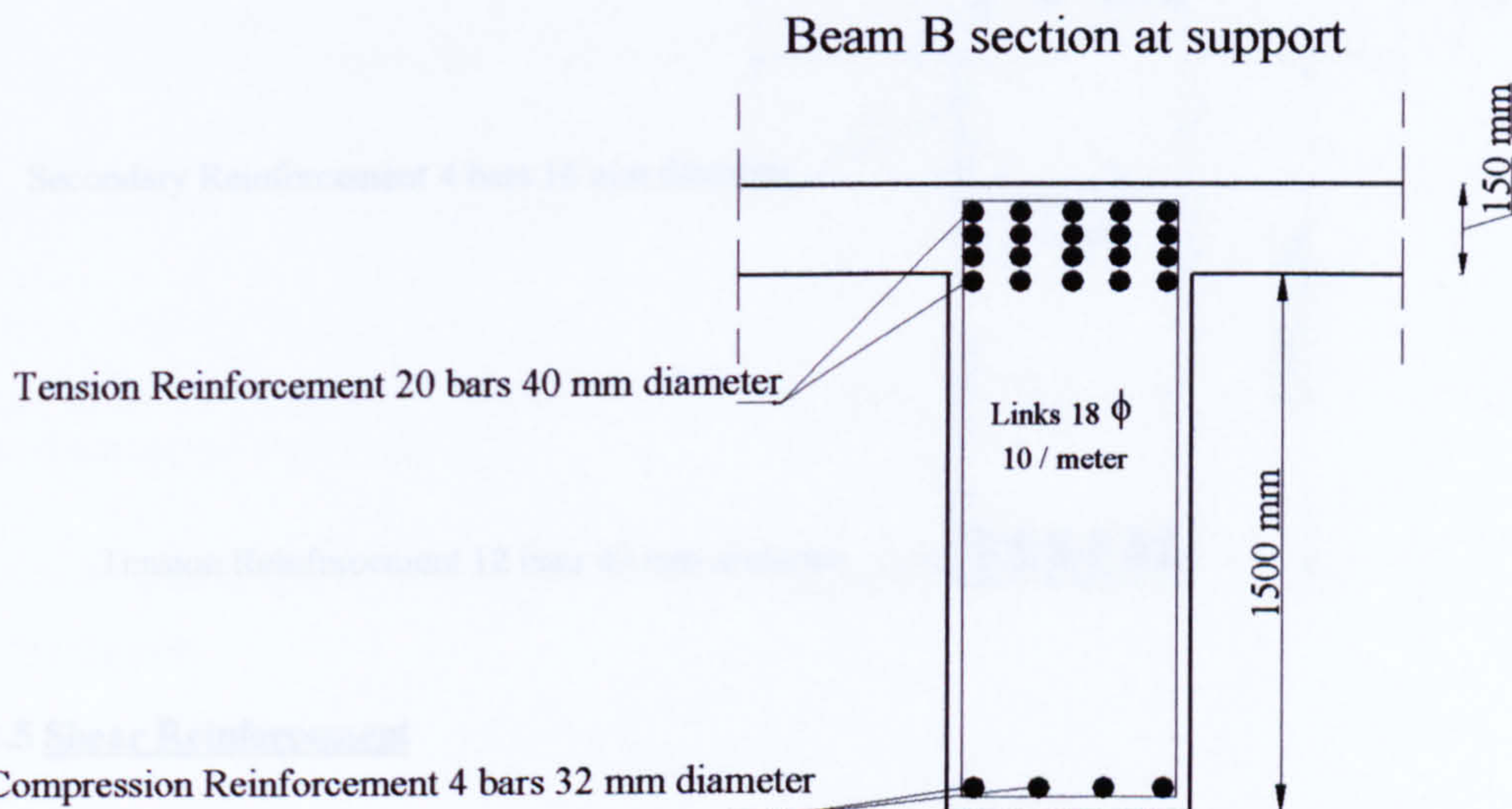
Area of tension reinforcement  $A_{sb2} := \frac{k_0 \cdot F_{cug} \cdot b_B \cdot d_{efl}^2}{0.95 \cdot F_y \cdot z_{1b}} + A_{sb1}$   $A_{sb2} = 2.469 \times 10^4 \text{ mm}^2$

**20 bars of T40 are arranged in 4 layers with  $area_{sb2} := 25132.74 \text{ mm}^2$**

$$r_{Blt} := \frac{area_{sb2}}{(S_t + d_B) \cdot b_B} \cdot 100$$

$$r_{Blt} = 1.904$$

acceptable ratio



#### 7.1.4 Critical Section At Span Point Under Columns Above (positive moment)

$$k2_b := \frac{M2_b}{F_{cug} \cdot b_B \cdot d_{efl}^2}$$

$$k2_b = 0.11$$

compression reinforcement is not required

$$z2_b := d_{efl} \cdot \left[ 0.5 + \left( 0.25 - \frac{k2_b}{0.9} \right)^{\frac{1}{2}} \right]$$

$$z2_b := \text{if}(z2_b > 0.95d_{efl}, 0.95d_{efl}, z2_b)$$

$$z2_b = 1.329 \times 10^3 \text{ mm}$$

$$A_{sb3} := \frac{M2_b}{0.95 \cdot F_y \cdot z2_b}$$

$$A_{sb3} = 1.457 \times 10^4 \text{ mm}^2$$



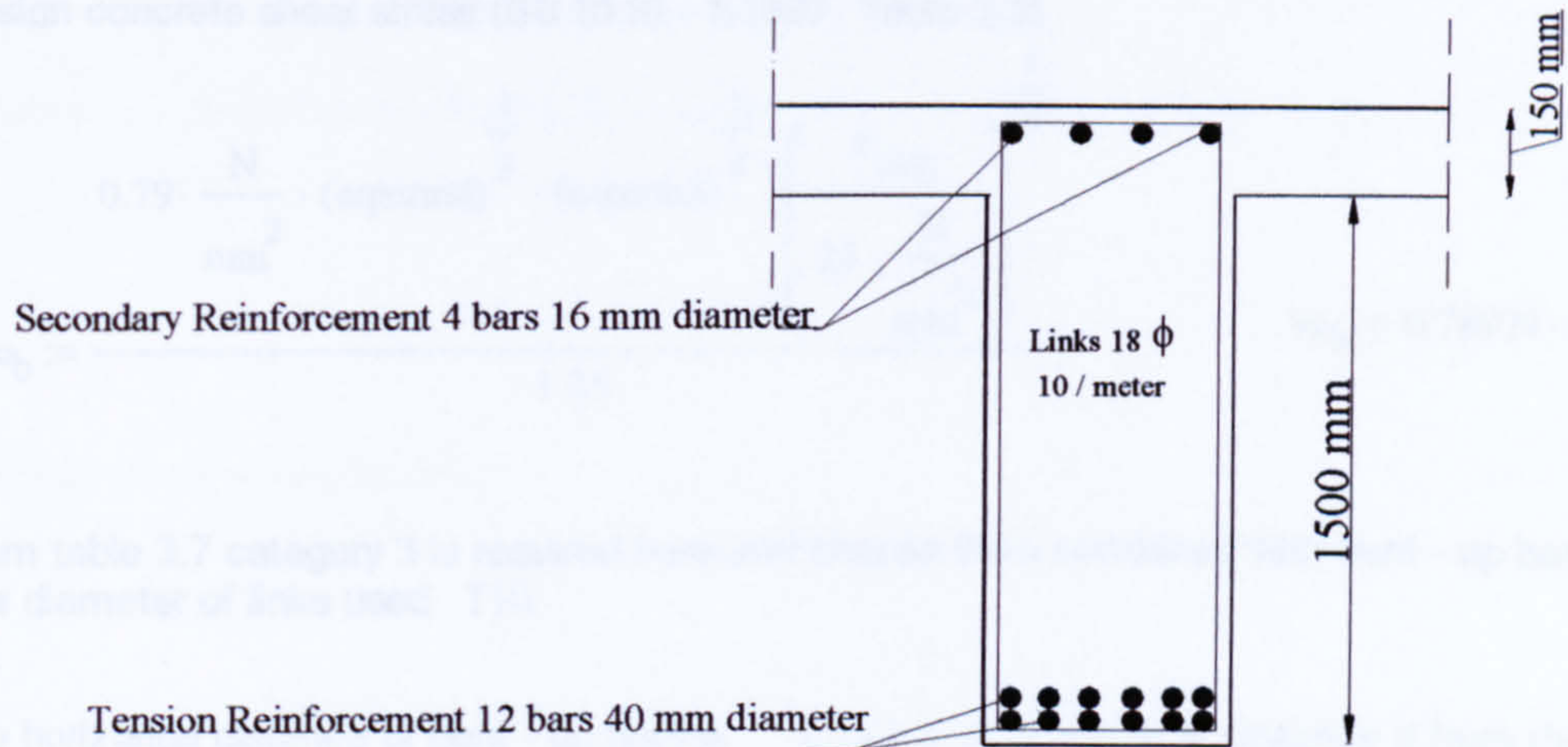
12 bars of T40 are arranged in 2 layers with  $area_{sb3} := 15079.64 \text{ mm}^2$

$$r_{B2t} := \frac{area_{sb3}}{(S_t + d_B) \cdot b_B} \cdot 100$$

$$r_{B2t} = 1.142$$

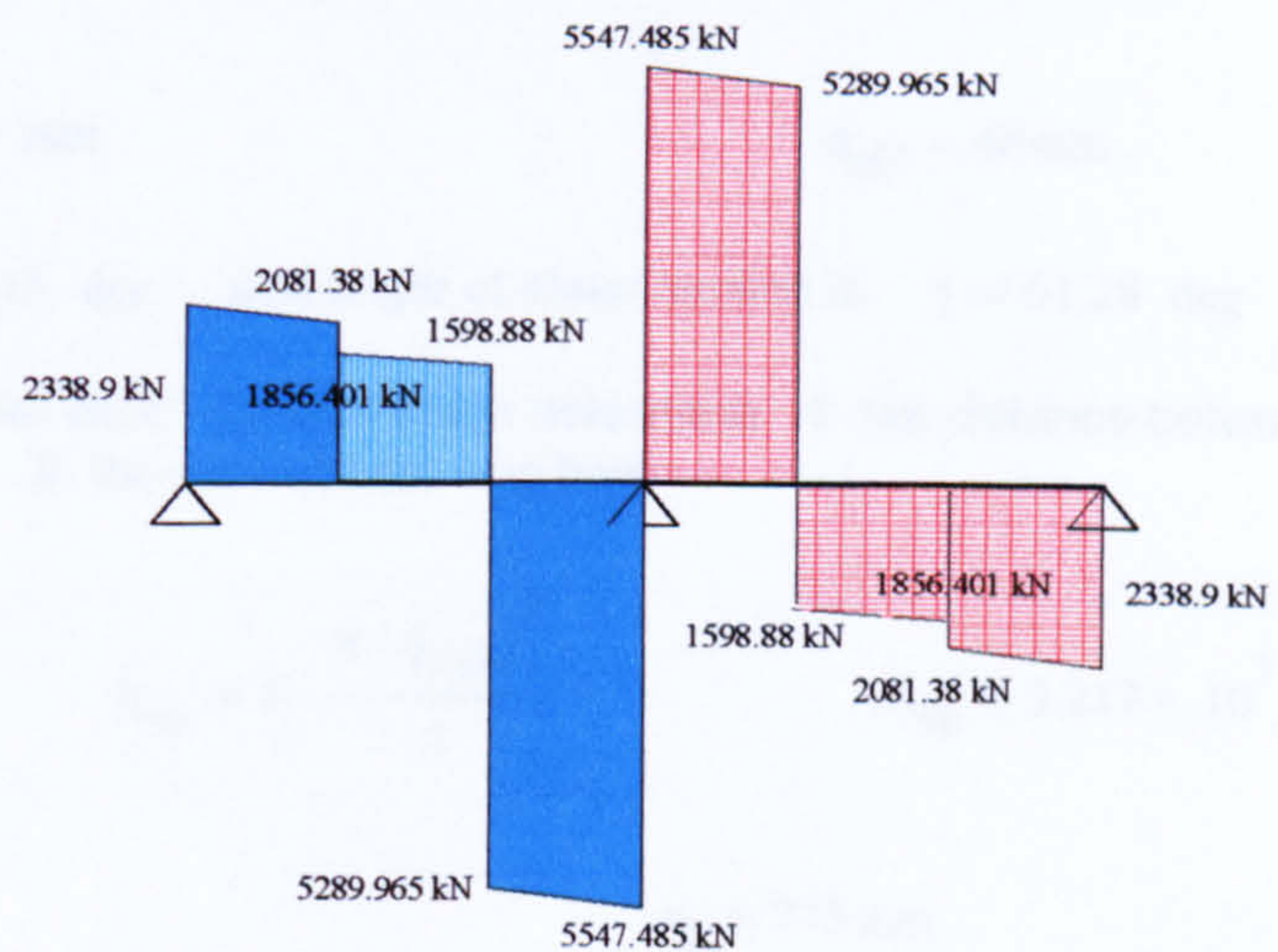
acceptable ratio

Beam B section at point under columns above



### 7.1.5 Shear Reinforcement

SHEAR FORCE DIAGRAM OF BEAM (B)



Ultimate shear stress

$$v_b := \frac{FS_b}{b_B \cdot d_{efl}}$$

$$v_b = 4.474 \text{ N} \cdot \text{mm}^{-2}$$



$$\text{eqterm3} := \frac{400 \cdot \text{mm}}{d_{\text{ef1}}}$$

$$\text{eqterm3} := \text{if}(\text{eqterm3} < 1, 1, \text{eqterm3})$$

$$\text{eqterm3} = 1$$

The check of shear depends on the tension reinforcement of section of span under column above i.e areasb3

$$\text{eqterm4} := \frac{100 \cdot \text{areasb3}}{b_B \cdot d_{\text{ef1}}}$$

$$\text{eqterm4} := \text{if}(\text{eqterm4} < 3, \text{eqterm4}, 3)$$

$$\text{eqterm4} = 1.216$$

Design concrete shear stress (BS 8110 - 1:1997, Table 3.8)

$$v_{c_b} := \frac{0.79 \cdot \frac{\text{N}}{\text{mm}^2} \cdot (\text{eqterm4})^{\frac{1}{3}} \cdot (\text{eqterm3})^{\frac{1}{4}} \cdot \left( \frac{F_{\text{cug}}}{25 \cdot \frac{\text{N}}{\text{mm}^2}} \right)^{\frac{1}{3}}}{1.25}$$

$$v_{c_b} = 0.789 \text{ N} \cdot \text{mm}^{-2}$$

From table 3.7 category 3 is required here and choose links combined with bent - up bars. The diameter of links used T10.

The horizontal distance of bent - up bars is  $s_t := 1.5 \cdot d_{\text{ef1}}$  starts at distance d from the face of the support.

$$s_t = 2.325 \times 10^3 \text{ mm}$$

Effective depth of compression reinforcement of section of beam that used for calculation of concrete shear strength is

$$d_{\text{ef3}} := \text{cover}_b + 8 \cdot \text{mm}$$

$$d_{\text{ef3}} = 48 \text{ mm}$$

Angle of bent - up bars is  $\alpha := 45 \cdot \text{deg}$  and angle of shear section is  $\gamma := 61.28 \cdot \text{deg}$

Choose 4 bars 32 mm diameter for bent - up bars which determine 1- the distance between every two bent - up bars (sb). 2- the area of bent - up bars.

$$\phi_{\text{bent}} := 32 \cdot \text{mm}$$

$$A_{\text{sb}} := 4 \cdot \frac{\pi \cdot \phi_{\text{bent}}^2}{4}$$

$$A_{\text{sb}} = 3.217 \times 10^3 \text{ mm}^2$$

$$s_b := \frac{s_t}{3}$$

$$s_b = 775 \text{ mm}$$

Links must be provided to resist one - half the shear i.e for bent - up bars or links, the shear force is

$$f_s := \frac{FS_b}{2}$$

$$f_s = 2.774 \times 10^3 \text{ kN}$$



$$V_{bent} := A_{sb} \cdot 0.95 \cdot F_y \cdot (\cos(\alpha) + \sin(\alpha) \cdot \cot(\gamma)) \cdot \frac{d_{ef1} - d_{ef3}}{s_b}$$

$$V_{bent} = 2.982 \times 10^3 \text{ kN}$$

Acceptable to resist shear by bent - up bars

**With respect to links**

$$\phi 2_b := 10 \text{ mm}$$

Total cross - section area of links at the neutral axis for 2 legs of T10 is

$$A_{sv} := 2 \cdot \frac{\pi \cdot \phi 2_b^2}{4}$$

$$A_{sv} = 157.08 \text{ mm}^2$$

Ultimate shear stress for links

$$v_{bl} := \frac{f_s}{b_B \cdot d_{ef1}}$$

$$v_{bl} = 2.237 \text{ N} \cdot \text{mm}^{-2}$$

Spacing of links through the span of beam is

$$s_v := \frac{A_{sv} \cdot 0.95 \cdot F_y}{b_B \cdot (v_{bl} - v_{cb})}$$

$$s_v = 59.262 \text{ mm}$$

Max links spacing is  $s_{vm} := 0.75 \cdot d_{ef1}$

$$s_{vm} = 1.162 \times 10^3 \text{ mm}$$

The final spacing for links for this beam is  $s_{vf} := 55.6 \text{ mm}$ . i.e 18 links T10 / meter

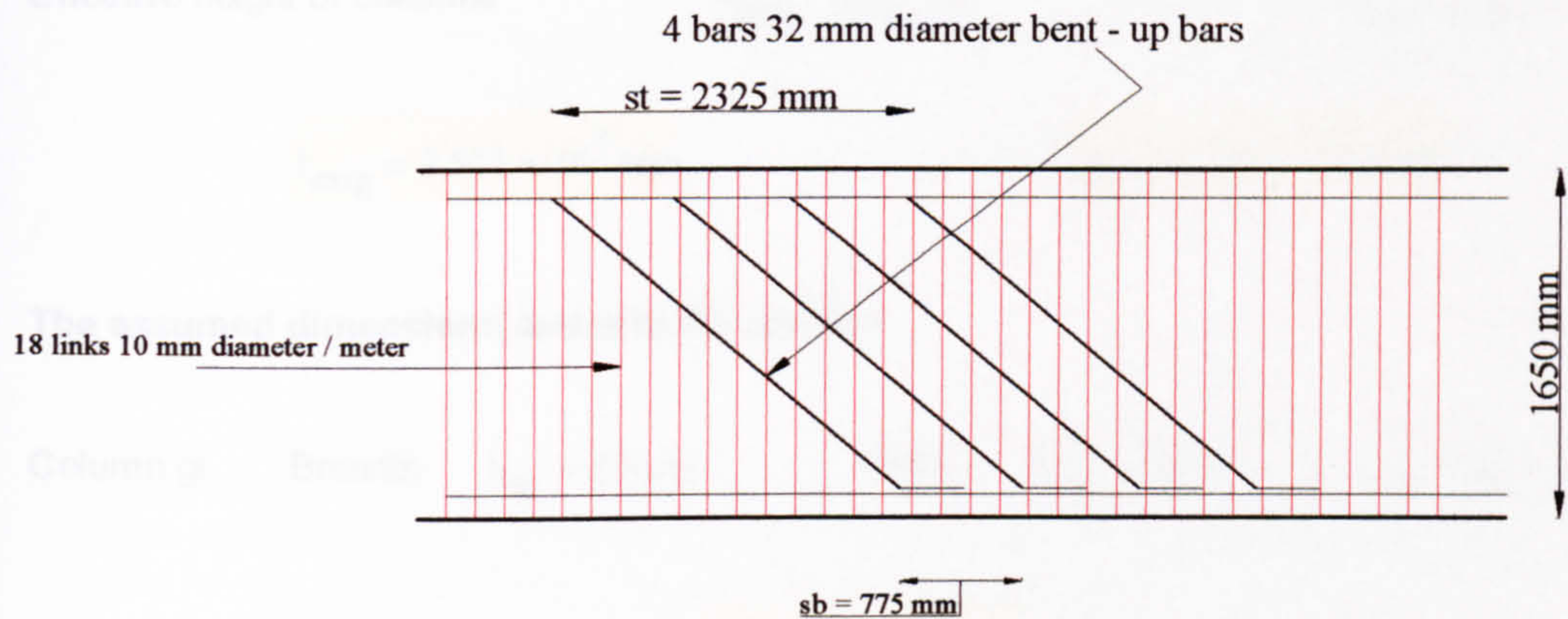
#### Note:

1- Due to the beam being singly reinforced section under column above secondary steel bars should be provided to stabilize shear links i.e 4 T16 for the beam section as secondary steel bars.

2- The bent - up bars combined with links used only for the section right and left of the central support but for other sections of beam its enough to use links only.



**Form of shear reinforcement of beam section near from central support**



**7.1.6 Deflection Check**

service stress  $fs_b := \frac{2 \cdot F_y \cdot A_{sb3}}{3 \cdot area_{sb3}}$   $fs_b = 296.279 \text{ N} \cdot \text{mm}^{-2}$

Modification Factor  $fm_b := 0.55 + \frac{477 \cdot \frac{N}{\text{mm}^2} - fs_b}{120 \cdot \left( 0.9 \cdot \frac{N}{\text{mm}^2} + \frac{M2_b}{b_B \cdot d_{efl}^2} \right)}$   $fm_b = 0.834$

Allowable span to depth ratio is  $SD_{rb} := 26 \cdot \frac{10 \cdot m}{l_B} \cdot fm_b$   $SD_{rb} = 18.071$

Actual span to depth ratio  $SD_{ab} := \frac{l_B}{d_{efl}}$   $SD_{ab} = 7.742$

**The beam is satisfactory with respect to deflections**

**7.2 Design Of Ground Floor Columns**

**7.2.1 Internal Column (unbraced columns)**

Clear height of column  $l_{0ig} := h_c - (d_B + S_t)$   $l_{0ig} = 3.35 \times 10^3 \text{ mm}$



From BS8110 - 1(table 3.19), effective height coefficients of columns are  $\beta := 0.75$

Effective height of columns

$$l_{exig} := l_{0ig} \cdot \beta$$

$$l_{eyig} := l_{0ig} \cdot \beta$$

$$l_{exig} = 2.513 \times 10^3 \text{ mm}$$

$$l_{eyig} = 2.513 \times 10^3 \text{ mm}$$

**The assumed dimensions and area for column**

Column gi

Breadth

$$b_{gi} := 800 \text{ mm}$$

Width

$$w_{gi} := 800 \text{ mm}$$

$$A_{gi} := b_{gi} \cdot w_{gi}$$

$$A_{gi} = 6.4 \times 10^5 \text{ mm}^2$$

**Check of column type ( short - slender)**

$$r_{xig} := \frac{l_{exig}}{w_{gi}}$$

$$r_{yig} := \frac{l_{eyig}}{b_{gi}}$$

$$r_{xig} = 3.141$$

$$r_{yig} = 3.141$$

Then the column is short columns because  $r_x$  and  $r_y < 10$  for this unbraced column .

**Design Loading for Columns**

The area of floor that this column type carries  $A_{fig} := 12 \cdot \text{m} \cdot 8 \cdot \text{m}$

$$A_{fig} = 9.6 \times 10^7 \text{ mm}^2$$

*Load form slab on column*  $LC_{sig} := n \cdot A_{fig}$

$$LC_{sig} = 993.047 \text{ kN}$$

Loads from beam B3 on column

$$LC_{B3ig} := \left[ (l_B - 2 \cdot b_{B2}) + (l_{B3} - b_B - b_{B3}) \right] \cdot b_{B3} \cdot d_{B3} \cdot \rho \cdot 1.4$$

$$LC_{B3ig} = 60.814 \text{ kN}$$

Loads from beam B2 on column  $LC_{B2ig} := d_{B2} \cdot b_{B2} \cdot (2 \cdot l_{B2} - b_B \cdot 2) \cdot \rho \cdot 1.4$

$$LC_{B2ig} = 65.264 \text{ kN}$$

Loads from beam B on column  $LC_{Big} := d_B \cdot b_B \cdot l_B \cdot \rho \cdot 1.4$

$$LC_{Big} = 474.647 \text{ kN}$$

There are concentrated loads from columns above and for this internal column there are two point loads right and left of central support



Loads from columns above  $LC_{cig} := 2 \cdot (N_{1i} - 0.25 \cdot LC_{1i}) \cdot \frac{8}{12}$

$$LC_{cig} = 8.572 \times 10^3 \text{ kN}$$

Tota axial loads on column except self weight

$$LC_{ig} := LC_{sig} + LC_{B3ig} + LC_{B2ig} + LC_{Big} + LC_{cig}$$

$$LC_{ig} = 1.017 \times 10^4 \text{ kN}$$

**Self weight of column**

$$L_{cig} := A_{gi} \cdot l_{0ig} \cdot \rho \cdot 1.4$$

$$L_{cig} = 70.67 \text{ kN}$$

All columns are designed as axially loaded and to compensate for the effect of eccentricities, the ultimate load from the floor immediately above the column is multiplied by factor 1.25. (Manual for the design of reinforced concrete building structures, the institution of structural engineers).

**Design of column Cgii**

Total axial load of column  $N_{gii} := LC_{ig} \cdot 1.25 + L_{cig}$

$$N_{gii} = 1.278 \times 10^4 \text{ kN}$$

Vertical steel bars of column  $A_{scgii} := \frac{N_{gii} - 0.35 \cdot F_{cug} \cdot A_{gi}}{0.7 \cdot F_y - 0.35 \cdot F_{cug}}$

$$A_{scgii} = 1.24 \times 10^4 \text{ mm}^2$$

16 bars  $\phi$  32 with area  $area_{cgui} := 12867.96 \text{ mm}^2$

Check of minimum and maximum steel bars area of column such that the minimum is  $r = 0.4\%$  and maximum =  $6\%$

$$r_{cgi} := \frac{area_{cgui}}{A_{gi}} \cdot 100$$

$$r_{cgi} = 2.011$$

(Acceptable ratio)

Links diamete for column not less than 6mm and the links diameter for this column is

$$\phi_{cgi} := 0.25 \cdot 32 \text{ mm}$$

$$\phi_{cgi} = 8 \text{ mm}$$

So that the links diameter of this column is 8mm (T8)

Max spacing for links is  $s_{cgi} := 12 \cdot 32 \text{ mm}$

$$s_{cgi} = 384 \text{ mm}$$

So that the used spacing for this column links is 250 mm i.e 4 T8 / meter



**7.2.2 External Column (unbraced columns)****The assumed dimensions and area for column**

Column  $g_e$       Breadth  $b_{ge} := 800\text{mm}$       Width  $w_{ge} := 600\text{mm}$        $A_{ge} := b_{ge} \cdot w_{ge}$

$$A_{ge} = 4.8 \times 10^5 \text{ mm}^2$$

**Check of column type (short - slender)**

$$r_{xeg} := \frac{l_{exig}}{w_{ge}}$$

$$r_{xeg} = 4.188$$

$$r_{yeg} := \frac{l_{eyig}}{b_{ge}}$$

$$r_{yeg} = 3.141$$

Then the column is short columns because  $r_x$  and  $r_y < 10$  for this unbraced column .

**Design Loading for Columns**

The area of floor that this column type carries  $A_{feg} := 6.125 \cdot \text{m} \cdot 8 \cdot \text{m}$        $A_{feg} = 4.9 \times 10^7 \text{ mm}^2$

Load form slab on column  $LC_{seg} := n \cdot A_{feg}$        $LC_{seg} = 506.868 \text{ kN}$

Loads from beam B3 on column

$$LC_{B3eg} := \left[ \left( \frac{l_B}{2} - \frac{b_{B1}}{2} \right) + (l_{B3} - b_B - b_{B3}) \right] \cdot b_{B3} \cdot d_{B3} \cdot \rho \cdot 1.4$$

$$LC_{B3eg} = 42.273 \text{ kN}$$

Loads from beam B1 on column  $LC_{B1eg} := d_{B1} \cdot b_{B1} \cdot (l_{B1} - b_B) \cdot \rho \cdot 1.4$        $LC_{B1eg} = 23.732 \text{ kN}$

Loads from beam B on column  $LC_{Beg} := \left( \frac{l_B}{2} + b_{B1} \right) \cdot b_B \cdot d_B \cdot \rho \cdot 1.4$        $LC_{Beg} = 247.212 \text{ kN}$

Loads from walls on column above the beam B1  $LC_{wf} := l_{B1} \cdot l_0 \cdot L_w \cdot 1.4$        $LC_{wf} = 82.6 \text{ kN}$

There are concentrated loads from columns above around central support and for this external column there is a part from this point load.

Loads from columns above  $LC_{ceg} := (N_{1i} - 0.25 \cdot LC_{1i}) \cdot \frac{4}{12}$        $LC_{ceg} = 2.143 \times 10^3 \text{ kN}$



Also there is axial load from columns above this external column  $LC_{cfeg} := N_{1f} - 0.5 \cdot LC_{1f}$

$$LC_{cfeg} = 4.145 \times 10^3 \text{ kN}$$

Total axial loads on column except self weight

$$LC_{eg} := LC_{seg} + LC_{B3eg} + LC_{B1eg} + LC_{Beg} + LC_{wf} + LC_{ceg} + LC_{cfeg}$$

$$LC_{eg} = 7.191 \times 10^3 \text{ kN}$$

**Self weight of column**

$$L_{ceg} := A_{ge} \cdot l_{0ig} \cdot \rho \cdot 1.4$$

$$L_{ceg} = 53.002 \text{ kN}$$

All columns are designed as axially loaded and to compensate for the effect of eccentricities, the ultimate load from the floor immediately above the column is multiplied by factor 1.5. (Manual for the design of reinforced concrete building structures, the institution of structural engineers).

**Design of column Cgie**

$$\text{Total axial load of column } N_{gie} := LC_{eg} \cdot 1.5 + L_{ceg}$$

$$N_{gie} = 1.084 \times 10^4 \text{ kN}$$

$$\text{Vertical steel bars of column } A_{scgie} := \frac{N_{gie} - 0.35 \cdot F_{cug} \cdot A_{ge}}{0.7 \cdot F_y - 0.35 \cdot F_{cug}}$$

$$A_{scgie} = 1.337 \times 10^4 \text{ mm}^2$$

$$\text{8 bars T40 + 8 bars T25 with area } area_{cgie} := 13980. \text{ mm}^2$$

Check of minimum and maximum steel bars area of column such that the minimum is  $r = 0.4\%$  and maximum =  $6\%$

$$r_{cge} := \frac{area_{cgie}}{A_{ge}} \cdot 100$$

$$r_{cge} = 2.913$$

(Acceptable ratio)

Links diameter for column not less than 6mm and the links diameter for this column is

$$\phi_{cge} := 0.25 \cdot 40 \text{ mm}$$

$$\phi_{cge} = 10 \text{ mm}$$

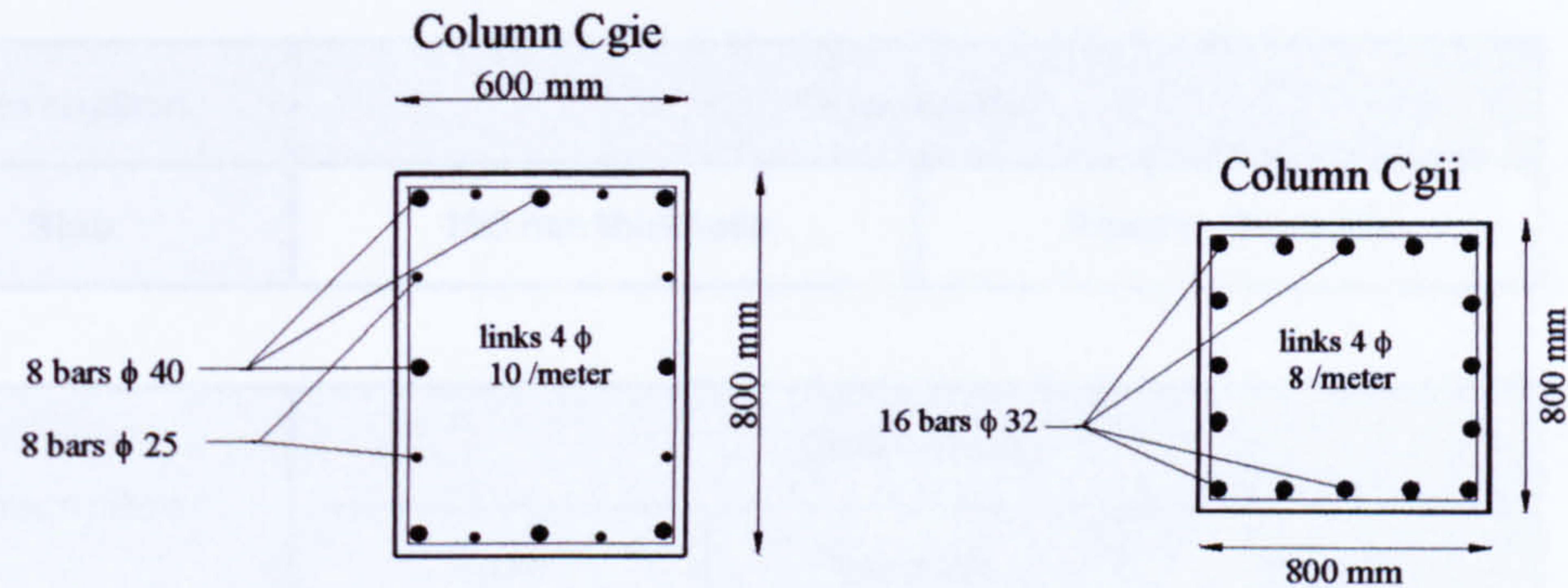
So that the links diameter of this column is 10mm (T10)

$$\text{Max spacing for links is } s_{cge} := 12 \cdot 25 \text{ mm}$$

$$s_{cge} = 300 \text{ mm}$$

So that the used spacing for this column links is 250 mm i.e 4 T10 / meter



**Ground Floor Columns of Building****8. Analytical Approach For Blockwork Of External Panels Of Building**

In this section the walls on beam B1 will be replaced by a diagonal compression struts to include the structural effects of wall panels without explicit modelling in the finite element representation.

Stafford Smith & Riddington (1978) recommend that the area of such a strut should be equal to one tenth of the diagonal length of the panel times the wall thickness.

$$\text{Diagonal length } L_D := \left[ (h_f)^2 + (l_{B1})^2 \right]^{\frac{1}{2}} \quad L_D = 8.732 \times 10^3 \text{ mm}$$

$$\text{Wall thickness } W_t := 250 \cdot \text{mm}$$

$$\text{Area of the strut section } a_s := \frac{1}{10} \cdot L_D \cdot W_t$$

$$a_s = 2.183 \times 10^5 \text{ mm}^2$$

By choosing dimensions equal to the area obtained above, it was found that these dimensions as follow:

$$\text{Breadth of strut } B_s := 300 \cdot \text{mm} \quad \text{and depth of strut } D_s := 750 \cdot \text{mm}$$

$$\text{The actual area of strut is } a_{sa} := B_s \cdot D_s \quad a_{sa} = 2.25 \times 10^5 \text{ mm}^2$$



**9. Summary of dimensions of the structural elements of the building**

Description	Dimensions	
Slab	150 mm thickness	Panels 4 m x 4m

Description	Dimensions		
	Span	Breadth	Depth
Beam B3	8000 mm	250 mm	400 mm
Beam B2	8000 mm	250 mm	550 mm
Beam B1	8000 mm	250 mm	400 mm
Beam B	12000 mm	800 mm	1500 mm
Bracing CS (Compression Strut)	8732 mm	300 mm	750 mm

Description	Columns	Dimensions		
		Breadth	Width	Height
Corner Columns From First to Ninth Floor	C9	250 mm	250 mm	3500 mm
	C8	250 mm	250 mm	3500 mm
	C7	250 mm	250 mm	3500 mm
	C6	300 mm	300 mm	3500 mm
	C5	300 mm	300 mm	3500 mm
	C4	300 mm	300 mm	3500 mm
	C3	350 mm	350 mm	3500 mm
	C2	350 mm	350 mm	3500 mm
	C1	350 mm	350 mm	3500 mm



<b>Facade Columns From First to Ninth Floor</b>	C9f	250 mm	250 mm	3500 mm
	C8f	250 mm	250 mm	3500 mm
	C7f	300 mm	300 mm	3500 mm
	C6f	300 mm	300 mm	3500 mm
	C5f	350 mm	350 mm	3500 mm
	C4f	350 mm	350 mm	3500 mm
	C3f	400 mm	400 mm	3500 mm
	C2f	400 mm	400 mm	3500 mm
	C1f	400 mm	400 mm	3500 mm
<b>Internal Columns From First to Ninth Floor</b>	C9i	250 mm	250 mm	3500 mm
	C8i	250 mm	250 mm	3500 mm
	C7i	350 mm	350 mm	3500 mm
	C6i	350 mm	350 mm	3500 mm
	C5i	450 mm	450 mm	3500 mm
	C4i	450 mm	450 mm	3500 mm
	C3i	450 mm	450 mm	3500 mm
	C2i	500 mm	500 mm	3500 mm
	C1i	500 mm	500 mm	3500 mm
<b>Ground Floor Columns</b>	Cgii	800 mm	800 mm	5000 mm
	Cgie	800 mm	600 mm	5000 mm



**10. Important Notes****Modification of some columns reinforcement**

- Column C9 (Page 25)

After check the design of this column section (using a Columns Assessment Computer Program) as a biaxial bending section, It is found that the percentage of steel bars reinforcement is insufficient due to the axial load of this floor column is low and bending moments around its section axes are high. The appropriate (final) reinforcement of this column section is:

4 bars of T16 + 4 bars of T12 with area  $area_{c9fi} := 1256.64 \text{ mm}^2$

Check of minimum and maximum steel bars area of column such that the minimum is  $r = 0.4\%$  and maximum =  $6\%$

$$r_{c9fi} := \frac{area_{c9fi}}{A_g} \cdot 100 \quad r_{c9fi} = 2.011 \quad (\text{Acceptable ratio})$$

Links diameter for column less than 6mm and the links diameter for this column is

$$\phi_{c9fi} := 0.25 \cdot 16\text{mm} \quad \phi_{c9fi} = 4 \text{ mm}$$

So that the links diameter of this column is 6mm (T6)

$$\text{Max spacing for links is } s_{c9fi} := 12 \cdot 12\text{mm} \quad s_{c9fi} = 144 \text{ mm}$$

So that the used spacing for this column links is 125 mm i.e 8 T6 / meter

- Column C9f (Page 34)

After check the design of this column section (using a Columns Assessment Computer Program) as a uniaxial bending section, It is found that the percentage of steel bars reinforcement is insufficient due to the axial load of this floor column is low and bending moment around its section axis is high. The appropriate (final) reinforcement of this column section is:

4 bars of T16 + 4 bars of T12 with area  $area_{c9fi} := 1256.64 \text{ mm}^2$

Check of minimum and maximum steel bars area of column such that the minimum is  $r = 0.4\%$  and maximum =  $6\%$

$$r_{c9fi} := \frac{area_{c9fi}}{A_{gf}} \cdot 100 \quad r_{c9fi} = 2.011 \quad (\text{Acceptable ratio})$$

Links diameter for column less than 6mm and the links diameter for this column is



$$\phi_{c9ffl} := 0.25 \cdot 16\text{mm}$$

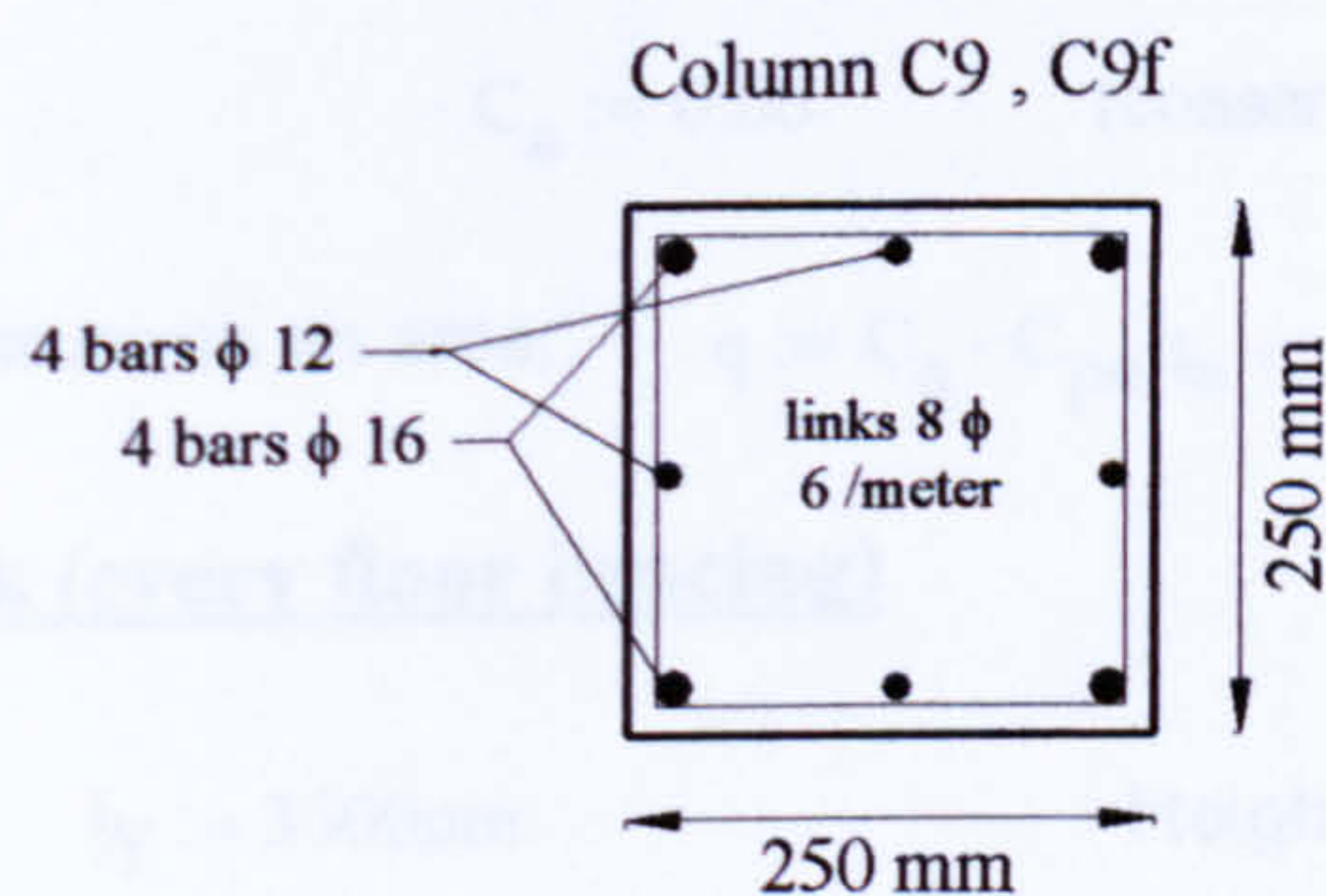
$$\phi_{c9ffl} = 4\text{ mm}$$

So that the links diameter of this column is 6mm (T6)

$$\text{Max spacing for links is } s_{c9ffl} := 12 \cdot 12\text{mm}$$

$$s_{c9ffl} = 144\text{ mm}$$

So that the used spacing for this column links is 125 mm i.e 8 T6 / meter



## 11. Stability Of Building

Lateral stability in two orthogonal directions should be provided by a system of strongpoints within the structure so as to produce a 'braced' structure, i.e. one in which the columns will not be subject to sway moments. Hence the multi-storey RC building will require to be braced. The ten-storey RC building is braced as shown in Fig. II.1. The stability check of the ten-storey RC building is satisfied as follows:

### conservative wind load calculation based on the requirements of BS6399

Basic wind speed	$V_b := 22 \cdot \text{m} \cdot \text{s}^{-1}$ (conservative)	BS6399, Flg.6
Altitude factor	$S_a := 1.04$ (conservative)	BS6399 cl 2.2.2.2, with 36.5 m building height
Direction factor	$S_d := 1$ (conservative)	BS6399 cl 2.2.2.3, 240 degrees
Seasonal Factor	$S_s := 1$ (conservative)	BS6399 cl 2.2.2.4
Probability Factor	$S_p := 1$ (conservative)	BS6399 cl 2.2.2.5
Site wind speed	$V_s := V_b \cdot S_a \cdot S_d \cdot S_s \cdot S_p$	$V_s = 22.88 \text{ m s}^{-1}$
BS 6399 cl 2.2.2		



Terrain and building factor  $S_b := 1.95$  (conservative) *BS6399 table 4*  
( $H_e = 30\text{m}$ ,  $>100\text{km}$  from sea)

Effective wind speed (*BS 6399 cl 2.2.3*):  $V_e := S_b \cdot V_s$   $V_e = 44.616\text{m s}^{-1}$

Dynamic pressure (*BS6399 cl 2.1.2*)  $q_s := \left(0.613 \cdot V_e^2\right) \cdot \text{Pa} \cdot \text{m}^{-2} \cdot \text{s}^2$

$$q_s = 1.22\text{kN} \cdot \text{m}^{-2}$$

### External Surface Pressure

External pressure coefficients  $C_{pe} := -1.6$  (conservative) *BS6399 cl 2.4 & 2.5*

Size effect factor  $C_a := 0.86$  (conservative) *BS6399 cl 2.1.3.4*

Conservative wind pressure on an area:  $q := C_a \cdot C_{pe} q_s$   $q = -1.679\text{kN} \cdot \text{m}^{-2}$

### 11.1 Stability Check (every floor bracing)

Height of Floor (1 - 9)  $h_f := 3500\text{mm}$

Height of Building  $h := 36.5 \cdot \text{m}$

Span of Building in Two Orthogonal Directions  $\text{span} := 24 \cdot \text{m}$

Horizontal Loading at Every Floor (due to wind pressure)  $f_f := \text{span} \cdot h_f \cdot q \cdot -1$

$$f_f = 141.039\text{kN}$$

As the floors of building (first to ninth floor) is 3-bay (8 m span for every bay), then the horizontal force is distributed on 3 bracing, i.e. the horizontal force for every bracing will be

$$\text{span}_{\text{bay}} := 8 \cdot \text{m} \quad f_{fb} := \frac{f_f}{3}$$

$$f_{fb} = 47.013\text{kN}$$

Force in bracing  $f_b := f_{fb} \cdot \left[ \frac{\left( \text{span}_{\text{bay}}^2 + h_f^2 \right)^{\frac{1}{2}}}{\text{span}_{\text{bay}}} \right]$   $f_b = 51.315\text{kN}$

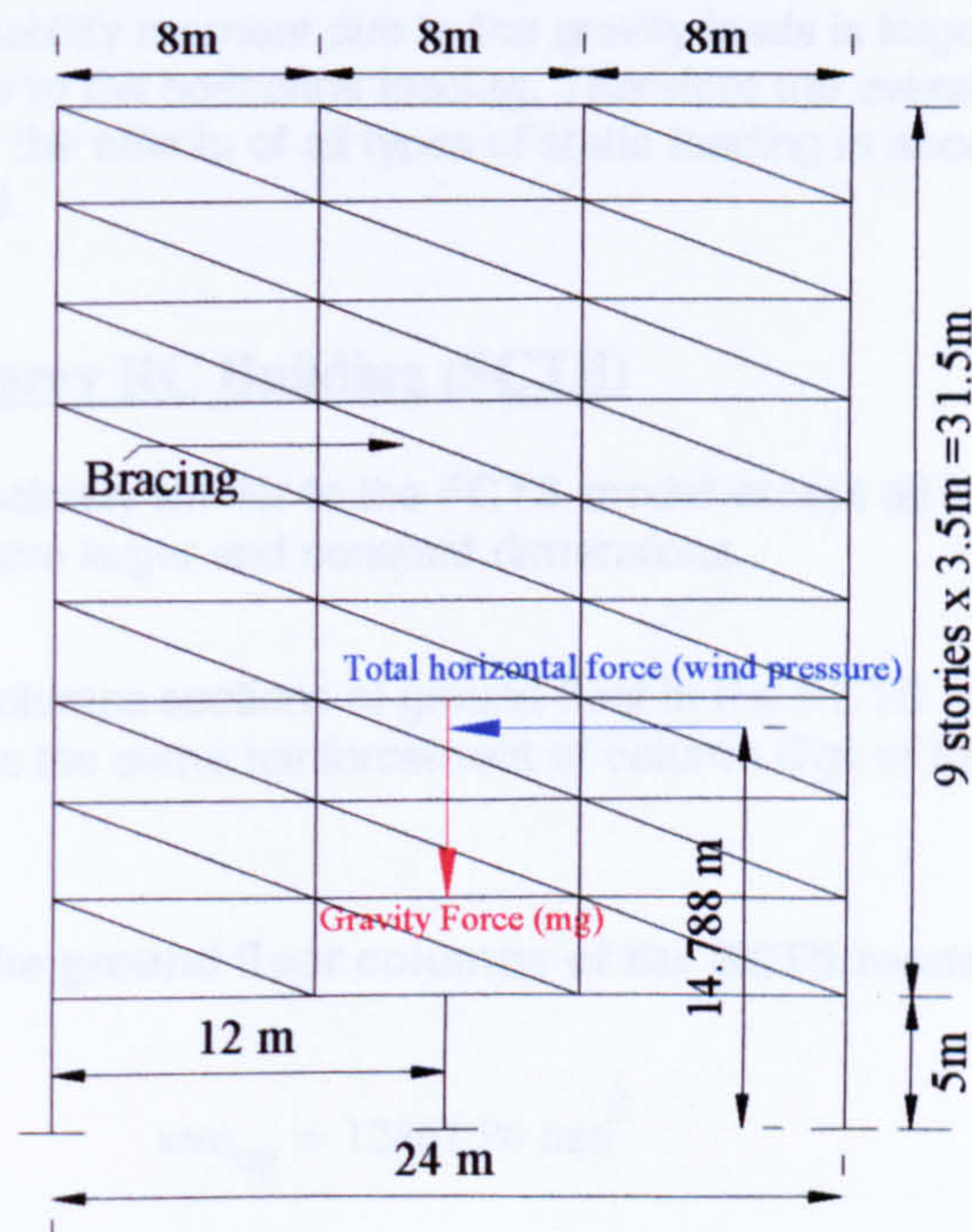
Then the applied tensile stress for bracing is  $\sigma_{tb} := \frac{f_b}{a_{sa}}$  ( $a_{sa}$  is the area of building bracing, refer to section 8)



$$\sigma_{tb} = 0.228 \text{ N} \cdot \text{mm}^{-2}$$

From the applied value of tensile stress above of the building bracing, it can be concluded that the bracing is subjected to low tensile stress. Therefore the lateral stability of building floors may be satisfied.

### **11.2 Stability Check (global building structure)**



Calculations of Building Overturning Moments

The overall stability of building depends on the resulting overturning moment from the horizontal forces (wind pressure), and the gravity forces of building, see figure above.

Total Horizontal Loading (total wind pressure on building)  $f_{wt} := \text{span} \cdot h \cdot q \cdot -1$

$$f_{wt} = 1.471 \times 10^3 \text{ kN}$$

The overturning moment around bottom corner of building due to the total horizontal force

$$m_{op} := f_{wt} \cdot 14.788 \cdot \text{m}$$

$$m_{op} = 2.175 \times 10^4 \text{ kN} \cdot \text{m}$$

The mass of building is  $\text{mass}_B := 6003200 \text{ Kg}$

The Gravity Force of Building is  $f_{gb} := \text{mass}_B \cdot 9.81 \cdot \text{N}$



$$f_{gb} = 5.889 \times 10^4 \text{ kN}$$

The stability moment around bottom corner of building due to the gravity force

$$m_{sg} := f_{gb} \cdot 12 \cdot m$$

$$m_{sg} = 7.067 \times 10^5 \text{ kN} \cdot m$$

From the values of moments due to the total horizontal loading & gravity force, it can be seen that the value of stability moment due to the gravity loads is larger than the overturning moment due to the horizontal loading. Therefore the overall global building structure is stable under the effects of all types of static loading in accordance with the requirements of BS8110.

### **Second Case Ten-Storey RC Building (SCTS)**

The SCTS model is absolutely similar to the FCTS model except all columns of the ground floor were modified to have larger and constant dimensions.

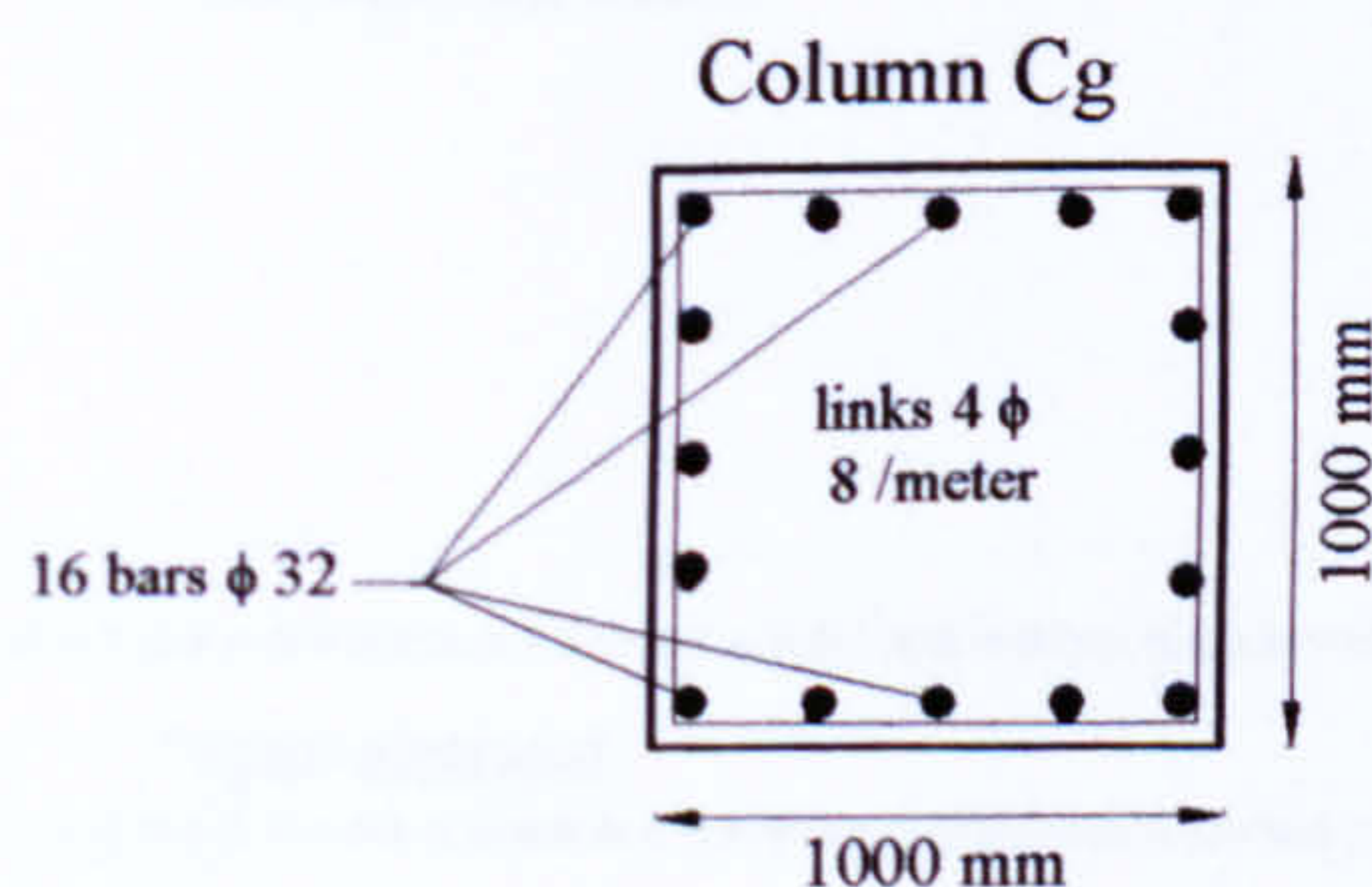
The Dimensions of all columns sections of ground floor in the SCTS model are 1m x 1m. Also the reinforcement is the same reinforcement of column Cgii of the ground floor of the FCTS model.

#### **Area of Steel Bars of the ground floor columns of the SCTS model**

$$16 \text{ bars } \phi 32 \text{ with area } \quad \text{area}_{cg} := 12867.96 \text{ mm}^2$$

The column links is 4 T8 / meter

#### **Ground Floor Columns of the SCTS model**





**APPENDIX III****ANSYS Input Data Batch File Of Transient Dynamic Analysis Of FCTS  
Under Both Horizontal And Vertical Earthquake Together**

```

/batch
/com,ANSYS RELEASE 5.7
/com, Structural
/prep7
c*****
/title, Transient Dynamic Analysis of FCTS under H+V EQ
c*****
c*****Element type*****
c*****
et,1,shell63          *elastic 4node shell element
keyopt,1,1,0
keyopt,1,2,0
keyopt,1,3,0
keyopt,1,5,2
keyopt,1,6,2
keyopt,1,7,0
keyopt,1,8,0
keyopt,1,9,0
c*****
et,2,beam44           *3D tapered beam
keyopt,2,2,0
keyopt,2,6,1
keyopt,2,9,9
keyopt,2,10,0
keyopt,2,7,0
keyopt,2,8,0
c*****
et,3,beam44           *3D tapered beam
keyopt,3,2,0
keyopt,3,6,1
keyopt,3,9,9
keyopt,3,10,0
keyopt,3,7,0
keyopt,3,8,0
c*****
et,4,beam44           *3D tapered beam
keyopt,4,2,0
keyopt,4,6,1
keyopt,4,9,9
keyopt,4,10,0
keyopt,4,7,0
keyopt,4,8,0
c*****
et,5,link8            *spar element
c*****
et,6,beam4            *3D elastic beam
keyopt,6,2,0
keyopt,6,6,1
keyopt,6,7,0
keyopt,6,9,9
keyopt,6,10,0

```



```

c*****
et,7,beam4          *3D elastic beam
keyopt,7,2,0
keyopt,7,6,1
keyopt,7,7,0
keyopt,7,9,9
keyopt,7,10,0
c*****
et,8,beam4          *3D elastic beam
keyopt,8,2,0
keyopt,8,6,1
keyopt,8,7,0
keyopt,8,9,9
keyopt,8,10,0
c*****
et,9,beam4          *3D elastic beam
keyopt,9,2,0
keyopt,9,6,1
keyopt,9,7,0
keyopt,9,9,9
keyopt,9,10,0
c*****
et,10,beam4         *3D elastic beam
keyopt,10,2,0
keyopt,10,6,1
keyopt,10,7,0
keyopt,10,9,9
keyopt,10,10,0
c*****
et,11,beam4         *3D elastic beam
keyopt,11,2,0
keyopt,11,6,1
keyopt,11,7,0
keyopt,11,9,9
keyopt,11,10,0
c*****
et,12,beam4         *3D elastic beam
keyopt,12,2,0
keyopt,12,6,1
keyopt,12,7,0
keyopt,12,9,9
keyopt,12,10,0
c*****
et,13,beam4         *3D elastic beam
keyopt,13,2,0
keyopt,13,6,1
keyopt,13,7,0
keyopt,13,9,9
keyopt,13,10,0
c*****
c*****Real constants of elements*****
c*****
r,1,0.15,0.15,0.15,0.15,,
c*****
r,2,0.1,1.33333333E-3,5.20833333E-4,0.125,0.2,,
rmodif,2,13,0,-0.275,0,
rmodif,2,21,0.125,0.2,
rmodif,2,7,0.1,1.33333333E-3,5.20833333E-4,0.125,0.2,,
rmodif,2,16,0,-0.275,0,
rmodif,2,23,,

```



```

rmodif,2,19,,,
rmodif,2,25,,,,,,
rmodif,2,31,,,,,,
rmodif,2,37,,,,,,
rmodif,2,43,,,,,,
rmodif,2,49,,,,, ,
rmodif,2,55, ,
c*****
r,3,0.1375,3.466145833E-3,7.161458333E-4,0.125,0.275, ,
rmodif,3,13,0,-0.35,0,
rmodif,3,21,0.125,0.275,
rmodif,3,7,0.1375,3.466145833E-3,7.161458333E-4,0.125,0.275, ,
rmodif,3,16,0,-0.35,0,
rmodif,3,23,,,
rmodif,3,19,,,
rmodif,3,25,,,,,,
rmodif,3,31,,,,,,
rmodif,3,37,,,,,,
rmodif,3,43,,,,,,
rmodif,3,49,,,,, ,
rmodif,3,55, ,
c*****
r,4,1.2,0.225,0.064,0.4,0.75, ,
rmodif,4,13,0,-0.825,0,
rmodif,4,21,0.4,0.75,
rmodif,4,7,1.2,0.225,0.064,0.4,0.75, ,
rmodif,4,16,0,-0.825,0,
rmodif,4,23,,,
rmodif,4,19,,,
rmodif,4,25,,,,,,
rmodif,4,31,,,,,,
rmodif,4,37,,,,,,
rmodif,4,43,,,,,,
rmodif,4,49,,,,, ,
rmodif,4,55, ,
c*****
r,5,0.225, ,
c*****
r,6,0.0625,3.255208333E-4,3.255208333E-4,0.25,0.25, ,
c*****
r,7,0.09,6.75E-4,6.75E-4,0.3,0.3, ,
c*****
r,8,0.1225,1.250520833E-3,1.250520833E-3,0.35,0.35, ,
c*****
r,9,0.16,2.133333333E-3,2.133333333E-3,0.4,0.4, ,
c*****
r,10,0.2025,3.4171875E-3,3.4171875E-3,0.45,0.45, ,
c*****
r,11,0.25,5.208333333E-3,5.208333333E-3,0.5,0.5, ,
c*****
r,12,0.64,0.034133333,0.034133333,0.8,0.8, ,
c*****
r,13,0.48,0.0144,0.0256,0.8,0.6,0,
c*****
c*****Concrete material properties of elements*****
c*****
mp,1,0
mp,ex,1,,20000000000
mp,prxy,1,,0.2
mp,dens,1,,4778.5

```



```

mp,ex,2,,200000000000
mp,prxy,2,,0.2
mp,dens,2,,2400
c*****
c*****Generation of slab & beam Nodes*****
c*****
n,1,0,0,0
ngen,25,1,1,1,1,1,0,0,
ngen,25,25,1,25,1,0,0,1,
ngen,10,625,1,625,1,0,3.5,0
c*****
c*****Generation of slab & beam elements*****
c*****
type,1
mat,1
real,1
e,1,26,27,2
egen,24,1,1,1,1
egen,24,25,1,24,1
egen,10,625,1,576,1
type,4
mat,2
real,4
e,1,2
egen,24,1,576,1,576,1
egen,4,200,576,1,578,1
type,3
mat,2
real,3
e,9,34
egen,24,25,5857,5857,1
egen,2,8,5857,5880,1
type,2
mat,2
real,2
e,1,26
egen,24,25,5905,5905,1
egen,2,4,5905,5928,1
egen,3,8,5929,5952,1
egen,2,4,5977,6000,1
e,101,102
egen,24,1,6025,6025,1
egen,3,200,6025,6048,1
type,3
mat,2
real,3
egen,10,625,5857,5904,1
type,2
mat,2
real,2
egen,10,625,5905,6096,1
type,2
mat,2
real,2
e,626,627
egen,24,1,8257,8257,1
egen,2,600,8257,8280,1
type,3
mat,2
real,3

```



```

e,826,827
egen,24,1,8305,8305,1
egen,2,200,8305,8328,1
type,2
mat,2
real,2
egen,9,625,8257,8304,1
type,3
mat,2
real,3
egen,9,625,8305,8352,1
c*****
c*****Generation of elements & nodes of ground floor columns*****
c*****
n,6251,0,-5,0
ngen,3,1,6251,6251,1,12,0,0
ngen,4,3,6251,6253,1,0,0,8
ngen,5,12,6251,6262,1,0,1,0
c*****
type,12
mat,2
real,12
e,6252,6264
egen,4,12,9129,9129,1
egen,4,3,9129,9132,1
e,6300,13
e,6303,213
e,6306,413
e,6309,613
type,13
mat,2
real,13
e,6251,6263
egen,4,12,9149,9149,1
egen,4,3,9149,9152,1
egen,2,2,9149,9164,1
e,6299,1
e,6302,201
e,6305,401
e,6308,601
e,6301,25
e,6304,225
e,6307,425
e,6310,625
c*****
c*****Generation of elements & nodes of first floor columns*****
c*****
n,6311,0,0.875,0
ngen,4,1,6311,6311,1,8,0,0
ngen,4,4,6311,6314,1,0,0,8
ngen,3,16,6311,6326,1,0,0.875,0
c*****
type,8
mat,2
real,8
e,1,6311
e,6311,6327
egen,2,16,9190,9190,1
e,6343,626
egen,2,3,9190,9191,1

```



```

e,25,6314
e,6346,650
egen,2,12,9190,9191,1
egen,2,3,9197,9198,1
e,601,6323
e,6355,1226
e,625,6326
e,6358,1250
type,9
mat,2
real,9
e,6312,6328
e,6328,6344
egen,2,1,9205,9206,1
egen,2,12,9205,9208,1
e,6315,6331
e,6331,6347
egen,2,3,9213,9214,1
egen,2,4,9213,9216,1
e,9,6312
e,6344,634
e,17,6313
e,6345,642
e,609,6324
e,6356,1234
e,617,6325
e,6357,1242
e,201,6315
e,6347,826
e,225,6318
e,6350,850
e,401,6319
e,6351,1026
e,425,6322
e,6354,1050
type,11
mat,2
real,11
e,6316,6332
e,6332,6348
egen,2,1,9237,9238,1
egen,2,4,9237,9240,1
e,209,6316
e,6348,834
e,217,6317
e,6349,842
e,409,6320
e,6352,1034
e,417,6321
e,6353,1042
c*****
c*****Generation of elements & nodes of second floor columns*****
c*****
ngen,2,16,6343,6358,1,0,1.75,0
ngen,3,16,6359,6374,1,0,0.875,0
c*****
type,8
mat,2
real,8
e,6359,6375

```



```

e,6375,6391
egen,2,3,9253,9254,1
egen,2,12,9253,9256,1
e,626,6359
e,6391,1251
e,650,6362
e,6394,1275
e,1226,6371
e,6403,1851
e,1250,6374
e,6406,1875
type,9
mat,2
real,9
e,6360,6376
e,6376,6392
egen,2,1,9269,9270,1
egen,2,12,9269,9272,1
e,6363,6379
e,6379,6395
egen,2,3,9277,9278,1
egen,2,4,9277,9280,1
e,634,6360
e,6392,1259
e,642,6361
e,6393,1267
e,1234,6372
e,6404,1859
e,1242,6373
e,6405,1867
e,826,6363
e,6395,1451
e,850,6366
e,6398,1475
e,1026,6367
e,6399,1651
e,1050,6370
e,6402,1675
type,11
mat,2
real,11
e,6364,6380
e,6380,6396
egen,2,1,9301,9302,1
egen,2,4,9301,9304,1
e,834,6364
e,6396,1459
e,842,6365
e,6397,1467
e,1034,6368
e,6400,1659
e,1042,6369
e,6401,1667
c*****
c*****Generation of elements & nodes of third floor columns*****
c*****
ngen,2,16,6391,6406,1,0,1.75,0
ngen,3,16,6407,6422,1,0,0.875,0
c*****
type,8

```



```

mat,2
real,8
e,6407,6423
e,6423,6439
egen,2,3,9317,9318,1
egen,2,12,9317,9320,1
e,1251,6407
e,6439,1876
e,1275,6410
e,6442,1900
e,1851,6419
e,6451,2476
e,1875,6422
e,6454,2500
type,9
mat,2
real,9
e,6408,6424
e,6424,6440
egen,2,1,9333,9334,1
egen,2,12,9333,9336,1
e,6411,6427
e,6427,6443
egen,2,3,9341,9342,1
egen,2,4,9341,9344,1
e,1259,6408
e,6440,1884
e,1267,6409
e,6441,1892
e,1859,6420
e,6452,2484
e,1867,6421
e,6453,2492
e,1451,6411
e,6443,2076
e,1475,6414
e,6446,2100
e,1651,6415
e,6447,2276
e,1675,6418
e,6450,2300
type,10
mat,2
real,10
e,6412,6428
e,6428,6444
egen,2,1,9365,9366,1
egen,2,4,9365,9368,1
e,1459,6412
e,6444,2084
e,1467,6413
e,6445,2092
e,1659,6416
e,6448,2284
e,1667,6417
e,6449,2292
c*****
c*****Generation of elements & nodes of fourth floor columns*****
c*****
ngen,2,16,6439,6454,1,0,1.75,0

```



```
ngen,3,16,6455,6470,1,0,0.875,0
```

```
c*****
```

```
type,7
```

```
mat,2
```

```
real,7
```

```
e,6455,6471
```

```
e,6471,6487
```

```
egen,2,3,9381,9382,1
```

```
egen,2,12,9381,9384,1
```

```
e,1876,6455
```

```
e,6487,2501
```

```
e,1900,6458
```

```
e,6490,2525
```

```
e,2476,6467
```

```
e,6499,3101
```

```
e,2500,6470
```

```
e,6502,3125
```

```
type,8
```

```
mat,2
```

```
real,8
```

```
e,6456,6472
```

```
e,6472,6488
```

```
egen,2,1,9397,9398,1
```

```
egen,2,12,9397,9400,1
```

```
e,6459,6475
```

```
e,6475,6491
```

```
egen,2,3,9405,9406,1
```

```
egen,2,4,9405,9408,1
```

```
e,1884,6456
```

```
e,6488,2509
```

```
e,1892,6457
```

```
e,6489,2517
```

```
e,2484,6468
```

```
e,6500,3109
```

```
e,2492,6469
```

```
e,6501,3117
```

```
e,2076,6459
```

```
e,6491,2701
```

```
e,2100,6462
```

```
e,6494,2725
```

```
e,2276,6463
```

```
e,6495,2901
```

```
e,2300,6466
```

```
e,6498,2925
```

```
type,10
```

```
mat,2
```

```
real,10
```

```
e,6460,6476
```

```
e,6476,6492
```

```
egen,2,1,9429,9430,1
```

```
egen,2,4,9429,9432,1
```

```
e,2084,6460
```

```
e,6492,2709
```

```
e,2092,6461
```

```
e,6493,2717
```

```
e,2284,6464
```

```
e,6496,2909
```

```
e,2292,6465
```

```
e,6497,2917
```



```

c*****
c*****Generation of elements & nodes of fifth floor columns*****
c*****
ngen,2,16,6487,6502,1,0,1.75,0
ngen,3,16,6503,6518,1,0,0.875,0
c*****
type,7
mat,2
real,7
e,6503,6519
e,6519,6535
egen,2,3,9494,9495,1
egen,2,12,9494,9497,1
e,2501,6503
e,6535,3126
e,2525,6506
e,6538,3150
e,3101,6515
e,6547,3726
e,3125,6518
e,6550,3750
type,8
mat,2
real,8
e,6504,6520
e,6520,653
egen,2,1,9510,9511,1
egen,2,12,9510,9513,1
e,6507,6523
e,6523,6539
egen,2,3,9518,9519,1
egen,2,4,9518,9521,1
e,2509,6504
e,6536,3134
e,2517,6505
e,6537,3142
e,3109,6516
e,6548,3734
e,3117,6517
e,6549,3742
e,2701,6507
e,6539,3326
e,2725,6510
e,6542,3350
e,2901,6511
e,6543,3526
e,2925,6514
e,6546,3550
type,10
mat,2
real,10
e,6508,6524
e,6524,6540
egen,2,1,9542,9543,1
egen,2,4,9542,9545,1
e,2709,6508
e,6540,3334
e,2717,6509
e,6541,3342
e,2909,6512

```



```

e,6544,3534
e,2917,6513
e,6545,3542
c*****
c*****Generation of elements & nodes of sixth floor columns*****
c*****
ngen,2,16,6535,6550,1,0,1.75,0
ngen,3,16,6551,6566,1,0,0.875,0
c*****
type,7
mat,2
real,7
e,6551,6567
e,6567,6583
egen,2,3,9558,9559,1
egen,2,12,9558,9561,1
e,3126,6551
e,6583,3751
e,3150,6554
e,6586,3775
e,3726,6563
e,6595,4351
e,3750,6566
e,6598,4375
egen,3,1,9558,9559,1
egen,3,4,9558,9559,1
egen,3,4,9560,9561,1
egen,3,1,9562,9563,1
e,3134,6552
e,6584,3759
e,3142,6553
e,6585,3767
e,3326,6555
e,6587,3951
e,3350,6558
e,6590,3975
e,3526,6559
e,6591,4151
e,3550,6562
e,6594,4175
e,3734,6564
e,6596,4359
e,3742,6565
e,6597,4367
type,8
mat,2
real,8
e,6556,6572
e,6572,6588
egen,2,1,9608,9609,1
egen,2,4,9608,9611,1
e,3334,6556
e,6588,3959
e,3342,6557
e,6589,3967
e,3534,6560
e,6592,4159
e,3542,6561
e,6593,4167

```



```

c*****
c*****Generation of elements & nodes of seventh floor columns*****
c*****
ngen,2,16,6583,6598,1,0,1.75,0
ngen,3,16,6599,6614,1,0,0.875,0
c*****
type,6
mat,2
real,6
e,6599,6615
e,6615,6631
egen,2,3,9624,9625,1
egen,2,12,9624,9627,1
e,3751,6599
e,6631,4376
e,3775,6602
e,6634,4400
e,4351,6611
e,6643,4976
e,4375,6614
e,6646,5000
type,7
mat,2
real,7
e,6600,6616
e,6616,6632
egen,2,1,9640,9641,1
egen,2,12,9640,9643,1
e,6603,6619
e,6619,6635
egen,2,3,9648,9649,1
egen,2,4,9648,9651,1
e,3759,6600
e,6632,4384
e,3767,6601
e,6633,4392
e,4359,6612
e,6644,4984
e,4367,6613
e,6645,4992
e,3951,6603
e,6635,4576
e,3975,6606
e,6638,4600
e,4151,6607
e,6639,4776
e,4175,6610
e,6642,4800
type,8
mat,2
real,8
e,6604,6620
e,6620,6636
egen,2,1,9672,9673,1
egen,2,4,9672,9675,1
e,3959,6604
e,6636,4584
e,3967,6605
e,6637,4592
e,4159,6608

```



```

e,6640,4784
e,4167,6609
e,6641,4792
c*****
c*****Generation of elements & nodes of eighth and ninth floor columns*****
c*****
ngen,2,16,6631,6646,1,0,1.75,0
ngen,3,16,6647,6662,1,0,0.875,0
ngen,2,16,6679,6694,1,0,1.75,0
ngen,3,16,6695,6710,1,0,0.875,0
c*****
type,6
mat,2
real,6
e,6647,6663
e,6663,6679
egen,4,1,9688,9689,1
egen,4,4,9688,9691,1
egen,4,4,9692,9695,1
egen,2,48,9688,9719,1
e,4376,6647
e,6679,5001
e,4384,6648
e,6680,5009
e,4392,6649
e,6681,5017
e,4400,6650
e,6682,5025
e,4576,6651
e,6683,5201
e,4584,6652
e,6684,5209
e,4592,6653
e,6685,5217
e,4600,6654
e,6686,5225
e,4776,6655
e,6687,5401
e,4784,6656
e,6688,5409
e,4792,6657
e,6689,5417
e,4800,6658
e,6690,5425
e,4976,6659
e,6691,5601
e,4984,6660
e,6692,5609
e,4992,6661
e,6693,5617
e,5000,6662
e,6694,5625
e,5001,6695
e,6727,5626
e,5009,6696
e,6728,5634
e,5017,6697
e,6729,5642
e,5025,6698
e,6730,5650

```



```

e,5201,6699
e,6731,5826
e,5209,6700
e,6732,5834
e,5217,6701
e,6733,5842
e,5225,6702
e,6734,5850
e,5401,6703
e,6735,6026
e,5409,6704
e,6736,6034
e,5417,6705
e,6737,6042
e,5425,6706
e,6738,6050
e,5601,6707
e,6739,6226
e,5609,6708
e,6740,6234
e,5617,6709
e,6741,6242
e,5625,6710
e,6742,6250
c*****
c*****Generation of bracing elements of model*****
c*****
type,5
mat,2
real,5
e,609,1226
egen,3,8,9816,9816,1
egen,9,625,9816,9818,1
e,1,634
egen,3,8,9843,9843,1
egen,9,625,9843,9845,1
e,601,1026
e,401,826
e,201,626
egen,9,625,9870,9872,1
e,25,850
egen,3,200,9897,9897,1
egen,9,625,9897,9899,1
c*****
c*****Boundary conditions of model*****
c*****
d,6251,ux,0
d,6251,uy,0
d,6251,uz,0
d,6251,rotx,0
d,6251,roty,0
d,6251,rotz,0
d,6252,ux,0
d,6252,uy,0
d,6252,uz,0
d,6252,rotx,0
d,6252,roty,0
d,6252,rotz,0
d,6253,ux,0
d,6253,uy,0

```



```
d,6253,uz,0
d,6253,rotx,0
d,6253,roty,0
d,6253,rotz,0
d,6254,ux,0
d,6254,uy,0
d,6254,uz,0
d,6254,rotx,0
d,6254,roty,0
d,6254,rotz,0
d,6255,ux,0
d,6255,uy,0
d,6255,uz,0
d,6255,rotx,0
d,6255,roty,0
d,6255,rotz,0
d,6256,ux,0
d,6256,uy,0
d,6256,uz,0
d,6256,rotx,0
d,6256,roty,0
d,6256,rotz,0
d,6257,ux,0
d,6257,uy,0
d,6257,uz,0
d,6257,rotx,0
d,6257,roty,0
d,6257,rotz,0
d,6258,ux,0
d,6258,uy,0
d,6258,uz,0
d,6258,rotx,0
d,6258,roty,0
d,6258,rotz,0
d,6259,ux,0
d,6259,uy,0
d,6259,uz,0
d,6259,rotx,0
d,6259,roty,0
d,6259,rotz,0
d,6260,ux,0
d,6260,uy,0
d,6260,uz,0
d,6260,rotx,0
d,6260,roty,0
d,6260,rotz,0
d,6261,ux,0
d,6261,uy,0
d,6261,uz,0
d,6261,rotx,0
d,6261,roty,0
d,6261,rotz,0
d,6262,ux,0
d,6262,uy,0
d,6262,uz,0
d,6262,rotx,0
d,6262,roty,0
d,6262,rotz,0
```



```

c*****
c*****Analysis type*****
c*****
antype,4
trnpt,full
c*****
c*****Load steps & Solution control options*****
c*****
outres,nsol,all          load step No.1
alphad,0.09
betad,0.09
time,0.1
kbc,1
c*****
acel,0,0.981,0,          gravity loads
lswrite,1,
c*****
c*****
time,0.2          load step No.2
kbc,1
c*****
acel,0,1.962,0,          gravity loads
lswrite,2,
c*****
c*****
time,0.3          load step No.3
kbc,1
c*****
acel,0,2.943,0,          gravity loads
lswrite,3,
c*****
c*****
time,0.4          load step No.4
kbc,1
c*****
acel,0,3.924,0,          gravity loads
lswrite,4,
c*****
c*****
time,0.5          load step No.5
kbc,1
c*****
acel,0,4.905,0,          gravity loads
lswrite,5,
c*****
c*****
time,0.6          load step No.6
kbc,1
c*****
acel,0,5.886,0,          gravity loads
lswrite,6,
c*****
c*****
time,0.7          load step No.7
kbc,1
c*****
acel,0,6.867,0,          gravity loads
lswrite,7,
c*****
c*****

```



```

time,0.8                                load step No.8
kbc,1
c*****
acel,0,7.848,0,                        gravity loads
lswrite,8,
c*****
c*****
time,0.9                                load step No.9
kbc,1
c*****
acel,0,8.829,0,                        gravity loads
lswrite,9,
c*****
c*****
deltim,0.1,0,0
time,15                                load step No.10
kbc,1
c*****
acel,0,9.81,0,                        gravity loads
lswrite,10,
c*****
c*****
deltim,0.01,0,0                        load step No.11
alphad,0.029
betad,0.028
time,25.19
kbc,1
c*****
flst,2,12,1,orde,2
fitem,2,6251
fitem,2,-6262
*dim,htime,table,1019,1,time
d,p51x,,%htime%,,,ux,uz,,, (horizontal displacement time-history)
flst,2,12,1,ORDE,2
fitem,2,6251
fitem,2,-6262
*dim,vtime,table,1019,1,time
d,p51x,,%vtime%,,,uy,,,, (vertical displacement time-history)
lswrite,11,
c*****
c*****Output control & solution*****
c*****
outres,nsol,all,                        solution for DOF at nodes
/config,nres,1500
/lgwrite,file,lgw,
/output,file,out,
/solu
lssolve,1,11,1,
finish

```



APPENDIX IV

Spreadsheet of Assessment Results

Transient Dynamic Analysis of FCTS (Under Horizontal Earthquake Only)  
Columns Assessment for Axial Load and Transverse Bending Moments

Bottom section of column  
Min. Applied Axial Load (+ compressive / - tensile)  
Absolute Maximum Bending Moments

General Information			Section Properties			F <sub>cu</sub> (N/mm <sup>2</sup> )	F <sub>y</sub> (N/mm <sup>2</sup> )	Applied Loads			Failure Surface Assessment			BS8110 Assessment		
Level	Column ID	FE No.	Height (mm)	Breadth (mm)	A <sub>s</sub> (mm <sup>2</sup> )			Axial (kN)	M <sub>xx</sub> (kN.m)	M <sub>zz</sub> (kN.m)	U <sub>mxx</sub> (kN.m)	U <sub>mzz</sub> (kN.m)	Margin	Acceptability	Margin	Acceptability
ground	A31	9129	800	800	12867.96	40	503.8	5560	1390	1570	2564.59	2564.59	1.02	PASSED	0.98	FAILED
ground	A32	9130	800	800	12867.96	40	503.8	5540	902	959	2564.67	2564.67	1.85	PASSED	1.57	PASSED
ground	A33	9131	800	800	12867.96	40	503.8	5530	498	351	2564.71	2564.71	5.03	PASSED	3.37	PASSED
ground	A34	9132	800	800	12867.96	40	503.8	5510	215	274	2564.78	2564.78	10.21	PASSED	5.89	PASSED
ground	B31	9133	800	800	12867.96	40	503.8	10300	1400	1490	1936.98	1936.98	0.85	FAILED	0.87	FAILED
ground	B32	9134	800	800	12867.96	40	503.8	10200	922	909	1956.87	1956.87	1.98	PASSED	1.39	PASSED
ground	B33	9135	800	800	12867.96	40	503.8	10200	445	329	1956.87	1956.87	9.25	PASSED	3.16	PASSED
ground	B34	9136	800	800	12867.96	40	503.8	10200	65.4	252	1956.87	1956.87	37.62	PASSED	6.82	PASSED
ground	C31	9137	800	800	12867.96	40	503.8	10200	1450	1490	1956.87	1956.87	0.84	FAILED	0.87	FAILED
ground	C32	9138	800	800	12867.96	40	503.8	10200	945	907	1956.87	1956.87	1.94	PASSED	1.37	PASSED
ground	C33	9139	800	800	12867.96	40	503.8	10200	438	328	1956.87	1956.87	9.44	PASSED	3.2	PASSED
ground	C34	9140	800	800	12867.96	40	503.8	10200	69.3	252	1956.87	1956.87	37.29	PASSED	6.77	PASSED
ground	D31	9141	800	800	12867.96	40	503.8	5490	1470	1580	2564.85	2564.85	0.97	FAILED	0.95	FAILED
ground	D32	9142	800	800	12867.96	40	503.8	5470	960	957	2564.9	2564.9	1.76	PASSED	1.53	PASSED
ground	D33	9143	800	800	12867.96	40	503.8	5460	467	343	2564.93	2564.93	5.28	PASSED	3.53	PASSED
ground	D34	9144	800	800	12867.96	40	503.8	5440	209	278	2564.97	2564.97	10.07	PASSED	5.89	PASSED
ground	A35	9145	800	800	12867.96	40	503.8	5500	546	879	2564.82	2564.82	2.56	PASSED	1.99	PASSED
ground	B35	9146	800	800	12867.96	40	503.8	10200	539	830	1956.87	1956.87	3.24	PASSED	1.75	PASSED
ground	C35	9147	800	800	12867.96	40	503.8	10200	576	832	1956.87	1956.87	3.11	PASSED	1.72	PASSED
ground	D35	9148	800	800	12867.96	40	503.8	5430	568	895	2564.98	2564.98	2.46	PASSED	1.94	PASSED
ground	A11	9149	600	800	13980.1	40	503.8	5440	935	732	2161.96	1905.57	1.72	PASSED	1.43	PASSED
ground	A12	9150	600	800	13980.1	40	503.8	5430	623	426	2162.9	1905.89	3.26	PASSED	2.25	PASSED
ground	A13	9151	600	800	13980.1	40	503.8	5420	366	170	2163.83	1906.2	8.18	PASSED	4.32	PASSED
ground	A14	9152	600	800	13980.1	40	503.8	5410	155	186	2164.77	1906.52	14.88	PASSED	6.95	PASSED
ground	B11	9153	600	800	13980.1	40	503.8	5390	1030	777	2166.62	1907.15	1.54	PASSED	1.32	PASSED
ground	B12	9154	600	800	13980.1	40	503.8	5380	685	426	2167.55	1907.47	3	PASSED	2.12	PASSED
ground	B13	9155	600	800	13980.1	40	503.8	5370	346	188	2168.47	1907.78	8.16	PASSED	4.38	PASSED
ground	B14	9156	600	800	13980.1	40	503.8	5360	8.51	275	2169.39	1908.09	14.1	PASSED	6.82	PASSED
ground	C11	9157	600	800	13980.1	40	503.8	4760	1090	780	2220.43	1925.8	1.41	PASSED	1.27	PASSED
ground	C12	9158	600	800	13980.1	40	503.8	4750	724	428	2221.22	1926.08	2.64	PASSED	2.05	PASSED
ground	C13	9159	600	800	13980.1	40	503.8	4740	361	187	2222	1926.36	6.86	PASSED	4.29	PASSED
ground	C14	9160	600	800	13980.1	40	503.8	4730	23.9	277	2222.78	1926.64	11.72	PASSED	6.61	PASSED
ground	D11	9161	600	800	13980.1	40	503.8	3520	1120	730	2281.68	1944.11	1.28	PASSED	1.27	PASSED
ground	D12	9162	600	800	13980.1	40	503.8	3510	756	420	2281.88	1943.21	2.15	PASSED	1.99	PASSED
ground	D13	9163	600	800	13980.1	40	503.8	3500	393	182	2282.08	1942.3	4.82	PASSED	4.06	PASSED



General Information			Section Properties			Fcu (N/mm <sup>2</sup> )		Fy (N/mm <sup>2</sup> )		Applied Loads			Failure Surface Assessment			BS8110 Assessment		
Level	Column ID	FE No.	Height (mm)	Breadth (mm)	As (mm <sup>2</sup> )					Axial (kN)	Mxx (kN.m)	Mzz (kN.m)	Umx (kN.m)	Umzz (kN.m)	Margin	Acceptability	Margin	Acceptability
ground	D14	9164	600	800	13980.1	40	503.8	3490	172	201	2282.28	201	1941.39	7.54	PASSED	6.14	PASSED	
ground	A51	9165	600	800	13980.1	40	503.8	3540	1060	743	2281.27	743	1945.91	1.32	PASSED	1.3	PASSED	
ground	A52	9166	600	800	13980.1	40	503.8	3520	711	428	2281.68	428	1944.11	2.22	PASSED	2.06	PASSED	
ground	A53	9167	600	800	13980.1	40	503.8	3510	419	178	2281.88	178	1943.21	4.64	PASSED	3.9	PASSED	
ground	A54	9168	600	800	13980.1	40	503.8	3500	179	202	2282.08	202	1942.3	7.4	PASSED	6.03	PASSED	
ground	B51	9169	600	800	13980.1	40	503.8	4770	1070	794	2219.64	794	1925.52	1.41	PASSED	1.28	PASSED	
ground	B52	9170	600	800	13980.1	40	503.8	4760	720	436	2220.43	436	1925.8	2.63	PASSED	2.04	PASSED	
ground	B53	9171	600	800	13980.1	40	503.8	4750	369	185	2221.22	185	1926.08	6.78	PASSED	4.24	PASSED	
ground	B54	9172	600	800	13980.1	40	503.8	4740	21.6	281	2222	281	1926.36	11.59	PASSED	6.55	PASSED	
ground	C51	9173	600	800	13980.1	40	503.8	5300	1040	791	2174.86	791	1909.96	1.5	PASSED	1.3	PASSED	
ground	C52	9174	600	800	13980.1	40	503.8	5290	692	434	2175.76	434	1910.27	2.91	PASSED	2.09	PASSED	
ground	C53	9175	600	800	13980.1	40	503.8	5280	347	186	2176.66	186	1910.58	8.03	PASSED	4.39	PASSED	
ground	C54	9176	600	800	13980.1	40	503.8	5260	10.1	279	2178.45	279	1911.19	13.48	PASSED	6.71	PASSED	
ground	D51	9177	600	800	13980.1	40	503.8	5370	995	748	2168.47	748	1907.78	1.61	PASSED	1.36	PASSED	
ground	D52	9178	600	800	13980.1	40	503.8	5360	665	435	2169.39	435	1908.09	3.03	PASSED	2.15	PASSED	
ground	D53	9179	600	800	13980.1	40	503.8	5350	342	168	2170.31	168	1908.41	8.64	PASSED	4.56	PASSED	
ground	D54	9180	600	800	13980.1	40	503.8	5340	149	190	2171.22	190	1908.72	14.63	PASSED	6.93	PASSED	
ground	A15	9181	600	800	13980.1	40	503.8	5390	310	492	2166.62	492	1907.15	4.45	PASSED	2.85	PASSED	
ground	B15	9182	600	800	13980.1	40	503.8	5350	334	625	2170.31	625	1908.41	3.4	PASSED	2.34	PASSED	
ground	C15	9183	600	800	13980.1	40	503.8	4720	367	630	2223.56	630	1926.92	2.97	PASSED	2.26	PASSED	
ground	D15	9184	600	800	13980.1	40	503.8	3470	339	511	2282.67	511	1939.57	2.93	PASSED	2.63	PASSED	
ground	A55	9185	600	800	13980.1	40	503.8	3490	326	517	2282.28	517	1941.39	2.96	PASSED	2.64	PASSED	
ground	B55	9186	600	800	13980.1	40	503.8	4730	343	639	2222.78	639	1926.64	3.01	PASSED	2.27	PASSED	
ground	C55	9187	600	800	13980.1	40	503.8	5250	344	635	2179.35	635	1911.5	3.26	PASSED	2.29	PASSED	
ground	D55	9188	600	800	13980.1	40	503.8	5330	324	502	2172.13	502	1909.03	4.24	PASSED	2.77	PASSED	
1	A11	9189			3890			3365.28										
1	A12	9190			3890			3365.28										
1	A13	9191			3880			3365.28										
1	A14	9192			3880			3365.28										
1	A52	9193	350	350	5180.48	30	503.8	2710	31.6	36.9	146.66	36.9	146.66	9.11	PASSED	3.16	PASSED	
1	A53	9194	350	350	5180.48	30	503.8	2710	14.3	3.57	146.66	3.57	146.66	99.02	PASSED	9.54	PASSED	
1	A51	9195	350	350	5180.48	30	503.8	2710	54.4	73.9	146.66	73.9	146.66	2.55	PASSED	1.63	PASSED	
1	A54	9196	350	350	5180.48	30	503.8	2710	14.7	37.8	146.66	37.8	146.66	13.08	PASSED	3.47	PASSED	
1	D12	9197	350	350	5180.48	30	503.8	2700	29.5	37	147.74	37	147.74	9.75	PASSED	3.22	PASSED	
1	D13	9198	350	350	5180.48	30	503.8	2700	15.2	3.71	147.74	3.71	147.74	89.16	PASSED	9.06	PASSED	
1	D52	9199			3750			3365.28										
1	D53	9200			3740			3365.28										
1	D11	9201	350	350	5180.48	30	503.8	2700	51.3	73.4	147.74	73.4	147.74	2.72	PASSED	1.66	PASSED	
1	D14	9202	350	350	5180.48	30	503.8	2690	15.2	38.2	148.82	38.2	148.82	13.14	PASSED	3.48	PASSED	
1	D51	9203			3750			3365.28										
1	D54	9204			3740			3365.28										
1	A22	9205	400	400	8947.25	30	503.8	2710	51.7	51	410.7	51	410.7	12.25	PASSED	5.94	PASSED	
1	A23	9206	400	400	8947.25	30	503.8	2710	22	17.6	410.7	17.6	410.7	52.8	PASSED	14.65	PASSED	



General Information			Section Properties			F <sub>cu</sub> (N/mm <sup>2</sup> )	F <sub>y</sub> (N/mm <sup>2</sup> )	Applied Loads			Failure Surface Assessment				BS8110 Assessment		
Level	Column ID	FE No.	Height (mm)	Breadth (mm)	A <sub>s</sub> (mm <sup>2</sup> )			Axial (kN)	M <sub>xx</sub> (kN.m)	M <sub>zz</sub> (kN.m)	U <sub>mxx</sub> (kN.m)	U <sub>mzz</sub> (kN.m)	Margin	Acceptability	Margin	Acceptability	
1	A42	9207	400	400	8947.25	30	503.8	2470	46.1	36.4	432.55	432.55	432.55	15.43	PASSED	7.12	PASSED
1	A43	9208	400	400	8947.25	30	503.8	2470	24.1	15.4	432.55	432.55	432.55	44.74	PASSED	14.28	PASSED
1	D22	9209	400	400	8947.25	30	503.8	2470	44.3	36.9	432.55	432.55	432.55	15.82	PASSED	7.31	PASSED
1	D23	9210	400	400	8947.25	30	503.8	2460	25.4	15.4	433.45	433.45	433.45	42.23	PASSED	13.7	PASSED
1	D42	9211	400	400	8947.25	30	503.8	2580	50	51.1	422.58	422.58	422.58	12	PASSED	6.05	PASSED
1	D43	9212	400	400	8947.25	30	503.8	2580	23.3	17.5	422.58	422.58	422.58	46.31	PASSED	14.15	PASSED
1	B12	9213	400	400	8947.25	30	503.8	4020	35.4	87.4	276.76	276.76	276.76	8.18	PASSED	2.82	PASSED
1	B13	9214	400	400	8947.25	30	503.8	4020	22.4	8.19	276.76	276.76	276.76	121.1	PASSED	11.13	PASSED
1	B52	9215	400	400	8947.25	30	503.8	3460	36.4	96.6	338.88	338.88	338.88	7.94	PASSED	3.15	PASSED
1	B53	9216	400	400	8947.25	30	503.8	3460	19.4	8.76	338.88	338.88	338.88	130.69	PASSED	15.38	PASSED
1	C12	9217	400	400	8947.25	30	503.8	3480	38.6	96.4	336.87	336.87	336.87	7.82	PASSED	3.12	PASSED
1	C13	9218	400	400	8947.25	30	503.8	3480	20	8.83	336.87	336.87	336.87	125.82	PASSED	14.87	PASSED
1	C52	9219	400	400	8947.25	30	503.8	3920	33.5	87.8	288.46	288.46	288.46	8.57	PASSED	2.95	PASSED
1	C53	9220	400	400	8947.25	30	503.8	3920	21.1	7.98	288.46	288.46	288.46	134.05	PASSED	12.28	PASSED
1	A21	9221	400	400	8947.25	30	503.8	2710	96	84.5	410.7	410.7	410.7	5.14	PASSED	3.29	PASSED
1	A24	9222	400	400	8947.25	30	503.8	2700	65.9	17.2	411.62	411.62	411.62	14.77	PASSED	5.73	PASSED
1	A41	9223	400	400	8947.25	30	503.8	2470	83	58	432.55	432.55	432.55	7.01	PASSED	4.07	PASSED
1	A44	9224	400	400	8947.25	30	503.8	2460	58	6.75	433.45	433.45	433.45	17.99	PASSED	7.14	PASSED
1	D21	9225	400	400	8947.25	30	503.8	2470	80.5	58.7	432.55	432.55	432.55	7.16	PASSED	4.15	PASSED
1	D24	9226	400	400	8947.25	30	503.8	2460	58.7	6.82	433.45	433.45	433.45	17.69	PASSED	7.05	PASSED
1	D41	9227	400	400	8947.25	30	503.8	2590	93.7	85.5	421.67	421.67	421.67	5.1	PASSED	3.36	PASSED
1	D44	9228	400	400	8947.25	30	503.8	2580	67	17.4	422.58	422.58	422.58	13.89	PASSED	5.75	PASSED
1	B11	9229	400	400	8947.25	30	503.8	4020	48.6	167	276.76	276.76	276.76	2.47	PASSED	1.52	PASSED
1	B14	9230	400	400	8947.25	30	503.8	4010	18.2	71.7	277.95	277.95	277.95	13.26	PASSED	3.6	PASSED
1	B51	9231	400	400	8947.25	30	503.8	3460	54.1	185	338.88	338.88	338.88	2.64	PASSED	1.68	PASSED
1	B54	9232	400	400	8947.25	30	503.8	3450	21.7	79	339.89	339.89	339.89	12.13	PASSED	3.97	PASSED
1	C11	9233	400	400	8947.25	30	503.8	3490	57	184	335.86	335.86	335.86	2.61	PASSED	1.67	PASSED
1	C14	9234	400	400	8947.25	30	503.8	3480	21	78.9	336.87	336.87	336.87	12.21	PASSED	3.95	PASSED
1	C51	9235	400	400	8947.25	30	503.8	3920	45.9	168	288.46	288.46	288.46	2.62	PASSED	1.59	PASSED
1	C54	9236	400	400	8947.25	30	503.8	3910	19.1	71.8	289.62	289.62	289.62	13.58	PASSED	3.74	PASSED
1	B22	9237	500	500	12867.96	30	503.8	5460	32.9	154	610.54	610.54	610.54	12.09	PASSED	3.73	PASSED
1	B23	9238	500	500	12867.96	30	503.8	5450	19.6	58	611.99	611.99	611.99	68.55	PASSED	9.58	PASSED
1	B42	9239	500	500	12867.96	30	503.8	5310	12.8	137	632.14	632.14	632.14	15.89	PASSED	4.49	PASSED
1	B43	9240	500	500	12867.96	30	503.8	5310	18.1	54.9	632.14	632.14	632.14	74.91	PASSED	10.48	PASSED
1	C22	9241	500	500	12867.96	30	503.8	5310	14.7	136	632.14	632.14	632.14	16.04	PASSED	4.5	PASSED
1	C23	9242	500	500	12867.96	30	503.8	5300	17.4	55	633.57	633.57	633.57	75.19	PASSED	10.52	PASSED
1	C42	9243	500	500	12867.96	30	503.8	5410	30.7	156	617.78	617.78	617.78	11.97	PASSED	3.74	PASSED
1	C43	9244	500	500	12867.96	30	503.8	5410	18.2	58.2	617.78	617.78	617.78	68.93	PASSED	9.7	PASSED
1	B21	9245	500	500	12867.96	30	503.8	5460	75.7	251	610.54	610.54	610.54	4.67	PASSED	2.23	PASSED
1	B24	9246	500	500	12867.96	30	503.8	5450	55.6	38.1	611.99	611.99	611.99	56.17	PASSED	9.13	PASSED
1	B41	9247	500	500	12867.96	30	503.8	5320	41.4	220	630.71	630.71	630.71	6.49	PASSED	2.71	PASSED
1	B44	9248	500	500	12867.96	30	503.8	5300	46.4	27.1	633.57	633.57	633.57	83.57	PASSED	11.62	PASSED
1	C21	9249	500	500	12867.96	30	503.8	5310	42.4	218	632.14	632.14	632.14	6.59	PASSED	2.74	PASSED



General Information			Section Properties			F <sub>cu</sub> (N/mm <sup>2</sup> )	F <sub>y</sub> (N/mm <sup>2</sup> )	Applied Loads			Failure Surface Assessment			BS8110 Assessment		
Level	Column ID	FE No.	Height (mm)	Breadth (mm)	A <sub>s</sub> (mm <sup>2</sup> )			Axial (kN)	M <sub>xx</sub> (kN.m)	M <sub>zz</sub> (kN.m)	U <sub>mxx</sub> (kN.m)	U <sub>mzz</sub> (kN.m)	Margin	Acceptability	Margin	Acceptability
1	C24	9250	500	500	12867.96	30	503.8	5300	44	26	633.57	633.57	91.49	PASSED	12.23	PASSED
1	C41	9251	500	500	12867.96	30	503.8	5420	74.3	254	616.33	616.33	4.63	PASSED	2.23	PASSED
1	C44	9252	500	500	12867.96	30	503.8	5400	58.3	39.4	619.22	619.22	51.62	PASSED	8.83	PASSED
2	A12	9253			3230			2941.17								
2	A13	9254			3230			2941.17								
2	A52	9255	350	350	4021.24	30	503.8	2380	14.6	41.3	132.3	132.3	9.12	PASSED	2.9	PASSED
2	A53	9256	350	350	4021.24	30	503.8	2380	1.35	1.7	132.3	132.3	3710.25	PASSED	62.78	PASSED
2	D12	9257	350	350	4021.24	30	503.8	2340	15.1	41.4	136.88	136.88	9.59	PASSED	2.98	PASSED
2	D13	9258	350	350	4021.24	30	503.8	2340	1.3	1.77	136.88	136.88	3802.66	PASSED	63.35	PASSED
2	D52	9259			3050			2941.17								
2	D53	9260			3050			2941.17								
2	A11	9261			3230			2941.17								
2	A14	9262			3230			2941.17								
2	A51	9263	350	350	4021.24	30	503.8	2380	28.5	83.1	132.3	132.3	2.27	PASSED	1.44	PASSED
2	A54	9264	350	350	4021.24	30	503.8	2380	13.6	41.8	132.3	132.3	9.06	PASSED	2.88	PASSED
2	D11	9265	350	350	4021.24	30	503.8	2350	29.9	83.2	135.74	135.74	2.36	PASSED	1.47	PASSED
2	D14	9266	350	350	4021.24	30	503.8	2340	14.7	42	136.88	136.88	9.41	PASSED	2.95	PASSED
2	D51	9267			3050			2941.17								
2	D54	9268			3050			2941.17								
2	A22	9269	400	400	7143.98	30	503.8	2630	68.9	25.9	341.22	341.22	11.4	PASSED	4.36	PASSED
2	A23	9270	400	400	7143.98	30	503.8	2630	1.09	9.56	341.22	341.22	337.02	PASSED	34.29	PASSED
2	A42	9271	400	400	7143.98	30	503.8	2170	63.4	16.2	384.57	384.57	12.38	PASSED	5.41	PASSED
2	A43	9272	400	400	7143.98	30	503.8	2160	1.06	4.51	385.49	385.49	597.43	PASSED	76.89	PASSED
2	D22	9273	400	400	7143.98	30	503.8	2180	63.3	16.6	383.65	383.65	12.4	PASSED	5.4	PASSED
2	D23	9274	400	400	7143.98	30	503.8	2170	1.22	4.58	384.57	384.57	579.28	PASSED	74.55	PASSED
2	D42	9275	400	400	7143.98	30	503.8	2510	68.3	26.3	352.75	352.75	11.19	PASSED	4.49	PASSED
2	D43	9276	400	400	7143.98	30	503.8	2510	1.34	9.05	352.75	352.75	324.98	PASSED	36.85	PASSED
2	B12	9277	400	400	7143.98	30	503.8	3520	21.2	61.4	247.43	247.43	13.73	PASSED	3.65	PASSED
2	B13	9278	400	400	7143.98	30	503.8	3520	2.62	3.35	247.43	247.43	2882.95	PASSED	59.78	PASSED
2	B52	9279	400	400	7143.98	30	503.8	3080	27.6	67.7	298.06	298.06	11.91	PASSED	3.92	PASSED
2	B53	9280	400	400	7143.98	30	503.8	3080	2.71	3.54	298.06	298.06	1758.4	PASSED	68.51	PASSED
2	C12	9281	400	400	7143.98	30	503.8	3080	27.1	67.5	294.92	294.92	12.01	PASSED	3.9	PASSED
2	C13	9282	400	400	7143.98	30	503.8	3080	2.49	3.35	295.97	295.97	2020.81	PASSED	72.22	PASSED
2	C52	9283	400	400	7143.98	30	503.8	3410	21.9	61.4	260.06	260.06	14.11	PASSED	3.83	PASSED
2	C53	9284	400	400	7143.98	30	503.8	3410	2.69	3.62	260.06	260.06	2373.46	PASSED	58.74	PASSED
2	A21	9285	400	400	7143.98	30	503.8	2630	137	43.1	341.22	341.22	3.87	PASSED	2.24	PASSED
2	A24	9286	400	400	7143.98	30	503.8	2620	66.8	8.5	342.19	342.19	13.91	PASSED	4.9	PASSED
2	A41	9287	400	400	7143.98	30	503.8	2170	126	30.1	384.57	384.57	4.58	PASSED	2.74	PASSED
2	A44	9288	400	400	7143.98	30	503.8	2160	61.4	11.2	385.49	385.49	13.56	PASSED	5.78	PASSED
2	D21	9289	400	400	7143.98	30	503.8	2180	126	30.9	383.65	383.65	4.56	PASSED	2.73	PASSED
2	D24	9290	400	400	7143.98	30	503.8	2170	61.8	11.5	384.57	384.57	13.45	PASSED	5.72	PASSED
2	D41	9291	400	400	7143.98	30	503.8	2520	136	43.8	351.8	351.8	3.91	PASSED	2.3	PASSED
2	D44	9292	400	400	7143.98	30	503.8	2510	66.7	8.69	352.75	352.75	13.63	PASSED	5.03	PASSED



General Information			Section Properties			F <sub>cu</sub> (N/mm <sup>2</sup> )	F <sub>y</sub> (N/mm <sup>2</sup> )	Applied Loads			Failure Surface Assessment			BS8110 Assessment		
Level	Column ID	FE No.	Height (mm)	Breadth (mm)	A <sub>s</sub> (mm <sup>2</sup> )			Axial (kN)	M <sub>xx</sub> (kN.m)	M <sub>zz</sub> (kN.m)	U <sub>mxx</sub> (kN.m)	U <sub>mzz</sub> (kN.m)	Margin	Acceptability	Margin	Acceptability
2	B11	9293	400	400	7143.98	30	503.8	3530	41.4	124	246.26	246.26	3.46	PASSED	1.81	PASSED
2	B14	9294	400	400	7143.98	30	503.8	3520	19.2	63.4	247.43	247.43	13.23	PASSED	3.58	PASSED
2	B51	9295	400	400	7143.98	30	503.8	3060	53.2	137	298.06	298.06	3.41	PASSED	1.95	PASSED
2	B54	9296	400	400	7143.98	30	503.8	3050	23	70.6	299.1	299.1	11.69	PASSED	3.86	PASSED
2	C11	9297	400	400	7143.98	30	503.8	3090	51.8	137	294.92	294.92	3.4	PASSED	1.93	PASSED
2	C14	9298	400	400	7143.98	30	503.8	3080	22.4	70.5	295.97	295.97	11.77	PASSED	3.83	PASSED
2	C51	9299	400	400	7143.98	30	503.8	3410	43.2	124	260.06	260.06	3.67	PASSED	1.9	PASSED
2	C54	9300	400	400	7143.98	30	503.8	3400	20.2	63.4	261.19	261.19	13.63	PASSED	3.76	PASSED
2	B22	9301	500	500	10360.96	30	503.8	4870	46.9	51.8	527.26	527.26	41.34	PASSED	8	PASSED
2	B23	9302	500	500	10360.96	30	503.8	4860	4.35	9.14	528.69	528.69	1530.29	PASSED	50.63	PASSED
2	B42	9303	500	500	10360.96	30	503.8	4730	35.1	62.1	547.12	547.12	39.68	PASSED	7.53	PASSED
2	B43	9304	500	500	10360.96	30	503.8	4730	3.86	7.48	547.12	547.12	1988.49	PASSED	63.32	PASSED
2	C22	9305	500	500	10360.96	30	503.8	4730	33.9	62.6	547.12	547.12	39.89	PASSED	7.52	PASSED
2	C23	9306	500	500	10360.96	30	503.8	4720	3.78	7.86	548.53	548.53	1857.16	PASSED	60.99	PASSED
2	C42	9307	500	500	10360.96	30	503.8	4830	45.3	51.4	532.98	532.98	42.75	PASSED	8.2	PASSED
2	C43	9308	500	500	10360.96	30	503.8	4820	4.36	8.93	534.4	534.4	1547	PASSED	52.19	PASSED
2	B21	9309	500	500	10360.96	30	503.8	4870	97	97.4	527.26	527.26	11.7	PASSED	4.17	PASSED
2	B24	9310	500	500	10360.96	30	503.8	4860	53.3	38.6	528.69	528.69	46.32	PASSED	8.15	PASSED
2	B41	9311	500	500	10360.96	30	503.8	4740	73	120	545.72	545.72	11.45	PASSED	3.85	PASSED
2	B44	9312	500	500	10360.96	30	503.8	4720	40.5	51.8	548.53	548.53	45.6	PASSED	8.58	PASSED
2	C21	9313	500	500	10360.96	30	503.8	4730	71.7	121	547.12	547.12	11.44	PASSED	3.84	PASSED
2	C24	9314	500	500	10360.96	30	503.8	4720	41	52.6	548.53	548.53	44.44	PASSED	8.45	PASSED
2	C41	9315	500	500	10360.96	30	503.8	4830	95	96.3	532.98	532.98	12.1	PASSED	4.27	PASSED
2	C44	9316	500	500	10360.96	30	503.8	4820	53.4	37.6	534.4	534.4	46.83	PASSED	8.26	PASSED
3	A12	9317			2650			2648.08								
3	A13	9318			2650			2648.08								
3	A52	9319	350	350	3220.13	30	503.8	2020	14.7	44.1	127.73	127.73	7.04	PASSED	2.59	PASSED
3	A53	9320	350	350	3220.13	30	503.8	2020	1.64	1.43	127.73	127.73	2661.94	PASSED	59.37	PASSED
3	D12	9321	350	350	3220.13	30	503.8	2010	15.1	44.2	128.73	128.73	7.03	PASSED	2.59	PASSED
3	D13	9322	350	350	3220.13	30	503.8	2010	1.77	1.4	128.73	128.73	2436.96	PASSED	56.42	PASSED
3	D52	9323	350	350	3220.13	30	503.8	2500	35.2	17.6	71.94	71.94	3.34	PASSED	1.78	PASSED
3	D53	9324	350	350	3220.13	30	503.8	2500	2.14	1.69	71.94	71.94	694.52	PASSED	27.15	PASSED
3	A11	9325			2650			2648.08								
3	A14	9326	350	350	3220.13	30	503.8	2640	39.9	19.9	52.12	52.12	1.37	PASSED	1.14	PASSED
3	A51	9327	350	350	3220.13	30	503.8	2020	29.7	89.7	127.73	127.73	1.78	PASSED	1.27	PASSED
3	A54	9328	350	350	3220.13	30	503.8	2020	16	46.8	127.73	127.73	6.24	PASSED	2.43	PASSED
3	D11	9329	350	350	3220.13	30	503.8	2010	31.2	89.8	128.73	128.73	1.78	PASSED	1.27	PASSED
3	D14	9330	350	350	3220.13	30	503.8	2000	17.3	46.8	129.73	129.73	6.23	PASSED	2.44	PASSED
3	D51	9331	350	350	3220.13	30	503.8	2500	72.6	36.1	71.94	71.94	0.79	FAILED	0.86	FAILED
3	D54	9332	350	350	3220.13	30	503.8	2490	39.3	20.6	73.28	73.28	2.73	PASSED	1.61	PASSED
3	A22	9333	400	400	5730.26	30	503.8	2330	68.1	8.77	308.88	308.88	11.46	PASSED	4.29	PASSED
3	A23	9334	400	400	5730.26	30	503.8	2320	4.97	1.01	309.87	309.87	788.46	PASSED	57.2	PASSED
3	A42	9335	400	400	5730.26	30	503.8	1960	63.8	15.8	344.54	344.54	10.81	PASSED	4.78	PASSED



General Information			Section Properties			F <sub>cu</sub> (N/mm <sup>2</sup> )	F <sub>y</sub> (N/mm <sup>2</sup> )	Applied Loads			Failure Surface Assessment			BS8110 Assessment	
Level	Column ID	FE No.	Height (mm)	Breadth (mm)	A <sub>s</sub> (mm <sup>2</sup> )			Axial (kN)	M <sub>ox</sub> (kN.m)	M <sub>zz</sub> (kN.m)	U <sub>mox</sub> (kN.m)	U <sub>mzz</sub> (kN.m)	Margin	Acceptability	Margin
3	A43	9336	400	400	5730.26	30	503.8	1960	5.15	1.88	344.54	344.54	414.18	56.21	PASSED
3	D22	9337	400	400	5730.26	30	503.8	1970	62.6	15.8	343.6	343.6	11.12	4.85	PASSED
3	D23	9338	400	400	5730.26	30	503.8	1960	5.13	1.76	344.54	344.54	423.38	56.98	PASSED
3	D42	9339	400	400	5730.26	30	503.8	2230	66.3	8.99	318.71	318.71	11.73	4.53	PASSED
3	D43	9340	400	400	5730.26	30	503.8	2220	4.98	0.99	319.68	319.68	694.76	58.79	PASSED
3	B12	9341	400	400	5730.26	30	503.8	3030	17.9	67	233.89	233.89	10.31	3.23	PASSED
3	B13	9342	400	400	5730.26	30	503.8	3020	0.8	4.36	235.06	235.06	2058.85	51.13	PASSED
3	B52	9343	400	400	5730.26	30	503.8	2690	19.3	73.8	271.91	271.91	9.4	3.38	PASSED
3	B53	9344	400	400	5730.26	30	503.8	2680	2.09	4.34	272.98	272.98	1256.4	53.81	PASSED
3	C12	9345	400	400	5730.26	30	503.8	2710	20	73.9	269.77	269.77	9.31	3.34	PASSED
3	C13	9346	400	400	5730.26	30	503.8	2710	2.11	4.34	269.77	269.77	1291.41	53.23	PASSED
3	C52	9347	400	400	5730.26	30	503.8	2920	17.2	66.8	246.59	246.59	10.82	3.43	PASSED
3	C53	9348	400	400	5730.26	30	503.8	2920	0.79	4.49	246.59	246.59	1804.85	52.17	PASSED
3	A21	9349	400	400	5730.26	30	503.8	2330	141	17.6	308.88	308.88	3.49	2.08	PASSED
3	A24	9350	400	400	5730.26	30	503.8	2320	77.5	8.52	309.87	309.87	9.34	3.81	PASSED
3	A41	9351	400	400	5730.26	30	503.8	1960	133	30.5	344.54	344.54	3.68	2.31	PASSED
3	A44	9352	400	400	5730.26	30	503.8	1950	73.4	13	345.48	345.48	9.16	4.31	PASSED
3	D21	9353	400	400	5730.26	30	503.8	1970	131	30.4	343.6	343.6	3.76	2.34	PASSED
3	D24	9354	400	400	5730.26	30	503.8	1960	72.7	12.8	344.54	344.54	9.32	4.34	PASSED
3	D41	9355	400	400	5730.26	30	503.8	2230	138	18.1	318.71	318.71	3.65	2.18	PASSED
3	D44	9356	400	400	5730.26	30	503.8	2220	76	8.71	319.68	319.68	9.51	4	PASSED
3	B11	9357	400	400	5730.26	30	503.8	3030	36	137	233.89	233.89	2.6	1.58	PASSED
3	B14	9358	400	400	5730.26	30	503.8	3020	18	73.6	235.06	235.06	8.74	2.98	PASSED
3	B51	9359	400	400	5730.26	30	503.8	2690	40.9	152	271.91	271.91	2.58	1.64	PASSED
3	B54	9360	400	400	5730.26	30	503.8	2680	23.3	81.4	272.98	272.98	7.79	3.05	PASSED
3	C11	9361	400	400	5730.26	30	503.8	2720	41.9	151	268.69	268.69	2.56	1.63	PASSED
3	C14	9362	400	400	5730.26	30	503.8	2710	23.4	81.2	269.77	269.77	7.78	3.02	PASSED
3	C51	9363	400	400	5730.26	30	503.8	2930	34.9	137	245.45	245.45	2.79	1.66	PASSED
3	C54	9364	400	400	5730.26	30	503.8	2920	17.7	73.5	246.59	246.59	9.12	3.13	PASSED
3	B22	9365	450	450	9650.97	30	503.8	4280	37.1	26.6	409.23	409.23	57.38	9.08	PASSED
3	B23	9366	450	450	9650.97	30	503.8	4280	2.16	2.8	409.23	409.23	6786.27	118.76	PASSED
3	B42	9367	450	450	9650.97	30	503.8	4160	30.3	35	423.44	423.44	54.53	9.6	PASSED
3	B43	9368	450	450	9650.97	30	503.8	4160	2.27	2.76	423.44	423.44	5964.94	123.12	PASSED
3	C22	9369	450	450	9650.97	30	503.8	4150	28.1	35.3	423.44	423.44	57.23	9.88	PASSED
3	C23	9370	450	450	9650.97	30	503.8	4150	2.22	2.82	424.62	424.62	5869.72	121.88	PASSED
3	C42	9371	450	450	9650.97	30	503.8	4250	34.6	26.1	412.81	412.81	62.82	9.73	PASSED
3	C43	9372	450	450	9650.97	30	503.8	4240	2.22	2.79	414	414	6449.24	119.85	PASSED
3	B21	9373	450	450	9650.97	30	503.8	4290	75.9	55	408.03	408.03	14.98	4.42	PASSED
3	B24	9374	450	450	9650.97	30	503.8	4280	40.2	29.5	409.23	409.23	48.65	8.34	PASSED
3	B41	9375	450	450	9650.97	30	503.8	4160	62.5	72	423.44	423.44	14.51	4.67	PASSED
3	B44	9376	450	450	9650.97	30	503.8	4150	33.6	38.3	424.62	424.62	45.66	8.78	PASSED
3	C21	9377	450	450	9650.97	30	503.8	4160	58.7	72.8	423.44	423.44	15.05	4.68	PASSED
3	C24	9378	450	450	9650.97	30	503.8	4150	32.3	38.8	424.62	424.62	46.46	8.76	PASSED



General Information			Section Properties			F <sub>cu</sub> (N/mm <sup>2</sup> )	F <sub>y</sub> (N/mm <sup>2</sup> )	Applied Loads			Failure Surface Assessment				BS8110 Assessment	
Level	Column ID	FE No.	Height (mm)	Breadth (mm)	A <sub>s</sub> (mm <sup>2</sup> )			Axial (kN)	M <sub>xx</sub> (kN.m)	M <sub>zz</sub> (kN.m)	U <sub>mxx</sub> (kN.m)	U <sub>mzz</sub> (kN.m)	Margin	Acceptability	Margin	Acceptability
3	C41	9379	450	450	9650.97	30	503.8	4250	71.6	53.9	412.81	412.81	16.29	PASSED	4.7	PASSED
3	C44	9380	450	450	9650.97	30	503.8	4240	38.6	28.8	414	414	51.57	PASSED	8.76	PASSED
4	A12	9381	300	300	3220.13	30	503.8	2120	23.4	10.8	51.86	51.86	4.05	PASSED	1.95	PASSED
4	A13	9382	300	300	3220.13	30	503.8	2120	0.88	0.86	51.86	51.86	1782.18	PASSED	45.62	PASSED
4	A52	9383	300	300	3220.13	30	503.8	1730	8.89	26.8	89.75	89.75	9.41	PASSED	3.05	PASSED
4	A53	9384	300	300	3220.13	30	503.8	1730	0.86	1.02	89.75	89.75	3548.8	PASSED	70.38	PASSED
4	D12	9385	300	300	3220.13	30	503.8	1730	9.34	26.8	89.75	89.75	9.32	PASSED	3.03	PASSED
4	D13	9386	300	300	3220.13	30	503.8	1730	0.86	1.02	89.75	89.75	3560.88	PASSED	70.33	PASSED
4	D52	9387	300	300	3220.13	30	503.8	2000	22.4	10.9	64.66	64.66	6.74	PASSED	2.52	PASSED
4	D53	9388	300	300	3220.13	30	503.8	2000	0.85	0.94	64.66	64.66	2597.22	PASSED	53.98	PASSED
4	A11	9389	300	300	3220.13	30	503.8	2120	47.8	21.8	51.86	51.86	0.97	FAILED	0.95	FAILED
4	A14	9390	300	300	3220.13	30	503.8	2110	25.1	11.8	52.97	52.97	3.65	PASSED	1.85	PASSED
4	A51	9391	300	300	3220.13	30	503.8	1730	17.8	54.7	89.75	89.75	2.36	PASSED	1.49	PASSED
4	A54	9392	300	300	3220.13	30	503.8	1730	9.52	28.7	89.75	89.75	8.24	PASSED	2.84	PASSED
4	D11	9393	300	300	3220.13	30	503.8	1730	18.9	54.7	89.75	89.75	2.33	PASSED	1.49	PASSED
4	D14	9394	300	300	3220.13	30	503.8	1720	10	28.7	90.6	90.6	8.23	PASSED	2.86	PASSED
4	D51	9395	300	300	3220.13	30	503.8	2000	45.7	22.3	64.66	64.66	1.62	PASSED	1.23	PASSED
4	D54	9396	300	300	3220.13	30	503.8	2000	23.9	12.1	64.66	64.66	5.83	PASSED	2.35	PASSED
4	A22	9397	350	350	5730.26	30	503.8	1990	48.4	5.96	241.28	241.28	12.6	PASSED	4.77	PASSED
4	A23	9398	350	350	5730.26	30	503.8	1980	2.32	1.09	242.13	242.13	1270.8	PASSED	88.84	PASSED
4	A42	9399	350	350	5730.26	30	503.8	1710	45.4	7.15	264.76	264.76	12.48	PASSED	5.44	PASSED
4	A43	9400	350	350	5730.26	30	503.8	1710	2.46	0.52	264.76	264.76	870.15	PASSED	98.05	PASSED
4	D22	9401	350	350	5730.26	30	503.8	1710	44.1	7.25	264.76	264.76	12.97	PASSED	5.58	PASSED
4	D23	9402	350	350	5730.26	30	503.8	1710	2.45	0.57	264.76	264.76	862.36	PASSED	97.51	PASSED
4	D42	9403	350	350	5730.26	30	503.8	1900	46.7	6.03	248.92	248.92	12.99	PASSED	5.07	PASSED
4	D43	9404	350	350	5730.26	30	503.8	1900	2.32	1.07	248.92	248.92	1114.53	PASSED	90.57	PASSED
4	B12	9405	350	350	5730.26	30	503.8	2530	11.7	45.8	192.59	192.59	13.23	PASSED	3.91	PASSED
4	B13	9406	350	350	5730.26	30	503.8	2530	0.47	2.14	192.59	192.59	3912.09	PASSED	84.35	PASSED
4	B52	9407	350	350	5730.26	30	503.8	2290	14.8	50.9	214.94	214.94	10.97	PASSED	3.88	PASSED
4	B53	9408	350	350	5730.26	30	503.8	2290	0.97	2.16	214.94	214.94	2395.48	PASSED	87.8	PASSED
4	C12	9409	350	350	5730.26	30	503.8	2320	15.6	51.4	212.22	212.22	10.69	PASSED	3.78	PASSED
4	C13	9410	350	350	5730.26	30	503.8	2320	0.98	2.15	212.22	212.22	2502.28	PASSED	86.75	PASSED
4	C52	9411	350	350	5730.26	30	503.8	2450	10.6	45.8	200.19	200.19	13.57	PASSED	4.09	PASSED
4	C53	9412	350	350	5730.26	30	503.8	2440	0.48	2.19	201.13	201.13	3339.81	PASSED	86.01	PASSED
4	A21	9413	350	350	5730.26	30	503.8	1990	99.2	12.3	241.28	241.28	4	PASSED	2.33	PASSED
4	A24	9414	350	350	5730.26	30	503.8	1980	52.7	6.91	242.13	242.13	10.94	PASSED	4.38	PASSED
4	A41	9415	350	350	5730.26	30	503.8	1710	93.3	14.4	264.76	264.76	4.34	PASSED	2.65	PASSED
4	A44	9416	350	350	5730.26	30	503.8	1700	50	6.95	265.59	265.59	10.9	PASSED	4.99	PASSED
4	D21	9417	350	350	5730.26	30	503.8	1710	90.9	14.6	264.76	264.76	4.5	PASSED	2.71	PASSED
4	D24	9418	350	350	5730.26	30	503.8	1710	48.9	7.01	264.76	264.76	11.28	PASSED	5.08	PASSED
4	D41	9419	350	350	5730.26	30	503.8	1900	95.8	12.7	248.92	248.92	4.24	PASSED	2.47	PASSED
4	D44	9420	350	350	5730.26	30	503.8	1900	51.1	6.87	248.92	248.92	11.27	PASSED	4.62	PASSED
4	B11	9421	350	350	5730.26	30	503.8	2540	23.7	93.1	191.63	191.63	3.54	PASSED	1.91	PASSED



General Information			Section Properties			F <sub>cu</sub> (N/mm <sup>2</sup> )	F <sub>y</sub> (N/mm <sup>2</sup> )	Applied Loads			Failure Surface Assessment				BS8110 Assessment	
Level	Column ID	FE No.	Height (mm)	Breadth (mm)	As (mm <sup>2</sup> )			Axial (kN)	M <sub>ox</sub> (kN.m)	M <sub>zz</sub> (kN.m)	U <sub>mox</sub> (kN.m)	U <sub>mzz</sub> (kN.m)	Margin	Acceptability	Margin	Acceptability
4	B14	9422	350	350	5730.26	30	503.8	2530	12	48.5	192.59	192.59	11.95	PASSED	3.7	PASSED
4	B51	9423	350	350	5730.26	30	503.8	2300	30.7	104	214.04	214.04	3.15	PASSED	1.89	PASSED
4	B54	9424	350	350	5730.26	30	503.8	2290	16.5	54.2	214.94	214.94	9.75	PASSED	3.63	PASSED
4	C11	9425	350	350	5730.26	30	503.8	2330	32.2	105	211.31	211.31	3.04	PASSED	1.84	PASSED
4	C14	9426	350	350	5730.26	30	503.8	2320	17.3	54.6	212.22	212.22	9.54	PASSED	3.55	PASSED
4	C51	9427	350	350	5730.26	30	503.8	2450	21.8	93	200.19	200.19	3.75	PASSED	2.01	PASSED
4	C54	9428	350	350	5730.26	30	503.8	2440	11.2	48.6	201.13	201.13	12.21	PASSED	3.87	PASSED
4	B22	9429	450	450	7143.97	30	503.8	3690	41.7	29.8	344.92	344.92	35.35	PASSED	6.81	PASSED
4	B23	9430	450	450	7143.97	30	503.8	3690	0.61	1.71	344.92	344.92	19835.03	PASSED	182.68	PASSED
4	B42	9431	450	450	7143.97	30	503.8	3590	33.7	40.4	357.34	357.34	33.32	PASSED	7.02	PASSED
4	B43	9432	450	450	7143.97	30	503.8	3580	0.61	1.58	358.56	358.56	19844.53	PASSED	203.06	PASSED
4	C22	9433	450	450	7143.97	30	503.8	3580	30.1	41.1	358.56	358.56	35.4	PASSED	7.1	PASSED
4	C23	9434	450	450	7143.97	30	503.8	3580	0.72	1.61	358.56	358.56	18259.45	PASSED	195.59	PASSED
4	C42	9435	450	450	7143.97	30	503.8	3660	37.8	29.3	348.68	348.68	40.14	PASSED	7.48	PASSED
4	C43	9436	450	450	7143.97	30	503.8	3660	0.64	1.66	348.68	348.68	19823.24	PASSED	188.48	PASSED
4	B21	9437	450	450	7143.97	30	503.8	3700	83.3	59	343.66	343.66	9.61	PASSED	3.4	PASSED
4	B24	9438	450	450	7143.97	30	503.8	3690	41	27.8	344.92	344.92	37.74	PASSED	6.99	PASSED
4	B41	9439	450	450	7143.97	30	503.8	3590	67.8	80.1	357.34	357.34	9.25	PASSED	3.53	PASSED
4	B44	9440	450	450	7143.97	30	503.8	3580	33.8	38.3	358.56	358.56	35.13	PASSED	7.34	PASSED
4	C21	9441	450	450	7143.97	30	503.8	3590	60.9	81.1	357.34	357.34	9.87	PASSED	3.57	PASSED
4	C24	9442	450	450	7143.97	30	503.8	3580	30.8	38.8	358.56	358.56	37.23	PASSED	7.4	PASSED
4	C41	9443	450	450	7143.97	30	503.8	3670	76.1	57.6	347.43	347.43	10.95	PASSED	3.72	PASSED
4	C44	9444	450	450	7143.97	30	503.8	3650	37.9	27	349.92	349.92	42.27	PASSED	7.61	PASSED
5	A12	9494	300	300	2513.27	30	503.8	1650	24	12.2	67.92	67.92	6.36	PASSED	2.46	PASSED
5	A13	9495	300	300	2513.27	30	503.8	1650	0.5	0.59	67.92	67.92	7725.45	PASSED	92.21	PASSED
5	A52	9496	300	300	2513.27	30	503.8	1460	10.7	28.1	83.58	83.58	6.73	PASSED	2.61	PASSED
5	A53	9497	300	300	2513.27	30	503.8	1460	0.56	0.78	83.58	83.58	4389.63	PASSED	84.43	PASSED
5	D12	9498	300	300	2513.27	30	503.8	1460	11.3	28.8	83.58	83.58	6.37	PASSED	2.53	PASSED
5	D13	9499	300	300	2513.27	30	503.8	1460	0.55	0.79	83.58	83.58	4406.25	PASSED	84.45	PASSED
5	D52	9500	300	300	2513.27	30	503.8	1560	22.4	12.4	75.64	75.64	8.38	PASSED	2.86	PASSED
5	D53	9501	300	300	2513.27	30	503.8	1560	0.5	0.49	75.64	75.64	9863.62	PASSED	113.66	PASSED
5	A11	9502	300	300	2513.27	30	503.8	1650	47.6	24	67.92	67.92	1.62	PASSED	1.24	PASSED
5	A14	9503	300	300	2513.27	30	503.8	1650	22.9	11.8	67.92	67.92	6.95	PASSED	2.57	PASSED
5	A51	9504	300	300	2513.27	30	503.8	1460	20.9	55.6	83.58	83.58	1.86	PASSED	1.32	PASSED
5	A54	9505	300	300	2513.27	30	503.8	1450	10.1	26.6	84.34	84.34	7.52	PASSED	2.78	PASSED
5	D11	9506	300	300	2513.27	30	503.8	1470	21.9	56.8	82.81	82.81	1.75	PASSED	1.28	PASSED
5	D14	9507	300	300	2513.27	30	503.8	1460	10.4	27.2	83.58	83.58	7.15	PASSED	2.69	PASSED
5	D51	9508	300	300	2513.27	30	503.8	1570	44.5	24.5	74.81	74.81	2.14	PASSED	1.43	PASSED
5	D54	9509	300	300	2513.27	30	503.8	1560	21.3	12.1	75.64	75.64	9.14	PASSED	3	PASSED
5	A22	9510	350	350	3926.99	30	503.8	1630	52.9	5.85	187.11	187.11	7.37	PASSED	3.36	PASSED
5	A23	9511	350	350	3926.99	30	503.8	1630	2.1	1.04	187.11	187.11	1013.39	PASSED	72.04	PASSED
5	A42	9512	350	350	3926.99	30	503.8	1430	51	8.26	202.26	202.26	7.29	PASSED	3.65	PASSED
5	A43	9513	350	350	3926.99	30	503.8	1430	2.26	0.29	202.26	202.26	769.68	PASSED	83.76	PASSED



General Information			Section Properties			F <sub>cu</sub> (N/mm <sup>2</sup> )	F <sub>y</sub> (N/mm <sup>2</sup> )	Applied Loads			Failure Surface Assessment			BS8110 Assessment		
Level	Column ID	FE No.	Height (mm)	Breadth (mm)	A <sub>s</sub> (mm <sup>2</sup> )			Axial (kN)	M <sub>xx</sub> (kN.m)	M <sub>zz</sub> (kN.m)	U <sub>mxx</sub> (kN.m)	U <sub>mzz</sub> (kN.m)	Margin	Acceptability	Margin	Acceptability
5	D22	9514	350	350	3926.99	30	503.8	1430	49.6	7.96	202.26	202.26	7.6	PASSED	3.75	PASSED
5	D23	9515	350	350	3926.99	30	503.8	1430	2.25	0.28	202.26	202.26	776.25	PASSED	84.3	PASSED
5	D42	9516	350	350	3926.99	30	503.8	1560	51.3	5.74	192.49	192.49	7.65	PASSED	3.55	PASSED
5	D43	9517	350	350	3926.99	30	503.8	1560	2.1	1.03	192.49	192.49	879.29	PASSED	73.51	PASSED
5	B12	9518	350	350	3926.99	30	503.8	2040	9.84	50.9	153.08	153.08	7.22	PASSED	2.81	PASSED
5	B13	9519	350	350	3926.99	30	503.8	2030	0.31	2	153.97	153.97	2778.59	PASSED	72.89	PASSED
5	B52	9520	350	350	3926.99	30	503.8	1900	14.5	56	165.27	165.27	6.14	PASSED	2.67	PASSED
5	B53	9521	350	350	3926.99	30	503.8	1900	1.02	1.99	165.27	165.27	1814.53	PASSED	68.97	PASSED
5	C12	9522	350	350	3926.99	30	503.8	1930	15.6	56.6	162.71	162.71	5.92	PASSED	2.6	PASSED
5	C13	9523	350	350	3926.99	30	503.8	1920	1.07	1.99	163.57	163.57	1847.45	PASSED	68.02	PASSED
5	C52	9524	350	350	3926.99	30	503.8	1970	9.17	50.8	159.26	159.26	7.47	PASSED	2.94	PASSED
5	C53	9525	350	350	3926.99	30	503.8	1970	0.31	2.04	159.26	159.26	2445.45	PASSED	73.7	PASSED
5	A21	9526	350	350	3926.99	30	503.8	1630	108	12.2	187.11	187.11	2.34	PASSED	1.64	PASSED
5	A24	9527	350	350	3926.99	30	503.8	1620	56.9	6.61	187.88	187.88	6.53	PASSED	3.13	PASSED
5	A41	9528	350	350	3926.99	30	503.8	1430	104	16.6	202.26	202.26	2.53	PASSED	1.79	PASSED
5	A44	9529	350	350	3926.99	30	503.8	1430	55.3	8.13	202.26	202.26	6.52	PASSED	3.39	PASSED
5	D21	9530	350	350	3926.99	30	503.8	1430	102	16	202.26	202.26	2.61	PASSED	1.83	PASSED
5	D24	9531	350	350	3926.99	30	503.8	1430	53.9	7.89	202.26	202.26	6.77	PASSED	3.48	PASSED
5	D41	9532	350	350	3926.99	30	503.8	1570	105	12.1	191.73	191.73	2.49	PASSED	1.73	PASSED
5	D44	9533	350	350	3926.99	30	503.8	1560	55.3	6.52	192.49	192.49	6.79	PASSED	3.29	PASSED
5	B11	9534	350	350	3926.99	30	503.8	2040	20	103	153.08	153.08	1.98	PASSED	1.39	PASSED
5	B14	9535	350	350	3926.99	30	503.8	2030	10	53.5	153.97	153.97	6.64	PASSED	2.7	PASSED
5	B51	9536	350	350	3926.99	30	503.8	1900	30.1	114	165.27	165.27	1.75	PASSED	1.31	PASSED
5	B54	9537	350	350	3926.99	30	503.8	1890	16.3	59.2	166.11	166.11	5.53	PASSED	2.53	PASSED
5	C11	9538	350	350	3926.99	30	503.8	1930	32.4	115	162.71	162.71	1.68	PASSED	1.27	PASSED
5	C14	9539	350	350	3926.99	30	503.8	1920	17.6	59.6	163.57	163.57	5.35	PASSED	2.46	PASSED
5	C51	9540	350	350	3926.99	30	503.8	1970	18.7	103	159.26	159.26	2.09	PASSED	1.45	PASSED
5	C54	9541	350	350	3926.99	30	503.8	1960	9.5	53.6	160.13	160.13	6.81	PASSED	2.8	PASSED
5	B22	9542	450	450	5180.48	30	503.8	3090	37	29.1	305.65	305.65	30.97	PASSED	6.25	PASSED
5	B23	9543	450	450	5180.48	30	503.8	3090	2.62	1.62	305.65	305.65	4957.54	PASSED	93.05	PASSED
5	B42	9544	450	450	5180.48	30	503.8	3000	32.1	37.8	316.79	316.79	27.81	PASSED	6.15	PASSED
5	B43	9545	450	450	5180.48	30	503.8	3000	2.63	2.29	316.79	316.79	3533.75	PASSED	87.81	PASSED
5	C22	9546	450	450	5180.48	30	503.8	3000	28	38.9	316.79	316.79	29.69	PASSED	6.23	PASSED
5	C23	9547	450	450	5180.48	30	503.8	3000	2.51	2.22	316.79	316.79	3797.91	PASSED	91.55	PASSED
5	C42	9548	450	450	5180.48	30	503.8	3070	32.9	28.6	308.15	308.15	35.59	PASSED	6.89	PASSED
5	C43	9549	450	450	5180.48	30	503.8	3060	2.63	1.85	309.4	309.4	4419.68	PASSED	91.09	PASSED
5	B21	9550	450	450	5180.48	30	503.8	3090	76.9	59.3	305.65	305.65	8.06	PASSED	3.02	PASSED
5	B24	9551	450	450	5180.48	30	503.8	3080	42	30.8	306.9	306.9	25.68	PASSED	5.61	PASSED
5	B41	9552	450	450	5180.48	30	503.8	3010	67.1	77.6	315.57	315.57	7.37	PASSED	2.97	PASSED
5	B44	9553	450	450	5180.48	30	503.8	3000	37.1	41.1	316.79	316.79	22.73	PASSED	5.56	PASSED
5	C21	9554	450	450	5180.48	30	503.8	3010	58.6	79.7	315.57	315.57	7.89	PASSED	3.02	PASSED
5	C24	9555	450	450	5180.48	30	503.8	2990	32.6	42.2	318.01	318.01	24.37	PASSED	5.66	PASSED
5	C41	9556	450	450	5180.48	30	503.8	3070	68.6	58.4	308.15	308.15	9.28	PASSED	3.32	PASSED



General Information			Section Properties			F <sub>cu</sub> (N/mm <sup>2</sup> )	F <sub>y</sub> (N/mm <sup>2</sup> )	Applied Loads			Failure Surface Assessment				BS8110 Assessment	
Level	Column ID	FE No.	Height (mm)	Breadth (mm)	As (mm <sup>2</sup> )			Axial (kN)	M <sub>xx</sub> (kN.m)	M <sub>zz</sub> (kN.m)	U <sub>mxx</sub> (kN.m)	U <sub>mzz</sub> (kN.m)	Margin	Acceptability	Margin	Acceptability
5	C44	9557	450	450	5180.48	30	503.8	3060	37.7	30.5	309.4	309.4	29.21	PASSED	6.14	PASSED
6	A12	9558	300	300	1608.49	30	503.8	1230	22.5	11.7	68.93	68.93	6.5	PASSED	2.46	PASSED
6	A13	9559	300	300	1608.49	30	503.8	1230	1.75	0.82	68.93	68.93	860.2	PASSED	32.25	PASSED
6	A52	9560	300	300	1608.49	30	503.8	1190	10.6	26.8	71.84	71.84	5.3	PASSED	2.25	PASSED
6	A53	9561	300	300	1608.49	30	503.8	1180	1.07	1.66	72.54	72.54	748.91	PASSED	33.31	PASSED
6	D12	9562	300	300	1608.49	30	503.8	1200	11	27.5	71.12	71.12	5	PASSED	2.17	PASSED
6	D13	9563	300	300	1608.49	30	503.8	1200	1.01	1.68	71.12	71.12	788.97	PASSED	32.85	PASSED
6	D52	9564	300	300	1608.49	30	503.8	1180	20.7	11.9	72.54	72.54	7.47	PASSED	2.74	PASSED
6	D53	9565	300	300	1608.49	30	503.8	1180	1.72	0.82	72.54	72.54	803.54	PASSED	34.21	PASSED
6	A11	9568	300	300	1608.49	30	503.8	1230	46.8	23.4	68.93	68.93	1.64	PASSED	1.19	PASSED
6	A14	9569	300	300	1608.49	30	503.8	1230	25.9	12.1	68.93	68.93	5.19	PASSED	2.18	PASSED
6	A51	9570	300	300	1608.49	30	503.8	1190	21.1	55.4	71.84	71.84	1.39	PASSED	1.09	PASSED
6	A54	9571	300	300	1608.49	30	503.8	1180	10.7	30	72.54	72.54	4.45	PASSED	2.06	PASSED
6	D11	9572	300	300	1608.49	30	503.8	1200	21.8	56.7	71.12	71.12	1.31	PASSED	1.06	PASSED
6	D14	9573	300	300	1608.49	30	503.8	1200	10.9	30.7	71.12	71.12	4.2	PASSED	1.98	PASSED
6	D51	9574	300	300	1608.49	30	503.8	1180	43.2	23.8	72.54	72.54	1.96	PASSED	1.32	PASSED
6	D54	9575	300	300	1608.49	30	503.8	1180	24	12.3	72.54	72.54	5.98	PASSED	2.42	PASSED
6	A22	9576	300	300	3669.38	30	503.8	1250	31.5	3.77	152.06	152.06	10.68	PASSED	4.58	PASSED
6	A23	9577	300	300	3669.38	30	503.8	1250	1.53	0.23	152.06	152.06	1074.61	PASSED	93.1	PASSED
6	A42	9578	300	300	3669.38	30	503.8	1160	30.7	4.69	158.92	158.92	10.48	PASSED	4.81	PASSED
6	A43	9579	300	300	3669.38	30	503.8	1160	1.58	0.16	158.92	158.92	832.08	PASSED	95.42	PASSED
6	B12	9580	300	300	3669.38	30	503.8	1580	4.9	30.3	125.76	125.76	11.7	PASSED	3.95	PASSED
6	B13	9581	300	300	3669.38	30	503.8	1580	0.29	1.36	125.76	125.76	2654.03	PASSED	86.49	PASSED
6	C12	9582	300	300	3669.38	30	503.8	1520	9.33	33.7	130.72	130.72	9.2	PASSED	3.54	PASSED
6	C13	9583	300	300	3669.38	30	503.8	1520	0.39	1.38	130.72	130.72	2199.98	PASSED	86.35	PASSED
6	B52	9584	300	300	3669.38	30	503.8	1490	8.7	33.4	133.17	133.17	9.45	PASSED	3.65	PASSED
6	B53	9585	300	300	3669.38	30	503.8	1490	0.44	1.39	133.17	133.17	1992.99	PASSED	86.14	PASSED
6	C52	9586	300	300	3669.38	30	503.8	1530	4.67	30.3	129.9	129.9	11.79	PASSED	4.07	PASSED
6	C53	9587	300	300	3669.38	30	503.8	1520	0.29	1.39	130.72	130.72	2277.83	PASSED	87.99	PASSED
6	D22	9588	300	300	3669.38	30	503.8	1150	30	4.51	159.68	159.68	10.8	PASSED	4.95	PASSED
6	D23	9589	300	300	3669.38	30	503.8	1150	1.57	0.2	159.68	159.68	811.6	PASSED	95.63	PASSED
6	D42	9590	300	300	3669.38	30	503.8	1210	30.8	3.7	155.12	155.12	10.87	PASSED	4.76	PASSED
6	D43	9591	300	300	3669.38	30	503.8	1210	1.51	0.22	155.12	155.12	990.85	PASSED	95.99	PASSED
6	A21	9592	300	300	3669.38	30	503.8	1250	64.7	7.72	152.06	152.06	3.55	PASSED	2.23	PASSED
6	A24	9593	300	300	3669.38	30	503.8	1250	34.4	3.89	152.06	152.06	9.36	PASSED	4.2	PASSED
6	A41	9594	300	300	3669.38	30	503.8	1160	63	9.53	158.92	158.92	3.66	PASSED	2.35	PASSED
6	A44	9595	300	300	3669.38	30	503.8	1150	33.7	4.66	159.68	159.68	9.18	PASSED	4.43	PASSED
6	B11	9596	300	300	3669.38	30	503.8	1580	10.1	61.8	125.76	125.76	3.34	PASSED	1.93	PASSED
6	B14	9597	300	300	3669.38	30	503.8	1570	5.14	32.4	126.6	126.6	10.43	PASSED	3.72	PASSED
6	B51	9598	300	300	3669.38	30	503.8	1500	17.8	68.2	132.35	132.35	2.8	PASSED	1.78	PASSED
6	B54	9599	300	300	3669.38	30	503.8	1490	9.1	35.8	133.17	133.17	8.43	PASSED	3.41	PASSED
6	C11	9600	300	300	3669.38	30	503.8	1520	19.1	68.8	130.72	130.72	2.71	PASSED	1.73	PASSED
6	C14	9601	300	300	3669.38	30	503.8	1520	9.81	36	130.72	130.72	8.24	PASSED	3.32	PASSED



General Information			Section Properties			F <sub>cu</sub> (N/mm <sup>2</sup> )	F <sub>y</sub> (N/mm <sup>2</sup> )	Applied Loads			Failure Surface Assessment			BS8110 Assessment		
Level	Column ID	FE No.	Height (mm)	Breadth (mm)	A <sub>s</sub> (mm <sup>2</sup> )			Axial (kN)	M <sub>xx</sub> (kN.m)	M <sub>zz</sub> (kN.m)	U <sub>mxx</sub> (kN.m)	U <sub>mzz</sub> (kN.m)	Margin	Acceptability	Margin	Acceptability
6	C51	9602	300	300	3669.38	30	503.8	1530	9.75	61.8	129.9	129.9	3.45	PASSED	1.99	PASSED
6	C54	9603	300	300	3669.38	30	503.8	1520	5.11	32.5	130.72	130.72	10.44	PASSED	3.82	PASSED
6	D21	9604	300	300	3669.38	30	503.8	1160	61.6	9.18	158.92	158.92	3.78	PASSED	2.4	PASSED
6	D24	9605	300	300	3669.38	30	503.8	1150	33	4.53	159.68	159.68	9.47	PASSED	4.53	PASSED
6	D41	9606	300	300	3669.38	30	503.8	1210	63.2	7.55	155.12	155.12	3.7	PASSED	2.32	PASSED
6	D44	9607	300	300	3669.38	30	503.8	1200	33.7	3.84	155.89	155.89	9.49	PASSED	4.39	PASSED
6	B22	9608	350	350	5730.27	30	503.8	2480	15.5	12.5	197.36	197.36	62.54	PASSED	10.25	PASSED
6	B23	9609	350	350	5730.27	30	503.8	2480	1.26	0.86	197.36	197.36	6840.21	PASSED	129.66	PASSED
6	B42	9610	350	350	5730.27	30	503.8	2410	13.6	16.5	203.94	203.94	53.52	PASSED	9.91	PASSED
6	B43	9611	350	350	5730.27	30	503.8	2410	1.29	1.09	203.94	203.94	5097.48	PASSED	125.88	PASSED
6	C22	9612	350	350	5730.27	30	503.8	2410	12	17	203.94	203.94	56.4	PASSED	9.9	PASSED
6	C23	9613	350	350	5730.27	30	503.8	2410	1.2	1.05	203.94	203.94	5633.46	PASSED	134.42	PASSED
6	C42	9614	350	350	5730.27	30	503.8	2460	13.8	12.3	199.25	199.25	70.98	PASSED	11.39	PASSED
6	C43	9615	350	350	5730.27	30	503.8	2460	1.22	0.95	199.25	199.25	6481.97	PASSED	132.21	PASSED
6	B21	9616	350	350	5730.27	30	503.8	2480	32.4	25.8	197.36	197.36	16.4	PASSED	4.92	PASSED
6	B24	9617	350	350	5730.27	30	503.8	2470	17.8	13.7	198.31	198.31	50.07	PASSED	9.05	PASSED
6	B41	9618	350	350	5730.27	30	503.8	2410	28.7	34.1	203.94	203.94	14.31	PASSED	4.77	PASSED
6	B44	9619	350	350	5730.27	30	503.8	2410	16	18.2	203.94	203.94	42.71	PASSED	8.87	PASSED
6	C21	9620	350	350	5730.27	30	503.8	2410	25.3	35.1	203.94	203.94	15.14	PASSED	4.78	PASSED
6	C24	9621	350	350	5730.27	30	503.8	2410	14.2	18.7	203.94	203.94	45.32	PASSED	8.88	PASSED
6	C41	9622	350	350	5730.27	30	503.8	2460	29	25.5	199.25	199.25	18.59	PASSED	5.44	PASSED
6	C44	9623	350	350	5730.27	30	503.8	2450	16.1	13.5	200.19	200.19	56.07	PASSED	9.94	PASSED
7	A12	9624	250	250	1709.03	30	503.8	833	12.4	6.19	59.07	59.07	10.47	PASSED	3.84	PASSED
7	A13	9625	250	250	1709.03	30	503.8	832	0.41	0.46	59.12	59.12	1886.59	PASSED	90.04	PASSED
7	A52	9626	250	250	1709.03	30	503.8	886	5.74	15	55.99	55.99	8.36	PASSED	3.18	PASSED
7	A53	9627	250	250	1709.03	30	503.8	884	0.54	0.42	56.11	56.11	1959.06	PASSED	76.61	PASSED
7	D12	9628	250	250	1709.03	30	503.8	902	5.86	15.3	55.04	55.04	8.06	PASSED	3.08	PASSED
7	D13	9629	250	250	1709.03	30	503.8	900	0.48	0.41	55.16	55.16	2387.53	PASSED	83.05	PASSED
7	D52	9630	250	250	1709.03	30	503.8	809	11.7	6.29	60.42	60.42	11.03	PASSED	4.08	PASSED
7	D53	9631	250	250	1709.03	30	503.8	807	0.42	0.45	60.53	60.53	1699.2	PASSED	91.99	PASSED
7	A11	9632	250	250	1709.03	30	503.8	834	25.3	12.2	59.01	59.01	3.21	PASSED	1.89	PASSED
7	A14	9633	250	250	1709.03	30	503.8	830	13.1	6.11	59.24	59.24	9.79	PASSED	3.69	PASSED
7	A51	9634	250	250	1709.03	30	503.8	887	11.3	30.4	55.93	55.93	2.46	PASSED	1.58	PASSED
7	A54	9635	250	250	1709.03	30	503.8	883	5.82	15.7	56.17	56.17	7.79	PASSED	3.06	PASSED
7	D11	9636	250	250	1709.03	30	503.8	903	11.5	31.2	54.98	54.98	2.32	PASSED	1.52	PASSED
7	D14	9637	250	250	1709.03	30	503.8	899	5.86	16.1	55.22	55.22	7.47	PASSED	2.95	PASSED
7	D51	9638	250	250	1709.03	30	503.8	810	23.9	12.4	60.36	60.36	3.45	PASSED	2.01	PASSED
7	D54	9639	250	250	1709.03	30	503.8	806	12.5	6.19	60.58	60.58	10.22	PASSED	3.89	PASSED
7	A22	9640	300	300	2060.89	30	503.8	903	34.2	3.26	108.09	108.09	5.39	PASSED	2.99	PASSED
7	A23	9641	300	300	2060.89	30	503.8	901	1.38	0.45	108.21	108.21	552.17	PASSED	65.35	PASSED
7	A42	9642	300	300	2060.89	30	503.8	887	33.8	5.1	109.04	109.04	5.3	PASSED	2.95	PASSED
7	A43	9643	300	300	2060.89	30	503.8	885	1.39	0.21	109.16	109.16	583.95	PASSED	72.02	PASSED
7	D22	9644	300	300	2060.89	30	503.8	883	33.2	4.91	109.28	109.28	5.44	PASSED	3.02	PASSED



General Information			Section Properties			F <sub>cu</sub> (N/mm <sup>2</sup> )	F <sub>y</sub> (N/mm <sup>2</sup> )	Applied Loads			Failure Surface Assessment			BS8110 Assessment		
Level	Column ID	FE No.	Height (mm)	Breadth (mm)	A <sub>s</sub> (mm <sup>2</sup> )			Axial (kN)	M <sub>xx</sub> (kN.m)	M <sub>zz</sub> (kN.m)	U <sub>mxx</sub> (kN.m)	U <sub>mzz</sub> (kN.m)	Margin	Acceptability	Margin	Acceptability
7	D23	9645	300	300	2060.89	30	503.8	882	1.36	0.21	109.34	109.34	591.76	PASSED	73.16	PASSED
7	D42	9646	300	300	2060.89	30	503.8	877	33.8	3.22	109.64	109.64	5.44	PASSED	3.06	PASSED
7	D43	9647	300	300	2060.89	30	503.8	875	1.36	0.43	109.75	109.75	520.87	PASSED	67.38	PASSED
7	B12	9648	300	300	2060.89	30	503.8	1140	3.86	33.3	93.13	93.13	5.63	PASSED	2.64	PASSED
7	B13	9649	300	300	2060.89	30	503.8	1140	0.28	1.13	93.13	93.13	1684.98	PASSED	73.1	PASSED
7	B52	9650	300	300	2060.89	30	503.8	1110	7.81	36.4	95.14	95.14	4.66	PASSED	2.35	PASSED
7	B53	9651	300	300	2060.89	30	503.8	1100	0.57	1.17	95.8	95.8	1195.74	PASSED	65.26	PASSED
7	C12	9652	300	300	2060.89	30	503.8	1130	8.4	36.8	93.81	93.81	4.52	PASSED	2.28	PASSED
7	C13	9653	300	300	2060.89	30	503.8	1130	0.62	1.17	93.81	93.81	1261.24	PASSED	63.05	PASSED
7	C52	9654	300	300	2060.89	30	503.8	1110	4.58	33.4	95.14	95.14	5.59	PASSED	2.66	PASSED
7	C53	9655	300	300	2060.89	30	503.8	1110	0.28	1.13	95.14	95.14	1542.68	PASSED	74.44	PASSED
7	A21	9656	300	300	2060.89	30	503.8	905	69.9	7.01	107.97	107.97	1.85	PASSED	1.46	PASSED
7	A24	9657	300	300	2060.89	30	503.8	899	36.8	3.95	108.33	108.33	4.8	PASSED	2.76	PASSED
7	A41	9658	300	300	2060.89	30	503.8	889	69.1	10.4	108.93	108.93	1.85	PASSED	1.44	PASSED
7	A44	9659	300	300	2060.89	30	503.8	883	36.4	5.18	109.28	109.28	4.77	PASSED	2.76	PASSED
7	D21	9660	300	300	2060.89	30	503.8	885	67.9	10.1	109.16	109.16	1.9	PASSED	1.47	PASSED
7	D24	9661	300	300	2060.89	30	503.8	880	35.8	5.03	109.46	109.46	4.89	PASSED	2.81	PASSED
7	D41	9662	300	300	2060.89	30	503.8	879	69.1	6.9	109.52	109.52	1.9	PASSED	1.49	PASSED
7	D44	9663	300	300	2060.89	30	503.8	873	36.4	3.92	109.87	109.87	4.84	PASSED	2.83	PASSED
7	B11	9664	300	300	2060.89	30	503.8	1150	8.1	67.9	92.46	92.46	1.65	PASSED	1.28	PASSED
7	B14	9665	300	300	2060.89	30	503.8	1140	4.25	35.3	93.13	93.13	5.09	PASSED	2.49	PASSED
7	B51	9666	300	300	2060.89	30	503.8	1110	16.3	74.1	95.14	95.14	1.41	PASSED	1.15	PASSED
7	B54	9667	300	300	2060.89	30	503.8	1100	8.83	38.6	95.8	95.8	4.2	PASSED	2.22	PASSED
7	C11	9668	300	300	2060.89	30	503.8	1130	17.6	74.8	93.81	93.81	1.35	PASSED	1.12	PASSED
7	C14	9669	300	300	2060.89	30	503.8	1130	9.49	38.9	93.81	93.81	4.08	PASSED	2.14	PASSED
7	C51	9670	300	300	2060.89	30	503.8	1110	9.59	67.9	95.14	95.14	1.7	PASSED	1.31	PASSED
7	C54	9671	300	300	2060.89	30	503.8	1100	4.98	35.5	95.8	95.8	5.05	PASSED	2.51	PASSED
7	B22	9672	350	350	3216.99	30	503.8	1860	16	14.1	155.38	155.38	36.61	PASSED	7.12	PASSED
7	B23	9673	350	350	3216.99	30	503.8	1860	0.86	0.63	155.38	155.38	9095.79	PASSED	138.5	PASSED
7	B42	9674	350	350	3216.99	30	503.8	1820	14.8	18.1	159.58	159.58	30.7	PASSED	6.54	PASSED
7	B43	9675	350	350	3216.99	30	503.8	1810	0.94	0.72	160.62	160.62	6748.09	PASSED	128.58	PASSED
7	C22	9676	350	350	3216.99	30	503.8	1820	13.2	18.7	159.58	159.58	32	PASSED	6.56	PASSED
7	C23	9677	350	350	3216.99	30	503.8	1810	0.88	0.71	160.62	160.62	7371.69	PASSED	136.1	PASSED
7	C42	9678	350	350	3216.99	30	503.8	1850	14.4	13.9	156.44	156.44	41.02	PASSED	7.75	PASSED
7	C43	9679	350	350	3216.99	30	503.8	1850	0.82	0.65	156.44	156.44	9186.08	PASSED	143.35	PASSED
7	B21	9680	350	350	3216.99	30	503.8	1870	33	29	154.32	154.32	9.66	PASSED	3.44	PASSED
7	B24	9681	350	350	3216.99	30	503.8	1860	17.5	15	155.38	155.38	31.75	PASSED	6.56	PASSED
7	B41	9682	350	350	3216.99	30	503.8	1820	30.7	37.1	159.58	159.58	8.27	PASSED	3.18	PASSED
7	B44	9683	350	350	3216.99	30	503.8	1810	16.4	19.2	160.62	160.62	26.62	PASSED	6.13	PASSED
7	C21	9684	350	350	3216.99	30	503.8	1820	27.5	38.3	159.58	159.58	8.62	PASSED	3.19	PASSED
7	C24	9685	350	350	3216.99	30	503.8	1810	14.8	19.8	160.62	160.62	27.73	PASSED	6.15	PASSED
7	C41	9686	350	350	3216.99	30	503.8	1850	29.9	28.5	156.44	156.44	10.86	PASSED	3.75	PASSED
7	C44	9687	350	350	3216.99	30	503.8	1840	15.9	14.8	157.49	157.49	35.22	PASSED	7.12	PASSED



General Information			Section Properties				Fcu (N/mm <sup>2</sup> )		Fy (N/mm <sup>2</sup> )		Applied Loads				Failure Surface Assessment				BS8110 Assessment	
Level	Column ID	FE No.	Height (mm)	Breadth (mm)	As (mm <sup>2</sup> )	Fcu (N/mm <sup>2</sup> )		Fy (N/mm <sup>2</sup> )		Axial (kN)	Mxx (kN.m)	Mzz (kN.m)	Urmxx (kN.m)	Urmzz (kN.m)	Margin	Acceptability	Margin	Acceptability	Margin	Acceptability
8	A12	9688	250	250	804.28	30	503.8	498	12.5	6.43	52.45	52.45	52.45	5.92	3.1	PASSED	5.92	PASSED	3.1	PASSED
8	A13	9689	250	250	804.28	30	503.8	496	0.32	0.42	52.54	52.54	52.54	700.5	82.71	PASSED	700.5	PASSED	82.71	PASSED
8	A22	9690	250	250	1608.49	30	503.8	568	17.8	1.61	53.98	53.98	53.98	4.44	2.86	PASSED	4.44	PASSED	2.86	PASSED
8	A23	9691	250	250	1608.49	30	503.8	567	0.92	0.2	53.98	53.98	53.98	239.98	51.44	PASSED	239.98	PASSED	51.44	PASSED
8	A42	9692	250	250	1608.49	30	503.8	603	17.7	2.44	53.87	53.87	53.87	4.58	2.8	PASSED	4.58	PASSED	2.8	PASSED
8	A43	9693	250	250	1608.49	30	503.8	601	0.91	0.14	53.88	53.88	53.88	302.79	53.98	PASSED	302.79	PASSED	53.98	PASSED
8	A52	9694	250	250	804.28	30	503.8	595	6.31	15.4	47.86	47.86	47.86	5.07	2.47	PASSED	5.07	PASSED	2.47	PASSED
8	A53	9695	250	250	804.28	30	503.8	594	0.4	0.31	47.91	47.91	47.91	1406.98	81.44	PASSED	1406.98	PASSED	81.44	PASSED
8	B12	9696	250	250	1608.49	30	503.8	726	1.74	17.6	53.23	53.23	53.23	5.56	2.87	PASSED	5.56	PASSED	2.87	PASSED
8	B13	9697	250	250	1608.49	30	503.8	724	0.2	0.79	53.24	53.24	53.24	664.06	59.03	PASSED	664.06	PASSED	59.03	PASSED
8	B22	9698	250	250	3220.13	30	503.8	1240	4.13	3.93	74.91	74.91	74.91	81.03	14.12	PASSED	81.03	PASSED	14.12	PASSED
8	B23	9699	250	250	3220.13	30	503.8	1240	0.4	0.32	74.91	74.91	74.91	5420.71	152.24	PASSED	5420.71	PASSED	152.24	PASSED
8	C12	9700	250	250	1608.49	30	503.8	739	3.92	19.1	53.13	53.13	53.13	4.7	2.51	PASSED	4.7	PASSED	2.51	PASSED
8	C13	9701	250	250	1608.49	30	503.8	737	0.19	0.8	53.15	53.15	53.15	706.49	58.89	PASSED	706.49	PASSED	58.89	PASSED
8	C22	9702	250	250	3220.13	30	503.8	1210	3.62	5.1	76.67	76.67	76.67	67.2	12.4	PASSED	67.2	PASSED	12.4	PASSED
8	C23	9703	250	250	3220.13	30	503.8	1210	0.38	0.34	76.67	76.67	76.67	4954.98	160.5	PASSED	76.67	PASSED	160.5	PASSED
8	D12	9704	250	250	804.28	30	503.8	611	6.35	15.8	47.05	47.05	47.05	4.92	2.38	PASSED	4.92	PASSED	2.38	PASSED
8	D13	9705	250	250	804.28	30	503.8	609	0.46	0.3	47.15	47.15	47.15	1336.13	73.15	PASSED	47.15	PASSED	73.15	PASSED
8	D22	9706	250	250	1608.49	30	503.8	603	17.5	2.36	53.87	53.87	53.87	4.66	2.84	PASSED	53.87	PASSED	2.84	PASSED
8	D23	9707	250	250	1608.49	30	503.8	601	0.89	0.14	53.88	53.88	53.88	312.06	55.11	PASSED	53.88	PASSED	55.11	PASSED
8	B42	9708	250	250	3220.13	30	503.8	1210	3.97	4.94	76.67	76.67	76.67	65.36	12.51	PASSED	76.67	PASSED	12.51	PASSED
8	B43	9709	250	250	3220.13	30	503.8	1210	0.4	0.34	76.67	76.67	76.67	4757.84	154.04	PASSED	76.67	PASSED	154.04	PASSED
8	B52	9710	250	250	1608.49	30	503.8	722	3.68	19	53.26	53.26	53.26	4.68	2.53	PASSED	53.26	PASSED	2.53	PASSED
8	B53	9711	250	250	1608.49	30	503.8	721	0.16	0.8	53.27	53.27	53.27	662.82	59.85	PASSED	53.27	PASSED	59.85	PASSED
8	C42	9712	250	250	3220.13	30	503.8	1240	3.81	3.87	74.91	74.91	74.91	88.07	14.93	PASSED	74.91	PASSED	14.93	PASSED
8	C43	9713	250	250	3220.13	30	503.8	1230	0.38	0.32	75.5	75.5	75.5	5583.67	160.17	PASSED	75.5	PASSED	160.17	PASSED
8	C52	9714	250	250	1608.49	30	503.8	702	1.99	17.7	53.39	53.39	53.39	5.31	2.84	PASSED	53.39	PASSED	2.84	PASSED
8	C53	9715	250	250	1608.49	30	503.8	701	0.23	0.79	53.4	53.4	53.4	574.63	58	PASSED	53.4	PASSED	58	PASSED
8	D42	9716	250	250	1608.49	30	503.8	561	17.8	1.62	53.99	53.99	53.99	4.39	2.86	PASSED	53.99	PASSED	2.86	PASSED
8	D43	9717	250	250	1608.49	30	503.8	560	0.9	0.2	54	54	54	236.22	52.17	PASSED	54	PASSED	52.17	PASSED
8	D52	9718	250	250	804.28	30	503.8	486	12	6.48	52.99	52.99	52.99	6.06	3.21	PASSED	52.99	PASSED	3.21	PASSED
8	D53	9719	250	250	804.28	30	503.8	485	0.33	0.43	53.04	53.04	53.04	613.97	79.91	PASSED	53.04	PASSED	79.91	PASSED
9	A12	9720	250	250	1256.64	30	503.8	199	11.8	6.52	61.06	61.06	61.06	3.33	3.49	PASSED	61.06	PASSED	3.49	PASSED
9	A13	9721	250	250	1256.64	30	503.8	198	0.82	1.22	61.02	61.02	61.02	29.93	31.52	PASSED	61.02	PASSED	31.52	PASSED
9	A22	9722	250	250	1256.64	30	503.8	255	19.6	1.22	63.15	63.15	63.15	3.11	3.06	PASSED	63.15	PASSED	3.06	PASSED
9	A23	9723	250	250	1256.64	30	503.8	253	0.88	0.15	63.08	63.08	63.08	65.89	62.63	PASSED	63.08	PASSED	62.63	PASSED
9	A42	9724	250	250	1256.64	30	503.8	332	19.5	2.73	64.83	64.83	64.83	3.48	2.99	PASSED	64.83	PASSED	2.99	PASSED
9	A43	9725	250	250	1256.64	30	503.8	330	0.85	0.32	64.8	64.8	64.8	96.52	58.29	PASSED	64.8	PASSED	58.29	PASSED
9	A52	9726	250	250	1256.64	30	503.8	280	6.67	14.7	63.92	63.92	63.92	3.28	3.16	PASSED	63.92	PASSED	3.16	PASSED
9	A53	9727	250	250	1256.64	30	503.8	279	1.56	0.88	63.9	63.9	63.9	32.16	27.97	PASSED	63.9	PASSED	27.97	PASSED
9	B12	9728	250	250	1256.64	30	503.8	354	2.06	19.7	65.13	65.13	65.13	3.71	3.06	PASSED	65.13	PASSED	3.06	PASSED
9	B13	9729	250	250	1256.64	30	503.8	352	0.17	0.82	65.1	65.1	65.1	134.56	68.87	PASSED	65.1	PASSED	68.87	PASSED
9	B22	9730	250	250	804.28	30	503.8	625	4	4.32	46.33	46.33	46.33	27.75	6.86	PASSED	46.33	PASSED	6.86	PASSED



General Information			Section Properties			F <sub>cu</sub> (N/mm <sup>2</sup> )	F <sub>y</sub> (N/mm <sup>2</sup> )	Applied Loads			Failure Surface Assessment				BS8110 Assessment	
Level	Column ID	FE No.	Height (mm)	Breadth (mm)	A <sub>s</sub> (mm <sup>2</sup> )			Axial (kN)	M <sub>xx</sub> (kN.m)	M <sub>zz</sub> (kN.m)	U <sub>mxx</sub> (kN.m)	U <sub>mzz</sub> (kN.m)	Margin	Acceptability	Margin	Acceptability
9	B23	9731	250	250	804.28	30	503.8	624	0.18	0.15	46.38	46.38	5983.87	PASSED	172.16	PASSED
9	C12	9732	250	250	1256.64	30	503.8	347	2.97	20.7	65.04	65.04	3.35	PASSED	2.82	PASSED
9	C13	9733	250	250	1256.64	30	503.8	345	0.16	0.85	65.01	65.01	124.38	PASSED	66.79	PASSED
9	C22	9734	250	250	804.28	30	503.8	611	3.91	5.21	47.05	47.05	22.98	PASSED	6.17	PASSED
9	C23	9735	250	250	804.28	30	503.8	610	0.17	0.16	47.1	47.1	5590.56	PASSED	179.06	PASSED
9	D12	9736	250	250	1256.64	30	503.8	290	6.64	15.1	64.11	64.11	3.31	PASSED	3.12	PASSED
9	D13	9737	250	250	1256.64	30	503.8	289	1.46	0.89	64.09	64.09	35.4	PASSED	29.24	PASSED
9	D22	9738	250	250	1256.64	30	503.8	335	19.4	2.66	64.87	64.87	3.53	PASSED	3.02	PASSED
9	D23	9739	250	250	1256.64	30	503.8	333	0.83	0.35	64.84	64.84	98.91	PASSED	58.74	PASSED
9	B42	9740	250	250	804.28	30	503.8	611	4.16	5.05	47.05	47.05	22.68	PASSED	6.17	PASSED
9	B43	9741	250	250	804.28	30	503.8	610	0.18	0.15	47.1	47.1	5144.93	PASSED	168.15	PASSED
9	B52	9742	250	250	1256.64	30	503.8	338	2.8	20.7	64.91	64.91	3.31	PASSED	2.83	PASSED
9	B53	9743	250	250	1256.64	30	503.8	337	0.14	0.84	64.9	64.9	121	PASSED	68.09	PASSED
9	C42	9744	250	250	804.28	30	503.8	622	3.88	4.26	46.48	46.48	28.6	PASSED	7.01	PASSED
9	C43	9745	250	250	804.28	30	503.8	620	0.16	0.15	46.59	46.59	6452.21	PASSED	185.45	PASSED
9	C52	9746	250	250	1256.64	30	503.8	345	2.15	19.8	65.01	65.01	3.61	PASSED	3.02	PASSED
9	C53	9747	250	250	1256.64	30	503.8	344	0.17	0.81	65	65	127.99	PASSED	68.86	PASSED
9	D42	9748	250	250	1256.64	30	503.8	253	19.6	1.22	63.08	63.08	3.1	PASSED	3.06	PASSED
9	D43	9749	250	250	1256.64	30	503.8	252	0.86	0.15	63.05	63.05	66.21	PASSED	63.39	PASSED
9	D52	9750	250	250	1256.64	30	503.8	198	11.5	6.48	61.02	61.02	3.39	PASSED	3.56	PASSED
9	D53	9751	250	250	1256.64	30	503.8	196	0.82	1.24	60.94	60.94	29.62	PASSED	31.18	PASSED
8	A11	9752	250	250	804.28	30	503.8	499	25.3	12.4	52.41	52.41	2.15	PASSED	1.55	PASSED
8	A14	9753	250	250	804.28	30	503.8	495	12.7	5.97	52.59	52.59	5.96	PASSED	3.12	PASSED
8	A21	9754	250	250	1608.49	30	503.8	570	36.7	3.44	53.97	53.97	1.64	PASSED	1.39	PASSED
8	A24	9755	250	250	1608.49	30	503.8	566	19.6	1.83	53.98	53.98	3.87	PASSED	2.6	PASSED
8	A41	9756	250	250	1608.49	30	503.8	604	36.5	5.12	53.87	53.87	1.64	PASSED	1.36	PASSED
8	A44	9757	250	250	1608.49	30	503.8	600	19.4	2.58	53.88	53.88	4.01	PASSED	2.56	PASSED
8	A51	9758	250	250	804.28	30	503.8	596	12.2	30.9	47.81	47.81	1.66	PASSED	1.24	PASSED
8	A54	9759	250	250	804.28	30	503.8	592	6.23	15.4	48.01	48.01	5.08	PASSED	2.48	PASSED
8	B11	9760	250	250	1608.49	30	503.8	727	3.77	36	53.22	53.22	1.8	PASSED	1.4	PASSED
8	B14	9761	250	250	1608.49	30	503.8	723	2.03	19.1	53.25	53.25	4.85	PASSED	2.63	PASSED
8	B21	9762	250	250	3220.13	30	503.8	1250	8.76	8.3	74.32	74.32	22.07	PASSED	6.6	PASSED
8	B24	9763	250	250	3220.13	30	503.8	1240	4.79	4.44	74.91	74.91	63.96	PASSED	12.23	PASSED
8	B41	9764	250	250	3220.13	30	503.8	1220	8.45	10.3	76.09	76.09	18.35	PASSED	5.93	PASSED
8	B44	9765	250	250	3220.13	30	503.8	1210	4.64	5.48	76.67	76.67	52.65	PASSED	11.15	PASSED
8	B51	9766	250	250	1608.49	30	503.8	724	7.62	38.9	53.24	53.24	1.52	PASSED	1.24	PASSED
8	B54	9767	250	250	1608.49	30	503.8	720	3.91	20.5	53.27	53.27	4.15	PASSED	2.35	PASSED
8	C11	9768	250	250	1608.49	30	503.8	740	8.15	39.2	53.12	53.12	1.5	PASSED	1.22	PASSED
8	C14	9769	250	250	1608.49	30	503.8	736	4.19	20.6	53.16	53.16	4.16	PASSED	2.33	PASSED
8	C21	9770	250	250	3220.13	30	503.8	1220	7.7	10.6	76.09	76.09	18.96	PASSED	5.89	PASSED
8	C24	9771	250	250	3220.13	30	503.8	1210	4.27	5.64	76.67	76.67	54.29	PASSED	11.09	PASSED
8	C41	9772	250	250	3220.13	30	503.8	1240	8.07	8.17	74.91	74.91	23.93	PASSED	7.07	PASSED
8	C44	9773	250	250	3220.13	30	503.8	1230	4.45	4.38	75.5	75.5	68.4	PASSED	13.11	PASSED



General Information			Section Properties			F <sub>cu</sub> (N/mm <sup>2</sup> )	F <sub>y</sub> (N/mm <sup>2</sup> )	Applied Loads			Failure Surface Assessment				BS8110 Assessment	
Level	Column ID	FE No.	Height (mm)	Breadth (mm)	As (mm <sup>2</sup> )			Axial (kN)	M <sub>xx</sub> (kN.m)	M <sub>zz</sub> (kN.m)	U <sub>mxx</sub> (kN.m)	U <sub>mzz</sub> (kN.m)	Margin	Acceptability	Margin	Acceptability
8	C51	9774	250	250	1608.49	30	503.8	704	4.32	36.3	53.38	53.38	1.75	PASSED	1.38	PASSED
8	C54	9775	250	250	1608.49	30	503.8	700	2.32	19.2	53.41	53.41	4.65	PASSED	2.6	PASSED
8	D11	9776	250	250	804.28	30	503.8	612	12.2	31.7	47	47	1.58	PASSED	1.2	PASSED
8	D14	9777	250	250	804.28	30	503.8	608	6.23	15.8	47.2	47.2	4.94	PASSED	2.4	PASSED
8	D21	9778	250	250	1608.49	30	503.8	604	36	4.97	53.87	53.87	1.67	PASSED	1.38	PASSED
8	D24	9779	250	250	1608.49	30	503.8	600	19.2	2.52	53.88	53.88	4.08	PASSED	2.59	PASSED
8	D41	9780	250	250	1608.49	30	503.8	563	36.5	3.43	53.99	53.99	1.64	PASSED	1.39	PASSED
8	D44	9781	250	250	1608.49	30	503.8	559	19.5	1.82	54	54	3.86	PASSED	2.61	PASSED
8	D51	9782	250	250	804.28	30	503.8	487	24.3	12.4	52.95	52.95	2.24	PASSED	1.61	PASSED
8	D54	9783	250	250	804.28	30	503.8	483	12.3	5.92	53.13	53.13	6.09	PASSED	3.23	PASSED
9	A11	9784	250	250	1256.64	30	503.8	201	24.3	14.1	61.13	61.13	1.59	PASSED	1.67	PASSED
9	A14	9785	250	250	1256.64	30	503.8	197	12.9	8.73	60.98	60.98	2.82	PASSED	2.97	PASSED
9	A21	9786	250	250	1256.64	30	503.8	256	39.9	2.58	63.19	63.19	1.51	PASSED	1.5	PASSED
9	A24	9787	250	250	1256.64	30	503.8	252	21.1	1.3	63.05	63.05	2.87	PASSED	2.84	PASSED
9	A41	9788	250	250	1256.64	30	503.8	333	39.9	5.7	64.84	64.84	1.55	PASSED	1.46	PASSED
9	A44	9789	250	250	1256.64	30	503.8	329	21.1	2.8	64.78	64.78	3.19	PASSED	2.78	PASSED
9	A51	9790	250	250	1256.64	30	503.8	281	14.3	30.4	63.94	63.94	1.51	PASSED	1.52	PASSED
9	A54	9791	250	250	1256.64	30	503.8	277	9.22	16.3	63.86	63.86	2.7	PASSED	2.67	PASSED
9	B11	9792	250	250	1256.64	30	503.8	355	4.1	40.3	65.14	65.14	1.63	PASSED	1.5	PASSED
9	B14	9793	250	250	1256.64	30	503.8	351	1.72	21.2	65.09	65.09	3.45	PASSED	2.89	PASSED
9	B21	9794	250	250	804.28	30	503.8	627	8.31	8.92	46.22	46.22	8.26	PASSED	3.31	PASSED
9	B24	9795	250	250	804.28	30	503.8	623	4.22	4.48	46.43	46.43	25.66	PASSED	6.58	PASSED
9	B41	9796	250	250	804.28	30	503.8	612	8.64	10.4	47	47	6.89	PASSED	2.99	PASSED
9	B44	9797	250	250	804.28	30	503.8	608	4.4	5.22	47.2	47.2	21.03	PASSED	5.93	PASSED
9	B51	9798	250	250	1256.64	30	503.8	339	5.84	42.3	64.93	64.93	1.47	PASSED	1.38	PASSED
9	B54	9799	250	250	1256.64	30	503.8	335	2.97	22.2	64.87	64.87	3.04	PASSED	2.64	PASSED
9	C11	9800	250	250	1256.64	30	503.8	348	6.22	42.4	65.05	65.05	1.47	PASSED	1.38	PASSED
9	C14	9801	250	250	1256.64	30	503.8	344	3.16	22.2	65	65	3.08	PASSED	2.63	PASSED
9	C21	9802	250	250	804.28	30	503.8	613	8.08	10.7	46.95	46.95	7.01	PASSED	2.99	PASSED
9	C24	9803	250	250	804.28	30	503.8	609	4.13	5.38	47.15	47.15	21.4	PASSED	5.94	PASSED
9	C41	9804	250	250	804.28	30	503.8	623	7.98	8.81	46.43	46.43	8.6	PASSED	3.39	PASSED
9	C44	9805	250	250	804.28	30	503.8	619	4.07	4.42	46.64	46.64	26.47	PASSED	6.74	PASSED
9	C51	9806	250	250	1256.64	30	503.8	346	4.31	40.4	65.02	65.02	1.6	PASSED	1.48	PASSED
9	C54	9807	250	250	1256.64	30	503.8	342	1.8	21.3	64.97	64.97	3.36	PASSED	2.86	PASSED
9	D11	9808	250	250	1256.64	30	503.8	292	14.3	31.2	64.15	64.15	1.51	PASSED	1.5	PASSED
9	D14	9809	250	250	1256.64	30	503.8	288	9.08	16.7	64.08	64.08	2.75	PASSED	2.65	PASSED
9	D21	9810	250	250	1256.64	30	503.8	336	39.7	5.54	64.89	64.89	1.57	PASSED	1.47	PASSED
9	D24	9811	250	250	1256.64	30	503.8	332	20.9	2.7	64.83	64.83	3.25	PASSED	2.81	PASSED
9	D41	9812	250	250	1256.64	30	503.8	254	39.9	2.59	63.12	63.12	1.5	PASSED	1.5	PASSED
9	D44	9813	250	250	1256.64	30	503.8	251	21.1	1.31	63.01	63.01	2.86	PASSED	2.84	PASSED
9	D51	9814	250	250	1256.64	30	503.8	199	23.8	14.1	61.06	61.06	1.61	PASSED	1.69	PASSED
9	D54	9815	250	250	1256.64	30	503.8	195	12.8	8.75	60.9	60.9	2.83	PASSED	2.98	PASSED



Transient Dynamic Analysis of FCTS (Under Horizontal Earthquake Only)

Assessment of Column B31 for Axial Load and Transverse Bending Moments During Seismic Excitation (Applied Earthquake loads Time-History) \*

Bottom section of column

Applied Axial Load

Absolute Maximum Bending Moments

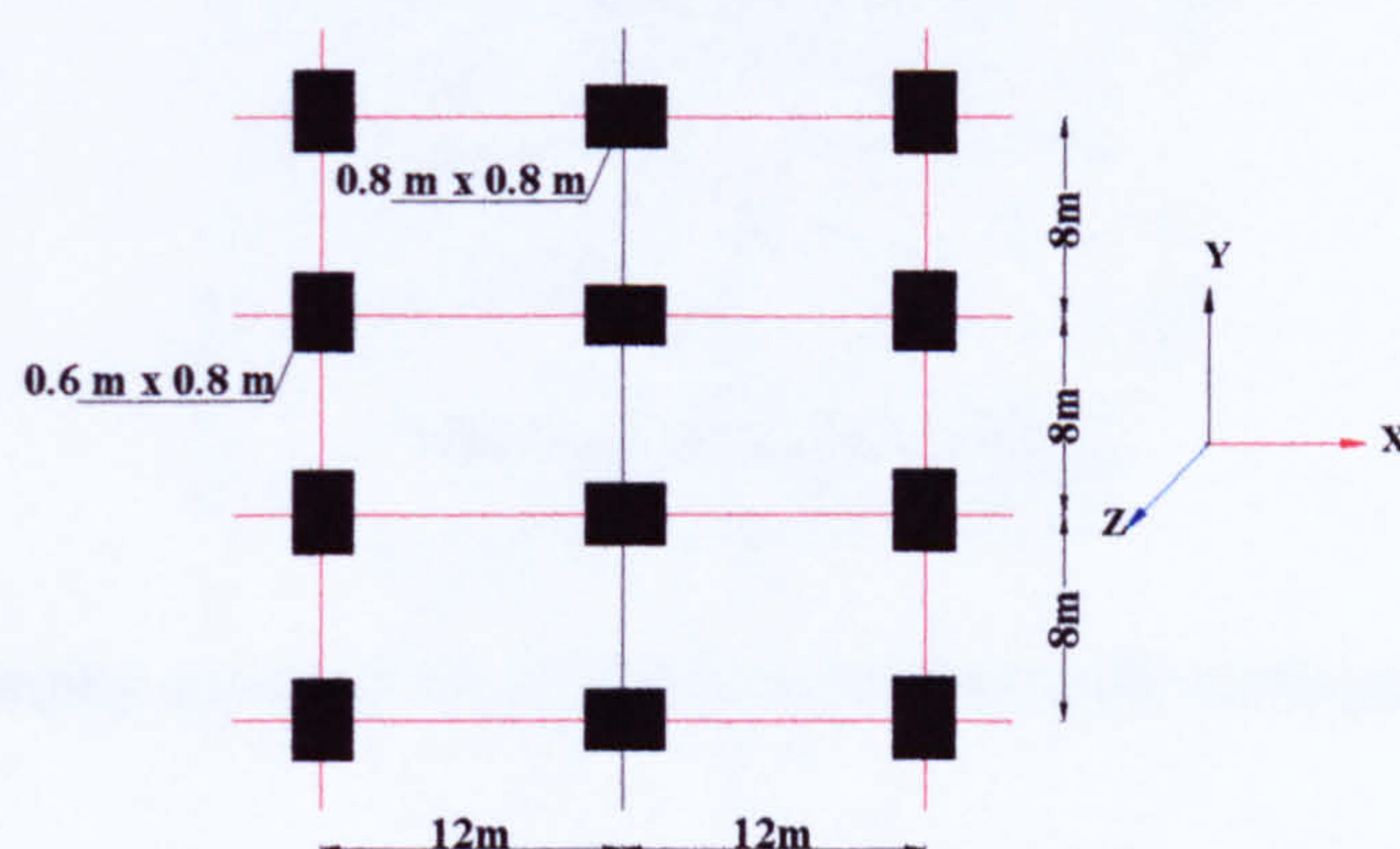
General Information			Section Properties			F <sub>cu</sub> (N/mm <sup>2</sup> )	F <sub>y</sub> (N/mm <sup>2</sup> )	Applied Loads			Failure Surface Assessment				BS8110 Assessment	
Level	Column ID	Time step (sec)	Height (mm)	Breadth (mm)	A <sub>s</sub> (mm <sup>2</sup> )			Axial (kN)	M <sub>xx</sub> (kN.m)	M <sub>zz</sub> (kN.m)	U <sub>mxx</sub> (kN.m)	U <sub>mzz</sub> (kN.m)	Margin	Acceptability	Margin	Acceptability
ground	B31	0.01	800	800	12867.96	40	503.8	10118.9	28.9	1.62	1972.85	1972.85	2002.79	PASSED	66.27	PASSED
ground	B31	0.02	800	800	12867.96	40	503.8	10118.8	33.03	6.48	1972.87	1972.87	1503.57	PASSED	54.05	PASSED
ground	B31	0.03	800	800	12867.96	40	503.8	10118.8	37.2	11.47	1972.87	1972.87	1141.44	PASSED	45.52	PASSED
All Rows Between Previous & Next Time Are Passed																
ground	B31	4.65	800	800	12867.96	40	503.8	10045.9	1254.68	1373.39	1987.12	1987.12	1.05	PASSED	0.97	FAILED
ground	B31	4.66	800	800	12867.96	40	503.8	10047	1311.21	1427.59	1986.91	1986.91	0.97	FAILED	0.93	FAILED
ground	B31	4.67	800	800	12867.96	40	503.8	10048.5	1357.24	1468.51	1986.62	1986.62	0.92	FAILED	0.9	FAILED
ground	B31	4.68	800	800	12867.96	40	503.8	10050.2	1385.87	1488.31	1986.29	1986.29	0.89	FAILED	0.89	FAILED
ground	B31	4.69	800	800	12867.96	40	503.8	10051.7	1399.03	1488.69	1985.99	1985.99	0.89	FAILED	0.89	FAILED
ground	B31	4.7	800	800	12867.96	40	503.8	10052.8	1395.34	1468.62	1985.78	1985.78	0.9	FAILED	0.89	FAILED
ground	B31	4.71	800	800	12867.96	40	503.8	10053.3	1374.61	1427.85	1985.68	1985.68	0.93	FAILED	0.92	FAILED
ground	B31	4.72	800	800	12867.96	40	503.8	10053.1	1335.81	1365.55	1985.72	1985.72	1	FAILED	0.95	FAILED
All Rows Between Previous & Next Time Are Passed																
ground	B31	4.78	800	800	12867.96	40	503.8	10041	941.91	810.82	1988.08	1988.08	2.16	PASSED	1.44	PASSED
ground	B31	4.79	800	800	12867.96	40	503.8	10038.7	859.49	702.17	1988.52	1988.52	2.65	PASSED	1.61	PASSED
ground	B31	4.8	800	800	12867.96	40	503.8	10036.7	779.07	597.6	1988.91	1988.91	3.31	PASSED	1.81	PASSED
All Rows Between Previous & Next Time Are Passed																
ground	B31	5.13	800	800	12867.96	40	503.8	10151.2	1206.22	1400.65	1966.51	1966.51	1.05	PASSED	0.96	FAILED
ground	B31	5.14	800	800	12867.96	40	503.8	10152	1260.67	1439.67	1966.35	1966.35	0.98	FAILED	0.93	FAILED
ground	B31	5.15	800	800	12867.96	40	503.8	10153.1	1299.96	1459.83	1966.13	1966.13	0.95	FAILED	0.91	FAILED
ground	B31	5.16	800	800	12867.96	40	503.8	10154.8	1324.41	1461.66	1965.8	1965.8	0.93	FAILED	0.91	FAILED
ground	B31	5.17	800	800	12867.96	40	503.8	10157.2	1333.7	1445.09	1965.32	1965.32	0.93	FAILED	0.91	FAILED
ground	B31	5.18	800	800	12867.96	40	503.8	10160.3	1340.33	1424.56	1964.71	1964.71	0.94	FAILED	0.92	FAILED
ground	B31	5.19	800	800	12867.96	40	503.8	10163.9	1349.8	1407.65	1964	1964	0.95	FAILED	0.92	FAILED
ground	B31	5.2	800	800	12867.96	40	503.8	10167.8	1358	1389.97	1963.23	1963.23	0.95	FAILED	0.93	FAILED
ground	B31	5.21	800	800	12867.96	40	503.8	10171.8	1356.73	1362.01	1962.44	1962.44	0.97	FAILED	0.94	FAILED
ground	B31	5.22	800	800	12867.96	40	503.8	10175.8	1344.65	1321.84	1961.66	1961.66	1	PASSED	0.96	FAILED
ground	B31	5.23	800	800	12867.96	40	503.8	10180.1	1322.13	1270.07	1960.81	1960.81	1.06	PASSED	0.98	FAILED
All Rows Between Previous & Next Time Are Passed																
ground	B31	10.17	800	800	12867.96	40	503.8	10086.3	288.77	277.94	1979.24	1979.24	16.46	PASSED	4.52	PASSED
ground	B31	10.18	800	800	12867.96	40	503.8	10084	298.61	267.28	1979.69	1979.69	16.47	PASSED	4.48	PASSED
ground	B31	10.19	800	800	12867.96	40	503.8	10082	306.36	254.71	1980.08	1980.08	16.66	PASSED	4.47	PASSED

\* This Column (B31) is included through the above spreadsheet of the global Assessment of the FCTS and is pointed out by the coloured row in the first page of this appendix

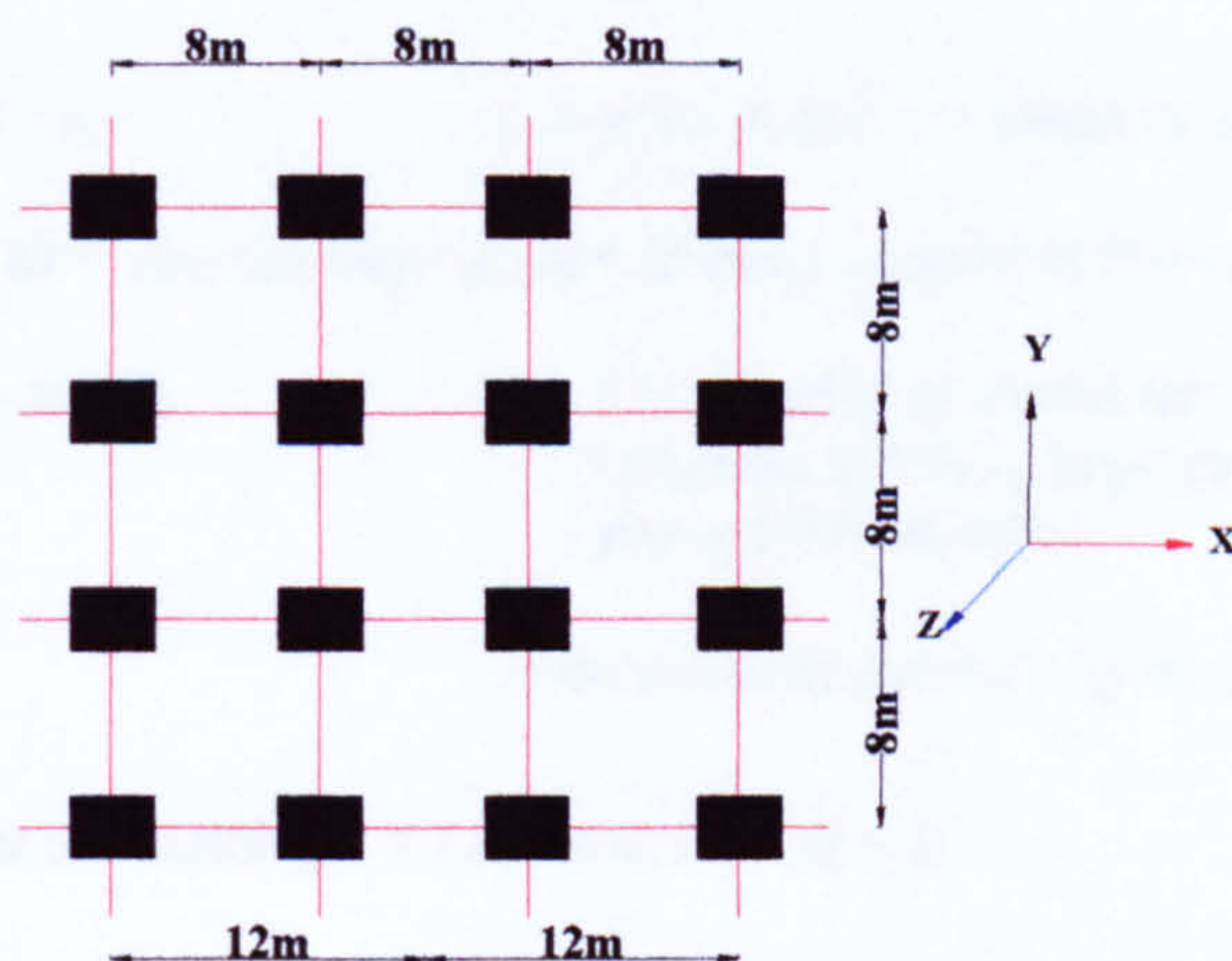


## Analytical Calculations For The Seismic Performance Of The 10 Storey RC Building

### The FCTS Model Under Horizontal Earthquake Only



**Plane of ground floor columns of the FCTS model**



**Plane of columns for other floors of the FCTS model**

(The dimensions of columns according to the Appendix II)

To calculate the peak ground acceleration that the FCTS model can withstand under the horizontal earthquake only, the overturning moment for the FCTS model was calculated as follows:

Gravity force of the building

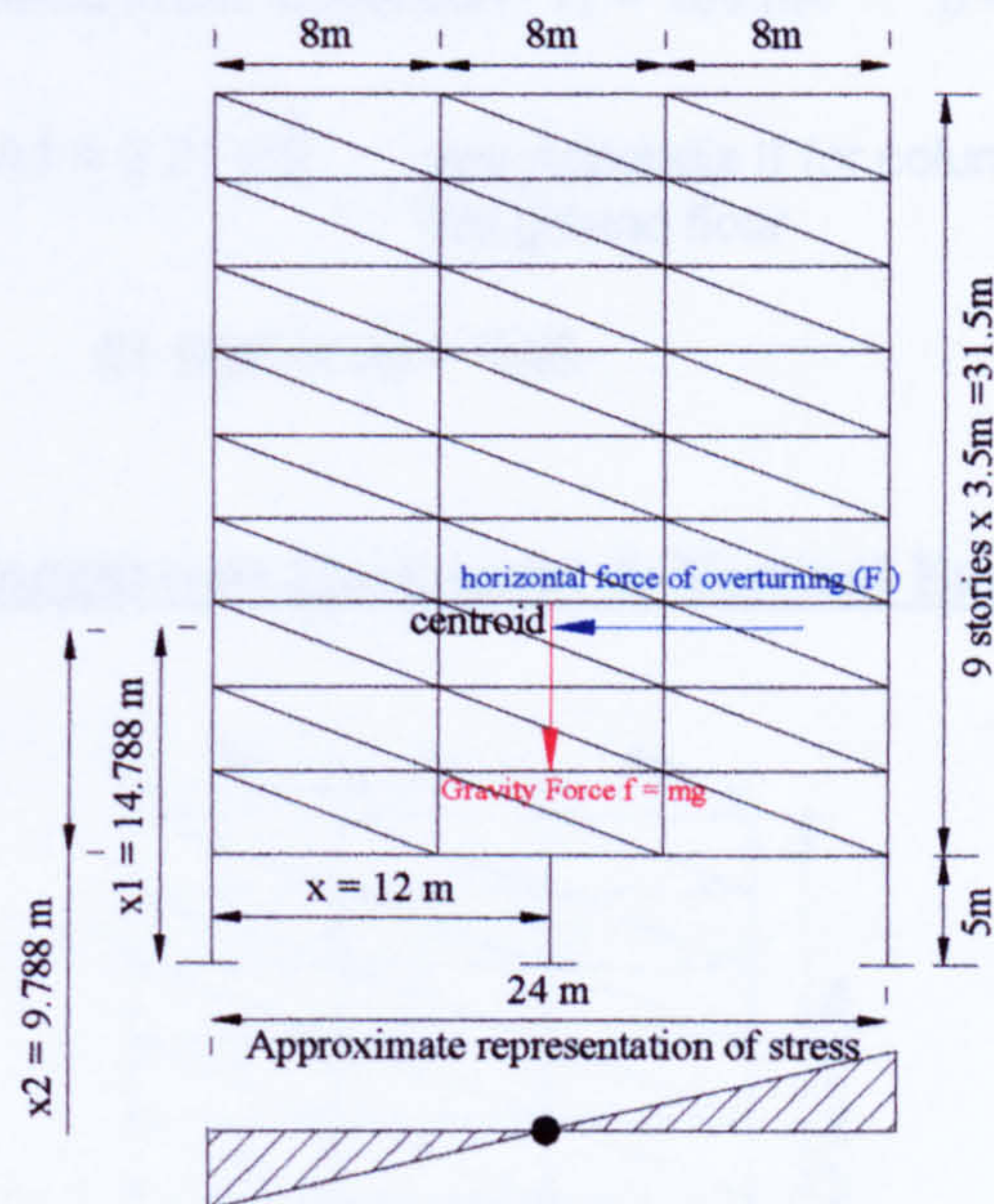
$$f := m \cdot g$$

$m$  = mass of building

$g$  = acceleration of gravity



## APPENDIX V



Overturning forces of the building under horizontal earthquake only

Assume horizontal overturning force =  $F_o = \beta mg$

$\beta$  = the peak value of the horizontal acceleration

$$x := 12\text{m}$$

For the building base

$$x_1 := 14.788\text{m}$$

For the first floor

$$x_2 := 9.788\text{m}$$

Direct stress for the building =  $f / A$

$A$  = sum of column areas of every floor

Bending stress =  $(M / I) \cdot x$        $M$  = overturning moment of building around the centroid

$x = 12\text{ m}$  as shown in the figure above

$I$  = moment of inertia for all columns in the  $x$ -direction around the centroid

$$M = \beta mg \cdot x_1$$

$$\text{Then Bending stress} = (\beta m g x_1 x) / I$$

From condition at zero stress for the building  $(f / A) - ((M / I) \cdot x) = 0$

$$\beta = I / x \cdot x_1 \cdot A$$

For the building base moment of inertia in the  $x$ -direction  $I = 553.212\text{ m}^4$

and total area of the columns  $A = 6.4\text{ m}^2$

see Appendix II for columns dimensions at the ground floor

$$\beta (\text{ground floor}) = 0.49$$



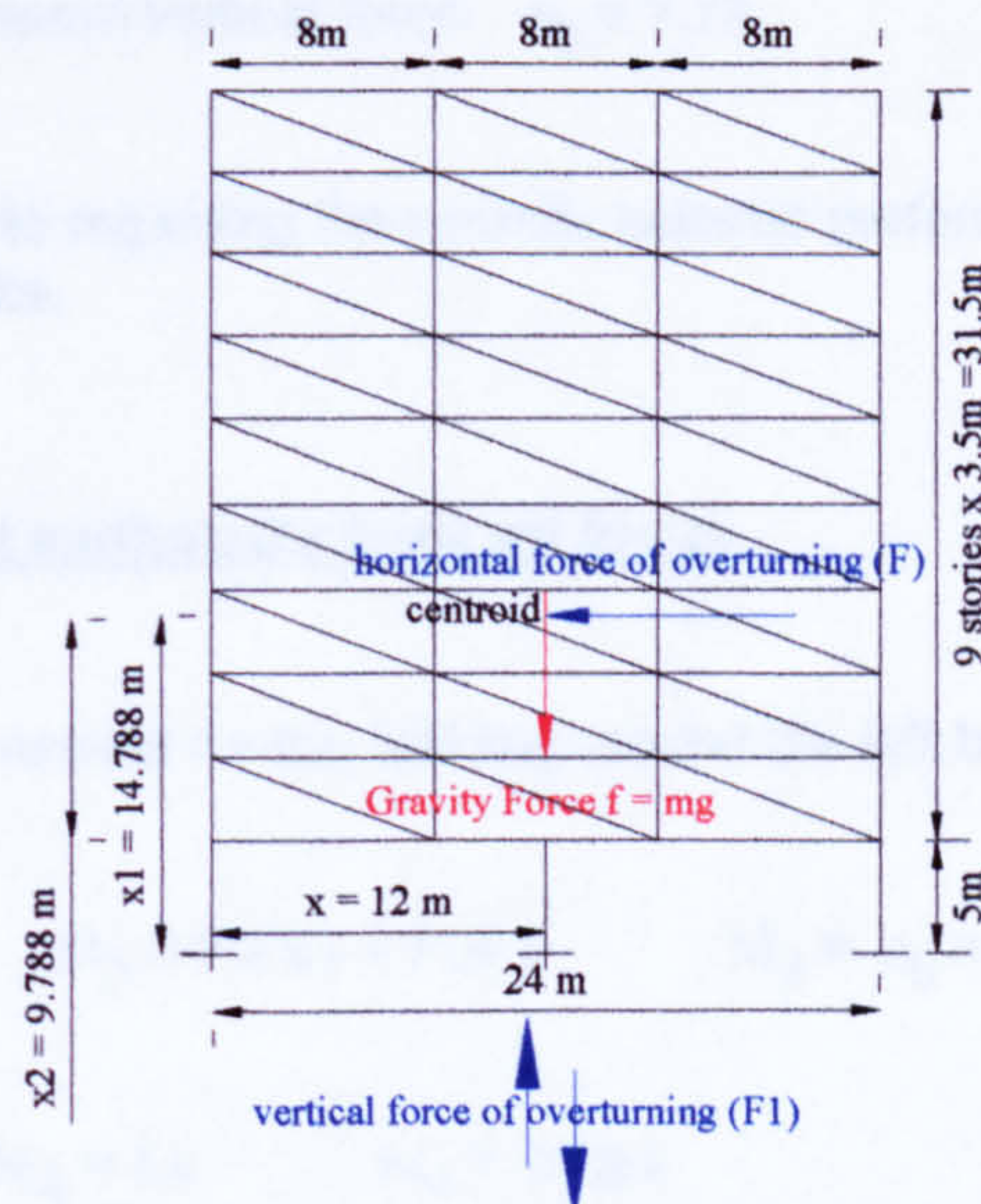
## APPENDIX V

For the first floor moment of inertia in the x-direction  $I_1 = 189 \text{ m}^4$        $\beta = I_1 / x \cdot x_2 \cdot A_1$

and total area of the columns  $A_1 = 2.77 \text{ m}^2$       see Appendix II for columns dimensions at the ground floor

$\beta_1$  (first floor) = 0.58

### The FCTS Model Under Concurrent Horizontal & Vertical Earthquake



Overturning forces of the building under concurrent horizontal & vertical earthquake

To calculate the peak acceleration of the concurrent horizontal and vertical earthquake that the building can withstand, it was assumed that there are horizontal and vertical overturning forces and the vertical force may be upward or downward. the overturning moment of the building was calculated around the left bottom corner of the building according to the stability conditions. the horizontal and vertical peak accelerations were calculated as follows:

#### First case of the vertical earthquake (downward force)

Gravity force  $f = m \cdot g$

Horizontal overturning force  $F_o = a_h \cdot m \cdot g$

Vertical overturning force  $F_{ov} = a_v \cdot m \cdot g$

$a_h$  is the value of the horizontal peak acceleration

$a_v$  is the value of the vertical peak acceleration

calculating the overturning moment for the building around the left bottom corner as shown in the figure above

the overturning moment       $M_1 = F_o \cdot x_1$        $M_1 = a_h \cdot m \cdot g \cdot x_1$



## APPENDIX V

the resisting moment  $M_2 = F_{ov}.x + f.x$   $M_2 = a_v.m.g.x + m.g.x$

By equating  $M_1$  &  $M_2$  then the result  $a_h.x1 = (a_v + 1) x$

Also as mentioned in chapter 2 , 3 the vertical earthquake = (2 / 3) the horizontal earthquake

$$a_v = (2 / 3) a_h$$

$$a_h = x / (x1 - (2/3)x)$$

Then in the case of the downward vertical force  $a_h = 1.77$   $a_v = 1.18$

This results are not acceptable regarding the realistic seismic performance of the RC buildings under the earthquake.

### Second case of the vertical earthquake (upward force)

calculating the overturning moment for the building around the left bottom corner as shown in the figure above

the overturning moment  $M_3 = F_o.x1 + F_{ov}.x$   $M_3 = a_h.m.g.x1 + a_v.m.g.x$

the resisting moment  $M_4 = f.x$   $M_4 = m.g.x$

By equating  $M_3$  &  $M_4$  then the result  $a_h.x1 + a_v.x = x$

Also as mentioned in chapter 2 , 3 the vertical earthquake = (2 / 3) the horizontal earthquake

$$a_v = (2 / 3) a_h$$

$$a_h = x / (x1 + (2/3)x)$$

Then in the case of the upward vertical force for the ground floor  
 $a_h = 0.53$   $a_v = 0.35$

For the first floor  $x2 = 9.788$  m  $a_h = x / (x2 + (2/3)x)$

Then in the case of the upward vertical force for the first floor  
 $a_h = 0.67$   $a_v = 0.44$